Yasuya Nomura

Morphological Aspects of Inner Ear Disease

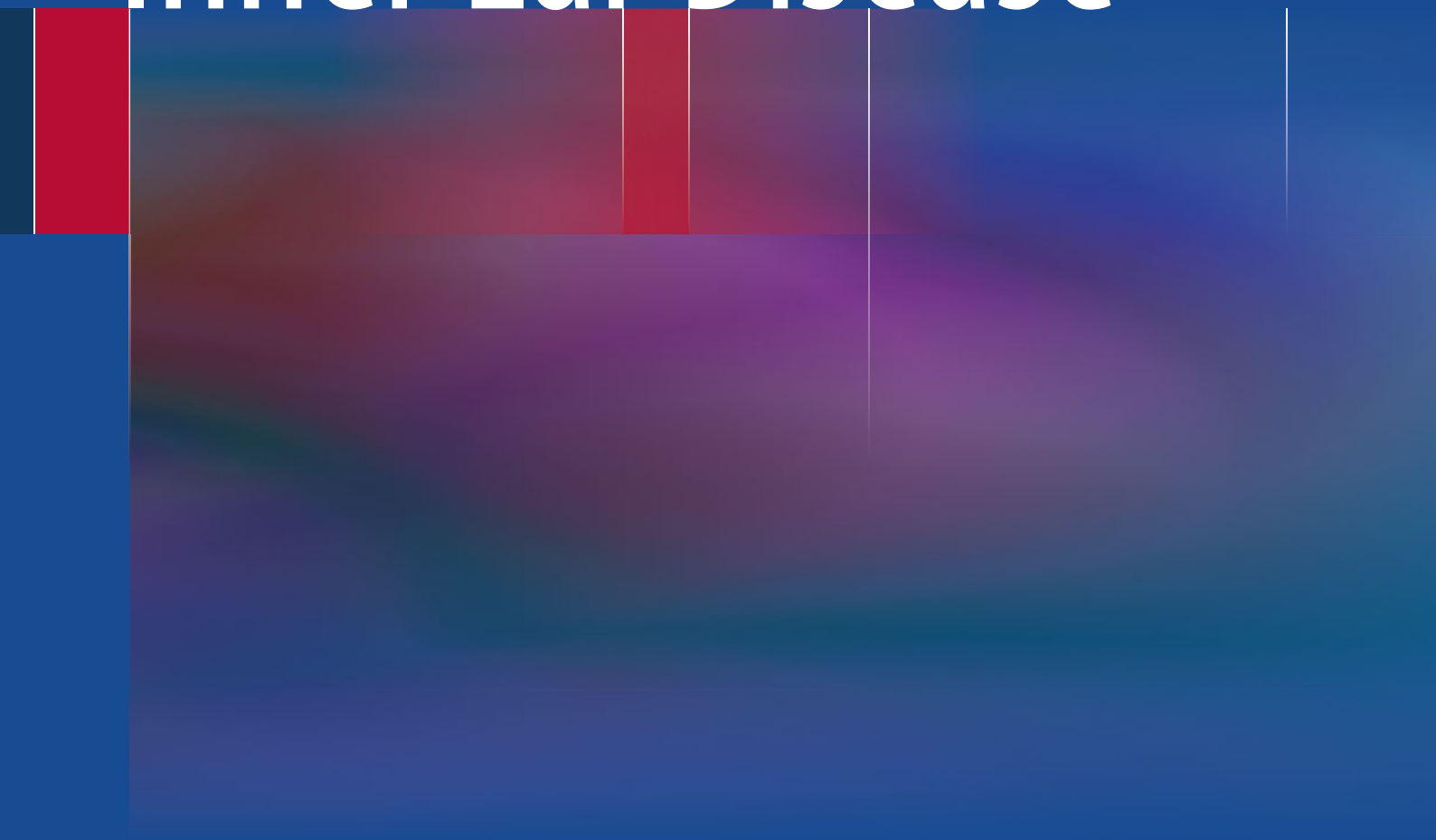

Springer

Morphological Aspects of Inner Ear Disease

Yasuya Nomura

Morphological Aspects of Inner Ear Disease

Springer

Yasuya Nomura
President
The Society for Promotion of International
Oto-Rhino-Laryngology
Tokyo, Japan

Professor Emeritus
The University of Tokyo
Tokyo, Japan

Visiting Professor
Showa University
Tokyo, Japan

ISBN 978-4-431-54203-2 ISBN 978-4-431-54204-9 (eBook)
DOI 10.1007/978-4-431-54204-9
Springer Tokyo Heidelberg New York Dordrecht London

Library of Congress Control Number: 2013950091

Preface

The inner ear is a beautiful organ particularly when it is shown in color. Its sensory cells lie in a hard cavern (the temporal bone) of a deep sea (the inner ear fluids). Color illustrations bring the organ forth out of darkness into a brilliant world and enable us to see glittering original shapes suggesting functional significance. Alfonso Corti published a paper with colored figures in 1851 describing the hearing organ that later bore his name. He no doubt would have published his paper using color photographs, had they been available 160 years ago.

Our knowledge of the pathophysiology of inner ear diseases is mainly based on histopathological studies of human temporal bones. However, the long gap in time between the onset of a disease and findings obtained from temporal bone specimens sometimes makes interpretation difficult. The specimens may appear before us years and years after the onset. During this time, diseased tissues will have been greatly altered in appearance due to cleansing and repairing processes. Aging also plays a part in this regard.

Experimental studies may be useful for obtaining information about ongoing changes occurring within the inner ear. They may teach us how the organ reacts to artificial stimuli in the acute stage and how the organ shows morphological changes that provide us with information on the integrity or mysteries of the inner ear. At the same time, in the results obtained, there may be a discrepancy between clinical and experimental work. Taking these facts into account, when seeing patients one must extend the imagination regarding the pathophysiology of diseases.

While revisiting old papers and photographs for the preparation of this book, I noticed several new findings that I had overlooked earlier. It was a pleasure for me to see old slides or photographs that glistened under new eyes. Advances in knowledge and experience will further unearth buried truths.

The contents of this book mainly comprise earlier works. I am grateful for those who have collaborated with me and shared both pleasures and difficulties with me. My gratitude also extends to other researchers who were kind enough to contribute to this book with their valuable scientific photographs. I greatly appreciate their generosity.

Tokyo, Japan — Yasuya Nomura

Contents

1 Structure of the Inner Ear 1
1.1 Phylogenesis of the Ear 1
1.2 The Inner Ear 1
1.2.1 Pars Superior 2
1.2.2 Pars Inferior 7
1.2.3 The Internal Auditory Canal 16
1.3 The Middle Ear 16
1.4 The External Ear 17
References 22

2 Inner Ear Fluid 23
2.1 Inner Ear Fluid 23
2.1.1 Perilymph and Endolymph 23
2.1.2 Cortilymph 23
2.1.3 The Cochlear Aqueduct 27
2.1.4 Perilymph and the Limbus Spiralis 29
2.1.5 Endolymph 30
2.2 Perilymphatic Fistula 30
2.2.1 Clinical Aspects 30
2.2.2 Changes of CSF and Middle Ear Pressures in Daily Life 34
2.2.3 Experimental Perilymphatic Fistula 36
2.2.4 Early Hearing Change with Perilymphatic Fistula 38
2.2.5 Vestibular Changes in Experimental Perilymphatic Fistula 38
References 50

3 Blood Vessels 51
3.1 Anatomy 51
3.1.1 Arteries and Veins 51
3.1.2 Capillaries of the Membranous Cochlea 55
3.1.3 Capillaries of the Vestibular Organs 61
3.2 Diseases of the Blood and Blood Vessels 63
3.2.1 Leukemia 63
3.2.2 Buerger's Disease 64
3.2.3 Cryoglobulinemia 67
3.2.4 Takayasu's Arteritis 74
3.2.5 Diabetes Mellitus 78
References 83

4 Sudden Deafness 85
4.1 Histopathology of Sudden Deafness 85
4.2 The Tectorial Membrane 86
4.3 Case Reports 87
4.3.1 Case 1 87
4.3.2 Case 2 88
4.3.3 Sudden Deafness in a Patient with Relapsing Polychondritis 90
4.3.4 Cochlear Neuronitis 92
4.4 Sudden Deafness and Asymptomatic Mumps 92
4.5 Vascular Disorders 97
4.6 Criteria for Diagnosis of Sudden Deafness in Japan 98
4.7 Postscript 99
References 99

5 Meniere's Disease 101
5.1 Discovery of Endolymphatic Hydrops in Meniere's Disease 101
5.2 Human Temporal Bone Study 102
5.3 Diagnosis of Endolymphatic Hydrops Using Gadolinium MRI 103
5.4 Experimentally Induced Endolymphatic Hydrops 107
5.5 Observation of Experimental Cochlear Hydrops Using OCT 107
5.6 Vestibular Evoked Myogenic Potentials 109
5.7 Gentamicin 110
References 114

6 Viral Diseases 117
6.1 Herpes Simplex Virus (HSV) 117
6.1.1 Herpes Classification 117
6.1.2 HSV and Sudden Deafness 118
6.1.3 Morphological Study 118
6.2 Cytomegalovirus 122
6.2.1 Introduction 122
6.2.2 Incidence of Congenital CMV Infection Among Newborns in Japan 123
6.2.3 Histopathology of the Temporal Bone in a Case of CMV 126
6.2.4 Experimental Cytomegalic Labyrinthitis 128
6.3 Mumps 137
6.3.1 Introduction 137
6.3.2 Morphological Studies 137
6.3.3 Criteria for Diagnosis of Mumps Deafness 143
6.3.4 Mumps and Sudden Deafness 143
6.3.5 Deafness in Mumps Patients 144
6.3.6 Deafness in Mumps Meningoencephalitis 145
References 145

7 Laser Irradiation of the Inner Ear 147
7.1 Introduction 147
7.2 Animal Experiments 148
7.2.1 The Cochlea 148
7.2.2 The Otolithic Organs 152
7.2.3 The Semicircular Canal 160
7.3 Clinical Applications 160
7.3.1 Irradiation of the Semicircular Canal 160
7.3.2 Irradiation of the Otolithic Organ 165
7.3.3 Surgical Procedure 167
References 179

8 Presbycusis 181
8.1 Nerve Fibers in the Osseous Spiral Lamina 181
8.2 Nerve Fibers in the Organ of Corti 182
8.3 Nerve Fibers Running Lateral to the Hair Cell Area 187
8.4 Degeneration of Sensory Hairs on the Outer Hair Cells 187
8.5 Strial Atrophy 190
8.6 Lipidosis of the Basilar Membrane 193
8.7 Prevention of Presbycusis 194
References 202

9 Anomalies 205
9.1 Cochlear Hyperplasia 205
9.1.1 Introduction 205
9.1.2 Cochlear Hyperplasia 205
9.2 Hypophosphatasia 206
9.2.1 Introduction 206
9.2.2 Case Report 206
9.3 Alagille Syndrome 210
9.3.1 Phylogenesis of the Semicircular Canal 210
9.3.2 Anomalies of the Semicircular Canal 213
9.4 Scheibe Dysplasia 214
9.4.1 Introduction 214
9.4.2 Dysplasia and Degeneration 215
9.4.3 Case Report 215
9.4.4 Comment 217
9.5 Mondini Dysplasia 219
9.5.1 Introduction 219
9.5.2 Characteristics of Mondini Dysplasia 220
9.5.3 Case Reports 223
References 228

Index 231

Structure of the Inner Ear

1

Abstract

Alfonso Corti described the hearing organ in detail in a monumental work with colored figures in 1851, only 160 years ago. The evolution of the ear began several hundred million years ago. The balance organ was established in its current state quite early, whereas the hearing organ developed late and took a long time to reach its present structure. The inner ear is known as the labyrinth, meaning "maze"; like a maze, this complicated structure in the temporal bone and its functional significance are hard to understand in detail, even in this era of molecular biology.

The inner ear is separated into two portions: the pars superior and the pars inferior. The balance organ belongs to the former, and the hearing organ with the saccule to the latter. In the vestibulum, two otolithic organs reside, separated by a thin membrane called the membrana limitans. Horseradish peroxidase (HRP), a tracer substance, does not spread beyond the membrana limitans to the pars superior when administered to the perilymphatic cistern through the oval window. Conversely, HRP administered to the perilymph of the lateral semicircular canal is confined within the pars superior. This separation is important when we consider drug delivery to the inner ear.

Keywords

Inner ear anatomy • Membrana limitans • Organ of Corti • Phylogenesis

1.1 Phylogenesis of the Ear

Phylogenetically, inner ear development preceded formation of the middle and external ear. The semicircular canal evolved from the lateral line organ during the Silurian period of the Paleozoic Era, and the utricle from the statocyst some 435–410 million years ago. Later, the saccule differentiated from a portion of the utricle. The first saccule appeared in *Petromyzontidae* (lampreys) as an evagination from the utricle. The utricle and canals were concerned with equilibrium, while the saccule served as a receptor for sound waves originating within the animal's body.

In the Devonian Period of the Paleozoic Era, about 410–350 million years ago, an outpouching termed the lagena cochleae differentiated from the saccule. Today, the sturgeon shows the lowest form of lagena. In the Mesozoic Era, about 250–65 million years ago, the wall of the lagena cochleae evolved into the pars basilaris, which further evolved to become the mammalian cochlea [1].

1.2 The Inner Ear

In Greek mythology, the labyrinth was a famous maze constructed by Daedalus, in which the Minotaur, a monster with a bull's body and a human head, was kept. The Minotaur roamed through the labyrinth and fed upon human victims until it was finally destroyed by Theseus. The name labyrinth was first used to describe the inner ear structure by Fallopius around 1550, but the first thorough description was that of Scarpa in "De auditu et olfactu" in 1789 [2]. In the Palace of Caserta, we can observe the labyrinthine pattern on the floor

Y. Nomura, *Morphological Aspects of Inner Ear Disease*, DOI 10.1007/978-4-431-54204-9_1,

Fig. 1.1 Labyrinthine pattern in the floor of Astrea's Room, Palace of Caserta, Italy (1815)

of Astrea's room as well as the story in the ceiling fresco (Fig. 1.1).

The inner ear has two openings to the middle ear: the oval window and the round window. The oval window is anchored by the footplate of the stapes. The annular ligament lies between the rim of the oval window and the footplate. Behind the footplate, there is a wide space called the vestibule. As the vestibule is filled with perilymph, the space is called the perilymphatic cistern. A vestibulum is an antechamber. The early etymology of the word is uncertain, but it is generally understood to be a place at the entrance of a building where outer clothing can be removed [2].

In the phylogenesis of the inner ear, the pars superior, which includes the utricle and semicircular canals, appeared before the pars inferior, composed of the saccule and cochlea. Each semicircular canal has two openings to the utricle: the ampullated end and the non-ampullated end. Therefore, the utricle originally had six openings. Over time, the non-ampullated ends of the anterior and posterior canals joined before entering the protruded part of the utricle, called the sinus superior utriculi. Later, this union became the common crus. The utricle lost one opening to the semicircular canals and retains five in all. The vestibule houses two otolithic organs: the utricle and saccule.

The coiled cochlea first appears in mammals, but in the lowest mammal, Ornithorhynchus (the duck-bill platypus of Australia), the cochlea makes only one-quarter turn, at the end of which persists a lagena. The whale has one and one-half cochlear turns, the horse has two, humans have two and three-quarters, the cat has three, and the pig has almost four [1] (Figs. 1.2 and 1.3).

The first foramen rotundum (round window) is found in the frog. The secondary tympanic membrane covers the foramen [1].

1.2.1 Pars Superior

1.2.1.1 Semicircular Canals

The anterior and posterior canals, termed the vertical canals, evolved earlier than the lateral canal. As the cochlea developed from the lagena, the anterior canal was pushed upward. Most of the anterior canal came to lie above the level of posterior canal. The anterior canal is called the superior canal.

A portion of the superior semicircular canal may form a ridge (arcuate ridge, eminentia arcuata) on the floor of the middle cranial fossa. Dehiscence of the bony wall of the ridge may result in superior canal dehiscence syndrome, a condition that leads to hearing and balance disorders. The posterior canal may form a projection in the anterior wall of the posterior cranial fossa (posterior surface of the petrous ridge) [3]. The lateral canal projects as a ridge on the medial wall of the mastoid cavity. This ridge has been called the surgical dome in fenestration surgery for otosclerosis.

The growth of the membranous (otic) labyrinth gives rise to the structure of the osseous labyrinth, which consists simply of spaces lined with periosteum (endosteum), surrounding and enclosing the membranous labyrinth. The membranous canals, much smaller than the osseous canals, are situated eccentrically in the perilymphatic space, so that they lie against the convex surface of the periosteal lining of the bony canals. Here, they are united by denser connective tissue than the trabeculae, which elsewhere bridge the perilymphatic spaces of the bony canals [3] (see also Figs. 7.32 and 7.33).

The ampullated ends of the superior and posterior semicircular canals empty through short, wide continuations into the utricle (Fig. 1.4).

1.2.1.2 The Utricle

The utricle or utriculus is an elongated portion of the membranous labyrinth receiving both ends of each semicircular canal. On the inferior surface of the utricle and extending slightly onto its lateral surface lies the macula, which contains sensory endings from the superior division of the vestibular nerve, the utricular nerve.

The macula of the utricle lies almost in the horizontal plane. The macula is fringed with marginal fibers (Figs. 1.5, 1.6 and 1.7). Through the oval window, the macula can be seen above as a white plaque in the vestibule.

1.2.1.3 Membrana Limitans

In 1920, de Burlet [4] described the *Grenzmembran*, which divided the *Spatium perilymphaticum* into *Spatium perilymphaticum superius* and *Spatium perilymphaticum inferius* (Figs. 1.8 and 1.9). In the upper perilymphatic space, there were *Bindegewebesbalken*, whereas no *Bindegewebesbalken* existed in the lower space.

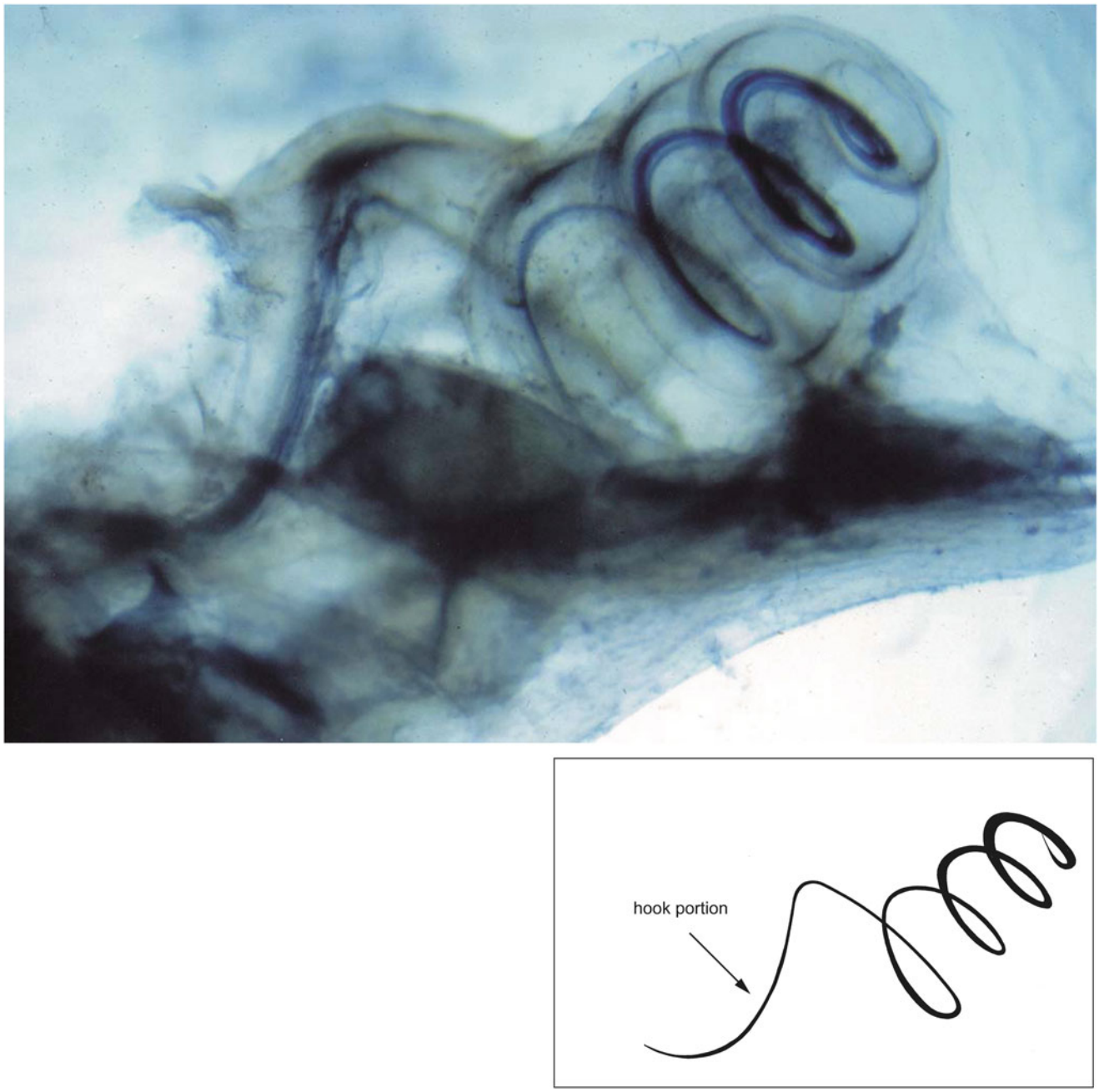

Fig. 1.2 Esterase activity in the organ of Corti. The guinea pig has four cochlear turns. Indoxyl acetate staining method reveals esterase activity localized mainly in the organ of Corti. The width of the *spiral winding* indicates the basilar membrane, which becomes wider from the base toward the apex. The *inset* shows its schema

The *Grenzmembran*, or membrana limitans, separates the perilymphatic space of the cochlea and saccule from that of the utricle and semicircular canals; in other words, it separates the pars superior from the pars inferior. The *Bindegewebesbalken* are the trabecular mesh between the membranous labyrinth and the periosteum (endosteum) of the osseous labyrinth of the pars superior.

Viewed with a light microscope, the membrana limitans appears to be a single layer of fibrocytes, but electron microscopy shows that the membrane is composed of several layers of thin cytoplasmic extensions of the fibrocytes. Hara and Kimura [5] observed that the membrana limitans was rectangular when viewed from the anterior side, with various surface curvatures and an invagination toward the internal

Fig. 1.3 Efferent nerve fibers in the cochlea. The organ of Corti and intraganglionic spiral bundle show acetylcholinesterase activity. Guinea pig, acetylcholinesterase stain, Gomori method

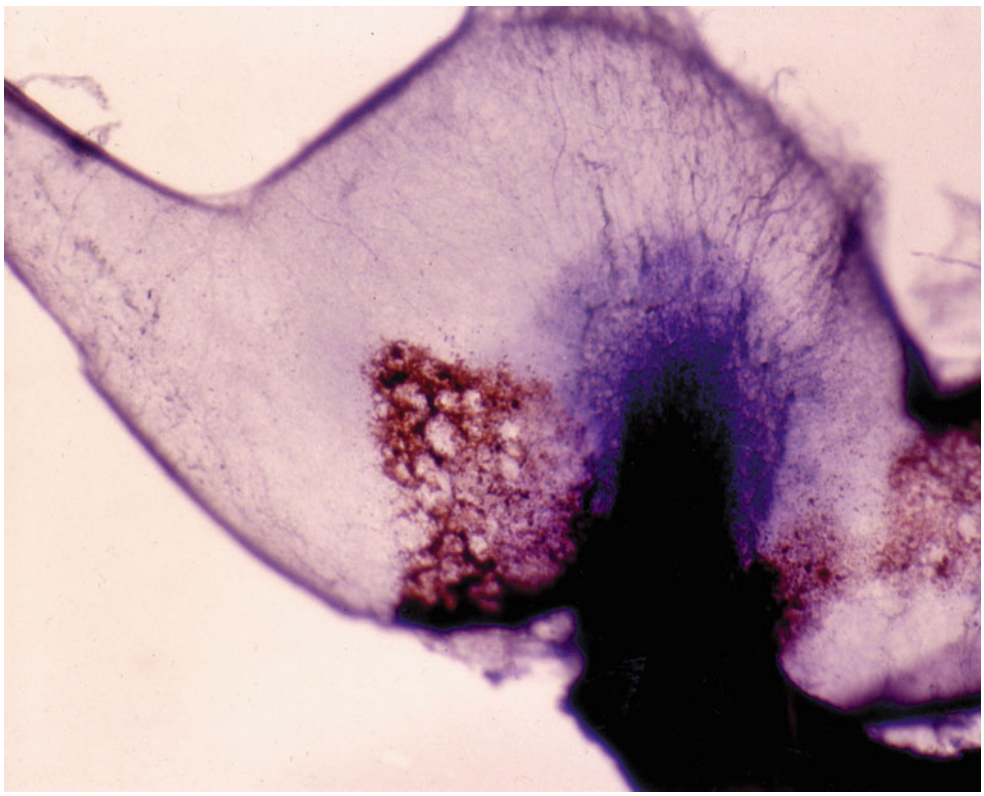

Fig. 1.4 The posterior ampulla with the singular nerve. The utricle lies to the right (not shown). Dark cell areas are observed. Seventy-one-year-old woman, staining in toto, HE stain

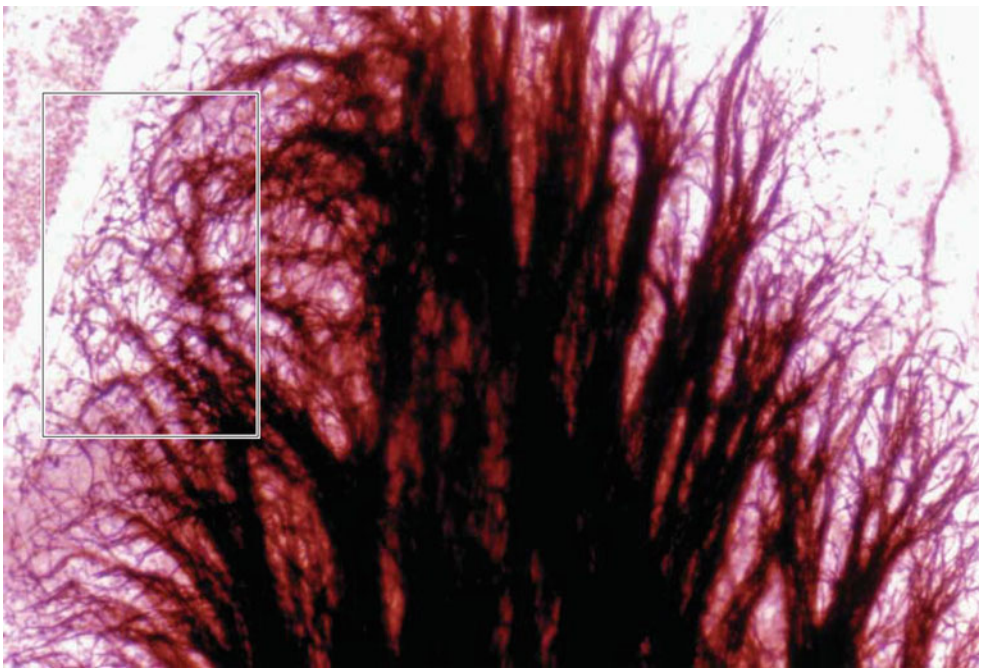

Fig. 1.5 Nerve fibers innervating the utricular macula. Fifty-nine-year-old man, Holmes stain (original ×6.5)

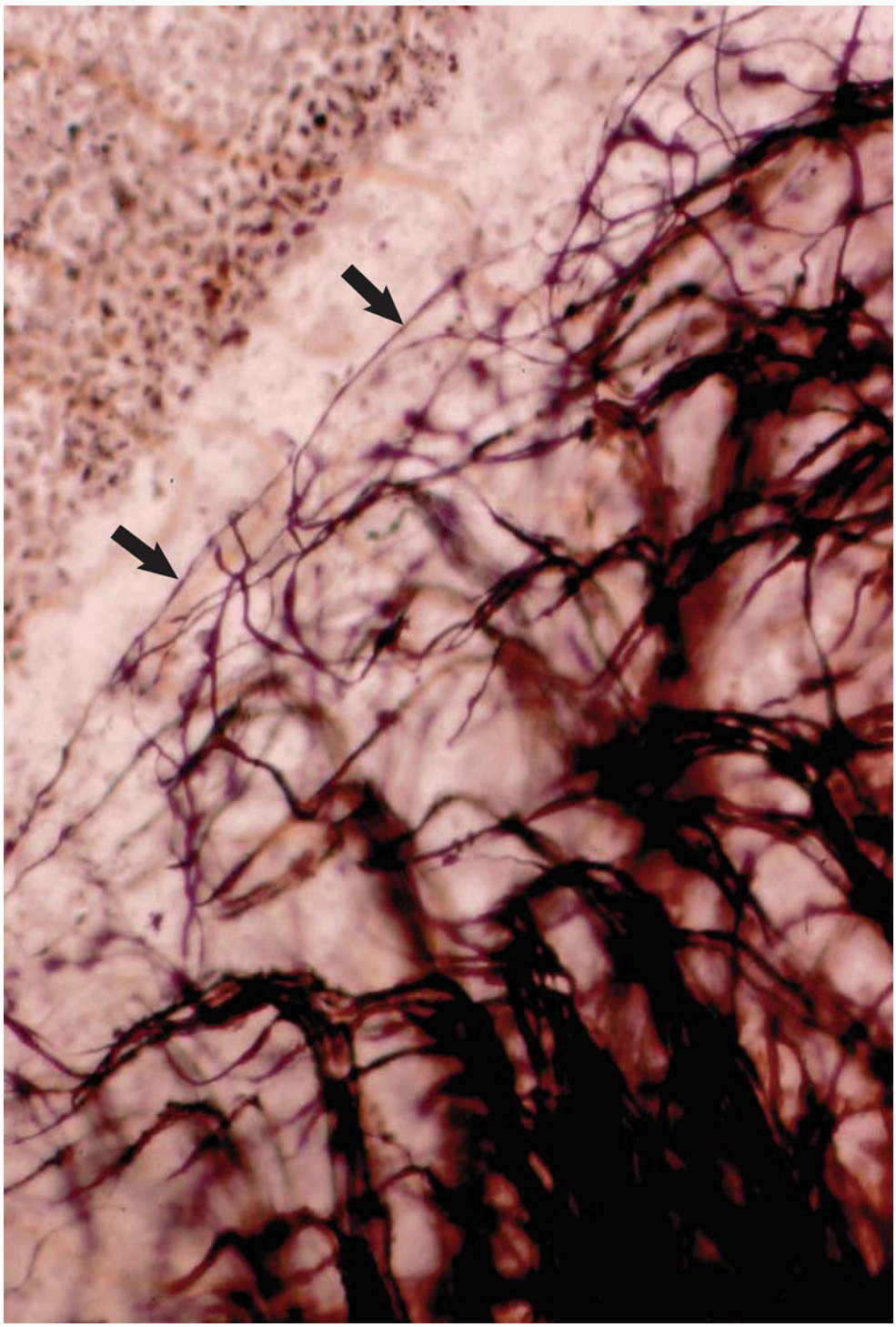

Fig. 1.6 Nerve fibers at the marginal area of utricular macula. Enlargement of the *inset* in Fig. 1.5. The macula is fringed with nerve fibers (*arrows*). Adjacent to the macula is the dark cell area (original ×16)

aperture of the vestibular aqueduct. When an absorbable gelatin sponge soaked with horseradish peroxidase, a tracer substance, was applied to the oval window after removal of the stapes, the tracer was found on the anterior side of the membrana limitans, and rarely on the posterior side. When tracer was applied to the perilymphatic space of the lateral semicircular canal, it was confined mostly to the posterior side of the membrana limitans. The tracer placed on either side of the membrana limitans failed to pass to the opposite side (Fig. 1.10).

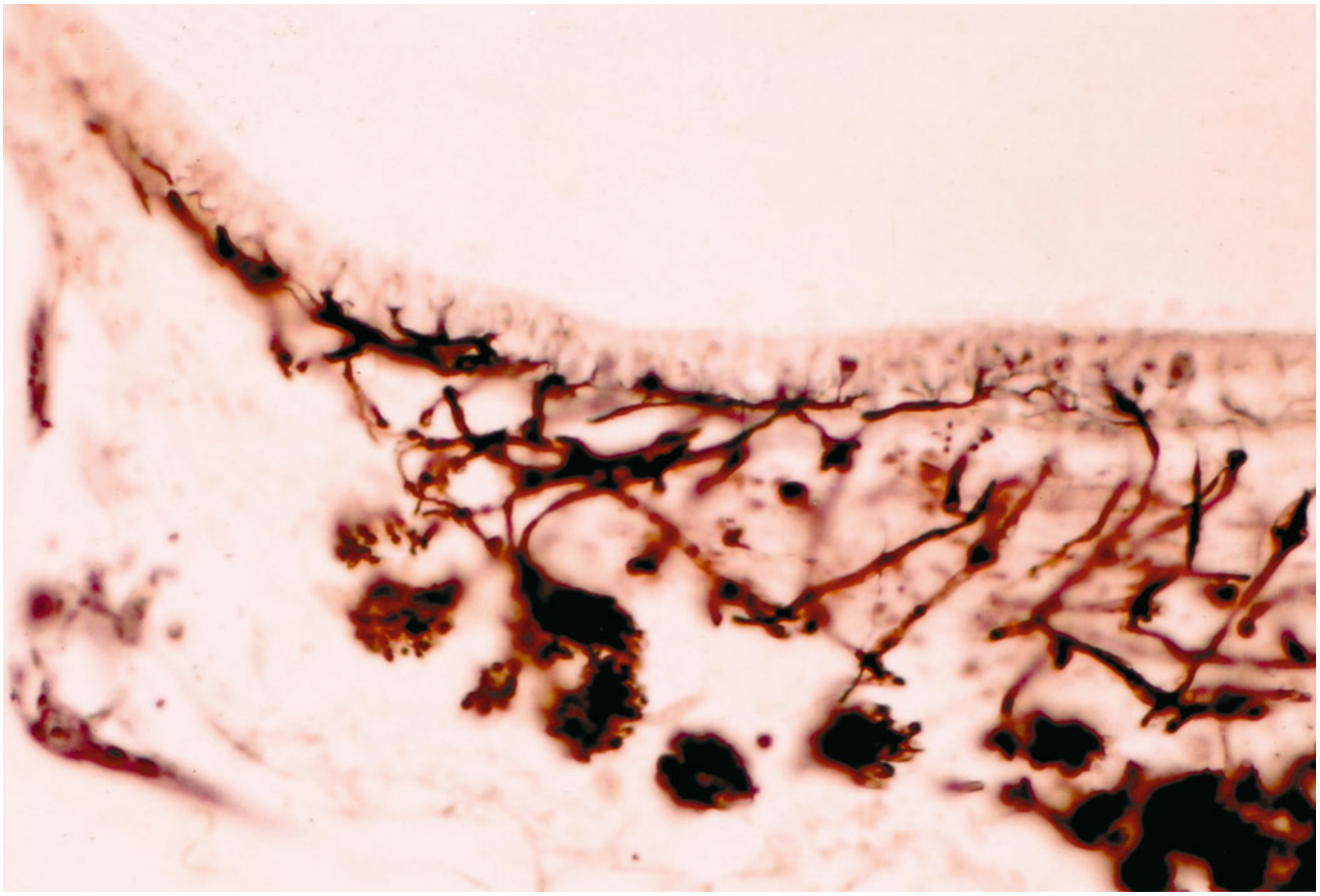

Fig. 1.7 Cross section of the utricular macula. Nerve chalices are seen in the sensory epithelium. Eighty-eight-year-old man, Holmes stain (original ×16)

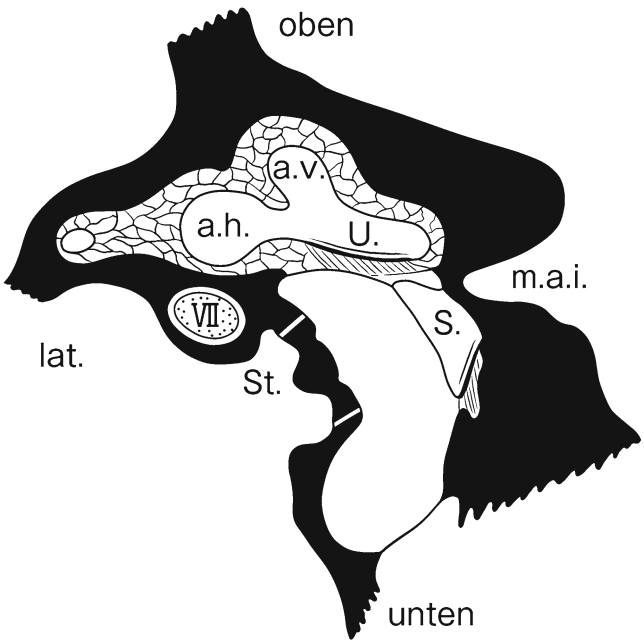

Fig. 1.8 Schema of the right labyrinth of a guinea pig [4]. The membrana limitans separates the pars superior from the pars inferior. The trabecular mesh exists in the perilymphatic space of the pars superior. *U* utricle, *S* saccule, *a.h.* lateral ampulla, *a.v.* superior ampulla, *m.a.i.* internal auditory canal, *St* stapes, *VII* facial nerve

Morphologically, the membrana limitans is a loosely organized barrier that may prevent or delay substances from reaching its opposite side.

1.2.2 Pars Inferior

1.2.2.1 The Saccule

The saccule or sacculus, diminutive form of saccus, is rounder than the utricle. Unlike the utricular macula, the saccular macula lies in a shallow bony depression, the spherical recess. The saccular macula lies at an approximate right angle to the utricular macula in the vestibule.

The saccular wall consists of mesothelial and epithelial cell layers. The anterior wall near the stapes is thickened by the presence of connective tissue between the layers and is called the reinforced area of the saccular membrane [6, 7] (Fig. 1.11). The saccular duct together with the utricular duct becomes the utriculosaccular duct, which communicates with the endolymphatic duct. The saccule is continuous with the cochlea through the tiny ductus reuniens (Fig. 1.12).

The macula sacculi is innervated by the saccular nerve, which arises mainly from the inferior division and partly

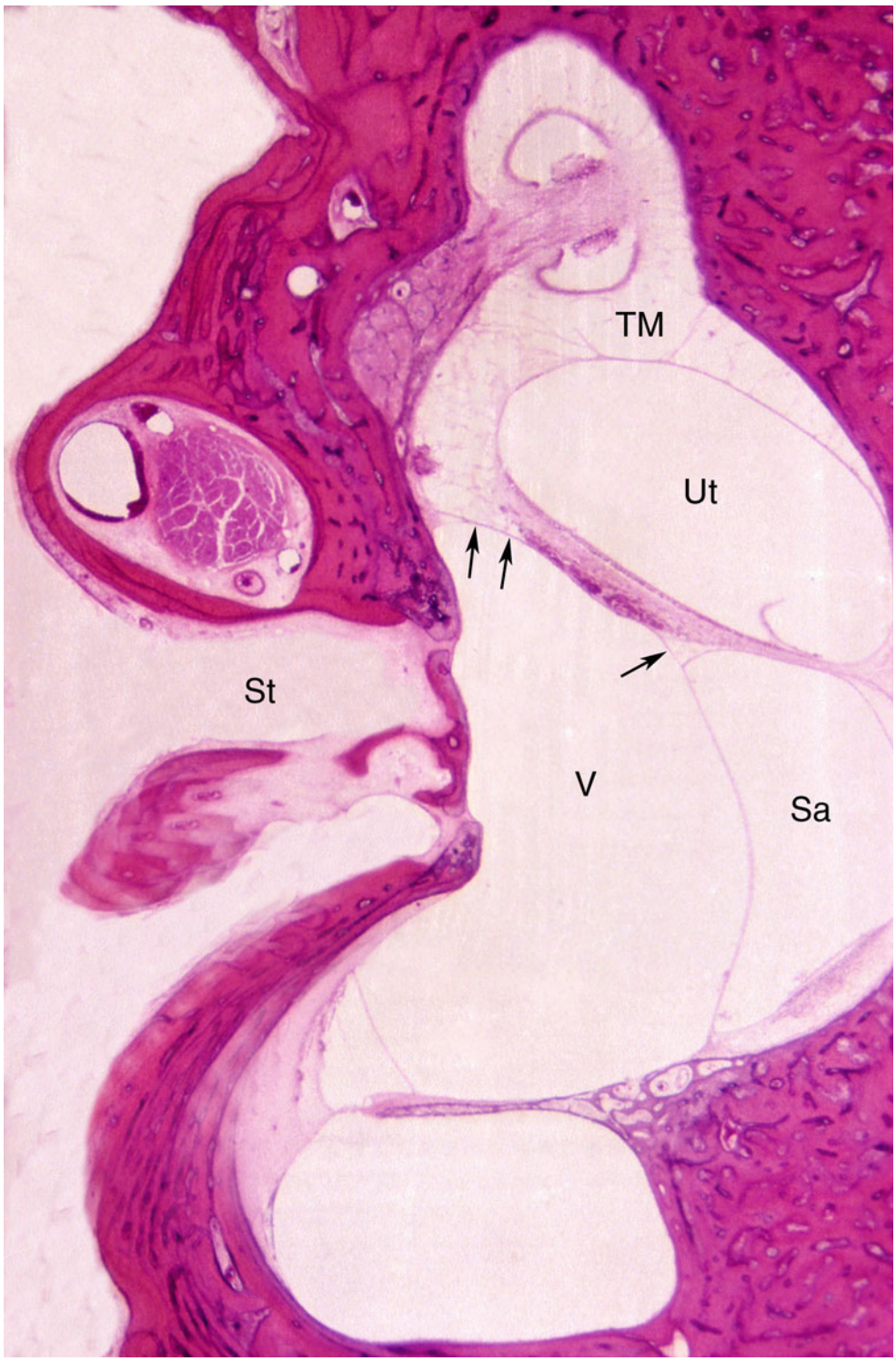

Fig. 1.9 Vertical section of a human temporal bone. *Arrows* indicate the membrana limitans extending partly over the saccular wall. *Ut* utricle, *Sa* saccule, *TM* trabecular mesh, *St* stapes, *V* vestibulum (original ×4)

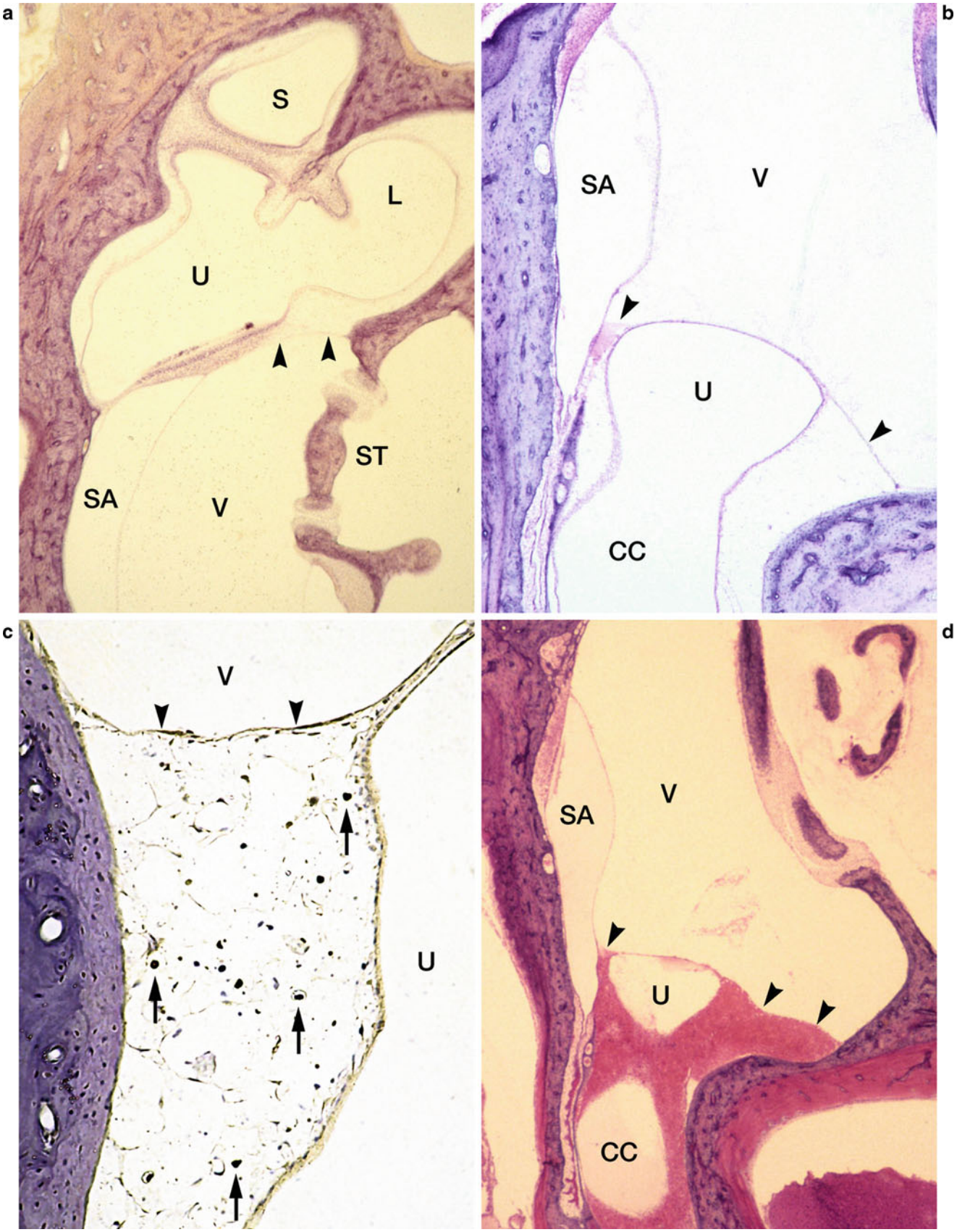

Fig. 1.10 Membrana limitans in the vestibulum of a guinea pig. (**a**) Membrana limitans (*arrows*) attaches to the superior rim of the oval window (original ×4). (**b**) Membrana limitans (*arrows*) invaginates toward the vestibular aqueduct (original ×4). (**c**) One week after HRP was introduced into the perilymphatic space of the lateral canal, tracer substance (*arrows*) is confined to the posterior side of the membrana limitans (original ×4). (**d**) Bleeding in the perilymphatic space of the utricle and common crus. Blood cells are confined to the perilymphatic space posterior to the membrana limitans (original ×4). *CC* crus commune, *S* superior ampulla, *SA* saccule, *ST* stapes, *U* utricle, *V* vestibulum HE stain (modified with author's permission) [5]

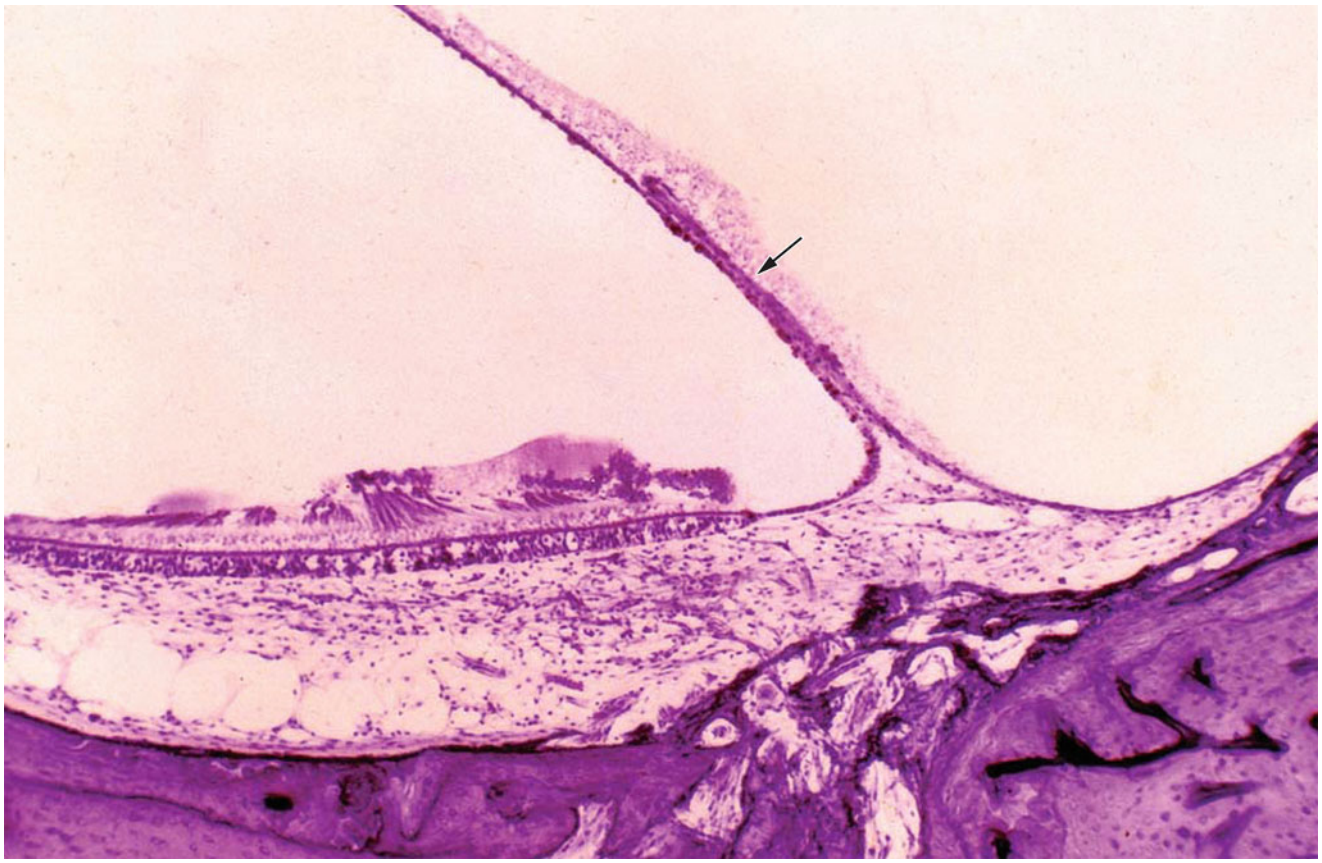

Fig. 1.11 The saccule. The saccule lies in a shallow bony depression, the spherical recess. The anterior portion of the saccular wall is thick and is called the reinforced area (*arrow*)

from the superior division of the vestibular nerve (Voit's nerve) (Fig. 1.13).

Voit [8] found that a part of the superior division of the vestibular nerve joined the saccular macula in the embryos of rabbits and monkeys (Semnopithecus maurus). Before this work, it was believed that the saccular macula was innervated by the ramulus maculae sacculi, belonging to the ramus inferior of the nervus vestibularis. Voit named this nerve the ramulus maculae sacculi pars inferior, and the nerve coming from the superior division the ramulus maculae sacculi pars superior (Voit's nerve).

The otoconia and saccular nerve of the saccular macula change with age. According to Johnsson [9], patients older than 60 years have large defects in the layer of statoconia (otoconia), while those under 30 years of age have a continuous layer of statoconia covering the entire neuroepithelium. He noted that patients with presbycusis had an obvious degeneration of the saccular nerve network, while utricular degeneration was mild.

1.2.2.2 The Cochlea

The promontory is the prominent area between the oval and round windows (Fig. 1.14). The name comes from the Latin *promunturium* or *promontorium*, which has been adopted by anatomists to describe several projecting areas in the body. The perilymphatic spaces in the cochlea, the scala vestibuli, and the scala tympani are compared to a winding U-tube. One end of the tube is anchored by the stapes footplate and the other by the round window membrane (Fig. 1.15). However, the membrane lies not at the end but at the side of the tube. The tube ends in a short blind sac, the vestibular cecum.

The footplate of the stapes is anchored in the oval window. Its anterior edge protrudes somewhat into the middle ear cavity, whereas its posterior edge fits to the frame of the window. Manipulation of the head of the stapes during ear surgery, with force directed posteriorly, parallel to the stapedial tendon, can dislocate the stapes from the oval window.

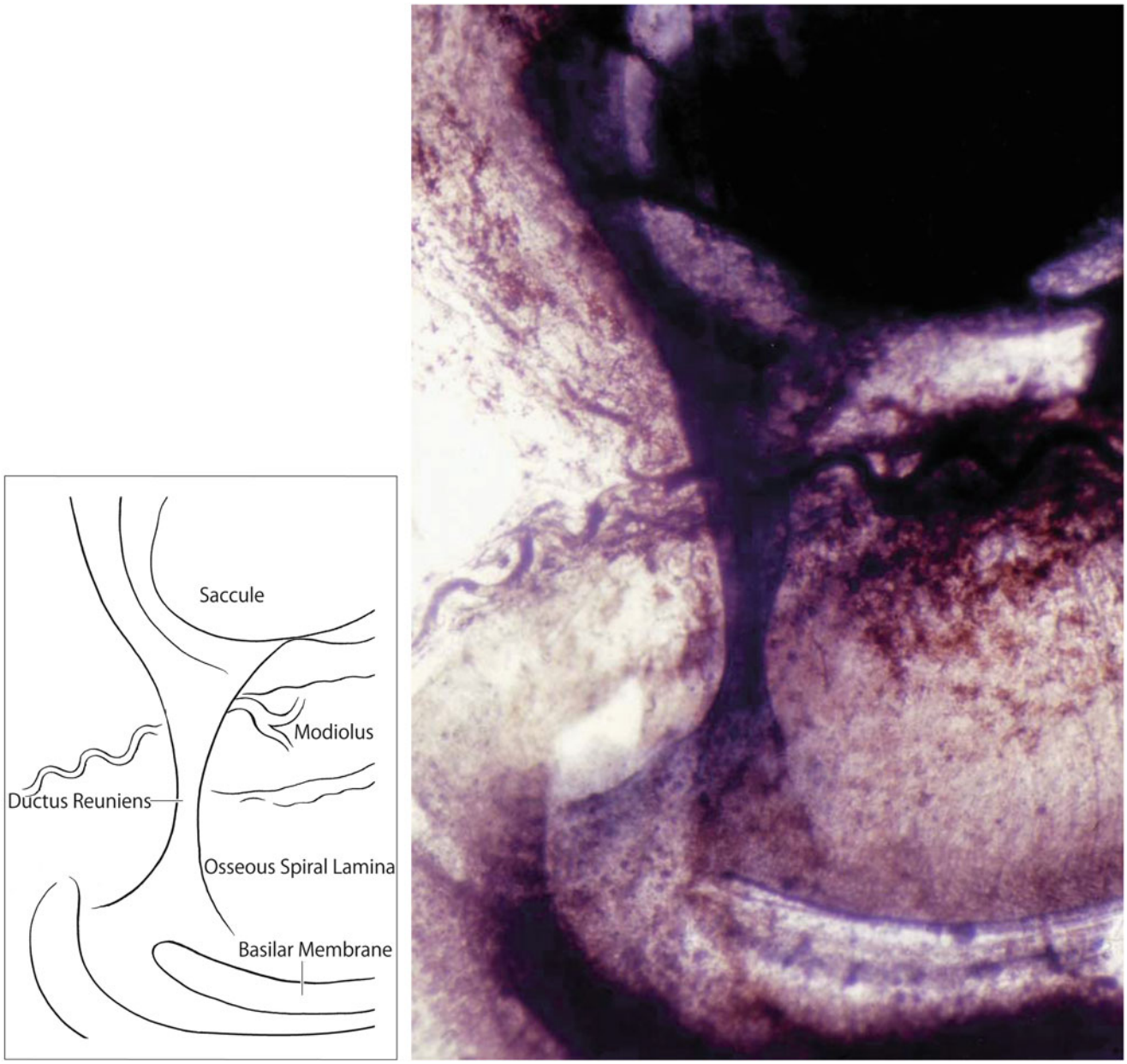

Fig. 1.12 Ductus reuniens. Funnel-shaped structures from the saccule and cochlea join to form the ductus reuniens. Eighty-three-year-old man, osmic acid stain

The upper surface of the vestibular lip of the limbus spiralis intersects at right angles the furrows produced by tooth-shaped elevations, called Huschke's teeth (Emil Huschke, German anatomist, 1797–1858) [10] (Fig. 1.16a,b). Between the auditory teeth are the interdental cells, to which the tectorial membrane is attached. The membrane remains attached even in severe atrophy of the fibrocytes of the limbus spiralis. Detachment of the tectorial membrane occurs with severe degeneration of the interdental cells, even when the underlying fibrocytes are intact. The interdental cells maintain the integrity of the tectorial membrane [11].

Corti (Marchese Alfonso Corti, Italian histologist, 1822–1888) published a paper entitled "Recherches sur l'organe de l'ouie des mammifères" in *Zeitschrift für wissenschaftliche Zoologie* in 1851 [12]. In 1854, Ernestus Reissner described the vestibular membrane. In the organ of Corti, there are several cell types that bear researchers' names: cells of Claudius (1856), Böttcher (1859), Deiters (1860), and Hensen (1863)

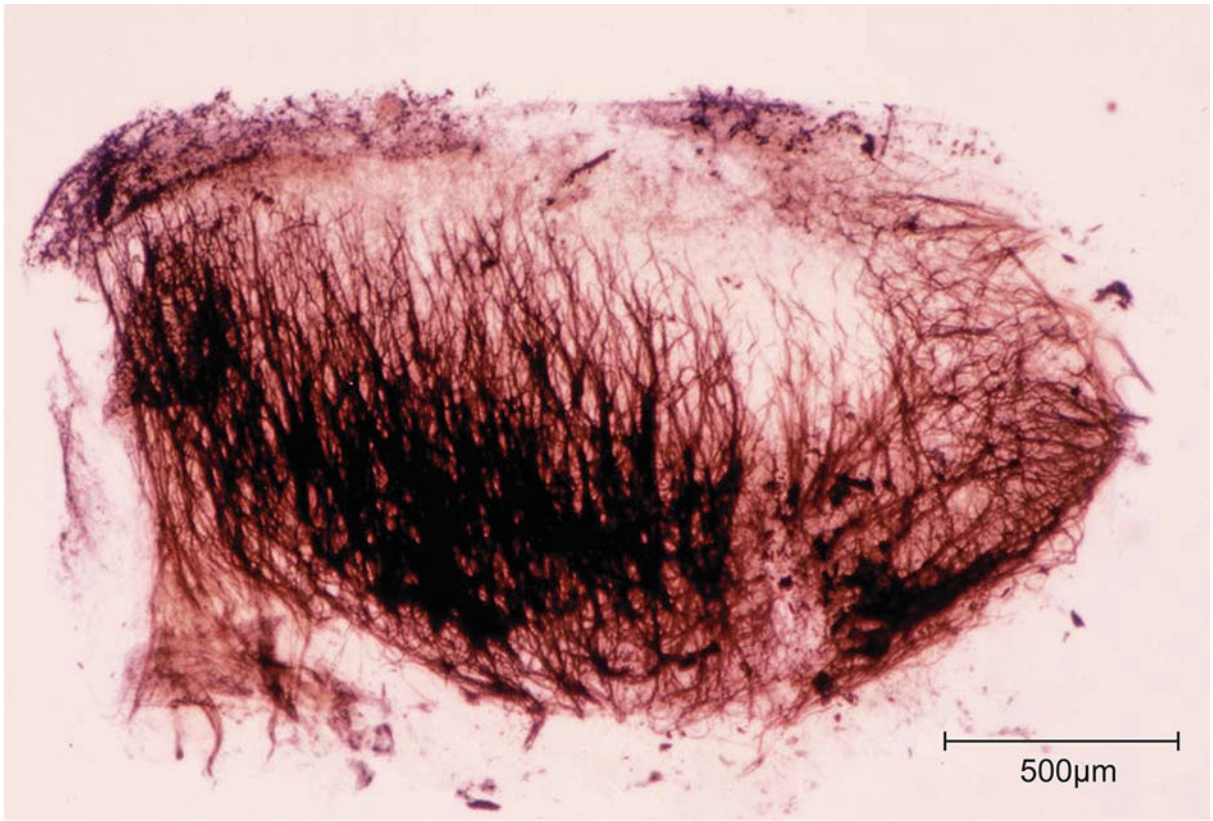

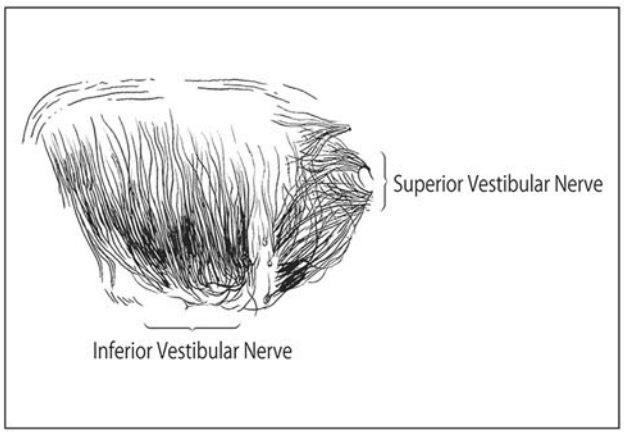

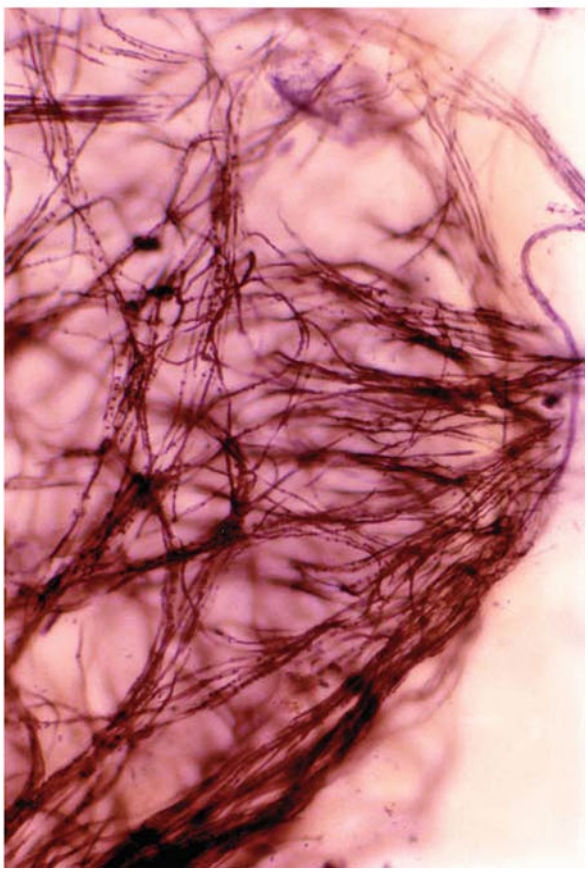

Fig. 1.13 Nerve fibers in the saccular macula. *Top*: The saccule is innervated by the inferior and superior divisions of the vestibular nerve. Loss of nerve fibers is marked (original ×2.5). *Bottom*: Enlarged photograph of the upper specimen showing nerve fibers from the superior division of the vestibular nerve (original ×16). Seventy-three-year-old man, Holmes stain

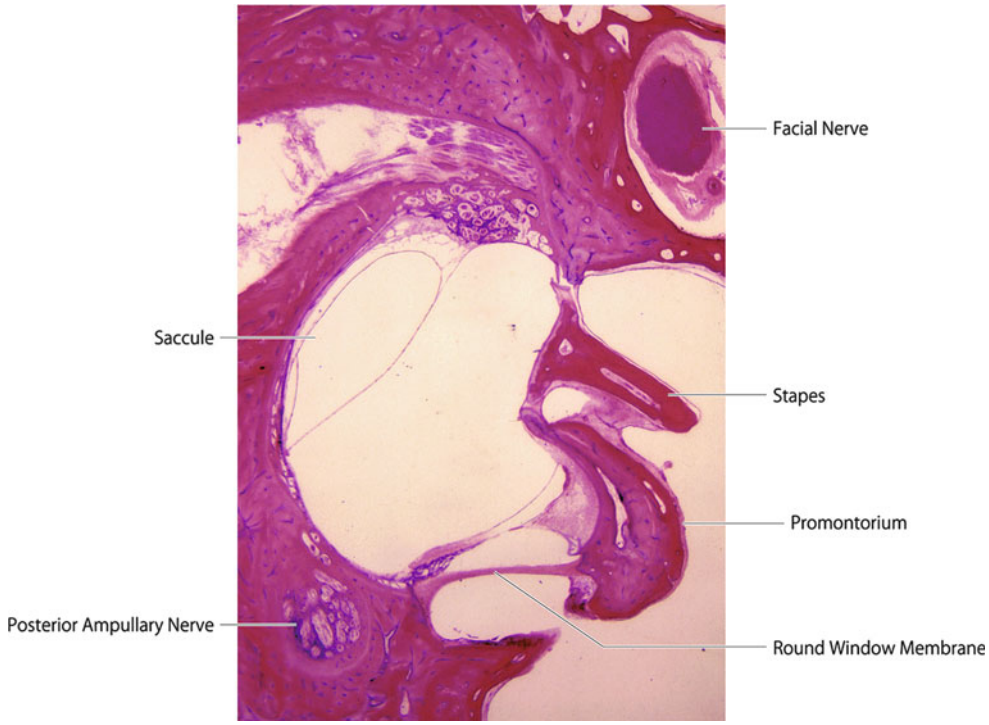

Fig. 1.14 Promontory between the oval and round windows. The singular nerve runs close to the round window, vestibulum, and osseous spiral lamina of the cochlea

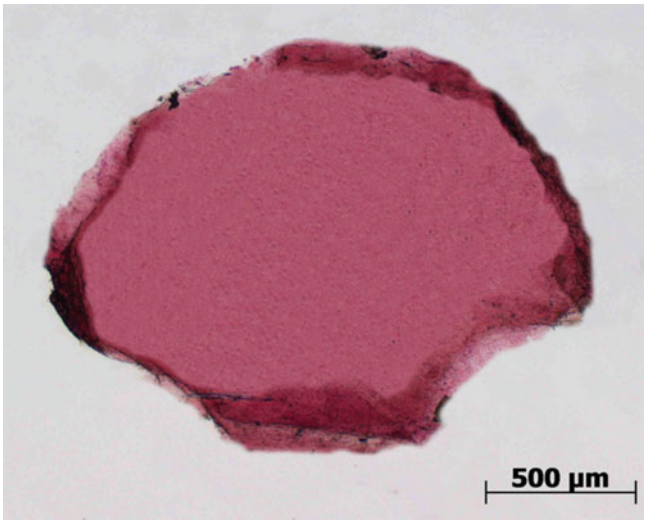

Fig. 1.15 The round window membrane (human). Seventy-three-year-old man, Kernechtrot staining (original ×2.5)

all were named between 1851 and 1863. The entire structure was named in honor of Corti [13] (Figs. 1.17 and 1.18).

Innervation of the Cochlea

The origin of the cochlear nerve is the spiral ganglion cell, located in Rosenthal's canal of the modiolus. The modiolus, named by Eustachius in 1563, is like the hub of a wheel from which the osseous spiral lamina radiates.

The dendrites from the spiral ganglion cells pass through the lamina to perforate its free edge (habenula perforata) and end in the organ of Corti. The spiral ganglion has two cell types. Type I spiral ganglion neurons are myelinated and lead to the inner hair cells. Each fiber has synaptic contact with only one inner hair cell, and each inner hair cell is innervated by approximately 10–30 fibers [14–16].

Type II spiral ganglion neurons, which are not myelinated, lead to the outer hair cells. More than 90 % of the afferent fibers originate at the inner hair cells. The outer hair cells are innervated by only about 10 % of the afferent nerve fibers, with many outer hair cells converging on a single fiber [14–16]. Similar ratios between neurons associated with the outer and inner hair cells have been founds in guinea pigs [17] and humans [18].

The efferent innervation of the cochlea also consists of two types of neurons. Non-myelinated lateral olivocochlear fibers originating from the lateral superior olivary nucleus run mainly to the ipsilateral cochlea, where they make synaptic contact with afferent dendrites associated with the inner hair cells. Myelinated medial olivocochlear fibers from the medial superior olivary nucleus provide an abundant efferent nerve supply predominantly to the outer hair cells of the contralateral cochlea. The functions of the efferent nerves

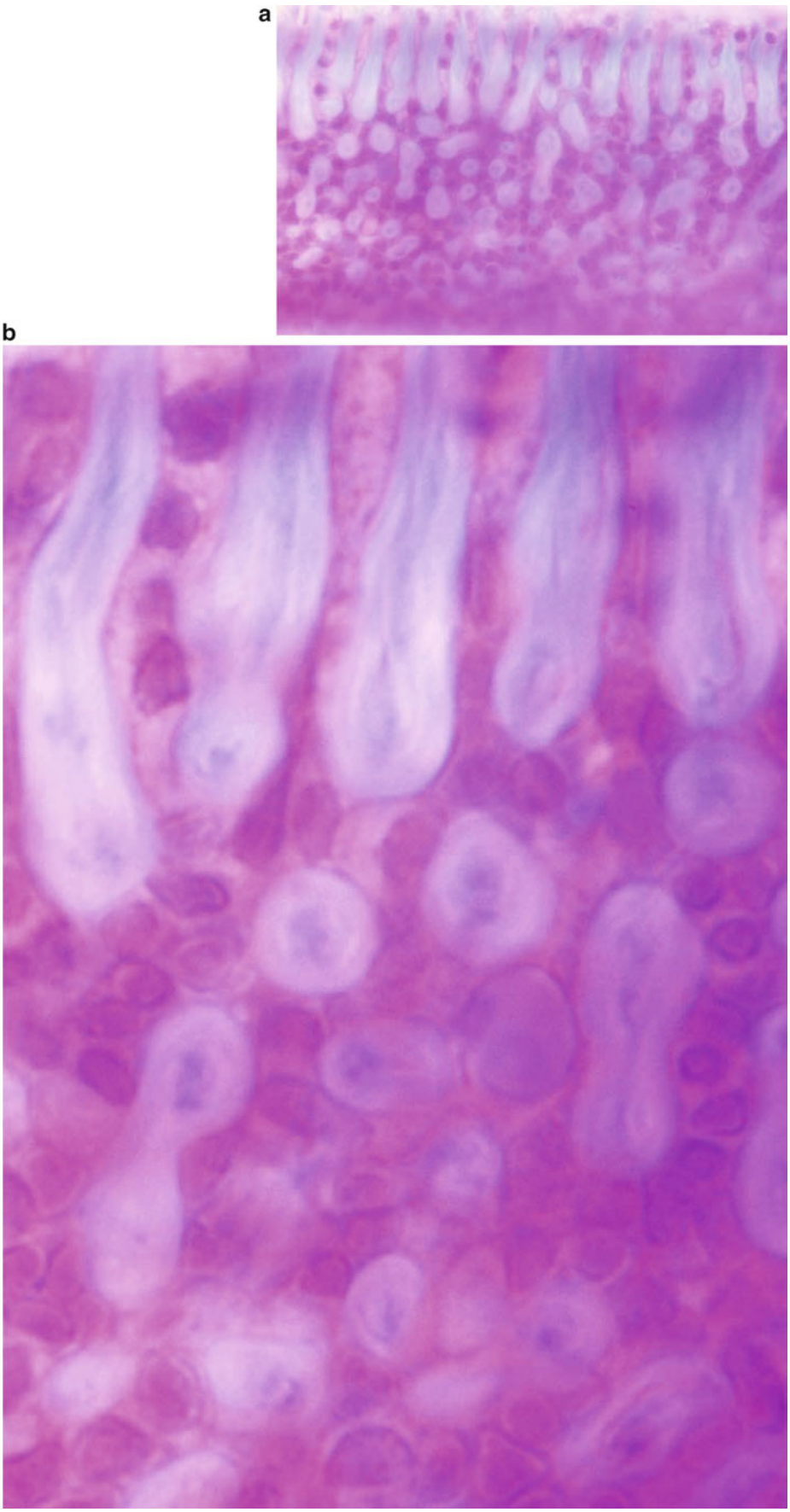

Fig. 1.16 Huschke's teeth (human). The vestibular lip of the limbus spiralis has ridges and furrows alternately (**a**, **b**). The interdental cells are situated in the furrows. An array of nuclei indicates arrangements of the interdental cells (**c**, **d**). (*a*) Original ×40, (*b*) original ×100 Masson staining, 74-year-old woman, (*c*) original ×20, (*d*) original ×100 Holmes staining, 73-year-old man, (*e*). A schema of interdental cells in the limbus spiralis C: organ of Corti *Arrow* indicates direction of the observations

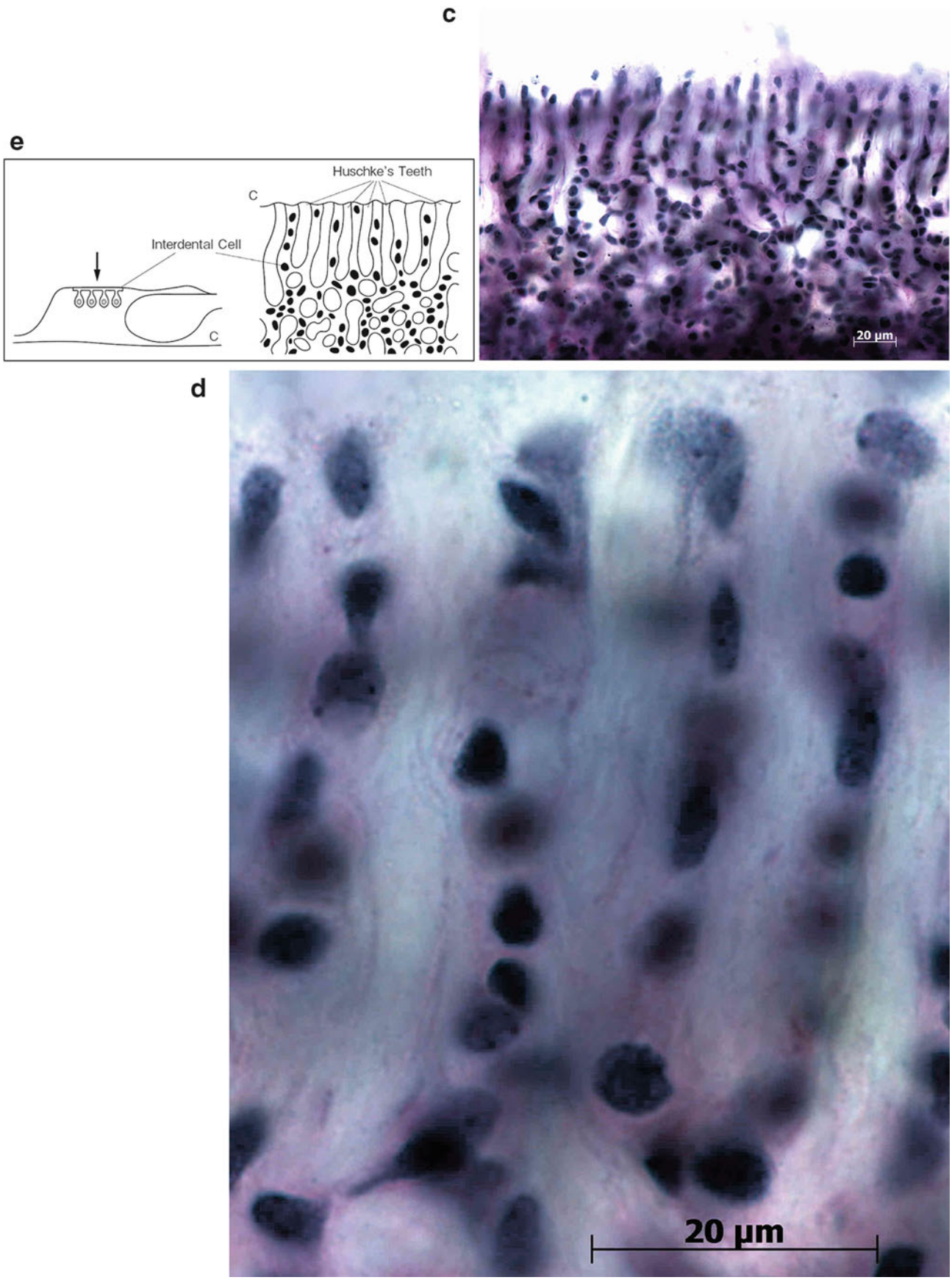

Fig. 1.16 (continued)

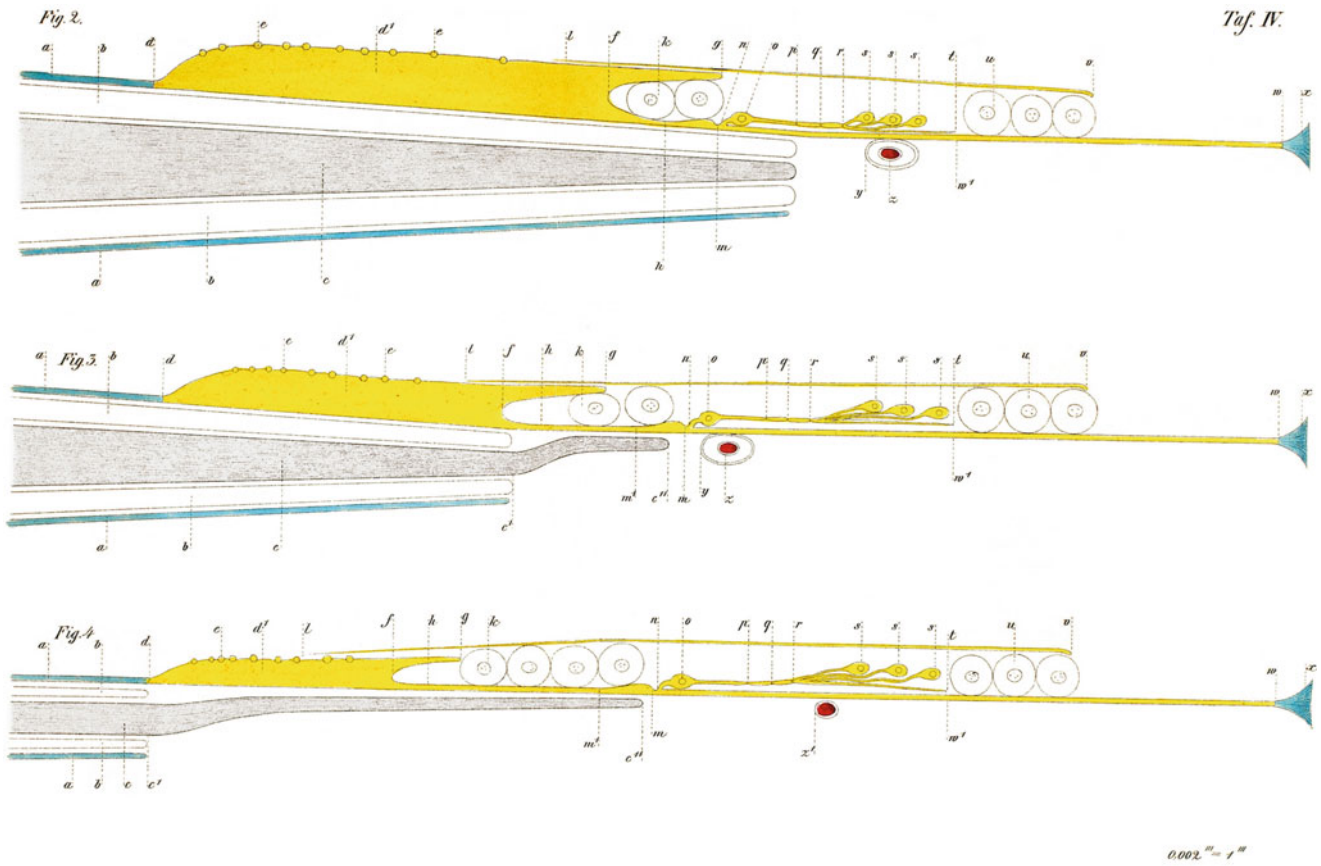

Fig. 1.17 The original figures of the organ of Corti [12]. Corti's colored figures of the hearing organ of the cat and dog (Courtesy of the Biological Sciences Library, University of Tokyo)

include improving the signal noise ratio, expanding the dynamic range in intensity coding, controlling cochlear amplification, and protecting the cochlea from loud sounds [16]. Within the tunnel of Corti run three kinds of nerve fibers: the medial fiber, basilar fiber, and tunnel spiral bundle. The medial efferent fiber crosses the middle portion of the tunnel. The basilar afferent fiber crosses the tunnel at the base. While crossing the tunnel of Corti, the medial fibers slant apically, whereas the basilar fibers slant toward the base [18, 19] (Fig. 1.19).

The tunnel spiral bundle consists of efferent fibers running at the junction of the inner pillar cells and the basilar membrane.

1.2.3 The Internal Auditory Canal

The cochlear nerve, vestibular nerve, and facial nerve run together with the labyrinthine artery within the internal auditory canal. At the fundus of the canal, the facial nerve and superior division of vestibular nerve are located above the crista transversa (transverse crest). The cochlear nerve and the inferior division of the vestibular nerve are located under the crista (Fig. 1.20).

Bill's bar (vertical crest; William F. House, American otologist, 1932–2012) is a ridge between the facial nerve and the superior division of the vestibular nerve.

1.3 The Middle Ear

The middle ear cavity is lined with mucosa, with different cell types, depending on location. Beneath the mucosa in the medial wall is Jacobson's nerve (tympanic nerve, Ludwig Levin Jacobson, Danish anatomist, 1783–1843), a branch of the glossopharyngeal nerve. After leaving the inferior ganglion or ganglion petrosum, the nerve enters the middle ear through the tympanic canaliculus, forming the tympanic plexus on the promontory.

Fibers from the caroticotympanic nerves join Jacobson's nerve. Many ganglion cells exist in the nerve (Fig. 1.21). The mucosa of the middle ear is supplied by sensory fibers of the glossopharyngeal nerve. Jacobson's nerve includes sensory, sympathetic and parasympathetic nerve fibers. Jacobson's nerve leaves the middle ear as the lessor petrosal nerve going to the otic ganglion. This nerve contains parasympathetic, presynaptic fibers. The postsynaptic fibers leave the otic ganglion to innervate the parotid gland by way of the auriculotemporal nerve.

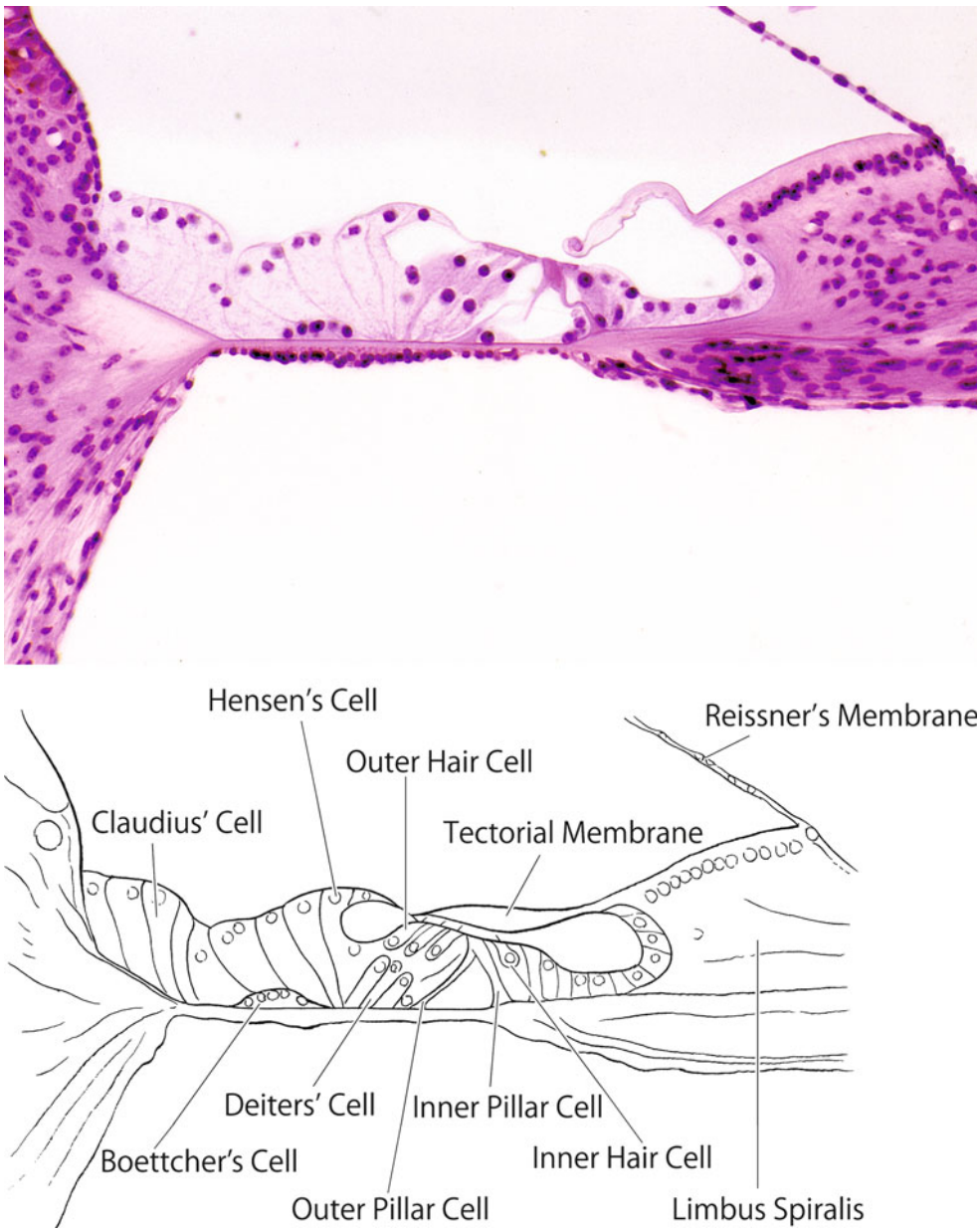

Fig. 1.18 The organ of Corti at the basal turn in a guinea pig (HE stain)

The head of the malleus and the body of the incus are located in the attic (epitympanic recess) of the middle ear, supported by the anterior and superior mallear ligaments and the posterior incudal ligament at the fossa incudis. Support may also be provided by mucosal folds (Fig. 1.22).

The chorda tympani arises from the vertical portion of the facial nerve about 4 mm above the stylomastoid foramen, and travels upward and forward into the iter chordae posterior to enter the tympanic cavity. The chorda tympani passes between the incus and malleus (Fig. 1.23). In passing the malleus, the chorda tympani lies on or above the tendon of the tensor tympani muscle. It leaves the tympanic cavity through the iter chordae anterius and emerges from the skull through the petrotympanic fissure.

1.4 The External Ear

The external ear consists of cartilaginous and bony parts.

The first branchial groove develops into the external auditory canal in the fourth week of gestation, whereas the other branchial grooves disappear. The floor of the external

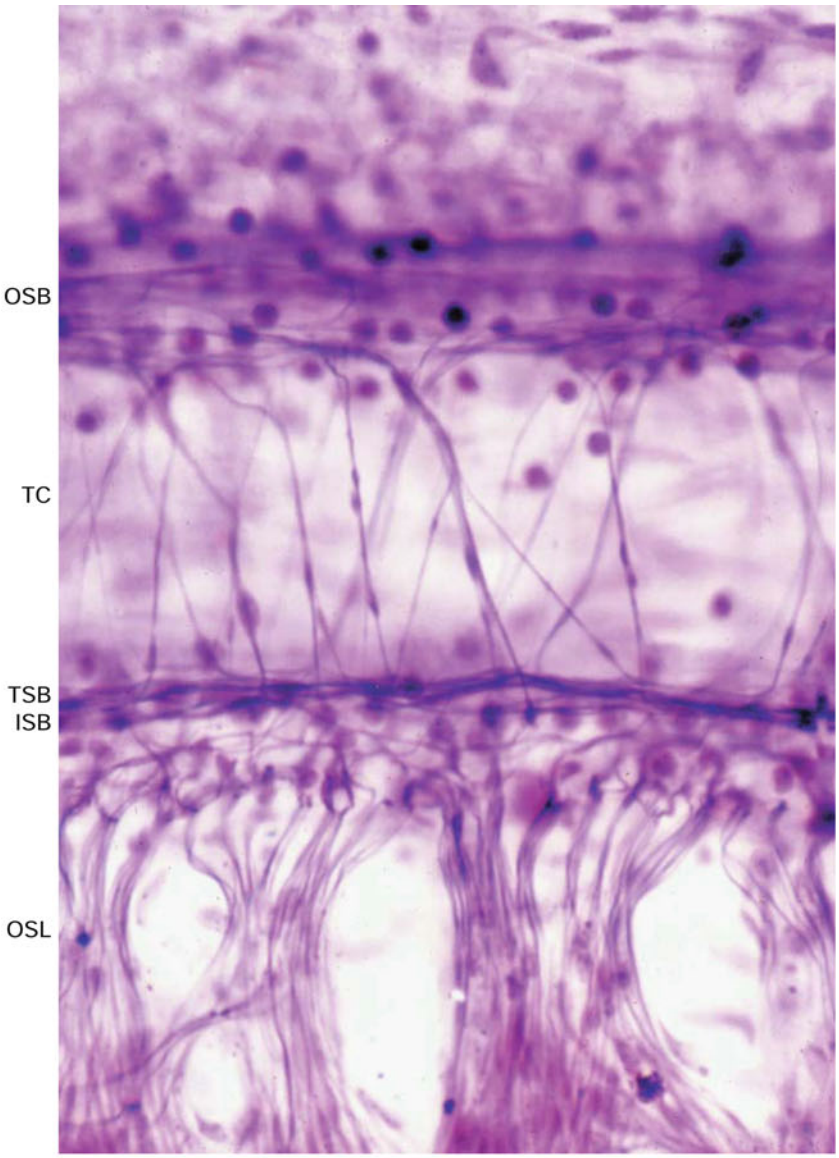

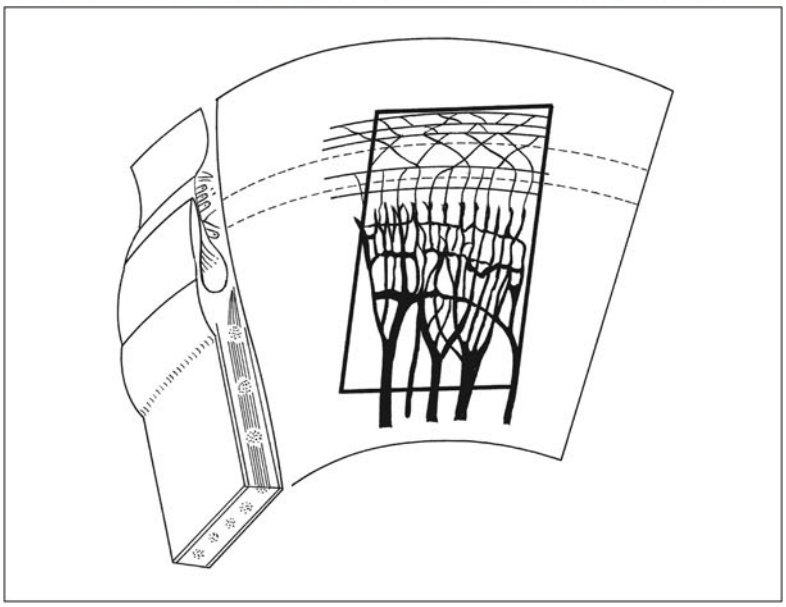

Fig. 1.19 Nerve fibers within the organ of Corti. Nerve fibers traveling to the outer hair cells cross the tunnel of Corti. From the osseous spiral lamina, the medial fibers cross the tunnel, slanting apically (to the *left* in the figure), whereas the basilar fibers slant toward the base (to the *right*). *OSL* osseous spiral lamina, *TSB* tunnel spiral bundle, *ISB* inner spiral bundle, *TC* tunnel of Corti, *OSB* outer spiral bundles. Seventy-four-year-old man, Holmes stain (original ×40) [18, 19]

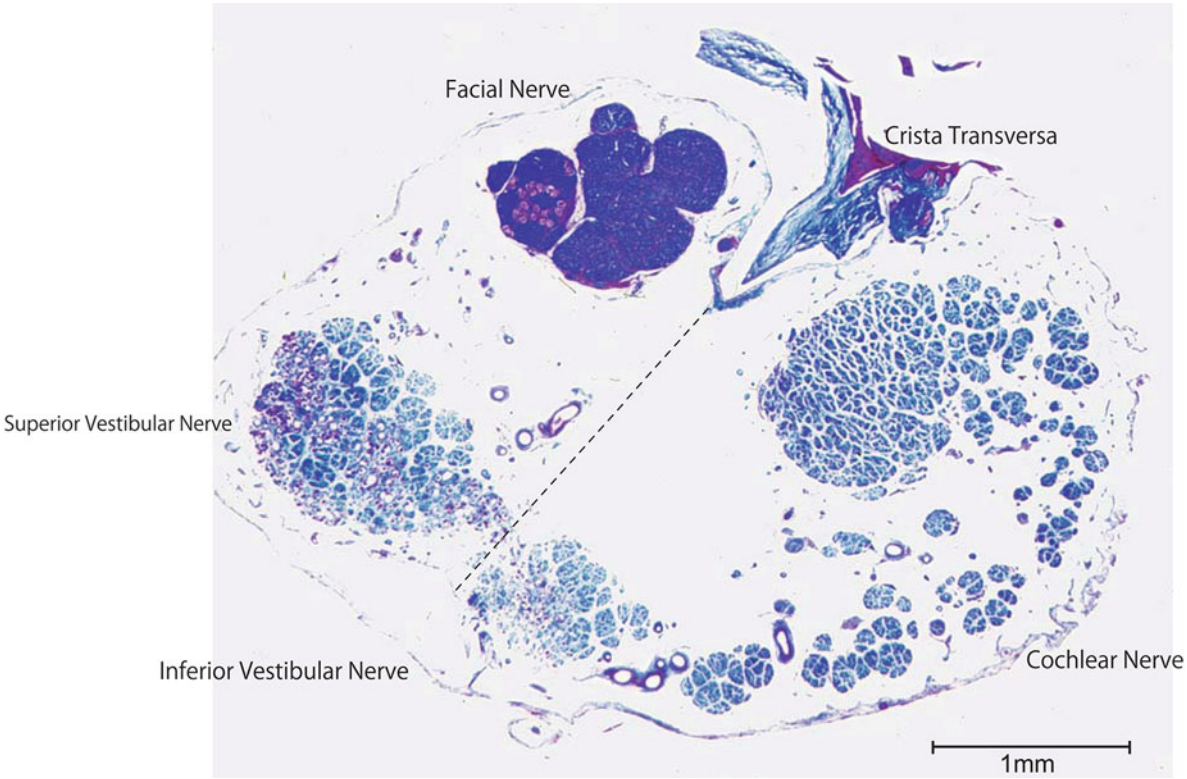

Fig. 1.20 Cross section of the internal auditory canal near the fundus. The *dotted line* shows the location of the crista transversa. The nerve fibers spread before passing through the tractus spiralis foraminosus to the basal turn of the cochlea. Eighty-year-old man, Azan stain, scale: 1 mm

Fig. 1.21 The tympanic nerve on the promontory. Many ganglion cells are present. They show positive acetylcholinesterase activity (original ×25)

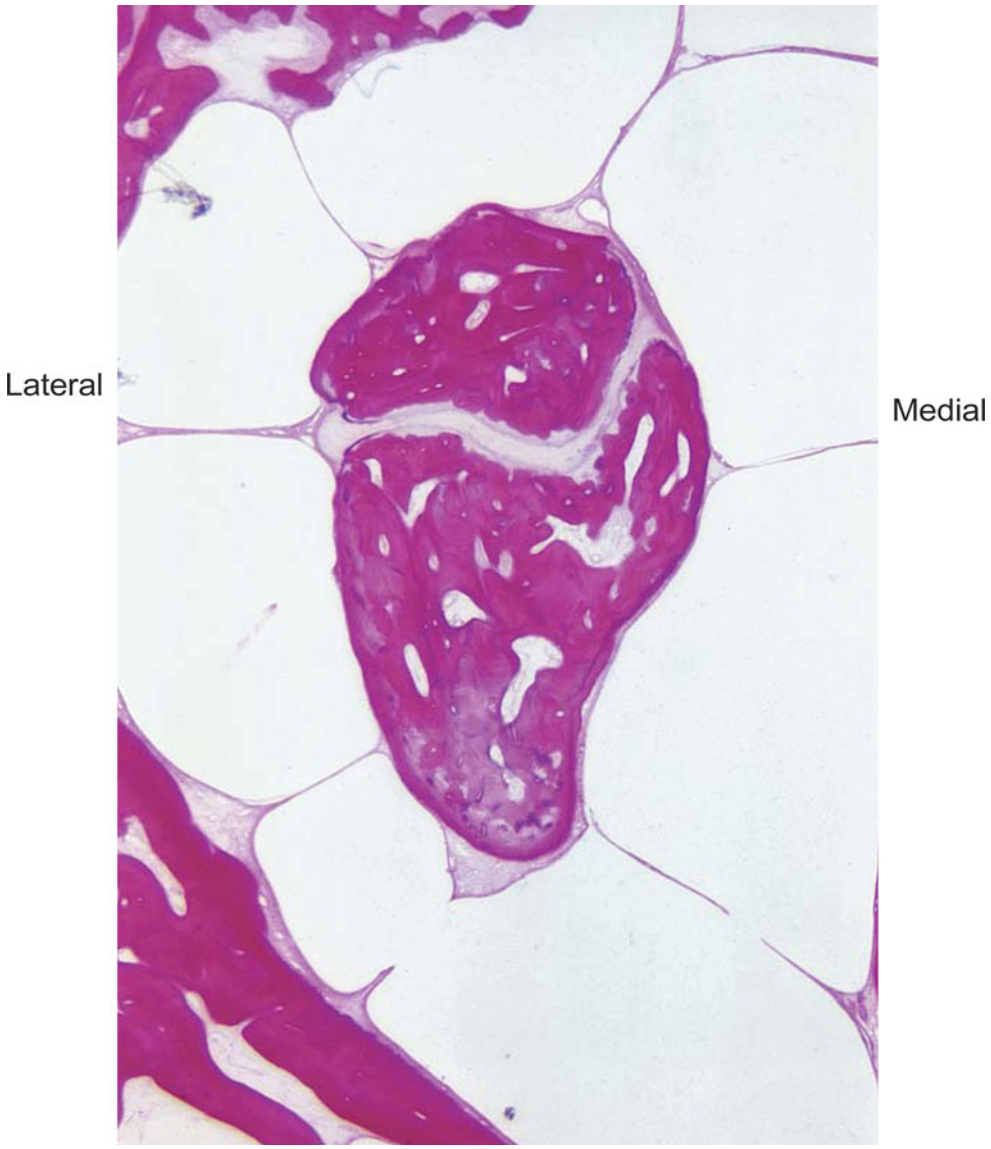

Fig. 1.22 Head of the malleus and body of the incus in the attic of the middle ear. The mucosal folds seem to sustain the ossicles from all directions

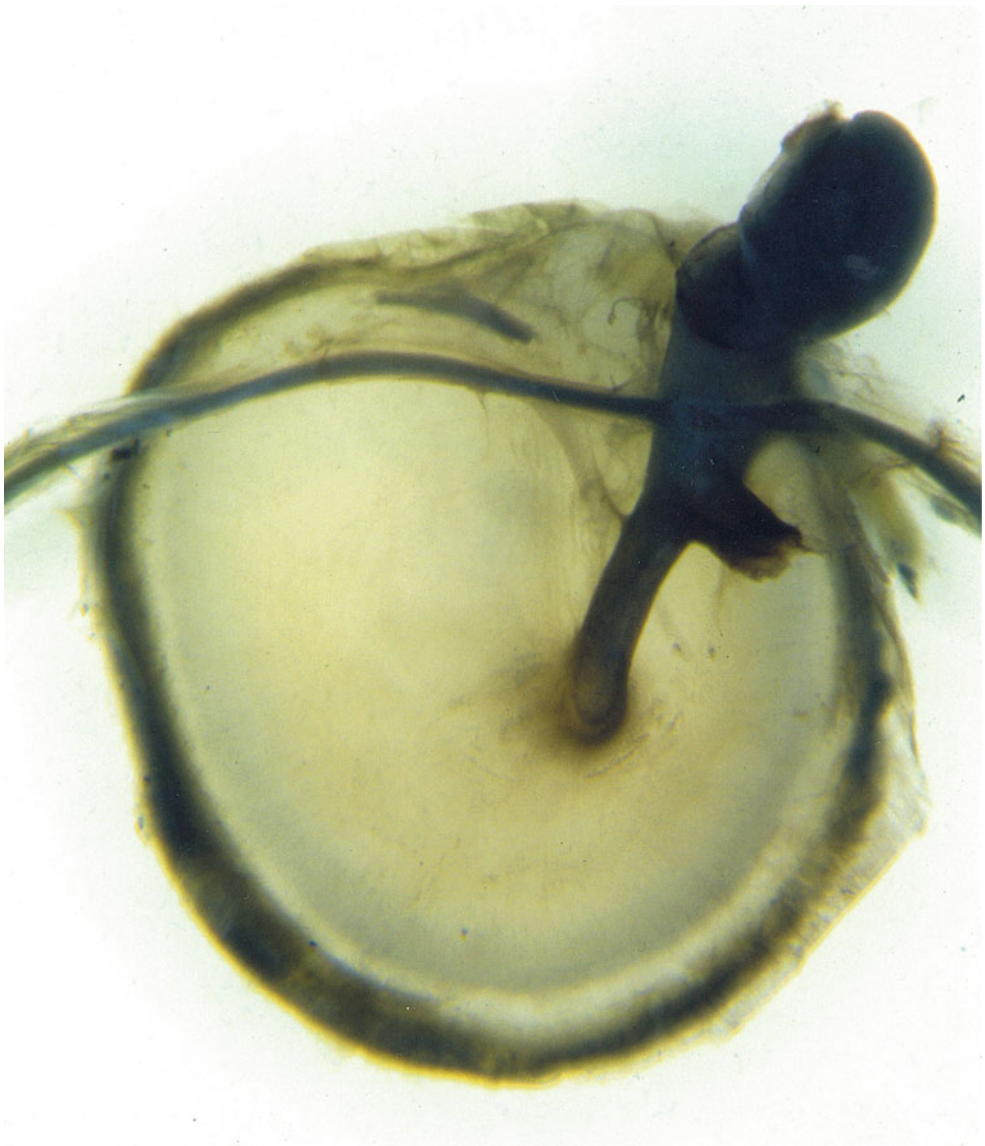

Fig. 1.23 The eardrum, malleus, tendon of the tensor tympani muscle, and chorda tympani as seen from inside the left tympanic cavity

auditory canal in newborns has no bony portion. The floor grows from the tympanic ring in early life. At the same time a bony canal roof is formed from the squama. Much of the definitive form of the external canal is completed by one year of age. A bony wall develops around the inner two-thirds of the canal and the lateral one-third is surrounded by cartilage. The canal reaches adult size by about the ninth year [20].

References

1. Guggenheim L (1948) Phylogenesis of the ear. Murray and Gee, Inc., Culver City
2. Skinner HA (1970) The origin of medical terms. Hafner Publishing Company, New York
3. Hollinshead WH (1958) Anatomy for surgeons: the head and neck, vol 1. A Hoeber-Harper Book, New York
4. de Burlet HM (1920) Der perilymphatische Raum des Meerschweinchenohres. Anat Anz 53:302–315
5. Hara M, Kimura RS (1993) Morphology of the membrana limitans. Ann Otol Rhinol Laryngol 104:625–630
6. Perlman HB (1940) Observations on a differentiated reenforced area of the saccular wall in man. Arch Otolaryngol 32:678–691
7. Igarashi M (1964) Comparative histological study of the reinforced area of the saccular wall in mammals. NASA Order No R-93
8. Voit M (1907) Zur Frage der Verästelung des Nervus acusticus bei den Säugetieren. Anat Anz 31:635–640
9. Johnsson L-G (1971) Degenerative changes and anomalies of the vestibular system in man. Laryngoscope 81:1682–1694
10. Huschke E (1835) Ueber die Gehörzahne, einen eigenthümlichen Apparat in der Schnecke des Vogelohrs. Arch Anat Physiol Wiss Med: 335–346
11. Kimura RS, Nye CL, Southard RE (1990) Normal and pathologic features of the limbus spiralis and its functional significance. Am J Otolaryngol 11:99–111
12. Corti A (1851) Recherches sur l'organe de l'ouie des mammifères. Z Wiss Zool 3:109–169
13. Schacht J, Hawkins JE (2004) Sketches of otohistory. Part 4: a cell by any other name: cochlear eponyms. Audiol Neurootol 9: 317–327
14. Spoendlin H (1969) Innervation patterns in the organ of Corti of the cat. Acta Otolaryngol 67:239–254
15. Spoendlin H (1985) Anatomy of cochlear innervation. Am J Otolaryngol 6:453–467
16. Stöver T, Diensthuber M (2012) Molecular biology of hearing. In: Laszig R (ed) Create the future. Rheinware, Germany, pp 53–78
17. Morrison D, Schindler RA, Wersäll J (1975) Quantitative analysis of the afferent innervation of the organ of Corti in guinea pig. Acta Otolaryngol 79:11–23
18. Nomura Y (1976) Nerve fibers in the human organ of Corti. Acta Otolaryngol 6:317–324
19. Nomura Y, Kirikae I (1967) Innervation of the human cochlea. Ann Otol Rhinol Laryngol 76:57–68
20. Pearson AA, Jacobson AD, VanCalcar RJ, Sauter RW (1970) The development of the ear. American Academy of Ophthalmology and Otolaryngology, Rochester

Inner Ear Fluid

2

Abstract

All sensory hair cells of the inner ear exist in extracellular fluid, but in some areas the fluid has the characteristics of intracellular fluid, as far as concentrations of K^+ and Na^+ are concerned. The membranous labyrinth contains the intracellular fluid-like endolymph, and is surrounded by a distinct extracellular fluid, the perilymph. The sensory hair cells of the cochlea are surrounded by extracellular fluid called cortilymph in a separate compartment. Excessive accumulation or leakage of any of these fluids may affect the functions of the whole or partial inner ear.

This chapter is concerned with perilymphatic fistula, signs and symptoms of which mimic Meniere's disease and sudden deafness. Because the pathophysiology of perilymphatic fistula formation is not clear, we have attempted to experimentally induce leakage of perilymph from the cochlear windows of guinea pigs by injecting artificial perilymph into the subarachnoid space or by suctioning a small amount of perilymph through the round window membrane. In these studies, the membranous labyrinth demonstrated various changes. The cochlea developed endolymphatic hydrops. The vestibular membranous labyrinth collapsed to a greater or lesser degree. In some experimental conditions, the organ of Corti showed cortilymphatic hydrops.

Keywords

Cerebrospinal fluid pressure • Cochlear aqueduct • Cortilymphatic hydrops • Experimental perilymphatic fistula • Perilymph • Perilymphatic fistula

2.1 Inner Ear Fluid

2.1.1 Perilymph and Endolymph

In 1760, Domenico Cotugno (Italian anatomist, 1736–1822) discovered the presence of fluid in the inner ear, which was thereafter called the "liquid of Cotugno." Later, Henri Marie Ducrotay de Blainville (French anatomist, 1777–1850) named the fluid "perilymph." The fluid within the membranous labyrinth was called "endolymph of Breschet" (Gilbert Breschet, French anatomist, 1784–1845). The vestibular membrane was described in 1854 by Ernst Reissner (German anatomist, 1824–1878), and has been called Reissner's membrane since that time.

2.1.2 Cortilymph

A third fluid space exists within the organ of Corti. Morphological studies have found no direct communication between the endolymphatic or perilymphatic spaces and the fluid within the organ of Corti. In 1960, Hans Engström [1] proposed the name "cortilymph" for the fluid filling the tunnel of Corti, the space of Nuel, the region around the hair cells, and the outer tunnel (Fig. 2.1).

Schuknecht and Seifi [2] perfused the scala tympani of a cat with a histochemical acetylcholinesterase staining solution, and found deposits of reaction product extending from holes in the lower shelf of the osseous spiral lamina to inside the organ of Corti (Fig. 2.2). Schuknecht believed that these

Y. Nomura, *Morphological Aspects of Inner Ear Disease*, DOI 10.1007/978-4-431-54204-9_2,

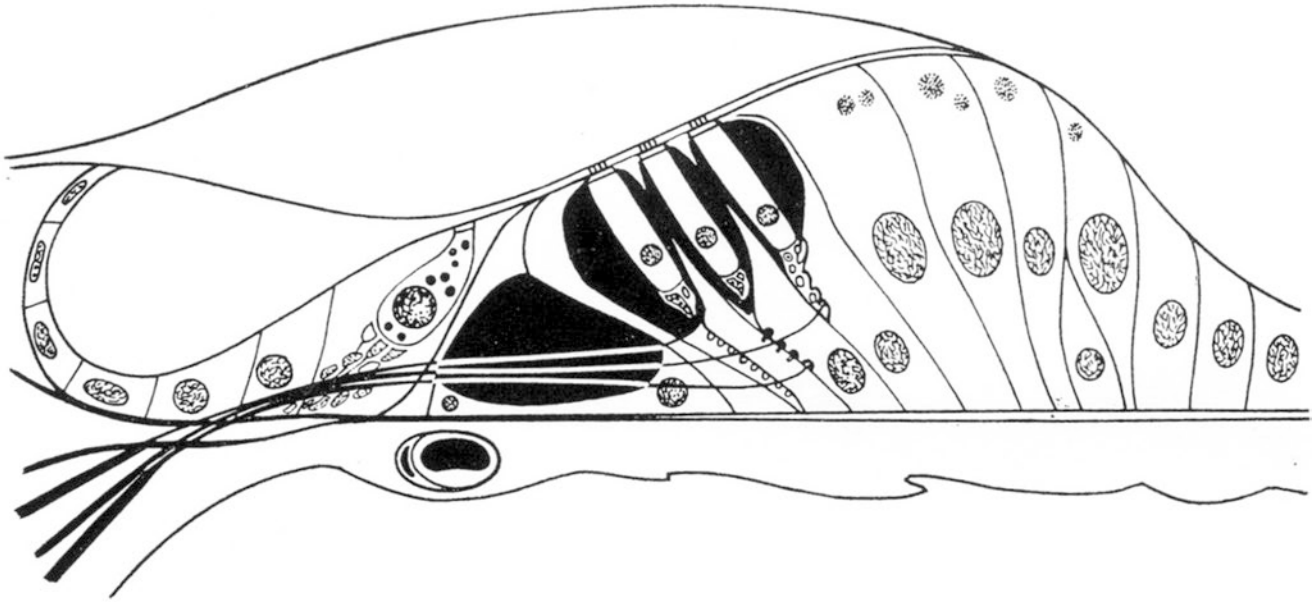

Fig. 2.1 The cortilymph occupies the space within the organ of Corti [1]. Engström H (1960) Acta Morphol Neerl Scand 3:195 Taylor & Francis Ltd. www.tandfonline.com

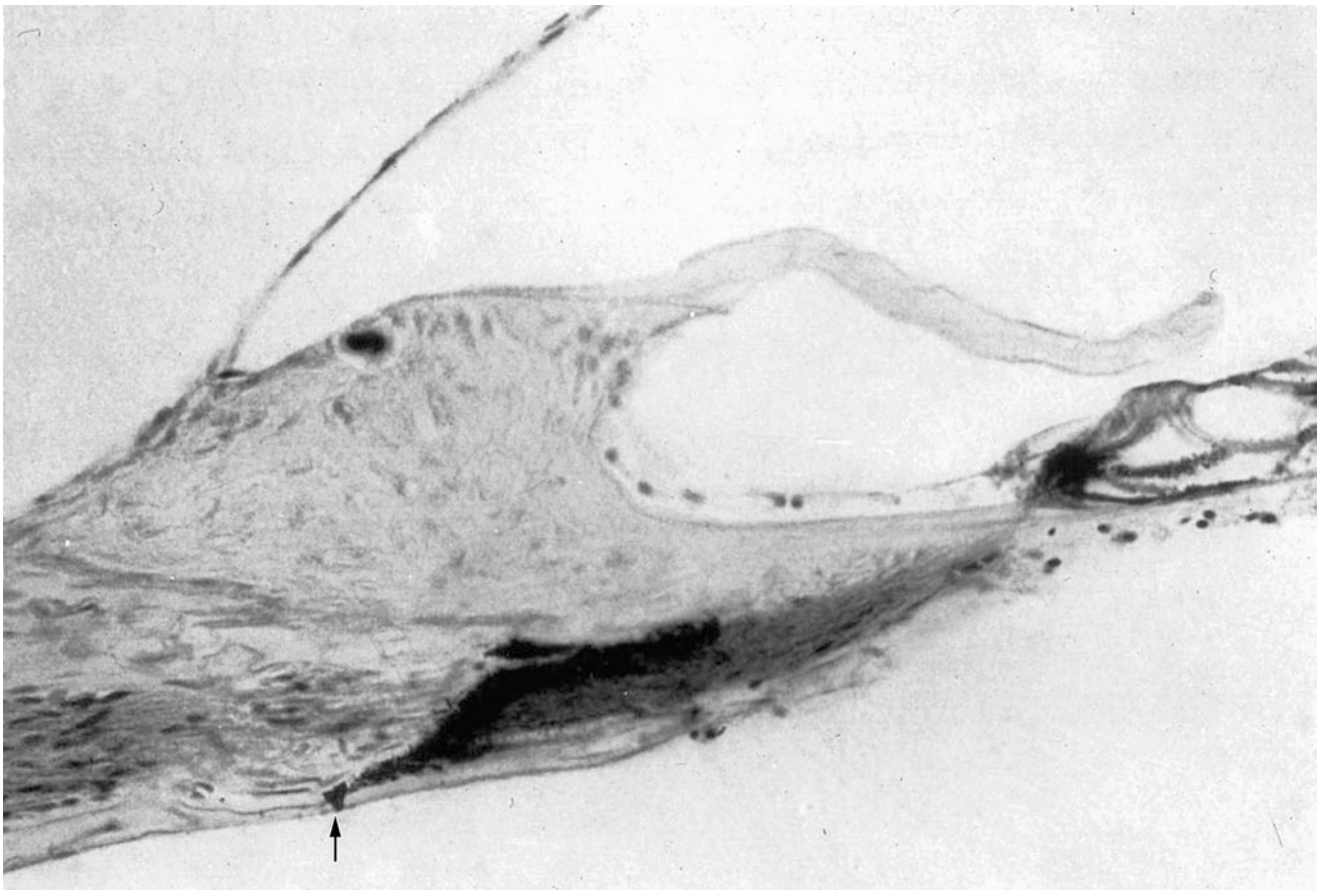

Fig. 2.2 Staining solution for acetylcholinesterase enters the osseous spiral lamina of a cat through a hole in the lower shelf. Reaction product is observed from the osseous spiral lamina to the organ of Corti. *Arrow*: Canaliculi perforantes Schuknechtii. Koelle's method (Courtesy of Dr. Schuknecht)

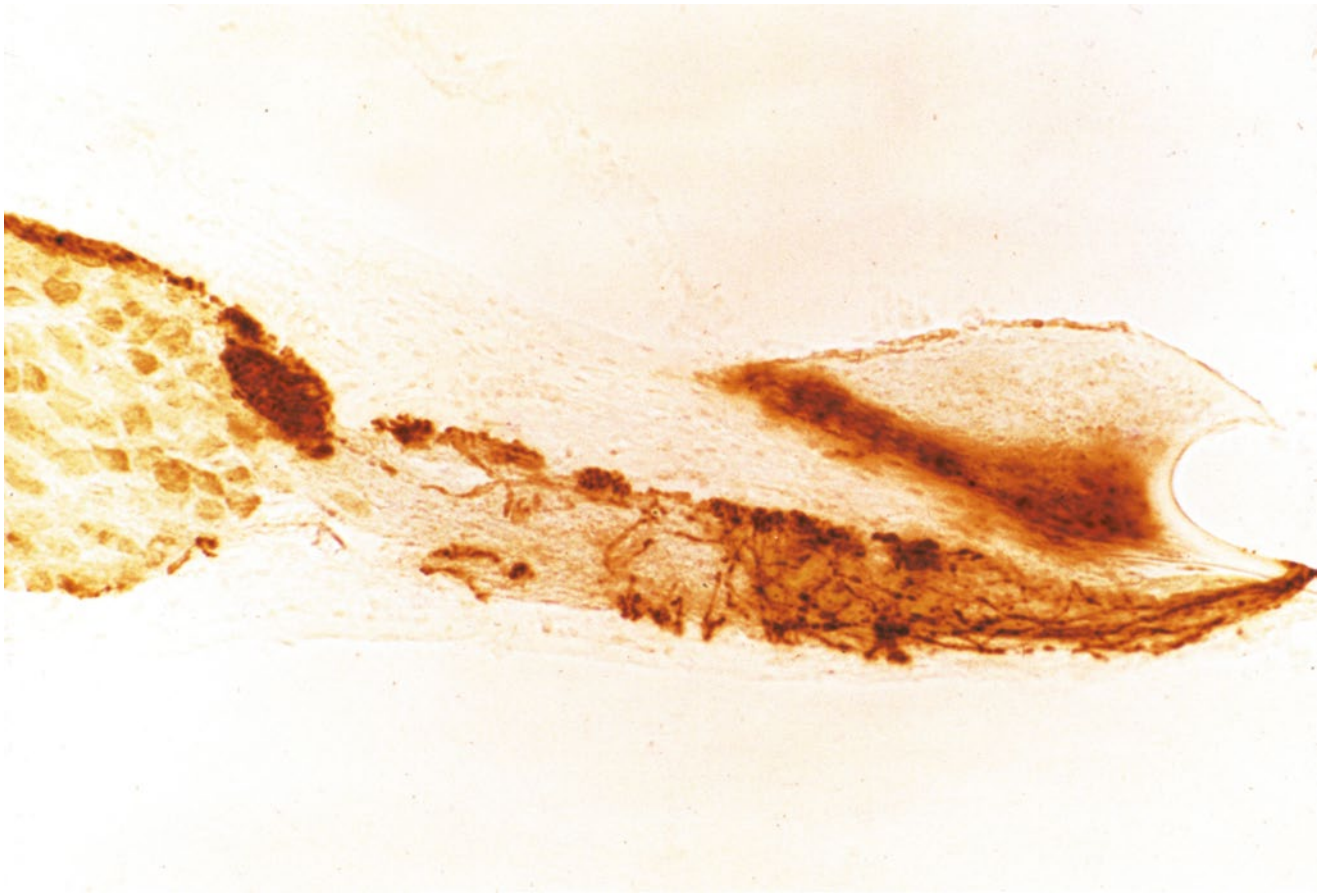

Fig. 2.3 Acetylcholinesterase activity in efferent fibers within the osseous spiral lamina of the cat. Strong activity is found in the intraganglionic spiral bundle and in the many small bundles adjacent to the upper and lower bony shelves. Frozen section, Gomori's method (original ×6.5)

were communicating perilymph channels from the scala tympani to the organ of Corti. The holes in the lower shelf of the osseous spiral lamina were named the "canaliculi perforantes Schuknechtii." They are located 0.2 mm from the habenula perforata in the cat. The staining solution flowed from the osseous spiral lamina through the habenula perforata into the organ of Corti. In a frozen specimen, however, no acetylcholinesterase reaction deposit could be found in the lower shelf of the osseous spiral lamina (Fig. 2.3).

Masuda et al. [3] demonstrated perilymphatic communication routes between the perilymph of the scala tympani and the cortilymph in guinea pigs by injecting inulin-methoxy-H3 through the round window membrane. Inulin accumulated not only in the habenula perforata and basilar membrane, but also in the cortilymph spaces, suggesting that the habenula perforata and basilar membrane are communication routes between the two spaces.

Nomura [4] perfused the scala tympani of guinea pigs using staining solution for succinic dehydrogenase with phenazine methosulfate. There were numerous holes in the lower shelf of the osseous spiral lamina through which the solution penetrated into the osseous spiral lamina (Fig. 2.4). Formation of reaction product, formazan, was rapid with phenazine methosulfate. Staining was observed along nerve fibers in the osseous spiral lamina. The staining solution passed from the osseous spiral lamina through the habenula perforata to the space in the organ of Corti (Fig. 2.5). The entire basilar membrane was eventually stained blue. But the first very rapid passage of solution into the organ of Corti was via a passageway between Deiters' cells and Hensen's cells (Fig. 2.6) [4]. According to Beagley [5], normal histological preparations showed fine canal-like intercellular spaces between Deiters' cells and Hensen's cells. Near the membrana reticularis, however, strong desmosomes join Hensen's cells to the outermost phalangeal process of Deiters' cells and this area seemed quite stable under the stress of acoustic trauma. By contrast, the base of the Hensen-Deiters' junction showed a wide cleft in some acoustically stimulated guinea pigs. Beagley was of the opinion that the Hensen-Deiters' split had protected the hair cells from acoustic stimuli.

From an electron microscopic study, Ishiyama and Ishiyama [6] noted that there was a wide gap between Deiters' cells and Hensen's cells adjacent to the basilar membrane (Fig. 2.7).

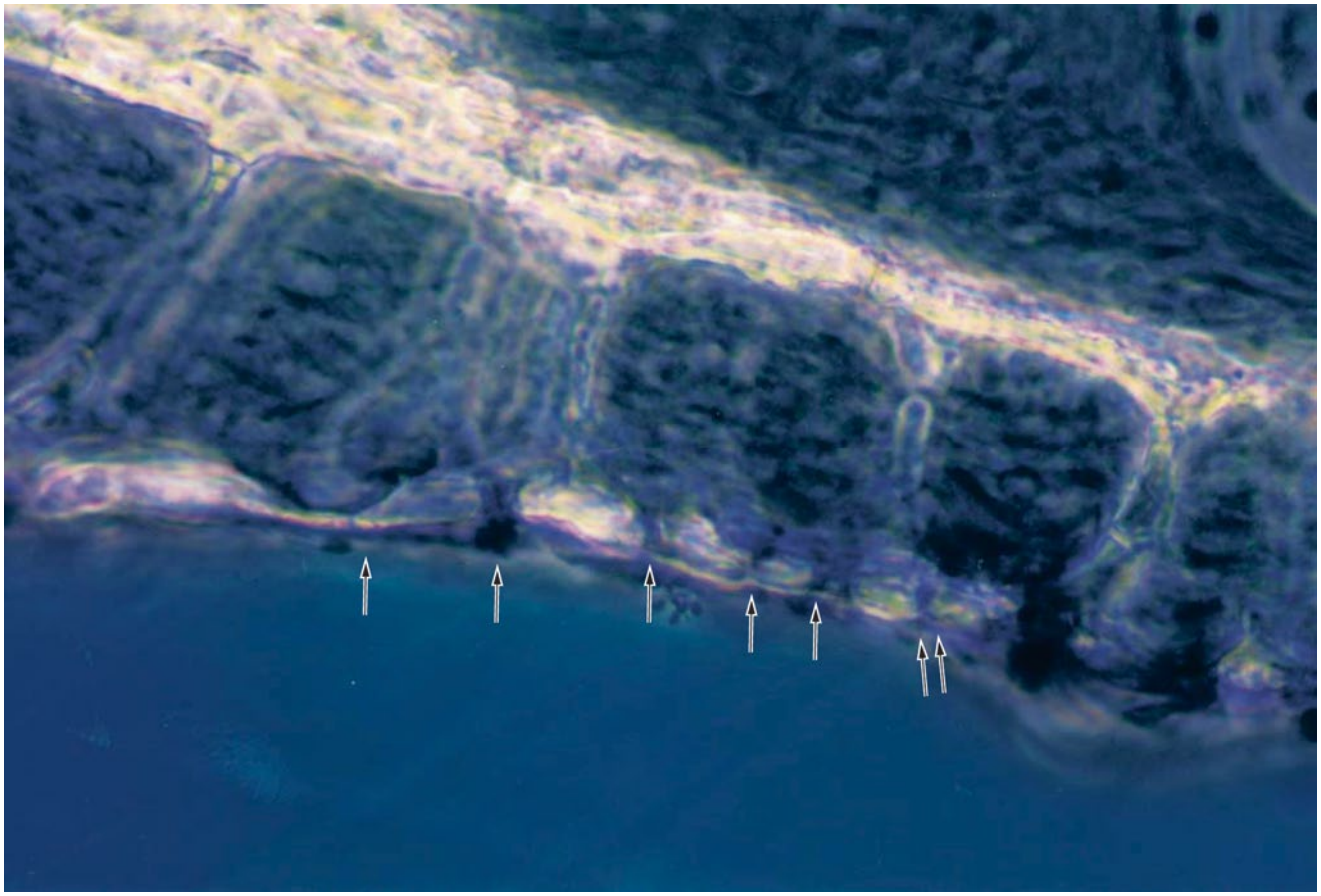

Fig. 2.4 Numerous holes (*arrows*) seen in the lower shelf of the osseous spiral lamina of the guinea pig. Staining solution for succinic dehydrogenase with phenazine methosulfate was introduced in the scala tympani (original ×16) [4]

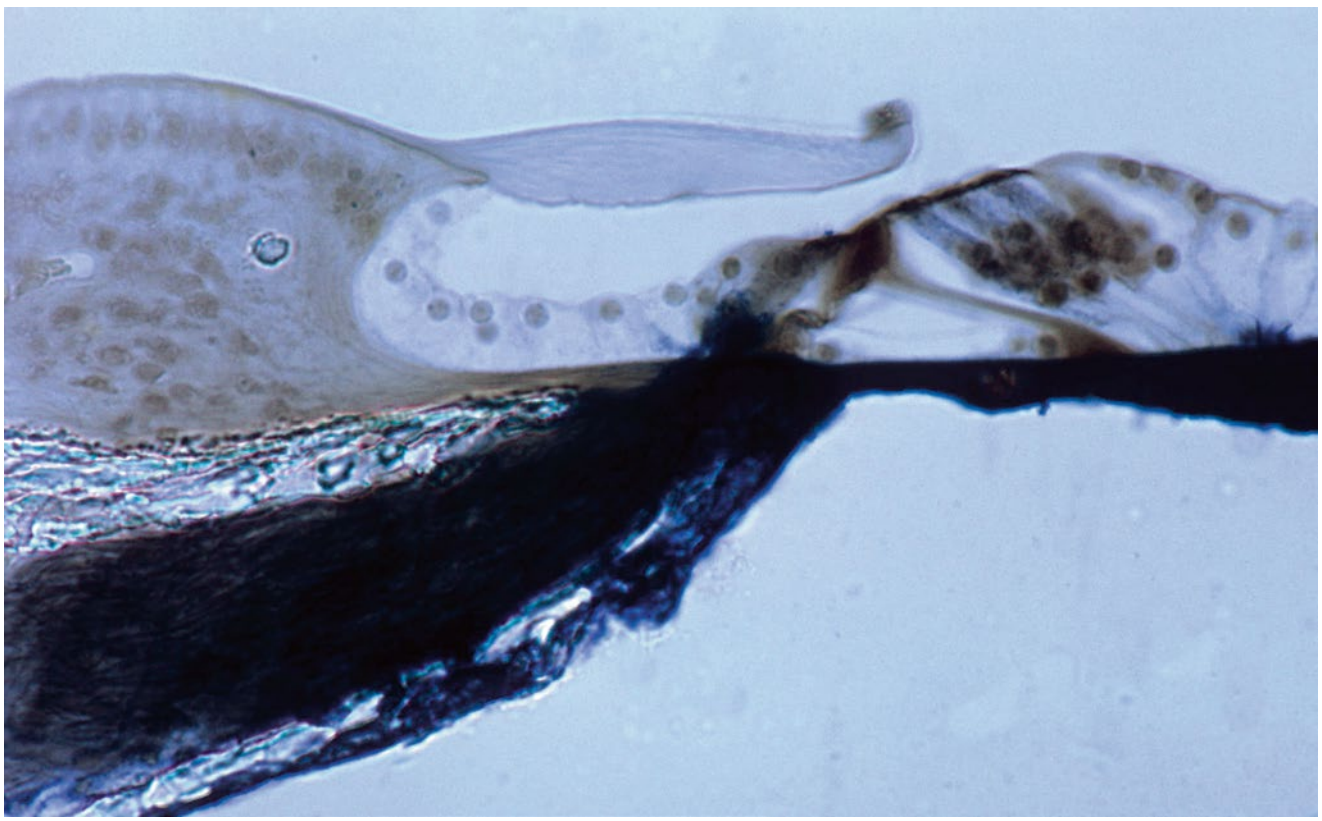

Fig. 2.5 Fluid passageway from the scala tympani to the organ of Corti. The solution entered through holes in the lower osseous spiral lamina to the inside the osseous spiral lamina of the guinea pig. The nerve fibers were stained. The solution entered the organ of Corti through the habenula perforata and basilar membrane (original ×6.5)

Fig. 2.6 Fluid passageway through the basilar membrane. Marker solution rapidly passed through the localized area of basilar membrane, and entered the organ of Corti through the space between Deiters' cell and Hensen's cell in the guinea pig (*arrow*). *Arrow* indicates a route for fluid into the organ of Corti (original ×40) [4]

In Nomura's study, after perfusion of the solution containing phenazine methosulfate, the organ of Corti became hydropic. Hensen's cells were pushed laterally, detached from the basilar membrane, and ballooned, so that there was a large space in the lateral part of the organ of Corti including the outer tunnel. This is the initial sign of formation of cortilymphatic hydrops. If hydropic conditions progress, the lateral portion of the membrana reticularis will be lifted (Fig. 2.8).

The pillar cells and Deiters' cells contain large numbers of tonofibrils. The pillar cells are firmly fixed to the basilar membrane. These cells together with the membrana reticularis strongly support the architecture of the organ of Corti. Hensen's cells have no contact with Deiters' cells at the base. The lateral aspect of the organ of Corti, where Hensen's cells are found, is the weakest and least able to tolerate increased pressure. Although the functions of Hensen's cells are not well understood, one role may be to release pressure within the organ of Corti.

As hydrops of the organ of Corti progresses with increasing osmotic pressure and/or diffusion from the scala tympani, the phalangeal processes of Deiters' cells and the pillar cells become slender, and hair cells disappear. The membrana reticularis and Hensen's cells become thin, but as a tough membrane they maintain the boundary of the organ of Corti (Fig. 2.9).

Djeric and Schuknecht [7] reported two cases of Hensen's cell cyst of the organ of Corti in human temporal bones. The cysts were bilaterally symmetrical. The authors postulated that the cysts might represent coalesced lipid droplets from Hensen's cells.

2.1.3 The Cochlear Aqueduct

The cochlear aqueduct and fundus of the internal auditory canal are communicating routes between the cerebrospinal fluid (CSF) and the perilymph (Fig. 2.10). The internal aperture of the cochlear aqueduct is located near the round window and the inferior cochlear vein (Fig. 2.11).

Gopen et al. [8] evaluated 101 temporal bones from subjects aged 0–100 years, and reported that the mean diameter of the narrowest portion of the cochlear aqueduct was 138 ± 58 μm, which occurred 200–300 μm from the cochlear

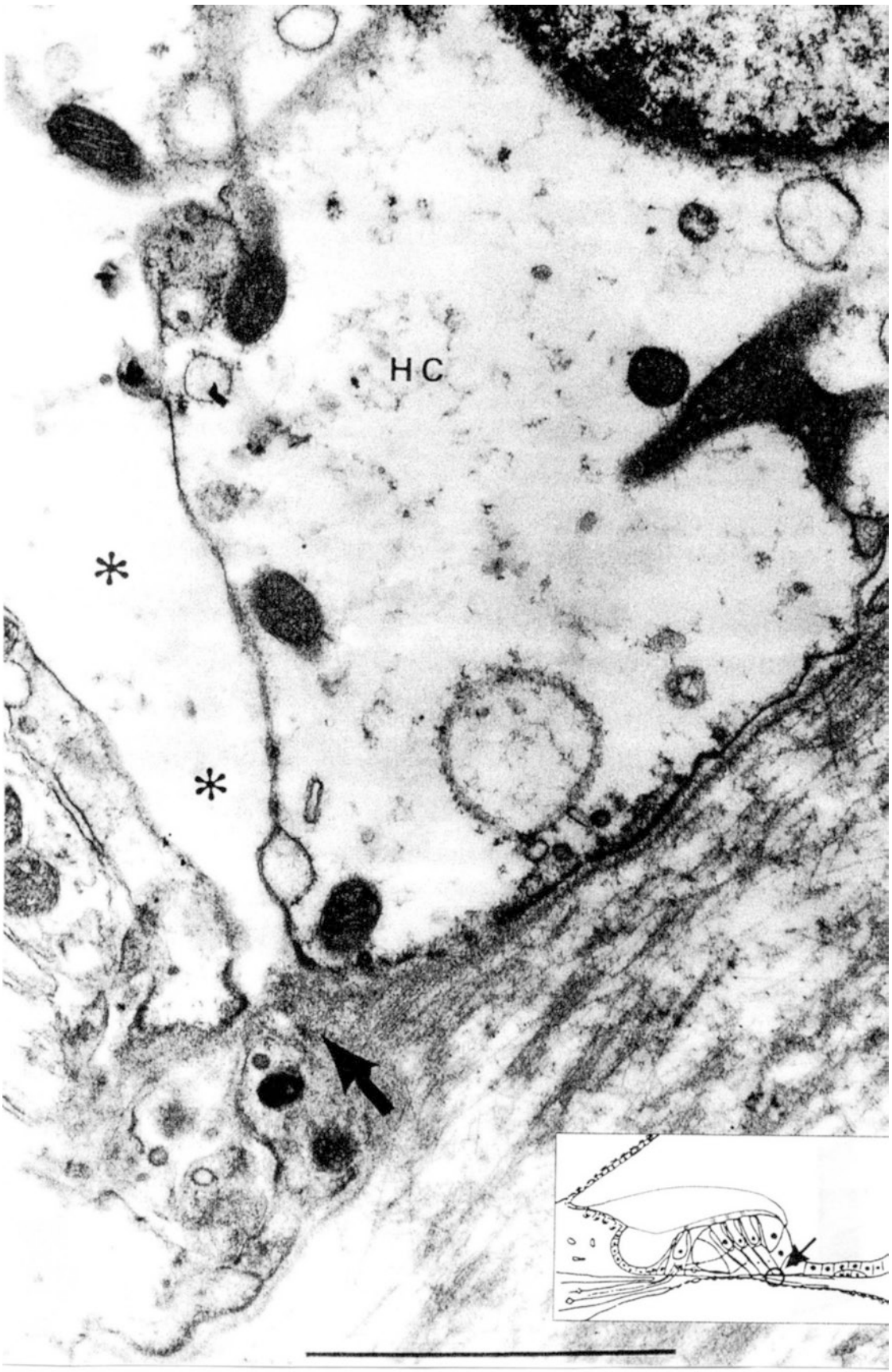

Fig. 2.7 There is a wide space between the junction (*asterisk*) of Deiters' cell and Hensen's cell. The inset shows the area of observation. *Arrow* indicates a route for fluid into the organ of Corti. *HC* Hensen's cell, scale: 1 μm (Courtesy of Drs. Ishiyama and Ishiyama) [6]

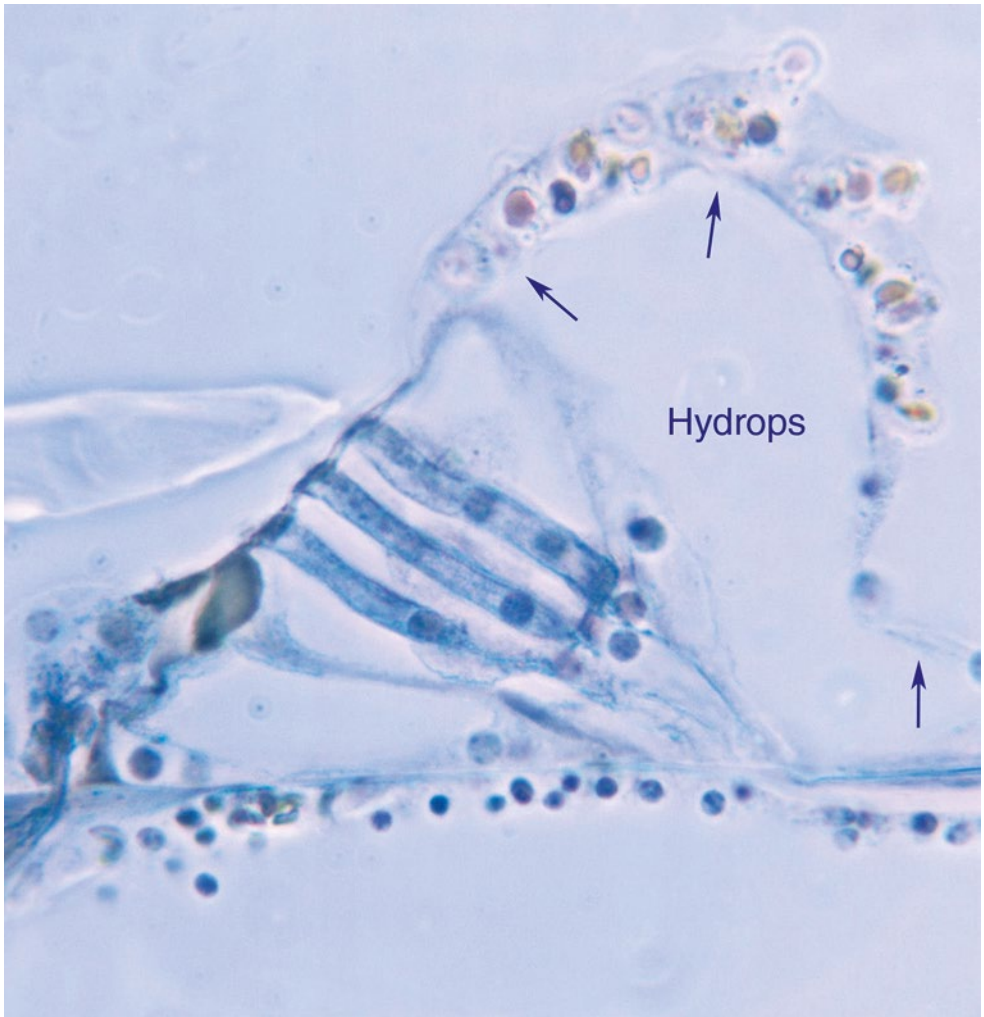

Fig. 2.8 Cortilymphatic hydrops. The organ of Corti is stained blue. Hensen's cell is detached from the basilar membrane. The split between Deiters' cell and Hensen's cell is enlarged. Hensen's cells are ballooned (*arrows*). Lateral part of the membrana reticularis is lifted. The inner pillar cell is crushed. Perfusion of the solution for staining succinic dehydrogenase with phenazine methosulfate, Guinea pig, original ×40

end of the aqueduct. They noted four types of aqueduct patencies: central lumen patent throughout the length of the aqueduct (34 %), lumen filled with loose connective tissue (59 %), lumen occluded by bone (4 %), and obliteration of the aqueduct (3 %). There was no correlation between age and narrowest diameter, or between age and type of patency.

The cochlear aqueduct is not a route for cerebrospinal fluid in cases of stapes gusher. Stapes gusher occurs in the cochlea when the fundus of the internal auditory canal is missing, and a wide communication exists between the internal auditory canal and the scala vestibuli (Fig. 2.12).

2.1.4 Perilymph and the Limbus Spiralis

The portion of the limbus spiralis facing the scala vestibuli was named the vasculoepithelial zone by Borghesan [9]. The zone is believed to be related to the production of perilymph constituents and is lined by osmiophilic cells [6, 10, 11]. The cells have also been shown to have Na^+/K^+-ATPase activity [12].

Hsu and Nomura [13] demonstrated strong carbonic anhydrase activity in the vasculoepithelial zone (Fig. 2.13). Carbonic anhydrase is an enzyme that assists the rapid conversion of carbon dioxide and water into carbonic acid, hydrogen, and bicarbonate ions.

$$CO_2 + H_2O \xrightarrow[\text{carbonic anhydrase}]{} HCO_3 - + H^+$$

Carbonic anhydrase is an important enzyme in the regulation of pH and fluid balance in different parts of the body, including the inner ear. Light and electron microscopic studies have shown diverse distribution of the enzyme in the inner ear. The stria vascularis and dark cells have strong carbonic anhydrase activity [13]. The neuroepithelia of the crista ampullaris show strong activity in the supporting cells, but sensory cells with nerve chalices show no activity, although the reaction products are found on the stereocilia (Fig. 2.14).

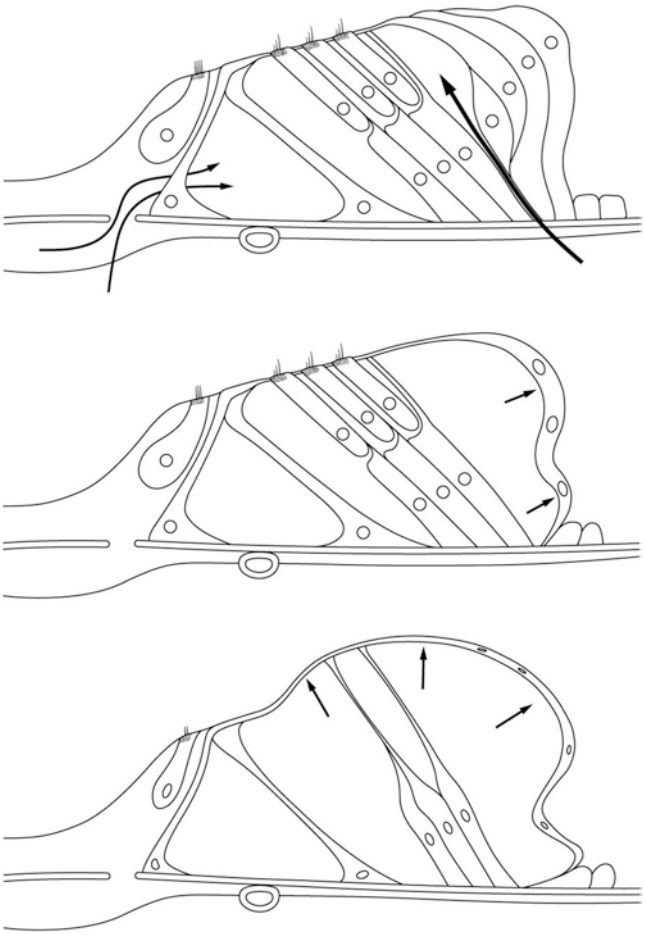

Fig. 2.9 Schema showing the process of cortilymphatic hydrops formation. Fluid enters the organ of Corti through the Deiters–Hensen's cell slit and habenula perforata. As the pillar cells and Deiters' cells are hardy, Hensen's cells are pushed laterally. As hydrops progresses, the pillar cells and Deiters' cell become elongated. The outer hair cells disappear

The inner ear maintains its functions through the actions of various cells and of enzymes such as carbonic anhydrase, Na^+/K^+-ATPase, and adenyl cyclase.

2.1.5 Endolymph

Endolymph is produced mainly in the stria vascularis and dark cell areas. Electrolyte concentrations in the endolymph are quite different from those in the perilymph. In 1954, Smith et al. [14] demonstrated a high potassium ion concentration and a low sodium ion concentration in the endolymph, while the reverse was found in the perilymph.

Unlike the utricle and ampullae of the semicircular canals, the saccule has no dark cell areas. Hydrops of the saccule is often quite marked in patients with Meniere's disease. The origin of the endolymph in these cases is probably the stria vascularis.

The membrana reticularis divides the cortilymph from the endolymph. When the cuticular plate of the outer hair cells disappears, repair of the membrana reticularis will take place simultaneously. The area of the cuticular plate is tightly enclosed by the surrounding phalanxes of Deiters' cells and the heads of the pillar cells, so that no contamination occurs between the endolymph and the cortilymph. When the stria vascularis is damaged by laser irradiation, rapid repair takes place to maintain the scala media.

Endolymphatic hydrops is described in the chapter on Meniere's disease.

2.2 Perilymphatic Fistula

2.2.1 Clinical Aspects

Perilymph may leak into the tympanic cavity from the inner ear in cases of temporal bone trauma, including ear surgery. However, leakage can occur without apparent cause, leading to signs and symptoms of inner ear malfunction. This condition is called spontaneous perilymphatic fistula.

Perilymphatic fistula is suggested if any of the following symptoms is evident:

- Tinnitus, hearing loss, fullness of the ear, dizziness, and disequilibrium, occurring immediately after straining, nose blowing, or any other physical activity that causes a rapid increase of cerebrospinal fluid (CSF) pressure. The same symptoms can also occur with a rapid change of atmospheric pressure that affects the middle ear pressure.
- Sensorineural hearing loss developing over a period of hours or a few days.
- Tinnitus or a sensation of running water within the ear.
- Dizziness when pressure in the external ear is artificially increased or decreased.
- Fullness of the ear, hearing loss, tinnitus, dizziness, and disequilibrium following a popping sound.

Perilymphatic fistula can also occur without hearing loss or dizziness. A definitive diagnosis can be made by confirming perilymph leakage or fluid from the oval and/or round window at exploratory tympanotomy or endoscopic inspection. The pathophysiology of perilymphatic fistula remains unclear, mainly because of the paucity of histopathological studies of the inner ear in patients with the disorder.

With exploratory tympanotomy, the areas near the oval and round windows can be reached. Fluid may be observed oozing around the stapes footplate without an apparent slit.

Because the round window membrane is nearly parallel to the floor of the external auditory canal in most cases, it is difficult to directly observe the membrane

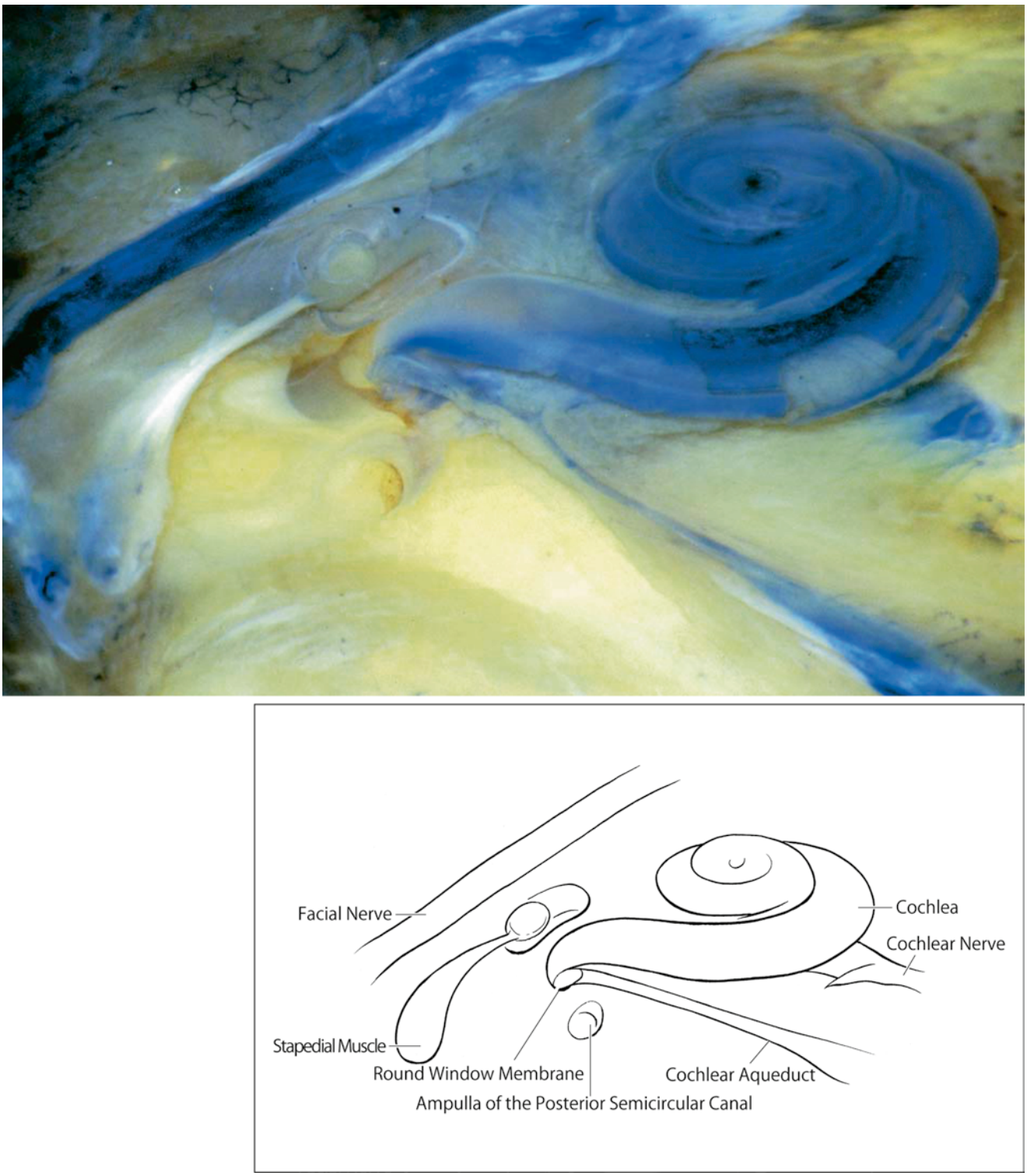

Fig. 2.10 Human cochlea and cochlear aqueduct. The internal aperture of the cochlear aqueduct is near the round window. Sudan Black B stain (original ×2.5)

(Fig. 2.15). Furthermore, a round window niche membrane is often observed in that area. Nomura [15] evaluated 100 temporal bones and found that only 30 lacked a recognizable membranous structure in the round window niche. Of the remaining 70, 13 had closed niches, 54 were perforated, and 3 had a reticulated structure. The closed type niche membrane may be mistaken for the round window membrane [15] (Fig. 2.16).

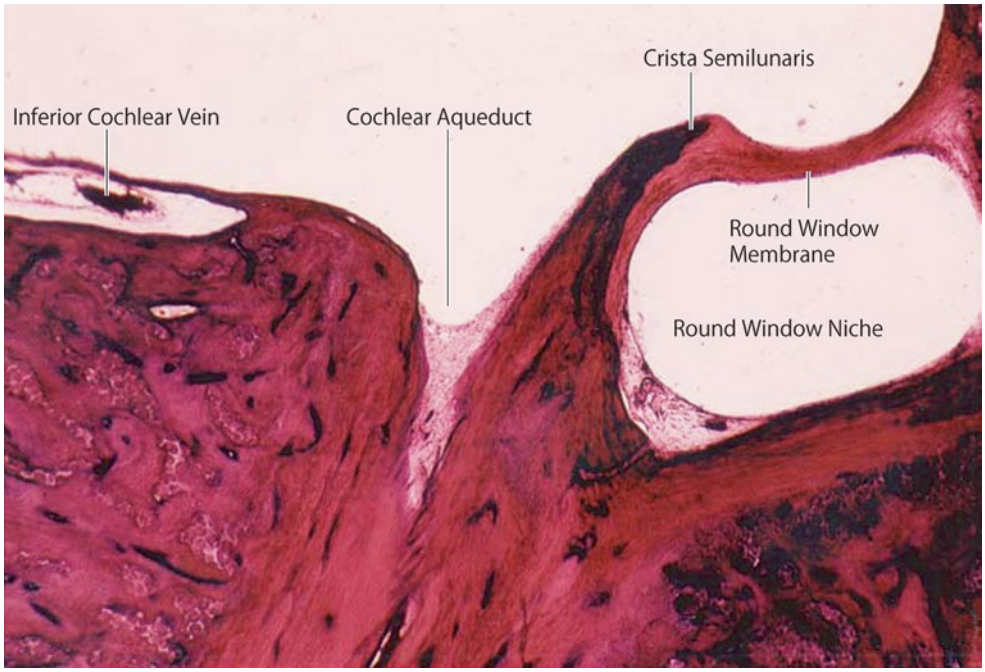

Fig. 2.11 The cochlear aqueduct's internal aperture near the round window. The inferior cochlear vein runs within the canal of Cotugno (original ×6.5)

Fig. 2.12 This temporal bone is from a patient with otopalatodigital syndrome. The bone shows fixation of the stapes, scala communis, defective modiolus, and a large communication between the internal auditory canal and scala vestibuli. No fundus of the internal auditory canal is observed. There is a risk of stapes gusher occurrence (Courtesy of Dr. Schuknecht)

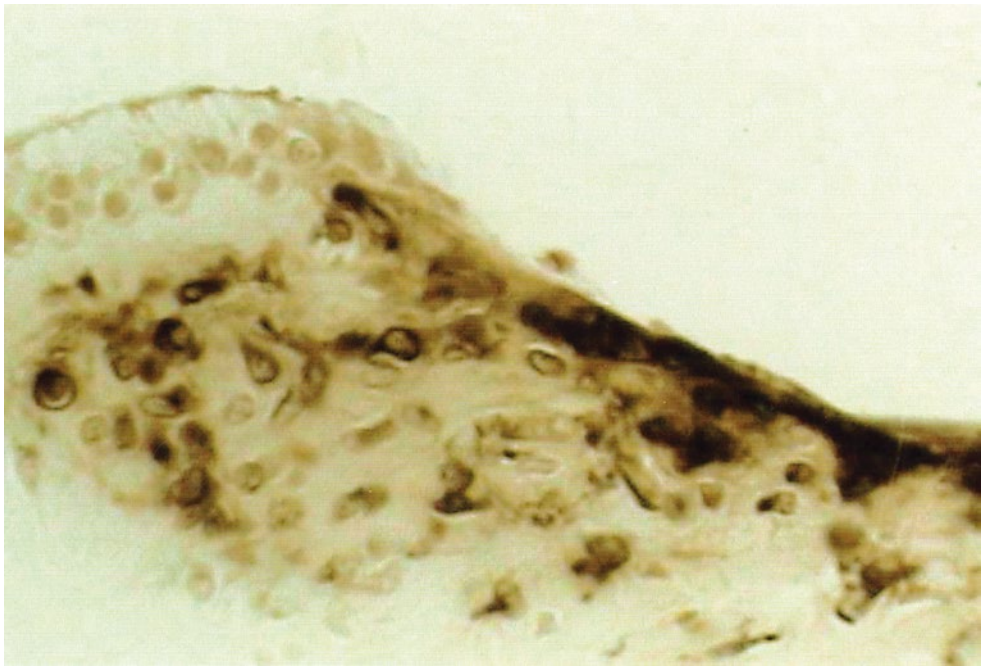

Fig. 2.13 Carbonic anhydrase activity in the limbus spiralis. The vasculoepithelial zone demonstrates strong enzyme activity. The interdental cell and its vicinity show no reaction. Guinea pig [13]

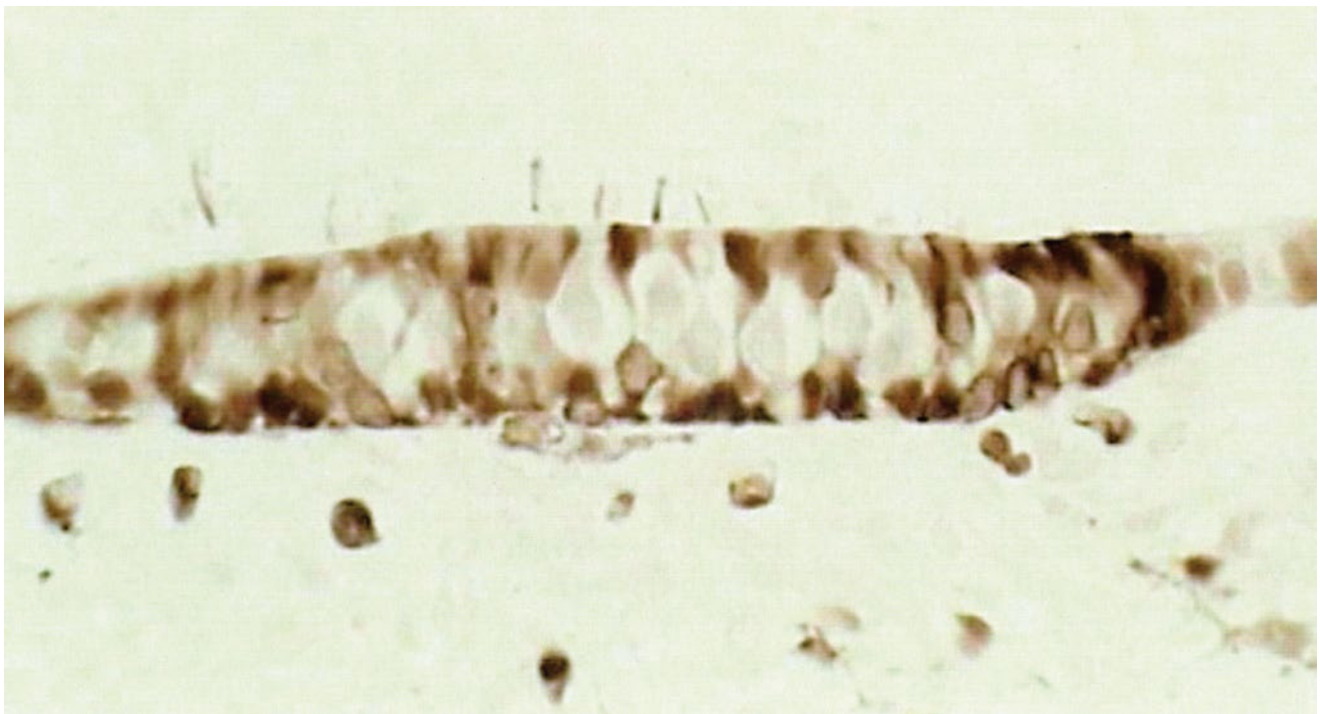

Fig. 2.14 Carbonic anhydrase activity in the neuroepithelia of the crista ampullaris. Supporting cells show carbonic anhydrase activity. The sensory cell and nerve chalice show no activity. The stereocilia show deposits of reaction products. Guinea pig (original ×40) [13]

In the same study, rupture of the oval window or round window membrane was observed when pressure was applied through the cochlear aqueduct or scala tympani of cadaver temporal bones. In the round window membrane, a slit-like fistula was observed, running parallel to the direction of the round window membrane fibers [15, 16] (Figs. 2.17 and 2.18). Round fistulae were not detected [15].

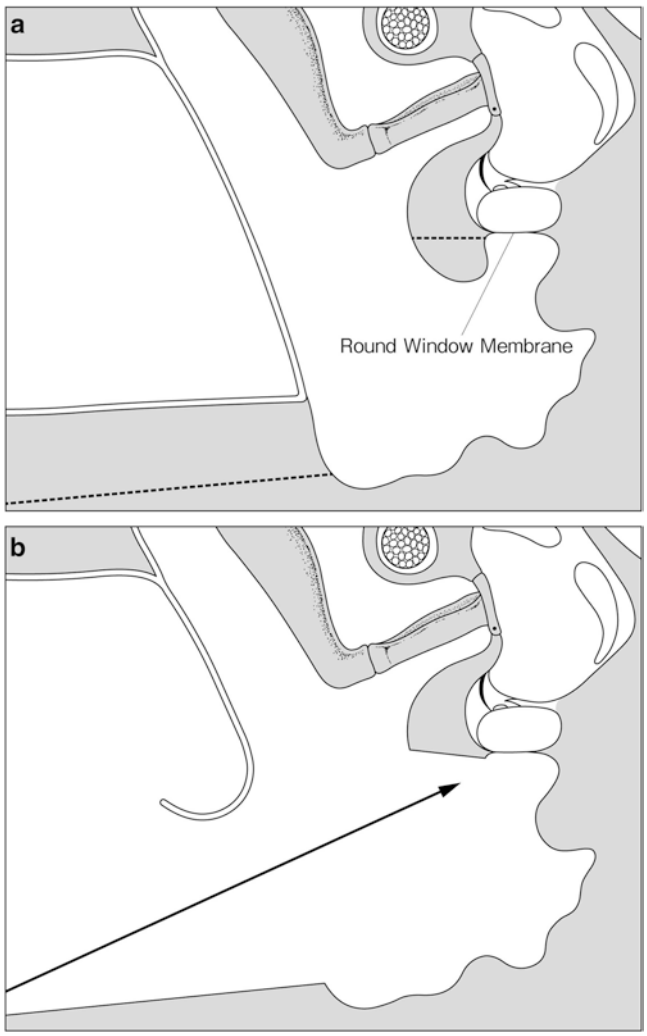

Fig. 2.15 The round window membrane can hardly be seen, even with exploratory tympanotomy. (**a**) Before tympanotomy, (**b**) during tympanotomy. Edge of the round window niche and the floor of the external auditory canal are removed

In cases of confirmed perilymph leakage, diagnosis of perilymphatic fistula can be made. In cases without confirmed perilymph leakage, can perilymphatic fistula be ruled out? The answer is "No." The signs and symptoms of the condition depend on the underlying pathology of the membranous labyrinth. Therefore, if the pathology persists after the fistula has been closed, patients may show ongoing signs of inner ear disease. The condition should be diagnosed as perilymphatic fistula even without confirmed perilymph leakage.

It has recently been reported that cochlin-tomoprotein is specifically present in the perilymph and can thus be used as a perilymph marker. Serum and CSF do not contain cochlin-tomoprotein. Perilymph is a mixture of plasma filtrated through the blood-labyrinth barrier [17], CSF, and constituents produced in the inner ear. The volume of perilymph is about 150 μL. If perilymphatic fistula occurs, the first few microliters that leak from the inner ear contain cochlin-tomoprotein. However, if leakage persists, the fluid may no longer contain the protein, or the protein concentration may be below the cut-off value of the test. In such cases, plasma filtrate and CSF leak from the inner ear.

Taking these circumstances into consideration, a diagnosis of perilymphatic fistula should be made clinically without performing exploratory tympanotomy, just as we routinely diagnose sudden deafness and Meniere's disease. Otherwise, clinical studies of perilymphatic fistula will not be promoted.

2.2.2 Changes of CSF and Middle Ear Pressures in Daily Life

Nose blowing is a not infrequent cause of perilymphatic fistula. Because patients usually do not recognize nose blowing as the cause of the condition, it is ignored. A diagnosis of spontaneous perilymphatic fistula may be made in such patients.

Goodhill [18] proposed the explosive and implosive routes in the pathogenesis of perilymphatic fistula. In the explosive route, high CSF pressure extends to the inner ear, resulting in fistula formation in the oval and/or round window. Conversely, high pressure in the middle ear exerts concomitant pressure on one or both of the windows, producing a fistula or fistulae via the implosive route.

2.2.2.1 Changes in CSF Pressure

To examine changes in CSF pressure in daily life, Sakikawa et al. [19] performed spinal taps on 23 hospitalized patients who required CSF examination for diagnosis of their medical problems. Their clinical diagnoses were vertigo (seven patients), sudden deafness (6), facial nerve paralysis (4), perilymphatic fistula (3), and other conditions (3).

During CSF pressure recording, the patients were asked to perform the following four actions: nose blowing with one nostril closed, nose blowing with both nostrils closed, breath holding, and sniffing. The results showed that nose blowing with both nostrils closed resulted in the greatest pressure elevation of the four actions. Resting CSF pressures ranged from 60 to 170 mmH_2O (mean, 112) in the 20 patients without perilymphatic fistula, and from 60 to 120 mmH_2O (mean, 120) in the three perilymphatic fistula patients. The mean value of maximum CSF pressure when nose blowing with both nostrils closed was 406 mmH_2O (range: 177–666) in 20 patients without fistula, while it was 523 mmH_2O (range: 449–598) in the three perilymphatic fistula patients.

Patients with perilymphatic fistula showed greater pressure changes than other patients (Fig. 2.19a). In some patients, nasopharyngeal pressure was measured in addition to CSF pressure (Fig. 2.19b). The study indicated that CSF pressure rose to more than 400 mmH_2O with nose blowing with both nostrils closed in 10 of 23 cases (7 of 20 non-perilymphatic

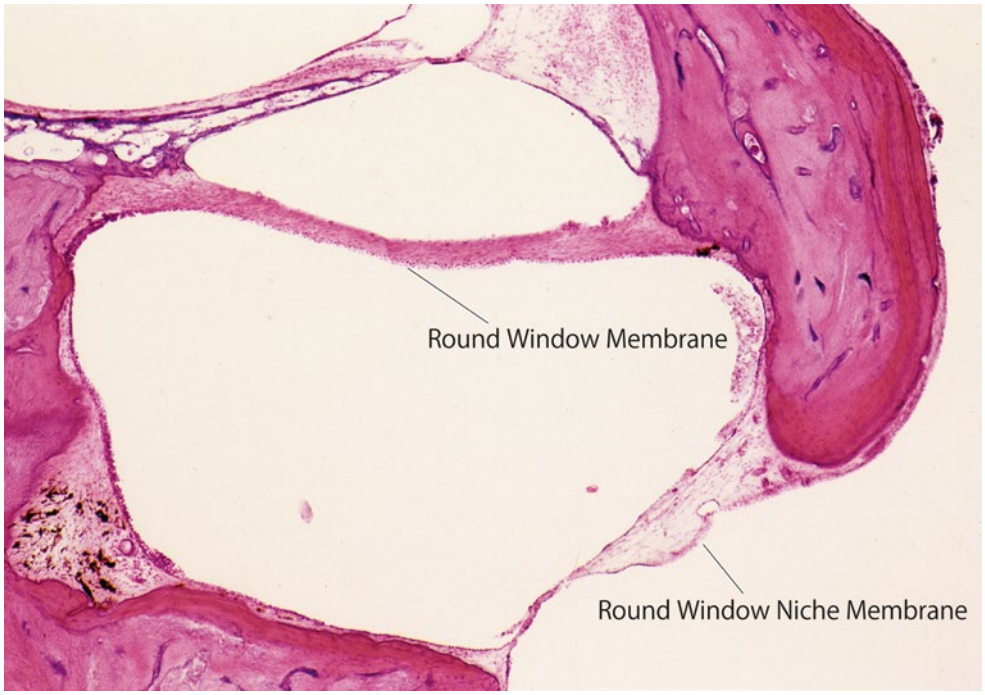

Fig. 2.16 The round window niche membrane closes the round window niche (closed type). The niche membrane may be mistaken for the round window membrane [15]

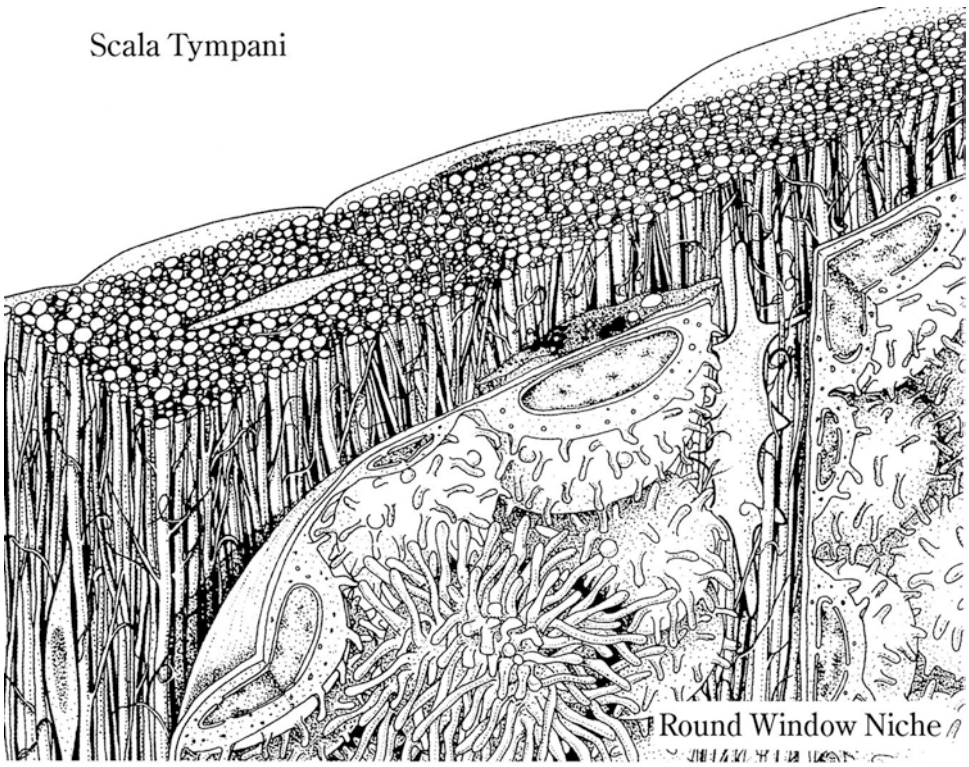

Fig. 2.17 Schema of the round window membrane (cross section). The membrane consists of three layers: the outer layer, which is a continuation of the mucosa of the tympanic cavity, the middle fibrous layer, and the inner mesothelial cell layer [16]

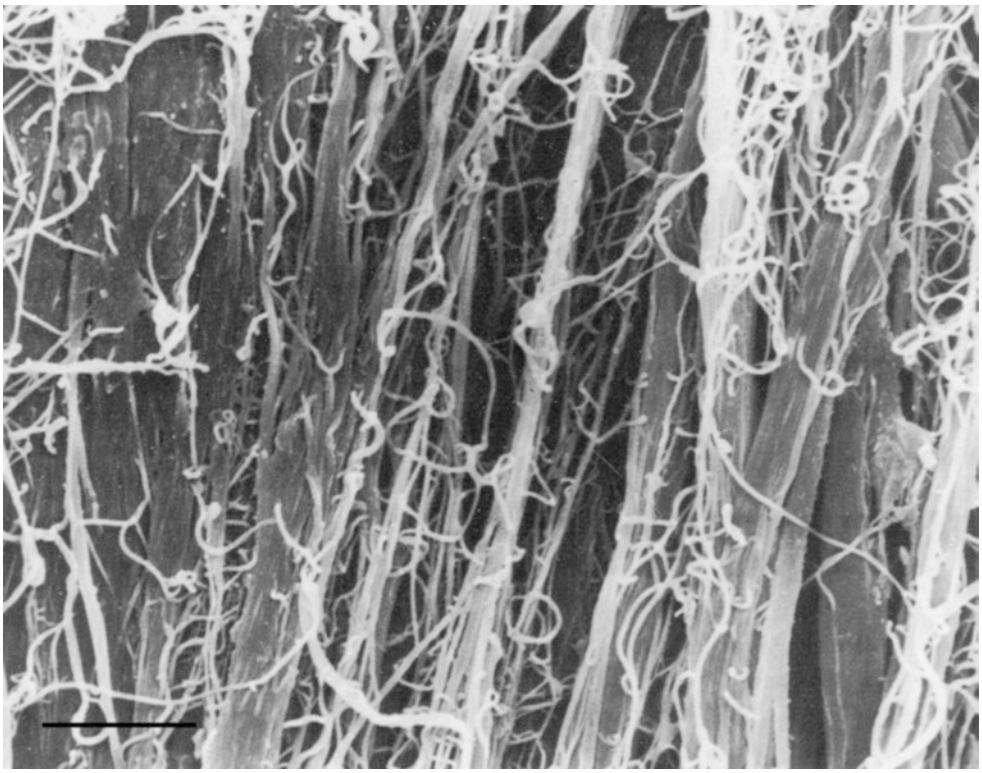

Fig. 2.18 The middle layer of the human round window membrane. Bundles of collagen fibers are seen. The fibers fan out from the crista semilunaris toward the bony edge of the round window. Scale: 3 μm (original ×4,500) [15]

fistula cases, and all perilymphatic fistula cases). Conversely, sniffing lowered CSF pressure in all cases.

2.2.2.2 Changes in Middle Ear Pressure

Changes in middle ear pressure in daily life have also been examined [20]. Eighteen patients with eardrum perforation were enrolled. Changes in middle ear pressure before and during nose blowing with both nostrils closed were recorded using a pressure monitor. Effects of sniffing and Eustachian catheterization were also examined.

During nose blowing with both nostrils closed, the mean pressure change was 252 mmH_2O (range: 163–340 mmH_2O). In 10 of 18 patients, middle ear pressure was unchanged during sniffing. These results suggest that sniffing only slightly influences middle ear pressure in people with competent Eustachian tubes. During Eustachian catheterization, the middle ear pressure changes ranged from 408 to 1,033 mmH_2O (mean, 776 mmH_2O).

The study showed that changes in middle ear pressure during nose blowing with both nostrils closed were large and rapid (Fig. 2.20). The amplitude of the pressure change in the middle ear during nose blowing was 230 mmH_2O.

2.2.2.3 Pressure Gradient

Nose blowing influences CSF pressure as well as middle ear pressure. The mean maximum CSF pressure during nose blowing was more than 400 mmH_2O. The mean middle ear pressure during nose blowing was 252 mmH_2O. Therefore, the pressure gradient across the cochlear windows is about 150 mmH_2O during nose blowing. During sniffing, middle ear pressure is unchanged. These results suggest that nose blowing may be an important cause of perilymphatic fistula via the explosive route, while sniffing is not likely to cause perilymphatic fistula.

Rupture of the cochlear windows was observed when artificial perilymph was injected into the subarachnoid spaces of guinea pigs. Ten of 14 ears showed cochlear window rupture. The pressure applied was 400 mmH_2O in nine of ten ears. Three animals in which no rupture occurred with pressure increases of 400 mmH_2O showed rupture of the round window membrane when the middle ear pressure decreased to −1,000 mmH_2O. The pressure gradient across the round window membrane is very important in the development of perilymphatic fistula [15].

2.2.3 Experimental Perilymphatic Fistula

With Goodhill's concept of explosive and implosive routes of fistula formation in mind, Hara et al. [21] injected artificial perilymph into the CSF of guinea pigs to produce high CSF pressure. This resulted in rupture of one or both windows on one or both sides. This method is an experimental perilymphatic fistula model of the explosive route. An alternate

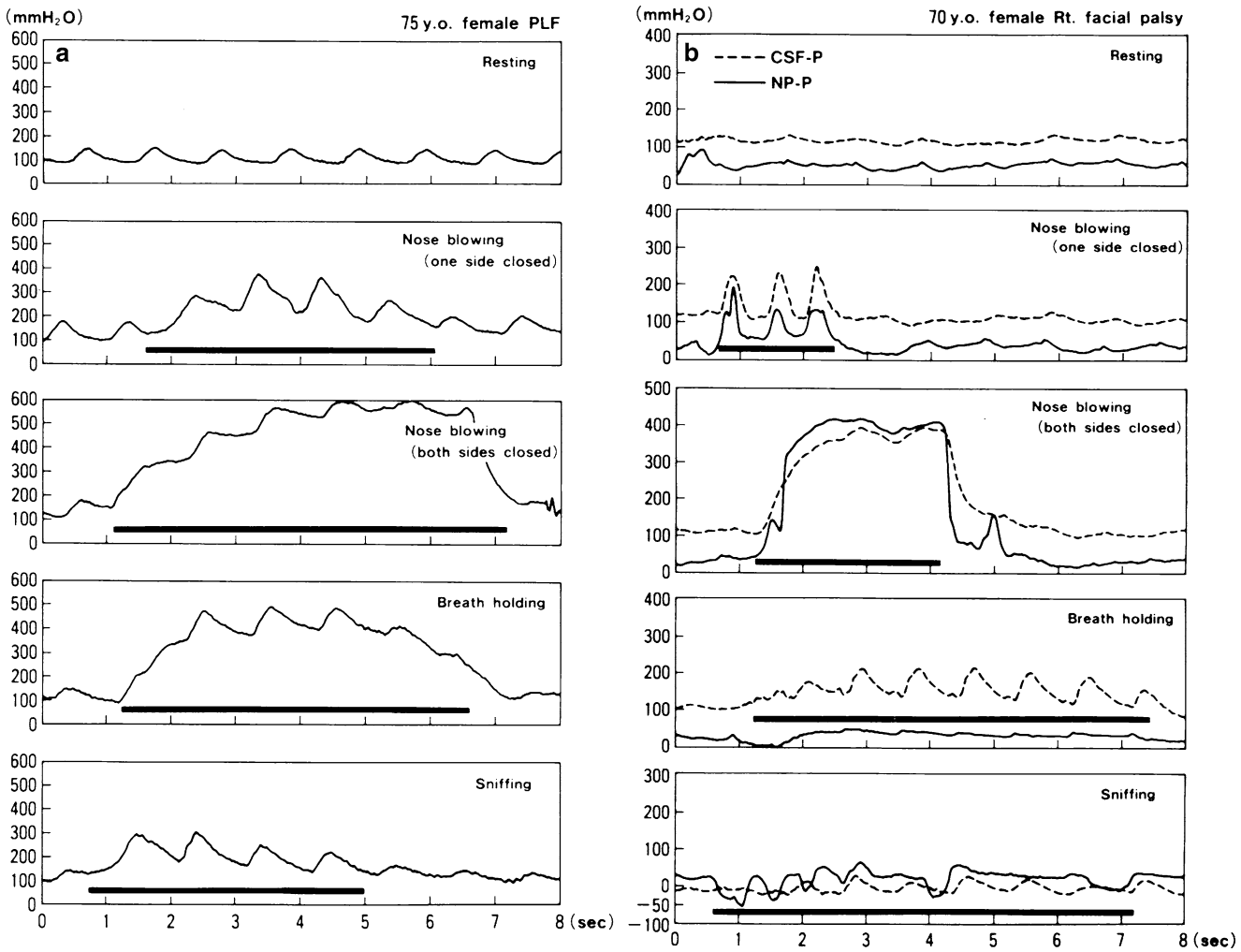

Fig. 2.19 (**a**) Changes in cerebrospinal fluid pressure (CSF-P) with nose blowing and other actions in a 75-year-old woman with perilymphatic fistula. Maximum CSF-P (mmH_2O) from the *top*: at rest, 136; nose blowing with one nostril closed, 381; nose blowing with both nostrils closed, 598; breath holding, 503; and sniffing, 290. *Black bar* indicates duration of actions. (**b**) Changes in CSF-P and nasopharyngeal pressure (NP-P) in a 70-year-old woman with facial palsy on the left side. When she blew her nose, both the CSF-P and NP-P increased equally. In breath holding, the NP-P was unchanged, while CSF-P increased. When she sniffed, both CSF-P and NP-P decreased [19]

method of producing an explosive route model is suctioning a small amount of perilymph (4 μL) through the round window. Hara and colleagues found that these methods produce similar changes in the membranous labyrinth. The speed of injection or suction and the volume of injected artificial perilymph or suctioned perilymph are important factors affecting changes in the membranous labyrinth and should be measured. However, in the preliminary experiment, no measurements were made.

It is interesting that these procedures resulted in the formation of endolymphatic hydrops in the cochlea (Fig. 2.21). This condition appeared to be temporary and resolved by the time the fistula closed. The organ of Corti remained normal. Decreased perilymph pressure and relatively increased endolymph pressure may be responsible for the formation of hydrops. Not only bulging of Reissner's membrane, but also bowing of the basilar membrane was observed in some animals (Fig. 2.22) [22]. The organ of Corti was compressed. The membrana reticularis showed a marked indentation between the first and second rows of the outer hair cells. The tectorial membrane was trapped and kinked. Another indentation occurred at the junction of the membrana reticularis and Hensen's cells. The pillar cells and outer hair cells were markedly bent (Fig. 2.23) [23].

In one case, marked hydrops was found in a guinea pig two months after injection of artificial perilymph (Fig. 2.24) [24]. The scala vestibuli disappeared because of marked distension of Reissner's membrane. The organ of Corti and stria vascularis were atrophic. A marked loss of connective tissue cells was observed in the limbus spiralis. The saccule was completely collapsed. This caused blockage of the longitudinal flow of endolymph, resulting in the formation of marked hydrops of the cochlea (Fig. 2.25).

Other findings observed in this series of experiments were collapse of Reissner's membrane (Fig. 2.26a), degeneration

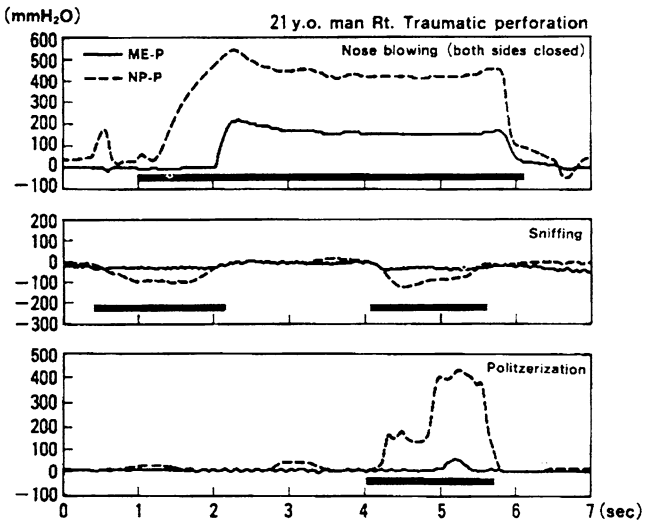

Fig. 2.20 Changes in middle ear pressure (ME-P) in a 21-year-old man with traumatic perforation. Both ME-P and nasopharyngeal pressure (NP-P) increased during nose blowing with both sides closed, but the amplitude of change of ME-P was less than half that of NP-P. The passive opening pressure of the Eustachian tube was 450 mmH_2O. When sniffing, NP-P decreased, while ME-P was unchanged. When politzerization was performed, ME-P increased slightly after NP-P increased to 400 mmH_2O. Black bar indicates duration of actions: from the top, nose blowing with both sides closed, sniffing, and politzerization [20]

of the organ of Corti (Fig. 2.26b) and cortilymphatic hydrops with a marked loss of the cellular elements of the organ of Corti (Figs. 2.9 and 2.27).

2.2.4 Early Hearing Change with Perilymphatic Fistula

In clinical cases of perilymphatic fistula, most patients complain of ear fullness, tinnitus, hearing impairment, and hyperacusis. Pure-tone audiometry reveals every kind of hearing impairment.

Audiograms taken soon after onset show low-tone sensorineural hearing loss [25] (Fig. 2.28a). Fullness of the ear with low-tone hearing loss may lead to misdiagnosis of Eustachian tube disorder.

Recovery of acute hearing loss in a case of perilymphatic fistula is presented in Figure 2.28b. Audiogram 1 was taken 16 h after onset and audiogram 2 taken 48 h after onset. Exploratory tympanotomy was performed on the fifth day. Fluid leakage from the round window niche was confirmed. A small amount of absorbable gelatin was placed to cover the round window membrane. Audiogram 3 shows the patient's hearing 12 days after onset. Low-tone sensorineural hearing loss and dominant negative SP in the electrocochleogram strongly suggest endolymphatic hydrops in the early stage of idiopathic perilymphatic fistula [25, 26].

2.2.5 Vestibular Changes in Experimental Perilymphatic Fistula

A characteristic finding of the vestibular labyrinth in cases of perilymphatic fistula is collapse. There is a trabecular mesh between the membranous labyrinth and surrounding bony wall in the pars superior of the inner ear (Fig. 2.29). When this mesh tears from the membranous labyrinth because of perilymph compromise, endolymph seepage occurs, resulting in collapse of the membranous labyrinth. The area and degree of collapse vary. The collapse of the pars superior can be classified as one of five types [27] (Fig. 2.30).

When the utricular wall is slightly collapsed, the trabecular mesh in that area disappears. The utricular macula remains intact (Figs. 2.30a and 2.31). However, the collapsed wall may touch the utricular macula if the degree of collapse is severe. The collapsed wall may scrape the otolithic membrane, stimulating the sensory cells of the utricular macula (Figs. 2.30b and 2.32). As the perilymph leaks, the collapsed utricular wall may vibrate, stimulating the sensory epithelium, resulting in dizziness (floating [irritable] labyrinth) [28] (Fig. 2.33). In the clinical setting, dizziness is often resolved after closure of the fistula, probably because the vibration of the membranous labyrinth ceases. Complete collapse of the utricular wall will not induce vibration of the wall (Fig. 2.30e).

The semicircular ducts show various changes in cases of experimental perilymphatic fistula. Collapse of the semicircular duct is the most common finding, and is particularly severe in the posterior ampulla (Fig. 2.34a–c). Marked collapse of the ampullary wall covers the crista ampullaris (Fig. 2.35). This resembles the histopathology of vestibular atelectasis [29] (Fig. 2.36).

Separation of two layers of the ampullary wall was observed without collapse in guinea pigs immediately after injection of artificial perilymph. The mesothelial lining of the ampulla maintained its normal shape. No tear in the trabecular mesh was observed. It is interesting to observe that the top of the cupula pulled down the epithelial lining of the ampullary wall. Perhaps the endolymph within the semicircular duct was suctioned, so that the epithelial lining together with the cupula was pulled, resulting in dissociation of the ampullary wall. The tip of the cupula seemed to adhere fairly tightly to the epithelial lining of the ampullary wall (Fig. 2.37a, b).

Caloric tests in guinea pigs with experimental perilymphatic fistulae revealed various changes: normal, no response, recovery, and caloric irregularity (Fig. 2.38). These responses

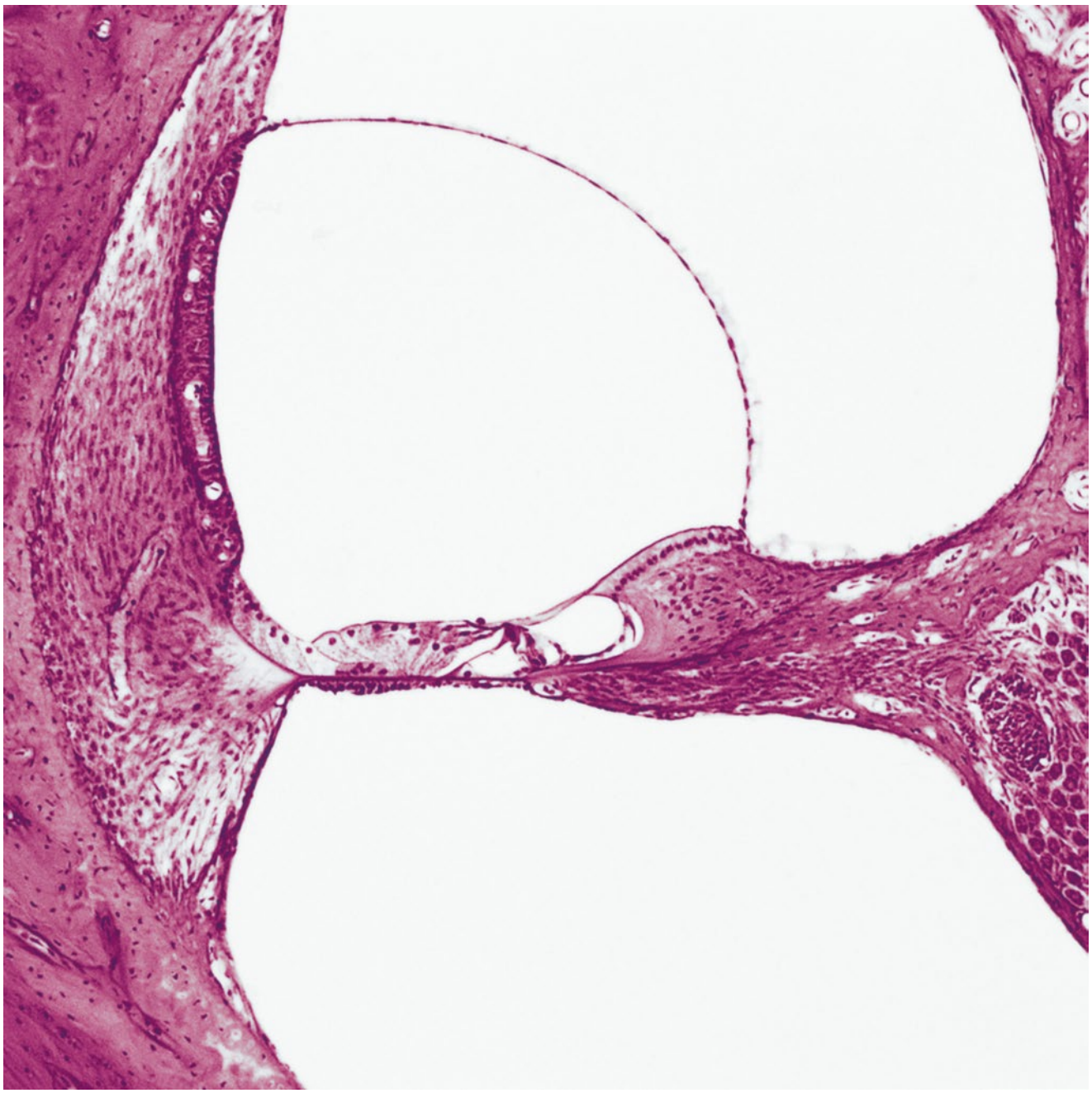

Fig. 2.21 Endolymphatic hydrops produced by experimental perilymphatic fistula in a guinea pig (injection method) [21]

may change with time. For example, no caloric response was observed 1 week after surgery in a particular animal, but it had recovered after another week [30–32] (Fig. 2.39).

Generally speaking, cochlear hydrops was observed with a normal vestibular system, although the saccule showed concomitant hydrops. Collapse of the vestibular system accompanied collapse of the scala media. However, the area and degree of collapse of the membranous vestibular labyrinth differs greatly from partial mild collapse to severe total collapse.

The experimental methods to produce perilymphatic fistulae described in this chapter are far from physiological conditions. Some of the results are difficult to understand. However, we can see mysteries hidden in the inner ear.

The variety of morphological changes observed in experimental perilymphatic fistula help us to consider the pathophysiology of inner ear disease when we see patients with the disorder. Keeping in mind the potential occurrence of the condition is of paramount importance.

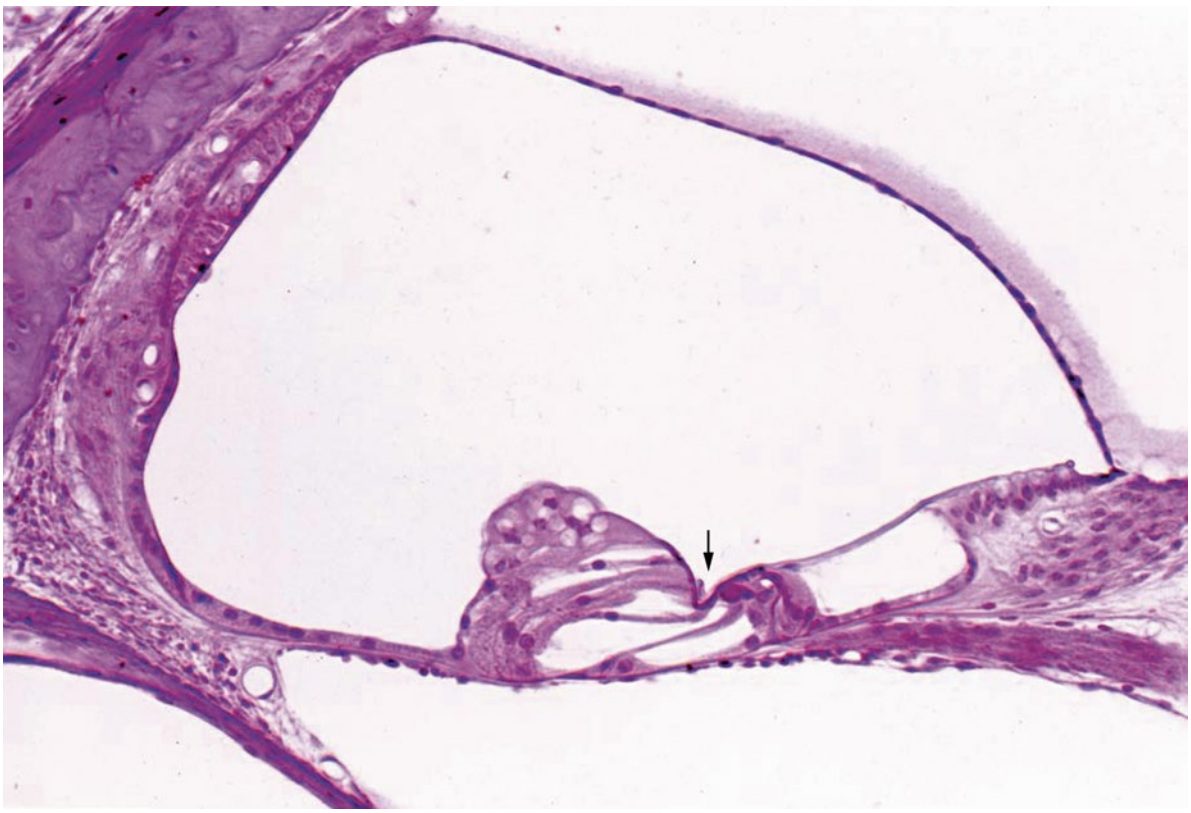

Fig. 2.22 Indentation of the membrana reticularis with hydrops in the guinea pig. The tectorial membrane is trapped at the indentation of the membrana reticularis (*arrow*). The basilar membrane shows a downward bowing (apical turn: original ×6.5) [22]

Fig. 2.23 Two notches (*arrows*) on the surface of the organ of Corti in the guinea pig. The right arrow indicates the area of the membrana reticularis between the first and second rows of outer hair cells. The tectorial membrane is trapped at the tip. The left arrow indicates the junction between the membrana reticularis and Hensen's cells (injection method, 1 month post-injection) (original × 40) [23]

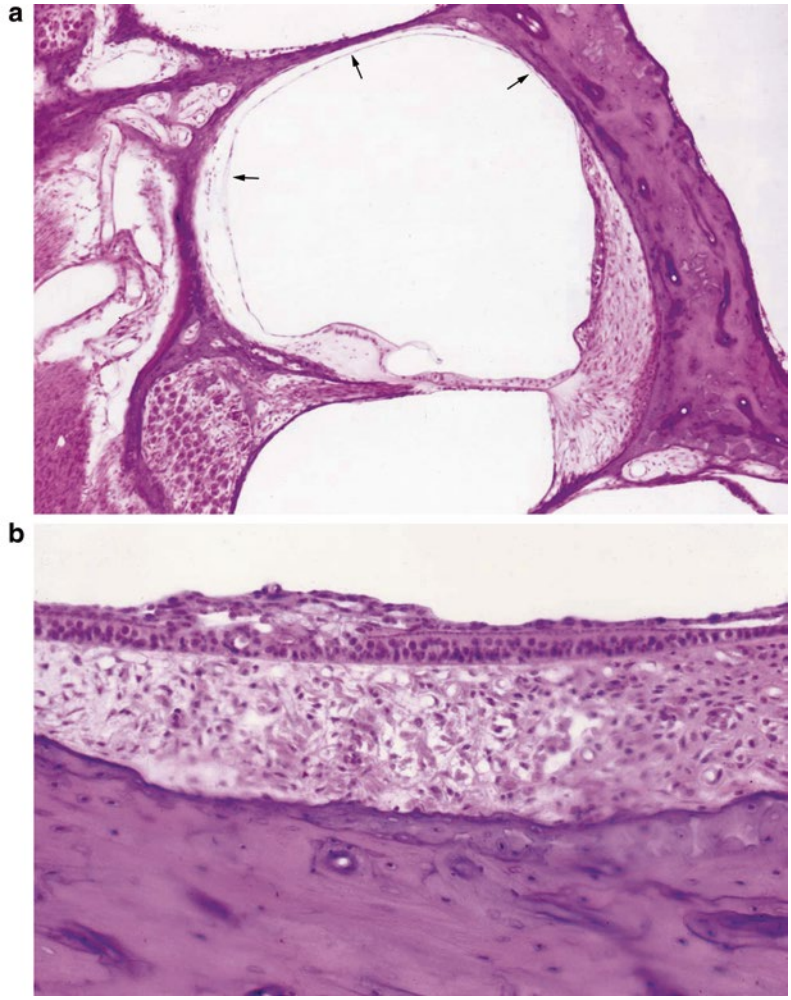

Fig. 2.24 Marked hydrops after experimental perilymphatic fistula formation in the guinea pig (injection method, 2 months post-injection). (**a**) The scala vestibuli is occupied by marked endolymphatic hydrops (*arrows*). The organ of Corti, limbus, and stria vascularis are atrophic. (**b**) Collapsed saccular wall covers the atrophic saccular macula [24]

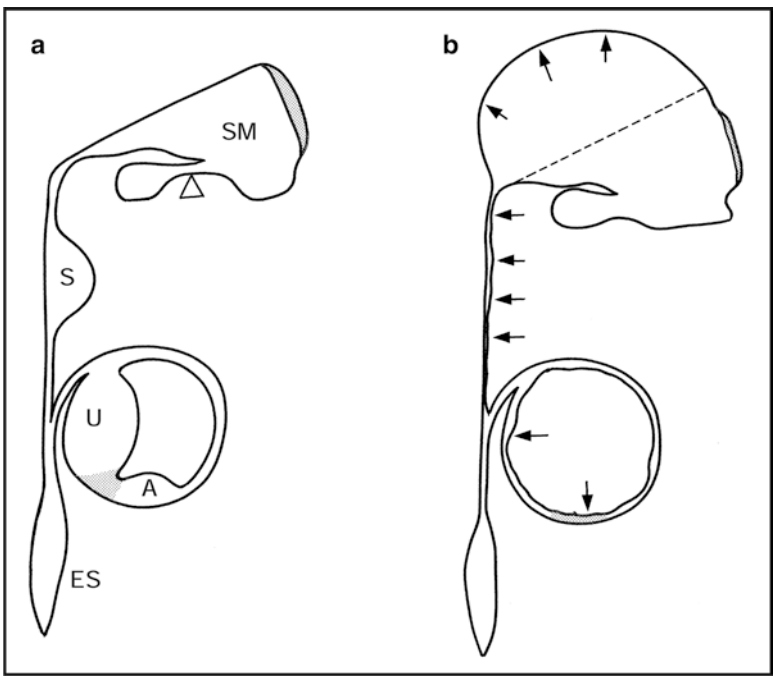

Fig. 2.25 Schema of cochlear hydrops formation by the collapsed saccule. Experimental perilymphatic fistula (**b**). The collapsed saccule inhibits the longitudinal flow of perilymph from the cochlea. (**a**) Normal membranous labyrinth, *SM* scala media, *S* saccule, *U* utricle, *A* ampulla, *ES* endolymphatic sac

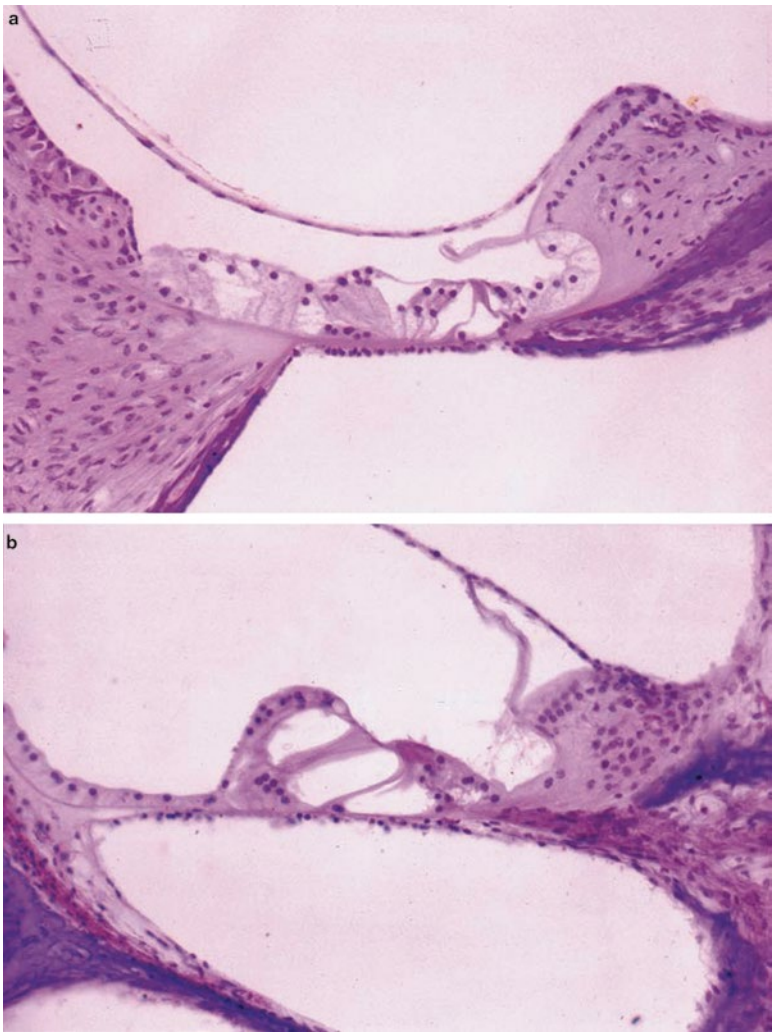

Fig. 2.26 Other cochlear changes in experimental perilymphatic fistula. (**a**) Collapsed Reissner's membrane (injection method, 1 month post). (**b**) Degeneration of the organ of Corti (suction method, 3 months post)

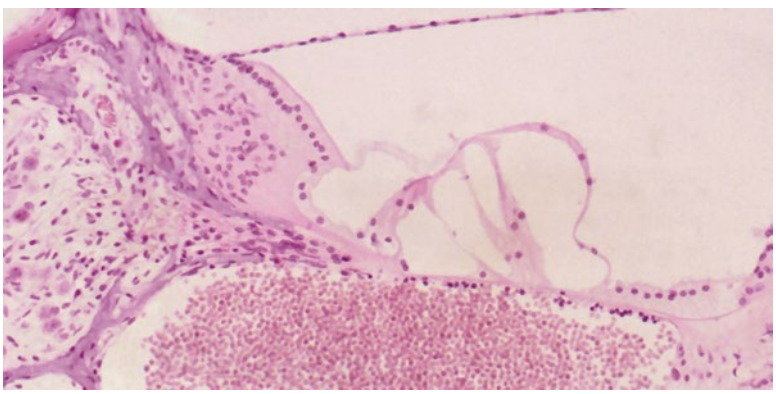

Fig. 2.27 Marked cortilymphatic hydrops. Most of the cells within the organ of Corti have disappeared. A few Deiters' cells and pillar cells remain in elongated shape. Marked loss of spiral ganglion cells. Massive hemorrhage remains in the scala tympani 1 month after injection (original ×16) [23]

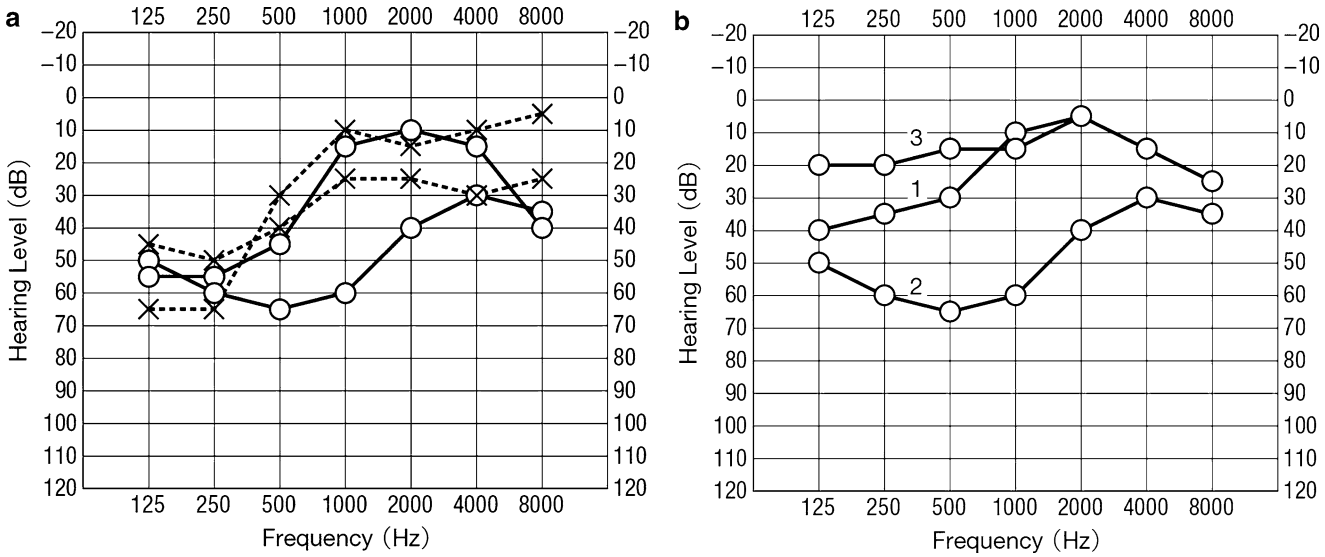

Fig. 2.28 Hearing changes in patients with perilymphatic fistula. (**a**) Hearing of four patients soon after the onset of perilymphatic fistula [25]. (**b**) Recovery of hearing after closure of the fistula. (*1*) Sixteen hours after onset, (*2*) forty-eight hours after onset, (*3*) exploratory tympanotomy was performed on the fifth day. Leakage from the round window niche was confirmed. The niche was closed using a small piece of absorbable gelatin. Audiogram was taken on the 12th day after onset [26]

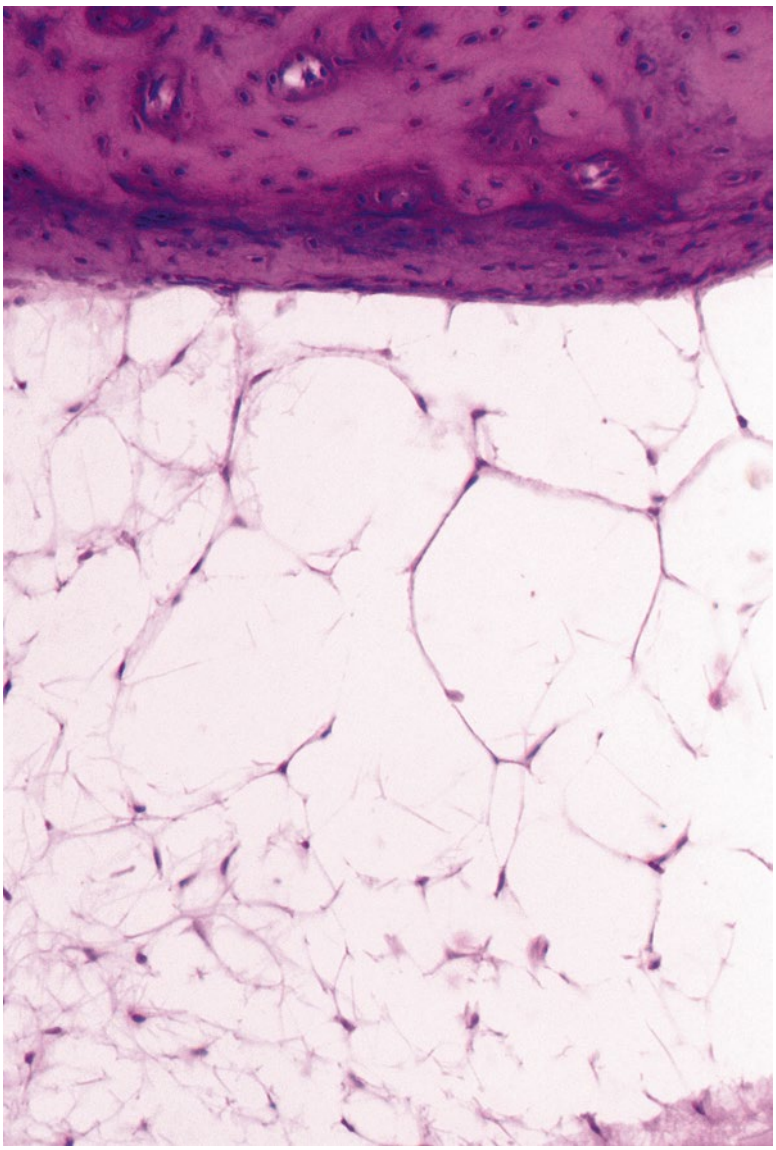

Fig. 2.29 Trabecular mesh in the vestibulum of the pars superior (guinea pig). The mesh exists between the membranous wall and surrounding bony wall (original ×25)

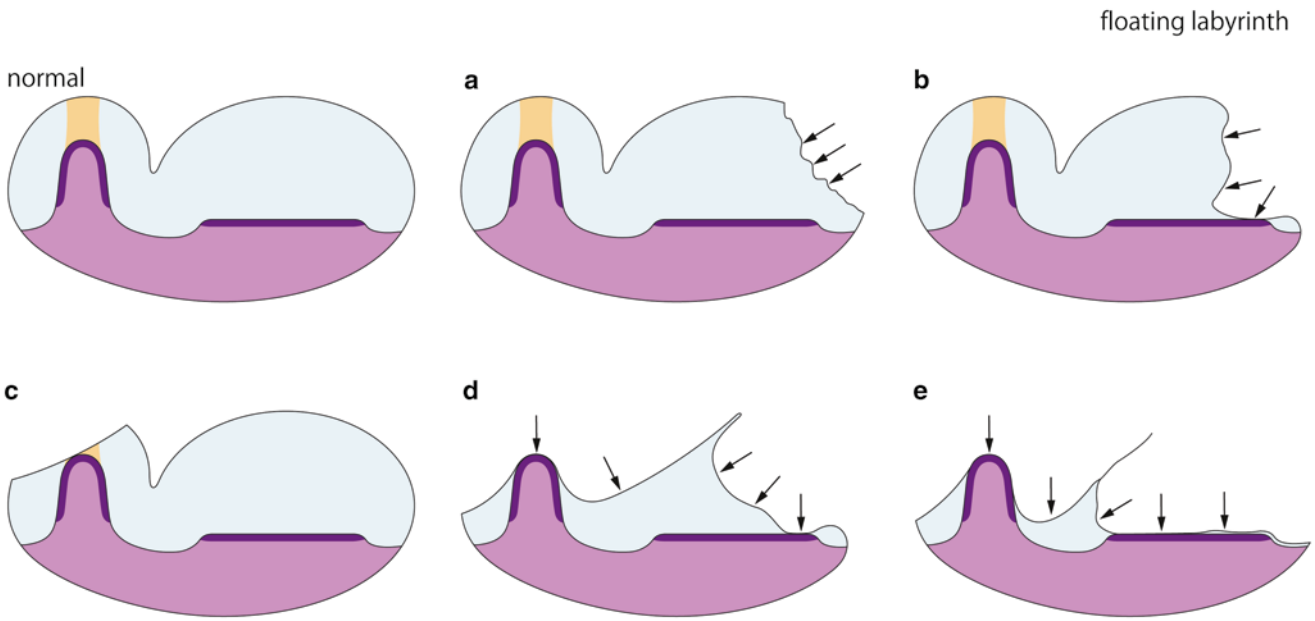

Fig. 2.30 Schema showing several types of vestibular collapse. (**a**) Mild collapse of the utricle. (**b**) Moderately collapsed utricular wall attaching to the utricular macula. (**c**) Collapse of the ampulla. (**d**) Marked collapse of the ampulla with moderate utricular collapse. (**e**) Marked collapse of the utricle and ampulla [27]

Fig. 2.31 Mild collapse of the utricular wall after experimental perilymphatic fistula. The trabecular mesh disappears only in the collapsed area (*arrow*: original ×2.5) [28]

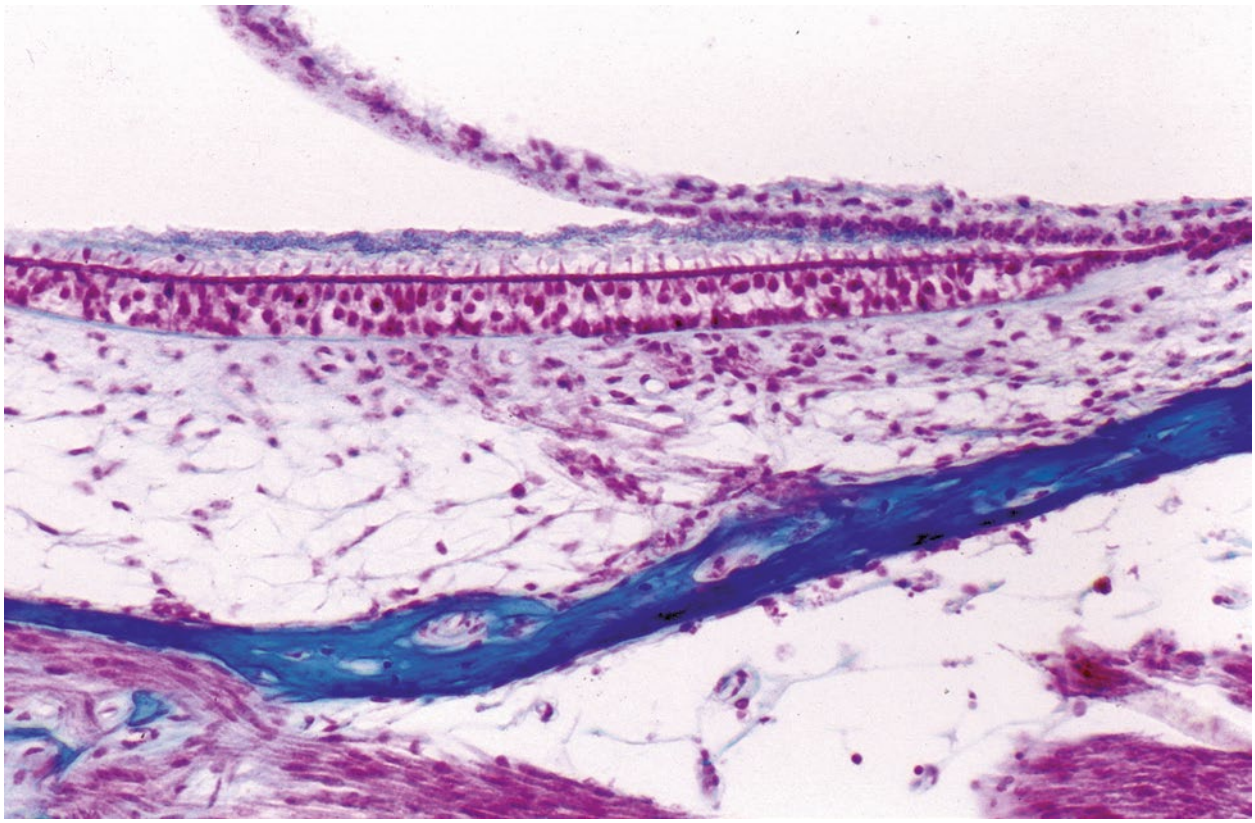

Fig. 2.32 Utricular wall partly collapsed onto the normal neuroepithelium of the macula (original ×16) [28]

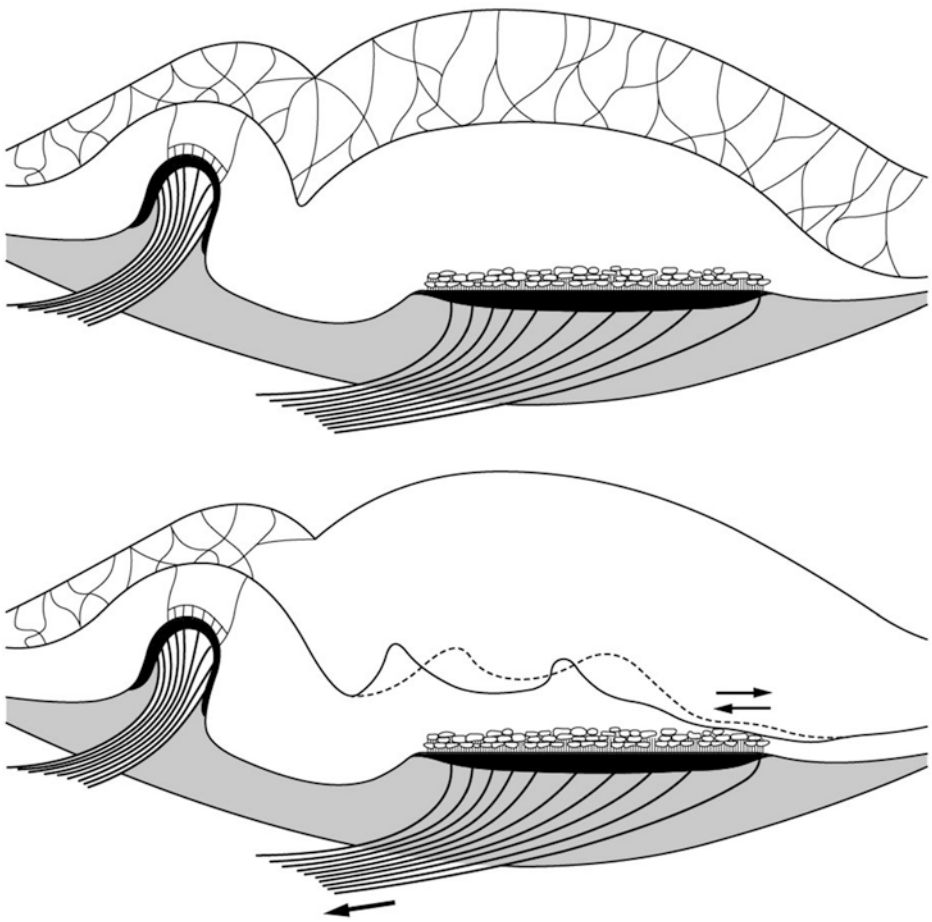

Fig. 2.33 Concept of the floating (irritable) labyrinth. The collapsed utricular wall stimulates the macula, causing dizziness [28]

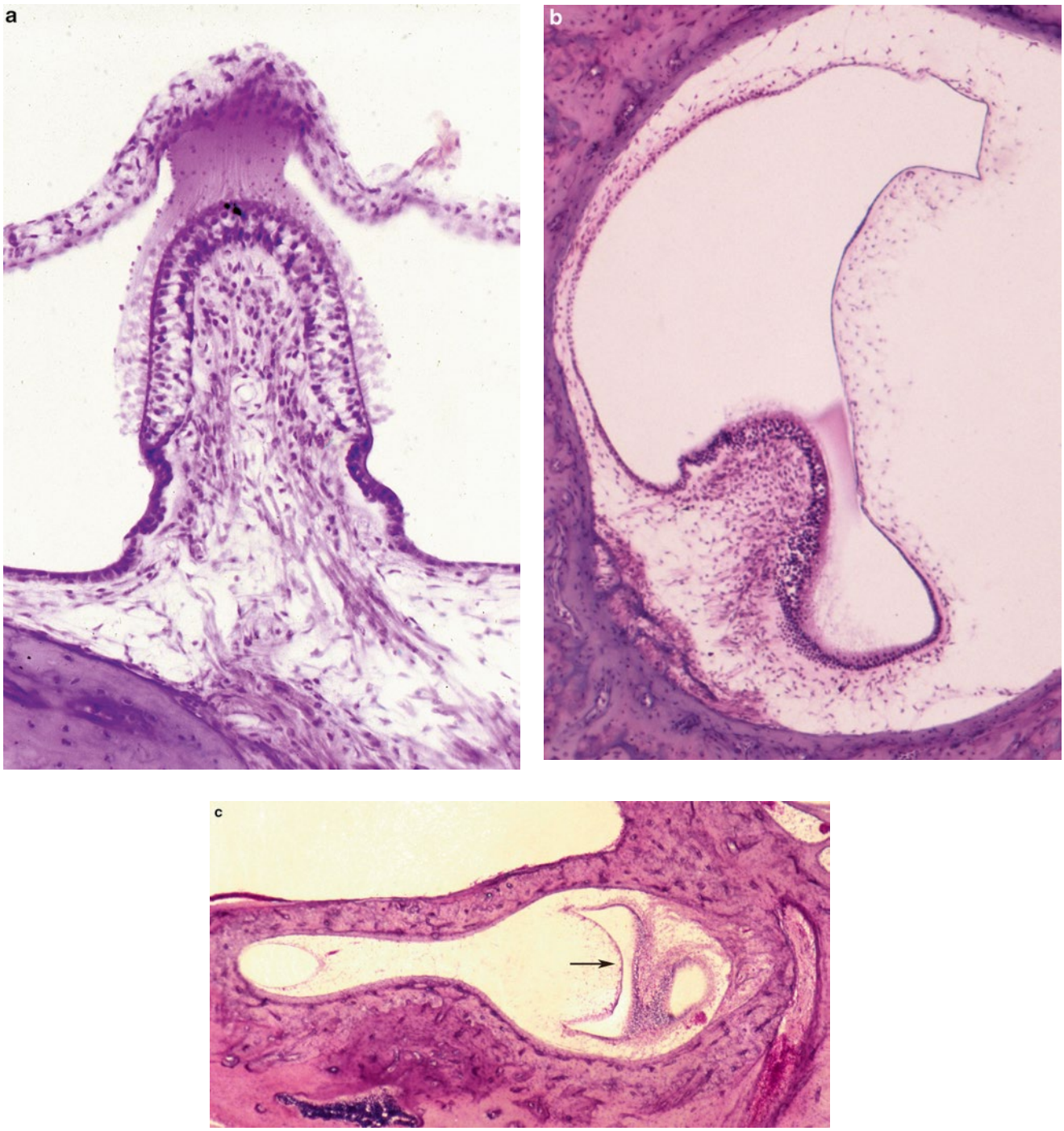

Fig. 2.34 Collapse of the ampullary wall of the guinea pig (suction method). (**a**) The cupula is compressed (original ×16). (**b**) Partial collapse of the posterior ampulla (original ×2.5). (**c**) Partial collapse (*arrow*) of the posterior ampulla ×10

Fig. 2.35 Marked collapse of the ampullary wall in the guinea pig

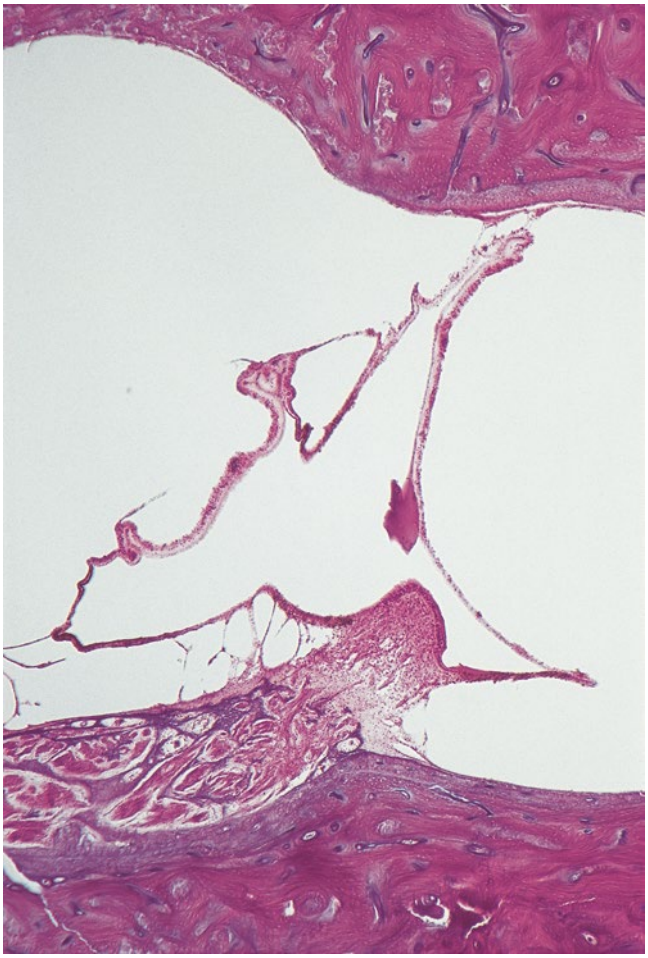

Fig. 2.36 Vestibular atelectasis. A human temporal bone specimen showing marked collapse of the ampullary wall (Courtesy of Dr. Merchant)

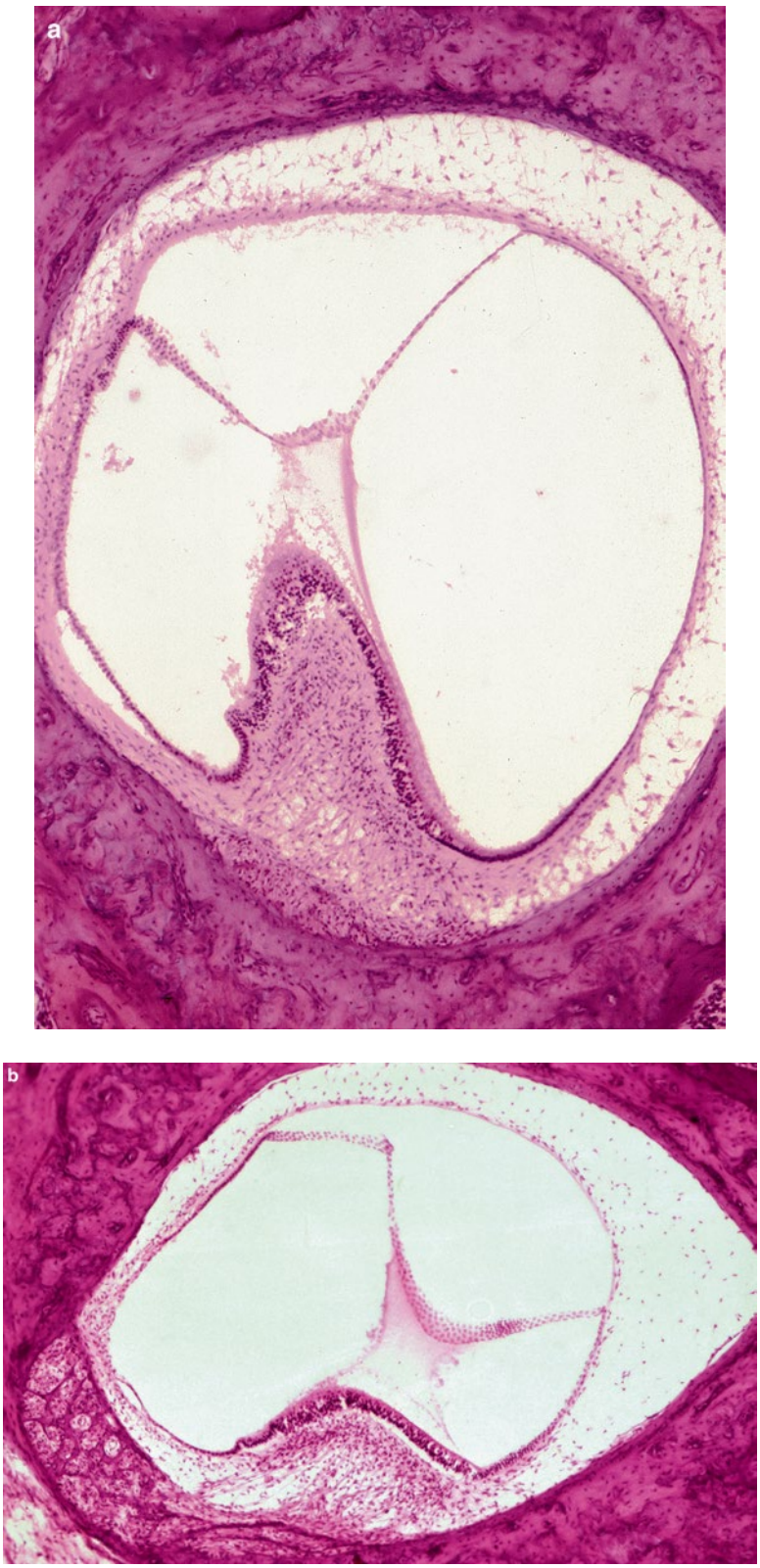

Fig. 2.37 Dissociation of ampullary wall. The epithelial cell layer is pulled from the mesothelial cell layer by the cupula. The trabecular mesh shows no change. (**a**) Anterior ampulla. The cochlea and saccule show mild hydrops. (original × 6.5) (**b**) Posterior ampulla. No change in the cochlea or other vestibular organs (immediately after injection). (original × 6.5) Guinea pigs

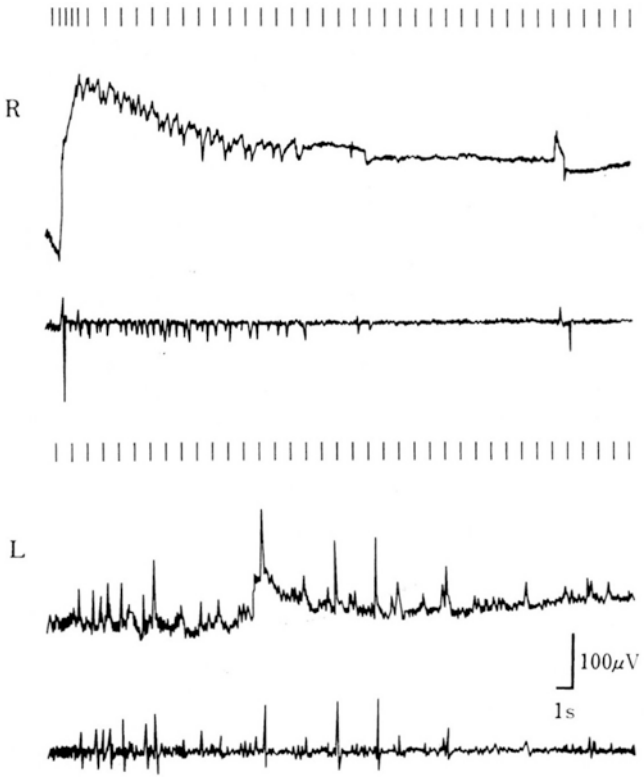

Fig. 2.38 Postoperative caloric test showing caloric irregularity. *L* Irregular waves of a longer duration are observed 1 week after surgery, *R* normal side, *Upper trace*: time base at 1 mark per second, *Second trace*: eye movement, *Third trace*: differentiated eye movements (eye velocity). Guinea pig (suction method) [22]

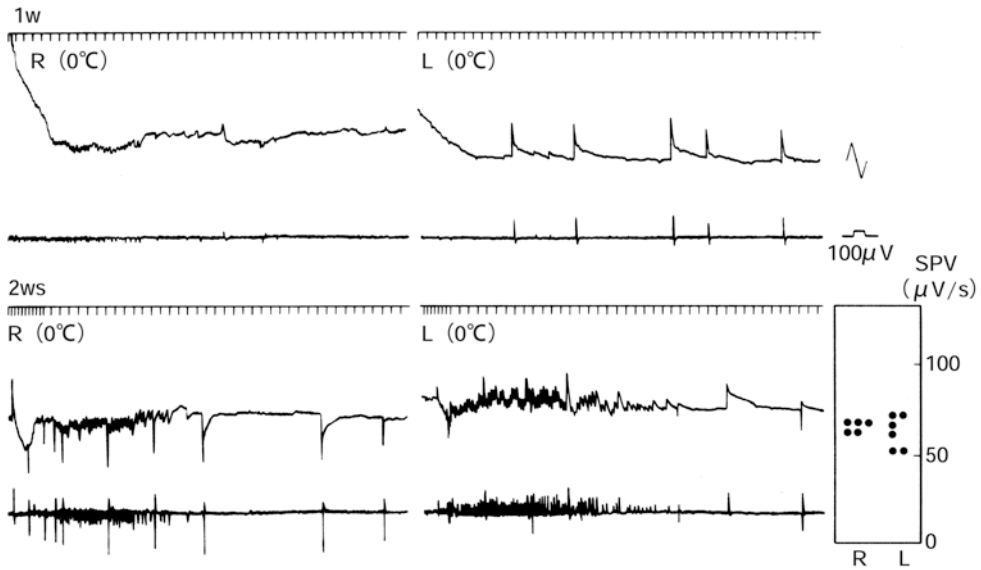

Fig. 2.39 Canal paresis converts to normal caloric response in an electronystagmogram (ENG). The caloric test 1 week after experimental perilymphatic fistula showed canal paresis, which had normalized 1 week later. *L* operated side, *R* normal side, *SPV* slow-phase velocity. Calculated from ENG recordings of the original nystagmus curve. *Upper trace*: Time base at 1 mark per second *Second trace*: Eye movement *Third trace*: Differentiated eye movements (eye velocity). Guinea pig (suction method) [32]

References

1. Engström H (1960) The cortilymph, the third lymph of the inner ear. Acta Morphol Neerl Scand 3:195–204 Taylor & Francis Ltd. www.tandfonline.com
2. Schuknecht HF, Seifi AE (1963) Experimental observations on the fluid physiology of the inner ear. Ann Otol Rhinol Laryngol 72:687–712
3. Masuda Y, Sando I, Hemenway WG (1971) Perilymphatic communication routes in guinea pig cochlea. Arch Otolaryngol 94: 240–245
4. Nomura Y (1968) The cortilymph—in relation to perilymphatic space. Pract Oto-Rhino-Laryngol 61:469–474
5. Beagley HA (1965) Acoustic trauma in the guinea pig. I. Electrophysiology and histology, II. Electron microscopy including the morphology of cell junctions in the organ of Corti. Acta Otolaryngol 60:437–451
6. Ishiyama E, Ishiyama K (2012) Atlas of the inner ear morphology, 3rd edn. Sozo Shuppan, Tokyo
7. Djeric D, Schuknecht HF (1989) Hensen's cell cyst of the organ of Corti. Acta Otolaryngol (Stockh) 108:55–61
8. Gopen Q, Rosowski J, Merchant SN (1997) Anatomy of the normal human cochlear aqueduct with functional implications. Hear Res 107:9–22
9. Borghesan E (1957) Modality of the cochlear humoral circulation. Laryngoscope 67:1266–1285
10. Ishiyama E, Keels EW, Weibel J (1970) New anatomical aspects of the vasculo-epithelial zone of the spiral limbus in mammals. Acta Otolaryngol (Stockh) 70:319–326
11. Kimura RS, Nye CL, Southard RE (1990) Normal and pathologic features of the limbus spiralis and its functional significance. Am J Otolaryngol 11:99–111
12. Schulte BA, Adams JC (1989) Distribution of immunoreactive Na, K-ATPase in gerbil cochlea. J Histochem Cytochem 37:127–134
13. Hsu CJ, Nomura Y (1985) Carbonic anhydrase activity in the inner ear. Acta Otolaryngol 418(Suppl):1–42
14. Smith CA, Lowry OH, Wu ML (1954) The electrolytes of the labyrinthine fluids. Laryngoscope 64:141–153
15. Nomura Y (1984) Otological significance of the round window. Adv Oto-Rhino-Laryngol 33:1–162
16. Nomura Y, Okuno T, Kawabata I (1983) The round window membrane. In: Pfaltz CR (ed) Modern perspectives in otology, vol 31. Adv Oto-Rhino-Laryngol, Karger, Basel pp 50–58
17. Juhn SK, Ryback LP (1981) Labyrinthine barriers and cochlear homeostasis. Acta Otolaryngol (Stockh) 91:529–534
18. Goodhill V (1971) Sudden deafness and round window rupture. Laryngoscope 81:1462–1474
19. Sakikawa Y, Kobayashi H, Nomura Y (1994) Changes in cerebrospinal fluid pressure in daily life. Ann Otol Rhinol Laryngol 103:959–963
20. Sakikawa Y, Kobayashi H, Nomura Y (1995) Changes in middle ear pressure in daily life. Laryngoscope 105:1353–1357
21. Hara M, Nomura Y, Saito K (1990) Histopathologic study of the perilymph-suctioned labyrinth. Ann Otol Rhinol Laryngol 99: 316–320
22. Nomura Y, Hara M, Young Y-H, Okuno T (1992) Inner ear morphology of experimental perilymphatic fistula. Am J Otolaryngol 13:32–37
23. Nomura Y, Hara M (1986) Experimental perilymphatic fistula. Am J Otolaryngol 7:267–275
24. Nomura Y, Hara M, Funai H, Okuno T (1987) Endolymphatic hydrops in perilymphatic fistula. Acta Otolaryngol (Stockh) 103:469–476
25. Fukaya T, Nomura Y (1988) Audiological aspects of idiopathic perilymphatic fistula. Acta Otolaryngol (Stockh) 456 (Suppl): 68–73
26. Fukaya T, Nomura Y (1987) Idiopathic perilymphatic fistula. Nippon Jibiinkoka Gakkai Kaiho (Tokyo) 91:233–239
27. Kukita N, Nomura Y (1994) Morphological changes of the vestibular labyrinth by experimental perilymph fistula. Showa Univ J Med Sci 6:97–103
28. Nomura Y, Okuno T, Hara M, Young Y-H (1992) "Floating" labyrinth: pathophysiology and treatment of perilymph fistula. Acta Otolaryngol (Stockh) 112:186–191
29. Merchant SN, Schuknecht HF (1988) Vestibular atelectasis. Ann Otol Rhinol Laryngol 97:565–576
30. Young Y-H, Nomura Y, Hara M (1992) Vestibular pathophysiologic changes in experimental perilymph fistula. Ann Otol Rhinol Laryngol 111:612–616
31. Young Y-H, Nomura Y, Hara M (1992) Caloric irregularity in experimentally induced perilymphatic fistula. Eur Arch Otorhinolaryngol 249:181–184
32. Young Y-H, Nomura Y (1995) Recovery of caloric function in experimental perilymph fistula. Ann Otol Rhinol Laryngol 104: 484–487

Blood Vessels

3

Abstract

Blood circulation is of paramount importance to maintaining the functions of the inner ear. However, because of the size and location of the labyrinth in the temporal bone, it is difficult to estimate clinically the details of its circulation. Histochemical staining of alkaline phosphatase allows clear visualization of the capillary networks of the inner ear. Studies of the distribution of capillaries in the inner ear sensory organs have shown that beneath the sensory epithelium dense capillary networks exist in the otolithic organs and semicircular canals. By contrast, the organ of Corti is poorly vascularized. Massive hemorrhage occurs in the inner ear in patients with blood diseases. Temporal bone histopathology reveals that cryoglobulinemia and diabetes mellitus cause pathological changes in the inner ear. A rolled-up tectorial membrane is often seen in viral labyrinthitis, though this finding may not be pathognomonic for viral infection. Vascular disturbances may also cause the formation of an encapsulated mass at the tip of the tectorial membrane, the size of which is generally smaller than those seen in viral labyrinthitis.

Keywords

Alkaline phosphatase • Buerger's disease • Cryoglobulinemia • Diabetes mellitus • Inner ear blood vessel • Leukemia • Takayasu's arteritis

3.1 Anatomy

3.1.1 Arteries and Veins

The artery of the inner ear arises from the vertebral artery system. The labyrinthine artery usually arises from the anterior inferior cerebellar artery (AICA), though occasionally it comes directly from the basilar artery. The endolymphatic sac is supplied with arterial blood from branches of the external carotid artery, i.e., the meningeal branch of the occipital artery and posterior meningeal artery. The latter is a branch of the ascending pharyngeal artery (Fig. 3.1).

The labyrinthine artery divides into the cochlear artery, vestibular artery, and vestibulocochlear artery in the internal auditory canal. Considerable variation exists in the exact manner of branching and distribution of the labyrinthine artery and its tributaries. The diameter of the labyrinthine artery is approximately 0.3 mm in humans.

The veins of the inner ear do not run through the internal auditory canal, with rare exceptions (Fig. 3.2). The vein of the cochlear aqueduct (inferior cochlear vein) runs within the canal of Cotugno and drains most of the venous blood from the cochlea into the inferior petrosal sinus or the superior bulb of the internal jugular vein. The vein of the vestibular aqueduct runs within the paravestibular canaliculus to join the sigmoid sinus. The venous drainage of the vestibular labyrinth is via the vein of the cochlear aqueduct and the vein of the vestibular aqueduct.

In the modiolus, modiolar arteries become tortuous before reaching the membranous labyrinth and the spiral ganglion (coiled arteriole). The interscalar septum separates the scala vestibuli from the scala tympani of the adjacent upper turn. It conveys radiating arterioles to the spiral ligament and stria

Y. Nomura, *Morphological Aspects of Inner Ear Disease*, DOI 10.1007/978-4-431-54204-9_3,

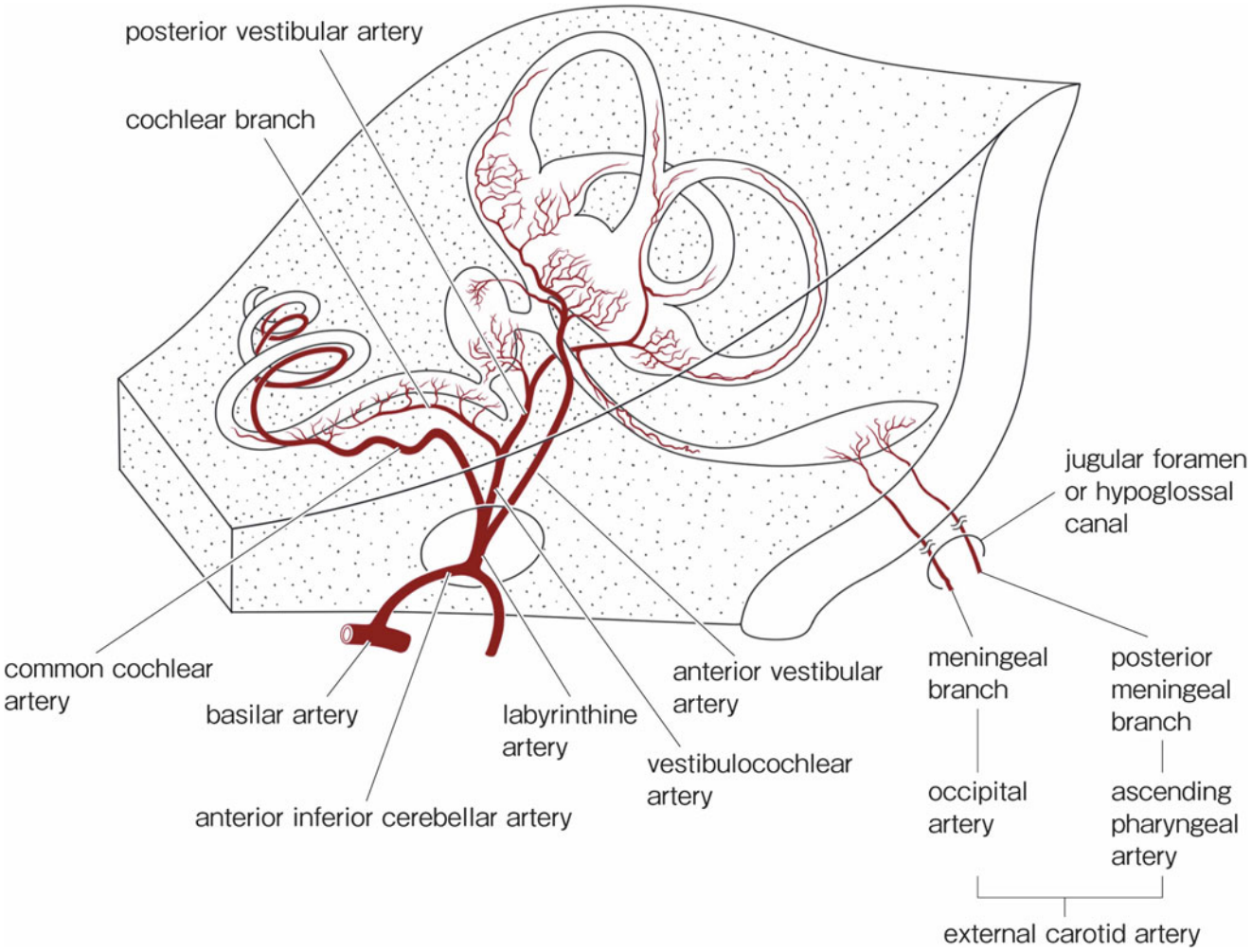

Fig. 3.1 Arteries of the inner ear

vascularis. Venules do not accompany the arterioles, but run in spiral form in the septum (Figs. 3.3 and 3.6).

In the interscalar septum, small bony canals radiate from the modiolus laterally to the spiral ligament, forming networks throughout the septum (Figs. 3.4 and 3.5). Arterioles and capillaries run within these canals. These vessels may be observed in a surface specimen of the interscalar septum after decalcification, dissection, and staining [1].

Arterioles run through the center of the wide bony canal. In other words, arterioles have a wide perivascular space. Pigmented cells are often seen attached to the arterioles. The cells contain melanosomes and premelanosomes, although the functional roles of the pigmented cells are not clear (Figs. 3.6, 3.7, 3.8, and 3.9).

Melanocytes are numerous in the human modiolus and their function is believed to be related to vasomotor control [2]. It has also been shown that drugs accumulate on inner ear melanin, confirmed by autoradiographic studies of lidocaine and its derivatives in rats [3].

Franz et al. [4] investigated melanocytes in the guinea pig modiolus using an electron microscope. Two different melanocyte types were observed. Type A was characterized by having spherical, uniformly pigmented stage IV melanosomes. No signs of melanogenesis were seen in this perivascular pigment cell form. Type B was very rarely observed and was characterized by fusiform to oval melanosomes in various stages of maturation. Connective tissue cells containing fusiform to oval melanosomes enclosed in membrane-bound vacuoles were frequently found. The connective tissue of the cochlear plexus seems to be derived from the leptomeninges.

To examine communication between spaces in the modiolus and the spiral ligament, Suzuki and Nomura [1] injected India ink under pressure into the modiolus. They found that India ink passed through the canal or channel of the interscalar septum to the upper spiral ligament. The bony channel ends at the margin of the interscalar septum. However, there is some continuation of the channel to the upper spiral ligament.

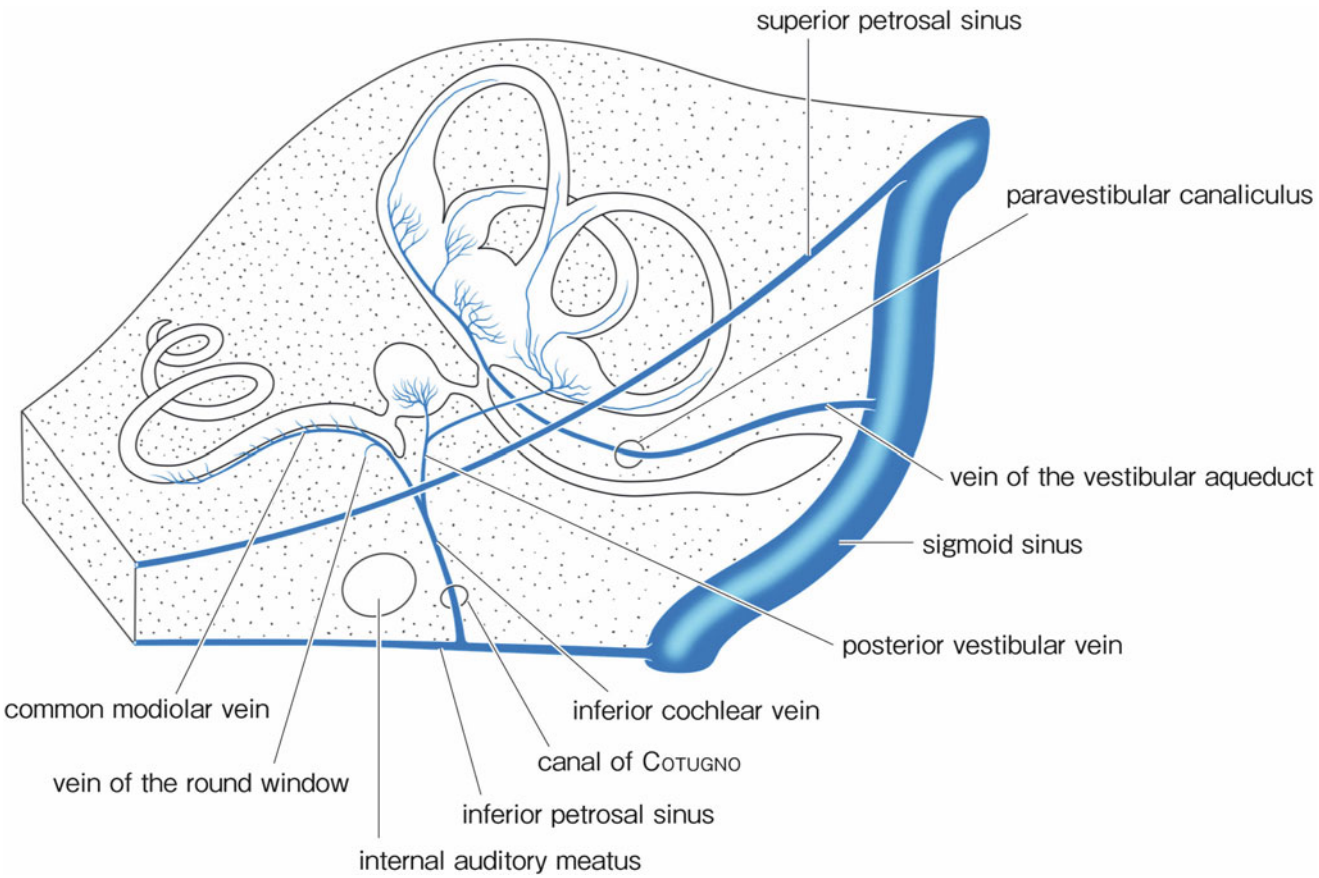

Fig. 3.2 Veins of the inner ear

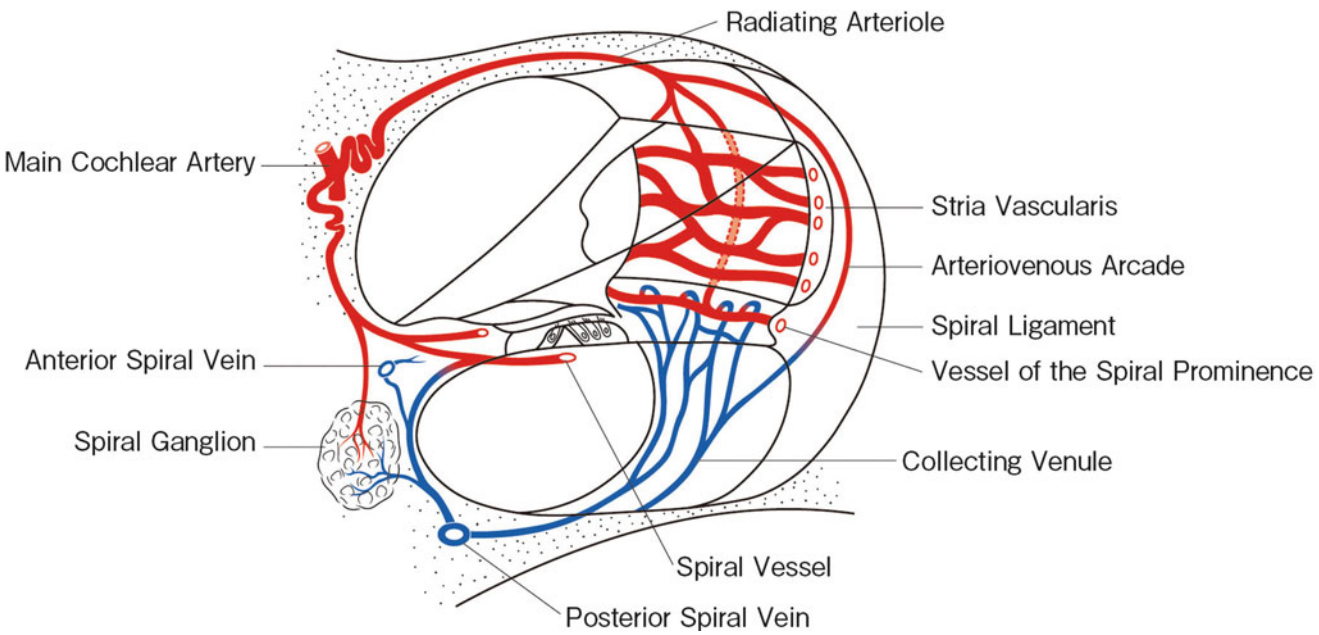

Fig. 3.3 Vascular system of the cochlea

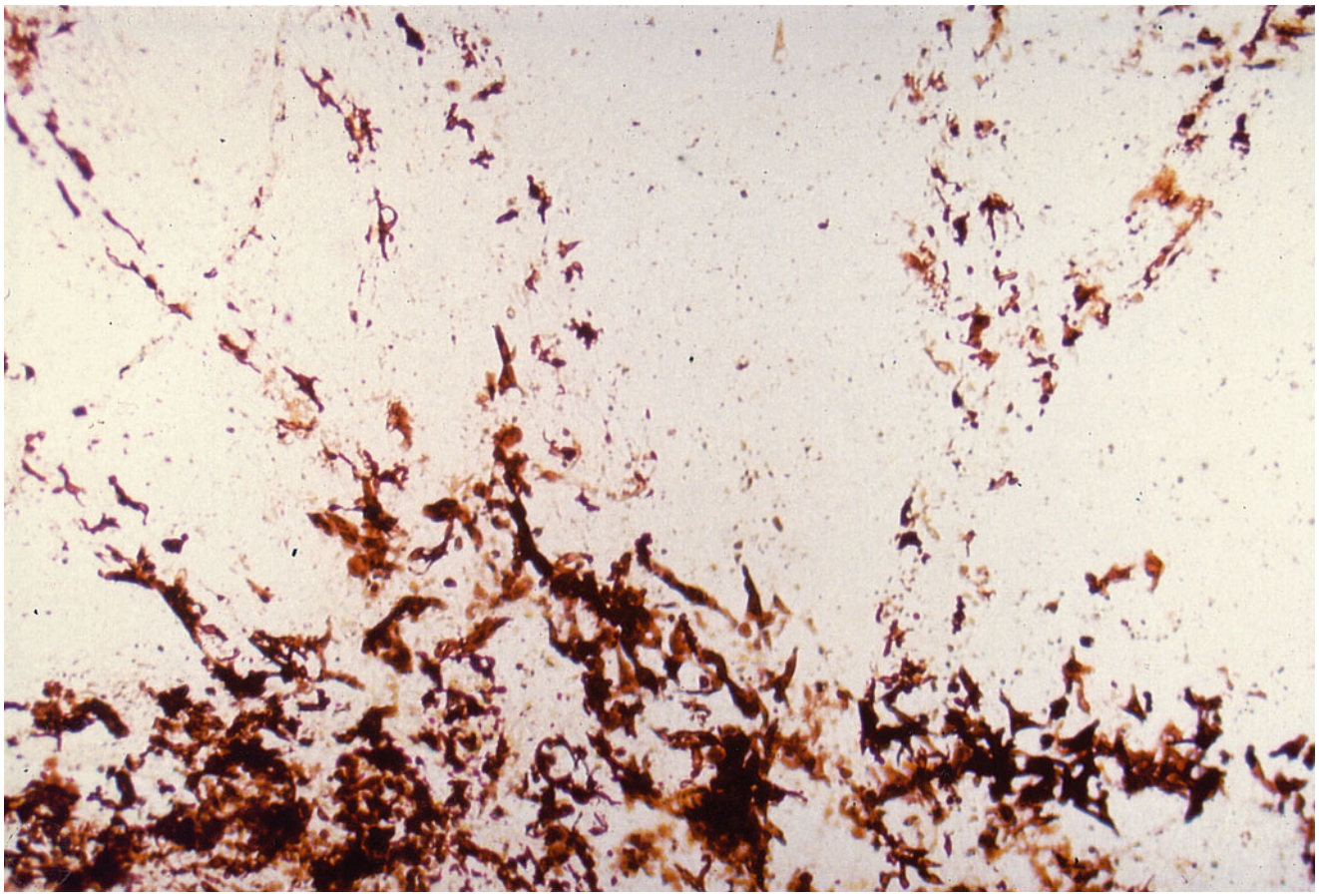

Fig. 3.4 Pigment cells in the interscalar septum, indicating the existence of canals. Abundant pigment cells are found in the modiolus (*below*). Fifty-year-old man, surface preparation, no stain (original ×6.5) [1]

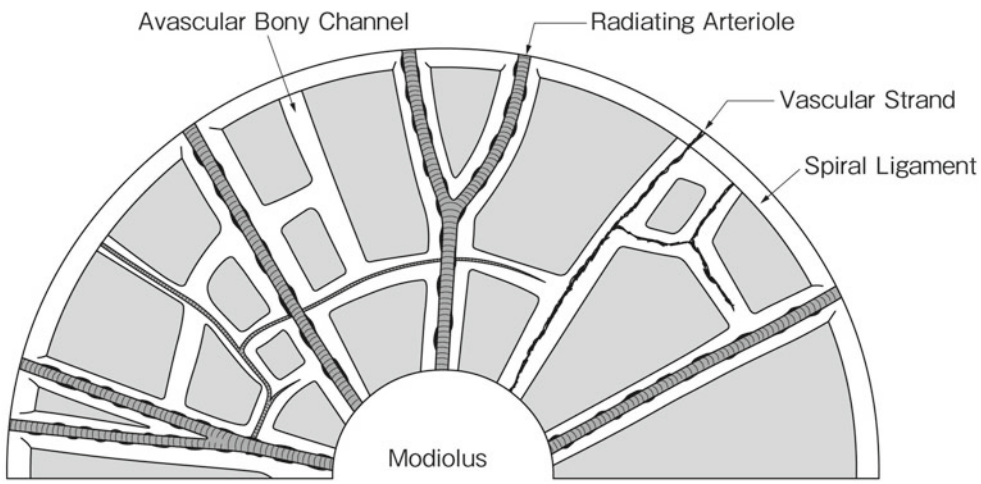

Fig. 3.5 Schema of the canalicular system in the human interscalar septum

The perivascular space around the radiating arteriole is constructed of loose connective tissue without bony tissue (Fig. 3.12). India ink was observed around the radiating arterioles (Figs. 3.10, 3.11, and 3.12), indicating that the perivascular channel is likely filled with cerebrospinal fluid (CSF).

The human modiolus facing the scala tympani has a thin and porous bony wall, and perilymph seems to pass freely through it (Fig. 3.13). The perivascular space may be involved in the formation and reabsorption of perilymph.

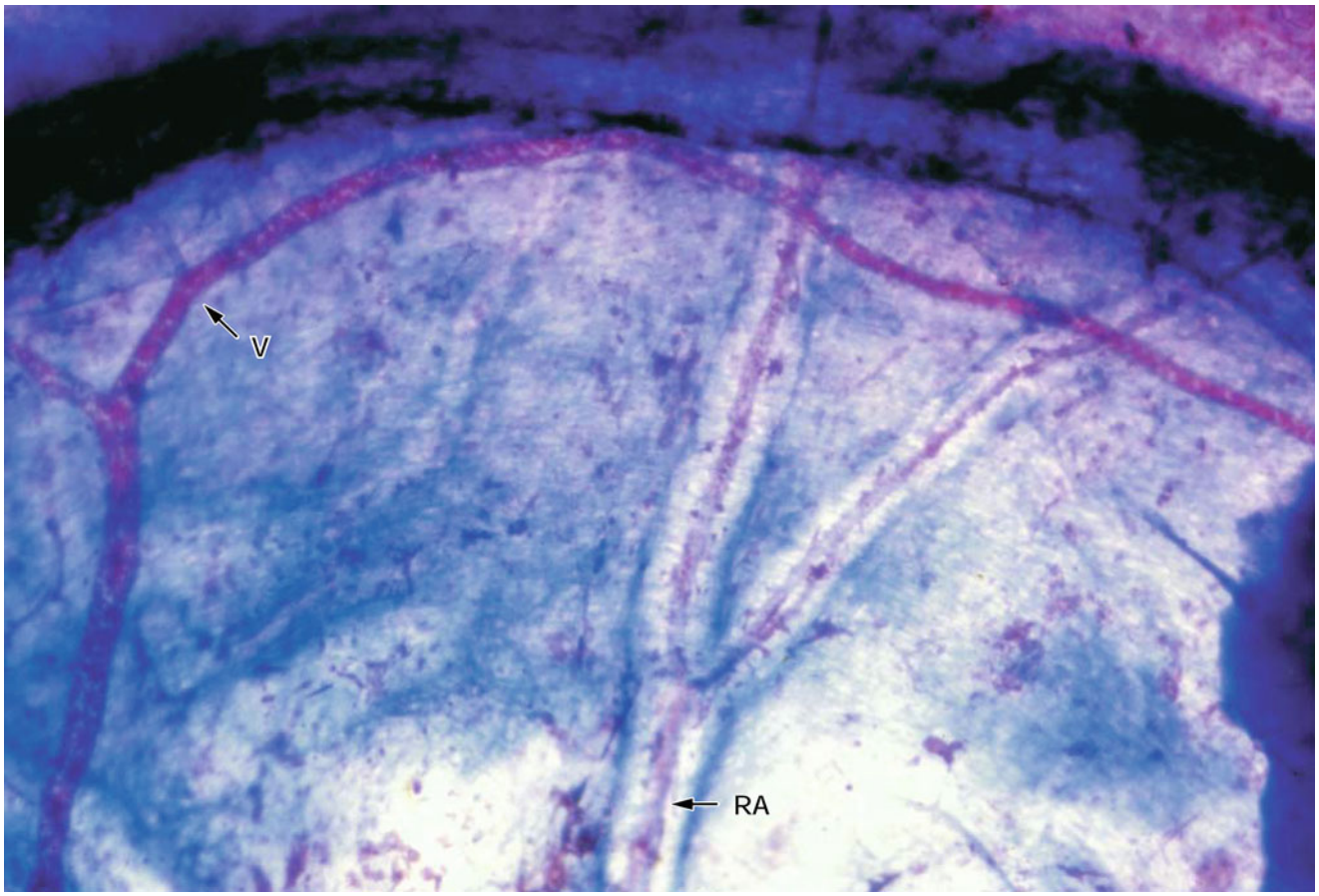

Fig. 3.6 Arterioles and venule in the septum. Arterioles (*RA*) run through the bony canal, while the venule (*V*) has no distinct canal. Azan staining (original ×6.5)

There are strand-like, atrophied vessels in the canals of the interscalar septum. Avascular canals are also observed (Figs. 3.14 and 3.15). The avascular canals may result from the disappearance of atrophied blood vessels. In the human inner ear, vascularization in the fetus is very dense, and in the infant, somewhat less so. A gradual involution of blood vessels takes place postnatally and continues with maturity and aging [5].

3.1.2 Capillaries of the Membranous Cochlea

To study the blood supply to the organ of Corti, Lawrence [6] inserted a probe approximately 25 μm long into a guinea pig's cochlea through a tiny hole in the cochlear wall to sever the arteriole going to the spiral ligament and stria vascularis. Loss of the arteriole resulted in degeneration of the spiral ligament, stria vascularis, and part of the spiral prominence, but had no effect on the organ of Corti. However, when Lawrence severed the arteriole in the modiolus going to the limbus and basilar membrane, hair cells were lost but the stria vascularis and spiral prominence remained healthy, indicating that capillary loops beneath the basilar membrane serve as the source of nutrients for the organ of Corti.

Capillary networks of the membranous labyrinth have been observed by injecting dyes, such as India ink and Prussian blue. Histochemistry is also useful for easy demonstration of the networks. Alkaline phosphatase staining is a histochemical method that can be used to demonstrate capillary networks in humans [7]. Burston's method for alkaline phosphatase staining may be used to study the membranous labyrinth as follows:

Fresh tissue is necessary for this histochemical study. After dissection, the tissue is soaked in the staining solution overnight at 4 °C. After washing in tap water, the tissue is fixed with formalin. After decalcification and dehydration, and mounting, the stained tissue is examined and trimmed under a microscope as a surface specimen before mounting.

In this staining method, alkaline phosphatase liberates naphthol compound from its substrate, for example, naphthol AS-MX phosphate. The naphthol compound is subsequently coupled to a diazonium salt such as Fast Blue RR to produce a blue azo dye at the site of enzyme activity.

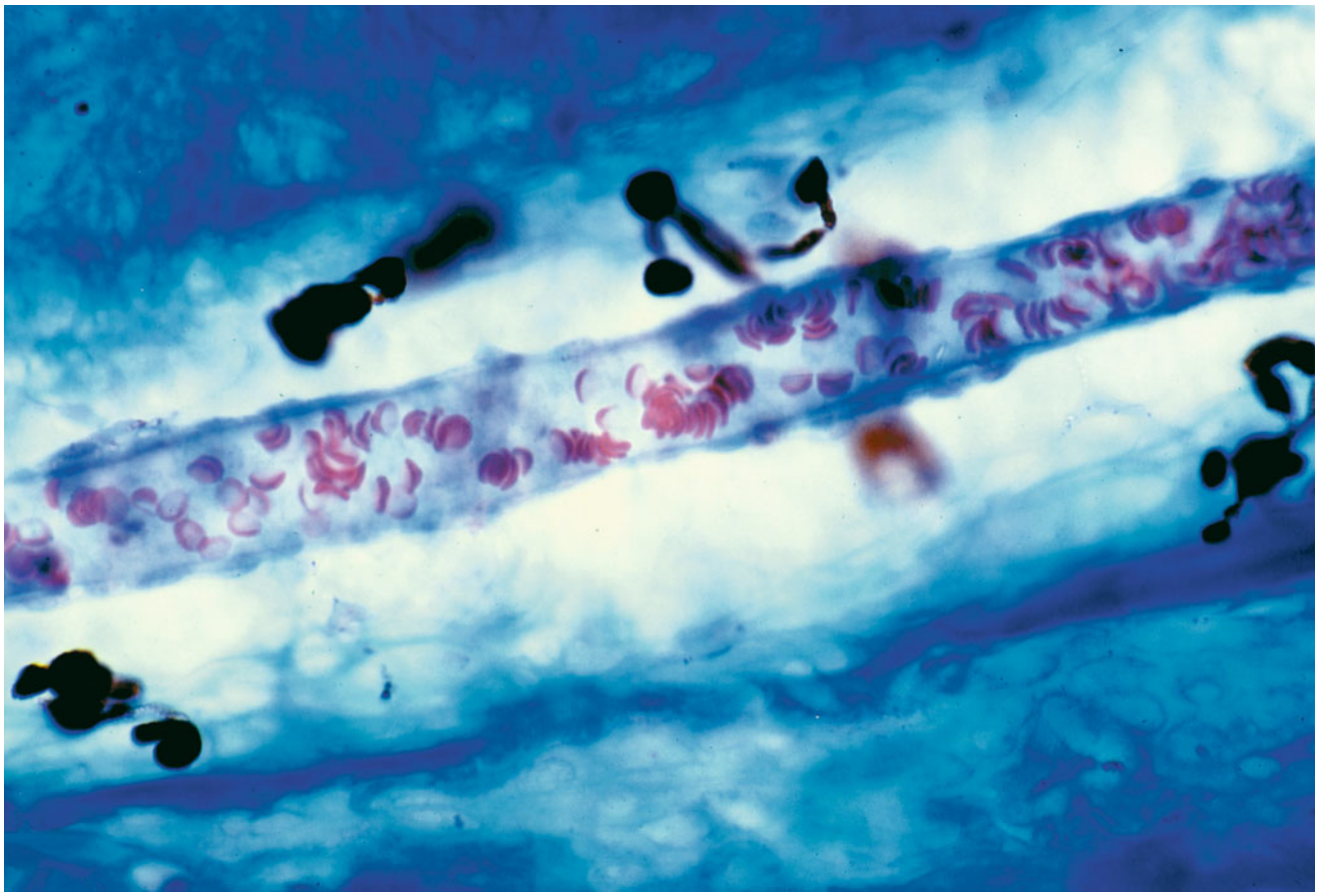

Fig. 3.7 Arteriole in the vascular canal of the septum. The diameter of the arteriole is 15 μm, while that of the vascular channel is 55 μm. Pigment cells are present in the canal. Seventy-one-year-old woman, Azan staining (original ×40) [1]

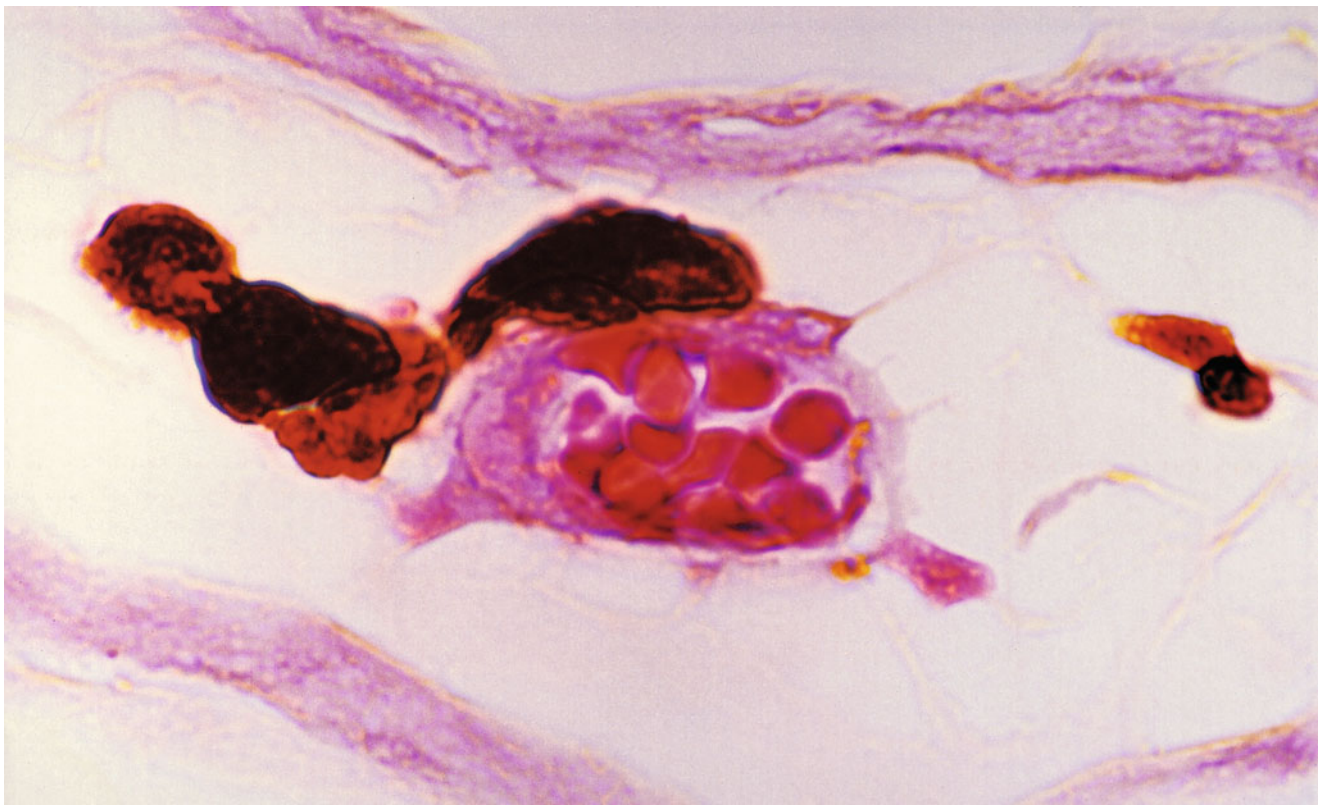

Fig. 3.8 Pigment cells adhering to the arteriole. Eighty-one-year-old woman, HE staining (original ×100) [1]

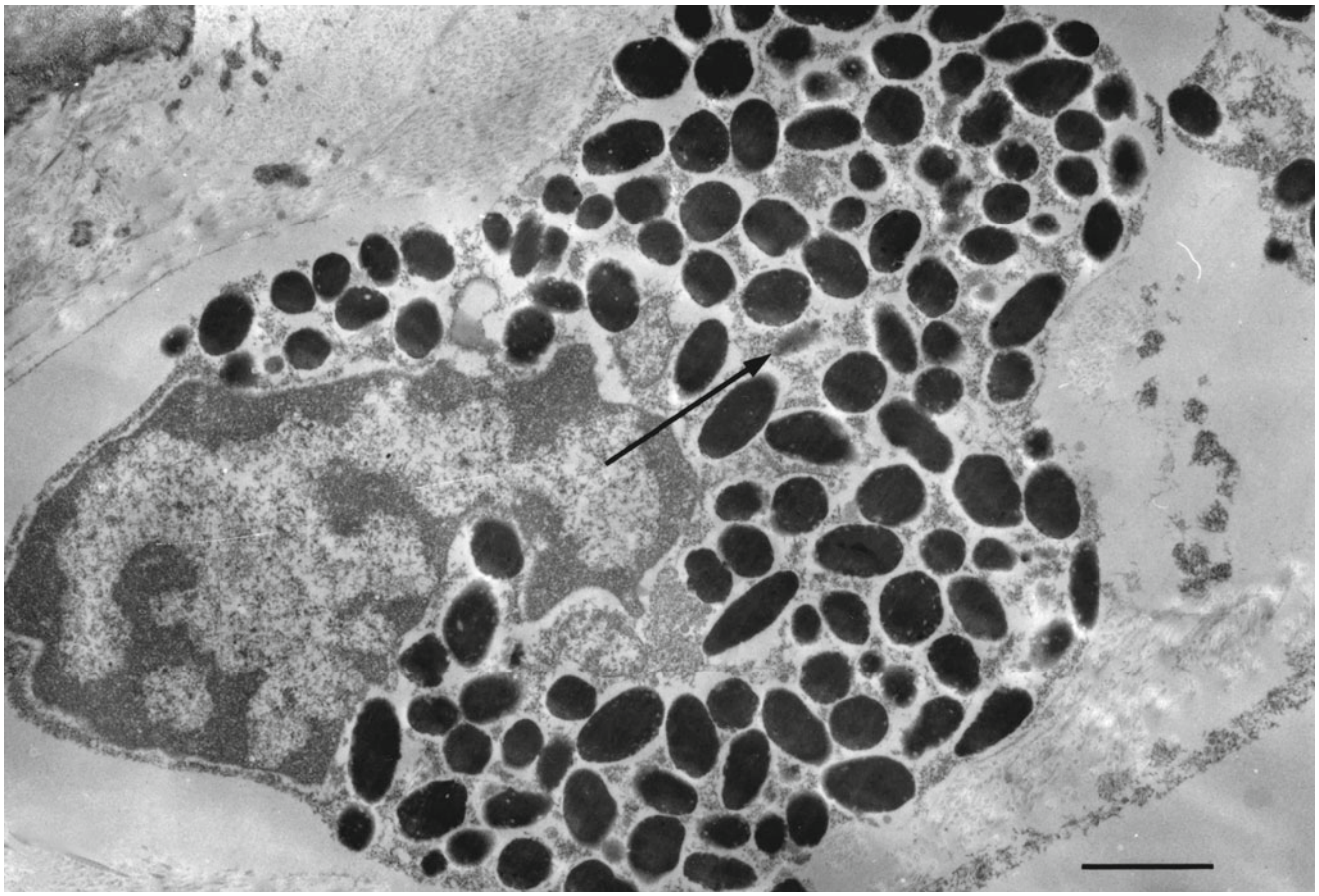

Fig. 3.9 Ultrastructure of a pigment cell. Melanosomes and premelanosomes (*arrow*) are observed. Sixty-one-year-old man (original ×12,000), scale: 1 μm [1]

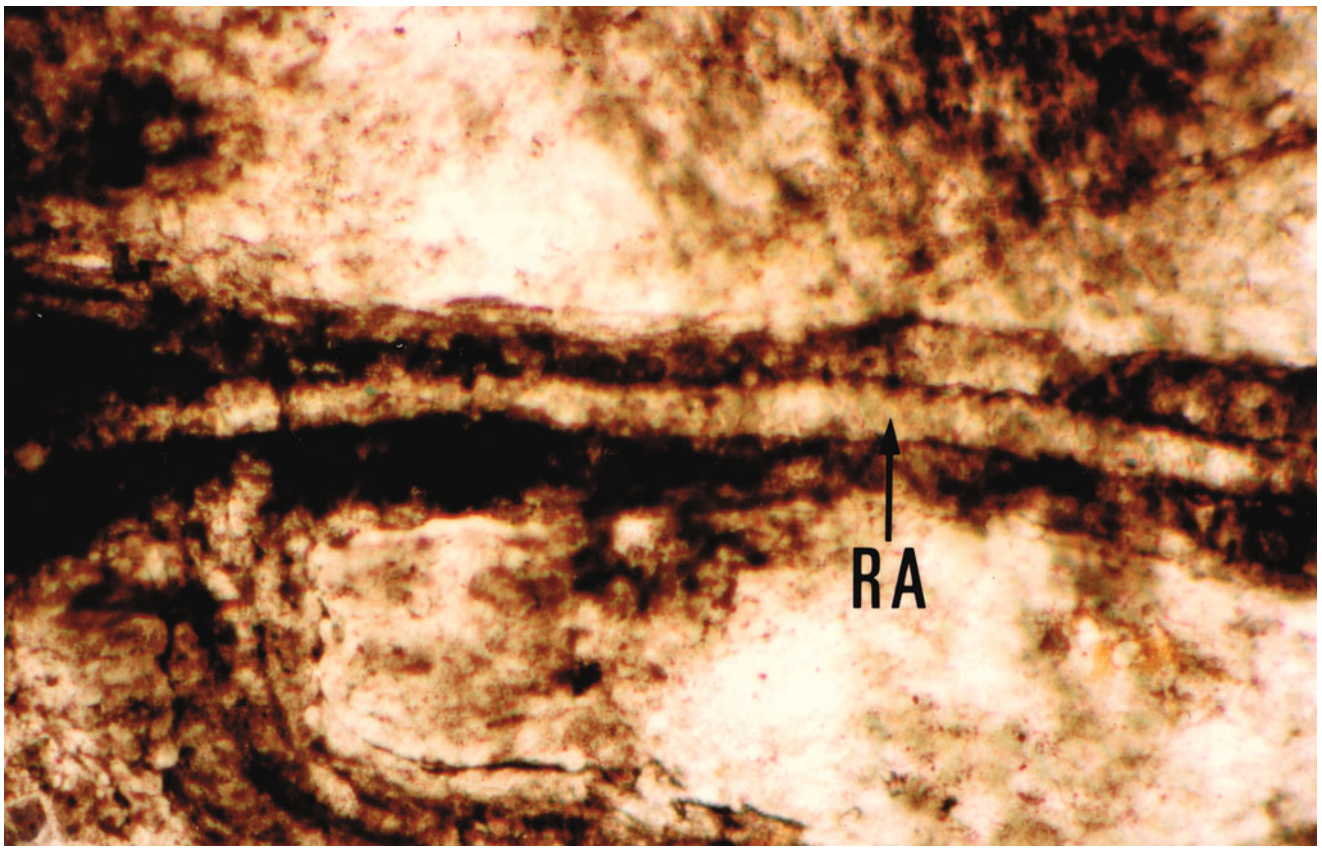

Fig. 3.10 India ink injected into the modiolus enters the vascular canal. *RA* radiating arteriole Sixty-eight-year-old man (original ×16) [1]

Fig. 3.11 India ink reaches the perivascular space of the upper spiral ligament. The space is surrounded by a thin bony wall. Sixty-one-year-old male, HE staining (original ×16) [1]

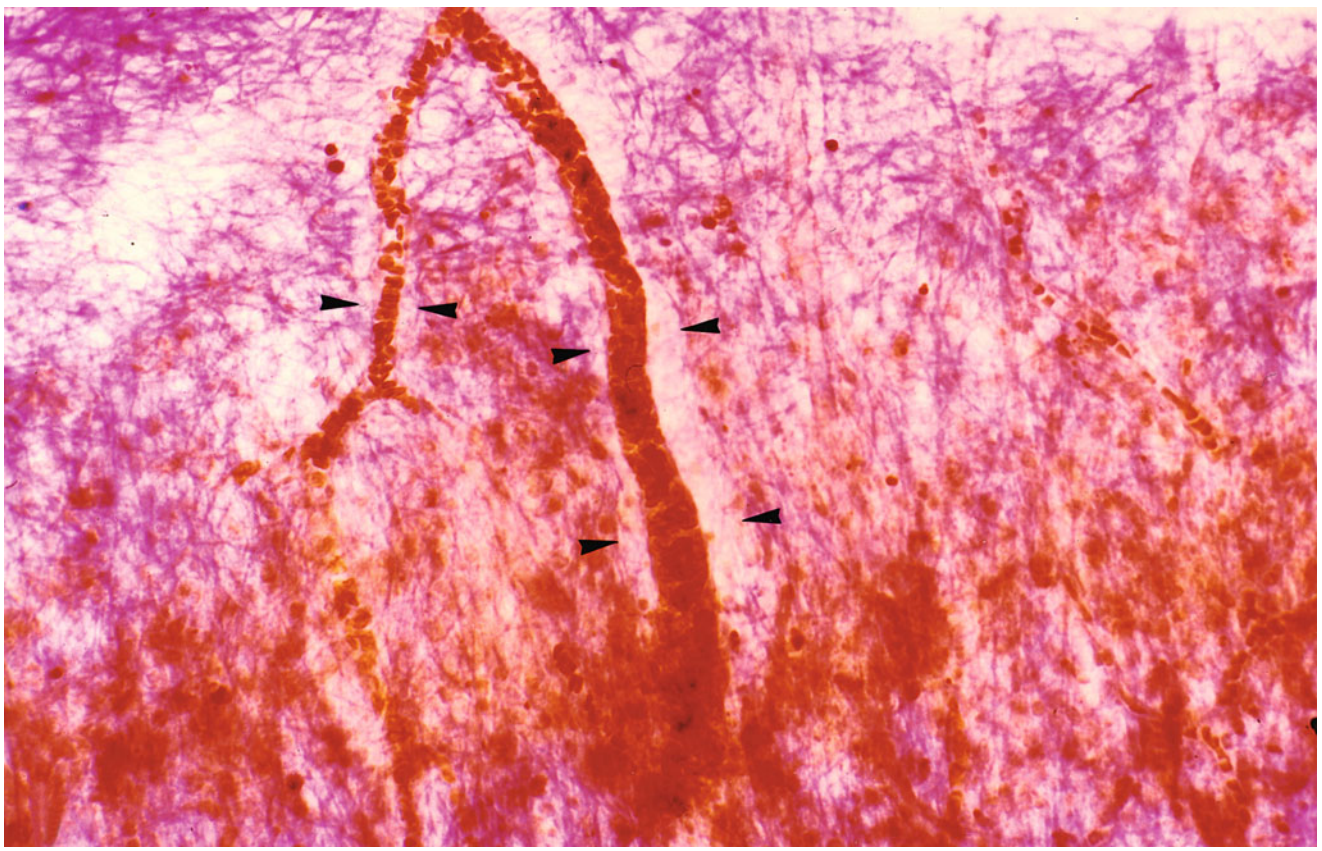

Fig. 3.12 Space is present around the radiating arterioles in the upper spiral ligament (*arrow heads*). There is no bony wall. Eight-four-year-old man, van Gieson staining (original ×16) [1]

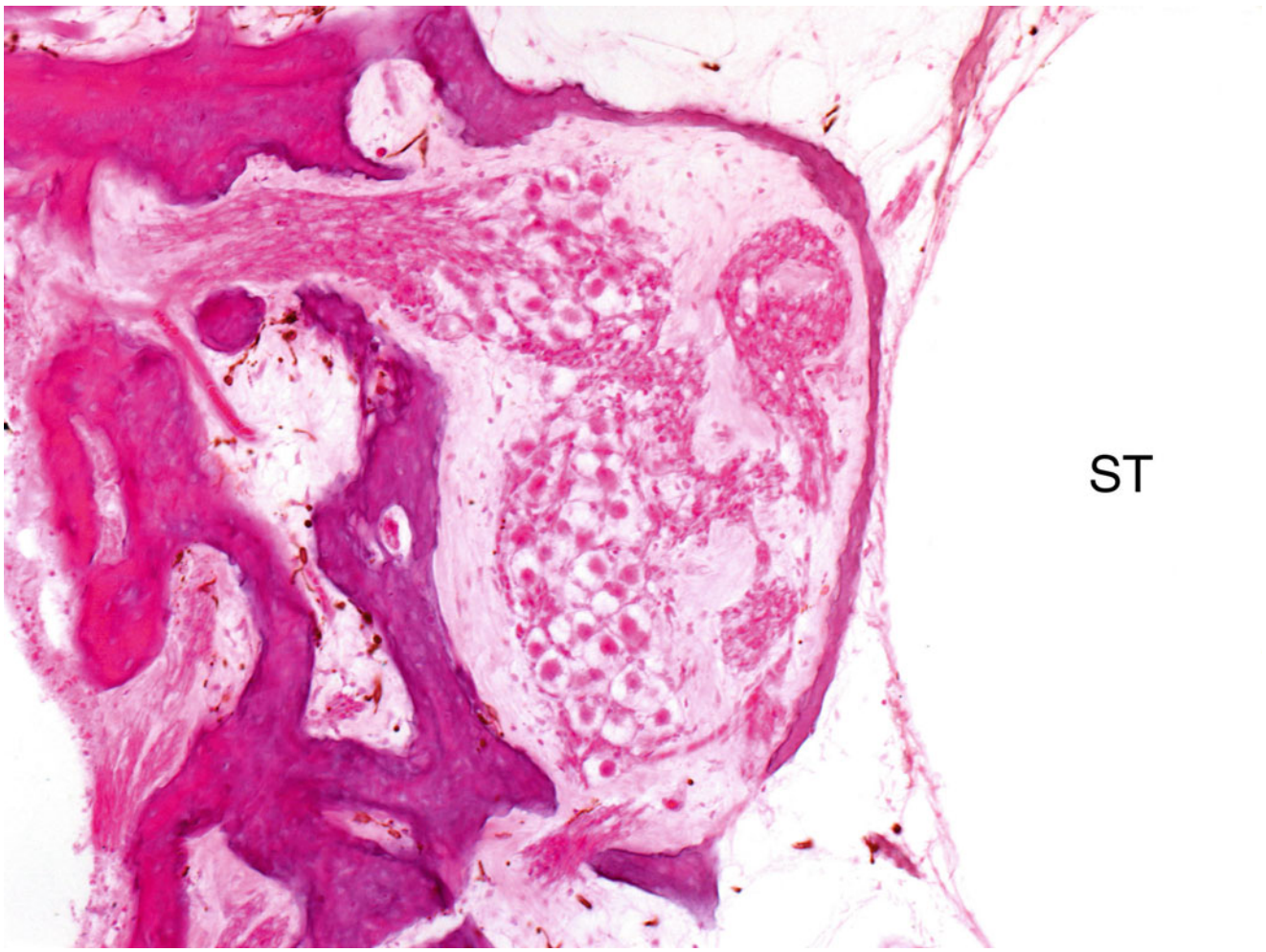

Fig. 3.13 Thin bony wall of the scala tympani of the human cochlea. Fluid communication between perilymph and cerebrospinal fluid in the modiolus is suggested. *ST* scala tympani

Blood vessels in the spiral ligament and stria vascularis are stained blue[1] or red,[2] depending on the diazonium salts used. Arterioles and venules are equally stained in humans. However, there are some species differences in staining results. Arterioles and capillaries are strongly stained in the cochlea of guinea pigs, but the venules, such as those in the lower spiral ligament, are weakly stained.

1 Blue stain	
Naphthol AS-MX phosphate	1.0 mg
Dimethylformamide	0.4 mL
Distilled water	12.0 mL
0.2 M propanediol buffer at pH 8.6	7.6 mL
Fast Blue RR	20.0 mg
2 Red stain	
Naphthol AS-TR phosxphate	5.0 mg
N-dimethyl formamide	0.5 mL
0.05 M tris buffer as pH 8.3	50.0 mL
Fast Red Violet LB	40.0 mg

Stained blood vessels of the stria vascularis and spiral ligament can be observed as surface specimens (Figs. 3.16 and 3.17). Strial capillaries will disappear in strial atrophy.

Branches of the radiating arterioles run in the spiral ligament to join the venules as arteriovenous arcades or join the vessel of the spiral prominence (Fig. 3.18). The spiral prominence and root cells are endowed with rich enzymatic activities (Fig. 3.19) [8].

Blood vessels in the osseous spiral lamina, organ of Corti, and limbus spiralis can also be clearly visualized [9, 10] (Figs. 3.20, 3.21, and 3.22). Capillaries in these structures are principally loops arranged in a coronal pattern. The loops run from the modiolus laterally in the osseous spiral lamina and underneath the basilar membrane, then return to the modiolus. It is interesting to note that no outer spiral vessel (vas spirale, the spiral vessel under the tunnel of Corti) is present beneath the organ of Corti in cats (Fig. 3.23).

The outer spiral vessel has many T-junctions composed of capillaries coming from and returning to the osseous spiral

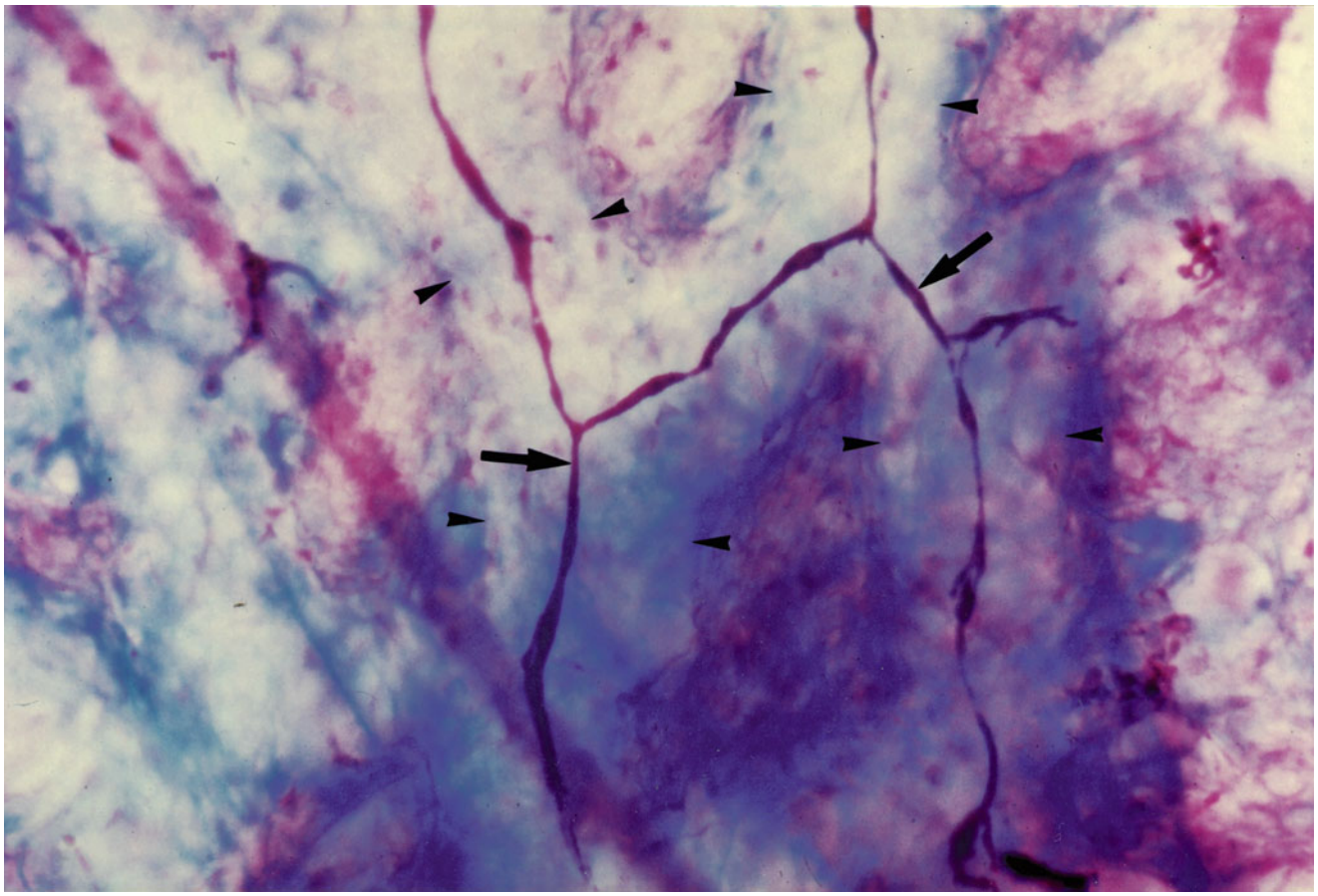

Fig. 3.14 Involution of blood vessel (*arrows*). *Arrowheads* indicate vascular channels. Eighty-three-year-old woman, Azan staining, (original ×16) [1]

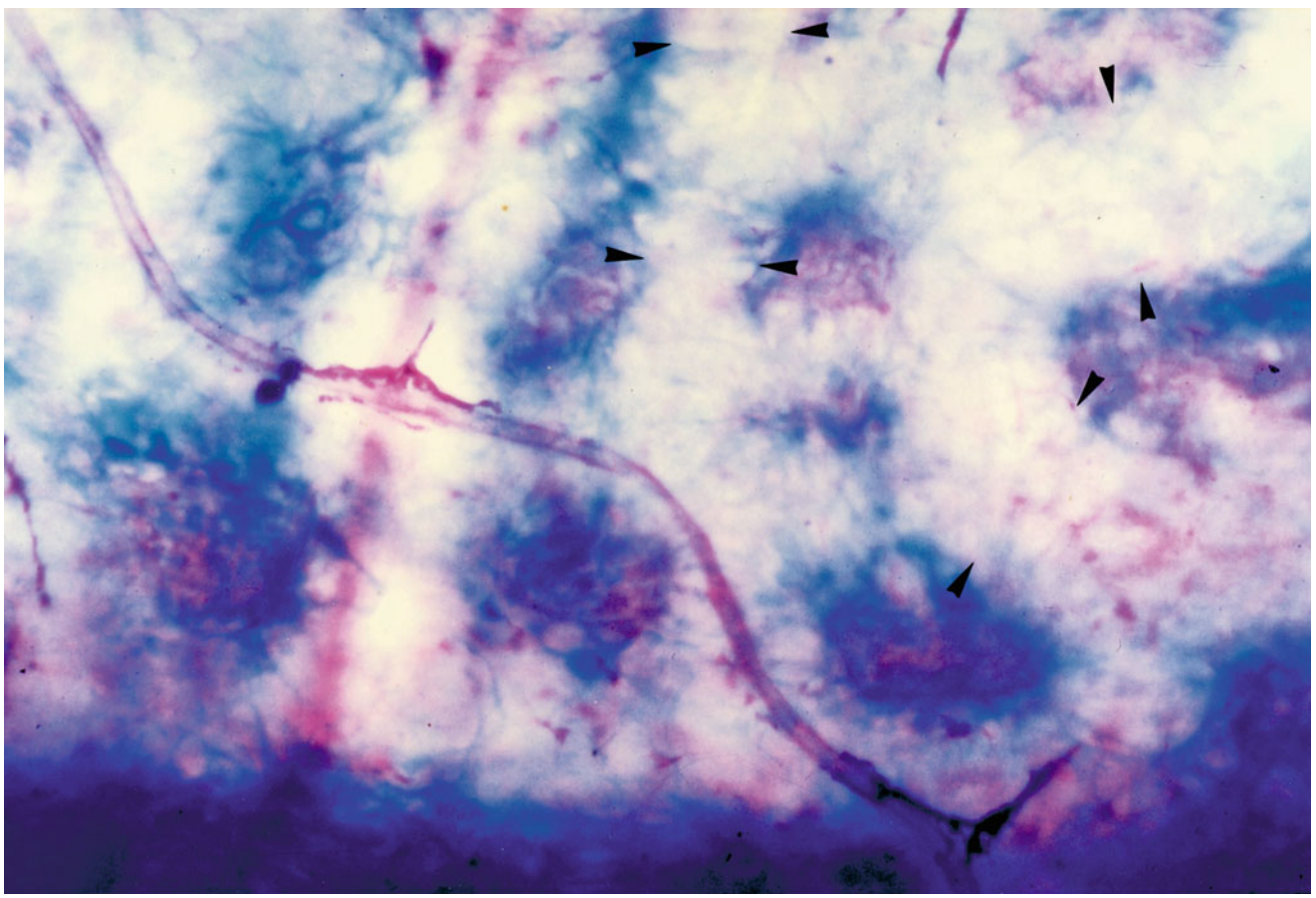

Fig. 3.15 Avascular channel (*arrowheads*). Eighty-three-year-old woman, Azan staining (original ×16) [1]

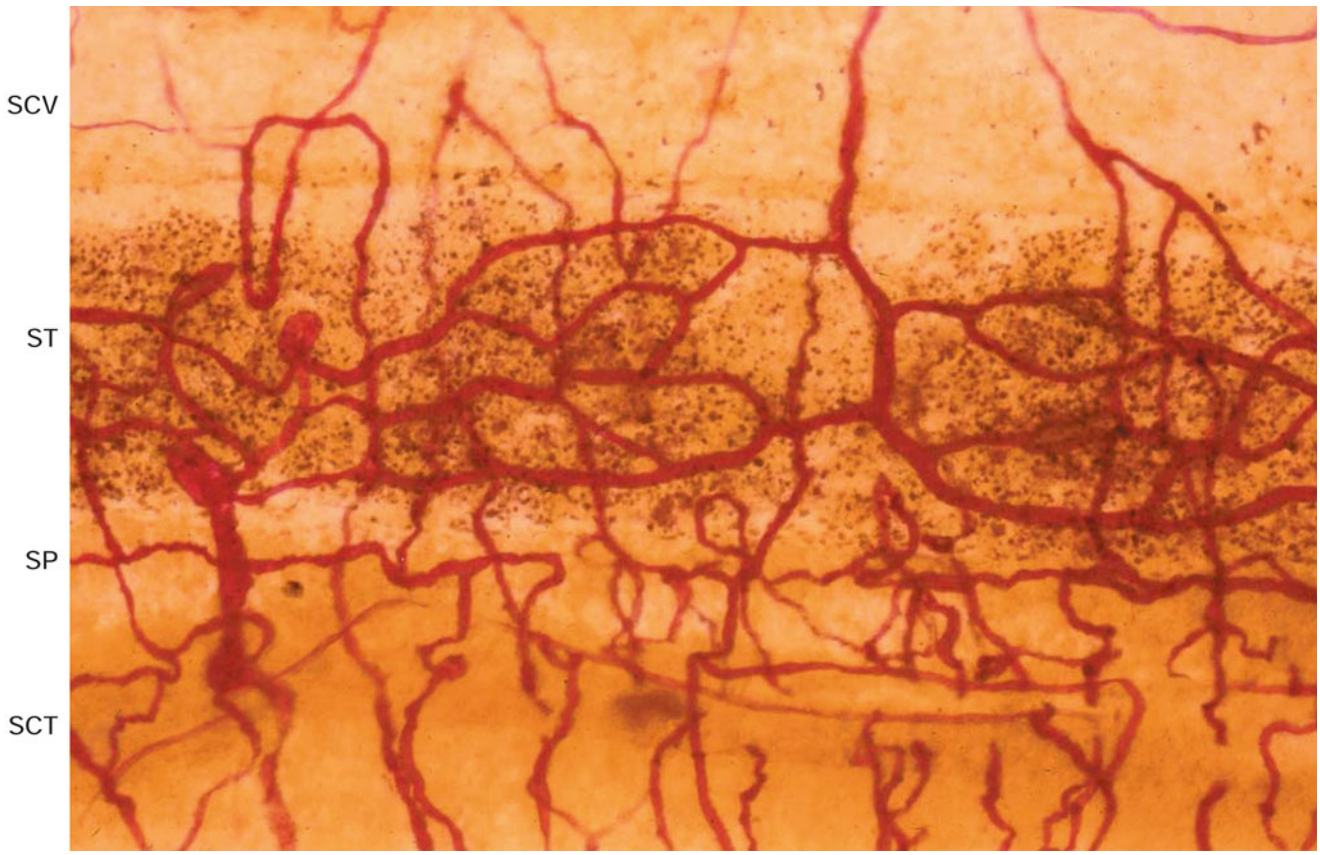

Fig. 3.16 Blood vessels of the stria vascularis and spiral ligament. *SCV* scala vestibuli, *ST* stria vascularis, *SP* spiral prominence, *SCT* scala tympani. Eighty-six-year-old woman, alkaline phosphatase staining (Burston), (original ×6.5)

lamina. Probably, the former convey arterial blood and the latter, venous blood. The staining results of alkaline phosphatase activity show us the direction of capillary blood flow in the T-junctions of the vas spirale in the guinea pig, because of weaker activity in venules than in arterioles [7].

Measurements of human outer spiral vessels were made using 40 fresh temporal bones from 30 patients, aged 4–85 years, median 49 years [10]. The length of a segment was measured from the basal end up to 28 mm. The lower basal turn was defined as extending from the basal end to 10 mm, the upper basal turn from 10 to 18 mm, and the middle turn from 18 to 28 mm.

Segments of the vas spirale in the middle turn ranged in length from 100 μm to 1 mm, with many segments measuring approximately 120 μm in length. In the lower basal turn, the lengths were distributed rather uniformly from 100 μm to more than 2 mm. The longest segment was 3.4 mm.

Comparing the capillary density in different areas of the osseous spiral lamina, morphometric measurement revealed that the 25 mm area (middle turn) of the osseous spiral lamina had capillary density about 1.5 times greater than of the 5 mm area (lower basal turn) [9]. It is uncertain whether this difference is due to aging. A marked loss of nerve fibers and organ of Corti in the lower basal turn in aged patients may correlate with capillary loss. Collapsed capillaries with weak alkaline phosphatase activity were observed in the osseous spiral lamina, indicative of a process of involution.

Corti described the vascular channel around the vas spirale in 1851 (Fig. 3.24) [11]. Avascular channels were present in the vas spirale, however, no strands were found within the channels (Figs. 3.22, 3.25 and 3.26).

Because the organ of Corti depends on capillaries of the osseous spiral lamina system for its oxygen supply and nutrients, microcirculation in the basal turn seems unfavorable compared with that of the vestibular sensory epithelia, where rich capillary networks develop.

3.1.3 Capillaries of the Vestibular Organs

In the vestibular organs, capillaries are well developed in the maculae of the utricle and saccule. Capillary density markedly decreases outside the maculae (Figs. 3.27 and 3.28) [12]. In the semicircular canals, a dense capillary network is observed in the crista ampullaris beneath the sensory epithelium. In the cat, the center of the sensory epithelium protrudes

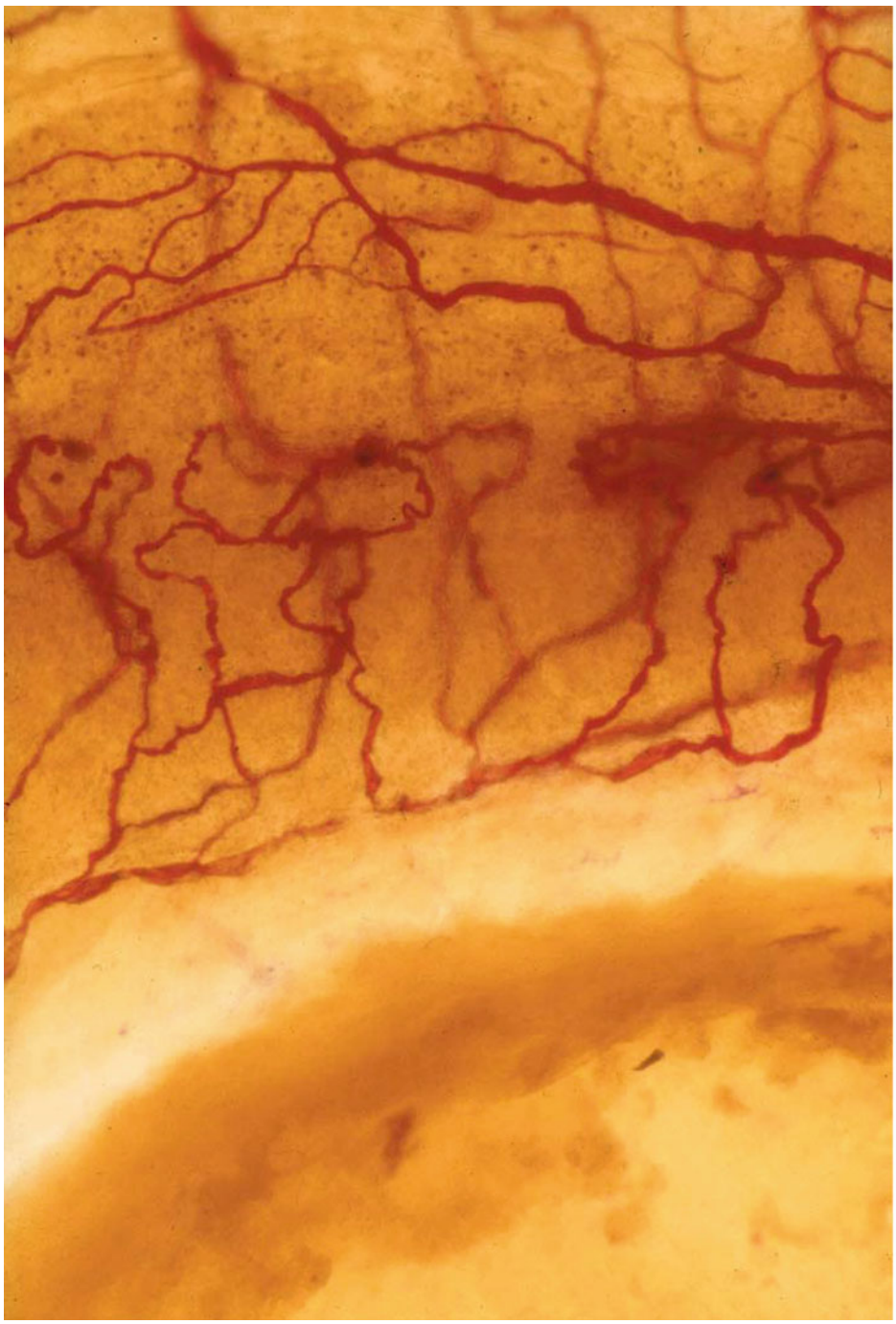

Fig. 3.17 Blood vessels of the stria vascularis and spiral ligament adjacent to the round window membrane (*RM*). Eighty-six-year-old man, alkaline phosphatase staining (Burston), (original ×6.5)

on the anterior and posterior crista ampullaris. In this area the epithelium is cylindrical, and no hair cells or nerve fibers are found (Fig. 3.29) [13]. We know that the sensory neuroepithelium of the vestibular organs performs the metabolic activities of glycolysis, the citric acid cycle, hexose monophosphate shunt, cytochrome oxidation system, and oxidative decarboxylation of alpha-keto acids [14]. Well-developed capillary networks support the vestibulocanal organs, which have high energy consumption because they react to continuous stimulation.

The planum semilunatum has a moderate distribution of capillaries, and the semicircular duct is less vascularized (Fig. 3.30).

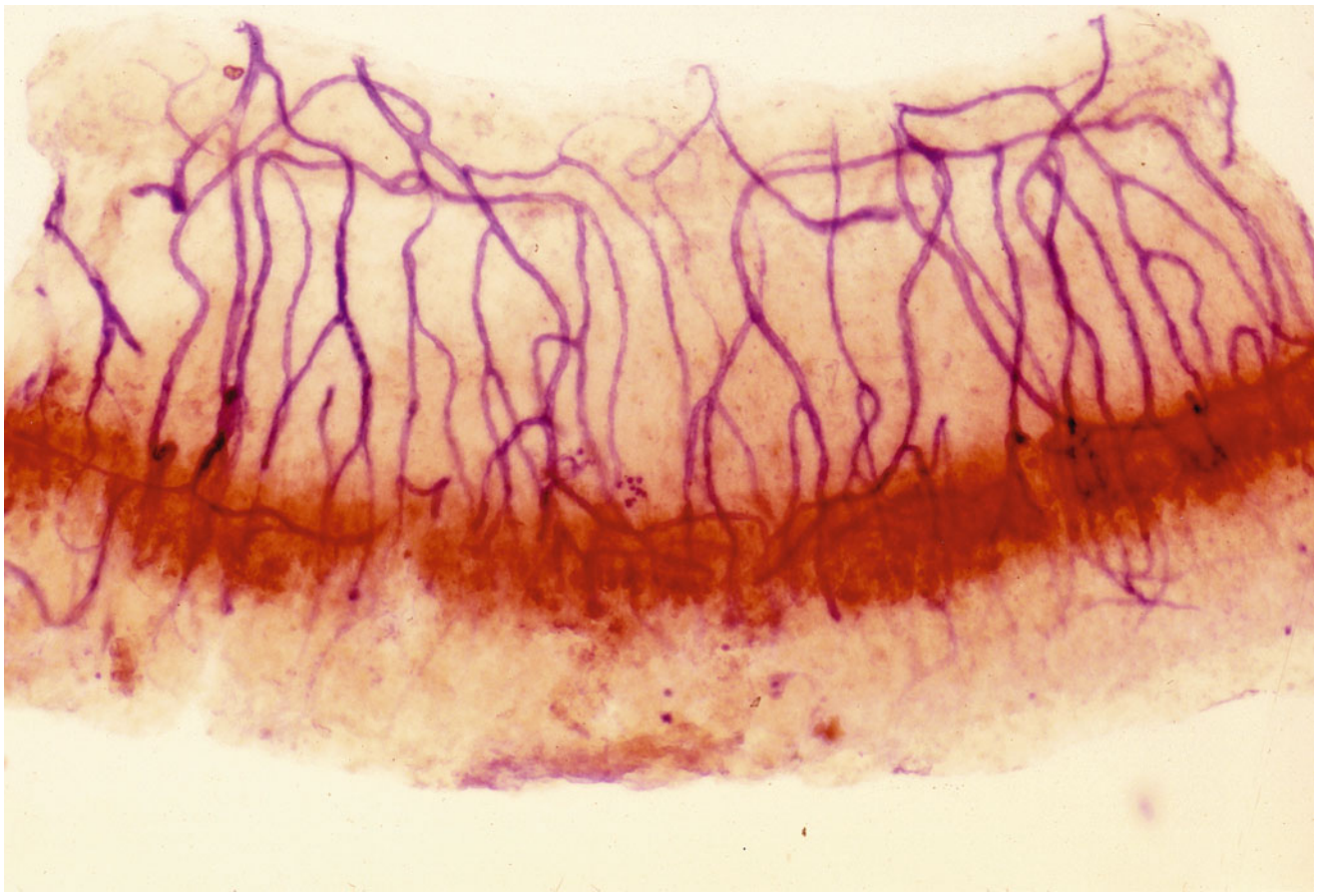

Fig. 3.18 Arteriovenous arcades in the spiral ligament and the root cells. Butylcholinesterase activity is present in the root cell. The blood vessels were stained to demonstrate alkaline phosphatase. The venules in the lower spiral ligament shows weak activity of alkaline phosphatase. The stria vascularis was removed. Guinea pig, double staining

3.2 Diseases of the Blood and Blood Vessels

Systemic diseases of the blood and blood vessels are known to affect the inner ear.

3.2.1 Leukemia

Leukemia often produces acute hearing loss and vertigo due to hemorrhage and leukemic infiltration in the inner ear. Even when there is no clinical evidence of ear disease, leukemic cells can infiltrate the inner ear. Development of otitis media was common in patients with leukemia in the pre-antibiotic era, causing inner ear complications. Aplastic anemia can also lead to massive hemorrhage in the inner ear.

3.2.1.1 Myeloid Leukemia

A 23-year-old woman developed a chronic fever of unknown origin of 38 °C in December 1967. In February 1968, she experienced gingival swelling and hemorrhage. A diagnosis of acute myeloid leukemia was made. She died in June 1968. At autopsy, hemorrhage was recognized in her pericardium, kidneys, stomach mucosa, subcutaneous tissues, and pleura. In the cochlea, massive hemorrhages were found in the scala tympani and Rosenthal's canal of the basal turn (Fig. 3.31).

A 16-year-old girl experienced repeated nosebleeds followed by purulent otitis media, mastoiditis, and facial palsy of the left side. Bleeding occurred from the eardrum. Nystagmus was observed with the fast phase toward the right side. Labyrinthitis occurred following acute otitis media. The middle ear cavity was filled with granulation tissue. Hemorrhage was observed with granulation formation in the inner ear (Figs. 3.32, 3.33, and 3.34). She died of acute myeloid leukemia.

Massive hemorrhage was observed in the modiolus and scala tympani of a 48-year-old man with acute myeloid leukemia (Fig. 3.35).

3.2.1.2 Aplastic Anemia

A 6-year-old boy developed bleeding from the nose and gingiva following a fever in June 1968. A diagnosis of aplastic

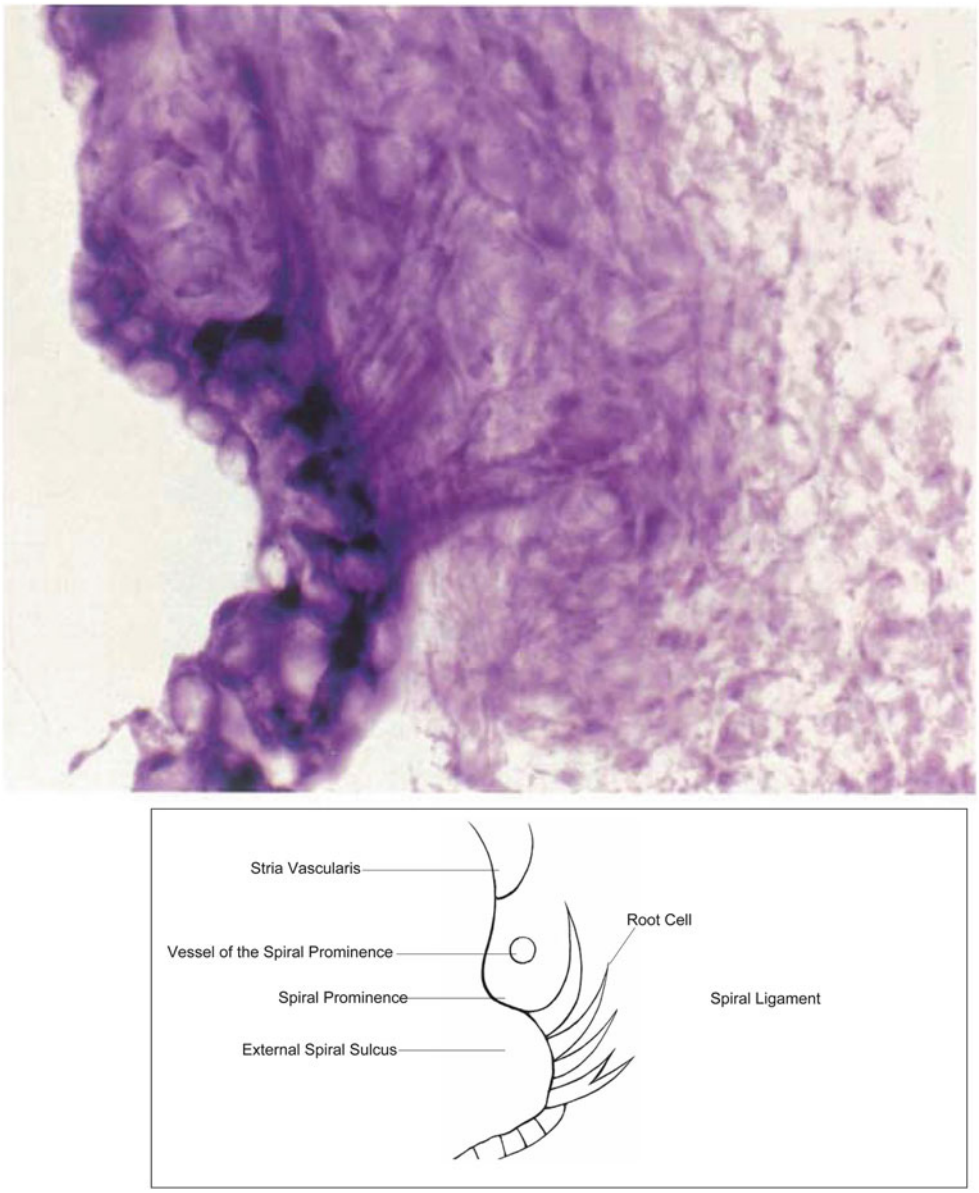

Fig. 3.19 NADH diaphorase activity in the root cells. Guinea pig. *NAD* Nicotinamide adenine dinucleotide

anemia was made. Soon thereafter, the boy complained of hearing loss in the left ear. Three days later, it was found that he was bleeding around the circumference of the left eardrum. One week later, the boy died. At autopsy, bleeding was found to have occurred in the digestive tract, heart, lungs, and around the urinary tract. Massive hemorrhage was found in the left temporal bone. Blood filled the tympanic cavity, antrum, and mastoid air cells. Blood was also found within the cochlea, vestibulum, semicircular canals, and internal auditory canal. Although blood was found in the perilymphatic space, none was found in the endolymphatic space (Fig. 3.36).

3.2.2 Buerger's Disease [15]

A 40-year-old man with Buerger's disease (thromboangiitis obliterans) developed sudden sensorineural hearing loss of the right ear with fullness of the ear and roaring tinnitus in June 1960. He was a heavy smoker. Five years earlier, he had developed intermittent claudication in his left leg and noted hearing loss in his left ear. In December 1959, he noticed that his right fingertips had become cold, cyanotic, and painful. An absence of pulsation in his right radial artery was noted. In February 1960, a 3 cm segment of the occluded radial artery was

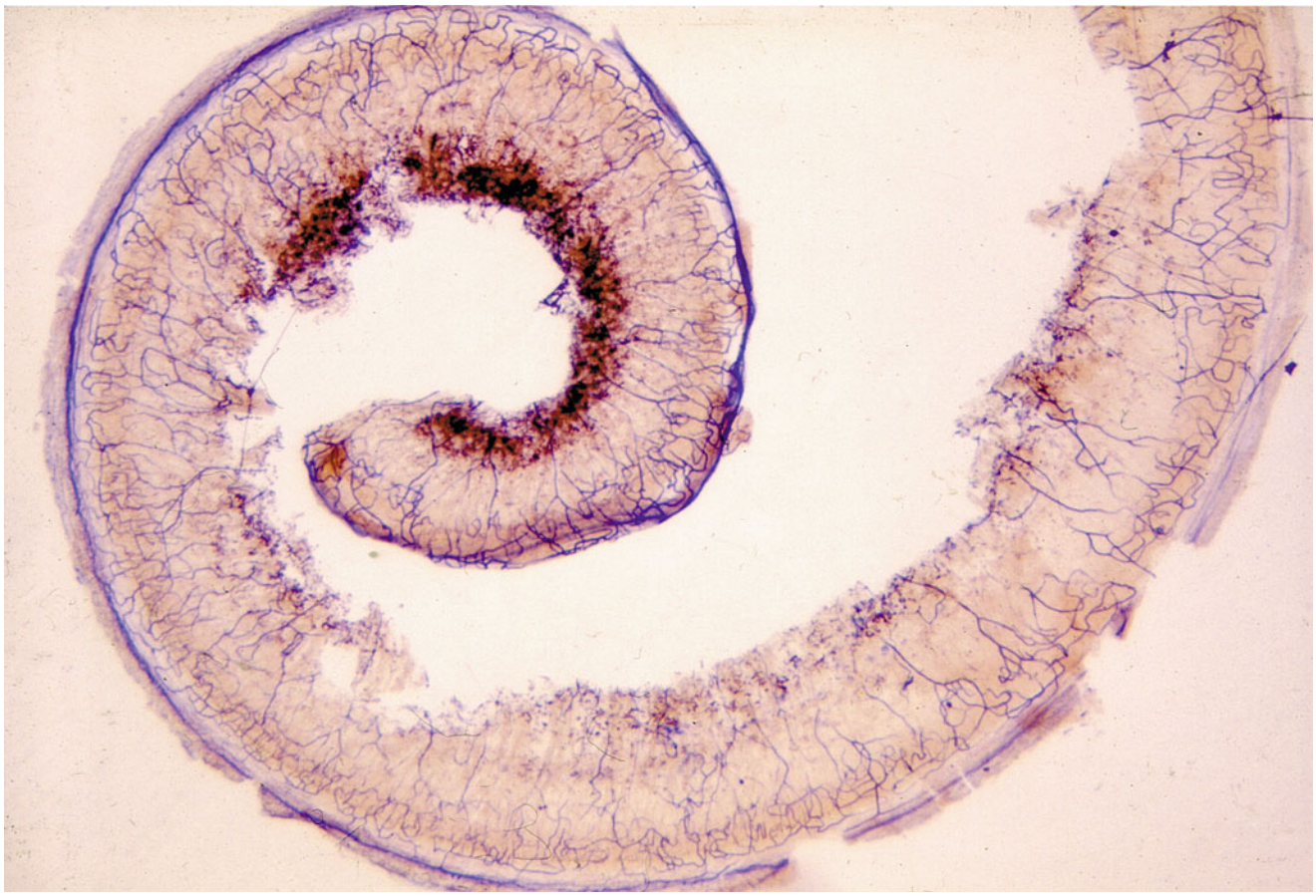

Fig. 3.20 Capillaries in the osseous spiral lamina with the organ of Corti of the whole cochlea. The capillary networks are dense in the osseous spiral lamina of the upper turn in comparison with the lower basal turn. Seventy-nine-year-old man, alkaline phosphatase staining (Burston), (original ×2.5) [9]

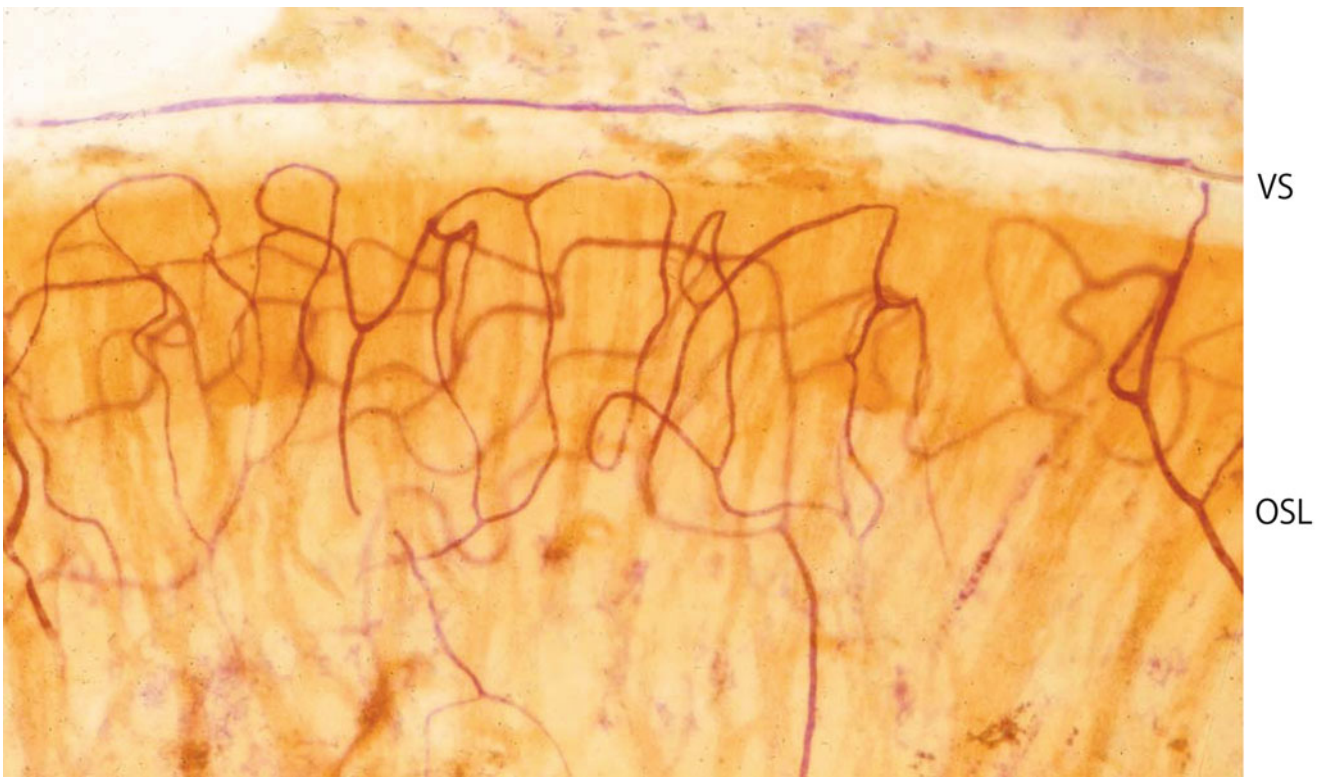

Fig. 3.21 A long spiral vessel (3 mm) in the lower basal turn. *VS* outer spiral vessel, *OSL* osseous spiral lamina. Forty-nine-year-old woman. alkaline phosphatase staining (original ×6.5)

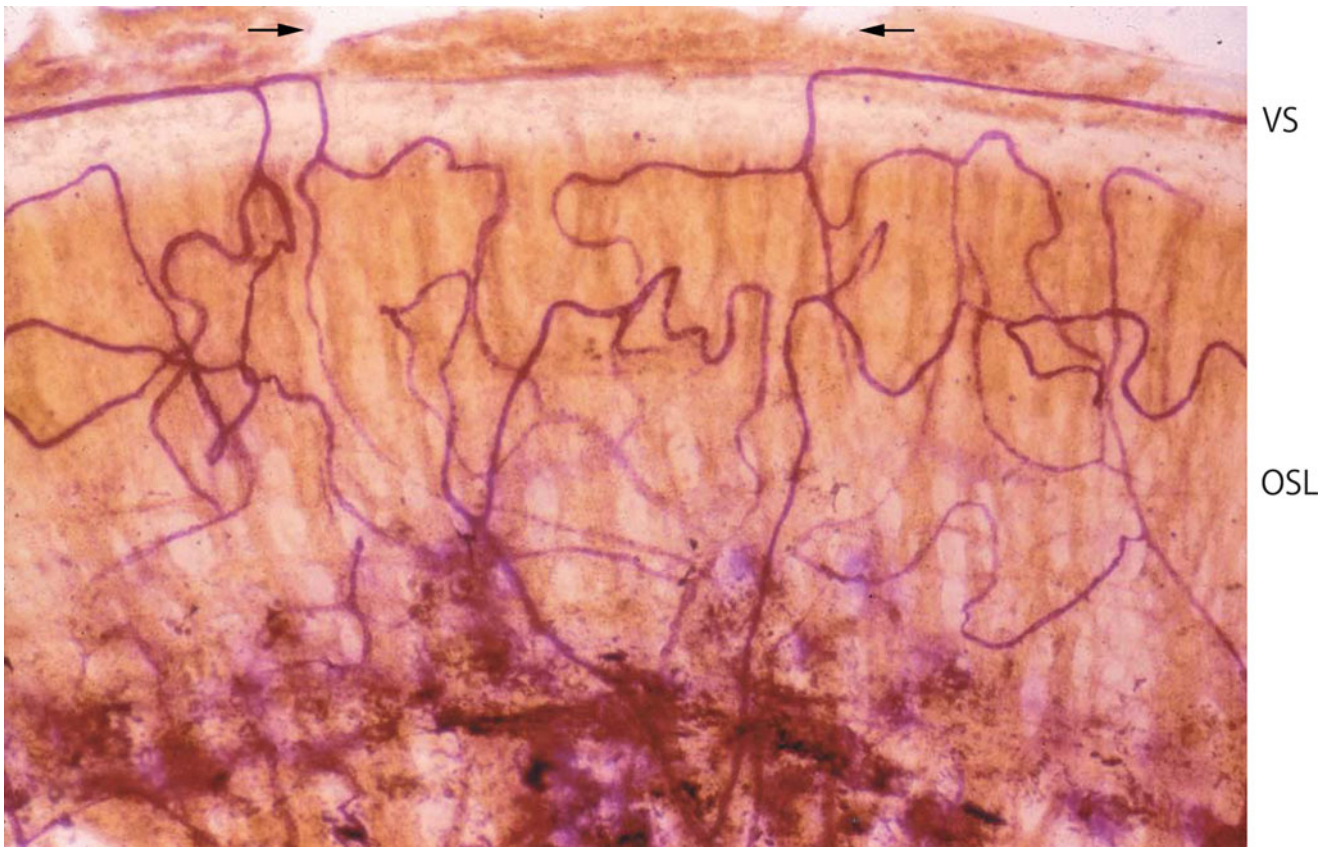

Fig. 3.22 The spiral vessel is partly missing as indicated by arrows. *VS* outer spiral vessel, *OSL* osseous spiral lamina, middle turn. Eighty-six-year-old woman, alkaline phosphatase staining (original ×6.5)

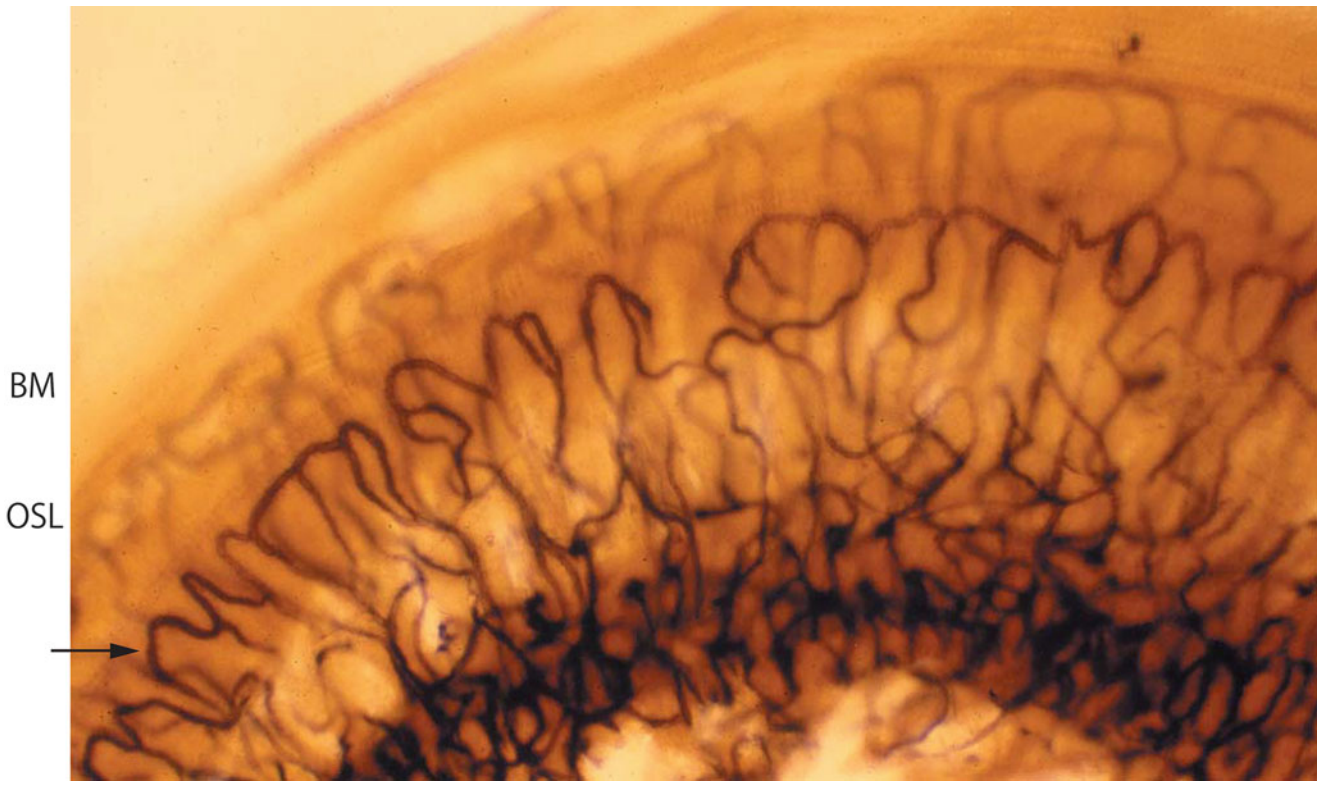

Fig. 3.23 The cat cochlea has no outer spiral vessel beneath the organ of Corti. Vascular loops in the limbus are clearly observed (*arrow*). *BM* basilar membrane, *OSL* osseous spiral lamina. Cat, alkaline phosphatase staining (original ×6.5)

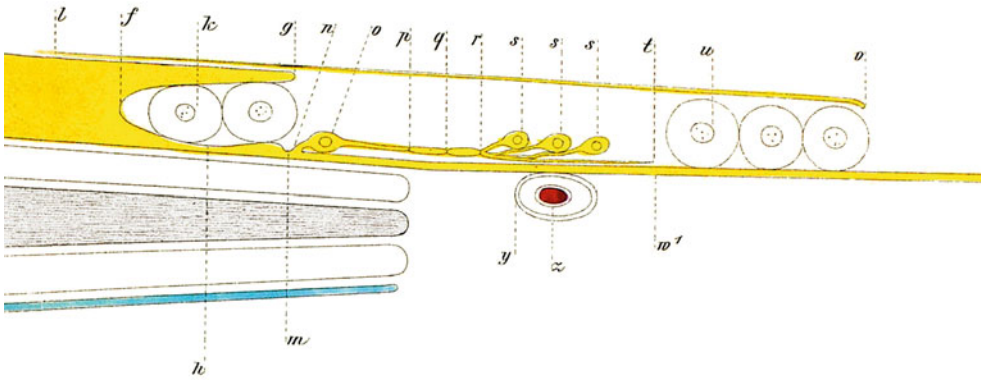

Fig. 3.24 Corti drew the vascular channel around the spiral vessel. *z* spiral vessel, *y* vascular channel [11]

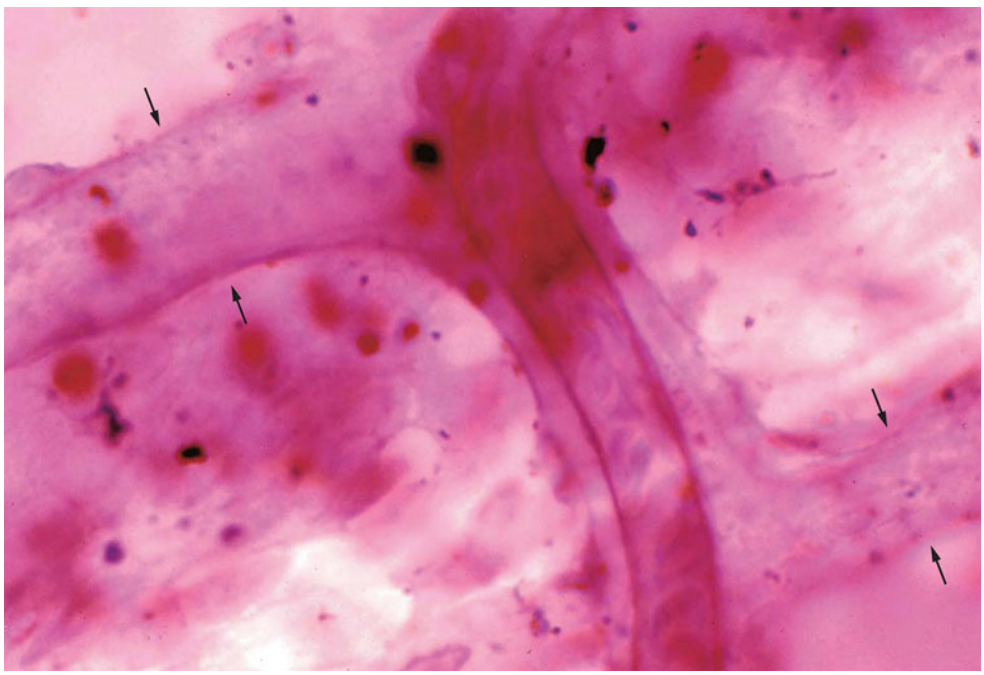

Fig. 3.25 Human vascular channel and avascular channel (*arrows*) (original ×100)

removed. Dense adhesions were seen around the artery. The histological diagnosis was thromboangiitis obliterans. Sensorineural hearing loss of sudden onset in the right ear occurred 4 months after surgery (Fig. 3.37). Angiography of the vertebrobasilar arterial system was performed. Visualization of the left anterior cerebral artery was a pathological finding, as this vessel is usually not observed in vertebral angiography. Insufficient filling of the arteries on the left side with opaque media was also pathological.

Thromboangiitis obliterans was considered a possible cause of acute sensorineural hearing loss in this patient, as disturbance of blood flow to the inner ear was conceivable. Cerebral involvement in patients with Buerger's disease is rare, with an incidence less than 0.5 % [16].

Today, the term "sudden deafness" would not be used to describe this patient's acute hearing loss in Japan, because he was suffering from a systemic disease of the blood vessels. The medical term "sudden deafness" should ideally be used exclusively to describe idiopathic sudden deafness.

3.2.3 Cryoglobulinemia [17]

Cryoglobulins are antibodies that precipitate reversibly at cold temperature. The signs and symptoms of cryoglobulinemia are purpura, arthralgia, Raynaud-like symptoms in the lower extremities, hematuria, and edema. These symptoms are due to altered physical and chemical properties of proteins.

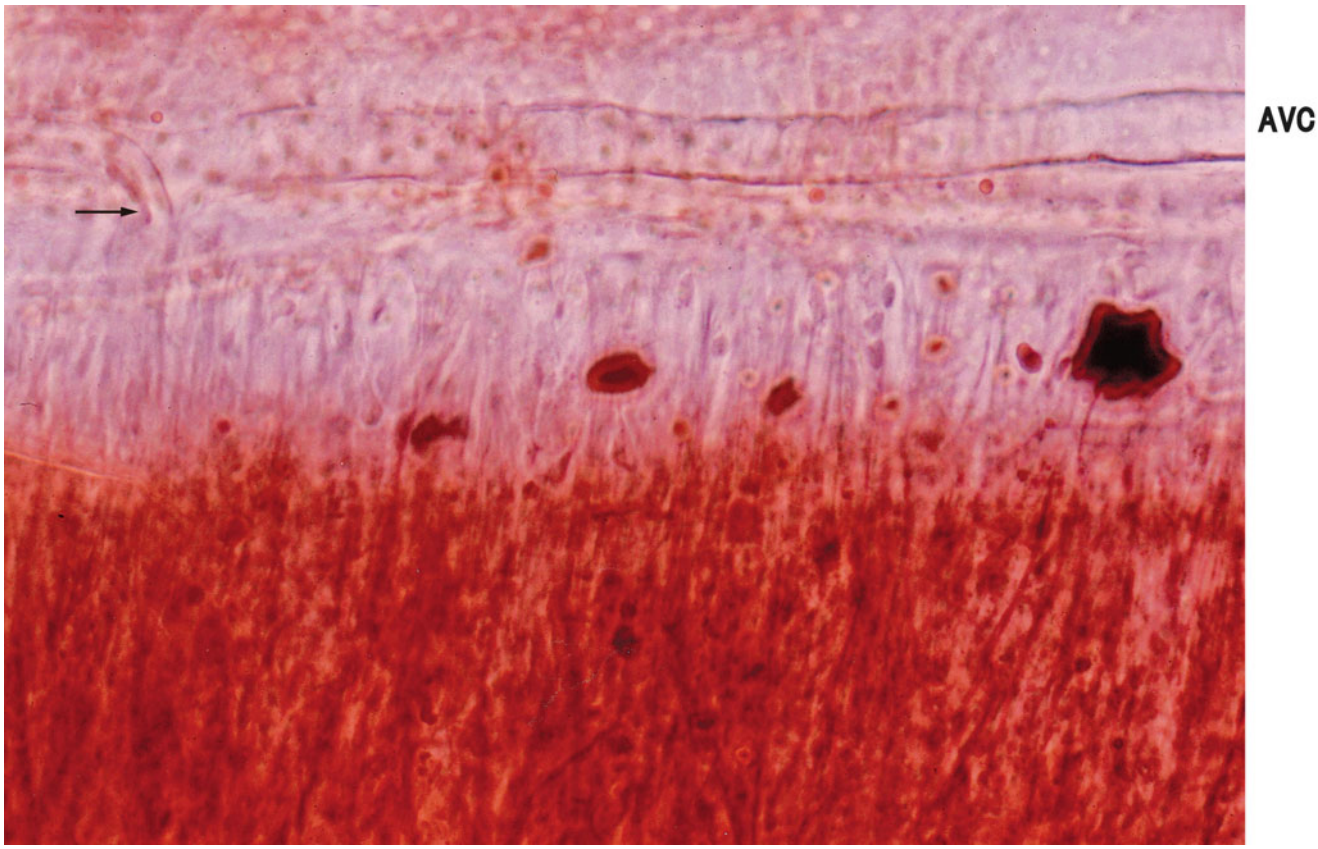

Fig. 3.26 A long segment of the avascular channel beneath the organ of Corti. *AVC* avascular channel 300 μm long, *arrow:* capillary joining the outer spiral vessel (original ×6.5)

When the extremities are exposed to cold, intravascular precipitation of cryoglobulins occurs.

A 44-year-old woman developed purpura and petechiae in her lower extremities in March 1960, symptoms that worsened every winter. In 1965, she experienced arthralgia in all joints after the birth of an apparently normal child. In 1968, a diagnosis of cryoglobulinemia was made, because refrigeration of her serum (4 °C) resulted in a whitish precipitate that resolved with exposure to warm temperatures.

After further examinations, a diagnosis of essential cryoglobulinemia of mixed type (IgG–IgA) was made. The patient received predonine, inositol hexanicotinate, and vitamin C. In 1972, she was admitted to The University of Tokyo Hospital because of exacerbation of ulcers on her lower extremities. Admission examination revealed her serum cryoglobulin level to be 150 mg/dL; the cryoglobulin was of mixed type (IgG and IgA); cryocrit was less than 2 %. The patient's C-reactive protein level was high, her anti-streptolysin O titer was 1,250 units/mL; the patient was RA-negative and had a negative direct Coombs test. The patient's erythrocyte sedimentation rate was 105 mm/h; serologic tests for syphilis were negative.

In March 1972, the patient first noted tinnitus and hearing loss of the left ear. During each subsequent winter and spring, her symptoms worsened. Funduscopic findings were bleeding and grade III (Keith-Wagener) hypertension. The patient developed dizziness in January 1978 and because her hearing loss was progressive, she was fitted with a hearing aid in August 1978. However, her hearing deteriorated to the point where the hearing aid was useless.

In September 1978, the patient was brought to our department on a stretcher, with a chief complaint of deafness. Upon inspection, her eardrums were normal; audiograms were indicative of bilateral total deafness. The patient had no spontaneous nystagmus; her nasal septum had a perforation about 1 cm in diameter. One week later, the patient died of bronchopneumonia.

Postmortem findings revealed systemic vasculitis of the medium to small arteries affecting several organs, with pronounced changes in her kidneys, liver, and colon. The inflammatory cell reaction was mild, and infiltrating cells were exclusively lymphocytes, with an absence of neutrophils. Intimal hyperplasia and adventitial fibrosis were the most common findings. Vasculitis of the arcuate and interlobar arteries in the kidneys had led to nephrosclerosis.

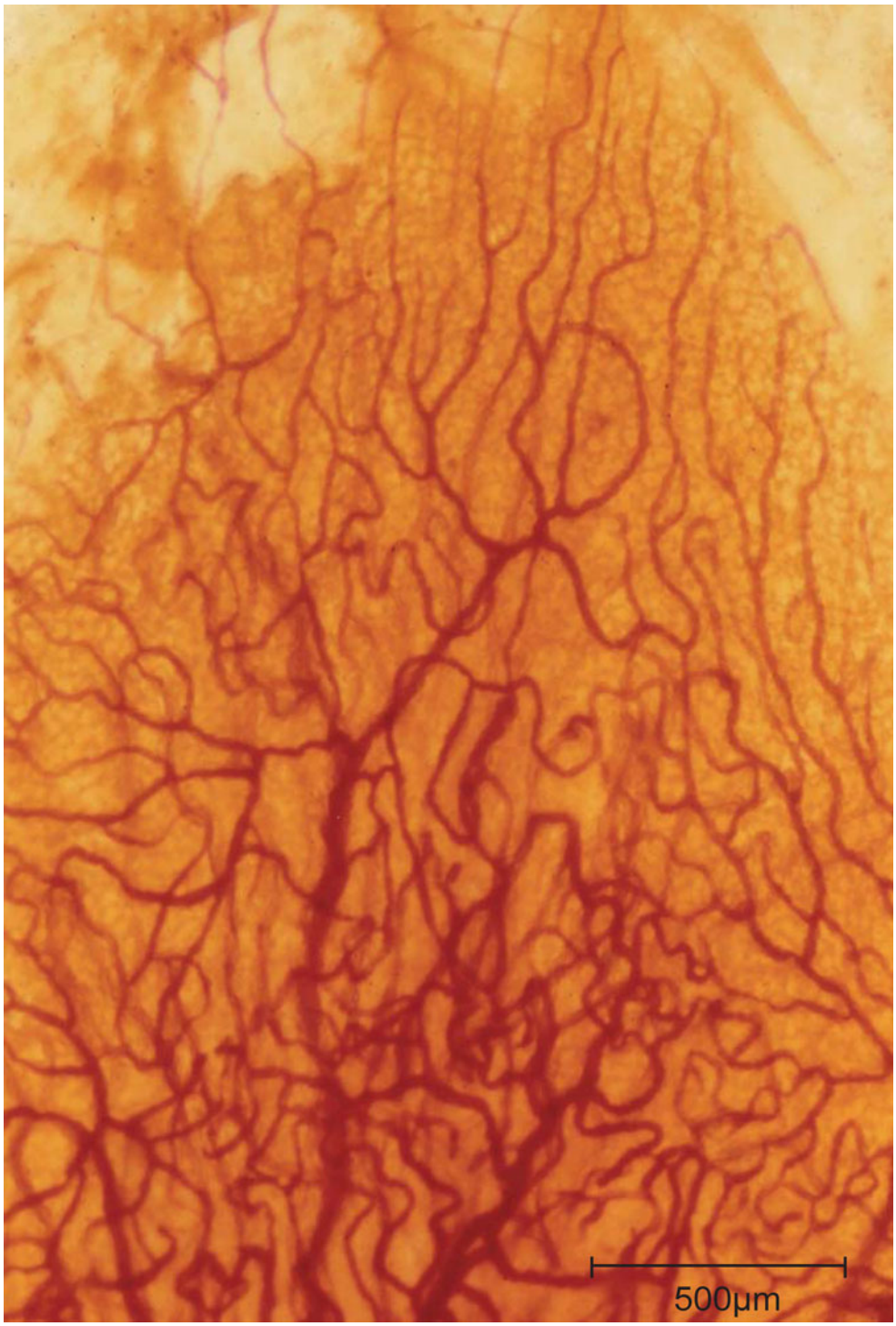

Fig. 3.27 Capillary network of human utricular macula. The dense network is restricted to the macular area. Scale: 500 µm Alkaline phosphatase staining (original ×6.5)

Several small ulcers were found in the colon, attributable to vasculitis of the mucosa.

The patient's left temporal bone was removed 5 h postmortem. The conventional celloidin embedding method was employed to prepare the bone for evaluation.

3.2.3.1 Cochlea

The organ of Corti was either missing or present as a mound on the basilar membrane in all cochlear turns. The spiral ganglion cells were relatively well preserved. The nerve fibers within the osseous spiral lamina were densely populated

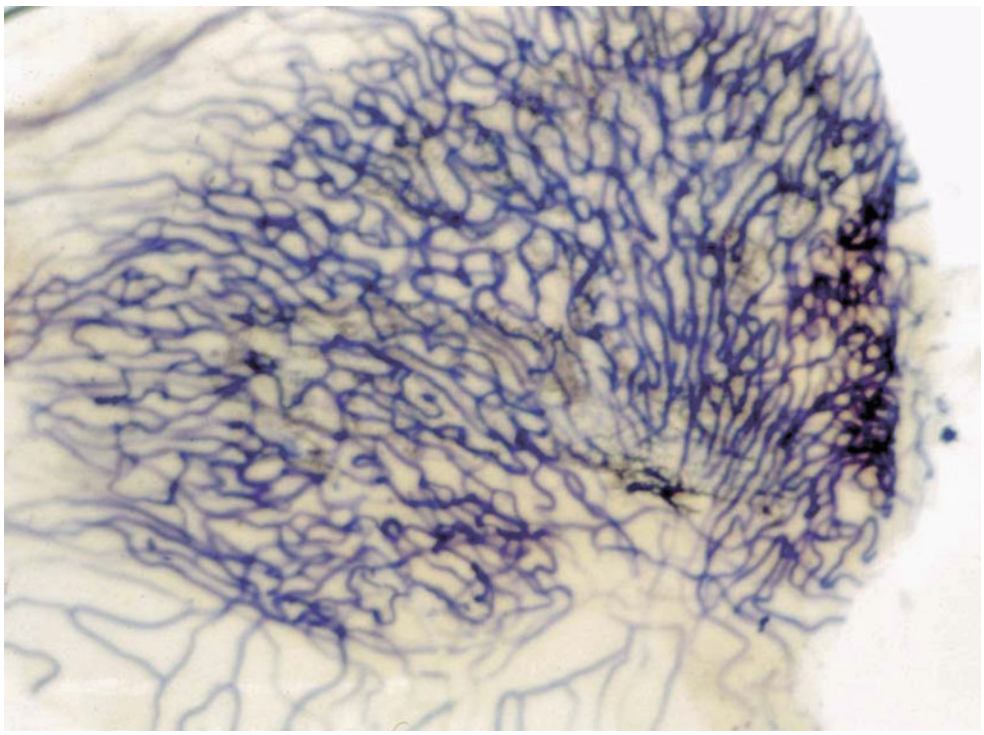

Fig. 3.28 Capillary network of the cat utricular macula. Macular capillaries show a dense network with active alkaline phosphatase activity, while capillaries outside the macula are sparse and less active (original ×2.5)

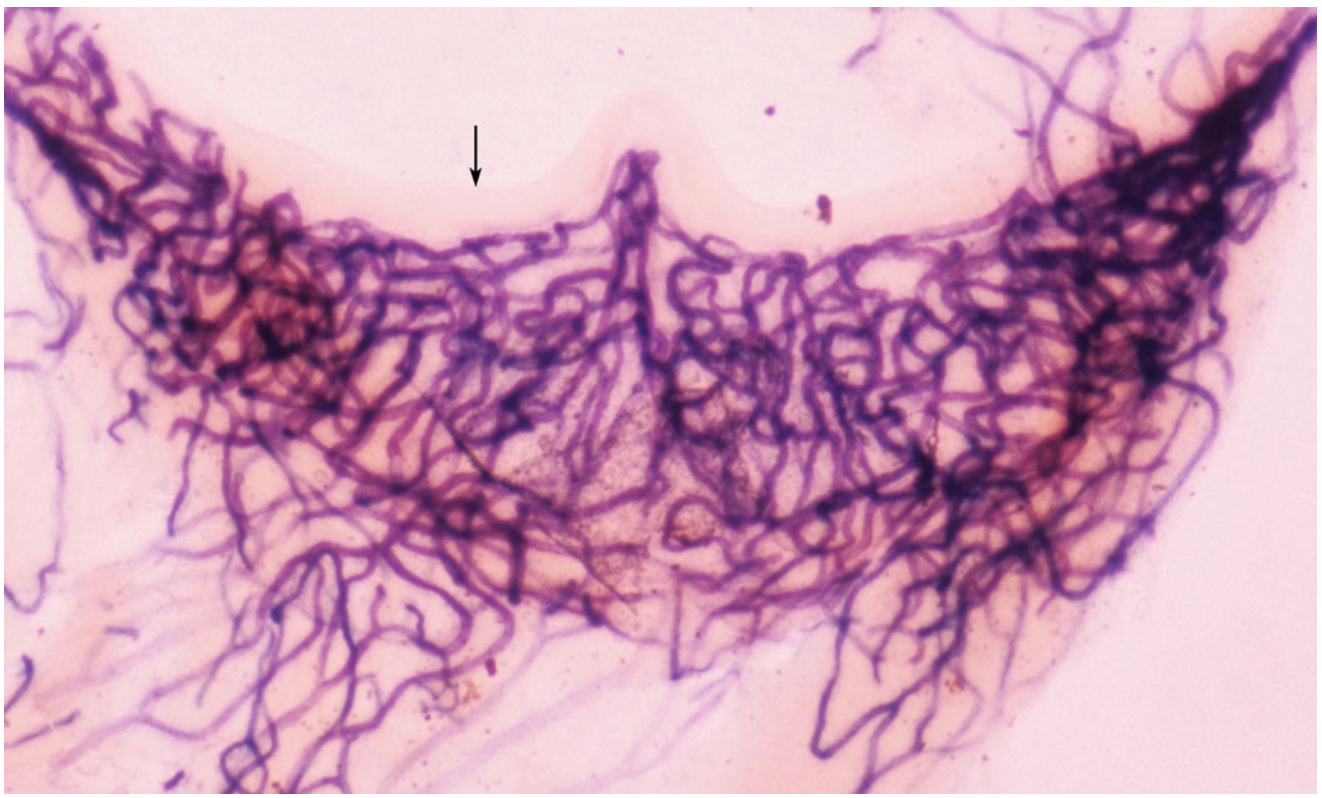

Fig. 3.29 Posterior crista ampullaris of the cat. A dense capillary network is observed underneath the sensory epithelium (*arrow*). Alkaline phosphatase staining (original ×6.5)

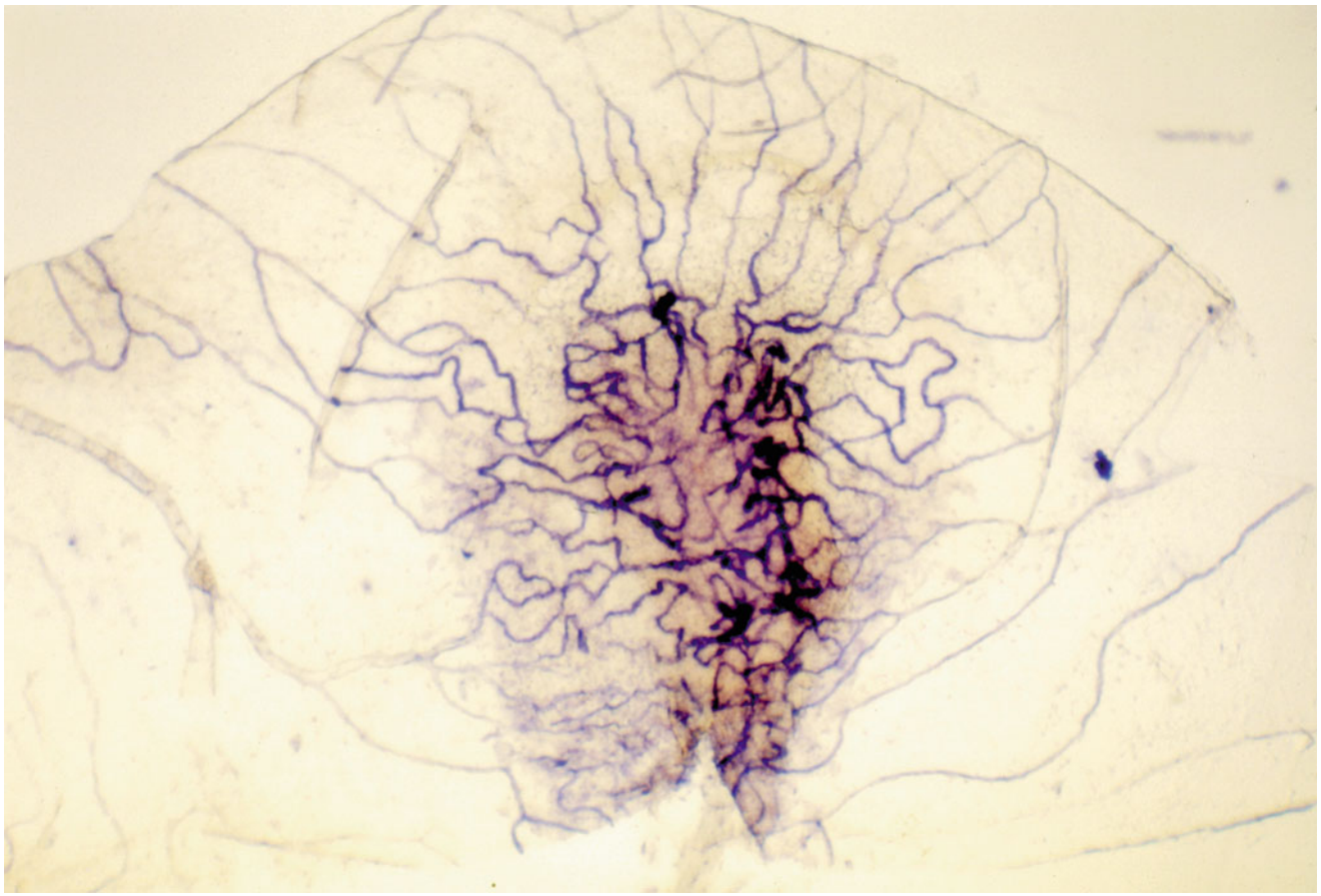

Fig. 3.30 The planum semilunatum of the lateral ampulla of the cat. Alkaline phosphatase staining (original ×6.5)

except in the basal turn (Fig. 3.38a). The tectorial membrane showed degenerative changes and had drooped into the inner sulcus. The remaining portion of the atrophic membrane was encapsulated and lay on the limbus spiralis, in which the interdental cells were missing. A part of the degenerated tectorial membrane adhered to Reissner's membrane (Fig. 3.38c).

The stria vascularis was atrophic throughout the cochlea and eosinophilic precipitate containing floating macrophages was found in the scala media. Reissner's membrane revealed bulging at the site of precipitate formation in the scala media. In the upper turn, heavy concentrations of proteinaceous exudate with fibrin-like crystals and occasional mononuclear cell infiltration were present.

New bone formation was marked in the scala tympani of the basal turn. The round window was completely closed by bony tissue (Fig. 3.38b). Toward the apex, the bony tissue decreased; here the scala tympani was occupied by connective tissue with melanocytes from the basal end up to the 7 mm area.

The blood vessels in the modiolus did not show vasculitis. However, some lymphocytic infiltration was present around the small modiolar artery (Fig. 3.38f).

3.2.3.2 Vestibule and Semicircular Canals

There was remarkable ossification in the patient's vestibule and semicircular canals (Fig. 3.38d). The sensory epithelium of the maculae and cristae was completely missing. Spaces of the vestibule and canals were almost completely occupied by bony tissue, adjacent to which was connective tissue with melanocytes (Fig. 3.38e). A space in the vestibule containing eosinophilic fluid with scattered histiocytes appeared originally to have been endolymphatic space. The superior and inferior divisions of the vestibular nerve showed a marked loss of fibers. The vestibular aqueduct, the paravestibular canaliculus, and the endolymphatic sac appeared almost normal.

In 32 mixed cryoglobulinemia patients, Berrettini et al. [18] found frequent audiovestibular involvement (34 %). Bilateral sensorineural hearing loss was found in seven

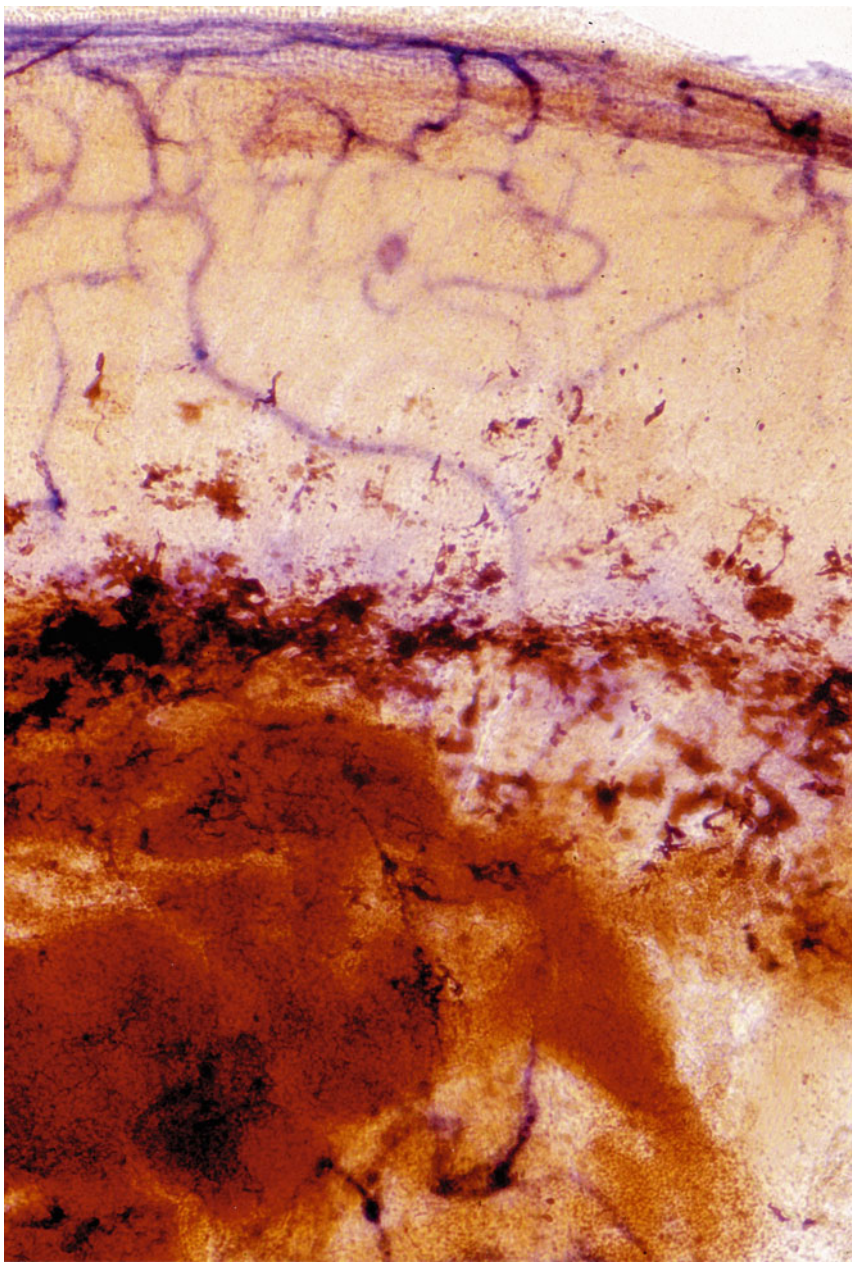

Fig. 3.31 Hemorrhage in the modiolus of a leukemic patient. Twenty-three-year-old woman, surface preparation, alkaline phosphatase staining (original ×6.5)

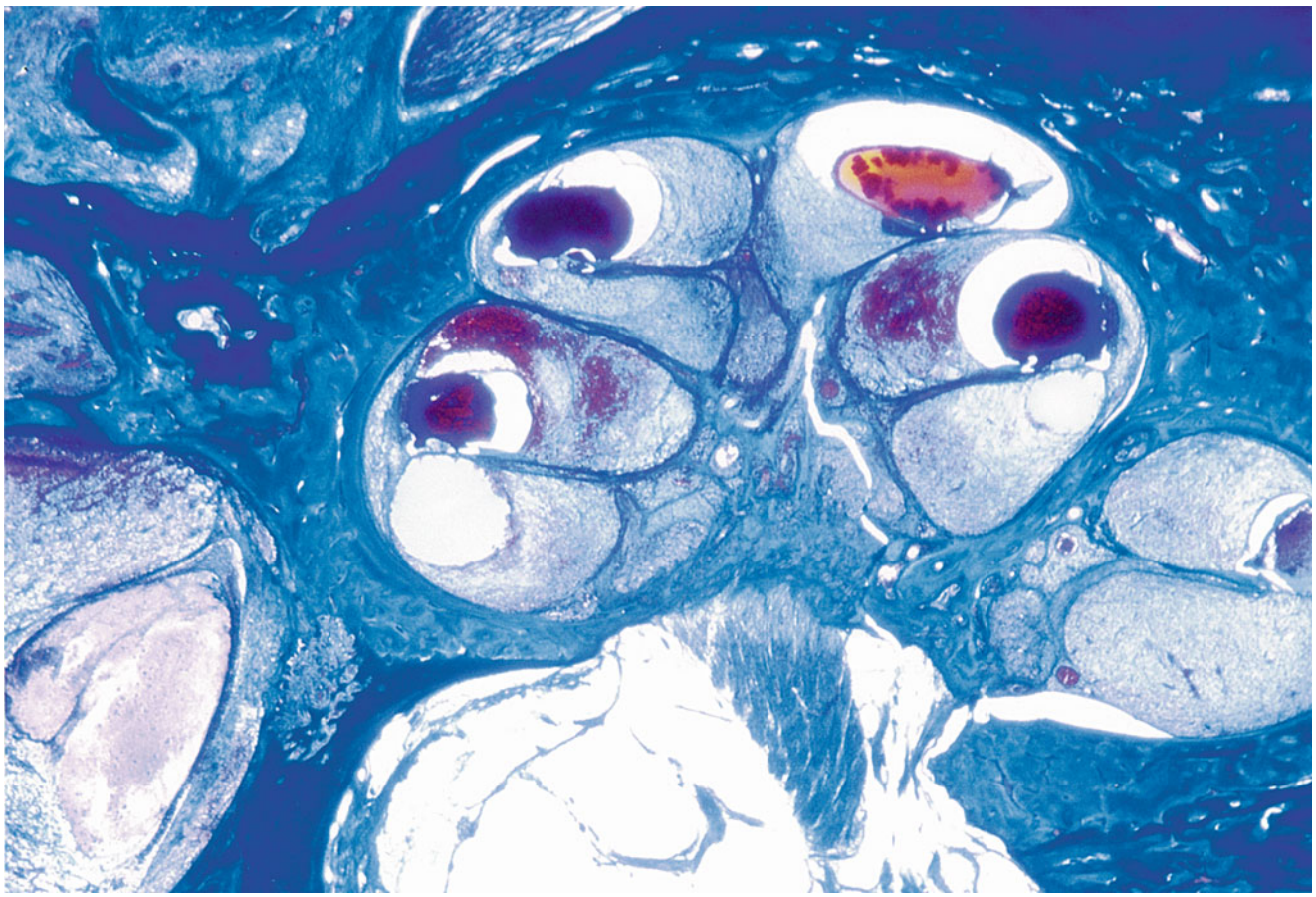

Fig. 3.32 Labyrinthitis in a 16-year-old girl with leukemia. Hemorrhage, granulation, and cell infiltration in the inner ear. Reissner's membrane is distended. Marked hemorrhage is observed in the scala media. The scalae vestibuli and tympani show cell infiltration and hemorrhage. Azan staining (original ×2.5)

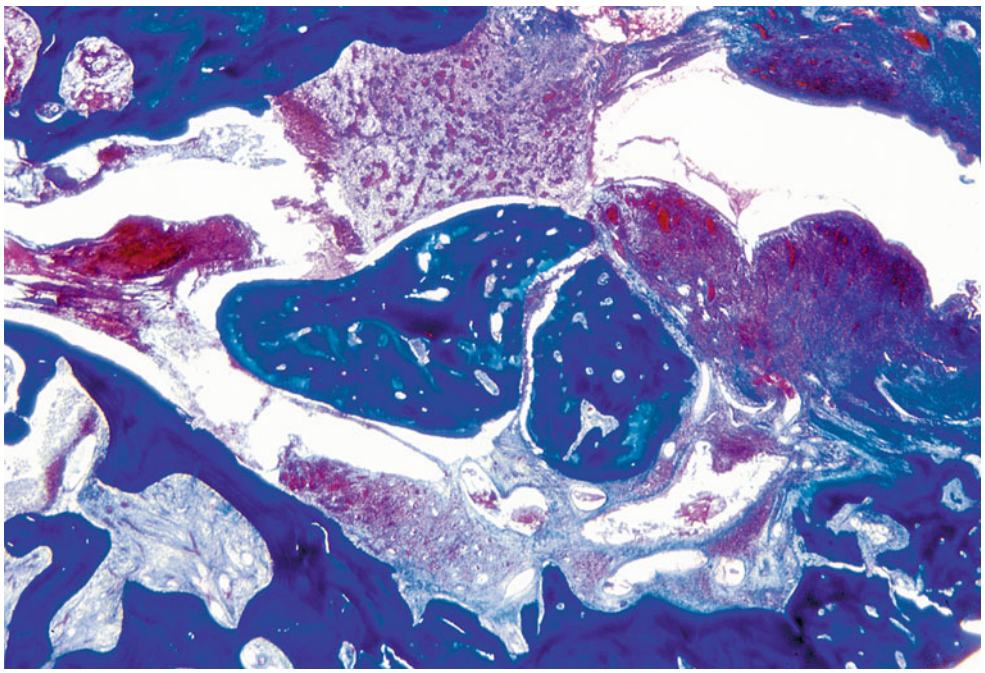

Fig. 3.33 Granulation with hemorrhage in the attic. Azan staining (original ×6.5)

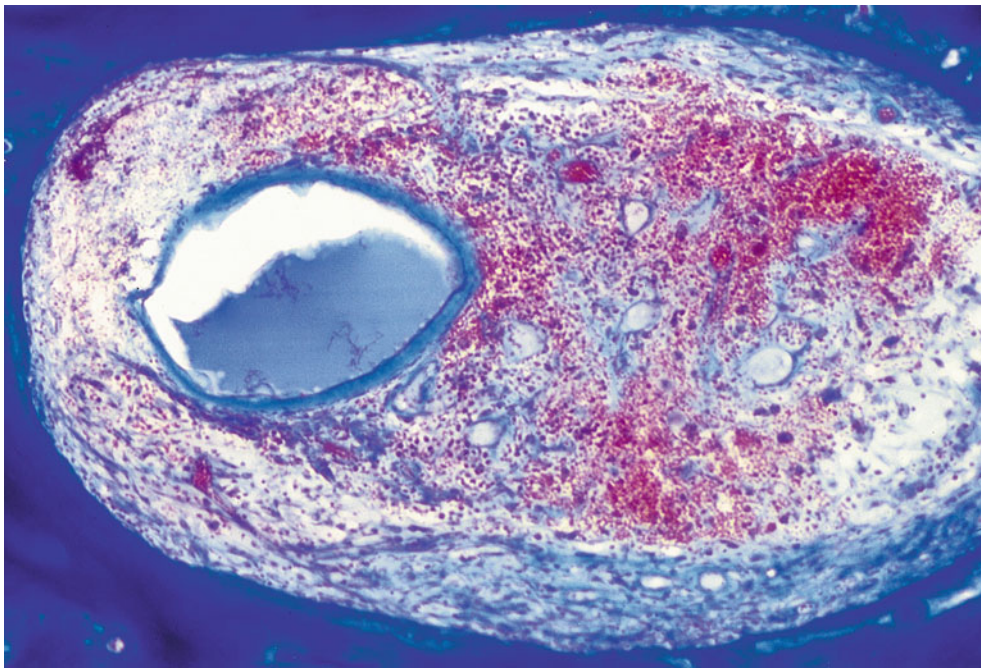

Fig. 3.34 The posterior semicircular canal shows hemorrhage, cell infiltration, and ossification. Basophilic coagulum is present in the semicircular duct (original ×16)

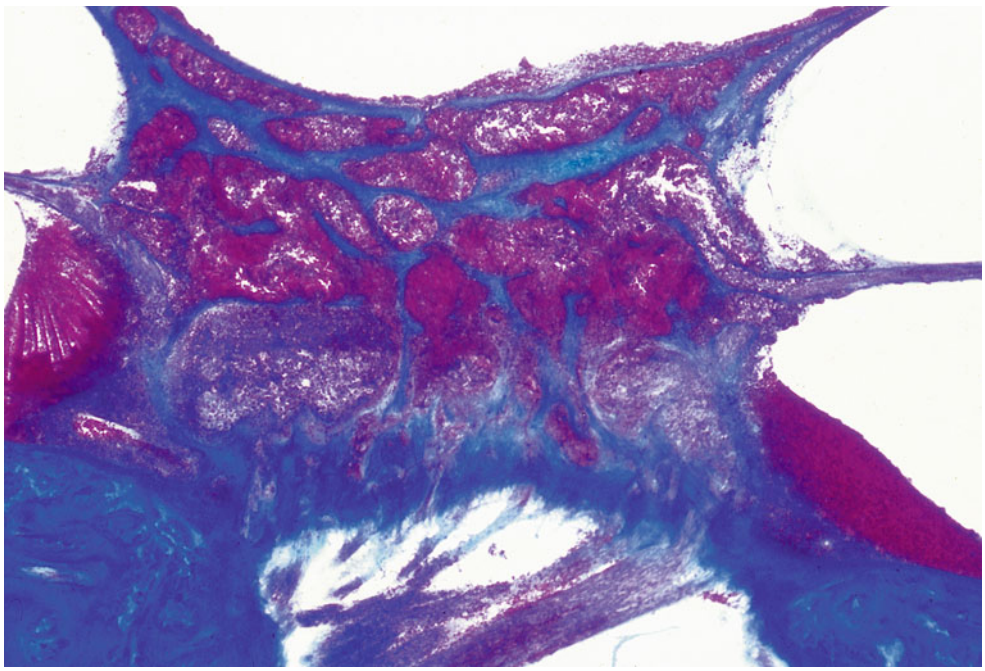

Fig. 3.35 Massive hemorrhage in the modiolus and scala tympani of a patient with acute myeloid leukemia. There is less hemorrhage in Rosenthal's canal and the internal auditory meatus. Forty-six-year-old man, Azan staining (original ×6.5)

patients (22 %), and altered vestibular function test results in another seven (22 %). Historical and clinical data showed a high incidence of benign paroxysmal positional vertigo in these patients. Immune complex-mediated microvascular involvement of the labyrinthine vessels is considered responsible for inner ear damage in mixed cryoglobulinemia.

3.2.4 Takayasu's Arteritis [19]

Takayasu's arteritis (pulseless disease, aortic arch syndrome) is a systemic autoimmune disease. Elevation of serum immune complexes, C-reactive protein, and erythrocyte sedimentation rate that precede hearing deterioration, and

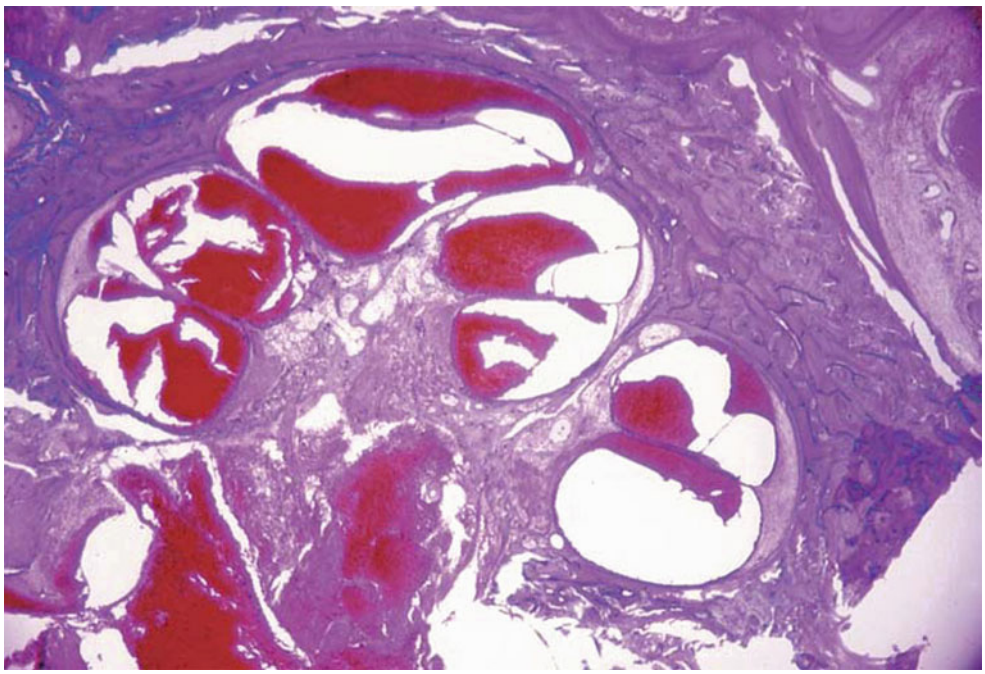

Fig. 3.36 Massive hemorrhage in the cochlea of a 6-year-old-boy with aplastic anemia. Hemorrhage is marked in the scala vestibuli, scala tympani, and internal auditory canal. Blood was not found in the scala media or Rosenthal's canal

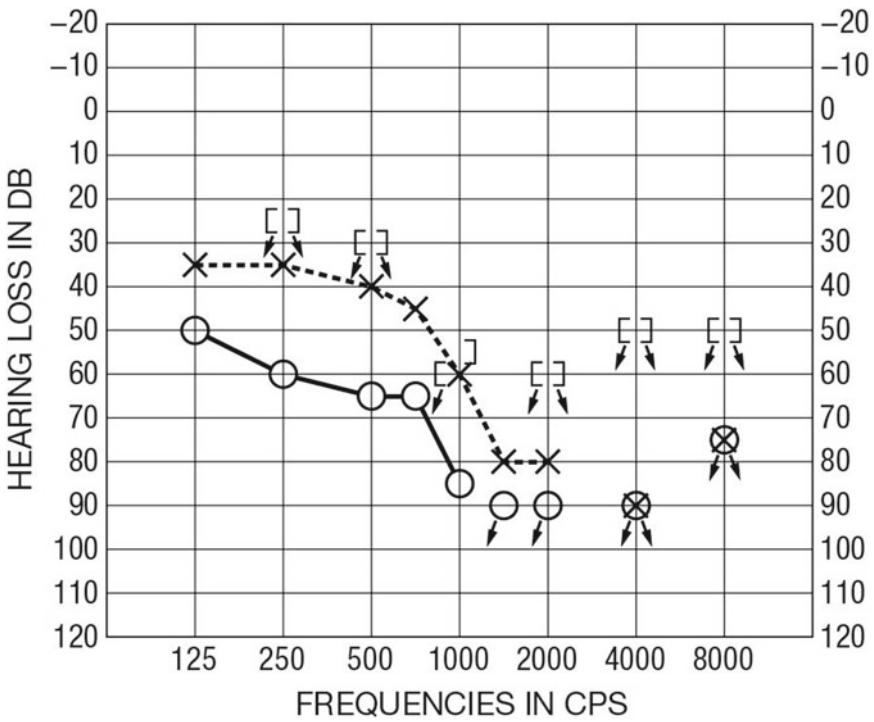

Fig. 3.37 Audiogram of a patient with Buerger's disease, July 1960 [15]

improvement with steroid therapy are indicative of autoimmune disease [20–22].

Thickening of the adventitia, necrosis of the media, and intimal thickening in the aorta are pathognomonic observations in this disease. The cause of the hearing loss associated with Takayasu's arteritis is unknown.

A 45-year-old woman developed bilateral insidious hearing loss. At 29 years of age, she had noted that her radial pulse

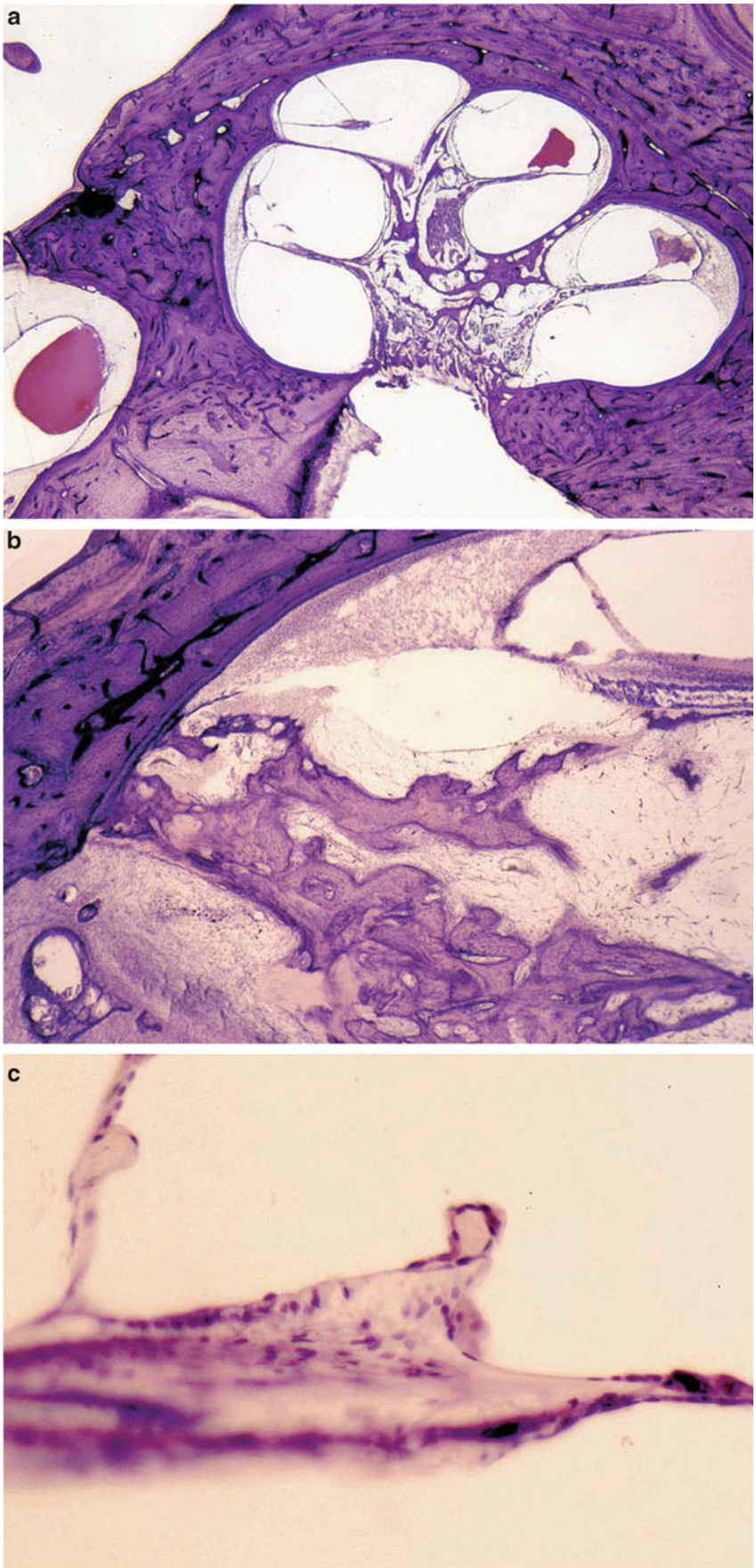

Fig. 3.38 A 62-year-old woman with cryoglobilinemia. (**a**) Accumulations of eosinophilic coagulum in part of the scala media and saccule (×4). (**b**) Near the round window, the scala tympani shows fibrosis and new bone formation. The round window is completely closed (×10). (**c**) The tectorial membrane is partly rolled-up at the vestibular lip of the limbus, covered by a single cell layer. Part of the membrane adheres to Reissner's membrane. Marked loss of interdental cells is evident. The osseous spiral lamia is devoid of nerve fibers (×65). (**d**) The vestibulum and semicircular canal show new bone formation. Accumulation of eosinophilic coagulum in the endolymphatic space is present (×10). (**e**) Cross section of the anterior semicircular canal shows new bone formation along the inside of the canal and around the semicircular duct (×25). (**f**) Cell infiltration in the perivascular space around the arteriole in the modiolus (original ×40) [17]

Fig. 3.38 (continued)

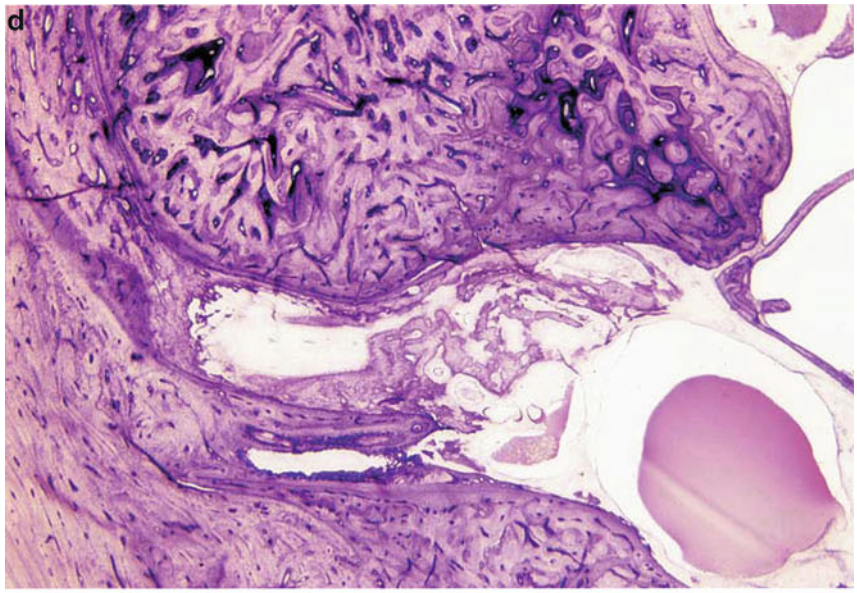

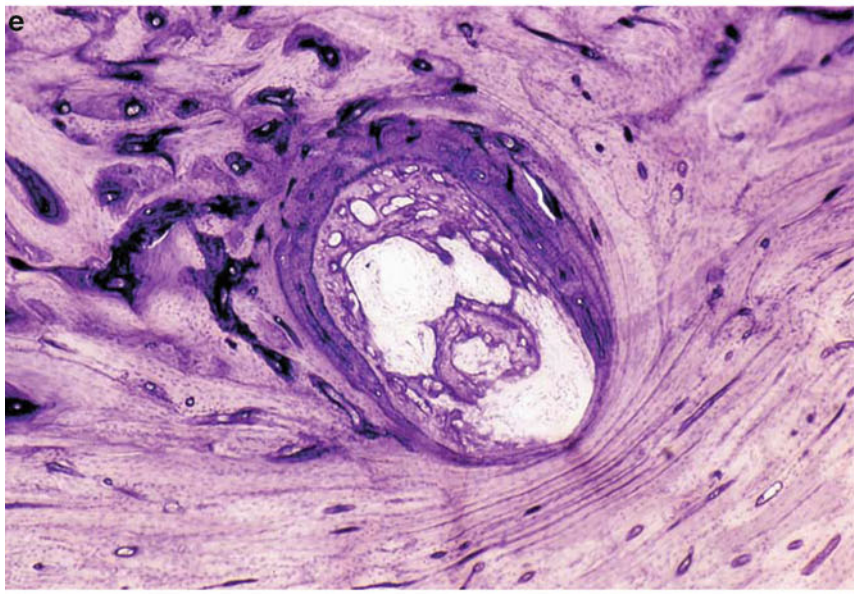

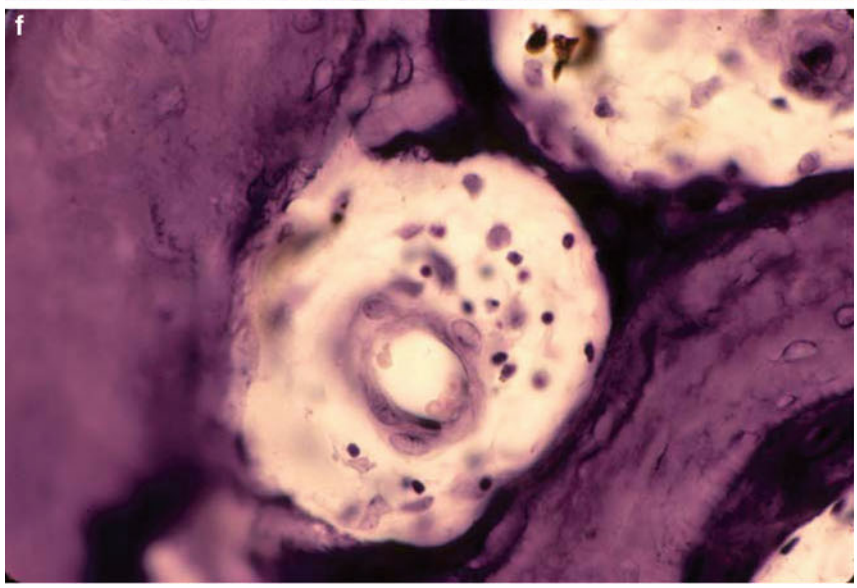

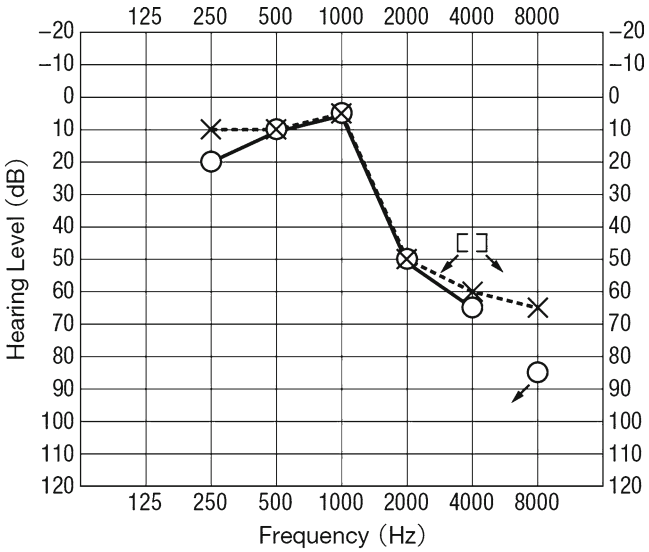

Fig. 3.39 Takayasu's arteritis. Audiogram of a 45-year-old woman [19]

was not palpable bilaterally. Angiographic examination at that time revealed bilateral obliteration of her subclavian arteries. The patient was diagnosed with Takayasu's arteritis, and was treated with corticosteroids. Her eventual cause of death was cardiac failure due to aortic insufficiency. Autopsy revealed dilatation of the aorta, the inner surface of which showed fine wrinkles and decreased elasticity. Histopathologically, there was thickening of the adventitia, disruption of elastic tissue of the media, and fibrous thickness of the intima. Marked focal lymphocytic infiltration was found. The arteries involved were the proximal portion of the pulmonary artery; the brachiocephalic trunk; the right axillary artery; the proximal portion of the right brachial artery; the left subclavian, axillary, and brachial arteries; and the entire length of the bilateral common and external carotid arteries. In contrast, the internal carotid arteries were remarkably well preserved. The vertebral arteries were also free from pathology. Blood vessels in the cranial cavity were normal.

An audiogram taken 4 months prior to the patient's death showed bilateral abrupt (sharp-cut) hearing loss at 1,000 Hz (Fig. 3.39). The temporal bones revealed almost complete loss of the outer hair cells in an area up to 13 mm from the basal end in the right ear, and in an area up to 12 mm in the left ear (Fig. 3.40). The inner hair cells were partly present in the same area in the right ear, but showed marked degeneration and loss in the left ear. In the remaining area of the cochleae, the inner and outer hair cells were well preserved. The cochlear neurons were almost totally absent in the basal turn bilaterally (Fig. 3.41).

The spiral vessel beneath the tunnel of Corti, the vas spirale, looked normal throughout the cochleae. In this case, the vessels within the cochleae and the internal auditory canals showed no pathology. The vertebral arteries were free from pathology. Thus, the hearing loss in this patient with Takayasu's disease did not result from vasculitis.

3.2.5 Diabetes Mellitus [24]

Diabetes mellitus is a systemic disease caused by abnormal glucose metabolism. Although it has been known for decades that diabetes mellitus causes sensorineural hearing loss, the histopathological changes associated with the disease are not yet fully understood.

Jørgensen [23] reported that many diabetic patients showed appreciable PAS-positive precipitates in the capillary walls of the stria vascularis. In some preparations, the capillary wall was 10–20 times thicker than normal. The PAS-positive substance was partly homogenous, partly organized in a net-like structure that resembled splitting of the basement membrane when viewed under high power. The strial changes were not associated with age, but were closely associated with the duration of diabetes.

Kariya et al. [24, 25] examined the temporal bones of patients with type 1 (insulin-dependent) and type 2 (non-insulin-dependent) diabetes mellitus from the temporal bone collection at the University of Minnesota, Department of Otolaryngology, Head and Neck Surgery. The temporal bones from patients with type 2 diabetes mellitus were divided into two groups: patients who had received insulin therapy and those treated with oral hypoglycemic drugs. Because there was a large difference in average age between the type 1 and type 2 groups, the researchers assembled an age-matched control group for each type (control groups 1 and 2).

In patients with both types of diabetes mellitus, the wall of the spiral modiolar artery was thick compared with the age-matched control groups (Fig. 3.42a). The wall thickening was similar in the type 1 group and type 2 group treated with hypoglycemic drugs. However, the vessel walls of type 2 patients on insulin therapy were thicker than those of the type 1 group. Because there was no significant difference in vessel wall thickness between the normal control groups 1 and 2, the difference in diabetic groups was not due to age, but to pathology of the vessel wall [26].

The vessel wall ratio was determined using the following formula:

$$\text{Vessel wall ratio}(\%) = \text{vessel wall thickness} / \text{outer diameter of the vessel} \times 100$$

There was a significant correlation between the right and left temporal bones in vessel wall thickness and vessel wall ratio in type 1 and type 2 diabetic patients.

Vessel wall thickness and vessel wall ratio were greater in patients with diabetes-related complications, e.g., hemodialysis,

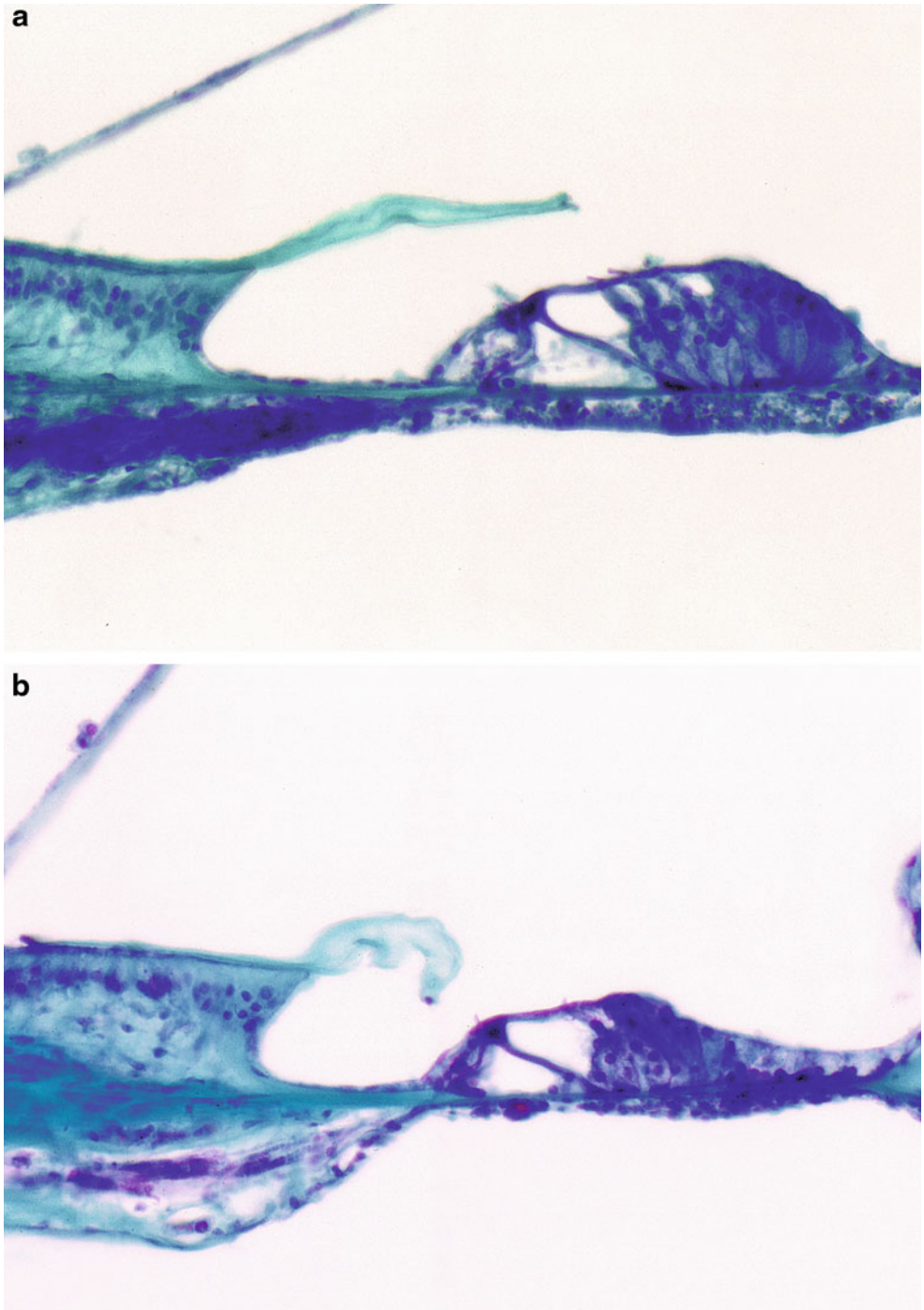

Fig. 3.40 Takayasu's arteritis. (**a**) The organ of Corti is preserved in the middle turn of the right cochlea. (**b**) The outer hair cells are missing in the first and second rows. Loss of the nerve fibers within the osseous spiral lamina is apparent in the lower basal turn of the right cochlea [19]

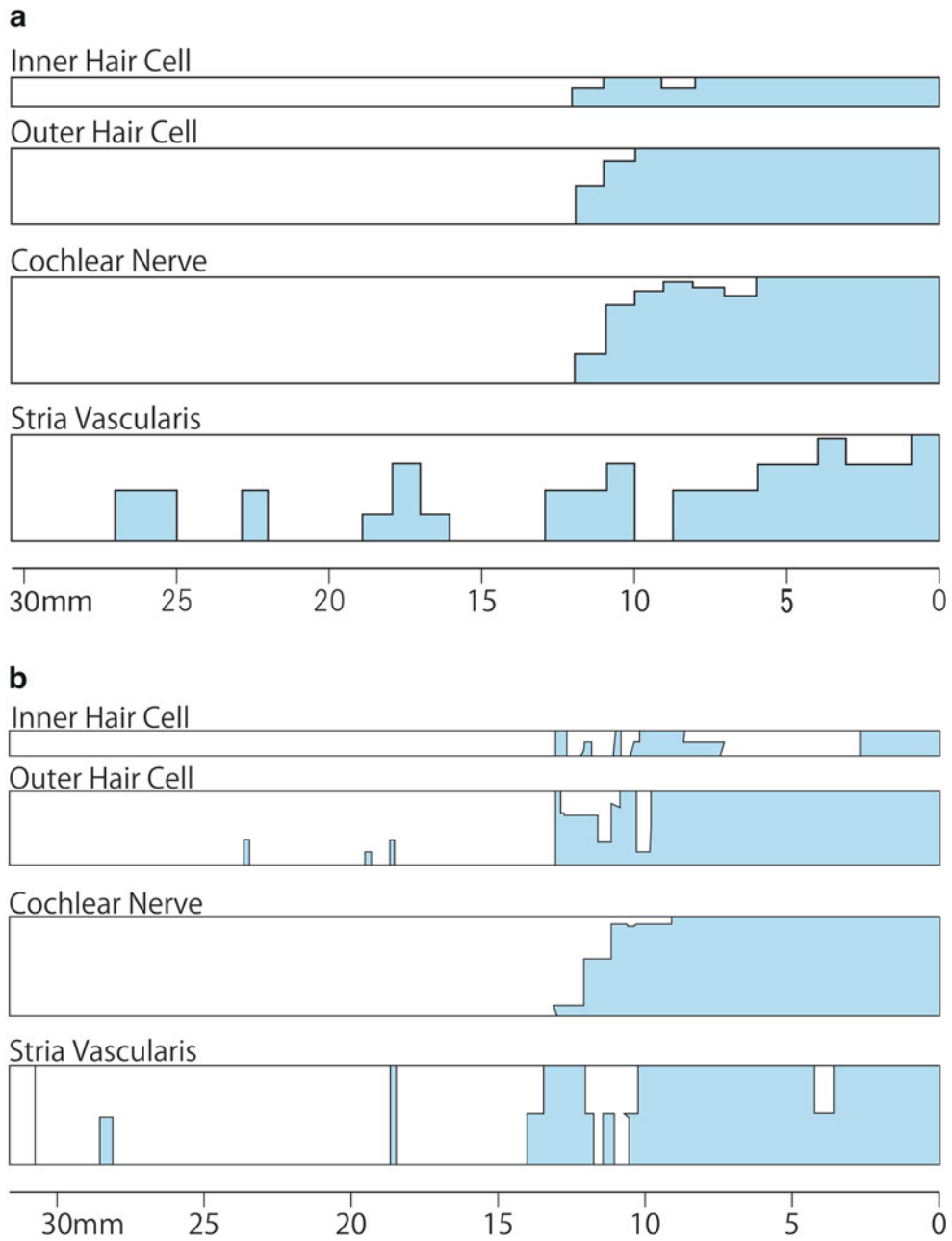

Fig. 3.41 Takayasu's arteritis. (**a**) Cochleogram of the left ear. (**b**) Cochleogram of the right ear. The *colored areas* indicate location and degree of cell loss [19]

diabetic retinopathy, diabetic neuropathy, diabetic cardiomyopathy, myocardial infarction, and hypertension, than in those without complications.

There is a close association between diabetes mellitus and arteriosclerosis. Various mediators produced in the endothelium of diabetic patients, including nitric oxide, prostanoids, endothelin, tissue-type plasminogen activator, plasminogen activator inhibitor-1, adhesion molecules, and inflammatory cytokines, cause endothelial dysfunction, leading eventually to arteriosclerosis and diabetic angiopathy.

The inner ear vascular wall is thickened in diabetic patients. This thickening can disrupt blood flow in the inner ear, resulting in sensorineural hearing loss.

Several changes are found in the cochlea of type 2 diabetic patients, including loss of the outer hair cells, thickening of the walls of the vas spirale and strial capillaries, and degeneration of the stria vascularis (Fig. 3.42b–d) [24–26].

Diabetes mellitus is known to be a risk factor for sudden deafness [27].

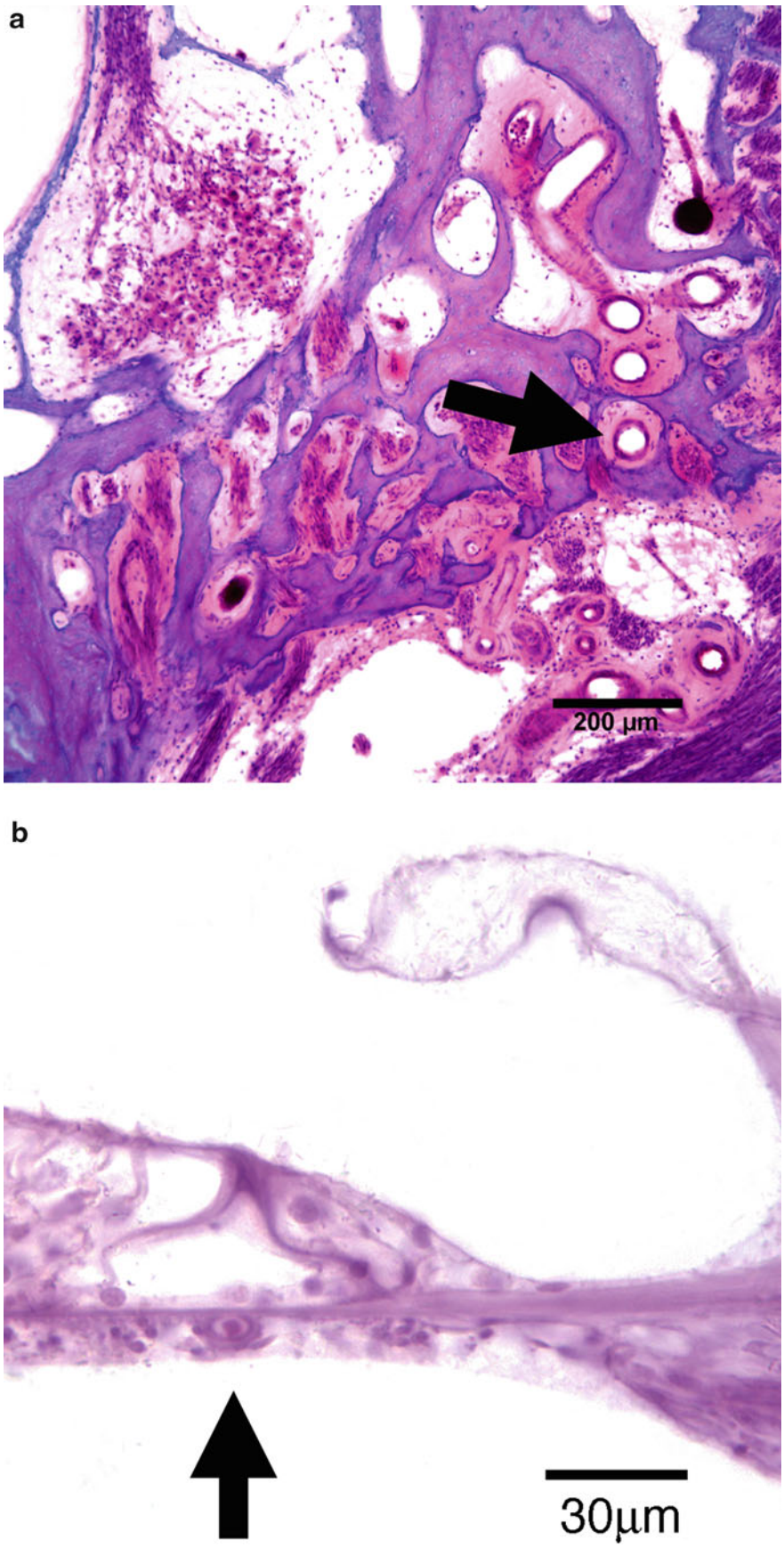

Fig. 3.42 Diabetes mellitus and the inner ear. (**a**) Vessels in the modiolus of the left cochlea in a patient with type 2 diabetes mellitus on insulin therapy. The vessel wall of the spiral modiolar artery is thickened (*arrow*). There is no decrease of spiral ganglion cells. Fifty-year-old man with type 2 diabetes mellitus (DM) in insulin therapy group [24]. (**b**) Spiral vessel wall thickening (*arrow*). Fifty-three-year-old woman with type 2 DM in insulin therapy group [24. (**c**) Decreased cell numbers in the spiral ligament. Fifty-six-year-old woman with type 2 DM in insulin therapy group [24]. (**d**) Atrophy of the stria vascularis. Fifty-six-year-old woman with type 2 DM in insulin therapy group [24] (Courtesy of Dr. Kariya)

Fig. 4.42 (continued)

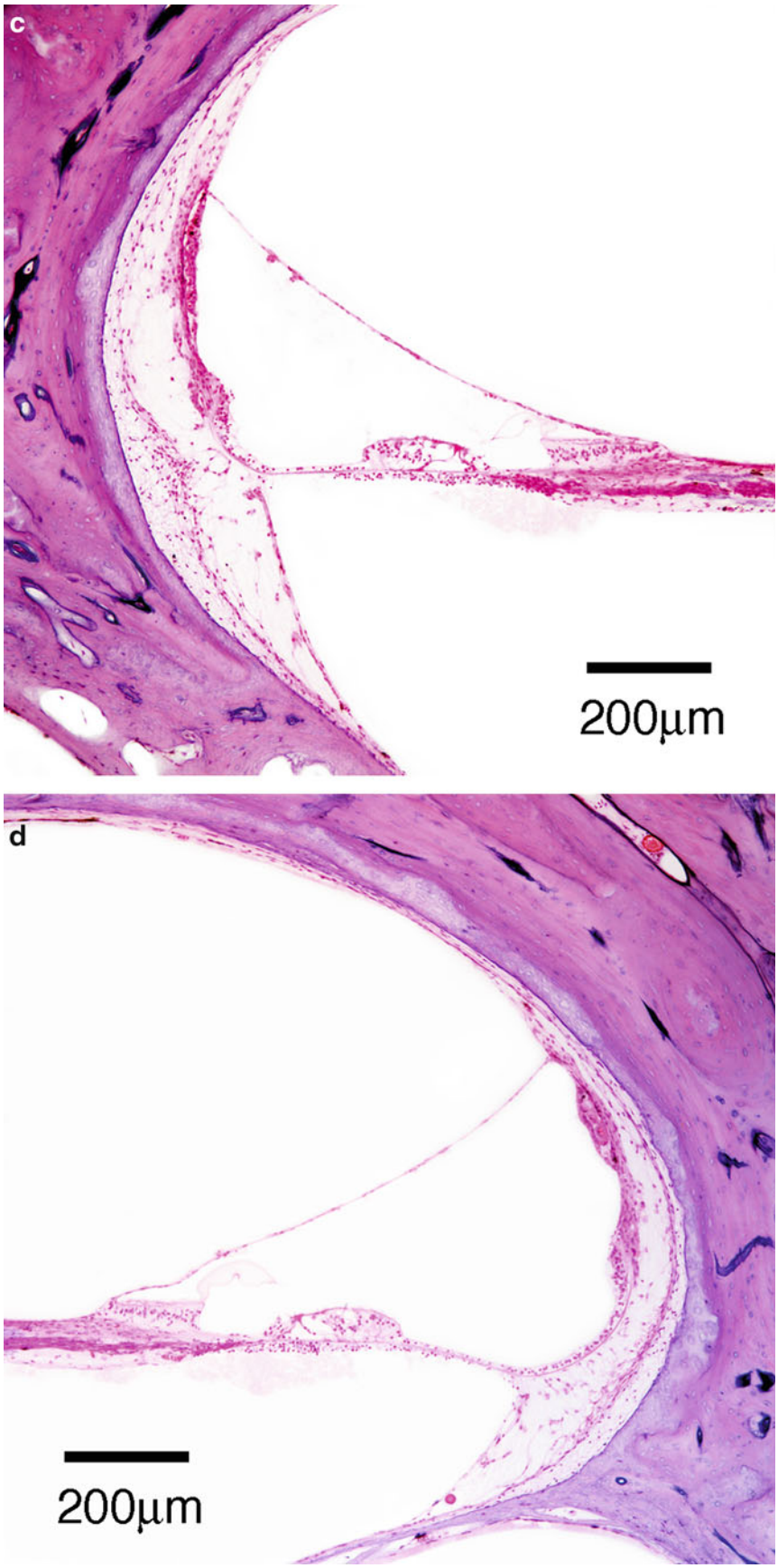

References

1. Suzuki A, Nomura Y (1994) The interscalar septum of the human cochlea. Showa Univ J Med Sci 6:105–109
2. La Ferriere KA, Arenberg IK, Hawkins JE, Johnsson LG (1974) Melanocytes of the vestibular labyrinth and their relationship to the microvasculature. Ann Otol Rhinol Laryngol 83:685–694
3. Wästerström SA (1984) Accumulation of drugs on inner ear melanin. Therapeutic and ototoxic mechanisms. Scand Audiol 23(Suppl):1–40
4. Franz P, Aharinejad S, Firbas W (1990) Melanocytes in the modiolus of the guinea pig cochlea. Acta Otolaryngol (Stockh) 109:221–227
5. Johnsson LG, Hawkins JE Jr (1972) Vascular changes in the human inner ear associated with aging. Ann Otol Rhinol Laryngol 81:364–376
6. Lawrence M (1966) Effects of interference with terminal blood supply on organ of Corti. Laryngoscope 76:1318–1337
7. Nomura Y, Hiraide F (1968) Cochlear blood vessel, a histochemical method of its demonstration. Arch Otolaryngol 88:231–237
8. Nomura Y, Ishii T, Ishii D (1970) The histochemistry of the spiral prominence. Arch kiln exp Ohren Nasen Kehlkopfheilkd 195:266–275
9. Kirikae I, Nomura Y, Hiraide F (1969) The capillary in the human cochlea. Acta Oto-laryngol 67:1–8
10. Nomura Y (1977) Vascular supply to the organ of Corti. Arch Oto-Rhino-Laryngol 214:213–220
11. Corti A (1851) Recherches sur l'organe de l'ouie des mammifères. Z Wiss Zool 3:109–169
12. Nomura Y, Hiraide F (1969) The capillary in the human vestibular labyrinth. Ann Otol Rhinol Laryngol 78:1220–1226
13. Retzius G (1884) Das Gehörorgan der Wirbelthiere. Morphologisch-histologische studien. II Das Gehörorgan der Vögel und der Säugethiere. Samson & Wallin, Stockholm
14. Nomura Y, Balogh K Jr (1964) Metabolic pathways in the vestibular labyrinth as revealed by histochemical technics. Acta Otolaryngol 57:484–492
15. Kirikae I, Nomura Y, Shitara T, Kobayashi T (1962) Sudden deafness due to Buerger's disease. Arch Otolaryngol 75:502–505
16. Lippman HI (1952) Cerebrovascular thrombosis in patients with Buerger's disease. Circulation 5:680–692
17. Nomura Y, Tsuchida M, Mori S, Sakurai T (1982) Deafness in cryoglobulinemia. Ann Otol Rhinol Laryngol 91:250–255
18. Berrettini S, Ferri C, La Civita L, Segnini G, Lombardini F, Bruschini P, Longombardo G, Sellari-Franceschini S (1995) Inner ear involvement in mixed cryoglobulinemia patients. Br J Rheumatol 34:370–374
19. Nomura Y, Kitamura K (1979) Abrupt (sharp cut) type sensorineural hearing loss-a human temporal bone study-. Auris Nasus Larynx 6:13–21
20. Kanzaki J, Ino T, Takahashi M, Koga k (1975) Clinical investigations on fluctuant hearing loss without vertigo. Audiol Japan 18:88–98
21. Kanzaki J, Ouchi T (1981) Steroid-responsive bilateral sensorineural hearing loss and immune complexes. Arch Otorhinolaryngol 230:5–9
22. Maruyoshi H, Toyama K, Kojima S, Kawano H, Ogata N, Miyamoto S, Sakamoto T, Yoshimura M, Ogawa H (2005) Sensorineural hearing loss combined with Takayasu's arteritis. Intern Med 44:124–128
23. Jørgensen BM (1964) Changes of aging in the inner ear, and the inner ear in diabetes mellitus. Histological studies. Acta Oto-Laryngol Suppl 188:125–128
24. Kariya S, Fukushima H, Nishizaki K (2011) Temporal bone histopathology in patients with diabetes mellitus. Pract Otol (Kyoto) 104(10):678–679
25. Kariya S, Cureoglu S, Fukushima H, Morita N, Baylan MY, Maeda Y, Nishizaki K, Paparella MM (2010) Comparing the cochlear spiral modiolar artery in type-1 and type-2 diabetes mellitus: a human temporal bone study. Acta Med Okayama 64:375–383
26. Fukushima H, Cureoglu S, Schachern PA, Paparella MM (2006) Effects of type 2 diabetes mellitus on cochlear structure in humans. Arch Otolaryngol Head Neck Surg 132:934–938
27. Japan intractable disease information center (www.nanbyou.or.jp), Sudden deafness

Sudden Deafness

4

Abstract

Sensorineural hearing loss of sudden onset may occur without apparent cause. In these cases it is essential to explore underlying diseases. The term "sudden deafness" has been used in two ways: either as a description of symptoms, or to mean idiopathic sudden deafness in which clinical examinations fail to find the cause. In patients with idiopathic sudden deafness, hearing may return spontaneously, or by treatment, may fail to return with treatment, or may show varying degrees of partial recovery. This chapter discusses causes of sudden deafness related to the histopathology of the tectorial membrane. In cases where histopathology points to viral infection as the cause, the clinical diagnosis of idiopathic sudden deafness changes to viral labyrinthitis. Asymptomatic mumps should be considered in cases of sudden deafness. Three studies evaluated IgM levels in patients with sudden deafness and found that 5–7 % were affected by asymptomatic mumps. Histopathological studies of the temporal bones from patients with sudden deafness are essential, but new approaches are needed for more complete understanding of the condition.

Keywords

Asymptomatic mumps • Cochlear neuronitis • Relapsing polychondritis • Sudden deafness • Tectorial membrane • Viral labyrinthitis

4.1 Histopathology of Sudden Deafness

Several diseases are known to cause sudden deafness as a symptom.

Idiopathic sudden deafness occurs without apparent cause and is unique in that hearing loss may be restored. According to the systematic review of Chau et al. [1], the suspected etiologies for patients suffering from sudden sensorineural hearing loss included idiopathic (71.0 %), infectious disease (12.8 %), otologic disease (4.7 %), trauma (4.2 %), vascular or hematologic disease (2.8 %), neoplasia (2.3 %), and other causes (2.2 %). If we could assess the cause of sudden deafness with histopathology, fewer cases would be labeled idiopathic.

There are many limitations to using temporal bone histopathology to determine the true etiology or pathology of sensorineural hearing loss. The findings may not represent the features of the disease, because of the long interval between the onset of disease and histopathological exam. Affected cells may degenerate and disappear. The repair process may have occurred and not be ongoing. Furthermore, in the time between the onset of sensorineural hearing loss and death, life-style related diseases and the aging process will definitely progress in the inner ear. Nevertheless, temporal bone studies may reveal elements of the etiology of the disease. Conversely, these studies may reveal nothing but normal findings. In these cases, more advanced methodology is needed to elucidate the cause of disease.

Cases of sudden deafness show similar histopathological findings to cases of viral labyrinthitis, i.e., atrophy of the organ of Corti, shrinkage of the tectorial membrane, and loss of hair cells. Pathological findings are restricted mainly to

Y. Nomura, *Morphological Aspects of Inner Ear Disease*, DOI 10.1007/978-4-431-54204-9_4,

the cochlea and saccule. The utricle and semicircular canals show either mild or no changes.

Schuknecht and Donovan [2] compared the pathologic findings in 12 ears with sudden deafness to those found in known cases of viral labyrinthitis caused by mumps, measles, rubella, and herpes zoster oticus. They found similar changes, especially in cases of mumps and rubella. This similarity is quite understandable because 5–7 % of patients with sudden deafness actually have mumps. This will be discussed further in this chapter and in Sect. 6.3, Mumps.

4.2 The Tectorial Membrane

Histopathology of the temporal bones in cases of sudden deafness often shows marked changes of the tectorial membrane. The tectorial membrane is generally detached from the surface of the organ of Corti in normal temporal bone cases, even when they are well preserved. Postmortem autolysis and the effects of aging are less pronounced in the tectorial membrane than in the other cells of the cochlea. This difference is because of the paucity of cellular components in the tectorial membrane, whose major components are fibrils and nonfibrillar matrix [3].

One commonly seen change in patients with viral diseases such as measles and mumps is "rolled-up" of the tectorial membrane. Rolled-up of the tectorial membrane is also reported in cases of sudden deafness, although not all cases show this change. The rolled-up tectorial membrane is covered by a single cell layer, indicating that this change did not occur postmortem (Figs. 4.1 and 4.2). Another common finding in patients with viral disease is loss of the interdental cells.

If the rolled-up change is caused by viral infection, we expect to induce similar changes in experimental animal models. In a study using guinea pigs, human herpes simplex virus (HSV type 1) was inoculated into the tympanic cavity or scala tympani of the basal turn of the cochlea. Inflammation occurred in the scala tympani of the basal turn, with less inflammation toward the apex. No cell infiltration was observed in the scala media. The tectorial membrane showed the rolled-up changes. HSV viral antigen was detected using a fluorescence method. Positive fluorescence was found within the tectorial membrane as well as in the interdental

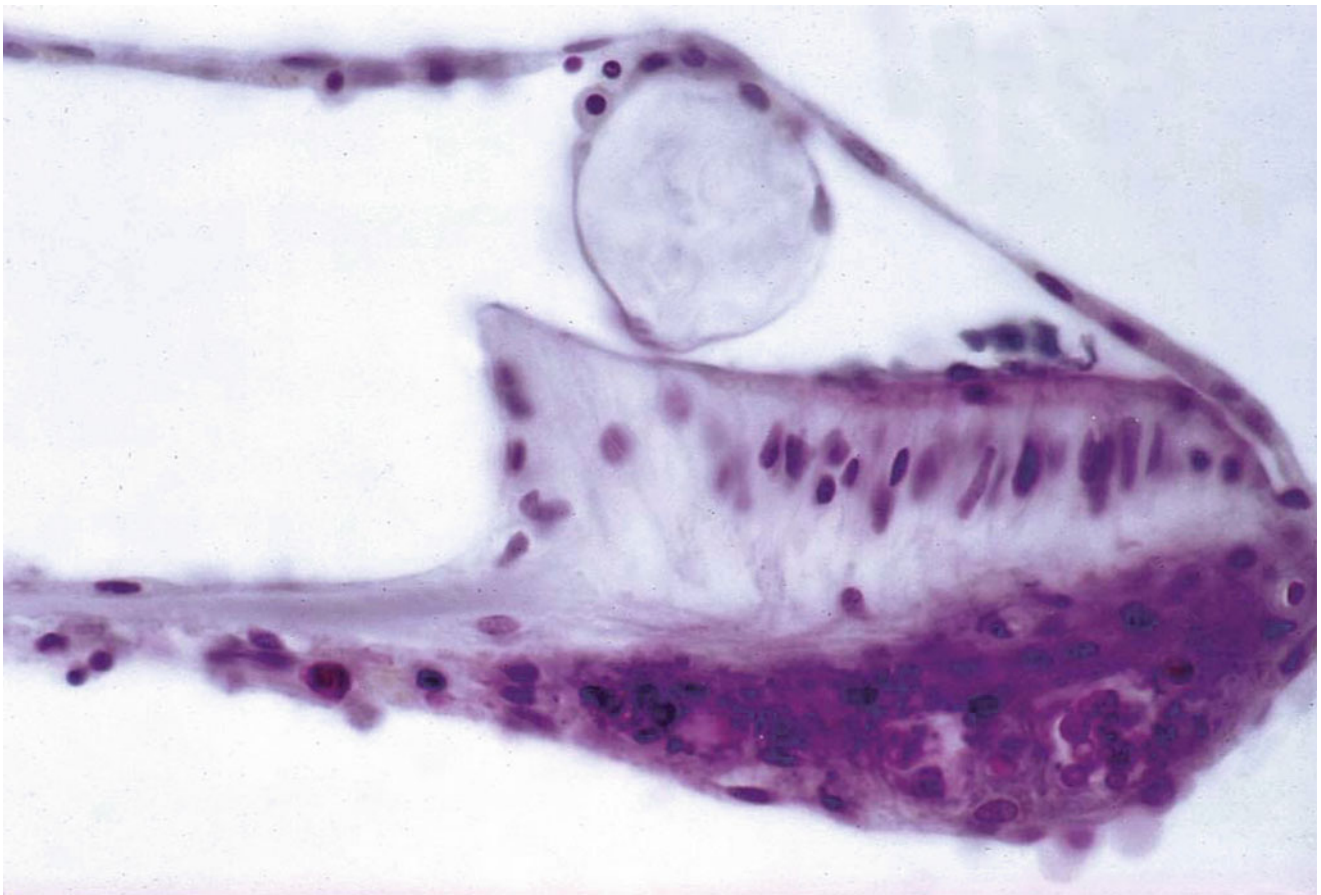

Fig. 4.1 Rolled-up tectorial membrane in a case of sudden deafness. The membrane surface is covered by a single cell layer. Loss of interdental cells is evident (Courtesy of Dr. Schuknecht)

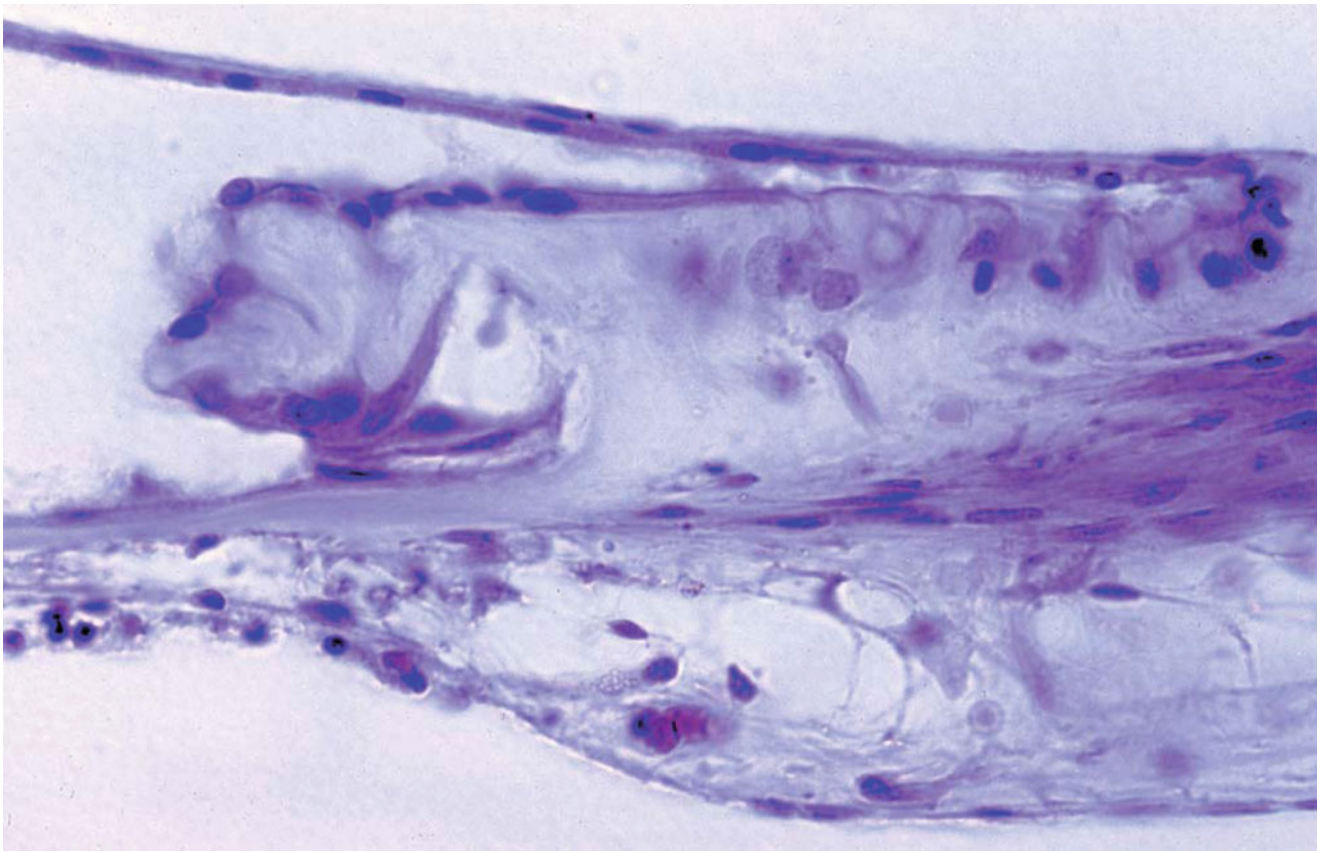

Fig. 4.2 Drooped and cohered tectorial membrane. The membrane is covered by a single layer of cells. The inner sulcus cells and interdental cells are missing. No nerve fibers are present in the osseous spiral lamina (Courtesy of Dr. Schuknecht)

cells (see Fig. 6.6) [4]. Other changes observed in the tectorial membrane after HSV inoculation were formation of large and small bulges on the membrane surface. Electron microscopic studies revealed virus particles approximately 10 nm in diameter within and around the bulges [5]. The contour of the dips in the imprints of the tectorial membrane demonstrated collapse or fusion [6].

4.3 Case Reports

4.3.1 Case 1

The tectorial membranes of a patient with bilateral sudden deafness showed marked changes [7].

A 46-year-old woman was astounded to learn that her three sons were drafted into the army on the same day in 1942. She noticed tinnitus in both ears before long, and developed bilateral hearing loss in the night, followed by vertigo. She stayed in bed for 1 month. In 1969, testing revealed hearing loss of 78 dB in the woman's right ear, and loss of 56 dB in her left ear (Figs. 4.3 and 4.6). In 1973, at the age of 77, the patient died by choking on phlegm.

4.3.1.1 The Right Temporal Bone

Pathological changes were found in the patient's cochlea and saccule. The lower basal turn of the organ of Corti was missing, and the upper basal turn had atrophied. In the middle turn, the inner and outer hair cells were partly missing and those remaining showed varying degrees of degeneration. The apical turn of the organ of Corti was atrophic.

The cochlear neurons were almost completely absent in the upper middle and basal turns. Twenty-five percent of neurons remained in the lower middle turn, and 75 % remained in the apical turn. The stria vascularis was atrophic and flat.

The tectorial membrane showed peculiarities in the basal turn. Many spherical structures, 3–4 μm in diameter, dotted both sides of the surface of the middle zone. At the tip of the marginal zone and the undersurface of the middle zone a larger round mass 15 μm in diameter was observed. The mass was located in the area between 10 and 15 mm from the basal end (Fig. 4.4a, b).

The saccular wall showed a perforation 750 μm in diameter and there was marked loss of the saccular neuroepithelium (Fig. 4.5). These findings may indicate the severity of the original involvement of the saccular macula.

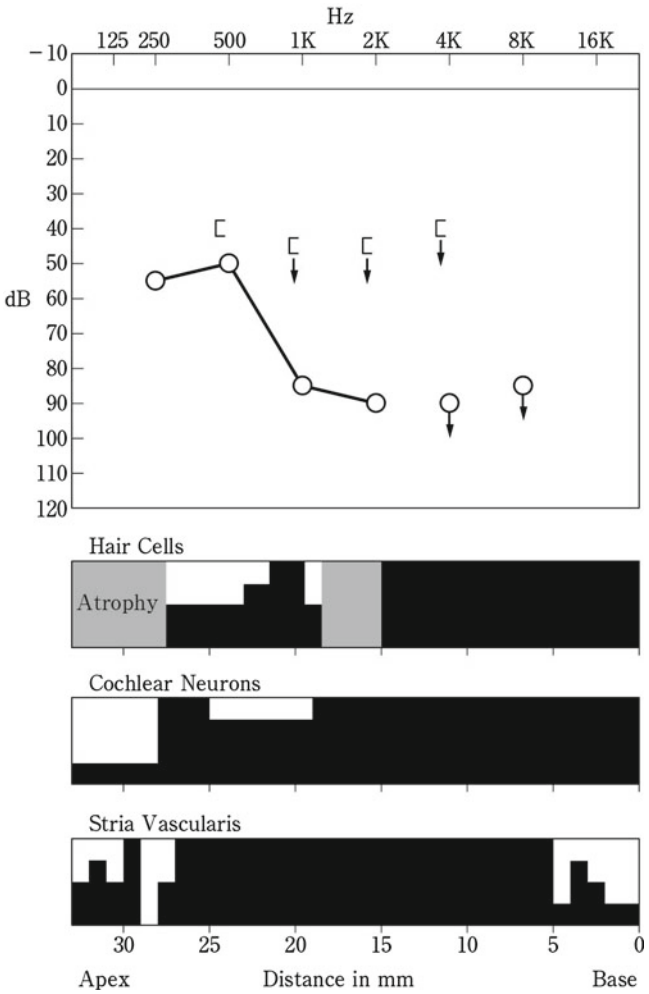

Fig. 4.3 Audiogram and cochleogram of the right ear (Case 1) [7]

4.3.1.2 The Left Temporal Bone

The organ of Corti was atrophic throughout all turns. The cochlear neurons were almost completely absent from the basal end up to the 17 mm area. The intraganglionic spiral bundle was missing in Rosenthal's canal. The stria vascularis was completely atrophic with the remnant of a thick-walled capillary. The spiral ligament was atrophic (Fig. 4.7).

The middle and marginal zones of the tectorial membrane drooped from the basal end up to the 10 mm area. A teardrop-shaped mass was attached to the undersurface of the membrane. In the 10–15 mm area, the thin limbal zone of the tectorial membrane was elevated by a cushion-like mass (18 μm thick) on the limbus (Fig. 4.8). The interdental cells were missing. From the 15 mm area to the apical end, the tectorial membrane was atrophic and flat, and adhered tightly to Reissner's membrane (Fig. 4.9a, b). No marked changes were seen in the utricle, saccule, or semicircular canals except for decreased neuroepithelium.

The pathological changes observed resulted from a combination of disease, repair, scarring, aging, and artifacts. Therefore, their interpretation needs deliberation. Because the tectorial membrane has no cellular element, changes caused by disease may persist unchanged for a long time. Although the rolled-up change was not found in this case, the many small particles on the surface of the tectorial membrane and the spherical substance at the tip of the right temporal bone resemble findings observed in experimental viral labyrinthitis of herpes simplex (see Fig. 6.7). The tectorial membrane of this patient's left ear was different from that of her right ear. Separation of the components of the membrane and loss of the interdental cells were common to both ears.

The tectorial membrane masses (bulges) were stained with alcian blue, toluidine blue, and PAS. They stained red in Azan specimens. As the tectorial membrane itself stains weakly or not at all with these techniques, the staining results suggest an alteration in the membrane's chemical properties and altered tissue substance. The substance must be hard, like keratin. This change (coagulation necrosis) occurred primarily in the middle zone.

The findings in this case are suggestive of viral infection. The patient's emotional stress possibly played an important role in decreasing her immunity, thereby allowing reactivation of latent viral infection.

The changes found in the tectorial membrane represented the final stage of progressive morphological changes, the initial stage of which causes deafness.

4.3.2 Case 2 [5]

A 20-year-old woman noticed profound hearing loss of sudden onset in her left ear with concurrent vertigo. An audiogram taken when she was 68 years of age revealed hearing loss of 70 dB in her left ear. She died at the age of 86. The temporal bone was removed 5 h postmortem. The organ of Corti was atrophic throughout the cochlea. The tectorial membrane was shrunken and drooped into the inner sulcus from the basal end to the 10 mm area. Its middle zone had formed a homogenous mass, suggesting further degenerative change of the tectorial membrane (Fig. 4.10). The tympanic lamella was missing (Figs. 4.11, 4.12, and 4.13). There was severe loss of spiral ganglion cells in the basal turn. The stria vascularis was atrophic throughout the cochlea.

The saccular wall had a permanent fistula approximately 800 μm in diameter (Fig. 4.13). Rolling of tissue at the edge of the fistula clearly prevented closure. The saccular macula revealed a profound loss of sensory epithelium. The utricular macula and cristae of the semicircular canals showed moderate loss of sensory epithelium. There was no connective tissue proliferation or new bone formation in the scalae of the cochlea.

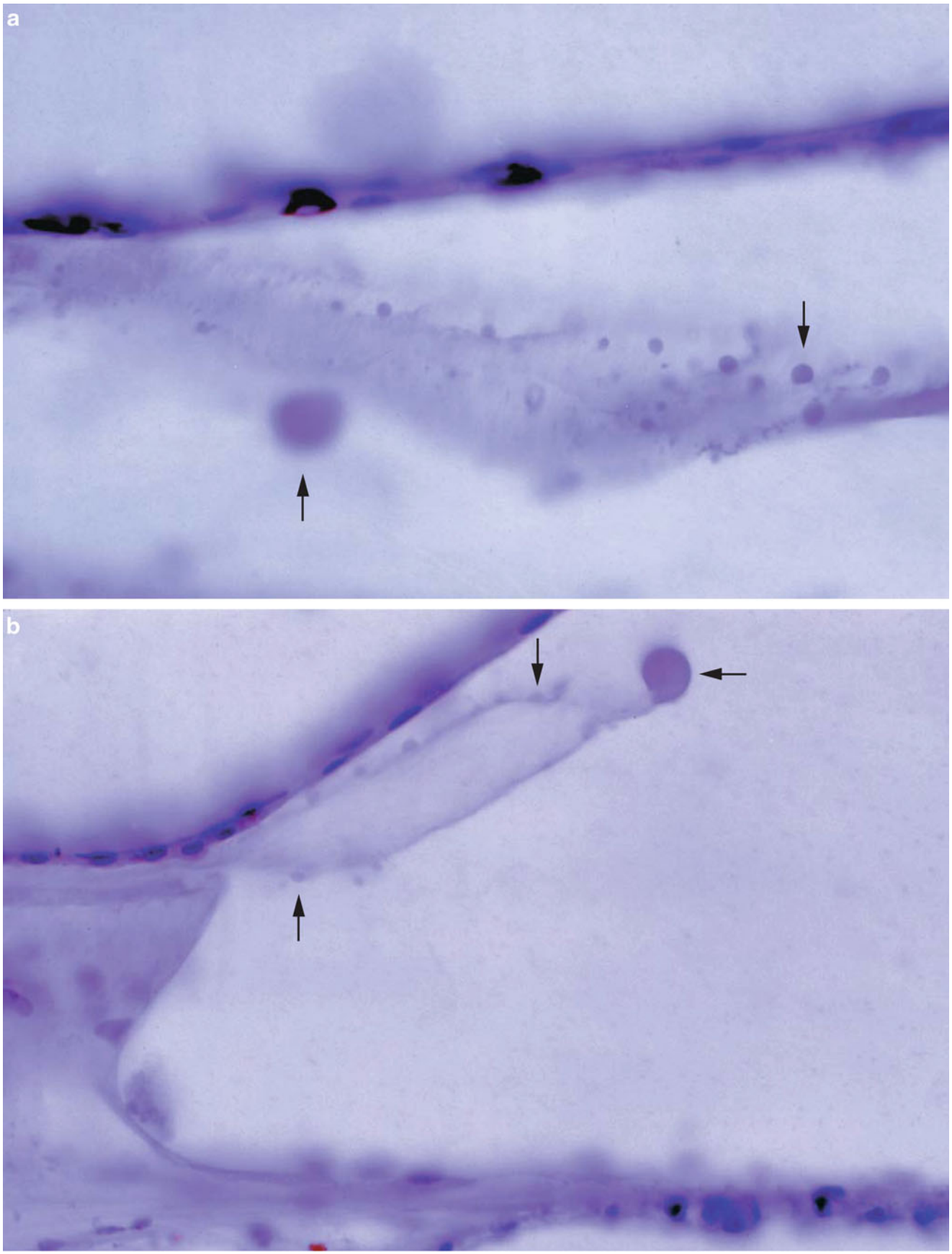

Fig. 4.4 Particles dotting the surface of the tectorial membrane of the right ear (*arrows*). (**a**) A larger mass is seen on the membrane's undersurface. (**b**) A larger mass is seen at the tip of the marginal zone. Small particles are seen on the surfaces of the tectorial membrane. The interdental cells and inner sulcus cells are missing [7]

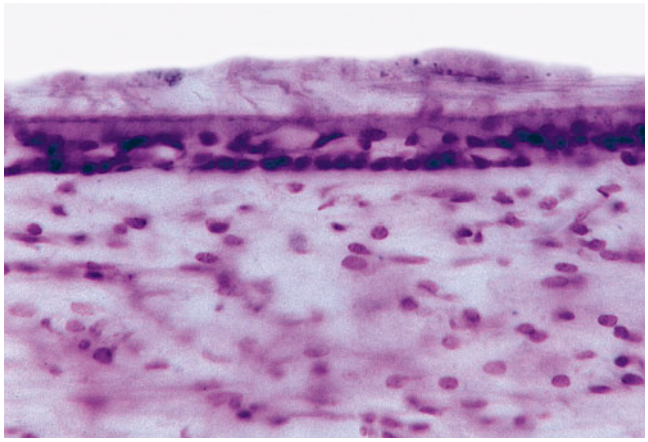

Fig. 4.5 Marked degeneration of the sensory epithelium and otolithic membrane of the saccule. No nerve fibers are observed beneath the sensory epithelium. Case 1, ×40

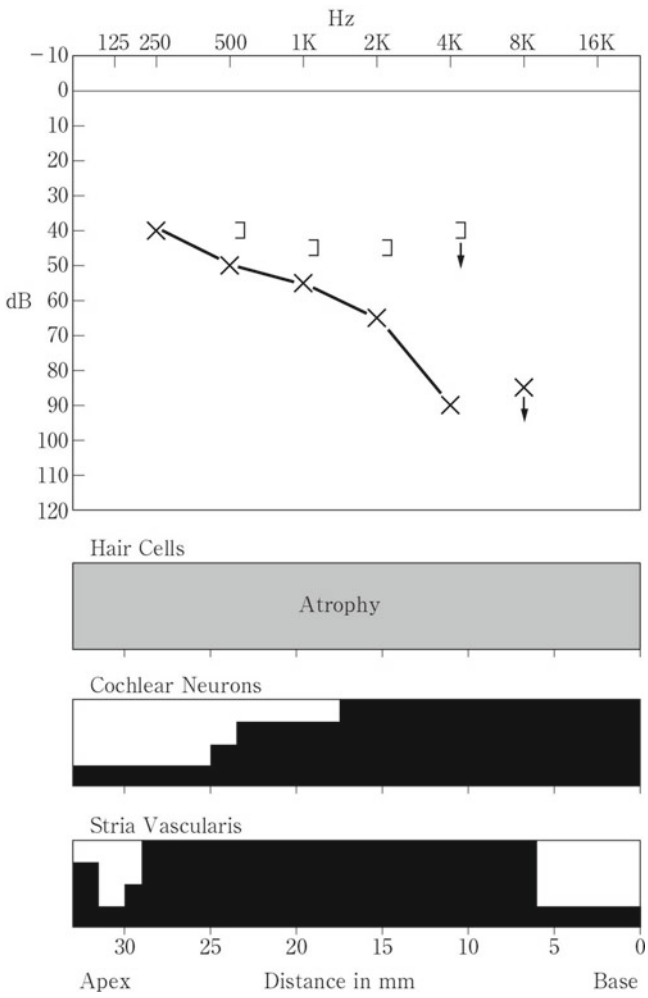

Fig. 4.6 Audiogram and cochleogram of the left ear (Case 1) [7]

There are at least three viral infection modalities: acute, latent, and reactivated latent infection.

In experimental viral labyrinthitis, cell infiltration may be observed in the cochlea several days after inoculation of virus. According to a histopathological study by Lindsay and Hemenway, an inflammatory reaction with escape of cells into the cochlear duct was found in an infant with measles 3.5 months after the acute stage of the disease [8]. In publications concerning sudden deafness, no specimens have shown cell infiltration in the scalae because of the long period between the onset of disease and death. Even the patient with the shortest period between the onset of sudden deafness and death (9 days) did not show cell infiltration in the cochlea [9].

Temporal bone findings from cases of sudden deafness are suggestive of viral infection of the inner ear. Pathology of the cochlea proceeds insidiously before symptoms appear and/or occurs in localized or limited areas. Reactivation of latent infection may cause subtle reaction in the tissue. Tissue reactions may differ with different viral species.

4.3.3 Sudden Deafness in a Patient with Relapsing Polychondritis

Hoshino et al. [10, 11] reported the case of a 57-year-old woman with relapsing polychondritis who developed acute profound sensorineural hearing loss in her left ear, followed the next day with loss in her right ear. Audiometry showed complete hearing loss in both ears. The patient was treated with steroids, an immunosuppressant (azathioprine), and antibiotics. Despite treatment, she took a gradual downhill course and died of gastrointestinal hemorrhage in October 1977, 1 year after her aural episodes. The patient's left ear was processed for scanning electron microscopy [10], and the right ear for study using the conventional celloidin method [11].

Light microscopic observation of the inner ear in the right temporal bone showed that the organ of Corti had degenerated and was compressed into a low mound throughout the entire cochlea. The tectorial membrane was covered by a layer of cells and had adhered to the membrana reticularis in the middle turn, or was tucked into the inner sulcus (Fig. 4.14).

The spiral ligament appeared normal at all sites except for the hook portion, where there was a patchy absence of spiral ligament cells. The stria vascularis showed sporadic patchy atrophy in every turn, but no granulomatous lesions were found. In the utricular and saccular maculae, the sensory epithelia showed marked degeneration. The saccular macula was composed only of a layer of flat cells. The sensory epithelia of the crista ampullaris of the three semicircular canals showed marked degeneration and were covered by a layer of cells.

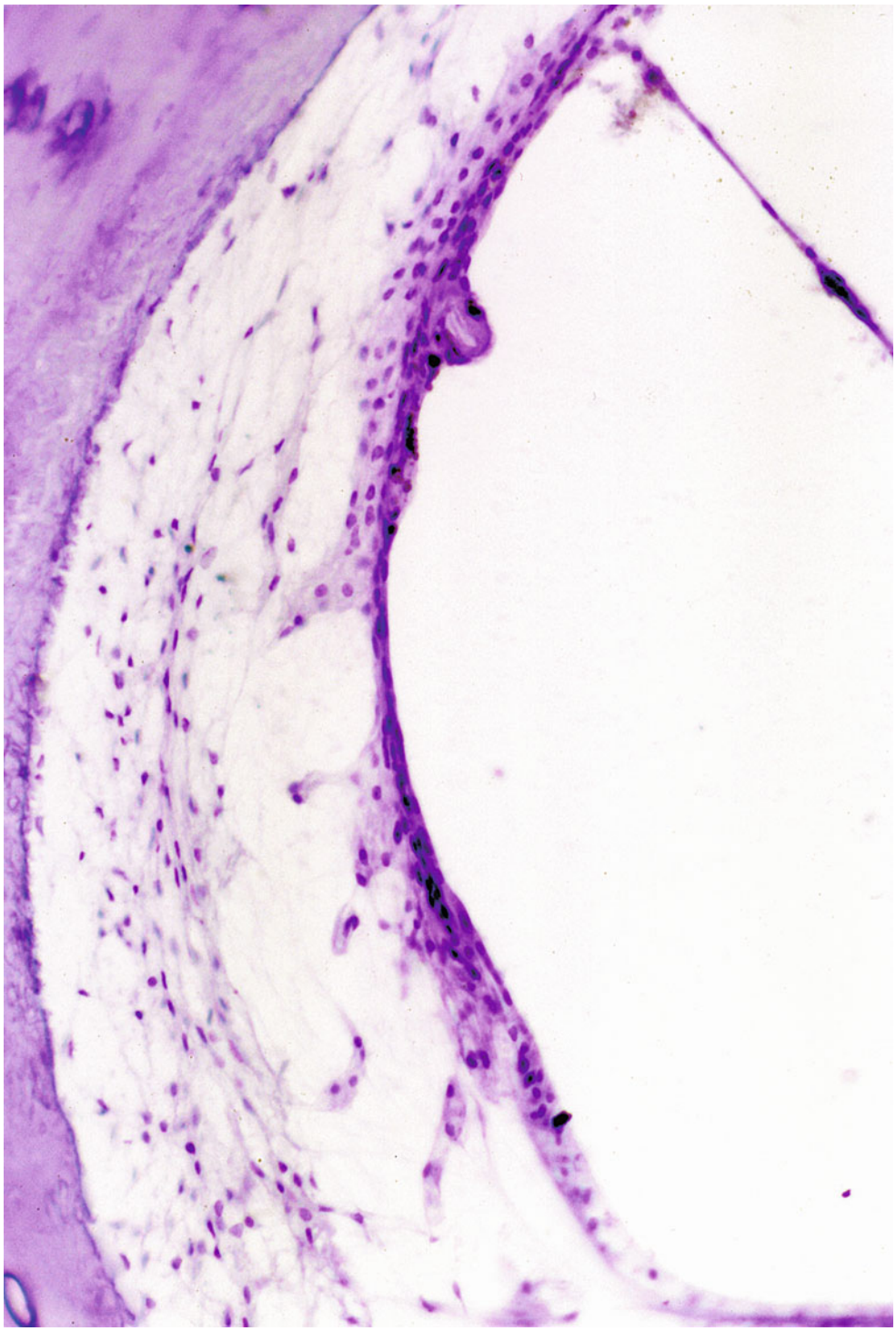

Fig. 4.7 Atrophy of the stria vascularis and spiral ligament. A thick-walled capillary remains in the atrophic stria. Case 1, left ear, ×40

A scanning electron microscope study of the left inner ear revealed marked degeneration of the organ of Corti in all turns. The tectorial membrane was rolled up and encapsulated. For the most part the tectorial membrane was lying on the inner sulcus. It was completely covered by a layer of thin flat cells (Fig. 4.15).

Based on these observations (marked atrophy of the organ of Corti, encapsulated and dislocated tectorial membrane with no noticeable decrease in myelinated nerve fibers), the authors suspected viral labyrinthitis as the cause of acute hearing loss in this case.

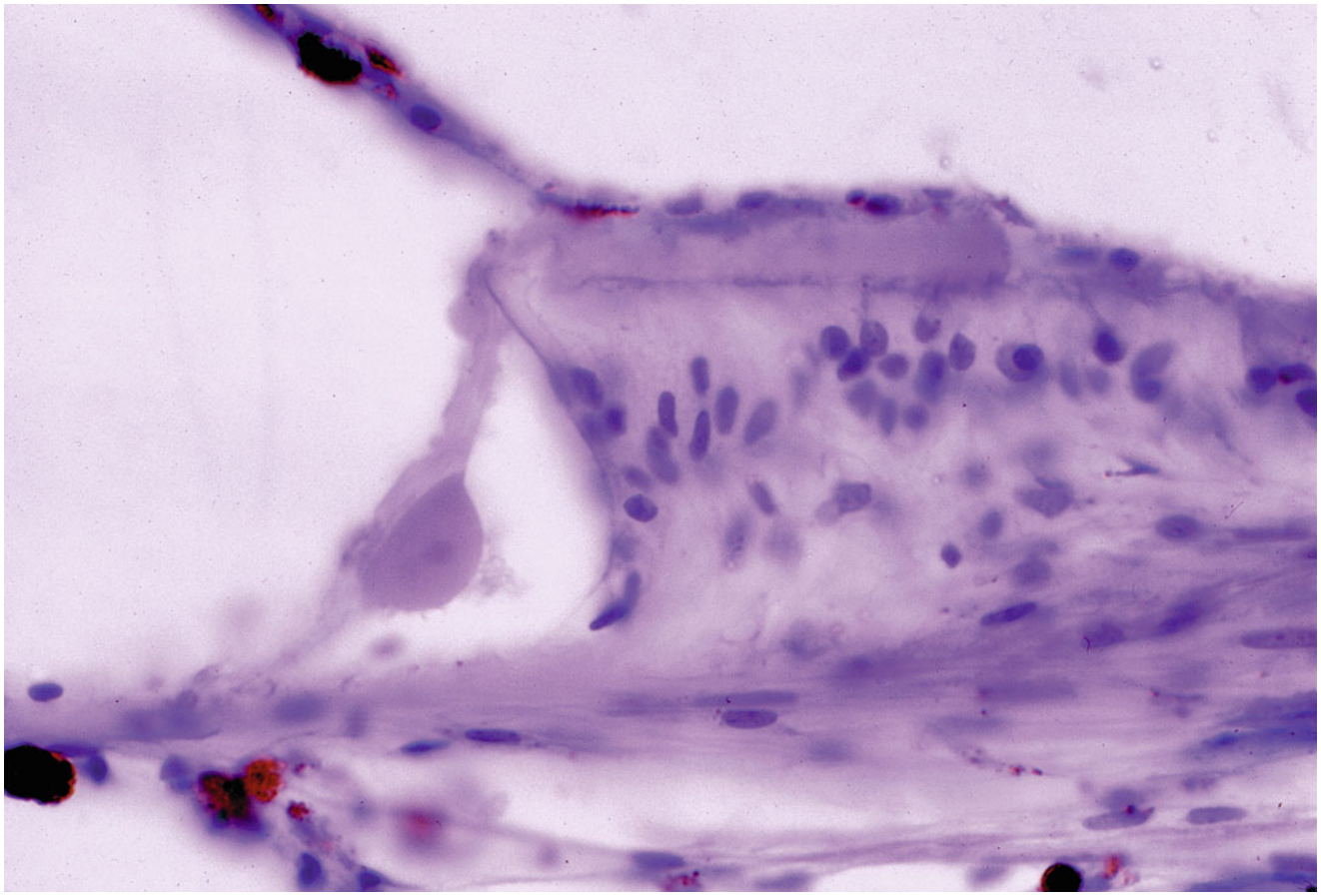

Fig. 4.8 Thickening of the limbal zone of the tectorial membrane. A teardrop-shaped mass is attached to the middle zone. Loss of interdental cells is evident. No nerve fibers are observed in the osseous spiral lamina. Case 1, left ear, ×40 [7]

4.3.4 Cochlear Neuronitis

Ishii and Toriyama [12] reported the case of a woman who had experienced sudden and profound hearing loss in the right ear at the age of 13 after having a cold, and who died of nasopharyngeal carcinoma at 41 years of age. An audiogram taken when the woman was 40 years old showed total deafness in the right ear. Caloric testing using 20 μL of water at 20 °C resulted in nystagmus of 110 s' duration on the right and no response on the left. Autopsy revealed that the tumor had invaded the meninges of the temporal bone, the cerebellopontine angle, and the flocculus of the left side.

The patient's right temporal bone showed a complete loss of cochlear neurons, but the organ of Corti was well-preserved (Figs. 4.16 and 4.17). As for the vestibular system, many nerve fibers were preserved and the end-organs seemed to be functional. The authors speculated that severe neuronitis of the cochlear nerve might have caused this patient's sudden deafness.

As the temporal bone showed no formation of new bone or fibrous tissue, a vascular lesion was not a likely cause of hearing loss in this case. Viral neuropathy remains plausible.

4.4 Sudden Deafness and Asymptomatic Mumps

Many viruses have been blamed for sudden deafness. Mumps is one such virus. Immunological tests are essential to diagnose viral diseases. IgM antibody appears early in the course of viral disease and IgM testing does not require paired sera to establish a diagnosis. Several papers have described IgM antibody testing to diagnose asymptomatic mumps in patients with sudden deafness. In the following three papers, the test was performed in adult patients with sudden deafness, all of whom met the criteria for diagnosis of the study group. According to these reports, the incidences of asymptomatic mumps among adults with sudden deafness were: 5.7 % [13], 6.9 % [14], and 7.2 % [15] (see Chap. 6, Sect. 3 Mumps).

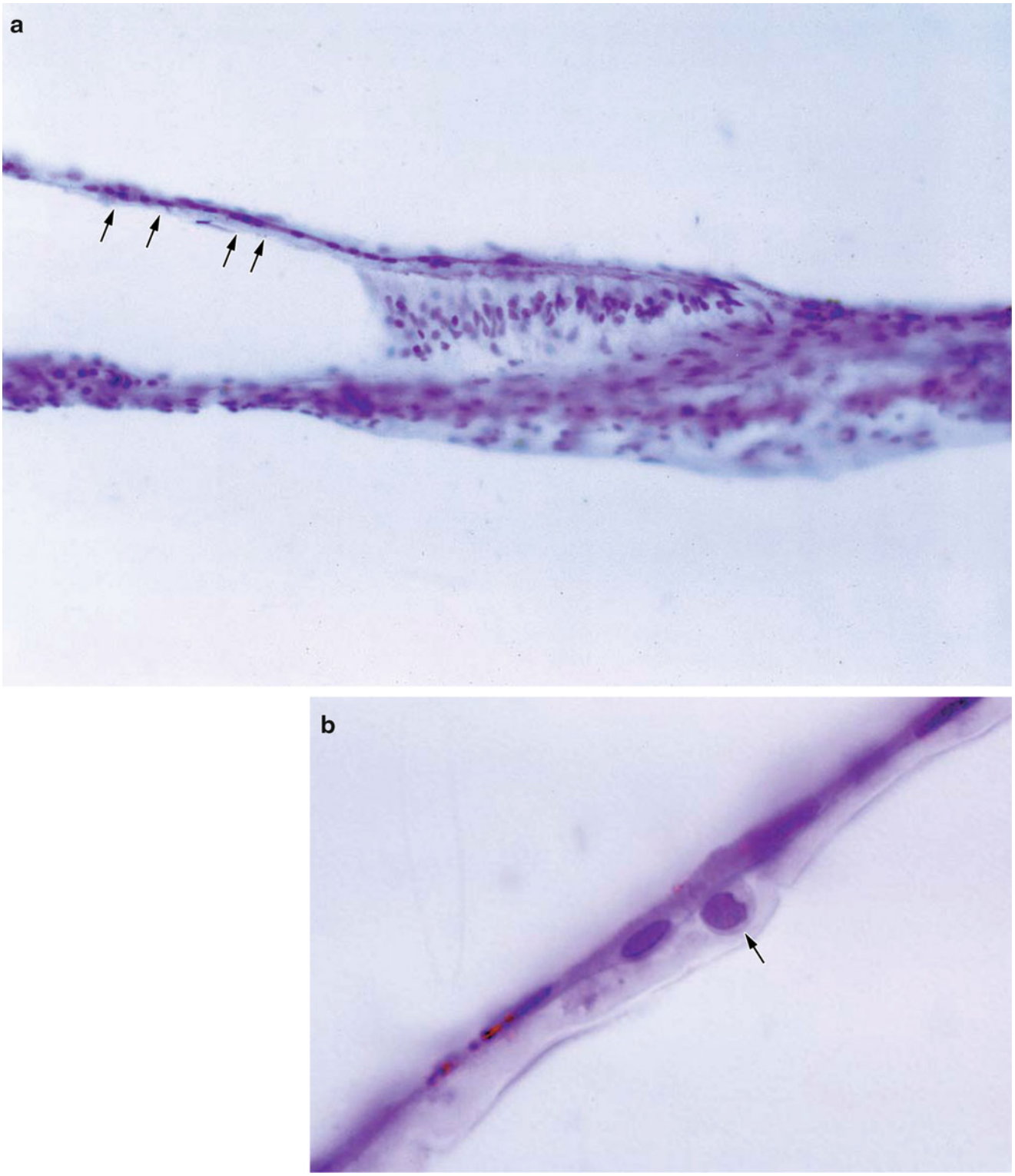

Fig. 4.9 (**a**) Flattened tectorial membrane attached to Reissner's membrane (*arrows*), apical turn (Case 1). (**b**) A histiocyte lies between the tectorial membrane and Reissner's membrane (*arrow*). Left ear [7]

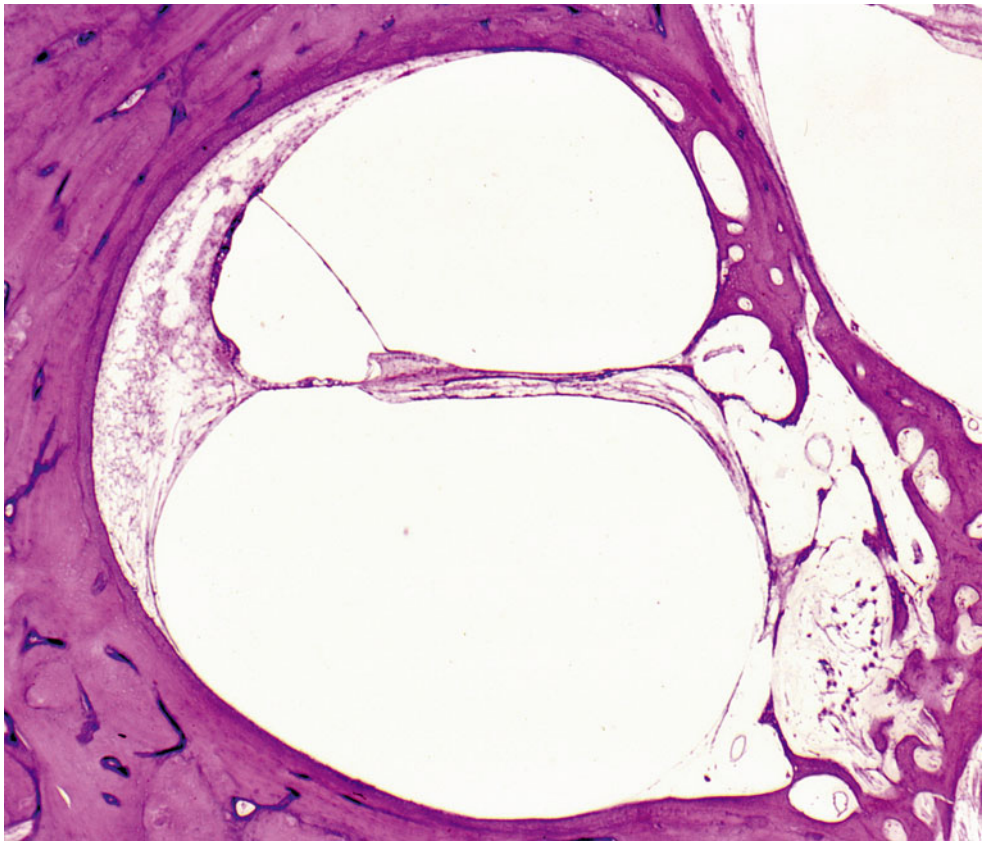

Fig. 4.10 Sudden deafness (Case 2). Atrophy is seen in the organ of Corti, stria vascularis, and spiral ligament. The spiral ganglion cells are markedly decreased in number (original ×2.5) [5]

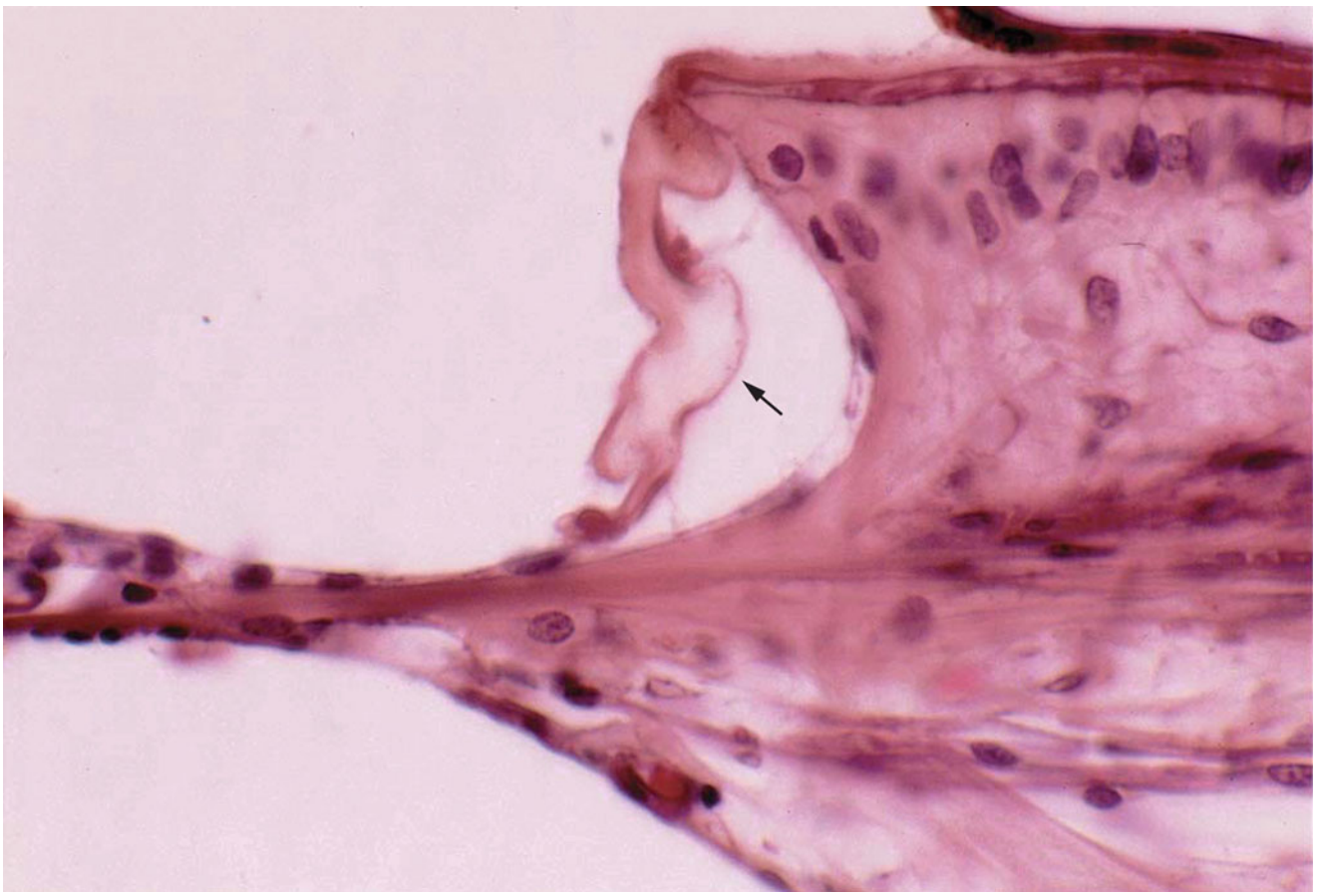

Fig. 4.11 Sudden deafness (Case 2). The tectorial membrane is drooping. The middle zone shows a homogenous elongated mass, suggesting an ongoing degenerative process (*arrow*) [5]

Fig. 4.12 The organ of Corti at the apical turn (Case 2). The outer hair cells are atrophic. No tympanic lamella exists (original ×100)

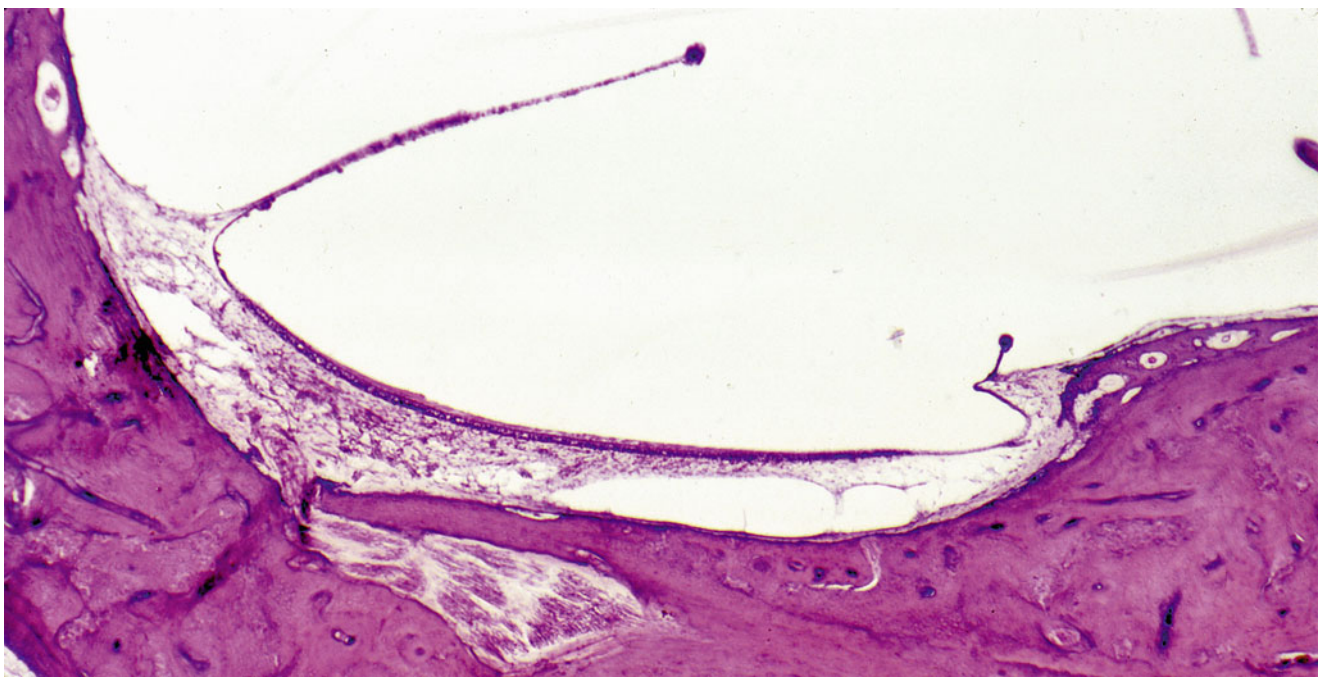

Fig. 4.13 Perforation of the saccular wall (Case 2). The saccular wall has a perforation 750 μm in diameter. The saccular macula is atrophic [5]

Fig. 4.14 A case of relapsing polychondritis. Organ of Corti in the middle turn. The degenerated and encapsulated tectorial membrane adheres to the degenerated organ of Corti (Courtesy of Dr. Hoshino) [11]

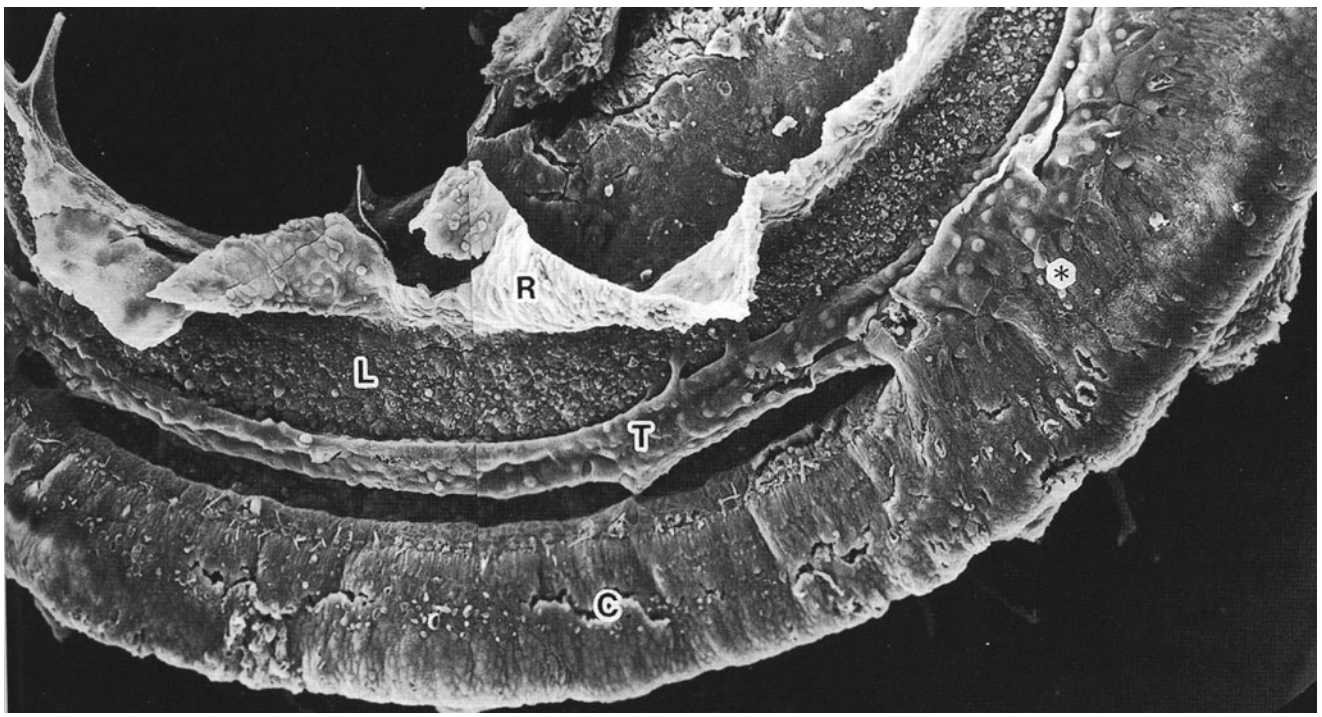

Fig. 4.15 Relapsing polychondritis. Surface view of the cochlear apical turn. The encapsulated tectorial membrane is lying for the most part on the inner sulcus. In the basal part the tectorial membrane is incorporated onto the organ of Corti. *C* organ of Corti, *T* tectorial membrane, *L* limbus spiralis, *R* Reissner's membrane, *asterisk* tectorial membrane partly unified with the organ of Corti (Courtesy of Dr. Hoshino) [10]

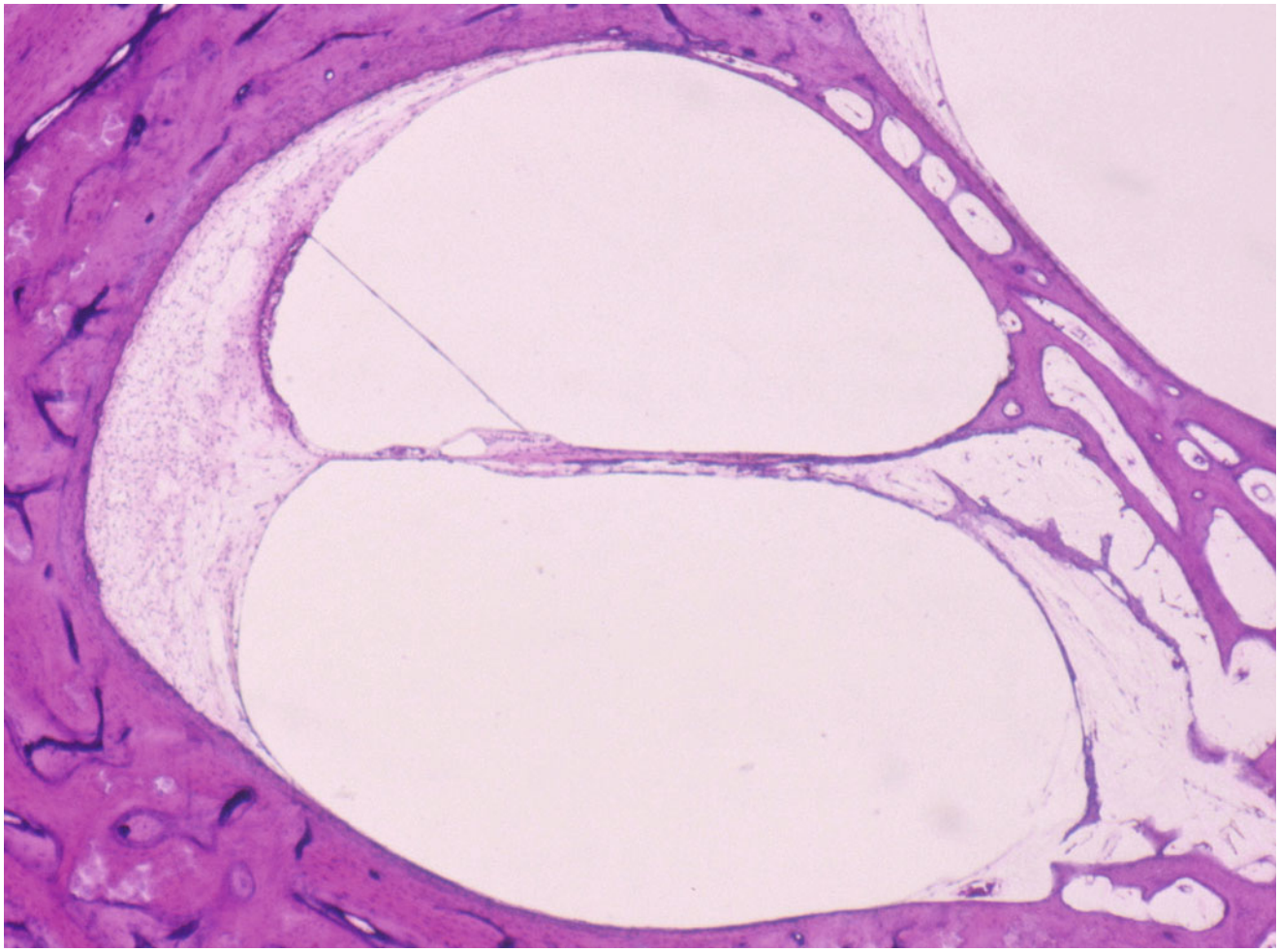

Fig. 4.16 Cochlear neuronitis. Basal turn. No ganglion cells are present in Rosenthal's canal (Courtesy of Dr. Ishii) [12]

Koga et al. [16] reported five pediatric patients with sudden deafness, one of whom had a positive mumps IgM test. This 21-month-old child had bilateral hearing loss, and asymptomatic mumps was the probable cause.

4.5 Vascular Disorders

Disturbance of blood circulation in the cochlea seems plausible as a cause of sudden deafness. The inner ear depends on a small labyrinthine artery for its oxygen and nutrient supply. Experiments by Kimura and Perlman [17, 18] demonstrated progressive changes in the inner ears of guinea pigs following obstruction of the anterior inferior cerebellar artery. In these animals the organ of Corti completely disappeared. The tectorial membrane, stria vascularis, spiral ligament, and spiral ganglion showed degeneration or disappearance. Vascular occlusion has been considered an attractive etiology for idiopathic sudden deafness.

The anterior vestibular artery is often a direct branch of the anterior inferior cerebellar artery and supplies the utricle and the superior and lateral ampullae. The posterior vestibular artery (vestibulocochlear artery) is a branch of the common cochlear artery and supplies the saccule, the posterior ampulla and a part of the cochlea.

Gussen [19] reported a case of sudden deafness and suggested circulatory disturbance of the posterior vestibular artery as the cause.

The patient was a 57-year-old man with sudden onset of dizziness lasting several seconds without nausea or vomiting, and unilateral deafness of the right side that began 3–4 h later. The patient was hospitalized 2 weeks later in congestive heart failure and severe renal failure. Audiometry at that time revealed total deafness in the right ear. The patient died 2 months after the onset of deafness.

At autopsy, subarachnoid hemorrhage with punctate cortical hemorrhage and arteriolar thickening involving the right superior cerebellar hemisphere were found. The pathological changes involved primarily the entire right cochlea, the saccule, and the ampulla of the posterior semicircular canal, and were consistent with vascular embarrassment of the temporal bone of 2 months' duration.

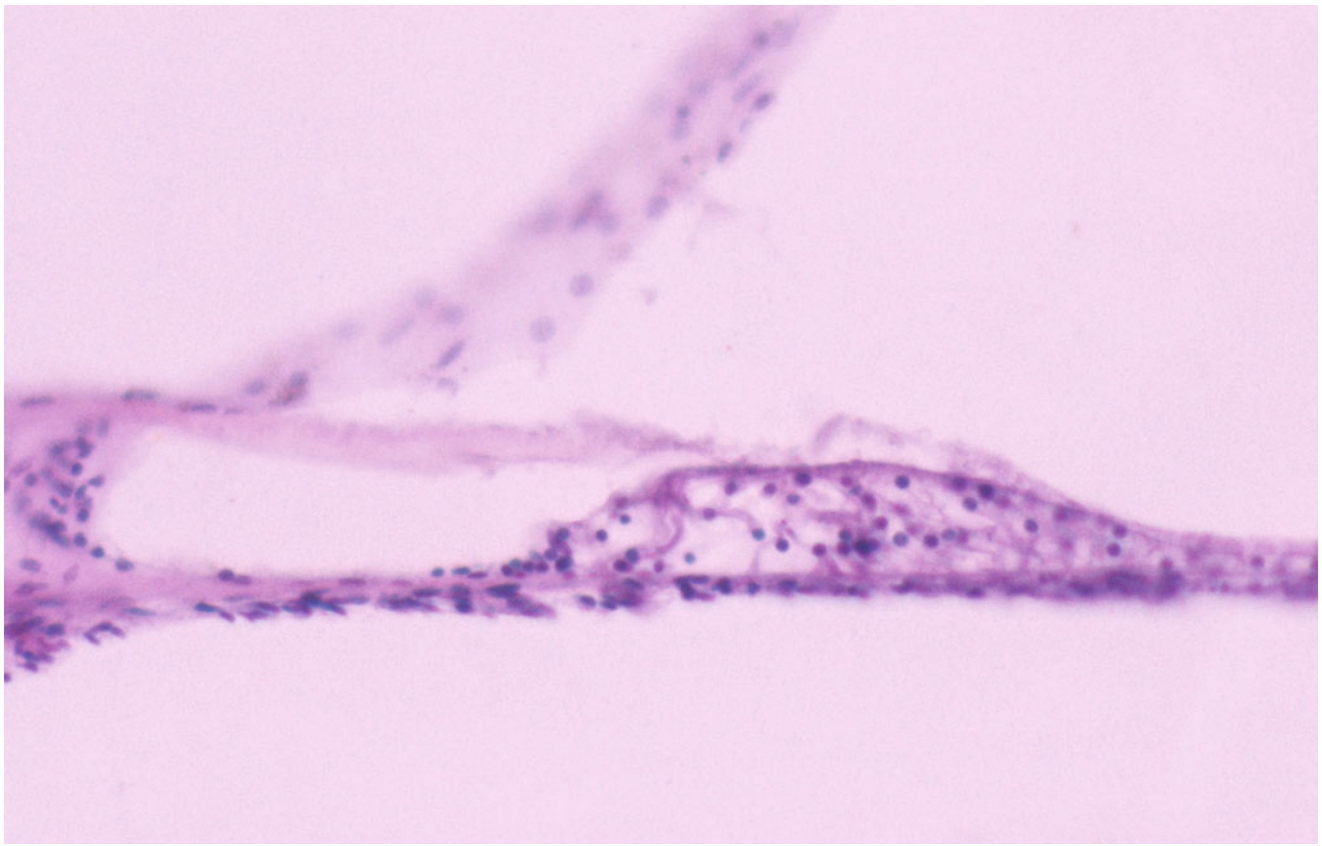

Fig. 4.17 Cochlear neuronitis. Organ of Corti in the middle turn. Hair cells and supporting elements including pillar cells are present (Courtesy of Dr. Ishii) [12]

The organ of Corti was absent throughout the entire cochlea. The tectorial membrane was present, but was either depressed into the inner sulcus or was fragmented or encapsulated on the limbus. The cells lining the inner sulcus were absent. The stria vascularis was atrophic throughout. The spiral ligament was markedly acellular in the hook and in the first part of the cochlea as well as in the middle and apical turns. The number of spiral ganglion cells was considerably decreased in the basal turn and somewhat decreased in the apical turn. Abundant nerve fibers were present in the modiolus and in proximal portions of the bony spiral laminae; however, there was considerable loss of nerve fibers distally, approaching the basilar membrane.

The vessels of the modiolus and internal auditory canal were congested. No fibrosis or bone formation was evident within the scalae of the cochlea.

The lining cells of the saccule were disrupted and the macula and otolithic membrane were absent, as were nerve fibers from the submacular region.

The crista of the posterior semicircular canal demonstrated loss of sensory and supporting cells and no cupula was evident.

The utricle and superior and lateral ampullae demonstrated postmortem disruption of the crista and macula. The utriculoendolymphatic valve was closed. The round window membrane was normal.

The endolymphatic duct and sac were filled with proteinaceous material and prominent clusters of foamy macrophages.

The pathological changes were consistent with the experiments of Kimura and Perlman. Although fibrosis and ossification within the cochlea had progressed extensively in 2 months in the experimental animals, Gussen's case did not show these changes. This difference was probably due to more complete vascular obstruction in the experimental animals.

Temporal bone histopathology shows that circulatory disturbance of the cochlea results in rolling of the tip of the tectorial membrane. The rolling is not as marked as that seen in viral infection.

4.6 Criteria for Diagnosis of Sudden Deafness in Japan

In 1973 the Sudden Deafness Study Group was organized under the auspices of the Ministry of Health and Welfare of Japan (Chairman: Professor Hiromu Miyake). The criteria for diagnosing sudden deafness were established to investigate

the clinical presentation, pathogenesis, and treatment of the disease in the study group.

In 2012 the Ministry of Health, Labor and Welfare, Acute Severe Hearing Loss Study Group (Chairman: Professor Kaoru Ogawa) revised the criteria.

Criteria for diagnosis of sudden deafness (2012)

Main Symptoms

1. Sudden onset
2. Sensorineural hearing loss, usually severe
3. Unknown etiology

For Reference

1. Hearing loss (i.e., hearing loss of 30 dB or more over three consecutive frequencies)
   a. Sudden onset of hearing loss, but may progressively deteriorate over 72 h
   b. No history of recurrent episodes
   c. Unilateral hearing loss, but may be bilateral at the onset
2. May be accompanied by tinnitus
3. May be accompanied by vertigo, nausea, and/or vomiting, without recurrent episodes
4. No cranial nerve symptoms other than from cranial nerve VIII

Definitive diagnosis: All of the above main symptoms are present.

If a patient with idiopathic sudden deafness is found to have other disease, such as mumps, the diagnosis of idiopathic sudden deafness should be changed. Instead, the case should be diagnosed as mumps deafness. With advances in medicine, causes of sudden deafness will become clear. But it will be a long time before the word "idiopathic" will be of no use.

4.7 Postscript

Patients with sudden deafness have a relatively high incidence of spontaneous recovery, most do not have vertigo, and the insult does not recur. Most temporal bone studies point to viral infection as a cause of sudden deafness. Most cases of irreversible sudden deafness are probably caused by viral labyrinthitis.

If the temporal bones of patients with complete recovery show normal findings without indication or suggestion of any cause of hearing loss, the diagnosis remains idiopathic sudden deafness.

This chapter mainly discussed the histopathology of the tectorial membrane in cases of viral labyrinthitis. Ideally, this content would be moved to the chapter on viral diseases. Regrettably, viral infection was not confirmed.

It is interesting to note that in experimental viral labyrinthitis, deformity of the imprint on the undersurface of the tectorial membrane occurs at an early stage of HSV-1 infection, while the outer hair cells appear intact [6]. If such change occurs and is reversible, it would be hard to discover cochlear pathology.

Functional disturbances of the stria vascularis and of the spiral ligament may play an important role in reversible idiopathic sudden deafness.

References

1. Chau JK, Lin JRJ, Atashband S, Irvine RA, Westerberg BD (2009) Systematic review of the evidence for the etiology of adult sudden sensorineural hearing loss. Laryngoscope 120:1011–1021
2. Schuknecht HF, Donovan ED (1986) The pathology of idiopathic sudden sensorineural hearing loss. Arch Otorhinolaryngol 243: 1–15
3. Raphael Y, Altschuler RA (2003) Structure and innervation of the cochlea. Brain Res Bull 60:397–422
4. Nomura Y, Kurata T, Saito K (1985) Cochlear changes after herpes simplex infection. Acta Otolaryngol (Stockh) 99:419–427
5. Nomura Y, Kurata T, Saito K (1985) Sudden deafness: Human temporal bone studies and an animal model. In: Nomura Y (ed) Hearing loss and dizziness. IGAKU-SHOIN Ltd, Tokyo, New York, pp 58–67
6. Saito K, Kurata T, Nomura Y (1985) Surface structure of the tectorial membrane with herpes simplex virus. 1984 Annual report of acute profound sensorineural hearing loss study group, Ministry of Health, Labor and Welfare, pp 165–168
7. Nomura Y, Hiraide F (1976) Sudden deafness. A histopathological study. J Laryngol Otol 90:1121–1142
8. Lindsay JR, Hemenway WG (1954) Inner ear pathology due to measles. Ann Otol Rhinol Laryngol 63:754–771
9. Schuknecht HF, Kimura RS, Naufal PM (1973) The pathology of sudden deafness. Acta Otolaryngol 76:75–97
10. Hoshino T, Kato I, Kodama A, Suzuki H (1978) Sudden deafness in relapsing polychondritis. A scanning electron microscopy study. Acta Otolaryngol 86:418–427
11. Hosino T, Ishii T, Kodama A, Kato I (1980) Temporal bone findings in a case of sudden deafness and relapsing polychondritis. Acta Otolaryngol 90:257–261
12. Ishii T, Toriyama M (1977) Sudden deafness with severe loss of cochlear neurons. Ann Otol Rhinol Laryngol 86:541–547
13. Nomura Y, Harada T, Sakata H, Sugiura A (1988) Sudden deafness and asymptomatic mumps. Acta Otolaryngol (Stockh) 456(Suppl): 9–11
14. Okamoto M, Shitara T, Nakayama M, Takamiya H, Nishimiya K, Ono Y (1994) Sudden deafness accompanied by asymptomatic mumps. Acta Otolaryngol (Stockh) 514(Suppl):45–48
15. Fukuda S, Chida E, Kuroda T, Kashiwamura M, Inuyama Y (2001) An anti-mumps IgM antibody level in the serum of idiopathic sudden sensorineural hearing loss. Auris Nasus Larynx 28(Suppl): S3–S5
16. Koga K, Kawashiro N, Nakayama T et al (1988) Immunological study on association between mumps and infantile unilateral deafness. Acta Otolaryngol (Stockh) 456(Suppl):55–60
17. Kimura R, Perlman HB (1958) Arterial obstruction of the labyrinth. Part I. Cochlear changes. Ann Otol Rhinol Laryngol 67:5–24
18. Kimura R, Perlman HB (1958) Arterial obstruction of the labyrinth. Part II. Vestibular changes. Ann Otol Rhinol Laryngol 67:25–40
19. Gussen R (1976) Sudden deafness of vascular origin: a human temporal bone study. Ann Otol Rhinol Laryngol 85:94–100

Meniere's Disease

5

Abstract

Since its first description in a paper by Prosper Ménière in 1861, the inner ear disorder consisting of malfunction of the vestibular and auditory systems has occupied a primary position in clinical and research fields in otology. Seventy-five years have passed since the discovery of endolymphatic hydrops in patients with Meniere's disease, and many features of the disorder have been elucidated, yet many remain unresolved.

This chapter introduces the following recent research: a histopathological study of the temporal bone, visualization of endolymphatic hydrops using gadolinium MRI, experimentally induced endolymphatic hydrops, optical coherence tomography for visualization of hydrops, vestibular evoked myogenic potentials in Meniere's disease, and the use of gentamicin as a treatment.

It is possible to visualize endolymphatic hydrops with the use of gadolinium in magnetic resonance images. Intratympanic or intravenous administration of gadolinium moves to the perilymph. In patients with endolymphatic hydrops, enlarged endolymphatic spaces occupy the perilymphatic space. Thus, reduced contrast media enhancement indicates an enlarged endolymphatic space, or hydrops. The clinical use of vestibular evoked myogenic potential testing will shed new light on the function of the otolithic organs in vestibular diseases, including Meniere's disease.

Keywords

Endolymphatic hydrops • Experiment • Gadolinium MRI • Gentamicin • Meniere's disease • Optical coherence tomography • Temporal bone histopathology • Vestibular evoked myogenic potential • Visualization of hydrops

5.1 Discovery of Endolymphatic Hydrops in Meniere's Disease

1938 was a memorable year in the history of Meniere's disease because it saw the publication of two papers concerning the histopathology of the temporal bone in patients with the disease. These papers were written by Yamakawa [1, 2] and by Hallpike and Cairns [3].

Yamakawa was professor and chairman at the Osaka Imperial University in Japan. He had studied the histopathology of the human temporal bone for 2 years under Professor Wittmaack in Germany. Yamakawa presented his paper entitled "*Über die pathologische Veränderungen bei einem Meniere-Kranken*" at the 42nd General Assembly of the Oto-Rhino-Laryngological Society of Japan on April 3 and 4, 1938 in Kyoto. This society was a section of the 10th Japanese Medical Congress. The patient described in the paper was Yamakawa's colleague, who was professor and chairman of Obstetrics and Gynecology at the same university. In his will, the patient requested that Yamakawa study his temporal bones.

The main change in this patient's temporal bone was distension of Reissner's membrane. The membrane was 1,240 μm long (normally 740 μm) in a portion of the basal turn, and it was 1,160 μm long (normally 740 μm) in the upper turn. Thus, it was almost twice its normal width. Yamakawa

Y. Nomura, *Morphological Aspects of Inner Ear Disease*, DOI 10.1007/978-4-431-54204-9_5,

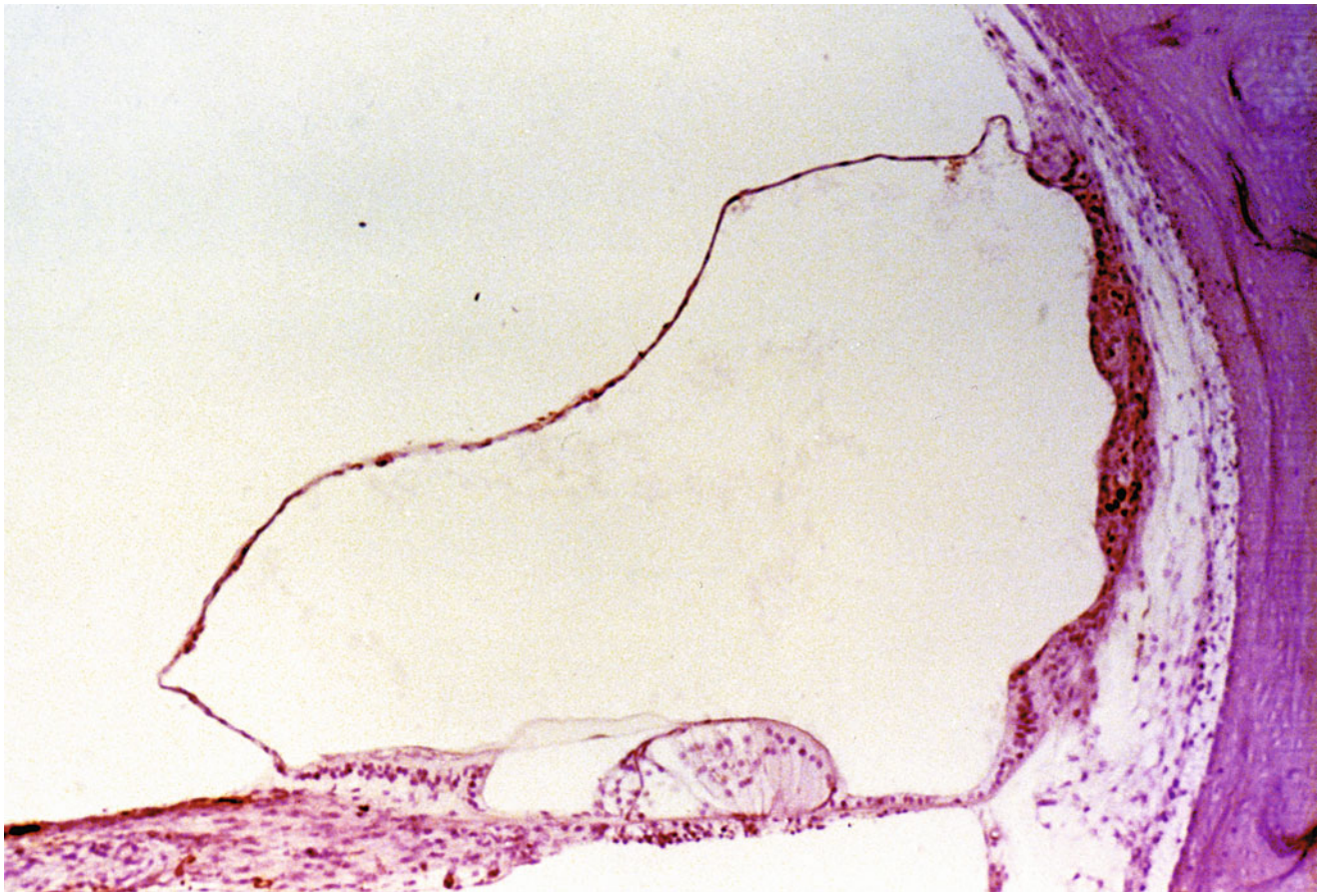

Fig. 5.1 Histopathology of a case of Meniere's disease reported by Professor Yamakawa. Reissner's membrane shows marked distension. The organ of Corti is normal (Courtesy of Professor Kubo)

described the shape of the distended Reissner's membrane as "bulging out to the perilymphatic space in the upper turn, while partly bulging and partly wavy in the lower turn." The organ of Corti and tunnel fibers appeared to be normal (Fig. 5.1). The spiral ganglion and Scalpa's ganglion were normal. The maculae sacculi and utriculi showed mild postmortem changes. Blood vessels were filled in the stria vascularis, and in several locations there were laminated uneven spherical calculi. Stimulation from the calculi results in increased endolymph secretion. This increase leads to functional disturbances of the inner ear sensory cells. Yamakawa thought that these changes would cause an attack of Meniere's symptoms. Restoration of the disturbed functions occurs after pressure decreases through diffusion and resorption of the endolymph and widening of Reissner's membrane.

Stahle [4] and Paparella et al. [5] described Yamakawa and his temporal bone studies in more detail.

Hallpike and Cairns published their paper in the *Journal of Laryngology and Otology* under the title "Observations on the pathology of Meniere's syndrome" [3]. They described hydrops in their patients as "gross dilatation of the saccule and scala media with obliteration of the perilymph spaces of the vestibule," (case 1) and "gross dilatation of the saccule and scala media with obliteration of the perilymph cistern of the vestibule and the scala vestibuli" (case 2). Their detailed descriptions of histopathological findings in Meniere's disease have greatly influenced research and clinical studies of the disease.

The term endolymphatic hydrops was not used in either paper published in 1938. How did researchers express "endolymphatic hydrops" at that time? Hallpike and Wright [6] used the term endolymphatic distension in their paper in 1939, Rollin [7] described *das Labyrinthhydrops*, Altmann and Fowler [8] discussed dilatation of the cochlear duct and dilatation of the endolymphatic system, Lindsay described labyrinthine dropsy in 1946 [9], and used the term labyrinthine hydrops in 1959 [10]. The term "endolymphatic hydrops" has gradually prevailed since the work of Henry Williams [11].

5.2 Human Temporal Bone Study

The term "endolymphatic hydrops" has been conceptually used as an alternative name for Meniere's disease, although the condition is not pathognomonic for Meniere's disease.

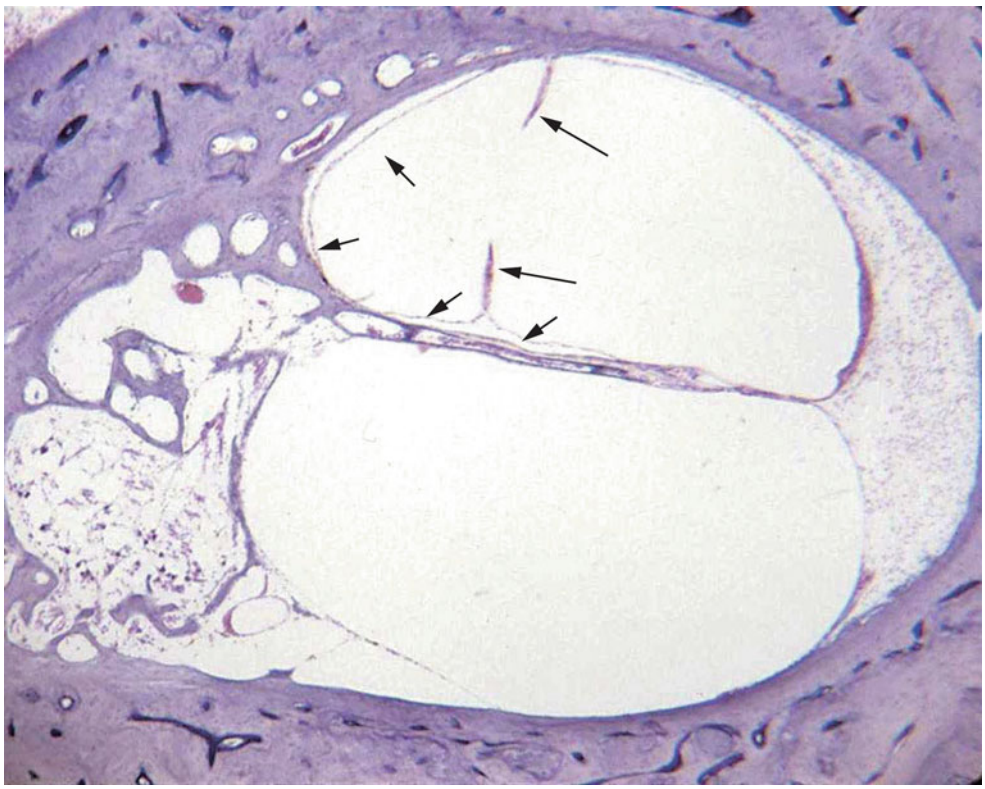

Fig. 5.2 Marked distension of Reissner's membrane. The scala vestibuli is completely occupied by the endolymphatic space. *Small arrows*: distended Reissner's membrane. *Large arrows*: infoldings (Courtesy of Dr. Okuno)

To understand the signs and symptoms of patients with Meniere's disease, we must investigate the sites and severity of inner ear hydrops in these patients.

Okuno and Sando [12] reported their histopathological study of 22 temporal bones from 16 individuals with Meniere's disease. The temporal bone specimens were from the collection of the Massachusetts Eye and Ear Infirmary. According to Okuno and Sando, endolymphatic hydrops was more often observed in the pars inferior (22/22) than in the pars superior (16/22) of the temporal bone (Fig. 5.2). Severe hydrops was observed most frequently in the saccule, followed by the cochlea, the utricle, and the three semicircular canals.

Saccular hydrops was observed in 19 of the 22 temporal bones. In 17 of these cases the saccular space had expanded laterally toward the footplate of the stapes, touched the footplate, and occupied the vestibular perilymphatic space inferolateral to the utricle.

Utricular endolymphatic hydrops was observed in 11 of 22 bones. In nine of these cases, the utricular membrane had expanded into the superomedial part of the vestibular perilymphatic space and then herniated into the common crus. The utricle had not expanded anterolaterally to the footplate of the stapes. The authors noted that hydrops was severe in individuals with a long history of Meniere's disease, whereas when the disease had been of shorter duration the hydrops was less severe.

Histopathologically, endolymphatic hydrops in Meniere's disease is classified into three groups (Fig. 5.3):

1. Severe hydrops in both the pars inferior and pars superior. Outpouching, infolding, and herniation are often observed (Fig. 5.3b). The severity of hydrops seems related to the severity of hearing loss.
2. Moderate cochlear hydrops accompanied by hydrops of the saccule, but by milder or no hydrops of the utricle or semicircular canals (Fig. 5.3c).
3. Hydrops with collapse of the membranous cochlea. The pars superior is normal in this group (Fig. 5.3d).

5.3 Diagnosis of Endolymphatic Hydrops Using Gadolinium MRI

Images of the inner ear can be obtained using gadolinium contrast agents.

Naganawa et al. [13] found that three dimensional fluid-attenuated inversion recovery (3D-FLAIR) imaging could minimize the ghost artifacts of fluid flow. The group studied the effects of contrast on the fluid of the inner ear [13, 14].

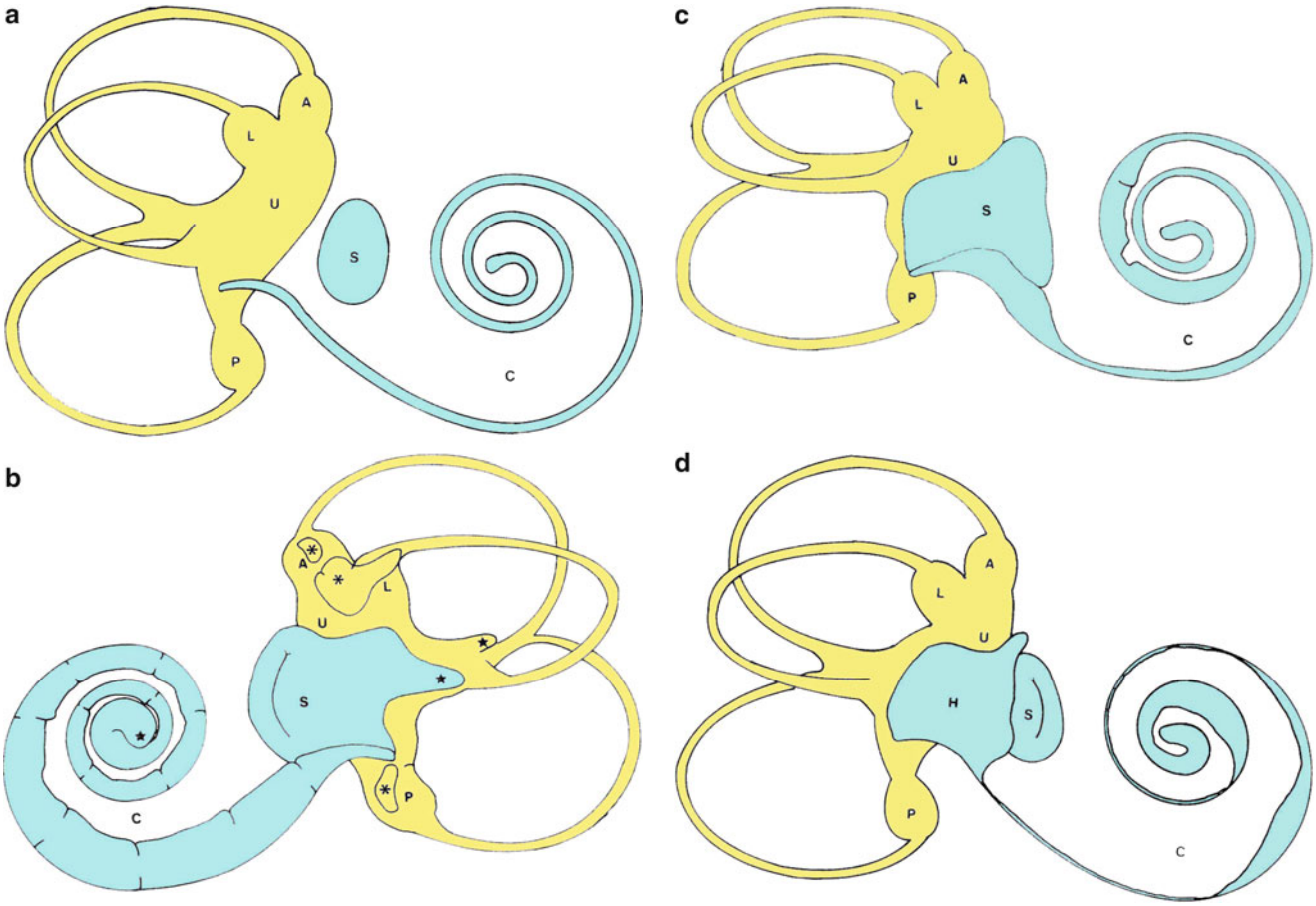

Fig. 5.3 Schematic representations of normal and pathological (hydrops and collapse) membranous labyrinths. (**a**) Normal membranous labyrinth. The pars superior is colored yellow, and the pars inferior blue. (**b**) Severe hydrops in both the pars inferior and the pars superior. Many infoldings are observed in the pars inferior, and three outpouchings (*asterisks*) are seen in the ampullae of the semicircular canals. The endolymphatic membrane at the apical turn has herniated through the helicotrema (*stars*). The saccular endolymphatic space occupies the vestibular perilymphatic space, attaching to the foot plate of stapes and herniating into the perilymphatic space of the nonampullated end of the lateral canal. The utricle has also expanded and herniated into the common crus. (**c**) Moderate hydrops in the cochlea and expansion of the saccular space filling the vestibule. (**d**) Hydrops and collapse in the cochlea. The hook portion of the basal turn (*H*) has expanded into the vestibule. *A* anterior semicircular canal, *C* cochlea, *L* lateral semicircular canal, *P* posterior semicircular canal, *S* saccule, *U* utricle (Modified with permission of the authors) (Courtesy of Drs. Okuno and Sando) [12]

Nakashima et al. [15] visualized endolymphatic hydrops in patients with Meniere's disease using intratympanic application of gadolinium. Using a 3 Tesla magnetic resonance imaging unit, they performed 3D-FLAIR imaging. Through the round window membrane in these patients, injected gadolinium entered the scala tympani of the basal turn, then spread toward the helicotrema and scala vestibuli. It also penetrated to the lower spiral ligament. One day after injection, gadolinium was observed in almost all areas of the perilymph. Six days after injection, gadolinium had almost disappeared from the inner ear.

Distension of Reissner's membrane prevents gadolinium from entering the scala vestibuli. Likewise, gadolinium cannot enter the perilymphatic cistern in cases of marked distension of the saccular wall and/or the utricular wall occupying the vestibule.

Gadolinium 3D-FLAIR images showed marked endolymphatic hydrops in patients with Meniere's disease. The cochlea and vestibule were occupied by endolymph, a change that was apparent when compared with images of the inner ear of normal subjects (Fig. 5.4a, c). There is no difference between T2-weighted images from individuals with and those without hydrops (Fig. 5.4b, d) [15].

A study of the distribution of gadolinium in the cochlear perilymph found differences depending on the method of delivery. In the intratympanic method, gadolinium-diethylenetriamine pentaacetic acid (Gd-DTPA, 500 mmol/L) was diluted eightfold with saline. In the intravenous method, a single dose (0.1 mmol/kg body weight) of Gd-DTPA-BMA was administered and heavily T2-weighted 3D-FLAIR was utilized. After intratympanic injection, gadolinium contrast agent distributed predominantly in the basal turn perilymph,

whereas it distributed more uniformly throughout the cochlear perilymph after intravenous injection [16]. The cochlear fluid was found to be most intensely enhanced 4 h after intravenous injection [14].

Visualization of endolymphatic hydrops is useful not only for diagnosis of Meniere's disease, but also for elucidation of its pathophysiology. Visualization will be of great help when selecting therapeutic modalities.

5.4 Experimentally Induced Endolymphatic Hydrops

In the cochlea, endolymph is produced by the stria vascularis. In the vestibular system, dark cells are considered responsible for endolymph production. The endolymphatic sac is the site of endolymph absorption, according to the longitudinal flow theory. Endolymphatic hydrops is believed to occur when the endolymphatic duct and/or sac is obliterated.

In 1964, Kimura successfully produced a guinea pig model of endolymphatic hydrops by obliterating the endolymphatic duct. His technique spread worldwide as a standard experimental method of producing endolymphatic hydrops and contributed to morphological and physiological studies of Meniere's disease [17–19].

The author received a set of experimental endolymphatic hydrops specimens from Dr. Kimura in September 2000. The specimen box was labeled with the following information:

Guinea Pig Hydrops
Blockage of endolymphatic duct
October 1980
Duncan Hartlay Strain
Weight: 438 g
Survival time: 4 months
Fixative: Heidenhain-Susa
Section: 20 μm serial
Stain: Hematoxylin-Eosin
Hydrops shown in: Cochlea,
Saccule, Utricle, Posterior +
Superior Ampullae

The specimens showed hydrops in almost all parts of the inner ear (Fig. 5.5a–d).

Experimental guinea pigs with hydrops demonstrated shifts in auditory thresholds, but they did not show signs of episodic vestibular disturbances.

The formation of hydrops seemed to result from blocking the longitudinal endolymph flow. However, because endolymph flows extremely slowly, blockage seems untenable as a complete explanation of hydrops. Type I and II fibrocytes in the spiral ligament are involved in inner ear fluid homeostasis, particularly with regard to K^+ cycling in the endolymph. These cells are engaged in transporting K^+ from the root cells to the stria vascularis. It has been demonstrated that these cells show cytochemical and ultrastructural lesions soon after endolymph flow blockage, before the formation of hydrops [20, 21].

There is some dispute about the relationship between symptoms and hydrops. It is uncertain which comes first, hydrops or vertigo [22].

5.5 Observation of Experimental Cochlear Hydrops Using OCT

Optical coherence tomography (OCT) is a type of echo tomography. It is non-contact and non-invasive technology, and is widely applied in ophthalmology clinics to examine the fovea centralis as a cross sectional image. Because the inner ear is confined within the hard otic capsule, it is presently difficult to obtain images of its structures. Recently, the cochlea has become an object of OCT research related to cochlear implantation, because knowledge of cochlear microanatomy is essential during cochleostomy [23, 24].

Kakigi [25] observed the cochlea of a guinea pig with experimentally induced endolymphatic hydrops using OCT. The endolymphatic duct of the left side was obliterated in this animal. Four weeks after surgery, the guinea pig was deeply anesthetized with ketamine and xylazine, then physiological saline was injected into the left ventricle and the animal was fixed with 10 % formalin. After fixation for a week, both temporal bones were removed and decalcified using ethylenediamine tetraacetic acid (EDTA) solution for 14 days. Images of the cochlea were obtained using Santec OCT systems controlled by Inner Vision (Santec Co., Komaki, Aichi, Japan). The center wavelength band was 1,320 nm and the scan range was 90 nm. The axial and lateral resolutions were 12.0 and 17.0 μm, respectively. The measurement speed was 50,000 lines/scan and the frame rate was 100 frames/s. The image depth and width were 6.0 and 10.0 mm, respectively.

Optical cross-sectional images of the cochlear turns showed moderate to marked endolymphatic hydrops (Fig. 5.6).

This technique does not require embedding and sectioning, so several types of processing artifacts can be avoided. After taking OCT images, the cochlea can be inspected using molecular biological and immunohistochemical techniques.

In the future, technological advancements will make it possible to obtain high resolution images, and to examine the inside of the temporal bone microanatomy in the clinical setting.

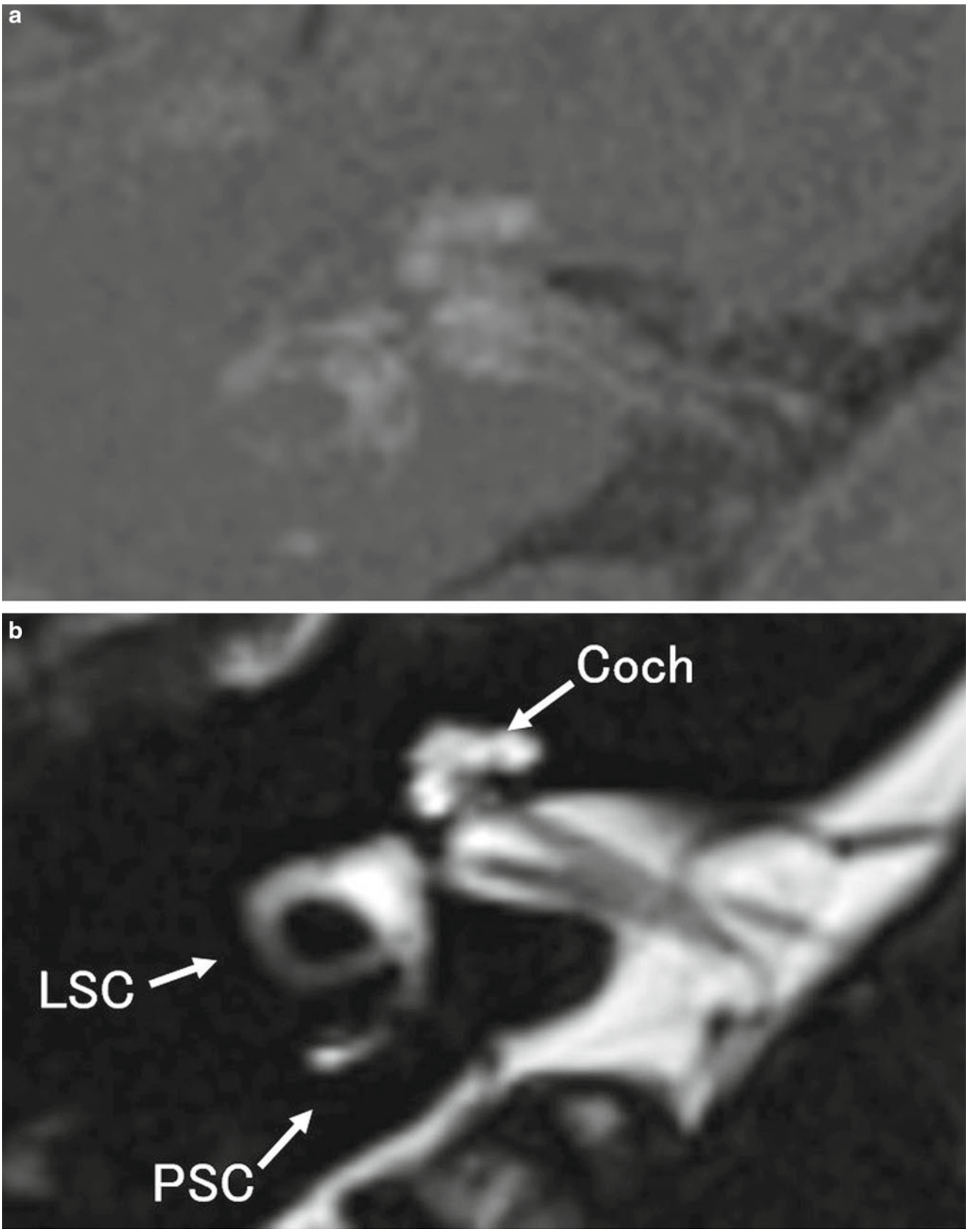

Fig. 5.4 MRI images of a normal inner ear and of the inner ear of a patient with Meniere's disease. To visualize the total inner ear fluid anatomy, T2-weighted images were obtained using 3D-SPACE sequence. To separately visualize the endolymph and perilymph anatomy, HYDROPS (HYbriD of Reversed image Of Positive endolymph signal and native image of positive perilymph Signal) images were obtained. Technical details of HYDROPS images have been reported previously [17]. (**a**) Normal. HYDROPS image. (**b**) Normal. T2-weighted image using 3D-SPACE sequence. *Coch* cochlea, *LSC* lateral semicircular canal, *PSC* posterior semicircular canal. (**c**) Meniere's disease. HYDROPS image. Hydrops is observed in the cochlea and vestibule (*arrows*). (**d**) Meniere's disease. T2-weighted image using 3D-SPACE sequence (Courtesy of Drs. Nakashima and Naganawa)

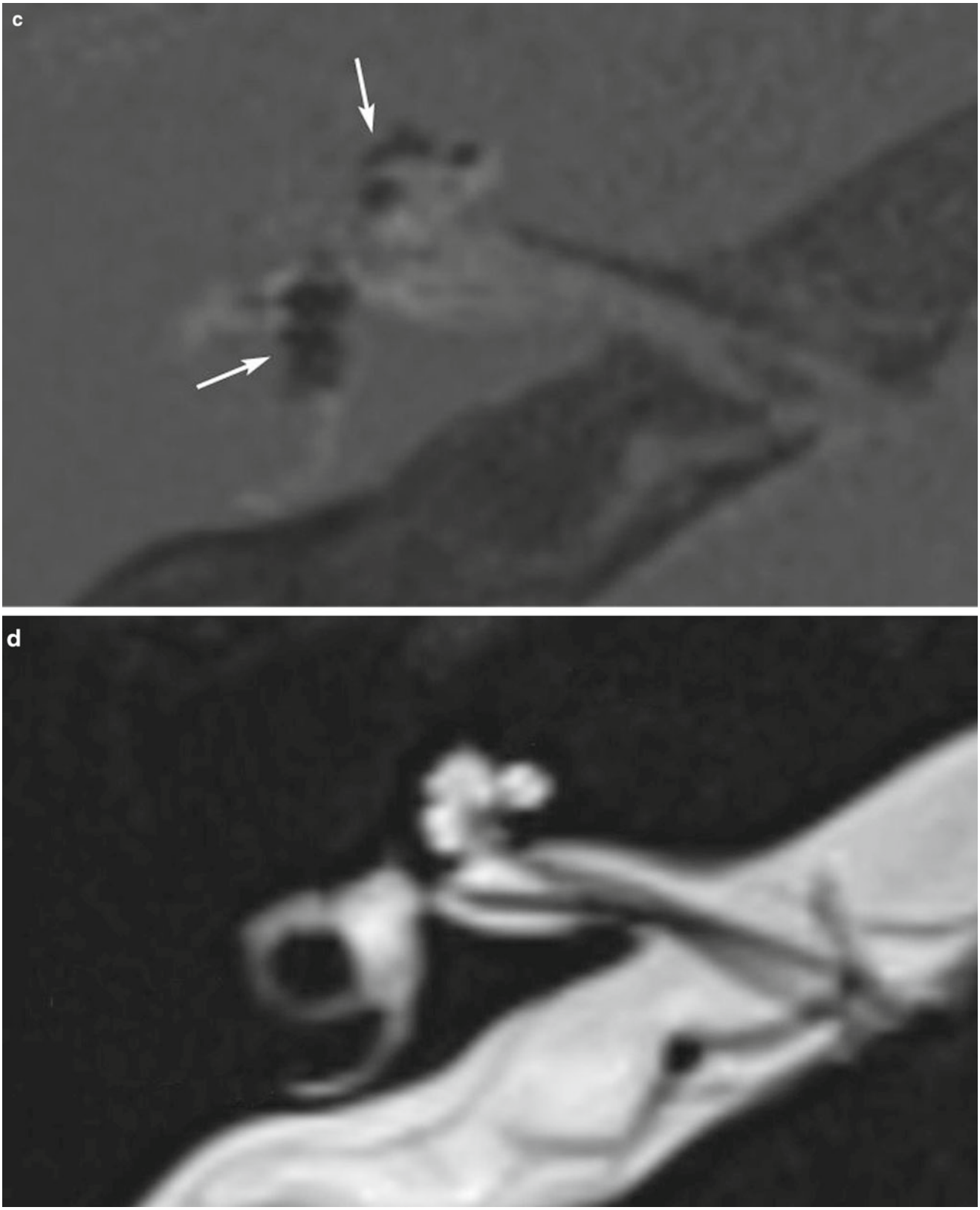

Fig. 5.4 (continued)

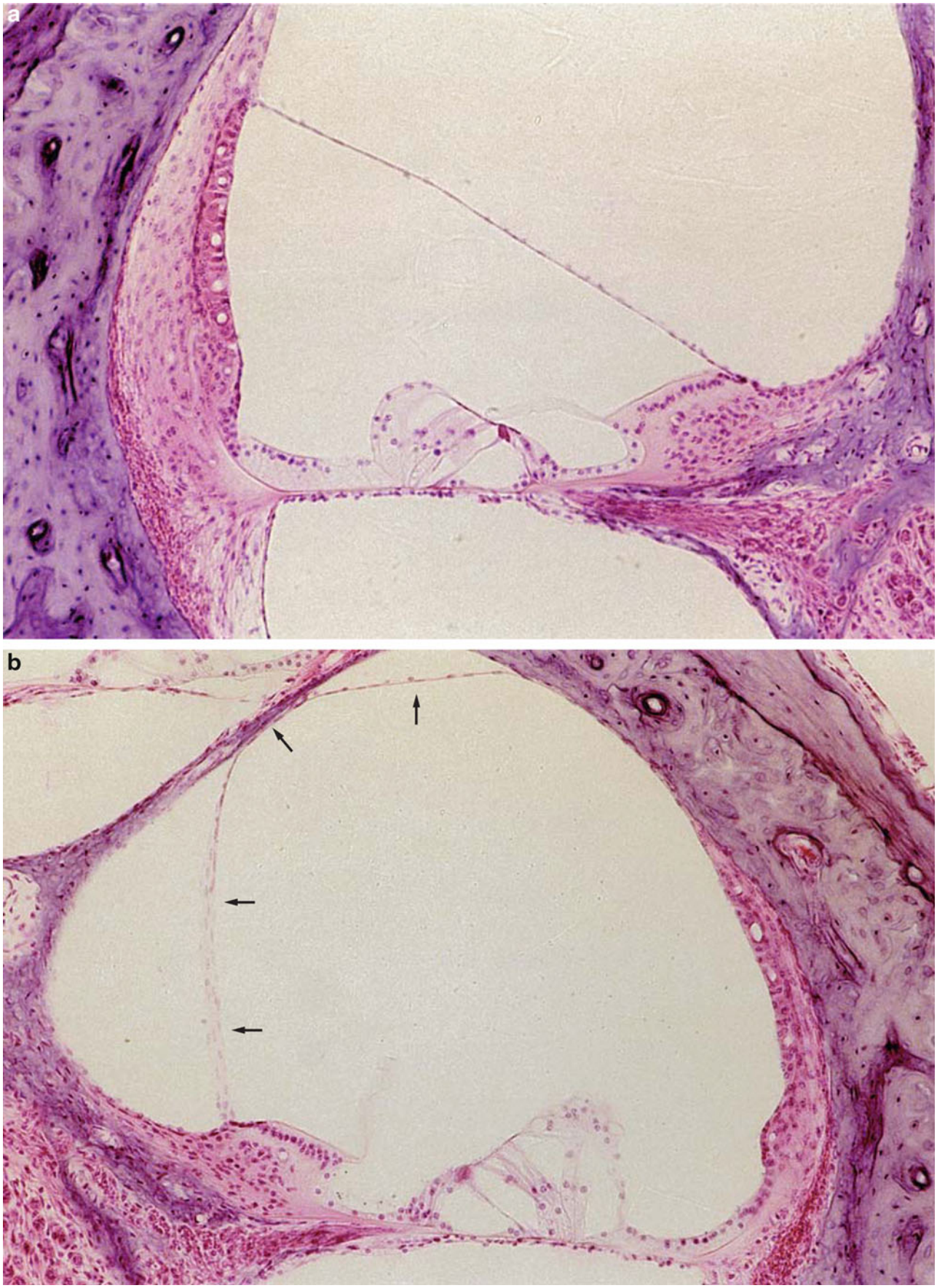

Fig. 5.5 Experimentally induced endolymphatic hydrops in the guinea pig. These specimens were made 4 months after obliteration of the endolymphatic duct and sac. (**a**) Control showing normal structure. (**b**) Markedly distended Reissner's membrane (*arrows*). (**c**) Normal structure on the control side *1*: endolymphatic duct, *2*: endolymphatic sac, *3*: operculum, *4*: lateral sinus. (**d**) Obliteration of the endolymphatic duct and sac (Courtesy of Dr. Kimura)

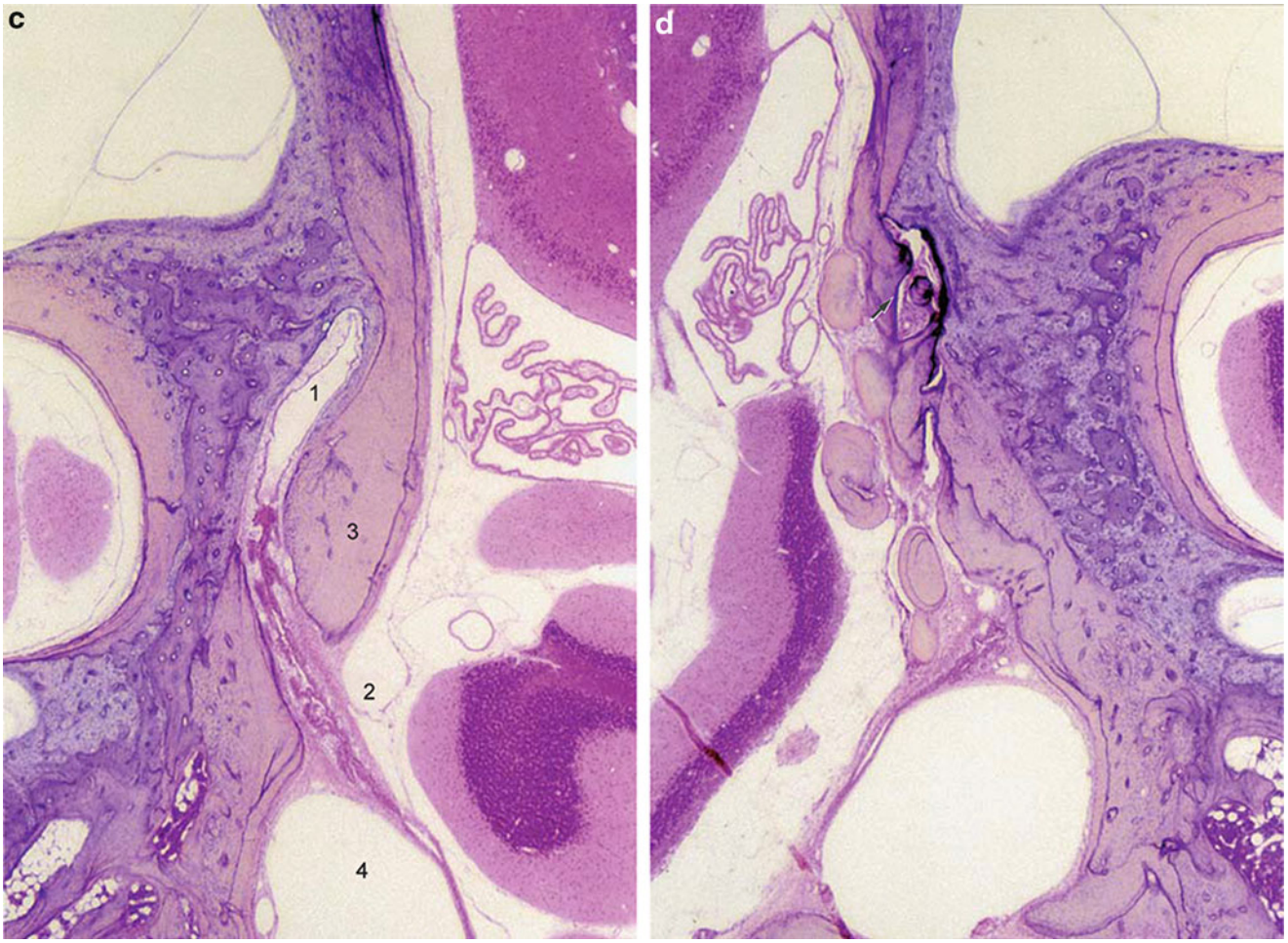

Fig. 5.5 (continued)

5.6 Vestibular Evoked Myogenic Potentials

Vestibular evoked myogenic potential (VEMP) testing has rapidly prevailed as the clinical test for patients with ear and neurotological diseases since Colebatch et al. published a paper on the subject in 1994 [26]. Cervical VEMPs (cVEMPs) are generated at the sternocleidomastoid muscle as a reflex induced by intense sound. The reflex begins at the saccule, travels via the inferior vestibular nerve to the lateral vestibular nucleus, then passes through the medial vestibulospinal tract to the motor neurons of the sternocleidomastoid muscle, where the evoked myogenic potentials are measured. Another method of measurement is using bone conduction of sound. The response can be recorded on the extraocular muscles, termed ocular VEMP (oVEMP). This reflex originates at the utricle and travels via the superior vestibular nerve along the vestibulo-ocular reflex pathway to the extraocular muscles.

Young (2013, Personal Communication) described three patients with Meniere's disease who showed different VEMP responses. The first patient, a 50-year-old man, had been suffering from attacks of vertigo and sensorineural hearing loss of the right ear for 8 months. Both oVEMP (nI–pI) and cVEMP (p13–n23) tests showed normal responses bilaterally (Fig. 5.7). The second patient, a 60-year-old woman, had a 2-year history of Meniere's disease of the left ear. Augmented oVEMP responses and reduced cVEMP responses were observed in the left ear, compared with the right. This condition is termed "VEMPs dissociation" (Fig. 5.8). The third patient, a 56-year-old woman, had experienced vertiginous episodes for 5 years. Both oVEMP and cVEMP tests revealed absent responses in the right ear, and normal responses in the left ear (Fig. 5.9). Her caloric test remained normal.

Loss of otolithic organs cannot guarantee resolution of vertigo. With the loss of semicircular canal function, patients might cease to experience vertigo.

Once the saccular wall ruptures during a Meniere attack, the collapsed or distorted saccule leads to absent or reduced cVEMPs. In this condition, the utriculo-endolymphatic valve

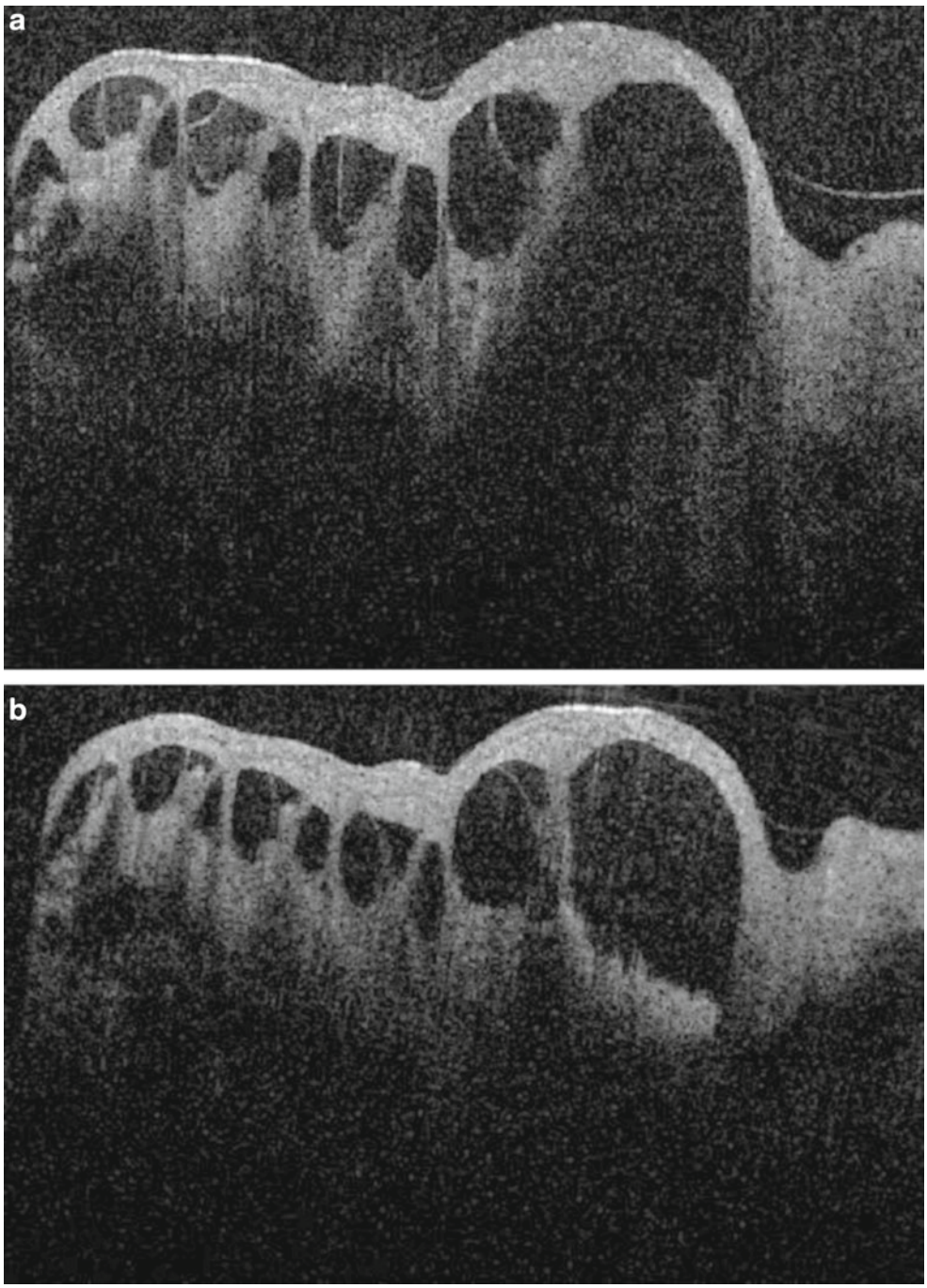

Fig. 5.6 Optical coherent tomography of the cochlea of the guinea pig. (**a**) All cochlear turns show hydrops 4 weeks after blockage of the endolymphatic duct. (**b**) Control (Courtesy of Dr. Kakigi)

closes to maintain normal pressure in the utricle and semicircular canals. Thus, augmentation of oVEMPs may result from a compensatory enlargement of utricular hydrops due to endolymphatic pressure elevation in the utricle. The augmentation is a transient and reversible state observed soon after a Meniere attack. Once the inner ear regains homeostasis, reopening of the utriculo-endolymphatic valve may cause relief of the utricular hydrops. Consequently, augmented oVEMPs resolve and normal responses return [27].

5.7 Gentamicin

Intratympanic application of aminoglycosides, such as streptomycin and gentamicin, has been used to treat intractable Meniere's disease. This technique is called chemical labyrinthectomy because chemicals destroy the sensory cells of the inner ear. The goal of this treatment is to control vertigo by destroying the vestibular system while maintaining hearing.

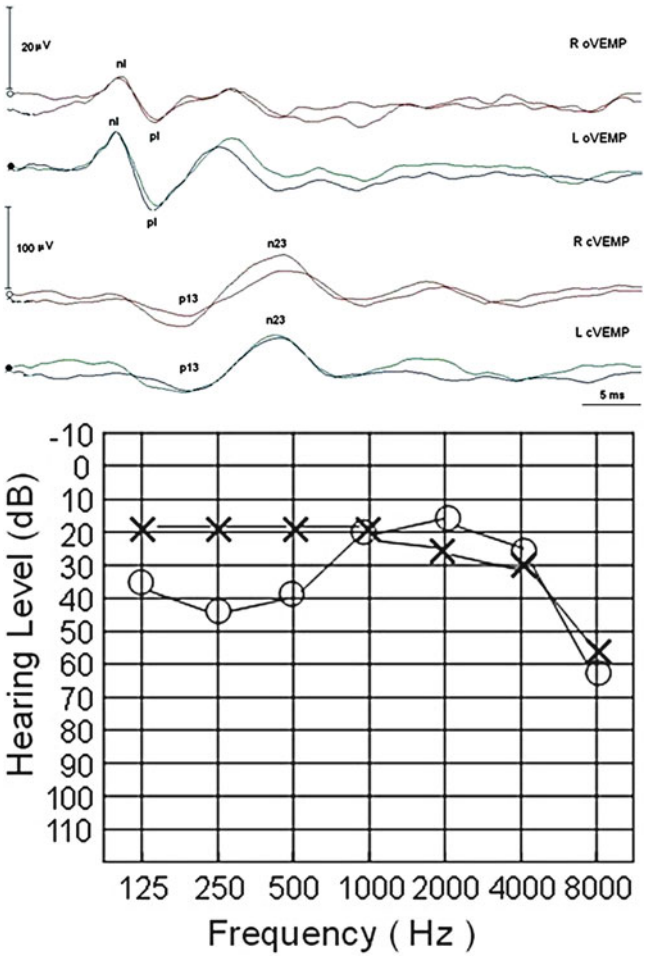

Fig. 5.7 VEMP test results and audiogram in a patient with Meniere's disease (Case 1). 50-year-old man. *Upper* figures show normal oVEMP bilaterally. *Lower* figures show normal cVEMP bilaterally

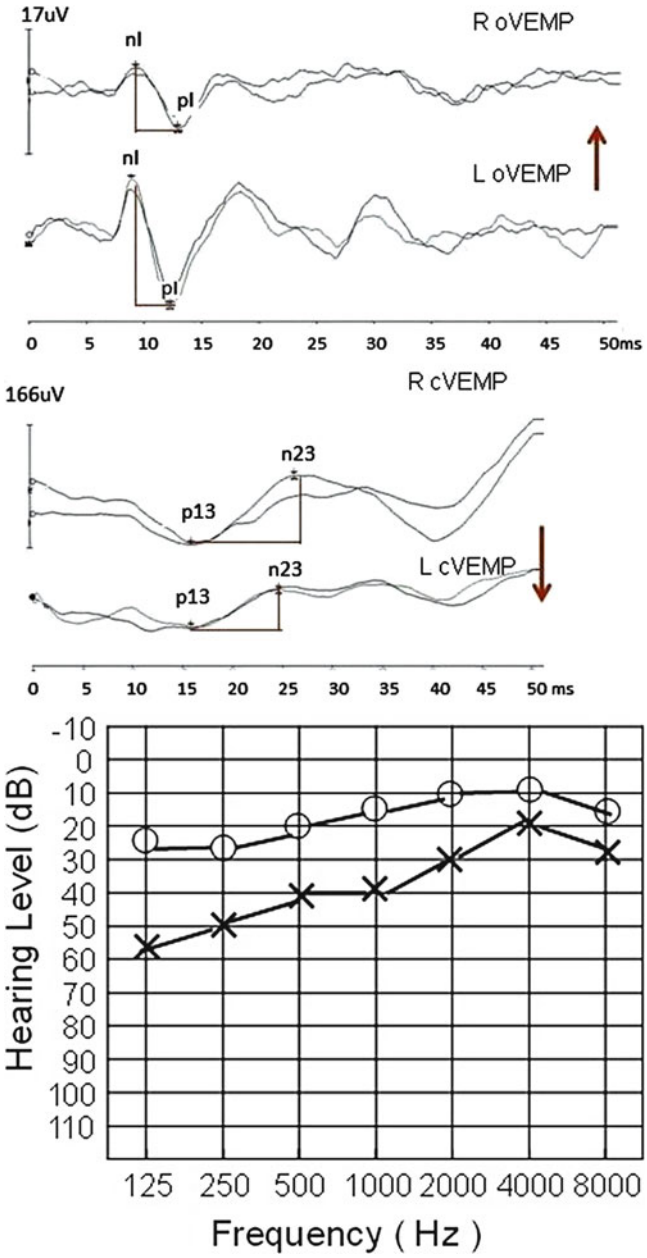

Fig. 5.8 VEMP test results and audiogram in a patient with Meniere's disease (Case 2). 60-year-old woman. Her left oVEMP shows an augmented response, while cVEMP shows reduced response. See text for explanation

Schuknecht [28] used intratympanic streptomycin for vestibular ablation in patients with Meniere's disease. In previous experiments, he had demonstrated that a saturated solution of streptomycin applied locally in the middle ear in cats caused degeneration of the vestibular and cochlear sensory epithelia.

Wersäll [29] introduced approximately 0.2 mL of a 50 % solution of gentamicin in saline into the bulla of guinea pigs once daily for 1–4 days. After 4 days, almost all of the sensory cells on the top of the crista had degenerated and only a few cells remained on the sides of the crista. In dilute solution experiments, even a 0.3 % gentamicin solution administered for 13 days caused severe changes in the vestibular sensory epithelia and degeneration of cochlear hair cells. Later, Wersäll [30] reported that the central part of the crista was most severely damaged, whereas the periphery of the crista, as well as the area close to the planum semilunatum, showed less change. The type I sensory cells were more severely damaged than type II. The sensory hairs showed successive stages of fusion and giant hair formation before the sensory cell disintegrated and disappeared.

Intratympanic gentamicin application has recently become a major treatment modality for intractable Meniere's disease. The reason for using gentamicin is that it is more vestibulotoxic than cochleotoxic. Intratympanic gentamicin is expected to destroy vestibular function while maintaining hearing.

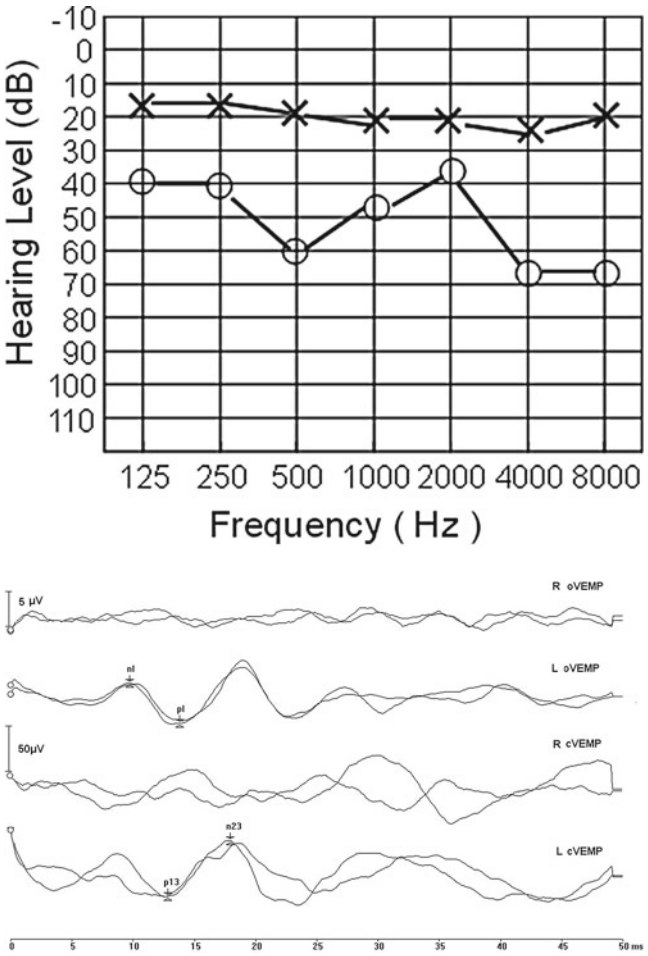

Fig. 5.9 VEMP test results and audiogram in a patient with Meniere's disease (Case 3). Fifty-six-year-old woman. The *right ear* shows absent responses in cVEMP and oVEMP. The *left ear* shows normal responses (Courtesy of Dr. Young)

Gentamicin appears to generate free radicals within the inner ear sensory cells. In one study, a variety of free-radical species were detected in the inner ear after gentamicin application, presumably initiating the apoptotic cascade [31]. It was reported that the c-Jun N-terminal kinase (JNK) signal pathway plays a role in gentamicin-induced cochlear and vestibular hair cell death [32]. Conversely, D-JNK-1 blocks this signal pathway and prevents hair cell death [32].

To study the inner ear lesions induced by gentamicin, it is mandatory to demonstrate the drug's distribution within the inner ear. Three methods of gentamicin administration have been described [33, 34]:

1. Intratympanic administration. Gentamicin (10 mg/0.25 mL) was injected into the middle ear of guinea pigs through the tympanic membrane.
2. Perilymphatic perfusion. One milliliter of phosphate-buffered solution containing gentamicin (5 mg/mL) was perfused from the scala tympani to the oval window for 15 min.
3. Intraperitoneal administration. Various doses of gentamicin (1–200 mg/kg) were injected intraperitoneally for 7 days.

Twenty-four to forty-eight hour after intratympanic administration of gentamicin (10 mg) in guinea pigs, the temporal bones were removed under deep anesthesia. An immunofluorescence method was employed to detect the presence of gentamicin in tissues. Specific fluorescence was found in the inner hair cells, outer hair cells, and tympanic panicle. There was no difference in fluorescence between cochlear turns. In the outer hair cells, specific fluorescence was strong in the subcuticular region and nucleus (Fig. 5.10). Rather uniform distribution of fluorescence was found in the cytoplasm of the inner hair cells. Deiters' cells, Hensen's cells, Reissner's membrane, and the lateral portion of the spiral ligament from the basal to the second turn also showed fluorescence.

When the gentamicin dose was reduced, for example to 2 or 1 mg, the subcuticular region of the outer hair cells continued to show strong fluorescence, while the inner hair cells and tympanic panicle lost fluorescence.

The stria vascularis showed no fluorescence in any of the experiments.

Intratympanic administration of 10 mg of gentamicin in the vestibular organs of guinea pigs produces strong specific fluorescence in type I hair cells in the crista ampullaris and utricle (Fig. 5.11). Nerve chalices of type I hair cells also showed strong fluorescence. Type II hair cells and supporting cells showed weak fluorescence, and the nerve fiber showed none. Dark cell areas showed a weak response.

Electron microscopy revealed massive antigen accumulation in the nerve chalices of type I hair cells. The antigens were located on the surface of the stereocilia.

After perilymphatic perfusion of gentamicin, an intense greenish fluorescence, indicative of the presence of gentamicin, was found in the outer hair cells, Deiters' cells, Hensen's cells, basilar membrane, and basilar crest. Weak fluorescence was found in Reissner's membrane and the tectorial membrane. No fluorescence was found in the stria vascularis or inner hair cells.

After intraperitoneal administration of gentamicin, intense fluorescence was demonstrated in the type I hair cells of the crista ampullaris and utricle. The nerve chalices also showed strong fluorescence. The type II hair cells, supporting cells, and dark cells showed no fluorescence.

The distribution and intensity of fluorescence varied according to the dose and duration of gentamicin application. The cytoplasm of the vestibular ganglion cells, Purkinje cells, and tubular epithelial cells of the renal cortex showed fluorescence.

Vulnerability of type I hair cells to streptomycin and gentamicin had already been reported by Wersäll et al., based on electron microscopy studies [30]. A strong affinity of amino-

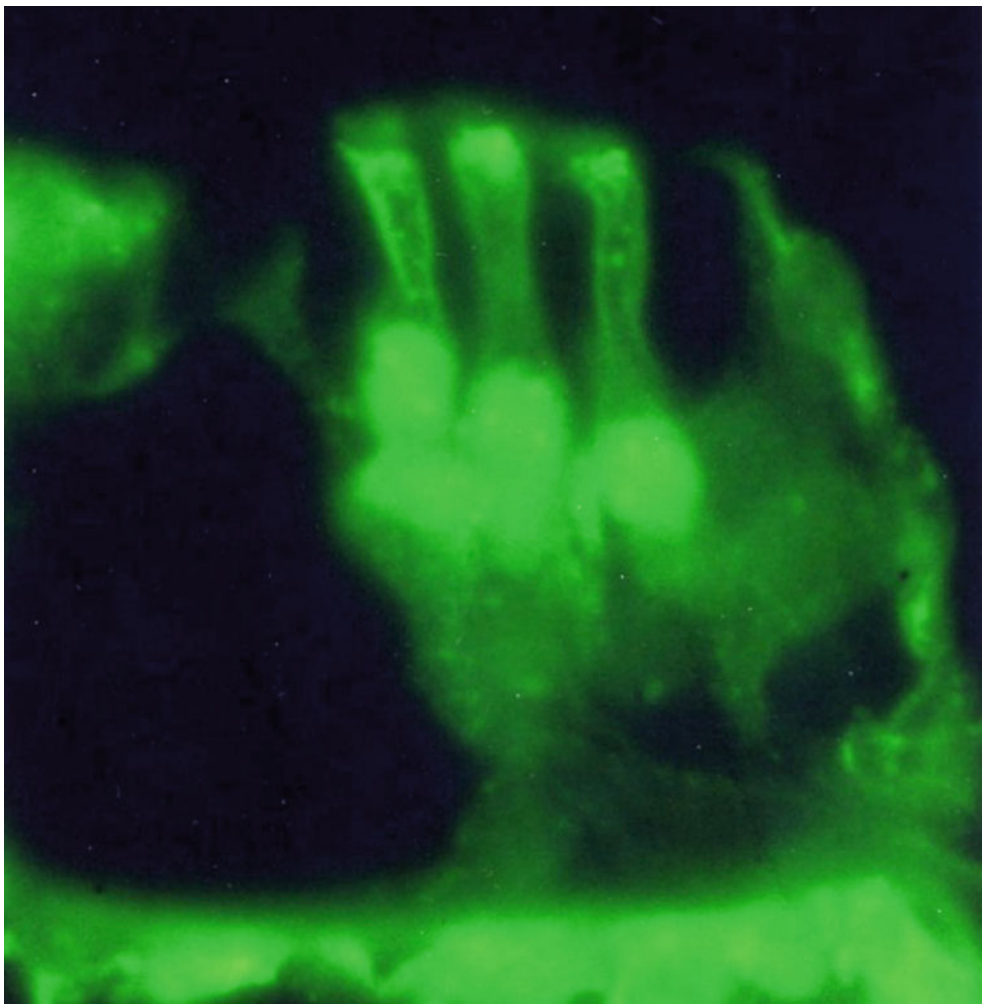

Fig. 5.10 Distribution of gentamicin in the organ of Corti. Ten milligram of gentamicin was administered into the tympanic cavity through the eardrum. Strong fluorescence indicates the presence of gentamicin. Fluorescence is observed in the subcuticular region and the nucleus of the outer hair cell. Guinea pig [33]

glycoside antibiotics for inositol phospholipid in the inner ear has been confirmed [35]. Gentamicin first attacks the cell membrane of the sensory cells. The number of receptors and membrane gradient will greatly influence the uptake of gentamicin. Generally, a close correlation has been found between the distribution of gentamicin and the presence of inner ear lesions.

Gentamicin administered near the round window produced lesions in the limbus, particularly in the basal turn. The regions close to the inner sulcus were most commonly affected. Detached tectorial membrane and severely degenerated sensory and interdental cells were observed in some specimens [36].

The route of gentamicin application is important when we use it clinically. Gentamicin or streptomycin applied to the lateral canal fenestra is toxic to all vestibular sensory cells located posterior to the membrana limitans, while very little effect is seen in the cochlear sensory cells [37, 38].

It has been postulated that a possible mechanism of gentamicin ototoxicity could be the damage inflicted on the vestibular dark cells. Several animal studies have shown that intratympanic application of gentamicin causes changes in dark cells prior to damage to the sensory neuroepithelium [39–41].

To verify the hypothesis that intratympanic gentamicin treatment in Meniere's disease can reduce endolymphatic hydrops, Fiorino et al. performed 3D-FLAIR gadolinium MRIs 1–3 weeks before and several months after administration. There was no evidence of reduced endolymphatic hydrops after treatment [42].

Recently, it has been suggested that occlusion of the lateral semicircular canal relieves vertiginous spells and preserves hearing in patients with Meniere's disease [43].

It should be noted that George Portmann described hydrops or hypertension in the endolymphatic compartments as the pathophysiological basis for Meniere's

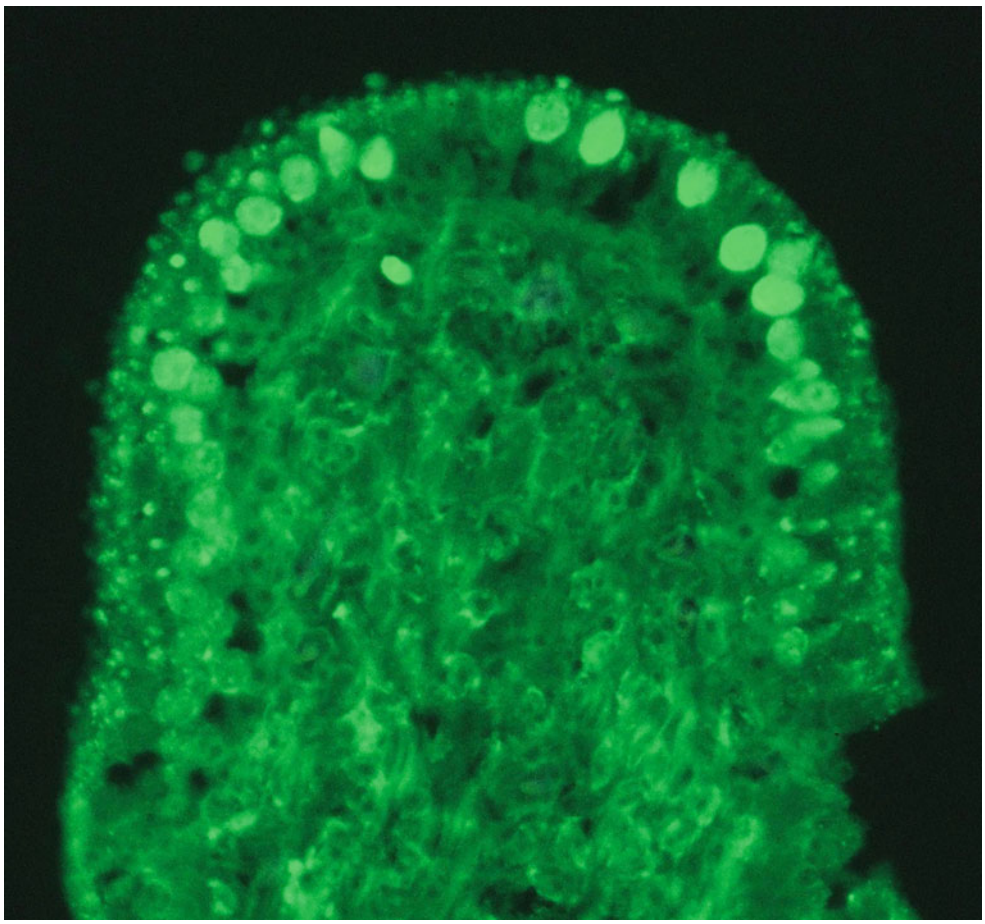

Fig. 5.11 Distribution of gentamicin in the crista ampullaris. Strong fluorescence appears in type 1 hair cells of the crista ampullaris after intratympanic application of gentamicin. In some animals, nerve chalices showed strong staining. Guinea pig [34] (Courtesy of Dr. Iwamori)

disease and invented endolymphatic sac surgery as a treatment in 1927, more than 10 years prior to the discovery of endolymphatic hydrops in the temporal bones of these patients.

References

1. Yamakawa K (1938) Hearing organ of a patient who showed Meniere's symptoms (in Japanese). J Otolaryngol Soc Jpn 44: 2310–2312
2. Yamakawa K (1938) Über die pathologische Veränderungen bei einem Meniere-Kranken. Z f Otol Tokyo 44:192–193
3. Hallpike CS, Cairns H (1938) Observations on the pathology of Meniere's syndrome. J Laryngol Otol 53:625–655
4. Stahle J (1989) Endolymphatic hydrops-fiftieth anniversary. Acta Otolaryngol (Stockh) 468(Suppl):11–16
5. Paparella MM, Morizono T, Matsunaga T (1992) Kyoshiro Yamakawa, MD, and temporal bone histopathology of Meniere's patient reported in 1938. Commemoration of the centennial of his birth. Arch Otolaryngol Head Neck Surg 118:660–662
6. Hallpike CS, Wright AJ (1939) On the histological changes in the temporal bone of a case of Meniere's disease. Proc R Soc Med 32(12):1646–1656
7. Rollin H (1940) Zur Kenntnis des Labyrinthhydrops und des durch ihn bedingten Ménière. Hals-Nasen-u Ohrenarzt 31:73–109
8. Altmann F, Fowler EP Jr (1943) Histological findings in Meniere's symptom complex. Ann Otol Rhinol Laryngol 52:52–80
9. Lindsay JR (1946) Labyrinthine dropsy. Laryngoscope 56:325–341
10. Lindsay JR (1959) Sudden deafness due to viral infection. Arch Otolaryngol 69:13–18
11. Williams HL, Horton BT, Day LA (1950) Endolymphatic hydrops without vertigo: its differential diagnosis and treatment. Arch Otolaryngol 51:557–581
12. Okuno T, Sando I (1987) Localization, frequency, and severity of endolymphatic hydrops and the pathology of the labyrinthine membrane in Meniere's disease. Ann Otol Rhinol Laryngol 96:438–445
13. Naganawa S, Koshikawa T, Nakamura T, Kawai H, Fukatsu H, Ishigaki T, Komada T, Maruyama K, Takizawa O (2004) Comparison of flow artifacts between 2D-FLAIR and 3D-FLAIR sequences at 3 T. Eur Radiol 14:1901–1908
14. Naganawa S, Komada T, Fukatsu H, Ishigaki T, Takizawa O (2006) Observation of contrast enhancement in the cochlear fluid space of healthy subjects using a 3D-FLAIR sequence at 3 Tesla. Eur Radiol 16:753–757
15. Nakashima T, Naganawa S, Sugiura M, Teranishi M, Sone M, Hayashi H, Katayama N, Ishida IM (2007) Visualization of endolymphatic hydrops in patients with Meniere's disease. Laryngoscope 117:415–420
16. Yamazaki M, Naganawa S, Kawai H, Sone M, Nakashima T (2012) Gadolinium distribution in cochlear perilymph: differences between

intratympanic and intravenous gadolinium injection. Neuroradiol 54:1161–1169
17. Kimura RS, Schuknecht HF (1965) Membranous hydrops in the inner ear of the guinea pig after obliteration of the endolymphatic sac. Pract Oto-rhino-laryngol 27:343–354
18. Kimura RS (1967) Experimental blockage of the endolymphatic duct and sac and its effect on the inner ear of the guinea pig: a study on endolymphatic hydrops. Ann Otol Rhinol Laryngol 76:664–687
19. Kimura RS (1968) Experimental production of endolymphatic hydrops. Otolaryngol Clin North Am 1:457–471
20. Ichimiya I, Adams JC, Kimura RS (1994) Changes in immunostaining of cochleas with experimentally induced endolymphatic hydrops. Ann Otol Rhinol Laryngol 103:457–468
21. Nadol JB Jr, Adams JC, Kim JR (1995) Degenerative changes in the organ of Corti and lateral cochlear wall in experimental endolymphatic hydrops and human Menière's disease. Acta Otolaryngol 519(Suppl):47–59
22. Merchant SN, Adams JC, Nadol JB Jr (2005) Pathophysiology of Meniere's syndrome: Are symptoms caused by endolymphatic hydrops? Otol Neurotol 26:74–81
23. Lin J, Staecker H, Jafri MS (2008) Optical coherence tomography imaging of the inner ear: A feasibility study with implications for cochlear implantation. Laryngoscope 117:341–346
24. Sepehr A, Djalilin HR, Chang JE, Chen Z, Wong BJ (2008) Optical coherence tomography of the cochlea in the porcine model. Laryngoscope 118:1449–1451
25. Kakigi A, Takubo Y, Egami N, Kashio M, Sakamoto T, Yamashita S, Yamasoba T (2013) Evaluation of the internal structure of the normal and pathological guinea pig cochleae using optical coherence tomography. 36th Midwinter research meeting of the association for research in otolaryngology, Baltimore (Abstract)
26. Colebatch JG, Halmagyi GM, Skuse NF (1994) Myogenic potentials generated by a click-evoked vestibulocollic reflex. J Neurol Neurosurg Psychiatry 57:190–197
27. Young Y-H (2013) Potential application of ocular and cervical vestibular-evoked myogenic potentials in Meniere's disease: a review. Laryngoscope 123:484–491
28. Schuknecht HF (1957) Ablation therapy in the management of Meniere's disease. Acta Otolaryngol (Stockh) 132(Suppl):1–42
29. Wersäll J, Lundquist P-G, Björkroth B (1969) Ototoxicity of gentamicin. J Infect Dis 119:410–416
30. Wersäll J, Björkroth B, Flock Å, Lundquist PG (1971) Sensory hair fusion in vestibular sensory cells after gentamicin exposure. Arch klin exp Ohr Nas Kehlk Heilk 200:1–14
31. Roland PS (2004) New developments in our understanding of ototoxicity. Ear Nose Throat J 83(Suppl 4):15–16
32. Wang J, Van de Water TR, Bonny C, de Ribaupierre F, Puel JL, Zine A (2003) A peptide inhibitor of c-Jun N-terminal kinase protects against both aminoglycoside and acoustic trauma-induced auditory hair cell death and hearing loss. J Neurosci 23(24):8596–8607
33. Nagai Y, Hayashida T, Nomura Y, Sada T, Iwamori M (1985) Immunohistochemical studies on ototoxicity of gentamicin. The 1984 annual report of acute profound deafness research committee of Japan pp 215–220
34. Hayashida T, Nomura Y, Iwamori M, Nagai Y, Kurata T (1985) Distribution of gentamycin by immunofluorescence in the guinea pig inner ear. Arch Otorhinolaryngol 242:257–264
35. Nagai Y, Iwamori M, Sakakibara K (1979) Immuno-biochemical analysis of ototoxicity. Annual report of acute profound deafness research committee of Japan, pp 44–47
36. Kimura RS, Nye CL, Southard RE (1990) Normal and pathologic features of the limbus spiralis and its functional significance. Am J Otolaryngol 11:99–111
37. Kimura RS, Iverson NA, Southard RE (1988) Selective lesions of the vestibular labyrinth. Ann Otol Rhinol Laryngol 97:577–584
38. Kimura RS, Lee K-S, Nye CL, Trehey JA (1991) Effects of systemic and lateral semicircular canal administration of aminoglycosides on normal and hydropic inner ears. Acta Otolaryngol (Stockh) 111:1021–1030
39. Assimakopoulos D (2003) Treatment of Meniere's disease by intratympanic gentamicin application. J Laryngol Otol 117:10–16
40. Park JC, Cohen GM (1982) Vestibular ototoxicity in the chick: effects of streptomycin on equilibrium and on ampullary dark cells. Am J Otolaryngol 1:17–27
41. Pender DJ (1985) Gentamicin tympanoclysis. Effects on the vestibular sensory cells. Am J Otolaryngol 6:358–367
42. Fiorino F, Pizzini FB, Barbieri F, Beltramello A (2012) Magnetic resonance imaging fails to show evidence of reduced endolymphatic hydrops in gentamicin treatment of Meniere's disease. Otol Neurotol 33(4):629–633
43. Charpiot A, Rohmer D, Gentine A (2010) Lateral semicircular canal plugging in severe Meniere's disease: a clinical prospective study about 28 patients. Otol Neurotol 31:237–240
44. Naganawa S, Yamazaki M, Kawai H, Bokura K, Sone M, Nakashima T (2012) Imaging of Ménière's disease by subtraction of MR cisternography from positive perilymph image. Magn Reson Med Sci 11:303–309

Viral Diseases

6

Abstract

Some viral infections are known to cause sensorineural hearing loss, which may occur suddenly as an acute single insult, or insidiously with a slowly progressive course. When hearing loss occurs during the course of systemic viral infection, it will be apparent that the infection is responsible for the hearing loss. However, hearing loss is not uncommonly categorized as being of "unknown etiology" and left undiagnosed.

To promote better understanding of viral labyrinthitis, we will present human temporal bone histopathology and animal experiment results concerning three viruses: herpes simplex virus, cytomegalovirus, and mumps virus.

In human temporal bone specimens from patients with viral labyrinthitis, the degenerated tectorial membrane often becomes rolled-up and encapsulated on the limbus spiralis or in the inner sulcus. Such findings are seen in patients with mumps and measles. In experimental herpes simplex virus labyrinthitis in guinea pigs, a rolled-up tectorial membrane with viral antigen deposition has been observed, along with bulges of varying sizes in the tectorial membrane. These bulges were found on the surface of the membrane as well as within it. With electron microscopy, virions were observed in and around the bulges. Similar findings were observed in a patient with bilateral sudden deafness. Reactivation of latent HSV infection was suspected in that case. However, not all cases of viral labyrinthitis show changes in the tectorial membrane.

Keywords

Cytomegalovirus • Experimental viral labyrinthitis • Herpes simplex virus • Human temporal bone histopathology • Mumps

6.1 Herpes Simplex Virus (HSV)

6.1.1 Herpes Classification

Human herpes virus has the following subfamilies:

1. *Alphaherpesvirinae*
   simplex virus
      HHV-1 = HSV-1: herpes simplex virus-1
      HHV-2 = HSV-2: herpes simplex virus-2
   varicella virus
      HHV-3 = VZV: varicella zoster virus
2. *Betaherpesvirinae*
   cytomegalovirus
      HHV-5 = CMV: cytomegalovirus
   roseolovirus
      HHV-6
      HHV-7
   Both cause roseola.
3. *Gammaherpesvirinae*
   lymphocryptovirus
      HHV-4 = EBV: Epstein-Barr virus
   rhadinovirus
      HHV-8 = KSHV: Kaposi's sarcoma-associated herpesvirus

Y. Nomura, *Morphological Aspects of Inner Ear Disease*, DOI 10.1007/978-4-431-54204-9_6,

6.1.2 HSV and Sudden Deafness

Hondo et al. [1] reported an association between HSV and sudden deafness. They studied the prevalence of HSV-1 in patients with sudden deafness by obtaining serum from patients during the acute phase of hearing loss and two to three times during the recovery phase of the disease. One hundred thirty-eight samples from 49 patients were submitted for neutralization testing (NT) and complement-fixation testing (CFT). Neutralizing antibodies against HSV-1 were present in 38 of 49 patients (78 %), a rate similar to that of the control group (77 %). No significant differences were found among different age groups. The CFT results were positive in 38 of 49 patients (78 %), significantly different from results in the control group, where 54 % of people tested positive. The difference between the NT and CFT results in the control group indicate no reactivation of latent HSV infection after initial infection in some individuals, resulting in the disappearance of CF antibody over time. The high incidence of CF antibodies among the patients with hearing loss suggests that if HSV causes the disease, the mechanism of infection may be related to reactivation of latent infection.

A significantly greater percentage of patients with hearing loss (43 %) had neutralizing antibodies against HSV-2 than the control group (20 %). All patients with antibodies against HSV-2 also had antibodies against HSV-1, suggesting that reinfection with HSV-1 precedes infection with HSV-2.

6.1.3 Morphological Study

6.1.3.1 Experimental HSV Labyrinthitis

In one study, HSV-1 and HSV-2 were isolated from the livers of neonates who died of disseminated HSV infection. The viruses were passaged in human embryonic fibroblasts. Virus titers of the strains were 9.2×10^7 pfu/mL (pfu, plaque-forming units) (type 1) and 3×10^6 pfu/mL (type 2).

Inoculation of the Middle Ear

The middle ear cavities of guinea pigs were inoculated with HSV solution (2×10^3 pfu/2 μL) through a hole in the tympanic bulla or tympanic membrane. Between 2 and 14 days after inoculation, the middle and inner ears were removed, fixed in buffered formalin, and decalcified using 10 % ethylenediamine tetraacetic acid (EDTA) solution. Conventional paraffin wax or celloidin were used for embedding. Viral antigen was detected in the inner ear by indirect immunofluorescence. Anti-HSV antiserum was obtained from rabbits after intracorneal inoculation with the virus and used as the primary antibody. Anti-rabbit IgG conjugated with fluorescein isothiocyanate (FITC) was used as the secondary antibody [2].

Results

HSV types 1 and 2 produced similar pathological changes [3].

A variable number of days after inoculation with the HSV solution, the labyrinths with the bullae were removed and processed. HSV infection of the middle ear caused bleeding, cell infiltration, fibrosis, and new bone formation in the mucosa. Immunofluorescence confirmed the presence of HSV antigen in middle ear infiltrates.

In one animal, the round window was found ruptured on day 11 after inoculation. Massive cell infiltration was observed in the scala tympani of the basal turn after round window rupture. Many multinuclear cells were present in the exudate. Some macrophages were found, each containing 4–5 neutrophils (emperipolesis) (Fig. 6.1) [4]. Inflammation extended to the organ of Corti through the basilar membrane. Exudate was present in the scala tympani of the entire cochlea, with less toward the apex. Mixed infection was considered.

Another animal showed marked cell infiltration and hemorrhage from the lower spiral ligament continuously to the scala tympani, and serous inflammation in the scala vestibuli and scala media 10 days after middle ear inoculation. The stria vascularis showed marked edema with disappearance of intermediate cells and was about twice as thick as normal. Edema was also observed in portions of the spiral ligament (Figs. 6.2a, b, 6.3) [4].

Invasion of middle ear infection also occurred without rupture of the round window membrane. In such cases, it was hard to distinguish the structure of the round window membrane because of the surrounding marked cell infiltration.

Inoculation of the Scala Tympani

HSV solution (2×10^3 pfu/2 μL) was inoculated directly into the scala tympani through the round window membrane using a fine needle. A small piece of absorbable gelatin was placed over the round window membrane and the skin incision was sutured after inoculation.

The scalae tympani and vestibuli were fibrotic 7 and 9 days after inoculation. This change was marked in the basal turn and less prominent toward the apical direction. Viral antigens were detected in the organ of Corti, Reissner's membrane, limbus spiralis, stria vascularis, spiral ganglion, and in fibrous tissue in the scalae tympani and vestibuli 6–12 days after virus inoculation into the scala tympani.

The organ of Corti degenerated after HSV inoculation. The nuclei of the hair cells disappeared first, while the cell bodies persisted for a time. Changes in the inner hair cells were less marked than in the outer hair cells. The supporting cells were resistant to infection. There was heavy distribution of antigen in the basal turn where morphological changes were prominent.

Electron microscopy showed HSV nucleocapsids in the nerve fibers and endings of afferent and efferent nerves beneath the outer hair cells (Fig. 6.4) [5]. The nerve fibers in the inner spiral bundle contained HSV nucleocapsids.

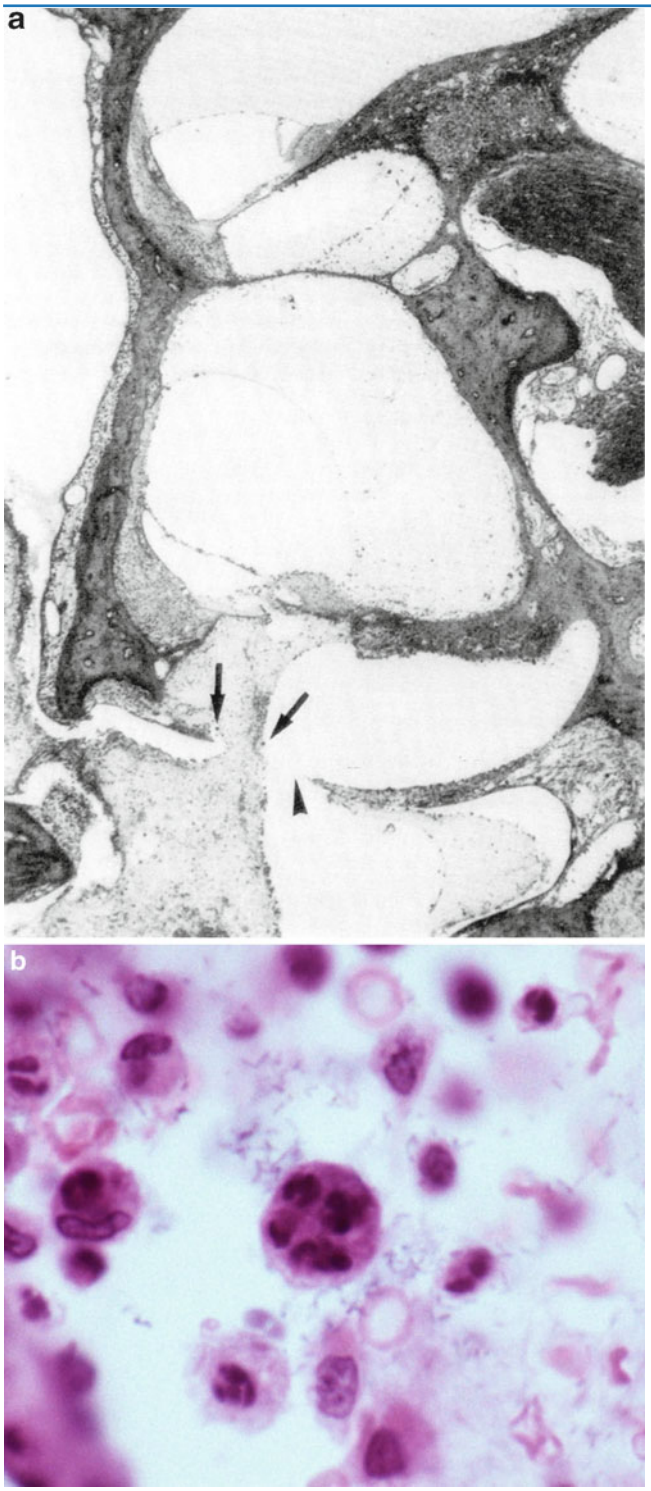

Fig. 6.1 Transtympanic HSV labyrinthitis. (**a**) Invasion of middle ear infection into the cochlea through the round window membrane. Exudate containing many multinuclear cells (*arrows*) has reached the scala tympani 11 days after inoculation of HSV-1 into the middle ear. *Arrowhead*: perforation of the round window membrane (original ×2.5). (**b**) High power view of the area indicated by the *left arrow* in (**a**). A macrophage contains four or five neutrophils (emperipolesis) (original ×40) [4]

After HSV infection, the tectorial membrane often detached from the limbus spiralis and became rounded or floated within the scala media. Detached tectorial membrane was trapped either by Reissner's membrane or by the stria vascularis (Figs. 6.4 and 6.5).

Sometimes degenerated tectorial membrane became a round mass, attached to Reissner's membrane, and was encapsulated by the epithelial cell layer of Reissner's membrane. Similarly, detached tectorial membrane trapped by the stria vascularis was covered by the marginal cells, and disappeared in the stria (Fig. 6.5). Within the stria vascularis, there was cell infiltration around the tectorial membrane. In the stria vascularis the tectorial membrane would be digested and disappear, while tectorial membranes attached to Reissner's membrane would remain unchanged for a long time.

Immunofluorescence studies revealed the distribution of HSV antigen. Particularly strong fluorescence was found on the surface of rolled-up tectorial membrane. The interdental cells also showed strong fluorescence (Fig. 6.6) [5].

Another tectorial membrane change was the presence of many small particles on the surface of the marginal and middle zones in the third turn. In HSV labyrinthitis, the matrix of the tectorial membrane showed aggregation of variably-sized masses on the surface, as well as within the tectorial membrane (Figs. 6.7 and 6.8a–c) [3, 6]. Similar findings were observed on the tectorial membrane of a patient who developed acute bilateral profound sensorineural hearing loss over the course of a single day (see text in Chap. 4, Sudden Deafness). Non-enveloped viral particles were found on the surface of the masses or bulges formed on the surface of the tectorial membrane in the experimental animals.

HSV particles consist of three main parts: the core, the characteristic shell (capsid), and the envelope [7]. It is rather unusual for HSV particles in the extracellular space to have no envelope. The unusual finding of non-enveloped virus particles in this case may be due to the presence of endolymph within the extracellular space.

The spiral ganglion cells are the preferred site of HSV infection. In the first days after inoculation, two types of intranuclear inclusion bodies appeared in the spiral ganglion: Cowdry type A and full type. The spiral ganglion cells gradually disappeared [8].

It is noteworthy that viral antigens were detected on the sixth day in the spiral ganglion not only on the inoculated side, but also on the non-inoculated side (Fig. 6.9) [5]. The opposite cochlea showed normal morphology, so the presence of virus there did not result from spread of viral inflammation from the inoculated cochlea. Potential routes of virus migration to the contralateral spiral ganglion include (1) through the CSF, (2) through the perineural space, (3) through the perilymph and CSF, or (4) hematogenous spread. The phenomenon of

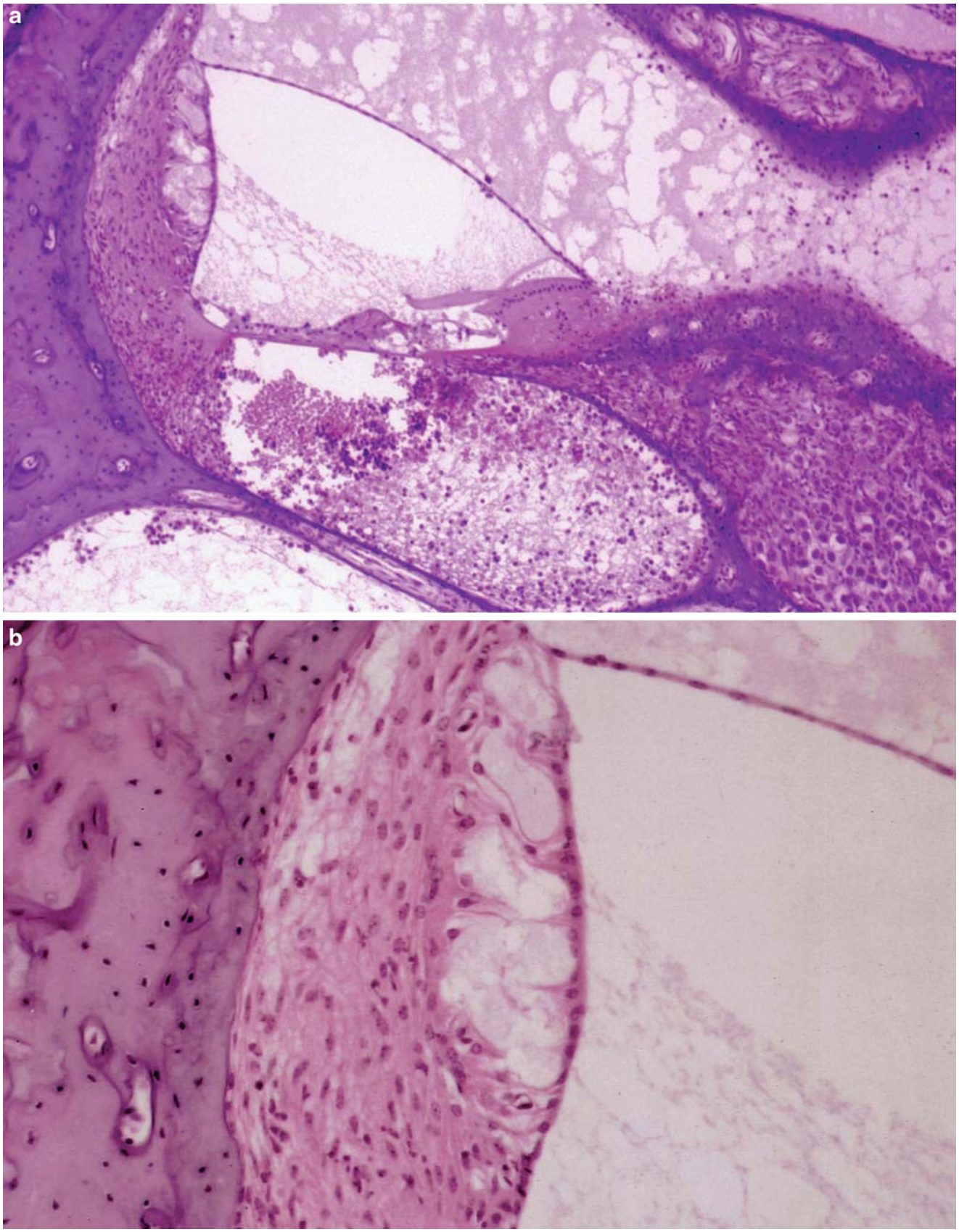

Fig. 6.2 Transtympanic HSV labyrinthitis. (**a**) Viral labyrinthitis 10 days after HSV-1 inoculation of the middle ear. Inflammation of the cochlea spreads mainly in the scala tympani of the basal turn through the round window. Marked hemorrhage and cell infiltration is observed in the lower spiral ligament and scala tympani. The stria vascularis shows marked edema and loss of the intermediate cells (original ×6.5). (**b**) Enlarged stria vascularis. Loss of intermediate cells and edema are marked. The spiral ligament is also edematous (original ×16) [4]

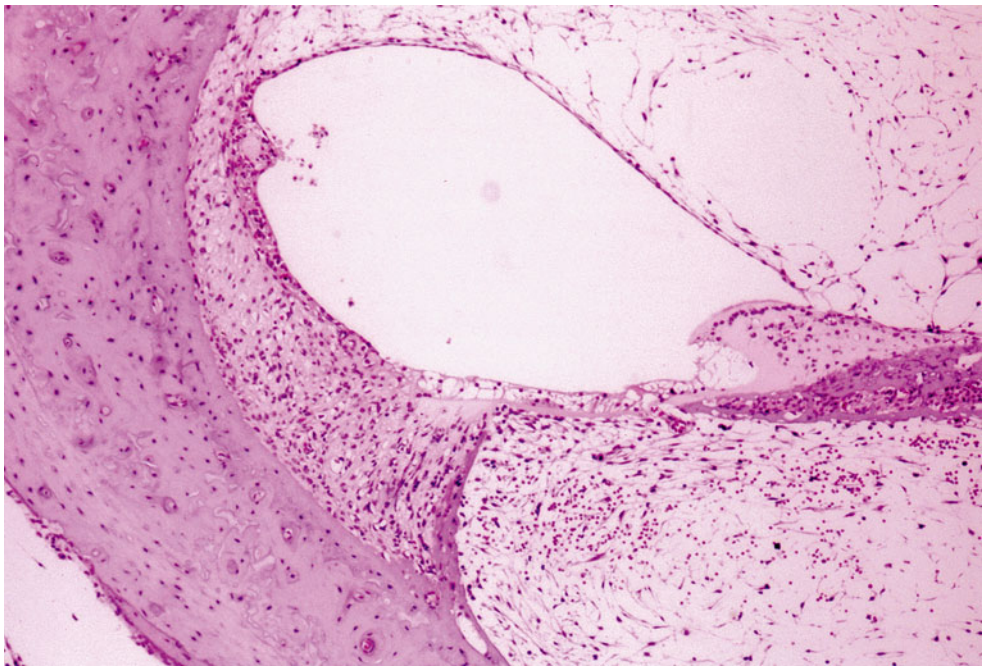

Fig. 6.3 Transtympanic HSV labyrinthitis. Seven days post-inoculation of the middle ear. Marked fibrosis in the scala tympani and scala vestibuli of the basal turn. The organ of Corti has degenerated. The stria vascularis is atrophic and has trapped the detached tectorial membrane (original ×6.5)

Schreiner may be involved. In the absence of morphological changes, the presence of HSV in the non-inoculated cochlea would be termed a latent infection. We attempted but failed to reactivate latent infection to induce drastic changes in the cochlea with administration of cyclophosphamide. If viral reactivation becomes possible, this method will be used to produce a model of acute profound sensorineural hearing loss.

Five to seven days after intralabyrinthine inoculation with HSV-1, the undersurface of the tectorial membrane showed several changes, while the hair cells and supporting cells showed no change.

Imprints exist on the undersurface of the tectorial membrane. Under a scanning electron microscope, partial exposure of the fibrous layer of the tectorial membrane was found after HSV infection, resulting from loss of the membrane matrix. Furthermore, changes were found in the imprint itself. The normal imprint consists of several elliptic dips arranged independently. In the infected tectorial membrane, the dips disintegrate, and may be fused (Fig. 6.10a–c) [9]. The coupling of the stereocilia with the deformed dip will interfere with normal sound transmission.

More advanced changes were observed in the cochlea 2 months after intralabyrinthine inoculation. The infected scala tympani revealed fibrosis and ossification. The stria vascularis had disappeared. Marked endolymphatic hydrops had developed. The organ of Corti had a strange appearance, with only the surface remaining as a thin membranous structure. The border cells, pillar cells, membrana reticularis, and Hensen's cells were probably involved in the formation of the structure. However, no visible cell elements were found inside the organ of Corti. No cellular infiltrates were observed within the cortilymphatic space (Fig. 6.11a, b).

Perhaps apoptosis had taken place in the hair cells and supporting cells. High osmolarity in the cortilymph induces influx of water from the scala tympani, resulting in the formation of cortilymphatic hydrops (see Chap. 2, Inner Ear Fluid).

6.1.3.2 Human Temporal Bone

To my knowledge, HSV labyrinthitis in human temporal bones has not been reported. We know from experiments that HSV infection results in peculiar and characteristic changes in the tectorial membrane. The changes seen with HSV labyrinthitis include rolling up of the tectorial membrane and formation of variably-sized particles resulting from condensation or aggregation of altered tectorial membrane constituents.

The patient with sudden deafness introduced in Chap. 4, in whom viral labyrinthitis was suspected, had tectorial membrane changes quite similar to those observed in experimental HSV labyrinthitis (Fig. 4.4).

Reptiles, a famous Escher lithograph, is suggestive of the viral life cycle. Many sleeping lizards (viruses) are hidden within a white page (a cell) in a drawing book. One of the viruses awakes and escapes from the cell for a walk, becoming gradually more vigorous. Finally, the virus is in high spirits and sits proud of its triumph on a regular dodecahedron (Fig. 6.12).

After its excursion, the virus returns to lie dormant in the cell. This illustrates the cycle of reactivation of latent HSV infection, although the nucleocapsid of HSV is a regular icosahedron.

Fig. 6.4 HSV nucleocapsids (*arrows*) in one of the efferent nerve endings beneath the first row of outer hair cells of the third turn. Scale: 0.5 μm × 31300 [5]

6.2 Cytomegalovirus

6.2.1 Introduction

Cytomegalovirus (CMV) belongs to the *Betaherpesvirinae* subfamily of *Herpesviridae*. It is also a member of the TORCH complex, i.e., Toxoplasmosis, Others, Rubella, CMV, and Herpes simplex virus. When these microorganisms infect pregnant women who lack immunity, severe complications may occur in the children before or after birth, without apparent symptoms in their mothers.

Cytomegalic inclusion diseases have been considered a leading cause of human congenital viral infection and hearing loss, including a progressive type of hearing loss in children [10]. According to Barbi et al. [11], more than 40 % of cases of deafness of unknown cause that need rehabilitation are attributable to CMV, which is most commonly the result of intrauterine infection. Infants can also be exposed to CMV through breast milk. Delayed onset of hearing loss after CMV infection is common. Infants with CMV and normal hearing at birth should be monitored for 6 years for hearing loss. Newborn infants with CMV can be treated with ganciclovir.

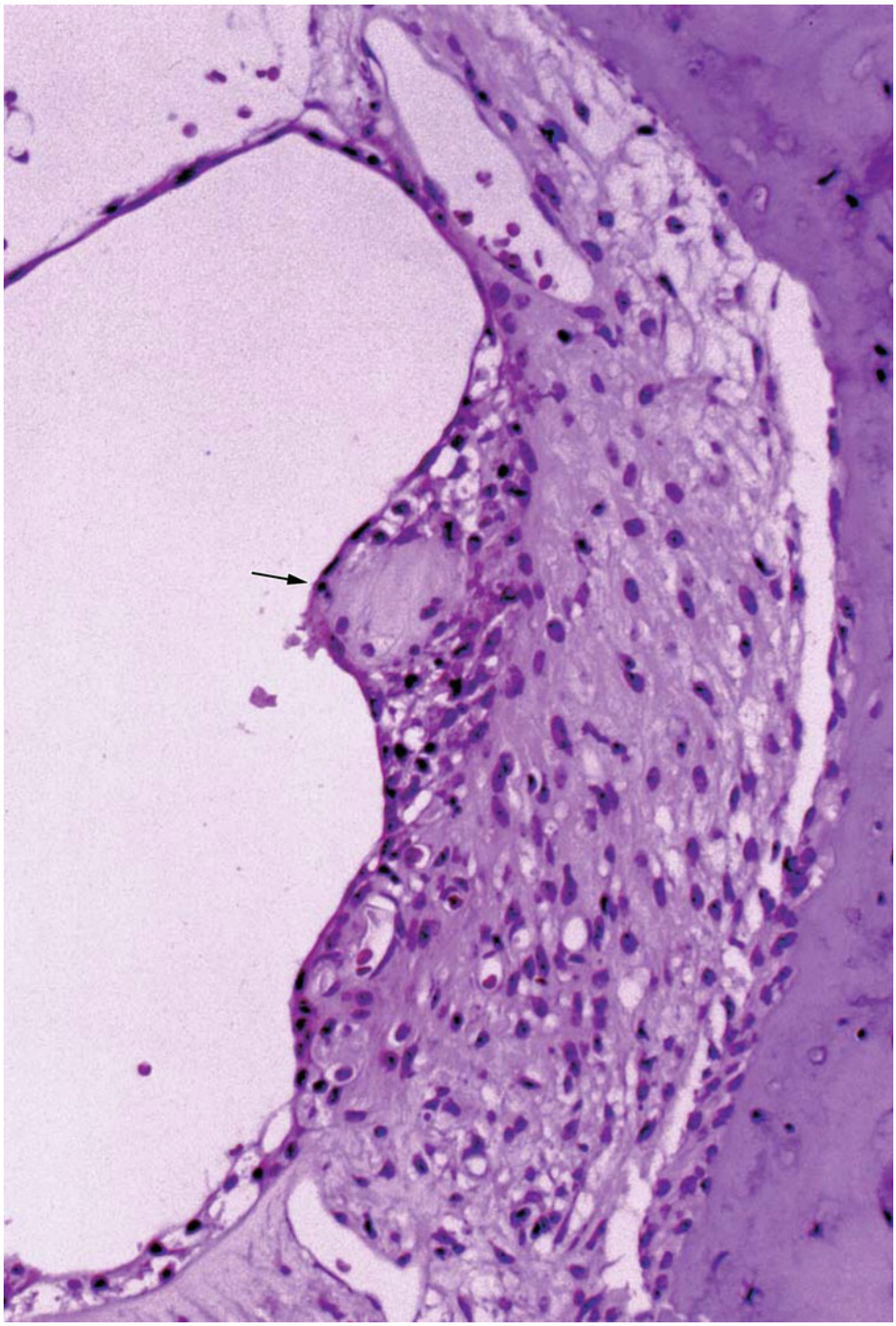

Fig. 6.5 The stria vascularis in viral labyrinthitis 7 days after intracochlear inoculation of HSV-1. The stria vascularis has trapped the detached tectorial membrane, which is covered by atrophic marginal cells. There is cell infiltration around the tectorial membrane. The *arrow* indicates the tectorial membrane (original ×16)

6.2.2 Incidence of Congenital CMV Infection Among Newborns in Japan

Because congenital CMV infection causes significant clinical consequences not only at birth but also with delayed otological and neurological sequelae, it is critical to establish a strategy for screening congenitally infected newborns. Koyano et al. [12] have recently developed a quantitative PCR assay using urine filter discs placed in diapers. The discs function directly as a PCR template without additional steps. Using these

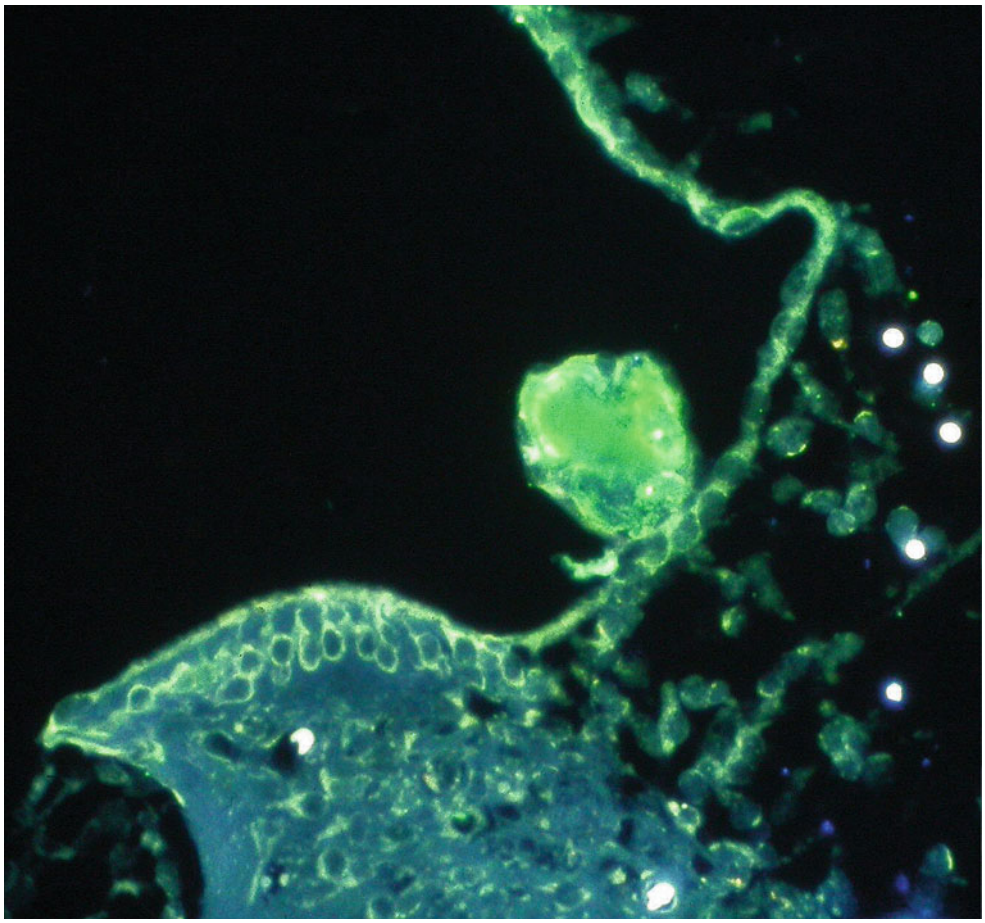

Fig. 6.6 Presence of HSV antigen in the rolled-up tectorial membrane 9 days after intracochlear inoculation. Intense fluorescence reaction in the rolled-up tectorial membrane indicates the presence of HSV antigen. Strong reaction is also found in Reissner's membrane and in the interdental cells (original ×16) [5]

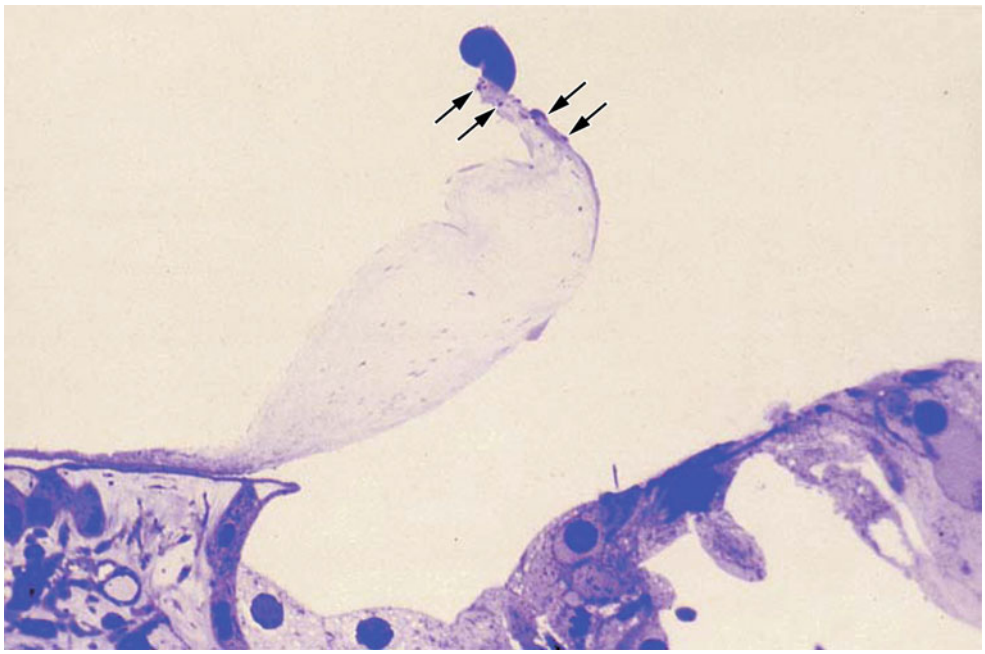

Fig. 6.7 Degeneration of the tectorial membrane. Seven days after intracochlear inoculation with HSV-1. Bulge formation at the tip of the marginal zone. Several small bulges are present nearby (*arrows*). Loss of interdental cells is observed. Toluidine blue staining (original ×16) [3]

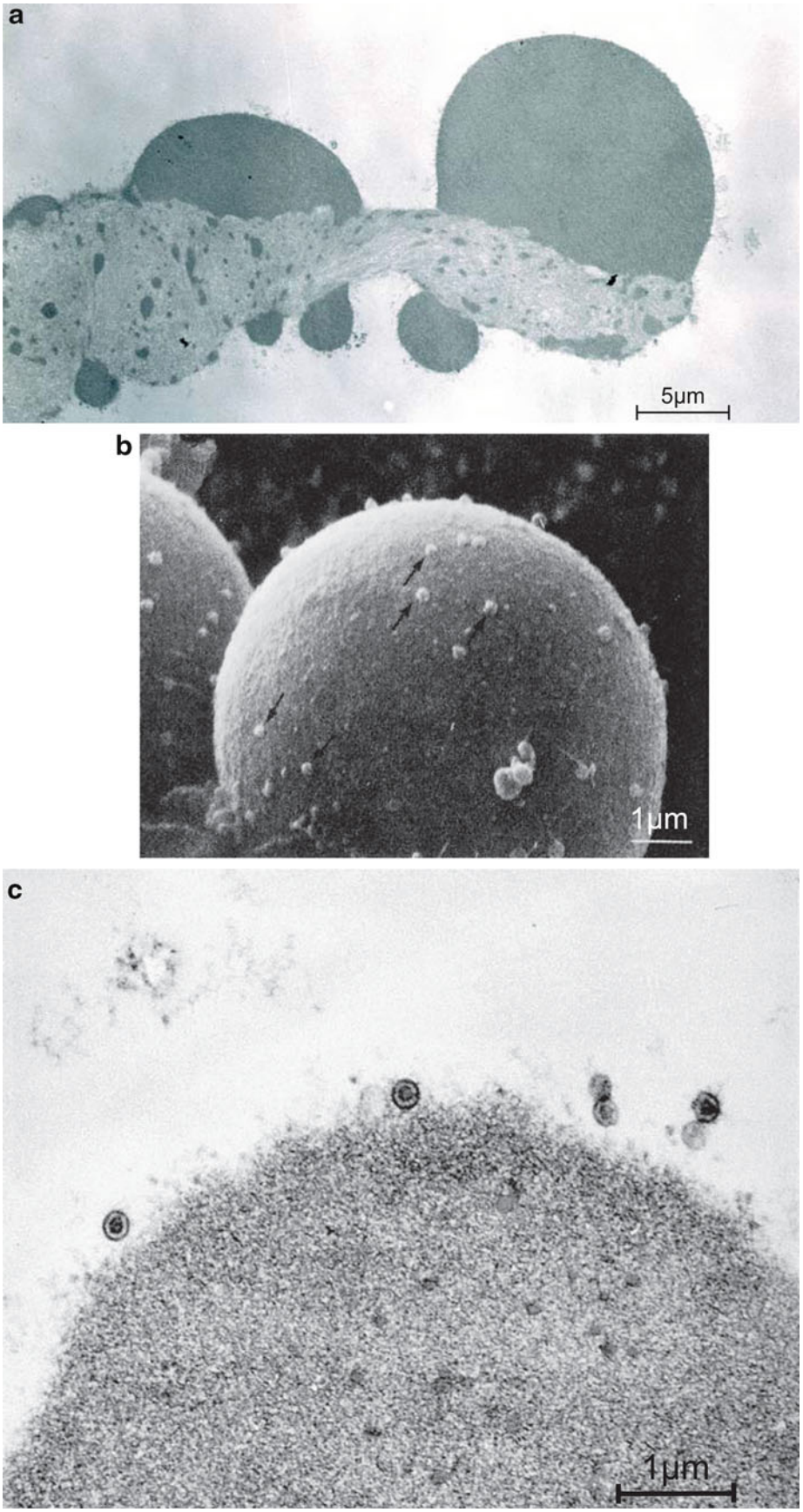

Fig. 6.8 Degenerated tectorial membrane with viral particles. (**a**) Transmission electron microscopic observation 9 days after intracochlear inoculation with HSV-1. Larger masses are present on the surface of the degenerating tectorial membrane. Many small masses are observed within the membrane (Bar: 5 μm, original ×7,500) [3]. (**b**) Scanning electron microscopic observation. A spherical mass on the surface of the tectorial membrane consisted of condensation of degenerated filaments. Many viral particles are seen on its surface (*arrows*) 7 days after intracochlear inoculation (Bar: 1 μm, original ×12,000) [9]. (**c**) Transmission electron microscopic observation. Viral particles on the surface of a bulge 9 days after intracochlear inoculation (Bar: 1 μm, original ×54,000 [3])

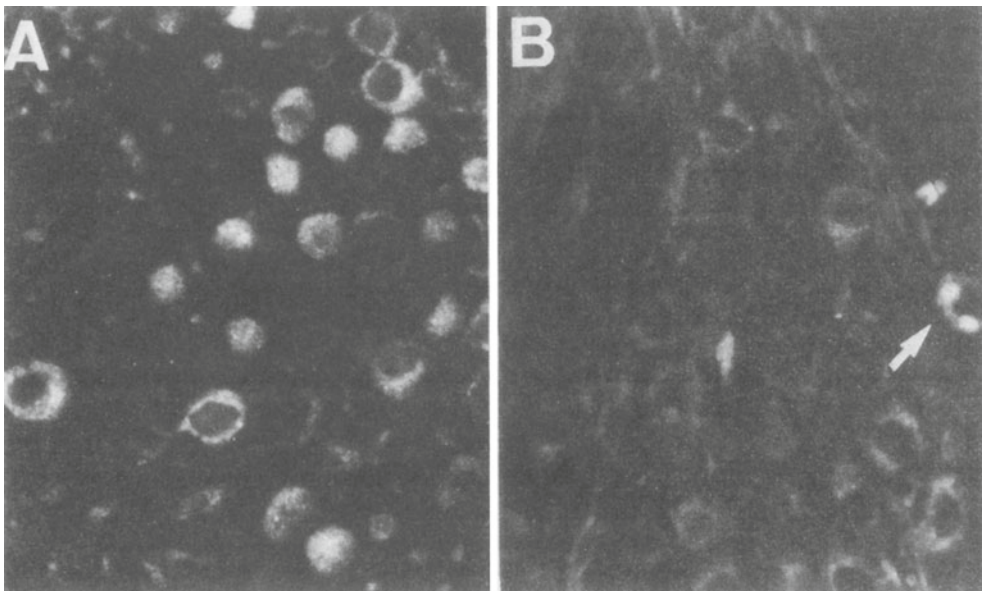

Fig. 6.9 HSV antigen in the spiral ganglion. (**a**) The inoculated side of the spiral ganglion shows the presence of HSV antigen. (**b**) The non-inoculated side of the ganglion shows the presence of antigen only sporadically. A single ganglion cell has HSV antigen in this photograph (*arrow*) (original ×16) [5]

discs, the researchers established a multicentric congenital CMV screening program.

More than 21,000 newborns were enrolled at 25 sites in geographically separate areas of Japan. Congenital CMV infection was identified in 0.31 % (95 % CI, 0.24 % to 0.39 %) of newborns. Thirty percent of these cases (20/66) had typical clinical manifestations and/or had pathological brain imaging results at birth. Audiological testing was conducted using auditory brainstem responses and auditory steady-state responses, and brain imaging was performed using CT and/or MRI. Almost two-thirds of the cases had siblings, a significantly higher rate than for uninfected newborns. When tested, most of these (21/25) were found to have CMV strains identical to those of their siblings. Siblings are a major risk factor for congenital CMV infection.

Ogawa et al. [13] tested 67 children with severe sensorineural hearing loss for CMV and GJB2 mutations. DNA specimens were prepared from dried umbilical cords. Congenital CMV infection was identified in 15 % of the patients, and GJB2 mutations were identified in 24 %. All CMV-positive children had developed sensorineural hearing loss before the age of 2 years. Most had no obvious clinical abnormality at birth.

6.2.3 Histopathology of the Temporal Bone in a Case of CMV

Myers and Stool [14] reported the case of a 3-day-old girl who died of cytomegalic inclusion disease that included exfoliative dermatitis, hepatosplenomegaly secondary to extramedullary hematopoiesis, biliary cirrhosis, and severe bronchopneumonia. Autopsy revealed cytomegalic inclusions in the convoluted tubules of the kidneys and many other organs. Inclusion-bearing cells were also seen in the temporal bones.

6.2.3.1 The Left Temporal Bone

The organ of Corti showed severe postmortem degenerative changes, but hair cells and supporting cells were seen in all turns of the cochlea. The tectorial membrane was present and normal although occasionally in an eccentric position. Inclusion-bearing cells were present in Reissner's membrane in all turns, but only in the inner epithelial cell layer and protruding into the scala media. The stria vascularis had degenerated, and inclusion-bearing cells were found in its superficial layer in all turns. Hydrops of the cochlear duct was found only in the apical turn. The cells of the spiral ganglion and Scarpa's ganglion had degenerated but seemed normal in number.

The sensory epithelium of the cristae of the posterior and superior semicircular canal had disintegrated and the cupulae were missing. Typical cytomegalic inclusion cells were found in the walls of all canals but never within the planum semilunatum or the sensory epithelium of the crista.

Several inclusion bodies were found in the utricular macula, though it is impossible to determine whether these were in sensory or supporting cells. Many inclusion-bearing cells were found in the membranous wall.

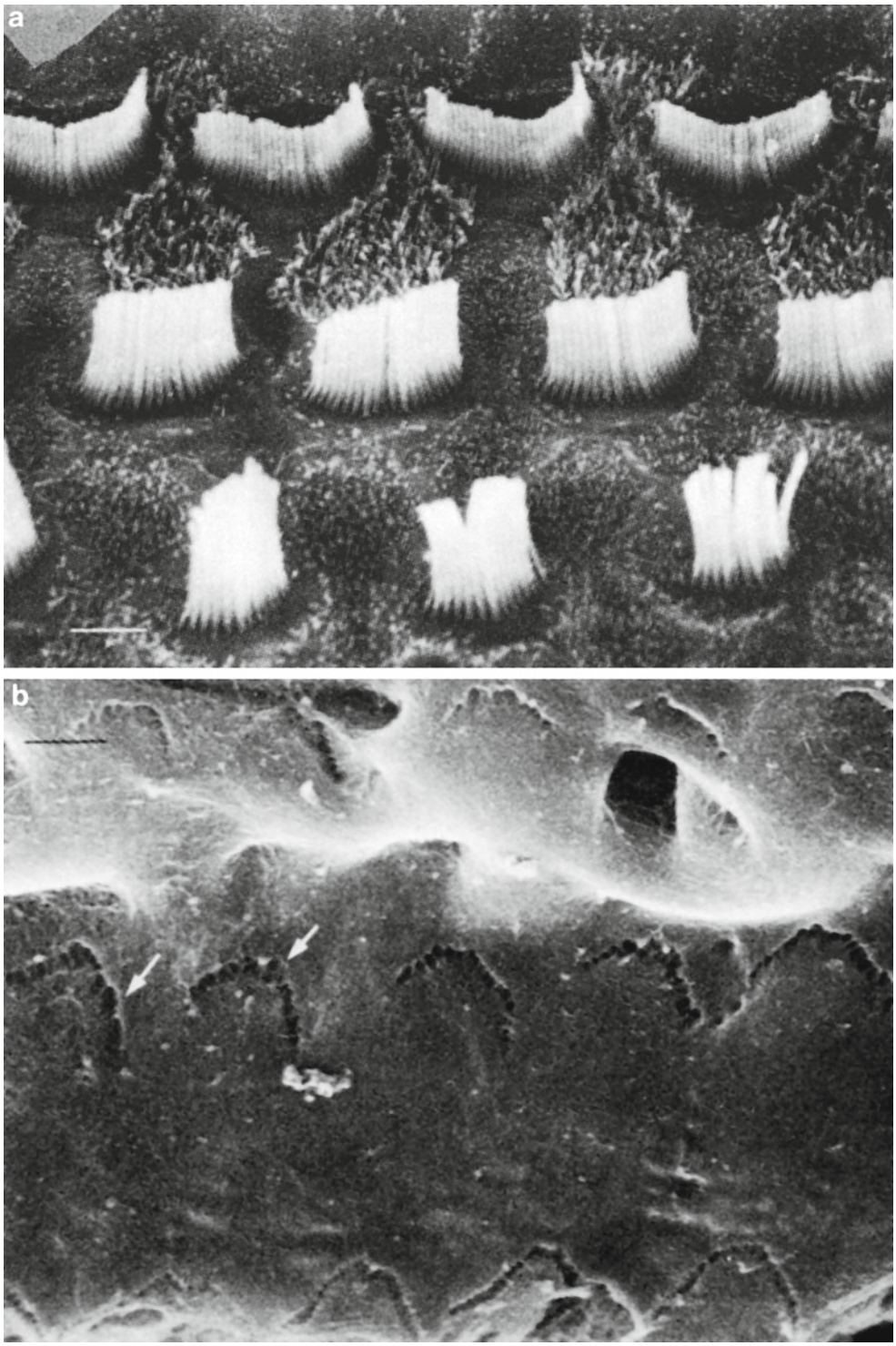

Fig. 6.10 The stereocilia and imprints. Scanning electron microscopic observations 7 days after intracochlear inoculation of HSV-1 (1×10^6 pfu/2μL). (**a**) Stereocilia of the outer hair cells. There are no apparent changes (Bar: 1 μm). (**b**) Dips in the imprints are destroyed (*arrows*) (Bar: 1 μm, original ×20,000). (**c**) Fusions of the imprint (*arrows*) and exposure of the fibrous layer (Bar: 1 μm, original ×20,000) [9]

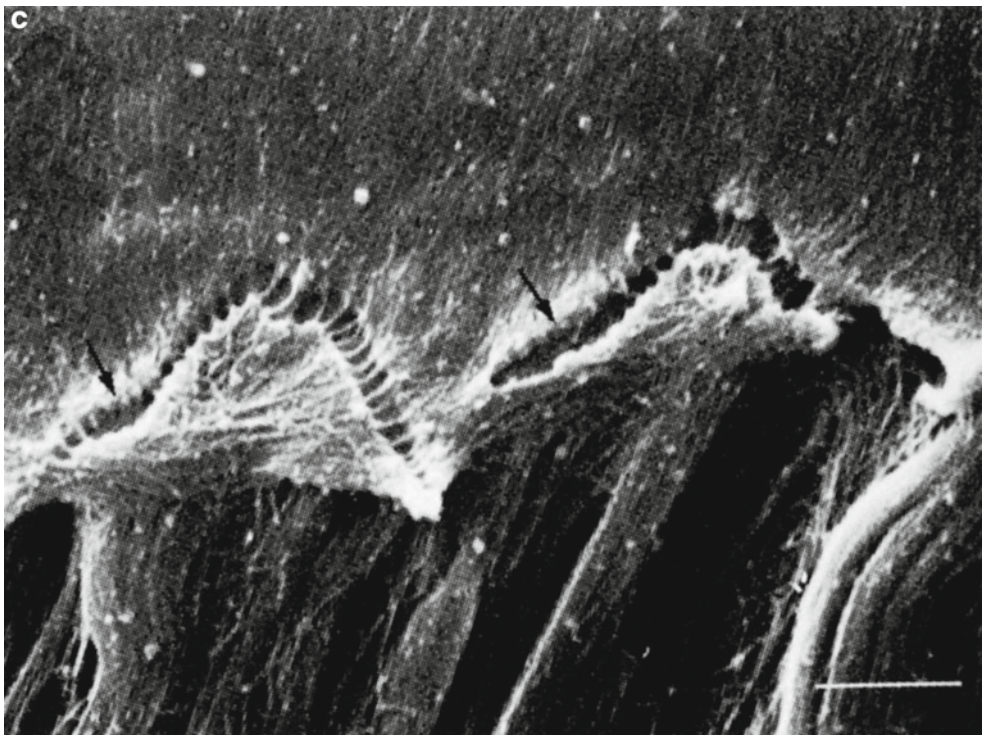

Fig. 6.10 (continued)

In the saccule, one inclusion-bearing cell was found in the macular epithelium. Numerous inclusion bodies were found in the membranous wall protruding into the endolymphatic space.

6.2.3.2 The Right Temporal Bone

No inclusion-bearing cells were found in the organ of Corti. The tectorial membrane was present and normal. There was marked endolymphatic hydrops along the entire cochlear duct. No inclusion-bearing cells were noted in the stria vascularis or Reissner's membrane, except for an occasional cell in the hook region. A large cystic structure was noted in the stria vascularis at the apical turn of the cochlea. The cells of the spiral ganglion and Scarpa's ganglion had degenerated but seemed normal in number.

All three semicircular canals were similar to those of the left ear. Many inclusion-bearing cells were found in the membranous wall of the utricle. The sensory epithelium of the macula had degenerated, but no inclusion-bearing cells were present. The saccule showed marked hydrops with many inclusion-bearing cells in the membranous wall. There was degeneration of the macular epithelium, and one inclusion-bearing cell was noted. There was minimal loss of otoconia.

Cytomegalic inclusion disease produces changes that are strikingly different from other forms of viral labyrinthitis. The presence of infected cells in the cochlea, saccule, utricle, and semicircular canals demonstrates the susceptibility of the entire ear to this virus. In the membranous labyrinth, the inner (endolymphatic) layer is epithelial in origin and these cells seem susceptible to the virus [14, 15]. The outer (perilymphatic) layer is probably mesothelial in origin, and these cells seem not to be involved in infection.

The tectorial membrane never showed a "rolled-up" appearance on the limbus spiralis, which is a prominent feature of the degenerative changes of other viral infections. Furthermore, the organ of Corti is not affected by CMV infection.

Davis et al. [16] reported their histopathologic examination of the temporal bone from a 22-day-old patient who had CMV infection of the entire membranous labyrinth without involvement of the sensory or neural structures. They postulated that blood-borne CMV virus had passed from the stria vascularis into the endolymphatic space and infected non-neurosensory epithelium.

6.2.4 Experimental Cytomegalic Labyrinthitis

6.2.4.1 Direct Inoculation of GPCMV to the Inner Ear

Katano et al. [17] performed direct inoculation of guinea pig cytomegalovirus (GPCMV) to the inner ear. Two microliter of GPCMV (2×10^3 $TCIN_{50}$/mL (TCID, Tissue Culture

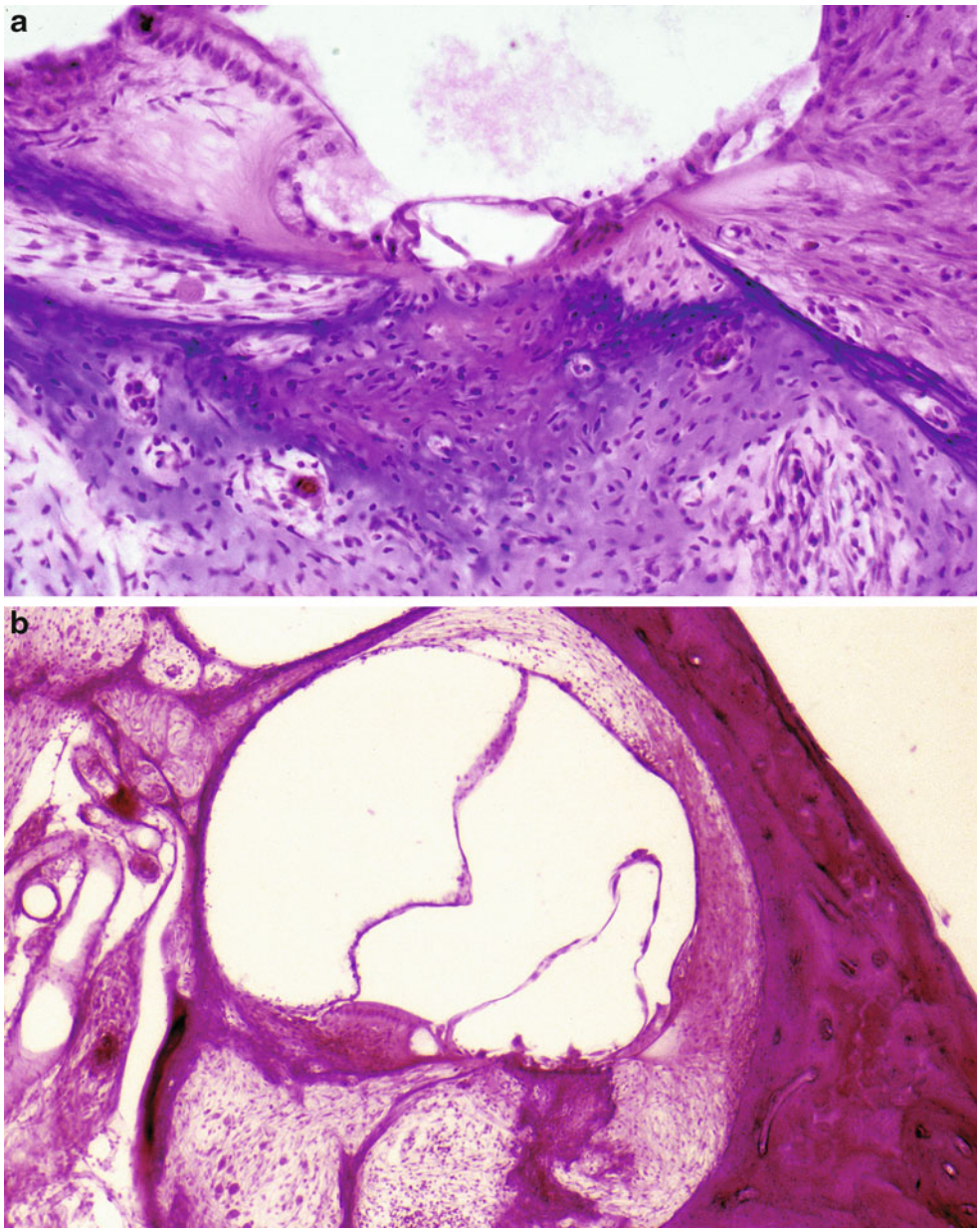

Fig. 6.11 Viral labyrinthitis 2 months after HSV inoculation of the scala tympani of the basal turn. (**a**) Ossified scala tympani of the basal turn. Surface of the organ of Corti remains. No hair cells or supporting cells remain. There is no cell infiltration within the organ of Corti. Nerve fibers in the osseous spiral lamina are missing (original ×6.5). (**b**) The organ of Corti has disappeared, leaving its surface as a bulge. The scala media shows endolymphatic hydrops with cortilymphatic hydrops. The scala tympani is filled with fibrous tissue and new bone. The osseous spiral lamina and Rosenthal's canal are enlarged. Marked loss of the spiral ganglion cells is observed (original ×2.5)

Infective Dose) were inoculated into the inner ear through the round window using 27 gauge needles. The round window was covered with absorbable gelatin after inoculation. Buffer solution was used as a control. The guinea pigs were sacrificed 9–12 days after inoculation.

Histologically, there was marked bleeding with inflammation in the labyrinth, particularly in the scala vestibuli, scala tympani, and spiral ganglion (Fig. 6.13a). The organ of Corti and limbus spiralis were relatively intact. The utricle, saccule, and semicircular ducts were atrophic, and slight inflammatory cell infiltration and bleeding were found in the perilymph region. Immunohistochemistry revealed that there were GPCMV-infected cells in the scala vestibuli, scala tympani, and spiral ganglion (Fig. 6.13b). As to Reissner's membrane, GPCMV-infected cells were detected only on the side facing the scala vestibuli, and not on the side facing the scala media (Fig. 6.13c). The stria vascularis showed severe congestion, but GPCMV antigen was not detected. No

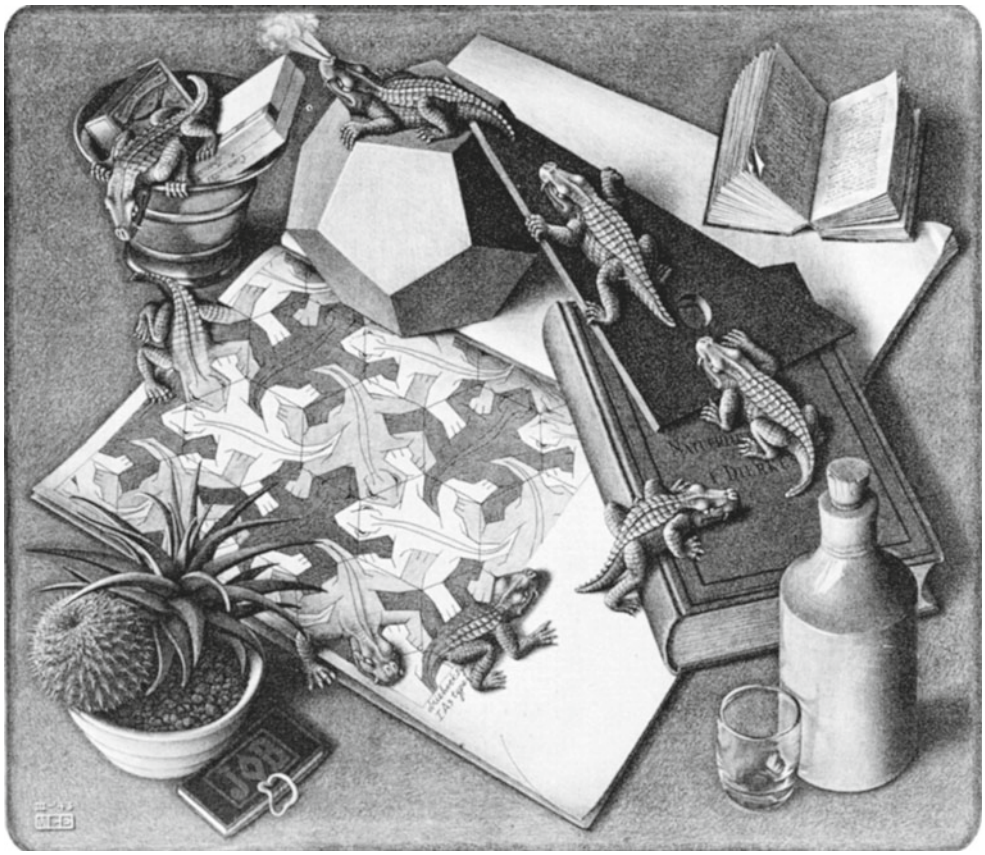

Fig. 6.12 *Reptiles*, a lithograph by M.C. Escher printed in 1943 (M.C. Escher's "Reptiles" © 2013 The M.C. Escher Company – The Netherlands. All rights reserved. www.mcescher.com)

GPCMV-antigen was detected in the utricle, saccule, semicircular ducts, or endolymphatic sac.

6.2.4.2 Vertical GPCMV Infection

Transplacental fetal infection with GPCMV has been investigated.

Katano et al. [17] inoculated GPCMV into the subcutaneous tissue of pregnant guinea pigs at 5 weeks of gestation. Five weeks later the pregnant guinea pigs were sacrificed before delivery and the fetuses examined. Severe bleeding was observed in the scala tympani (Fig. 6.14c). Remarkable changes found in the fetal cochleae included the presence of cytomegalic cells attached to Reissner's membrane, necrosis in the spiral ganglion, and vacuolar degeneration of the stria vascularis. GPCMV-infected cells were detected in the scala vestibuli, scala tympani, and spiral ganglion (Fig. 6.14b, d, f), but not in the endolymphatic areas, including the cochlear duct, utricle, saccule, and semicircular ducts. GPCMV antigen was detected not only in the inner ear, but also in the middle ear and kidneys (Fig. 6.14g, h). The localization of GPCMV-infected cells in vertically-infected fetuses was similar to that found with direct inoculation of GPCMV into the inner ear.

From these experiments, it was obvious that GPCMV was transmitted from mother to fetus across the placenta, and spread throughout the inner ear of the fetus, particularly to the perilymphatic spaces and spiral ganglion. No virus antigen was detected in the stria vascularis or in the organ of Corti.

It is noteworthy that both human CMV infection and guinea pig GPCMV infection spare the organ of Corti. However, contrary to the findings in human temporal bone studies, in experimental studies GPCMV-bearing cells were not found in the epithelial cell layer facing the endolymphatic compartments, but were present in the mesothelial cell layer facing the perilymphatic spaces [16]. The route of viral infection to the fetus is transplacental in both cases. The reason for the difference in virus distribution is not clear at present, but species-specific CMV differences may be responsible.

Similar experimental studies have been reported [4, 18]. In one, salivary gland suspensions containing 1×10^7 $TCID_{50}$/mL of GPCMV were prepared and diluted to 1×10^6 $TCID_{50}$/mL. A small volume of the GPCMV solution (2 μL) was inoculated into the middle ear of guinea pigs. The middle ear showed hemorrhage, round cell infiltration, and fibrosis from 5 to 14 days after inoculation. Inclusion bodies were present in the infiltrated cells in the middle ear mucosa. In one animal,

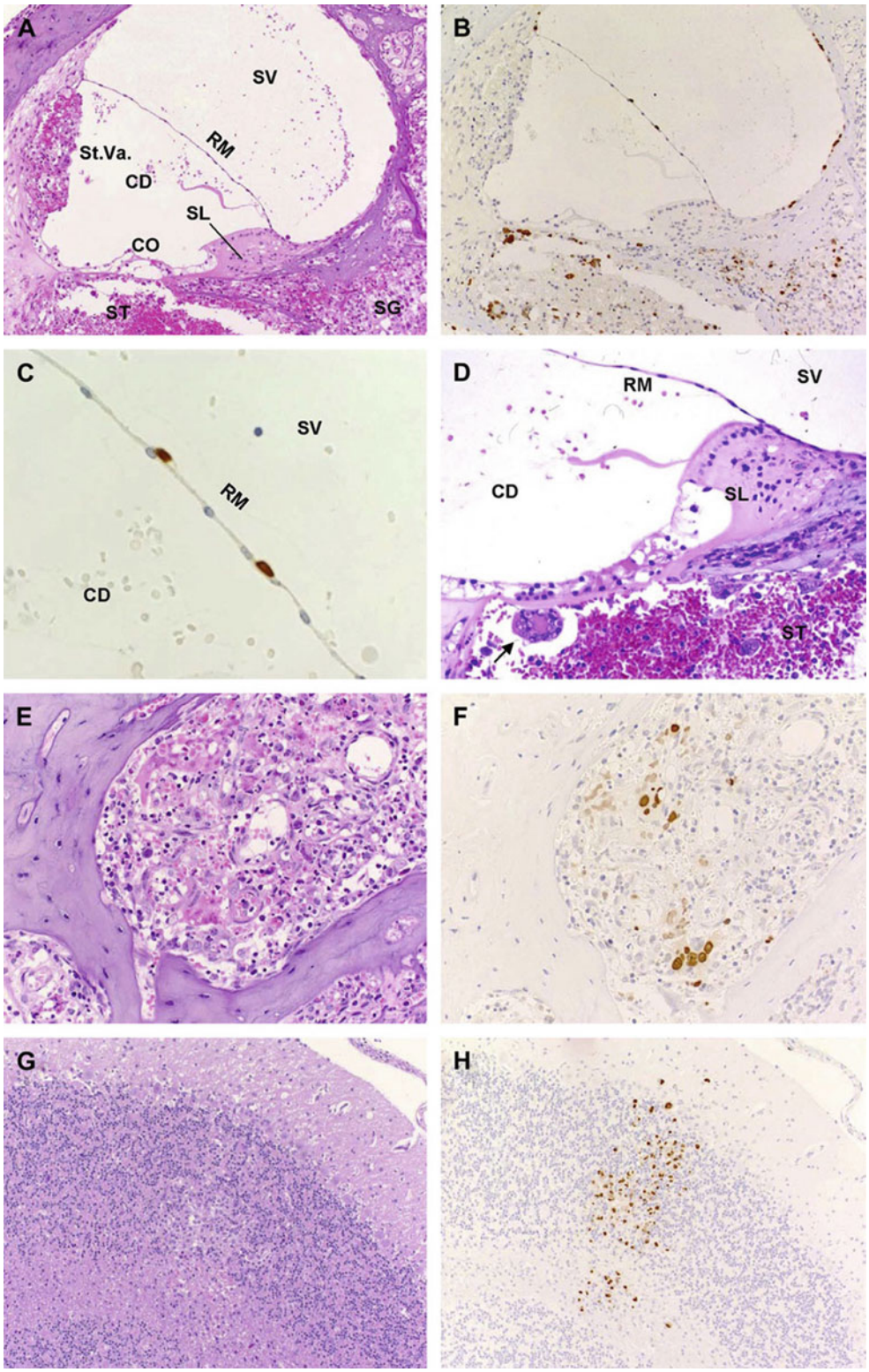

Fig. 6.13 Histopathology of guinea pigs inoculated with GPCMV in the inner ear [17]. *CD* cochlear duct, *CO* organ of Corti, *RM* Reissner's membrane, *SL* spiral limbus, *ST* scala tympani, *SV* scala vestibuli, *St.Va* stria vascularis. (**a**) Low magnification view of the cochlea. Bleeding and inflammatory cell infiltration are evident with HE staining. (**b**) Immunohistochemistry for GPCMV in a serial section of (**a**). GPCMV antigens were detected predominantly in the scala vestibuli, scala tympani, and spiral ganglion, but not in the stria vascularis or organ of Corti. (**c**) High power view of Reissner's membrane. GPCMV-infected cells are only present on the side facing the scala vestibuli, the mesothelial cell layer. No viral antigens were found on epithelial cells facing the scala media. Immunohistochemical staining. (**d**) Giant cells with remarkable intranuclear inclusion bodies are found in the scala tympani (*arrow*). Marked bleeding with inflammatory cell infiltration in the scala tympani (HE staining). (**e**) The spiral ganglion. Severe inflammation with bleeding is observed (HE staining). (**f**) Immunohistochemistry for GPCMV of the spiral ganglion. GPCMV antigens are detected in the spiral ganglion. (**g**) Cerebellum of GPCMV-inoculated guinea pig. Loss of cerebellar granule cells is evident (HE staining). (**h**) Immunohistochemistry for GPCMV in a serial section of (**g**). GPCMV antigens are detected at the site of cell loss

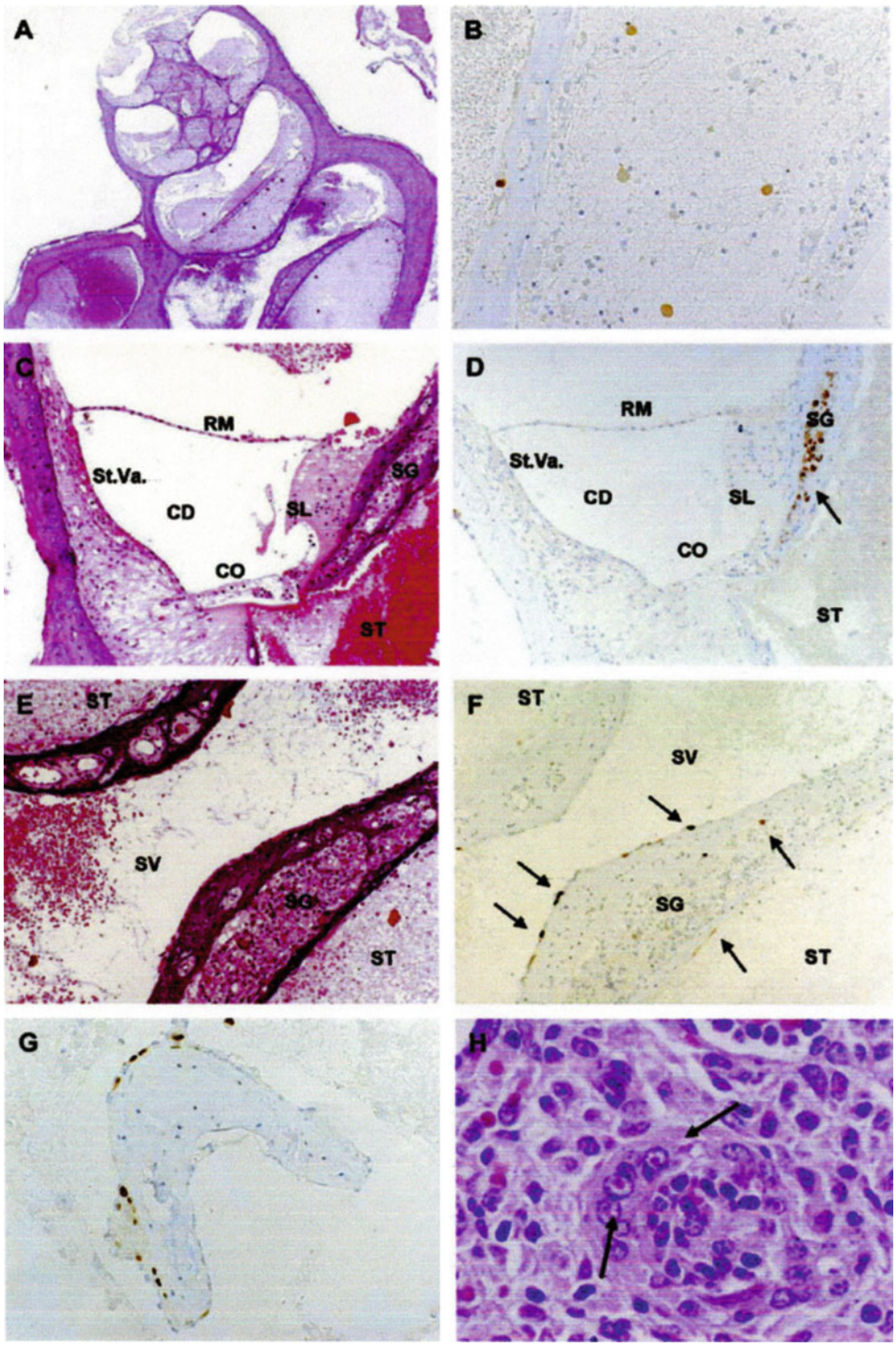

Fig. 6.14 Histopathology of the inner ear from the fetus of a GPCMV-inoculated mother [17]. (**a**) Low power view of the cochlea. Severe bleeding and inflammation are observed in the cochlea (HE staining). (**b**) High power view of GPCMV-infected cells in the spiral ganglion. Severe destruction of the spiral ganglion is observed. (**c**) Severe bleeding is observed in the scala tympani of the fetus (HE staining). (**d**) Immunohistochemistry reveals the presence of GPCMV-infected cells in the spiral ganglion (*arrow*). (**e**) High power view of the scala vestibuli, scala tympani, and spiral ganglion. Marked bleeding is observed in the scalae tympani and vestibuli. (**f**) Immunohistochemistry for GPCMV in a serial section of (**e**). GPCMV antigens are detected in the mesothelial cell layer of the scalae tympani and vestibuli, and within the spiral ganglion (*arrows*). (**g**) GPCMV antigens are found in the mucosa of the stapes. (**h**) Cytomegalic inclusion-bearing cells are found in the kidney (*arrows*) (HE staining)

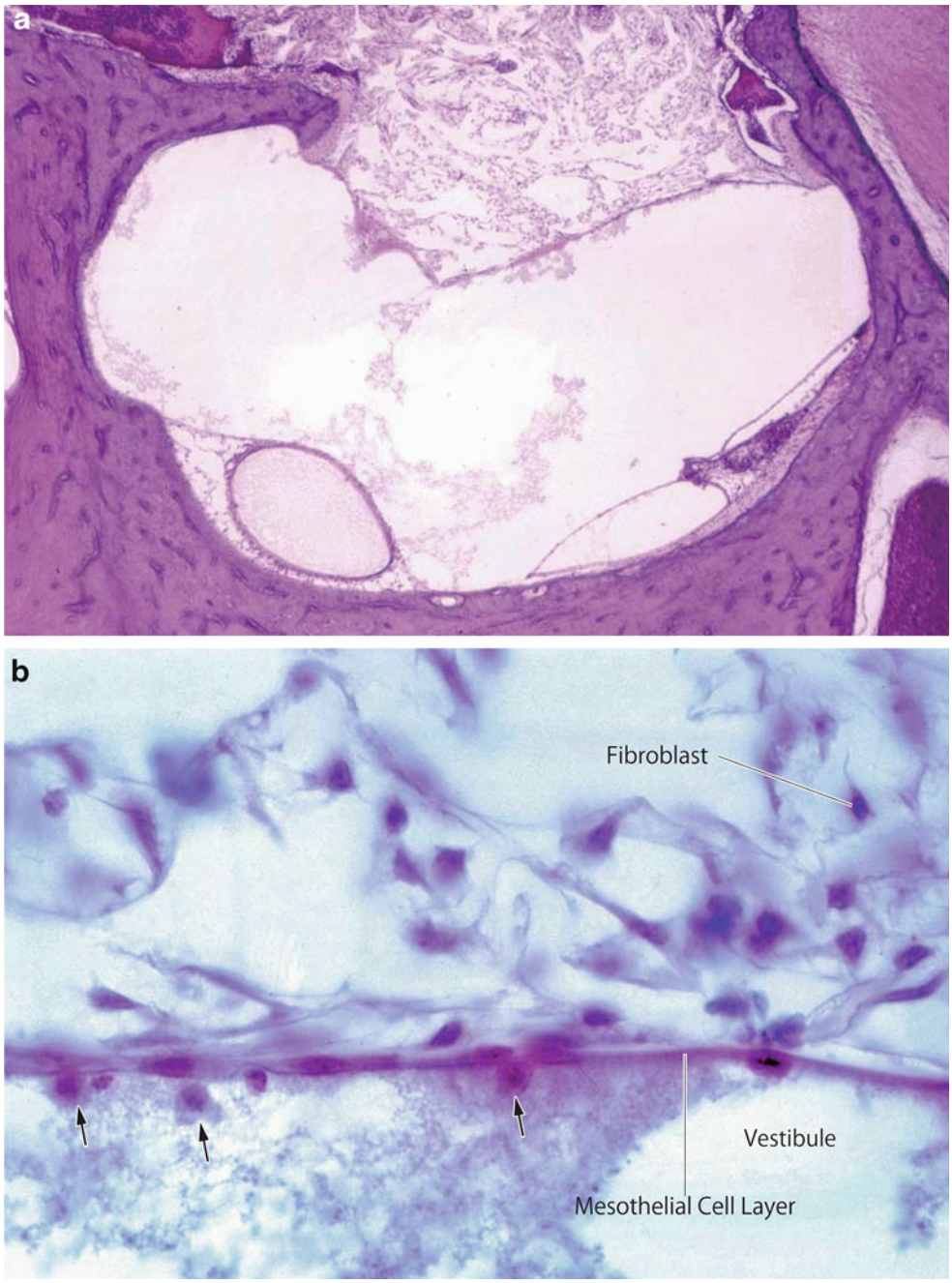

Fig. 6.15 Fourteen days after GPCMV inoculation into the middle ear [4]. (**a**) The stapes is displaced and the oval window is shielded by a mesothelial cell layer and fibroblasts. There is exudate in the vestibule, but no cell infiltration is observed. The saccule shows some changes (original ×2.5). (**b**) High power view of (**a**). *Arrows*: macrophages (original ×16). (**c**) Many macrophages are attached to wall of the scala vestibuli (original ×6.5). (**d**) High power view of the wall of the scala vestibule in (**c**). Presence of macrophages suggests that the cochlea receives information about GPCMV inflammation in the middle ear. *Arrows*: mesothelial cells (original ×100)

the stapes was displaced by inflammation 14 days after inoculation. The oval window was protected by fibroblasts covering the mesothelial cell layer, preventing invasion of infection to the inner ear (Fig. 6.15a, b). Many macrophages were attached to surface of the mesothelial cell layer (Fig. 6.15c, d). In contrast to the marked fibrosis in the middle ear cavity, the vestibule was relatively clear, although it contained a small amount of exudate, indicating the presence of serous labyrinthitis. In this animal, the round window area was clear and the cochlea showed clear space. However, a high power view revealed a few macrophages attached to the round window membrane and to the wall of

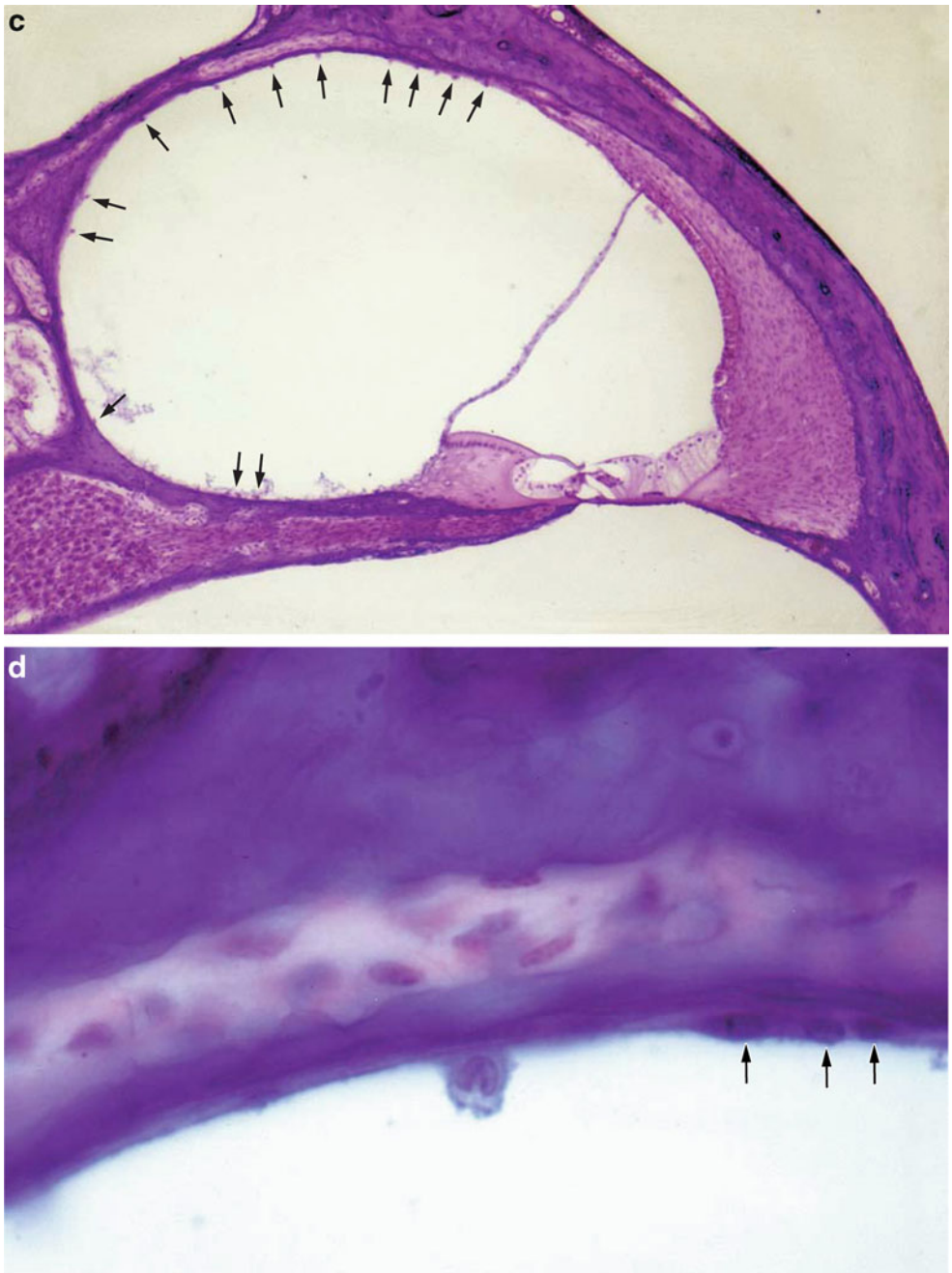

Fig. 6.15 (continued)

the perilymphatic space [4]. Another animal showed inclusion body-bearing cells in the spiral ganglion 9 days after middle ear inoculation (Fig. 6.16) [18].

The cochlea showed marked hemorrhage in the scala tympani and vestibule 2 months after direct inoculation of GPCMV into the cochlea through the round membrane. Inclusion body-bearing cells were present in the scala tympani of the basal turn where marked hemorrhage and cell infiltration occurred (Fig. 6.17). The organ of Corti had degenerated [4].

The stria vascularis was another site of viral invasion. Of the three cell layers, primarily the intermediate cells were affected and disappeared. The stria vascularis became thick and swollen, filled with exudate. The marginal cells, however, were tightly arranged.

Inclusion body-bearing cells were found protruding into the scala media from the epithelial cell layer of Reissner's membrane 46 days after CMV inoculation through the round window membrane. Marked hemorrhage and cell infiltration were observed in the scala media and scala vestibuli (Fig. 6.18) [18].

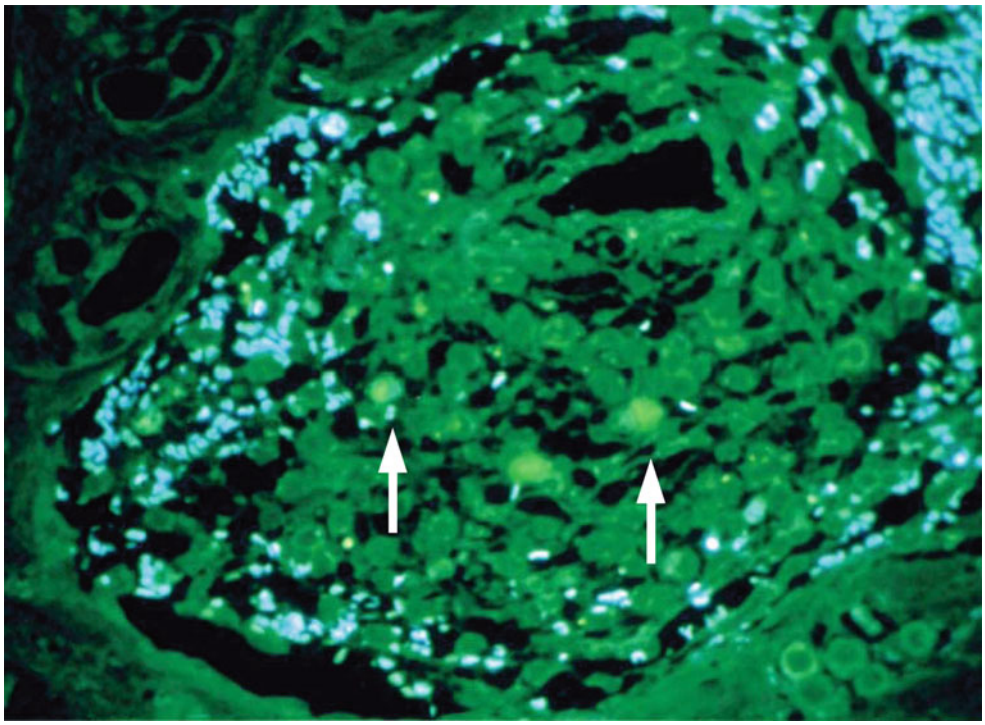

Fig. 6.16 The spiral ganglion showing presence of GPCMV antigen (*arrows*). 9 days after GPCMV inoculation to the middle ear. Fluorescence microscopy

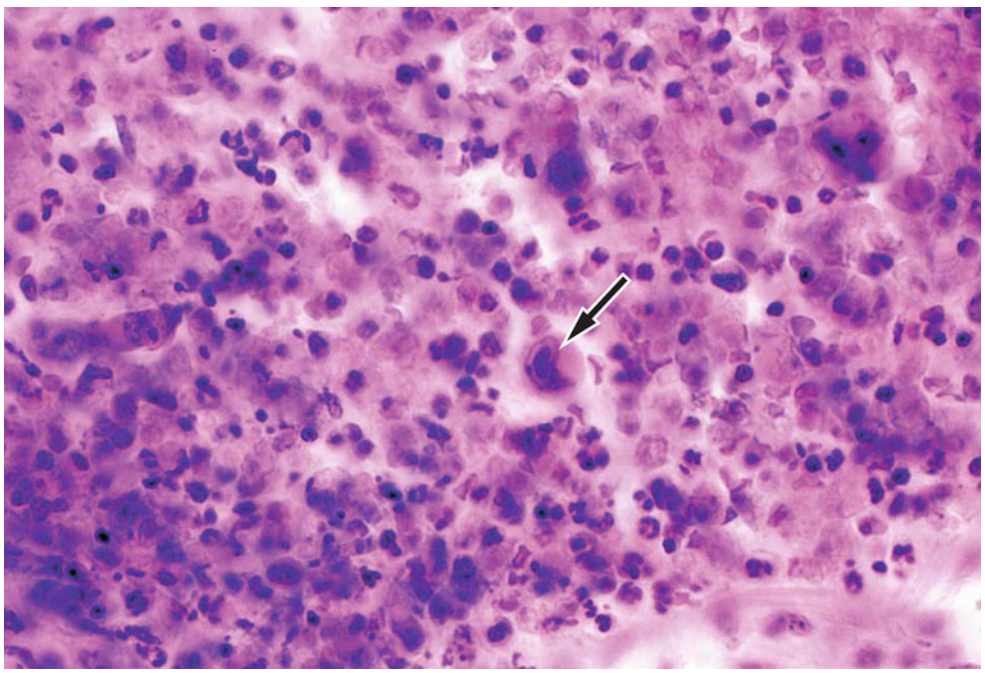

Fig. 6.17 Inclusion body-bearing cell (*arrow*) in the scala tympani, which is filled with cell infiltration and hemorrhage. Two months after inoculation of GPCMV into the scala tympani of the basal turn (×40) [4]

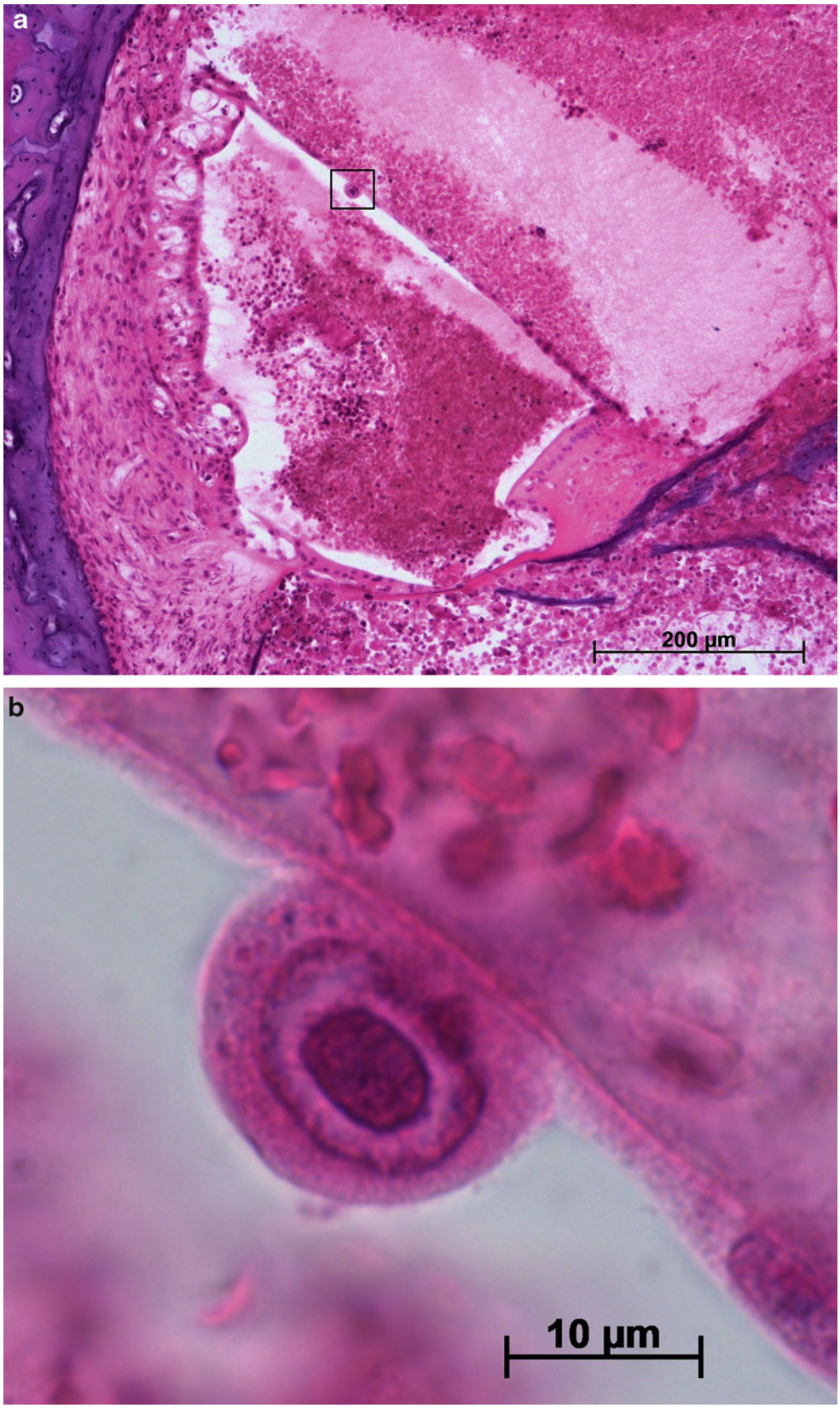

Fig. 6.18 GPCMV inoculation into the scala tympani. (**a**) Marked inflammation and hemorrhage are observed in the whole cochlea. The stria vascularis shows marked edema. Inclusion body-bearing cell protrudes into the scala media from the epithelial cell layer of Reissner's membrane (within the *square*) Original ×10. (**b**) High power view of the inclusion body-bearing cell shown in the inset of (**a**). 46 days after GPCMV inoculation into the scala tympani (original ×100) [18]

The site of viral antigen or cytomegalic cells in the labyrinth may differ depending on the route of infection and species differences, as well as the severity of infection. With the spread of hemorrhage and cell infiltration, cytomegalic cells may appear in both endolymphatic and perilymphatic spaces.

The organ of Corti is not susceptible to CMV or GPCMV. However, it degenerates when severe pathological changes occur in the scala tympani and/or scala media.

An electron microscopic study revealed that lymphocytes with intranuclear CMV passed through the basilar membrane to the widened spaces between Deiters' cells from the scala tympani infiltrate 7 days after inoculation. This suggests a possible route of viral infection of the organ of Corti [19].

The routes of virus invasion from outside to the inner ear are hard to identify. Several routes have been considered: (1) from middle ear infection via the oval and/or round windows, (2) hematogenous spread to the stria vascularis, (3) in cases of meningitis, via cerebrospinal fluid to the perilymph, (4) from the middle ear along the facial nerve through dehiscence of the facial canal, and (5) transplacental. These routes may be closely associated. Systemic viral infection may occur via hematogenous dissemination after viral inoculation of the middle ear.

After inoculation of virus into the middle ear, macrophages appear in the perilymphatic space, including on the round window membrane and the wall of the scala vestibuli of the lower basal turn, without apparent perforation of the cochlear windows or cell infiltration in the perilymph. This indicates interaction between the infected middle ear and the inner ear through the cochlear windows. Macrophages belong to the "mononuclear phagocyte system." Adsorption of virus particles to macrophages is the first step in virus-macrophage interaction [20].

6.2.4.3 Endolymphatic Duct Inoculation

In one study, GPCMV suspension was inoculated into the endolymphatic duct of guinea pigs [21]. Three weeks after inoculation the cochlea showed marked endolymphatic hydrops (Fig. 6.19a). No GPCMV inclusion bodies were found in the cochlea, the vestibule, or the semicircular canals. The organ of Corti was preserved. No cell infiltration was found in the perilymphatic spaces. However, the perilymph in all turns of the scala tympani contained exudate that stained faintly with HE. Exudate was also found in the scala vestibuli, but to a lesser degree. Many macrophages were found adhered to the wall of the scala tympani, particularly in the basal turn.

Although GPCMV-infected cells were not found in the inner ear, inoculated virus still might have some effect there. Macrophages scattered on the wall of the scala tympani of the first and second turns are reminiscent of the previously stated findings (Fig. 6.15c).

After GPCMV inoculation, the endolymphatic duct was occluded (Fig. 6.19c). The edge of the operculum covering the endolymphatic sac was destroyed and replaced by thick fibrous tissue. There was space inside the sac, but it was partly obliterated. Adjacent cerebellum was severely damaged.

The saccule showed marked hydrops. The utricle and semicircular ducts also showed hydrops. The endolymphatic space was clear throughout the whole inner ear.

Harris et al. [22] inoculated GPCMV virus into either the perilymphatic space or the endolymphatic sac of seronegative and seropositive animals. The seronegative animals showed progressive hearing loss with marked inflammation and degeneration of neural elements. With endolymphatic duct inoculation, endolymphatic hydrops with deafness developed in the seronegative animals. Seropositivity protected the hearing, though seropositive animals developed mild hydrops due to local inflammation without viral replication.

6.3 Mumps

6.3.1 Introduction

Mumps has been considered one of the causes of sudden deafness for decades. Patients with sudden deafness who have asymptomatic or silent mumps will not be recognized as mumps patients, unless someone considers the possibility and performs serological tests. Mumps infection without parotitis may be more common than is generally assumed and may remain undiagnosed [23].

Van Dishoeck and Bierman [24] performed serological tests and viral cultures of blood and stools from 66 patients with sudden severe unilateral hearing loss and found that four certainly had mumps and two others probably had mumps. None of these patients had parotitis or a previous history of mumps infection.

6.3.2 Morphological Studies

6.3.2.1 Histopathology of the Temporal Bone

There are limited numbers of histopathological studies of temporal bones from patients with mumps deafness.

Lindsay et al. [25] reported the case of a 6-year-old boy who had developed bilateral profound deafness following mumps infection at the age of 2 years. His eventual terminal illness was of sudden onset, progressing rapidly to coma and death. The final pathological diagnosis and cause of death after microscopic examination was inclusion cell encephalitis.

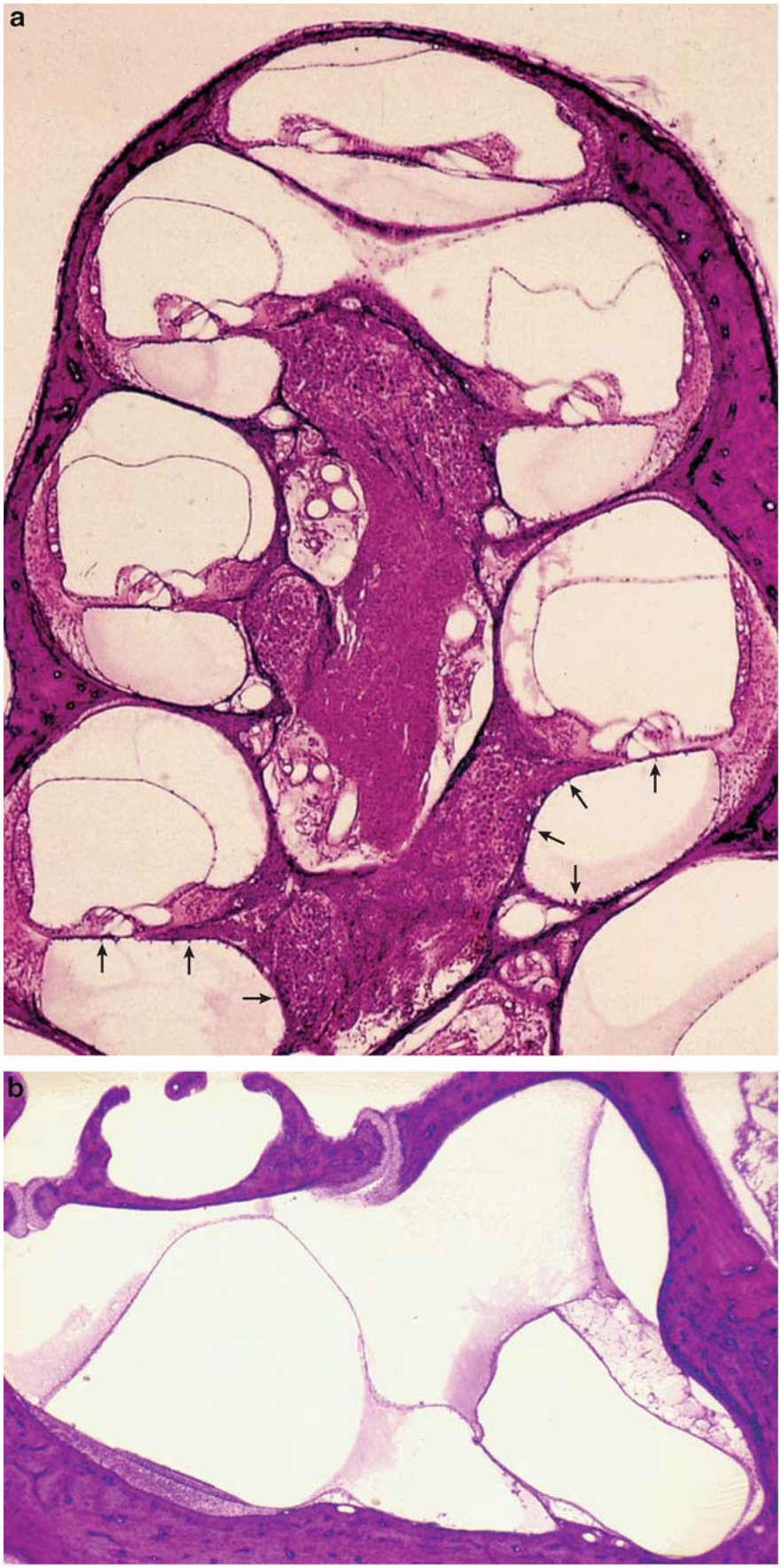

Fig. 6.19 Inoculation of GPCMV into the endolymphatic duct [21]. (**a**) Development of endolymphatic hydrops in all turns. The organ of Corti is preserved. There is precipitate in the perilymphatic space. The scala media is clear. Many macrophages are attached to the wall of the scala tympani of the basal turn (*arrows*). Three weeks after inoculation. HE staining (original ×1). (**b**) The saccule and utricle show hydrops. (**c**) Inoculated site. The endolymphatic duct is blocked. The cerebellum is severely damaged. (**d**) Normal side. *1*: endolymphatic duct, *2*: operculum, *3*: endolymphatic sac, *4*: sigmoid sinus

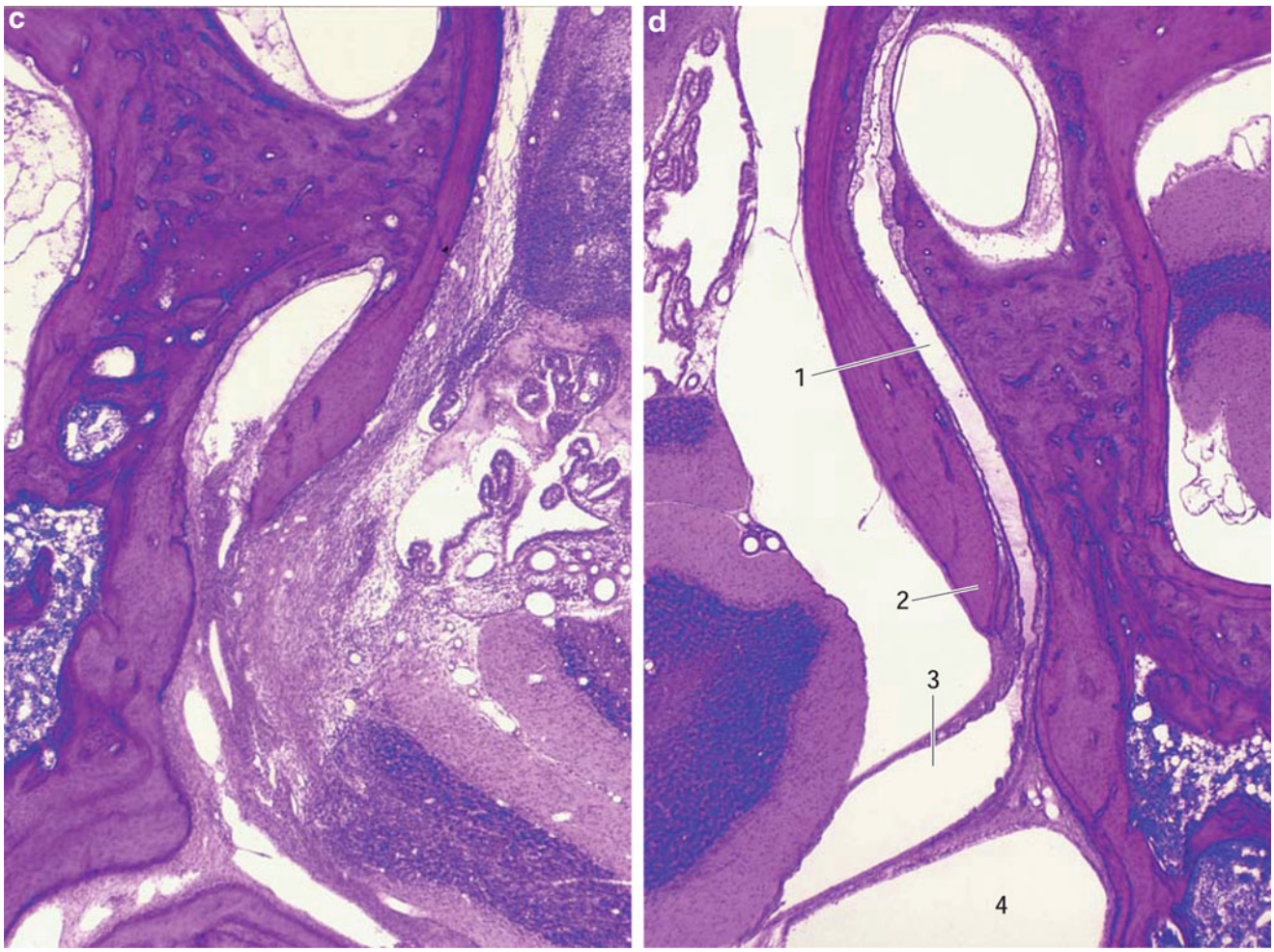

Fig. 6.19 (continued)

The Left Temporal Bone

The volume of endolymph appeared normal with no distortion of Reissner's membrane except in a few isolated areas where it was torn (artifact). The stria vascularis was completely lost in most of the basal and part of the middle turn. The tectorial membrane had degenerated in all turns (Fig. 6.20). It was detached from the limbus spiralis and lay on the basilar membrane as an encapsulated hyaline mass in the basal turn. In the middle turn it was a rolled-up mass surrounded by a single layer of flattened cells. The organ of Corti showed severe degeneration in the basal turn and less toward the upper turns. Nerve fibers and spiral ganglion cells were well preserved in the middle and apical turns but reduced in the basal turn. The utricle, saccule, and semicircular canals appeared normal.

The Right Temporal Bone

Reissner's membrane had collapsed in the middle and basal turns and appeared attached in some areas to the degenerated stria vascularis, spiral prominence, outer and inner sulcus cells, and the limbus. The stria vascularis had completely degenerated, although some remnants remained in the upper turn. The organ of Corti was completely missing in the basal and lower middle turns. The tectorial membrane had detached from the limbus in the basal and lower middle turns and a remnant was present on the basilar membrane as a small mound covered by flattened cells. In the middle turn it lay rolled-up in the angle between Reissner's membrane and the limbus. In the apical turn, the tectorial membrane remained attached but was thinned out and drooped into the inner sulcus and onto the organ of Corti (Fig. 6.21). The spiral ganglion cells were decreased in number in the lower basal turn, but normal in other turns.

The utricle, saccule, and semicircular canals appeared to be normal.

Smith and Gussen [26] reported the case of a 53-year-old woman who at age 40 had contracted a severe case of mumps from her daughter. Three years after infection, she failed a

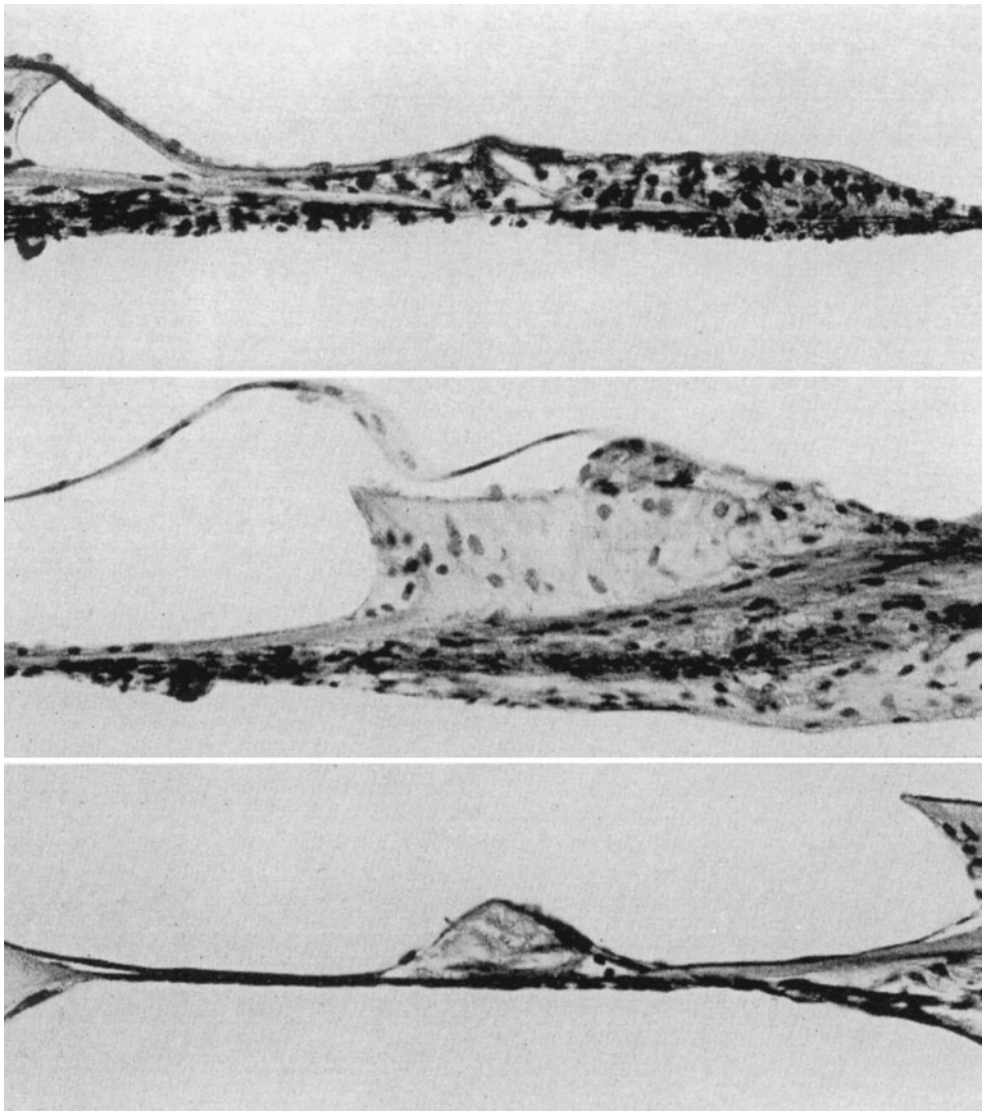

Fig. 6.20 The left temporal bone [25]. Photomicrographs showing the remnants of the tectorial membrane in the apical (*top*), middle, and basal turns of the left cochlea. The organ of Corti is present in the apical turn but is absent in the basal turn

pre-employment audiometric examination. After another 3 years, an otologist confirmed her bilateral sensorineural hearing loss. Later, the woman underwent a total abdominal hysterectomy, bilateral salpingo-oophorectomy, and partial omentectomy for adenocarcinoma that had invaded the uterus and ovaries. She received radiation therapy and cytotoxic drug therapy. A histopathological study of her temporal bones was performed 13 years after mumps infection.

The essential changes, bilaterally, were focal loss in the entire organ of Corti involving the majority of the lower basal turn and part of the upper basal turn, with occasional hair cell loss throughout the rest of the cochlea. Nerve fiber loss was prominent in the osseous spiral lamina of the involved basal turn regions.

These changes were similar to those in the case described by Lindsay et al. However, this patient had no atrophy of the stria vascularis. Small hyaline droplet formation was found along the edges of the tectorial membrane. A very pronounced change was severe degeneration of the outer sulcus cell area, most prominent in the basal turn.

A basophilic substance was found in the utricle and saccule, possibly representing degeneration of otoliths.

6.3.2.2 Experimental Mumps Labyrinthitis

Tanaka et al. [27] inoculated guinea pigs with mumps virus (Torii strain) directly into the cochlea through the round window membrane or via an intravascular injection. The cochleae were examined by immunofluorescence and electron microscopy.

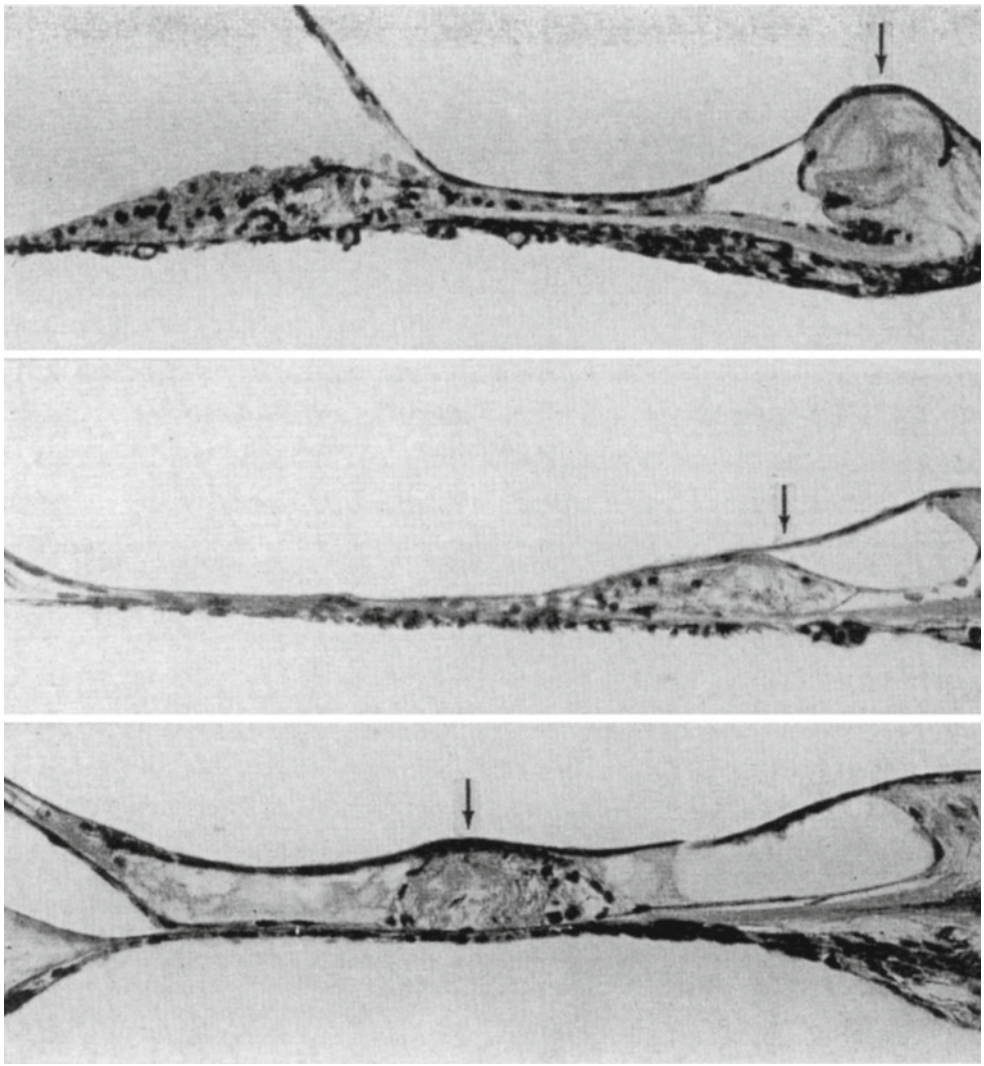

Fig. 6.21 The right temporal bone [25]. Photomicrographs of the apical (*top*), middle, and basal (*bottom*) turns of the right cochlea. In the middle and basal turns, Reissner's membrane is depressed, obliterating the scala media, and the organ of Corti is missing. In the apical turn the organ of Corti can be identified, but the tectorial membrane is no longer in position. *Arrows* indicate the degenerated tectorial membrane

Viral labyrinthitis was only produced by intracochlear inoculation.

Evidence of viral infection was confirmed by the presence of intracellular strands of nucleocapsid and mature virions budding at the endolymphatic space. These findings were prominent in both the stria vascularis and Reissner's membrane. When the stria vascularis was severely infected, shrinkage of intermediate cells and enlarged extracellular spaces were observed. On the other hand, when the cytological changes were mild, viral replication was not found. In general, the organ of Corti was severely damaged in the basal turn. After intravascular inoculation, viral antigen was detected in the stria vascularis, but cochlear lesions were not present.

Another experiment was performed in primates. Tanaka et al. [28] inoculated mumps virus into a unilateral cochlea of three monkeys (*Macaca irus*) and the inner ears were subsequently examined by immunofluorescent microscopy and transmission electron microscopy. Five microliters of the virus suspension was injected into the scala tympani through the round window membrane. The animals were sacrificed 14 days after inoculation. Serological studies confirmed titer elevation in neutralization tests.

In the immunohistochemical study, positive immunofluorescence was found in the stria vascularis.

With electron microscopy, observed changes were confined to the cochlea and did not involve the vestibular region. In the cochlea, the pathologic process involved all turns but

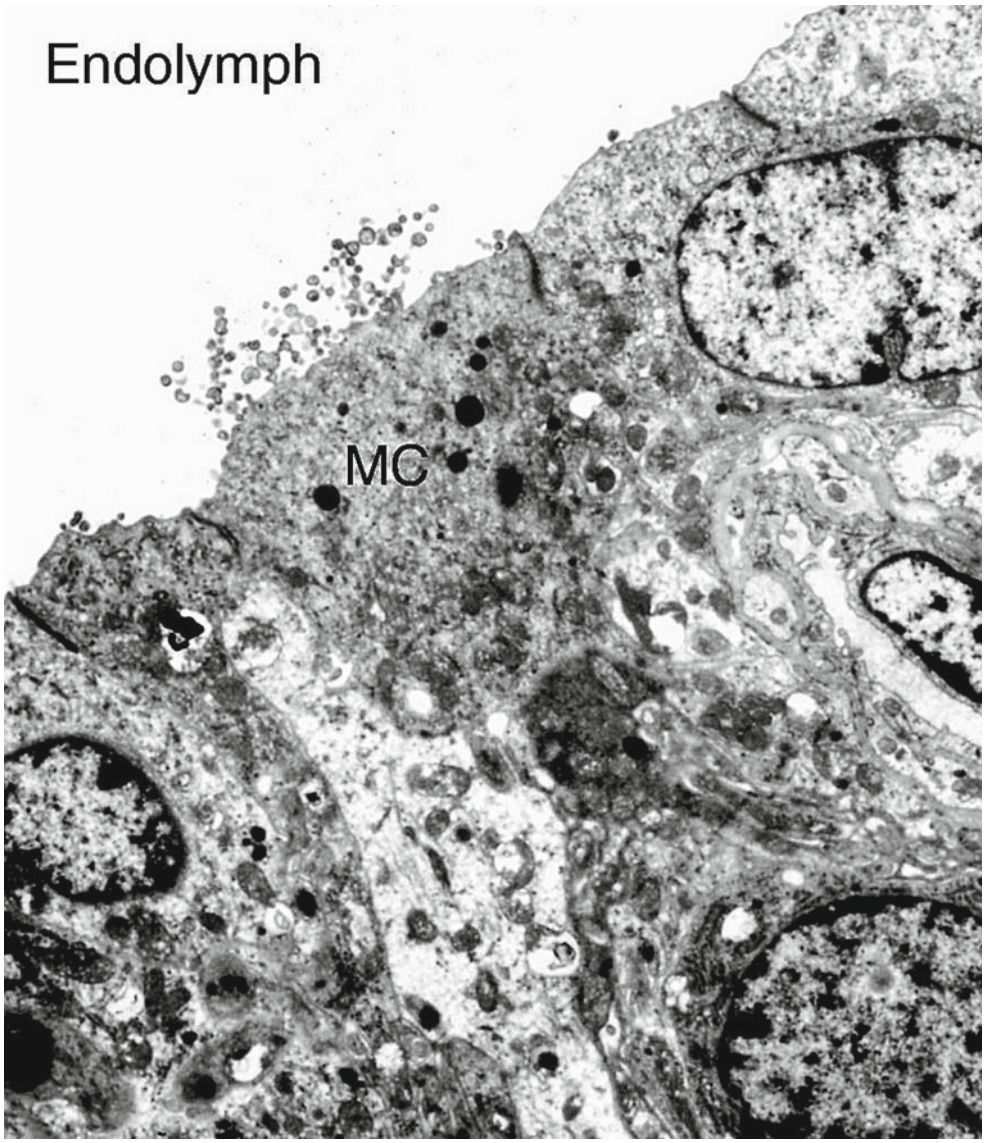

Fig. 6.22 Electron micrograph of the stria vascularis in the basal turn [28]. One of the marginal cells (*MC*) is shedding a large number of mature virions into the endolymph. The animal survived for 2 weeks after injection of virus suspension into the scala tympani through the round window membrane. Monkey (original ×8,200) (Courtesy of Dr. Tanaka)

was most prominent in the basal turn. Moderate fibrosis and cellular infiltration, mainly of macrophages and lymphocytes, were observed.

Marked pathologic changes were found in the organ of Corti and the stria vascularis. The organ of Corti had deteriorated to varying degrees throughout the cochlea. The outer hair cells had degenerated or disappeared. However, the inner hair cells were less susceptible and some remained intact without remarkable cytological changes. Degeneration of the stria vascularis was another characteristic feature and was most prominent in the upper basal turn. Marginal and intermediate cells were swollen, accompanied by distension of intercellular spaces and loss of complicated membrane specialization. There was morphological evidence of mumps virus replication in the marginal cells of the lower basal turn. Infected marginal cells had shed large numbers of mature virions into the endolymph, but the cytological integrity of these cells was usually maintained (Fig. 6.22).

These pathological features are in accordance with those of experimental mumps infection in guinea pigs, and thus are considered specific features of acute mumps labyrinthitis.

6.3.3 Criteria for Diagnosis of Mumps Deafness

Since 1972, the Ministry of Health and Welfare of Japan has established several investigation and research groups for intractable diseases in all medical fields. One hundred thirty diseases are listed as intractable at present. The following otological diseases are included: sudden deafness, idiopathic bilateral progressive deafness, mumps deafness, perilymphatic fistula, Meniere's disease, and low-tone sensorineural hearing loss.

In 1987, our study group devised a list of criteria for the diagnosis of mumps deafness. The following were the criteria as determined by the Acute Profound Hearing Loss Investigation and Research Group of the Japanese Ministry of Health and Welfare (Chairman: Professor Y. Nomura):

Criteria for diagnosis of mumps deafness [29]

Definitive

1. Patients with evident clinical signs of mumps, such as swelling of the parotid gland and submandibular gland, and acute severe hearing loss during the period from 4 days before to 18 days after the appearance of such swelling.
2. Patients without evident signs of mumps, but with a significant rise in anti-mumps serum antibody titer within 2–3 weeks after the onset of acute hearing loss.

Near definitive

Patients in whom IgM antibody to mumps virus is detected within 3 months after the onset of acute severe hearing loss.

For reference

Patients in whom mumps deafness is suspected clinically.

Our group decided that sensorineural hearing loss occurring between 4 days before and 18 days after the onset of clinical mumps can be considered to be caused by mumps. In this instance, serological testing is not necessarily required.

The serological test for mumps infection is based on a significant rise in mumps antibody titers in paired sera. The paired sera must be tested by the same laboratory using the same assay. A fourfold rise of titer or greater is significant.

Cases in which a patient's relative or friend has contracted mumps, or in which the patient fits the criteria for definitive diagnosis, but where the timing does not match are considered *For Reference*.

If the first serum sample is collected too late, the antibody titer may already be high. Furthermore, if a second sample is not obtained, the serological test is of no value.

6.3.4 Mumps and Sudden Deafness

In viral infection, virus specific IgM antibody is produced during the initial stage of infection. Therefore, detection of anti-virus IgM antibody is evidence of recent infection. Sakata et al. [30] found that mumps IgM antibody appeared in the serum soon after infection and remained present for 3 months. This means that if IgM antibodies for mumps are present, the patient has likely been infected with mumps within the past 3 months.

Between December 1986 and October 1987, serum samples were obtained from 53 adult patients with sudden deafness at The University of Tokyo Hospital, and kept in a deep freezer (−70 °C) until use. Of the 53 patients, 38 were men (age range, 23–59 years) and 15 were women (age range, 25–56 years). Sera were collected from the patients 6–42 days after the onset of sudden deafness [31].

For IgM antibody detection, peroxidase-conjugated monoclonal antibody to mumps virus was employed. The procedure was performed at the Department of Measles Virus, National Institute of Health. Antibody levels were evaluated by optical density measured at 492 nm using a photometer. The cut-off level was 0.35 OD_{492}. Values above 0.45 were classified as positive, while values between 0.36 and 0.44 were considered equivocal.

Among 53 patients, three were positive (5.7 %), one was equivocal, and 49 were negative. Audiograms of the three positive cases are shown in Fig. 6.23.

Case 1 was a 48-year-old woman who felt a rather unusual sensation when she touched her left ear at 3:00 p.m. on 1 February 1987. She noticed hearing loss in the same ear at 8:00 p.m. that day. No vertigo was noticed. She was admitted to the hospital on February 6. Steroids were given intravenously for 2 weeks. An audiogram taken 4 months after the onset showed partial recovery of her hearing at low frequencies (Fig. 6.23a). The interval between onset of deafness and blood sampling was 20 days. The OD_{492} value was 0.45, indicating positive mumps infection.

Case 2 was a 32-year-old man who developed acute dizziness and profound sensorineural hearing loss in his left ear on 7 July 1987. Caloric testing revealed canal paresis in that ear. The man's hearing was unchanged after treatment (Fig. 6.23b). Blood sampling was performed 24 days after the onset of disease. The patient's OD_{492} value was >1.90.

Case 3 was a 56-year-old woman who noticed hearing loss on waking on the morning of 9 September 1987. No vertigo was noticed. Steroid therapy was started immediately. An audiogram showed a pure-tone average of 72.5 dB. The patient's hearing had recovered to 32.5 dB a month later (Fig. 6.23c). Blood was drawn for IgM testing 11 days after the onset of hearing loss. The OD_{492} value was 0.88.

These results may confirm that even mumps deafness recovers considerably if steroid therapy starts immediately after the onset of deafness, and that hearing loss of 70 dB might be the limit of reversibility.

These patients were initially diagnosed with idiopathic sudden deafness, but after the IgM antibody test results their diagnoses changed to mumps deafness.

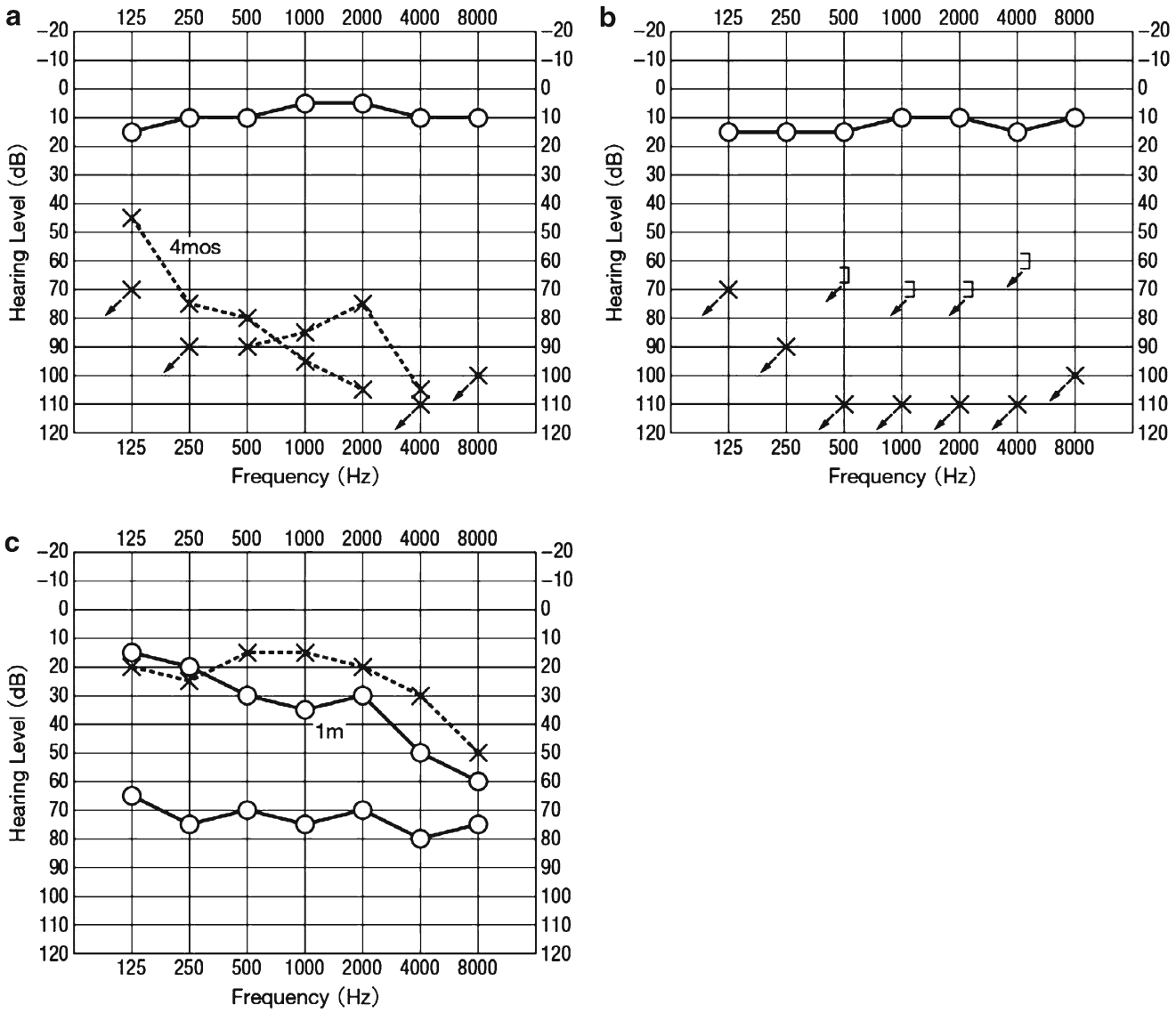

Fig. 6.23 Audiograms of three patients with sudden deafness accompanied by asymptomatic mumps. (**a**) Case 1: 48-year-old woman, (**b**) Case 2: 32-year-old man, (**c**) Case 3: 56-year-old woman [31]

Okamoto et al. [32] measured serum mumps antibody levels in 131 patients with sudden deafness. Positive IgM antibody results were obtained in 9 of 130 patients tested (6.9 %) and equivocal in six patients. IgG values were positive in 94 of 127 patients (74 %) and equivocal in 11 (8.7 %).

Fukuda et al. [33] measured IgM antibody for mumps in 69 patients with idiopathic sudden sensorineural hearing loss. Among 69 cases, 5 (7.2 %) were positive and 2 (2.9 %) were quasi-positive; the remaining 62 (89.9 %) were negative for IgM antibody. All positive IgM antibody cases were also positive for anti-mumps IgG antibody. Among 52 IgM-negative cases, 36 were positive for anti-mumps IgG antibody, eight were quasi-positive, and eight were negative.

The above data suggest that approximately 5–7 % of patients with idiopathic sudden deafness have silent mumps.

6.3.5 Deafness in Mumps Patients

Westmore et al. [34] were able to obtain a sample of perilymph from a patient with mumps who had developed sudden deafness. This 26-year-old woman with bilateral otosclerosis had previously undergone stapedectomy of the right ear with excellent results. One year after surgery she developed total deafness in the operated ear due to mumps. The patient presented 3 days after the onset of deafness. Considering the possibility that she might have a perilymphatic fistula, an

exploratory tympanotomy was performed. The Teflon piston was removed and a sample of perilymph was aspirated. Culture of the perilymph in primary monkey kidney tissue cultures grew mumps virus.

Okamoto et al. [35] compared the prognosis for hearing between two groups. One group included patients with idiopathic sudden deafness, and the other included patients with mumps deafness. All patients visited the same hospital within 7 days after the onset of deafness. The patients' audiograms showed that their hearing was off the scale in the range of 250–8,000 Hz on the affected side. There were 62 patients in the sudden deafness group with a male/female ratio of 28/34, whereas the mumps group included 39 patients with a ratio of 18/21. Marked hearing recovery[1] occurred in 41.2 % of patients in the sudden deafness group and slight recovery[2] was found in another 23.5 %. By contrast, marked recovery was seen in none of the mumps patients, and slight recovery in 26.5 %. These data confirm that normal hearing is rarely restored in mumps deafness.

6.3.6 Deafness in Mumps Meningoencephalitis

The incidence of deafness in patients with mumps meningoencephalitis differs in different studies. In a study by Azimi et al. [36], no evidence of hearing loss was found in 51 children with mumps meningitis. Mizushima and Murakami [37] found that mumps meningoencephalitis was not associated with deafness. Kanra et al. [38], on the other hand, found that the incidence of hearing loss was greater among patients with mumps meningoencephalitis than among those with uncomplicated mumps or among controls.

References

1. Hondo R, Kurata T, Nomura Y, Kanzaki J, Yanagita N, Koide J, Miyake H (1982) A seroepidemiological study of herpes simplex virus infection in the patients of sudden deafness. Otologia (Fukuoka) 28(Suppl 3):878–884
2. Kurata T, Hondo R, Sato S, Oda A, Aoyama Y, McCormick JB (1983) Detection of viral antigen in formalin-fixed specimens by enzyme treatment. Ann N Y Acad Sci 420:192–207
3. Nomura Y, Kurata T, Saito K (1985) Sudden deafness. Human temporal bone studies and an animal model. In: Nomura Y (ed) Hearing and dizziness. Igaku-Shoin, Tokyo, pp 58–67
4. Nomura Y, Hara M, Kurata T (1988) Experimental herpes simplex virus and cytomegalovirus labyrinthitis. Acta Otolaryngol (Stockh) 457(Suppl):57–66
5. Nomura Y, Kurata T, Saito K (1985) Cochlear changes after herpes simplex virus infection. Acta Otolaryngol (Stockh) 99:419–427
6. Saito K, Kurata T, Nomura Y (1984) Ultrastructure of the membranous cochlea with herpes simplex virus. 1983 Annual report of acute profound sensorineural hearing loss study group. Ministry of Health, Labor and Welfare, pp 111–113
7. Wildy P, Russell WC, Horne RW (1960) The morphology of herpes virus. Virology 12:204–222
8. Kurata T, Hondo R, Koide J, Nomura Y (1983) Experimental herpes simplex infection in the inner ear of guinea pig (IV). 1982 Annual report of acute profound sensorineural hearing loss study group. Ministry of Health, Labor and Welfare, pp 54–57
9. Saito K, Kurata T, Nomura Y (1985) Surface structure of the tectorial membrane with herpes simplex virus. 1984 Annual report of acute profound sensorineural hearing loss study group. Ministry of Health, Labor and Welfare, pp 165–168
10. Woolf NK (1990) Experimental congenital cytomegalovirus labyrinthitis and sensorineural hearing loss. Am J Otolaryngol 11:299–303
11. Barbi M, Binda S, Caroppo S, Ambrosetti U, Corbetta C, Sergi P (2003) A wider role for congenital cytomegalovirus infection in sensorineural hearing loss. Pediatr Infect Dis J 22(1):39–42
12. Koyano S, Inoue N, Oka A, Moriuchi H, Asano K, Ito Y, Yamada H, Yoshikawa T, Suzutani T (2011) Screening for congenital cytomegalovirus infection using newborn urine samples colleted on filter paper: feasibility and outcomes from a multicentre study. BMJ Open1:000118. doi:10.1136/bmjopen-000118
13. Ogawa H, Suzutani T, Baba Y, Koyano S, Nozawa N, Ishibashi K, Fujieda K, Inoue N, Omori K (2007) Etiology of severe sensorineural hearing loss in children:independent impact of congenital cytomegalovirus infection and GJB2 mutations. J Infect Dis 195:782–788
14. Myers EN, Stool S (1968) Cytomegalic inclusion disease of the inner ear. Laryngoscope 78:1904–1915
15. Strauss M (1990) Human cytomegalovirus labyrinthitis. Am J Otolaryngol 11:292–298
16. Davis LE, Spector GJ, Strauss M (1977) Cytomegalovirus endolabyrinthitis. Arch Pathol Lab Med 101:118–121
17. Katano H, Sato Y, Tsutsui Y, Sata T, Maeda A, Nozawa N, Inoue N, Nomura Y, Kurata T (2007) Pathogenesis of cytomegalovirus-associated labyrinthitis in a guinea pig model. Microbes Infect 9:183–191
18. Nomura Y, Harada T, Hara M (1988) Viral infection and the inner ear. ORL J Otorhinolaryngol Relat Spec 50:201–211
19. Saito K, Kurata T, Nomura Y (1988) Electron microscopic observations on the membranous cochlea after guinea pig cytomegalovirus infection. 1987 Annual report of the acute profound hearing loss study group. pp 47–49
20. Morgensen SC (1979) Role of macrophages in natural resistance to virus infections. Microbiol Rev 43:1–26
21. Nomura Y, Hara M, Okuno T, Yagi M, Kurata T, Nariuchi H (1989) Modality of endolymphatic hydrops. In: Nadol JB Jr (ed) Second international symposium on Meniere's disease. Kugler Ghedini Publications, Amsterdam, Berkeley, Milano, pp 89–96
22. Harris JP, Fan ST, Keitley EM (1990) Immunologic responses in experimental cytomegalovirus labyrinthitis. Am J Otolaryngol 11:304–308
23. Saunders WH, Lippy WH (1959) Sudden deafness and Bell's palsy: a common cause. Ann Otol Rhinol Laryngol 68:830–837
24. Van Dishoeck HA, Bierman TA (1957) Sudden perceptive deafness and viral infection; Report of the first one hundred patients. Ann Otol Rhinol Laryngol 66:963–980
25. Lindsay JR, Davey PR, Ward PH (1960) Inner ear pathology in deafness due to mumps. Ann Otol Rhinol Laryngol 69:918–935
26. Smith GA, Gussen R (1976) Inner ear pathologic features following mumps infection. Report of a case in an adult. Arch Otolaryngol 102:108–111
27. Tanaka K, Fukuda S, Suenaga T, Terayama Y (1988) Experimental mumps virus-induced labyrinthitis: immunohistochemical and ultrastructural studies. Acta Otolaryngol (Stockh) 456(Suppl):98–105

[1] More than 30 dB recovery in mean hearing level at the five frequencies (0.25, 0.5, 1, 2, and 4 kHz).

[2] Recovery of 10–29 dB in mean hearing level at the five frequencies.

28. Tanaka K, Fukuda S, Terayama Y, Toriyama M, Ishidoya J, Ito T, Sugiura A (1988) Experimental mumps labyrinthitis in monkeys (macaca irus)-Immunohistochemical and ultrastructural studies. Auris Nasus Larynx 15:89–96
29. Nomura Y (1988) Diagnostic criteria for sudden deafness, mumps deafness and perilymph fistula. Acta Otolaryngol (Stockh) 456(Suppl):7–8
30. Sakata H, Tsurudome M, Hishiyama M, Ito Y, Sugiura A (1985) Enzyme-linked immunosorbent assay for mumps IgM antibody: comparison of IgM capture and indirect IgM assay. J Virol Methods 12:303–311
31. Nomura Y, Harada T, Sakata H, Sugiura A (1988) Sudden deafness and asymptomatic mumps. Acta Otolaryngol (Stockh) 456(Suppl): 9–11
32. Okamoto M, Shitara T, Nakayama M, Takamiya H, Nishiyama K, Ono Y, Sano H (1994) Sudden deafness accompanied by asymptomatic mumps. Acta Otolaryngol 514(Suppl):45–48
33. Fukuda S, Chida E, Kuroda T, Kashiwamura M, Inuyama Y (2001) An anti-mumps IgM antibody level in the serum of idiopathic sudden sensorineural hearing loss. Auris Nasus Larynx 28(Suppl):S3–S5
34. Westmore GA, Pickard BH, Stern H (1979) Isolation of mumps virus from the inner ear after sudden deafness. Br Med J 1:14–15
35. Okamoto M, Shitara T, Higuchi A, Nakahara M (1984) Comparison of unilateral deafness in mumps and sudden deafness patients. Clinical Otology 11:154–155
36. Azimi PH, Cramblett HG, Haynes RE (1969) Mumps meningoencephalitis in children. JAMA 207:509–512
37. Mizushima N, Murakami Y (1986) Deafness following mumps: the possible pathogenesis and incidence of deafness. Auris Nasus Larynx 13(Suppl 1):55–57
38. Kanra C, Kara A, Cenqiz AB, Isik P, Ceyhan M, Atas A (2002) Mumps meningoencephalitis effect on hearing. Pediatr Infect Dis J 21:1167–1169

Laser Irradiation of the Inner Ear

7

Abstract

Laser can be used as a tool for inner ear surgery, particularly for the treatment of intractable vertigo. We found that argon laser selectively destroyed the maculae of the otolithic organs without injuring the wall of the membranous labyrinth, except for the dark cell area. The area of the maculae of the otolithic organs can be seen through the oval window after stapedectomy. The utricular macula is seen as a white plaque high in the vestibule. The recommended lasing site is the center of the plaque, or near its base, because nerve fibers and blood vessels enter the macula through the base. As for the human saccular macula, the saccular wall in the elderly contains many lipofuscin granules in its endothelial cell layer. Therefore, when lasing the saccular macula, sieve-like small perforations result in the saccular wall. These perforations may greatly influence the function of the cochlea.

Heat produced by laser irradiation of the semicircular canal can constrict the semicircular duct. This procedure does not require opening the canal for irradiation. Blue-lining the semicircular canal near the semicircular duct is essential. Because the duct adheres to the periosteum at the outer circumference of the canal, the blue line in this area is the best site to irradiate. This procedure is useful when attempting to immobilize the endolymph, such as for patients with intractable benign paroxysmal positional vertigo.

Laser surgery will eventually replace vestibular neurectomy. Its surgical field is within the scope of conventional ear surgery.

Keywords

Argon laser • Inner ear • Saccular macula • Semicircular canal • Semicircular duct • Surgery • Utricular macula • Vertigo

7.1 Introduction

Applications of laser as a treatment modality for inner ear disease have a long history. As early as 1965, Stahle and Högberg [1] irradiated the semicircular canals of pigeons using a Q-switched pulsed ruby laser and found a marked fibrotic reaction within the irradiated canal. The pigeons showed signs of labyrinthine irritation immediately after the procedure. Since then, the inner ear has been the subject of research aimed at developing laser surgery techniques [2–4].

In 1991, Anthony [5] reported lasing a pigment-marked blue-lined area of the posterior semicircular canal in two patients with benign paroxysmal positional vertigo (BPPV), and called this occlusion of the semicircular canal "partitioning." The lasing attempted to immobilize the endolymph of the posterior semicircular canal. Later, Anthony [6] thought that BPPV could be resolved by eliminating the otoliths from the utricle. Accordingly, the target organs for laser treatment have extended from the semicircular canals to the otolithic organ.

Among the various kinds of lasers, argon laser has been selected chiefly because it passes through the membranous vestibular labyrinth safely and selectively damages the sensory epithelium.

Y. Nomura, *Morphological Aspects of Inner Ear Disease*, DOI 10.1007/978-4-431-54204-9_7,

In this series of studies, the following two argon laser systems were used:

1. Coherent Medical Group Laser apparatus was incorporated in a Zeiss OMP1 operating microscope, spot size 100 μm
2. HGM Medical Laser System, Inc. ME-648, hand probe type, spot size 200 μm

Argon laser is a visible wavelength laser that has a range from 488 to 514.5 nm. The intensity of the argon laser in water falls to 1/10 its original surface value at a depth of 920 cm (penetration depth).

7.2 Animal Experiments

7.2.1 The Cochlea

7.2.1.1 Laser Irradiation of/Through the Round Window Membrane

Namba and Nomura [7] irradiated the round window membrane of guinea pigs (Takei strain) with an argon laser after pentobarbital anesthesia. The probe had an outer diameter of 600 μm, in which a glass fiber 200 μm in diameter was encased. One watt of power was applied for 0.5 s. The tip of the probe was approximated to the round window membrane about 1 mm from the target.

The irradiated round window membrane showed no microscopic changes. No burned spot or perforation was observed after application of the argon laser (Fig. 7.1). However, various changes were found within the cochlea. When the organ of Corti was irradiated, an area 300 μm in diameter completely disappeared, with formation of three slits in the basilar membrane. The direction of the slits was the same, parallel to the fibers of the basilar membrane. It seemed that the slits occurred secondary to micro-explosion of the organ of Corti. The basilar membrane itself seemed to permit passage of the argon laser beam (Fig. 7.2).

When the osseous spiral lamina of the basal turn was lased, the irradiated area was destroyed and the associated venule vaporized and coagulated, resulting in congestion of its periphery (Fig. 7.3). In another specimen, partial loss of the lower shelf of the osseous spiral lamina and loss of nerve fibers were seen on cross section. The upper shelf of the osseous spiral lamina was partly fractured and elevated. The limbus spiralis, tectorial membrane, and organ of Corti had degenerated (Fig. 7.4). Cyst formation in the stria vascularis was observed 2 days after irradiation. Because anatomy prevents direct access to the stria vascularis through the round window membrane, cyst formation might be a secondary effect. Though the secondary spiral lamina appeared intact, the adjacent lower spiral ligament was widely destroyed (Fig. 7.5) [8]. The basilar membrane showed a break. Claudius' cells near the break were lifted and attached to Reissner's membrane. The round window membrane remained intact (Fig. 7.6).

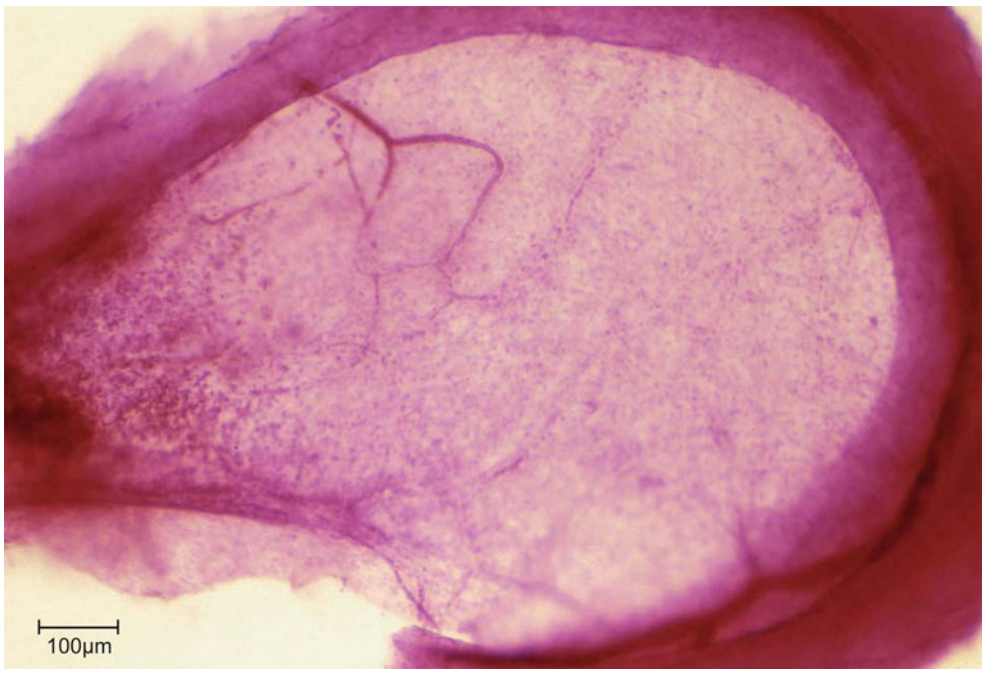

Fig. 7.1 The intact round window membrane after argon laser irradiation. Power 1.0 W × 0.5 s × 3 times. Beam diameter was 200 μm. Guinea pig, Kernechtrot staining, scale: 100 μm

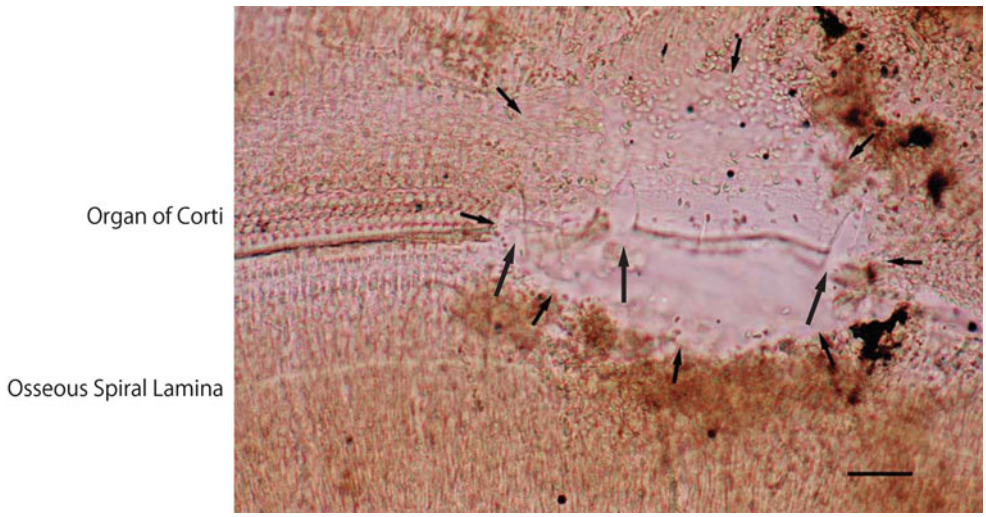

Fig. 7.2 Destruction of the organ of Corti immediately after irradiation [7]. Power 1.0 W×0.5 s. An area 300 μm in diameter disappeared (*arrows*). Three splits are found in the basilar membrane (*large arrows*). Scale: 50 μm

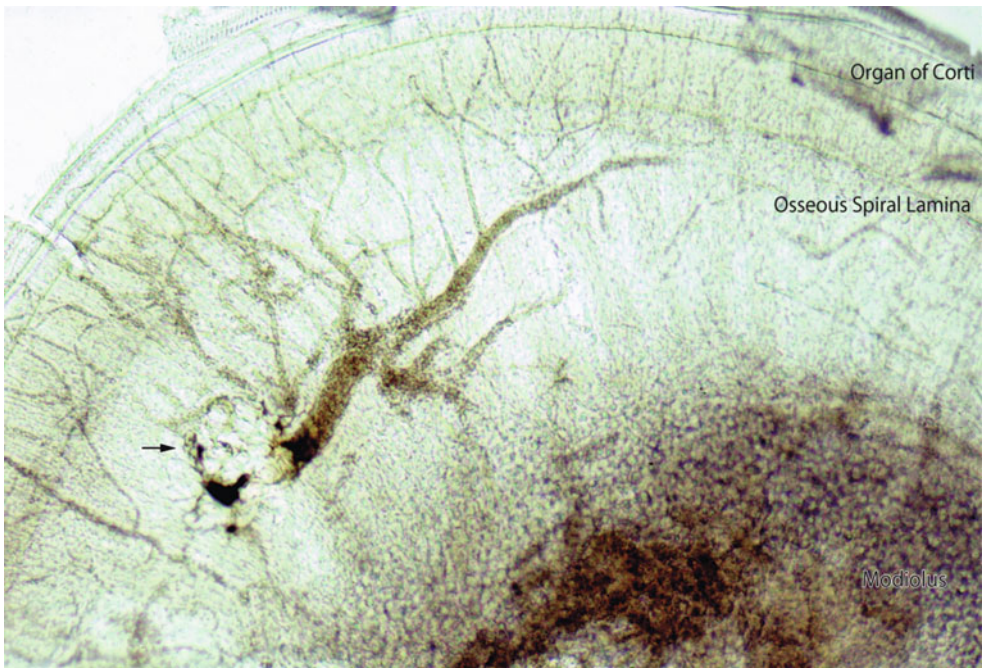

Fig. 7.3 Irradiation of the osseous spiral lamina through the round window membrane. The *arrow* indicates circular damage to the osseous spiral lamina. The venule running near the center of the explosion was involved, resulting in destruction and coagulation of the vessel. Its periphery is congested. Immediately after irradiation. The same animal whose intact round window membrane is shown in Fig. 7.1. Surface preparation, Nomarski microscope

7.2.1.2 Laser Irradiation of the Otic Capsule

The purpose of argon laser application to the bony wall of the cochlea is to produce localized loss or atrophy of the stria vascularis. In another study, the tip of the probe (diameter 200 μm) was advanced toward the otic capsule of the third cochlear turn, about 1 mm from the bony surface. The target was the stria vascularis [8].

The stria vascularis with spiral ligament was removed immediately after laser irradiation (800 mW×0.5 s) of the otic capsule of the third turn. Alkaline phosphatase staining was performed to confirm the effect of lasing on the strial capillary network. A circular coagulated area was found in the stria vascularis within which the strial capillaries showed no enzymatic activity (Fig. 7.7).

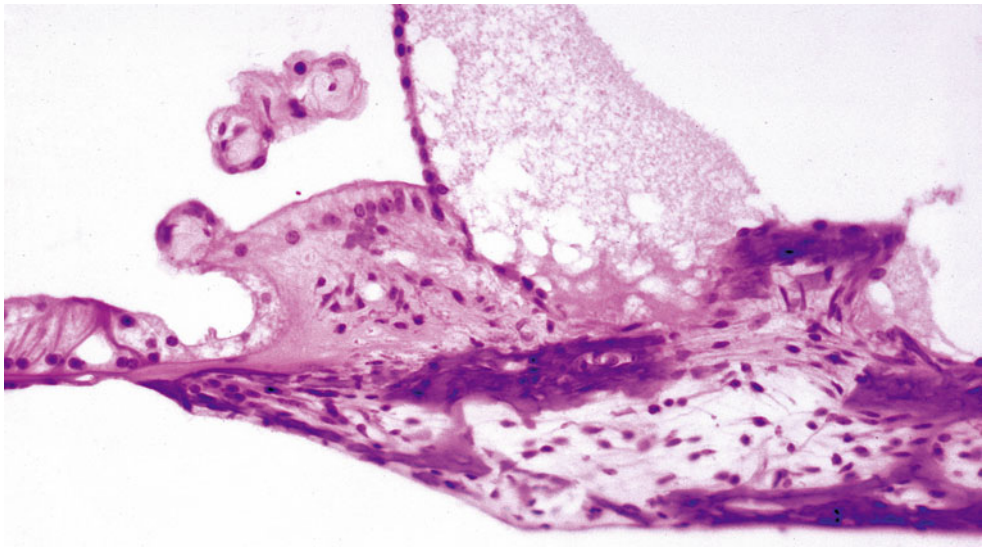

Fig. 7.4 Laser irradiation of the osseous spiral lamina through the round window membrane. There is loss of dendrites of the cochlear neurons in the osseous spiral lamina. A defect in the lower shelf and fracture of the upper shelf of the spiral lamina are seen. Partial loss of the interdental cells and degeneration of the tectorial membrane are evident. The organ of Corti and the internal sulcus cells have degenerated. Two days after irradiation (1 W × 0.5 s) (original ×16) [7]

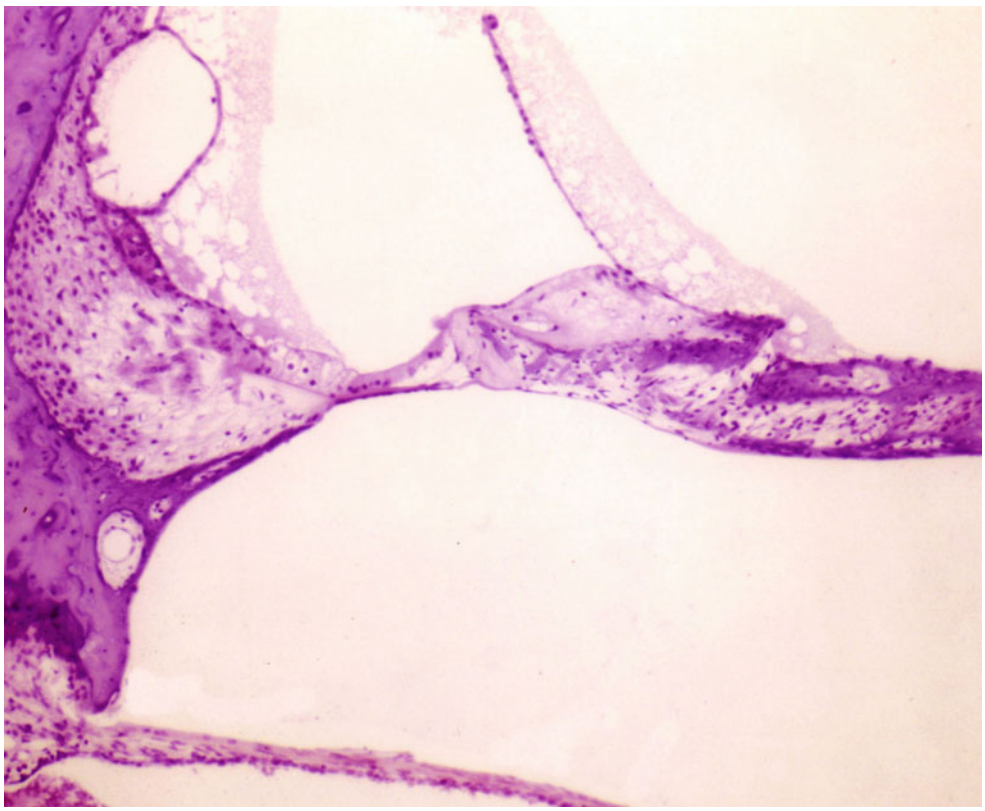

Fig. 7.5 Laser irradiation of the cochlea through the round window membrane. Laser beams hit the basilar membrane and the osseous spiral lamina, resulting in marked damage. A cyst has formed in the stria vascularis. The secondary spiral lamina appears intact but the adjacent lower spiral lamina is destroyed. Two days after irradiation (1 W × 0.5 s × 5 times) (original ×6.5) [8]

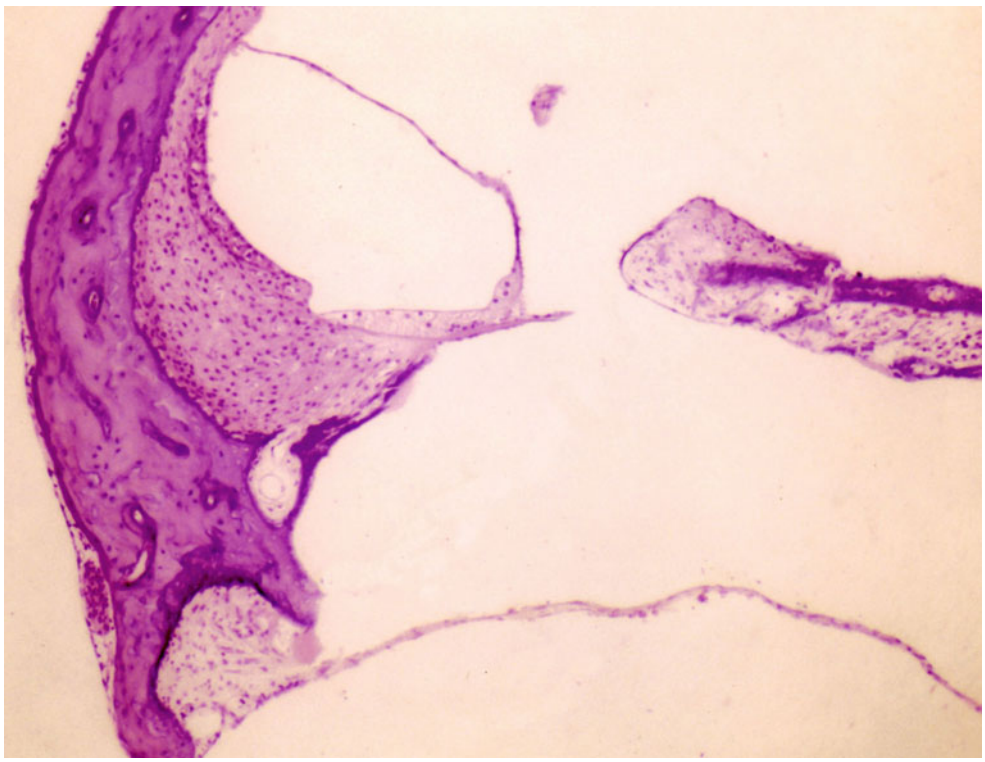

Fig. 7.6 Laser irradiation of the cochlea through the round window membrane. Laser beams hit the basilar membrane and the osseous spiral lamina, resulting in communication between the scalae tympani and vestibuli. Claudius' cells close the scala media together with Reissner's membrane (original ×6.5) [8]

A similar experiment was conducted using reduced laser power of 300 mW applied to the otic capsule [7]. This produced a charred area with an adjacent vaporized area in the capsule. The irradiated area showed a slight bulge covered by intact periosteum (Fig. 7.8). Strands connecting the remaining living tissues passed through the charred and lucent area. The strands may have been capillary remnants. Reissner's membrane appeared to have extended to cover the defect of the stria vascularis and spiral ligament. It is not clear whether the altered marginal cells of the stria vascularis participated in this process (Fig. 7.8). In another specimen, altered marginal cells remained and connected to Reissner's membrane. Several days later, cellular debris had cleared from the perilymphatic space, as well as from the scala media (Fig. 7.9).

Thirty-five days after laser irradiation (90 mW × 0.5 s), the stria vascularis was completely absent but the configuration of the scala media was preserved. The upper half of the spiral ligament was almost completely missing. The inner and outer hair cells had degenerated. Hensen's cells appeared preserved. No cellular debris remained in the scala media (Fig. 7.10).

The otic capsule did not show any changes after laser irradiation (50 mW × 0.5 s). However, the spiral ligament was atrophic and acellular behind the stria vascularis, which persisted as a single layer of altered marginal cells. The outer hair cells were atrophic and some lacked nuclei. The outer hair cells and the phalanx of Deiters' cells appeared to have fused. Hensen's cell appeared unchanged 30 days after laser application (Fig. 7.11).

The average thickness of the otic capsule of the third turn was 102 μm (mean of 12 animals) and the capsule did not show morphologic changes. This suggests that the laser beam passed through the bony wall and led to destruction of the spiral ligament and disappearance of the stria vascularis. However, the primary goal of inducing localized strial atrophy was unsuccessful. The laser power needed to be reduced to preserve an intact organ of Corti.

Using the photochemical reaction between the systemic injection of Rose Bengal and controlled green light irradiation of the cochlea, Ocho et al. [9] produced a localized degeneration of the stria vascularis with preservation of the outer hair cells. The photochemical reaction produced a reactive oxygen species, resulting in damage to the endothelium. This damage triggered platelet adhesion and aggregation at the site of endothelial injury, producing thrombi and affecting microcirculation in the lateral wall of the cochlea at the site of irradiation. The direction of irradiation was tangential to the target in the cochlear wall. The outer hair cells

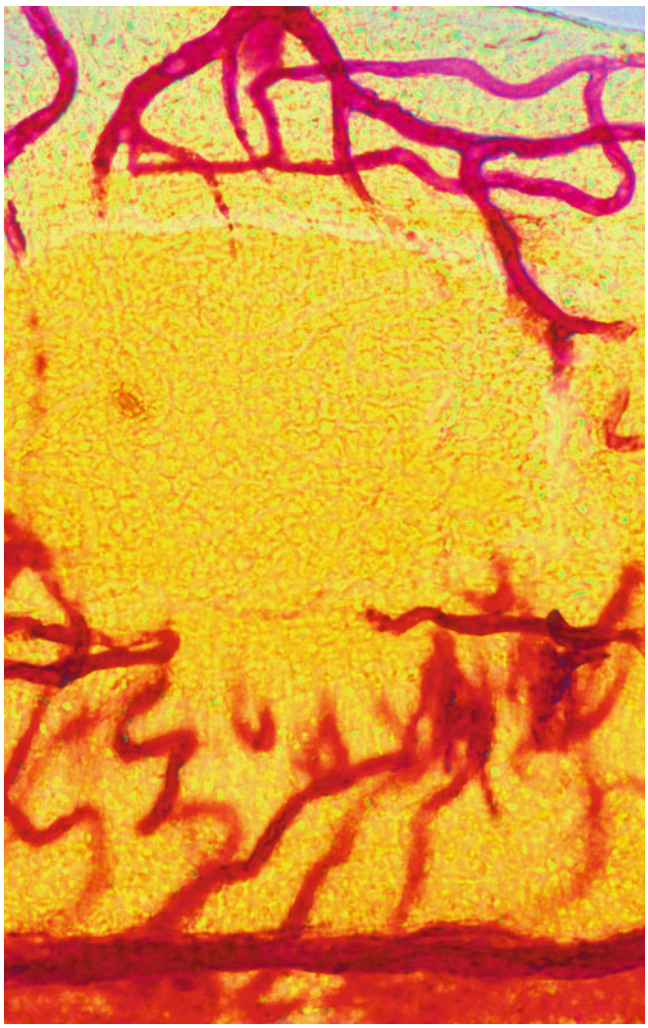

Fig. 7.7 Laser irradiation of the stria vascularis through the otic capsule of the third turn. The strial capillary in the coagulated area (about 300 μm in diameter) shows no alkaline phosphatase activity (0.8 W × 0.5 s). Guinea pig, alkaline phosphatase staining [8]

survived for 24 h after irradiation, then disappeared with loss of the stria vascularis [9, 10].

7.2.2 The Otolithic Organs

7.2.2.1 Laser Irradiation of the Utricular Macula

The utricular macula is located on the floor of the utricle and its area can be seen through the oval window as a white plaque in the upper portion of the vestibule.

An argon laser passes through the utricular wall without damaging it, except in the dark cell area. Melanin in the dark cell area is susceptible to the beam, resulting in perforation [11]. Irradiation of the macular area is safe, because the connective tissue layer beneath the sensory epithelium is relatively thick and almost no pigments or pigment cells exist there.

When irradiating the utricular macula of guinea pigs, stapedectomy should be performed carefully to allow replacement of the stapes in the oval window after irradiation.

A single irradiation with an argon laser (1–1.5 W for 0.5–1 s) is enough to erase the entire sensory area, including the otoliths, sensory epithelium, nerve fibers, and capillary networks. The beam is directed toward the center of the white plaque (Fig. 7.12) [11].

Histological changes seen in the utricular macula differ depending on the power and duration of irradiation, and the interval between irradiation and sacrifice. The sensory cells and supporting cells are most vulnerable to irradiation.

Histological Changes 10 Weeks After Argon Laser Irradiation of the Utricular Macula (1 W x 1 s)

Complete loss of the macula was observed with preservation of the utricular wall, saccular wall, and membrana limitans. The utricle showed a mild hydrops (Fig. 7.13) [12]. The nerve fibers underneath the sensory epithelium were also missing. The crista of the lateral semicircular canal remained intact (Fig. 7.14) [11]. Caloric testing response had returned to normal.

Immediately after irradiation, the supporting cells were partly missing and partly remained on the basement membrane as destroyed cells with pyknotic nuclei. The sensory cells were destroyed and elevated. The top surface of the sensory epithelium appeared undulated. There were clear spaces between the sensory cells and the basement membrane and/or remnants of the supporting cells. The basement membrane did not show any clear rupture under light microscopy (Fig. 7.15) [13]. Capillaries beneath the basement membrane were intact. When viewed with electron microscopy, nerve fibers in the subepithelial connective tissue layer showed marked distortion of their myelin sheaths with loss of neurofilaments.

The utricular macula of cynomolgus monkeys showed loss of sensory epithelium and nerve fibers in the subepithelial tissue 10 days after irradiation (2 W × 1 s). A beam 100 μm in diameter caused the loss of an area 250 μm in diameter in the sensory epithelium.

Under a light microscope the otolithic membrane appeared fairly well preserved for several days after irradiation (Fig. 7.16) [14].

The destroyed area seemed to have a sharp border with the remaining sensory epithelium. However, the stereocilia of the sensory cells were pulled out by elevation of the otolithic membrane (Fig. 7.17).

The otoliths disappeared from the utricular macula 2–3 weeks after irradiation. Under a scanning microscope, it was observed that half of the sensory epithelium had

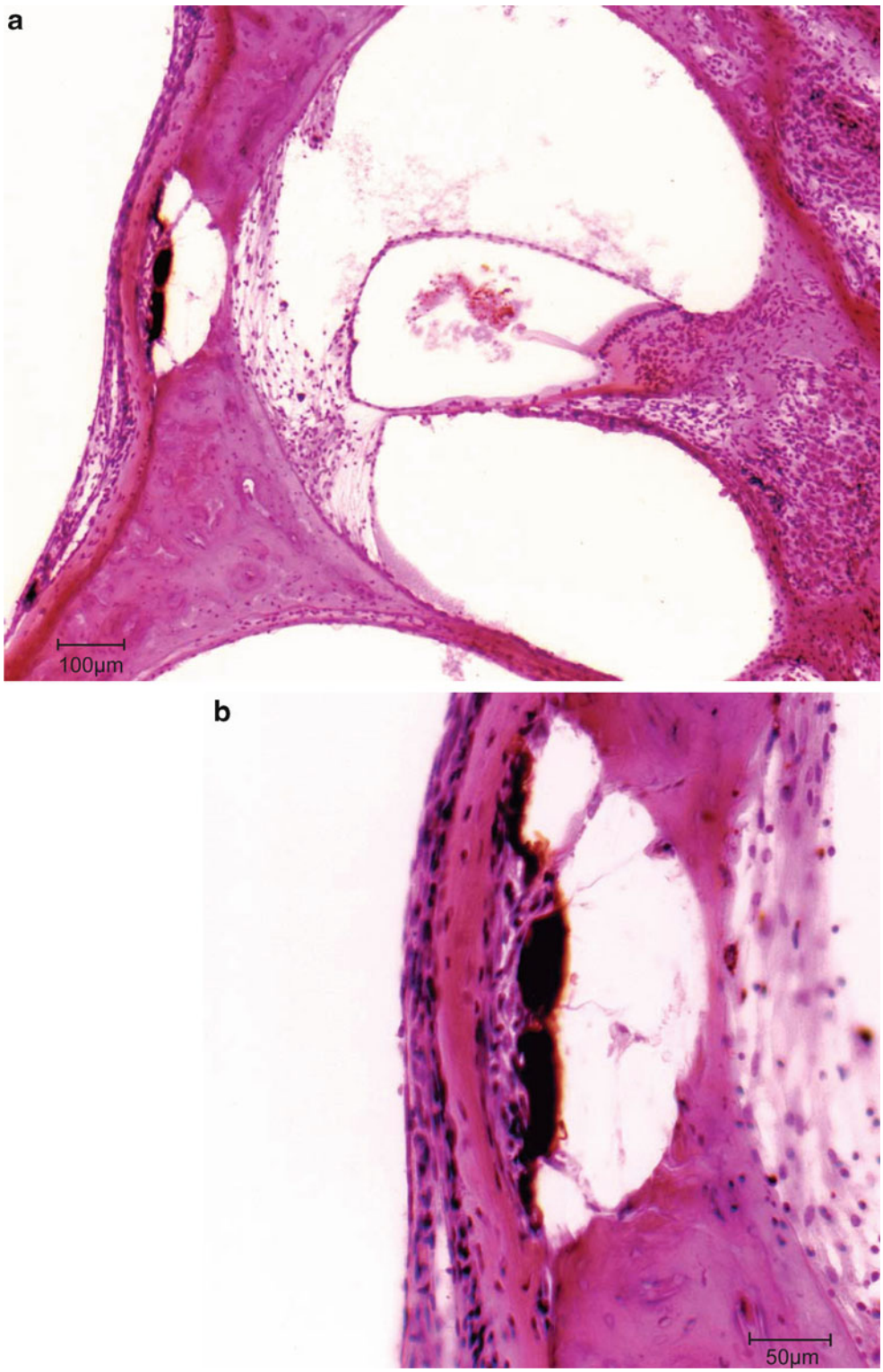

Fig. 7.8 Changes of the otic capsule and inside the cochlea [7]. (**a**) A carbonized area is present beneath the normal periosteum, which shows a bulge. Adjacent to the carbonized area is a vaporized region. The spiral ligament is defective and the stria vascularis is absent. The organ of Corti has been completely destroyed and has detached from the basilar membrane. Fifteen days after irradiation of the otic capsule adjacent to stria vascularis. The scala media is smaller but its boundary is preserved. Scale: 100 µm (original ×6.5). (**b**) Higher magnification of the section of (**a**). The power applied was 300 mW×0.5 s. The second turn of the cochlea of a guinea pig, 15 days after irradiation (original ×16), scale: 50 µm

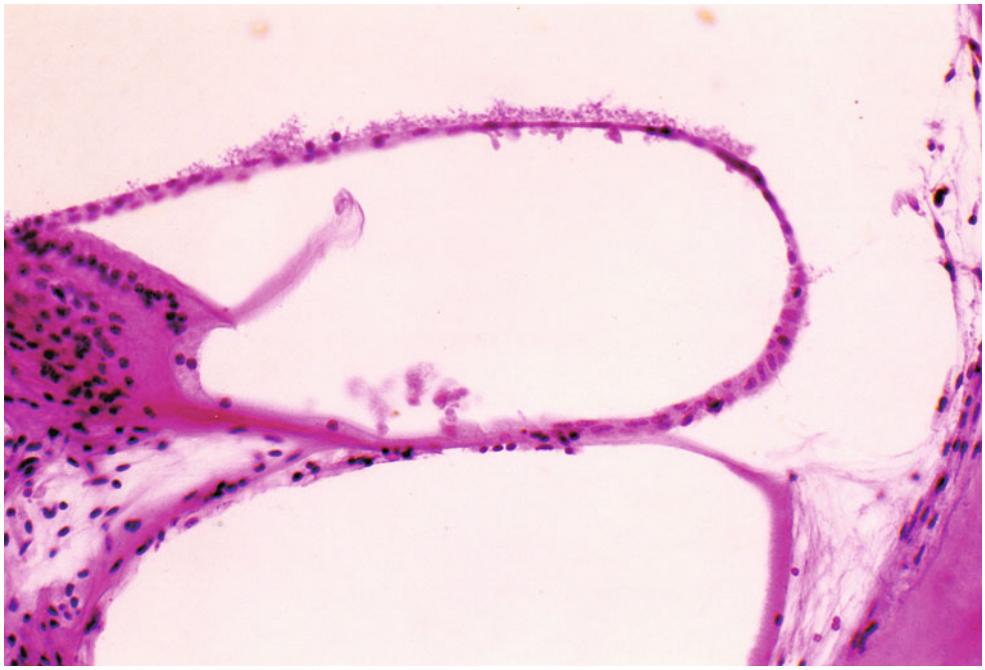

Fig. 7.9 More advanced stage. Irradiation of the otic capsule. In addition to loss of the stria vascularis, loss of the spiral ligament extends toward its lower portion. Dendrite loss in the osseous spiral lamina is more marked than that observed in Fig. 7.8. Twenty-six days after irradiation of 300 mW × 0.5 s (original ×16) [7]

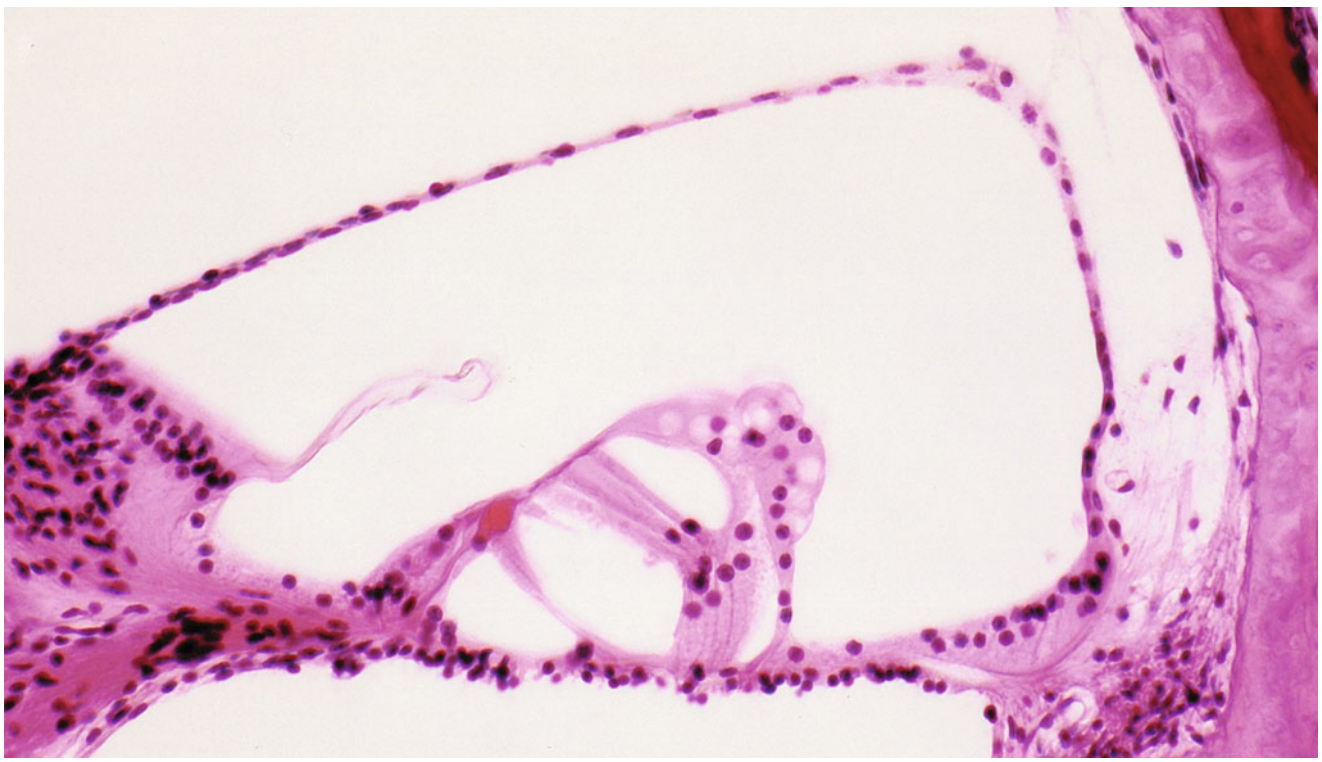

Fig. 7.10 Complete loss of the stria vascularis and near loss of the spiral ligament. The outer hair cells are elongated with shrunken nuclei. Reissner's membrane extends to cover the lost stria vascularis and spiral ligament. The endolymphatic compartment is preserved. Hensen's cells are fairly well preserved. 35 days after irradiation of the otic capsule (90 mW × 0.5 s). Guinea pig (original ×16) [7]

Fig. 7.11 Free floating, disintegrated strial cells in the scala media (*large arrow*). There is fusion of the anuclear atrophic hair cells with the phalanx of Deiters' cells (*small arrow*). The stria vascularis and spiral ligament are atrophic. Thirty days after argon laser irradiation of the otic capsule (50 mW × 0.5 s). Third turn of the cochlea, guinea pig (original ×16) [7]

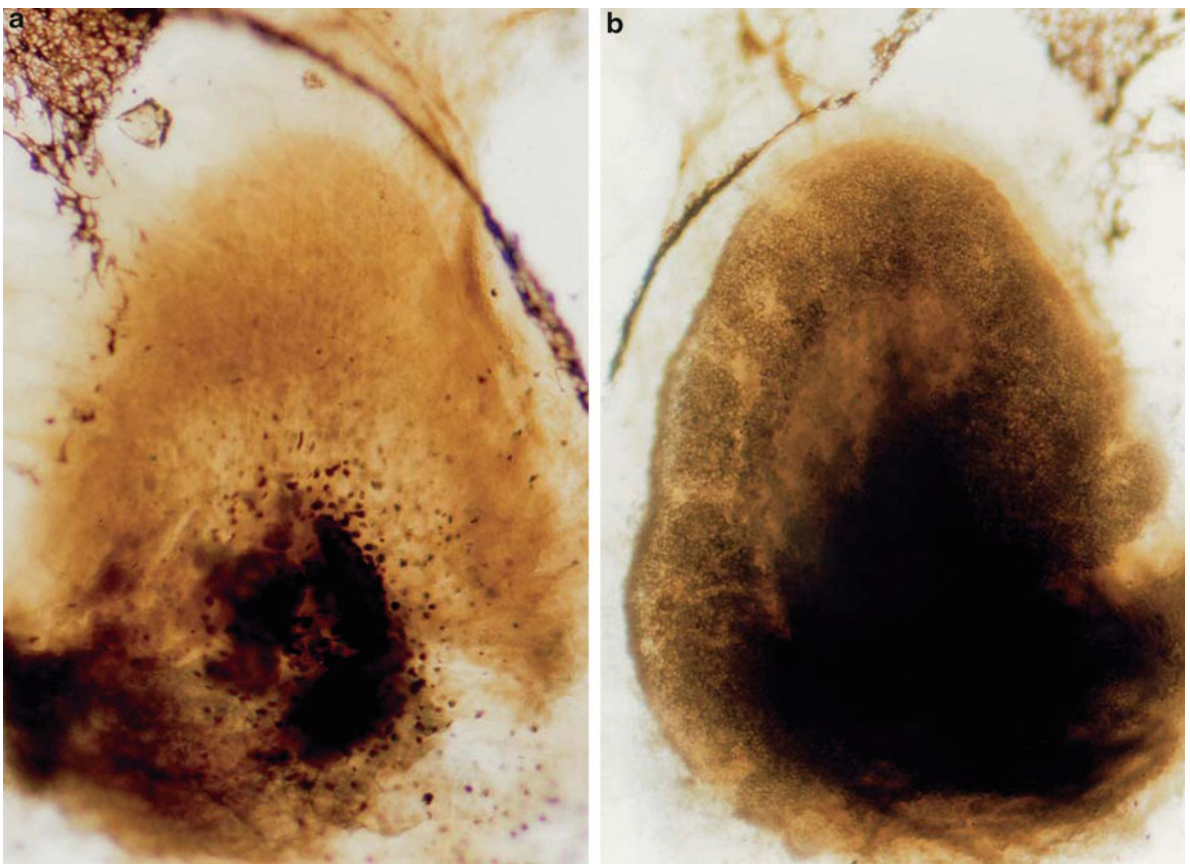

Fig. 7.12 Irradiation of the utricular macula [13]. (**a**) Complete loss of nerve fibers, sensory epithelium, and otoliths. Nineteen days after a single irradiation of 1.5 W × 0.5 s. (**b**) Control: The otoliths and dark-stained nerve fibers can be seen. Guinea pig, osmic acid staining, whole mount staining (original ×6.5)

Fig. 7.13 Irradiation of the utricular macula 10 weeks after irradiation [12]. (**a**) After stapedectomy, the utricular macula was irradiated by argon laser (1 W × 1 s). The stapes was replaced in the oval window after irradiation. The utricular macula has completely disappeared (*arrow*). Mild hydrops is seen in the utricle and semicircular duct. (**b**) Control: A cross section of normal utricular macula (*arrow*) is observed. Guinea pig, HE staining (original ×2.5)

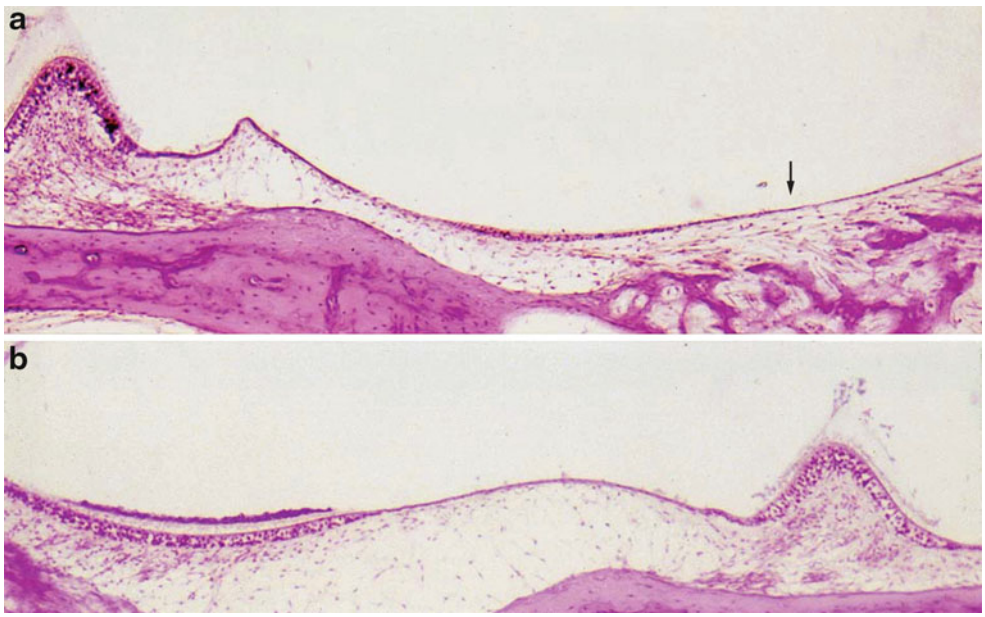

Fig. 7.14 Irradiation of the utricular macula [11]. (**a**) The utricular macula with nerve fibers is completely missing 10 weeks after irradiation (1 W × 0.5 s) (*arrow*). The subepithelial connective tissue is thin compared with the normal side. The crista ampullaris of the lateral canal lies on the same plane as the utricle. (**b**) Control: The utricular macula shows normal structure: otolithic membrane, sensory epithelium, and nerve fibers. Guinea pig (original ×6.5)

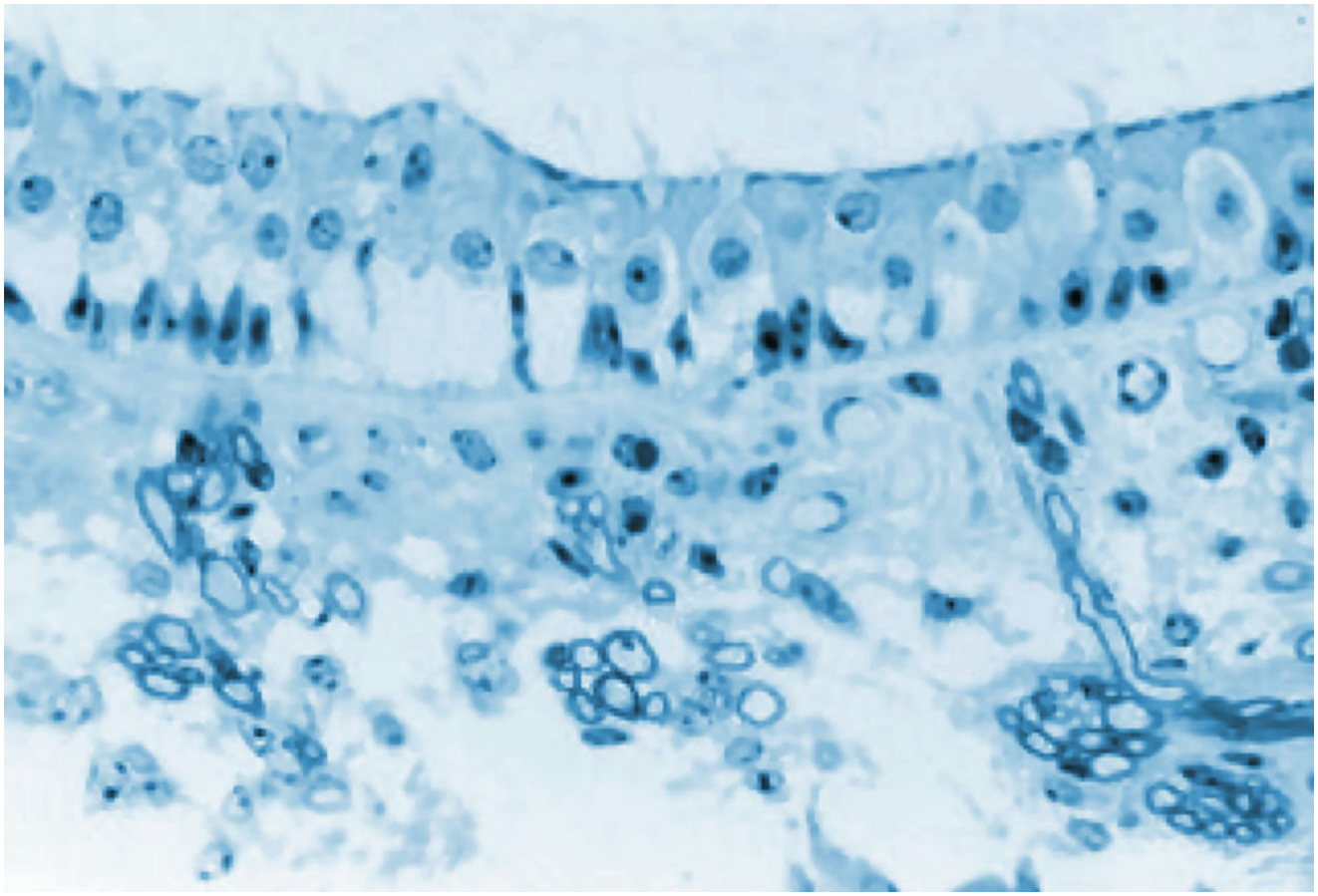

Fig. 7.15 The utricular macula immediately after irradiation. Sensory cells are destroyed and detached. There is marked loss of supporting cells. A lucent area is present between the basement membrane and the sensory cells. Myelinated nerve fibers in the subepithelial connective tissue show degenerated myelin sheaths and rare neurofilaments under an electron microscope. Guinea pig, toluidine blue staining (original ×40) [13]

disappeared 3 weeks after irradiation. A single layer of cuboidal cells covered the irradiated site. The cells were irregular in size and had no hairs on their surface (Fig. 7.18) [12].

Under a transmission electron microscope, the otoliths appeared irregularly arranged 2–5 days post-irradiation. Dispersed otolithic particles were surrounded and trapped by macrophages, in which they gradually lost their polygonal shape (Fig. 7.19) [15]. These macrophages dotted the membranous labyrinth of the pars superior, but none were observed after 3 weeks. There were masses of macrophages containing disintegrated otoliths in the dark cell area [15].

No tears in the membranous labyrinth were observed after irradiation. The membrana limitans and trabecular mesh were preserved. The utricle and semicircular canals sometimes developed mild hydrops after irradiation. Argon laser irradiation of the utricular macula can safely destroy all macular sensory components.

7.2.2.2 Laser Irradiation of the Saccular Macula

The saccular macula can be irradiated with argon laser through the oval window. Unlike utricular macula irradiation, in this case the laser beam passes through the saccular wall first, then the endolymph, the otolithic membrane, the sensory epithelium, and nerve fibers. Histological changes after irradiation are similar to those observed in the utricular macula.

In one study, the saccular macula of cynomolgus monkeys was irradiated using argon laser (1.0 W × 1.0 s × 3 times). Histopathological findings immediately after irradiation with a 200 μm diameter probe included pyknotic nuclei in the destroyed supporting cells of the basement membrane with destruction and dispersal of the sensory epithelium in an area 300 μm in diameter. A wide space between the basement membrane and dispersed sensory cells indicated a microexplosion within the sensory epithelium. The otolithic membrane was elevated without apparent changes. Capillaries remained beneath the basement membrane (Fig. 7.20) [14].

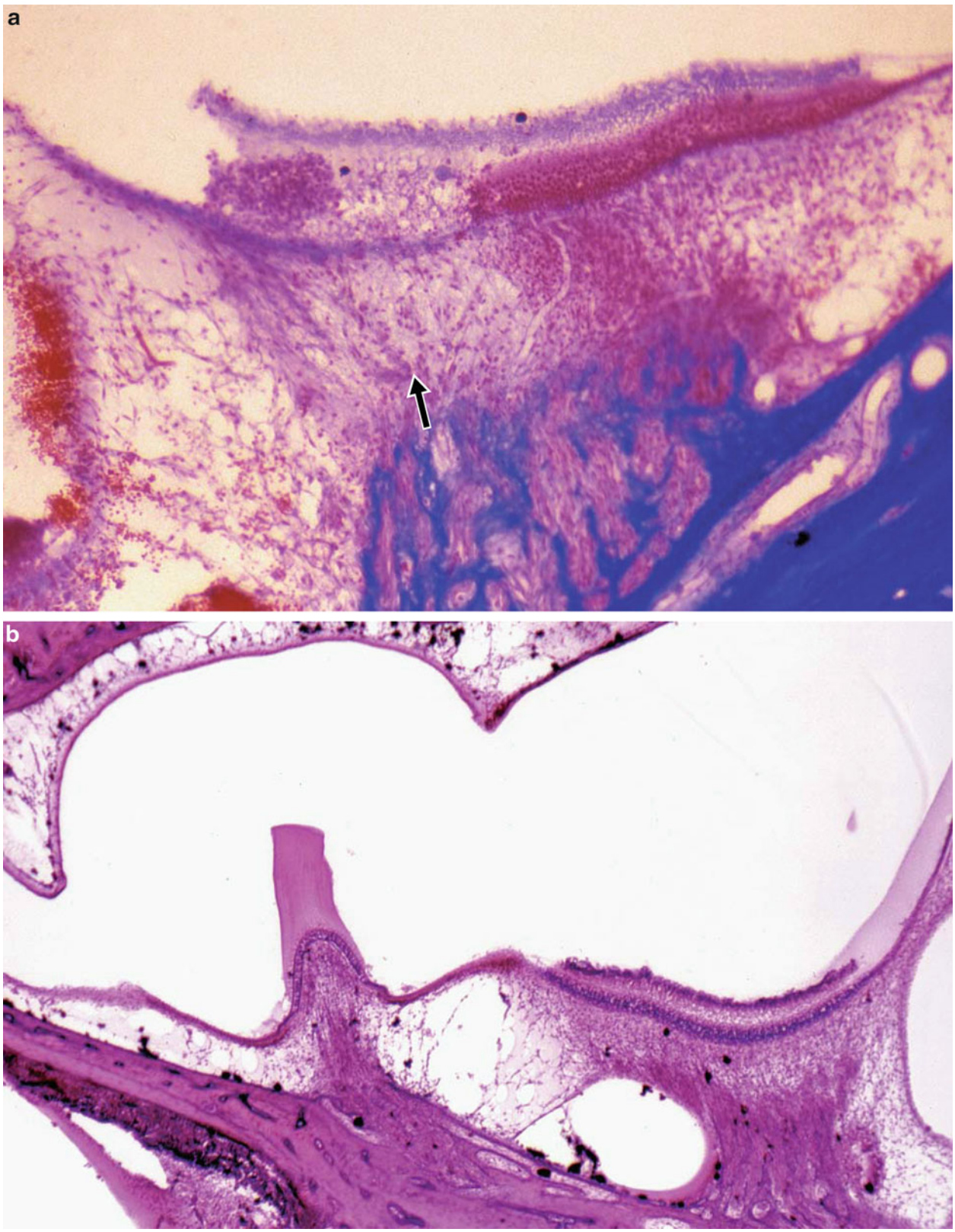

Fig. 7.16 Irradiation of the utricular macula [14]. (**a**) Laser irradiation (2 W × 1 s) of the utricular macula of a cynomolgus monkey. The sensory epithelium is destroyed in an area 250 μm in diameter. The otolithic membrane is preserved. Marked hemorrhage is observed in the remaining sensory epithelium. The *arrow* indicates the direction of irradiation (original ×6.5). (**b**) Control, showing the normal utricular macula and lateral crista ampullaris. 10 days after irradiation (original ×2.5)

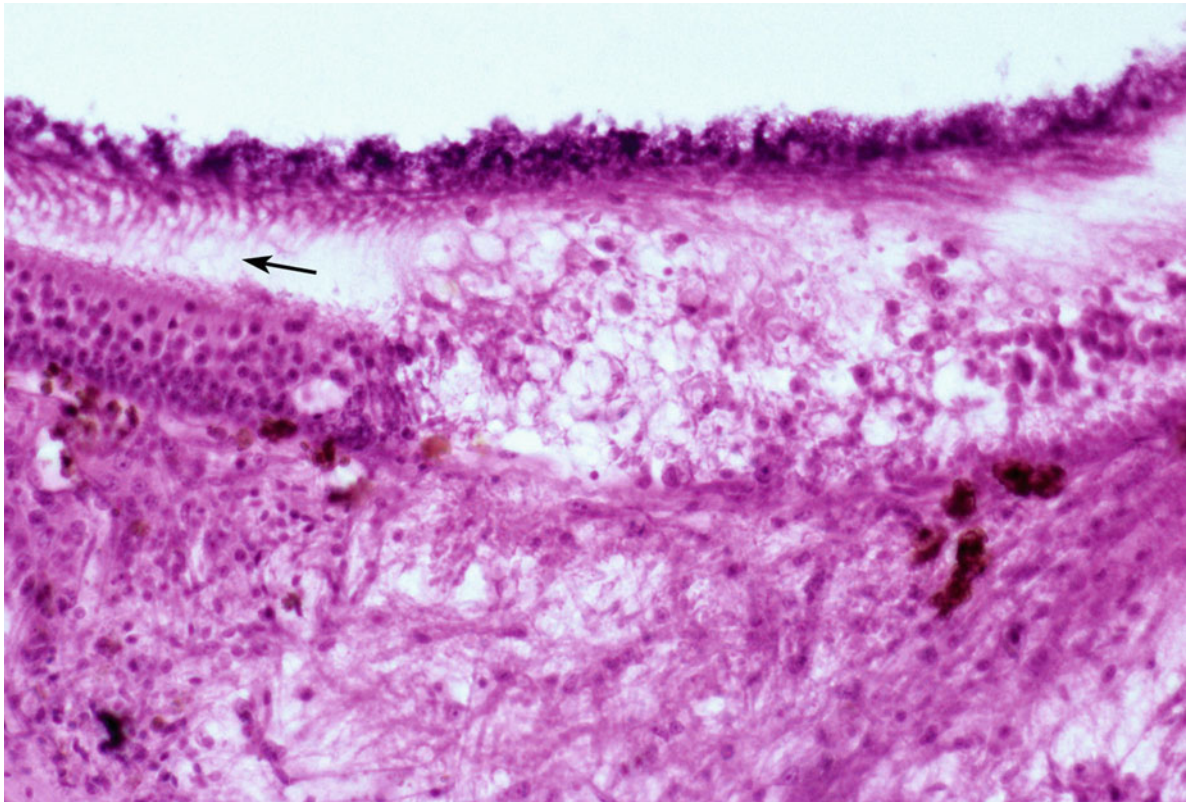

Fig. 7.17 High power view of the irradiated area of the utricular macula. Destruction and dispersal of the sensory epithelium have elevated the otolithic membrane, pulling out the stereocilia from the remaining sensory cells nearby (*arrow*). The basement membrane is destroyed. The subepithelial connective tissue layer shows marked destruction. Cynomolgus monkey (original ×16)

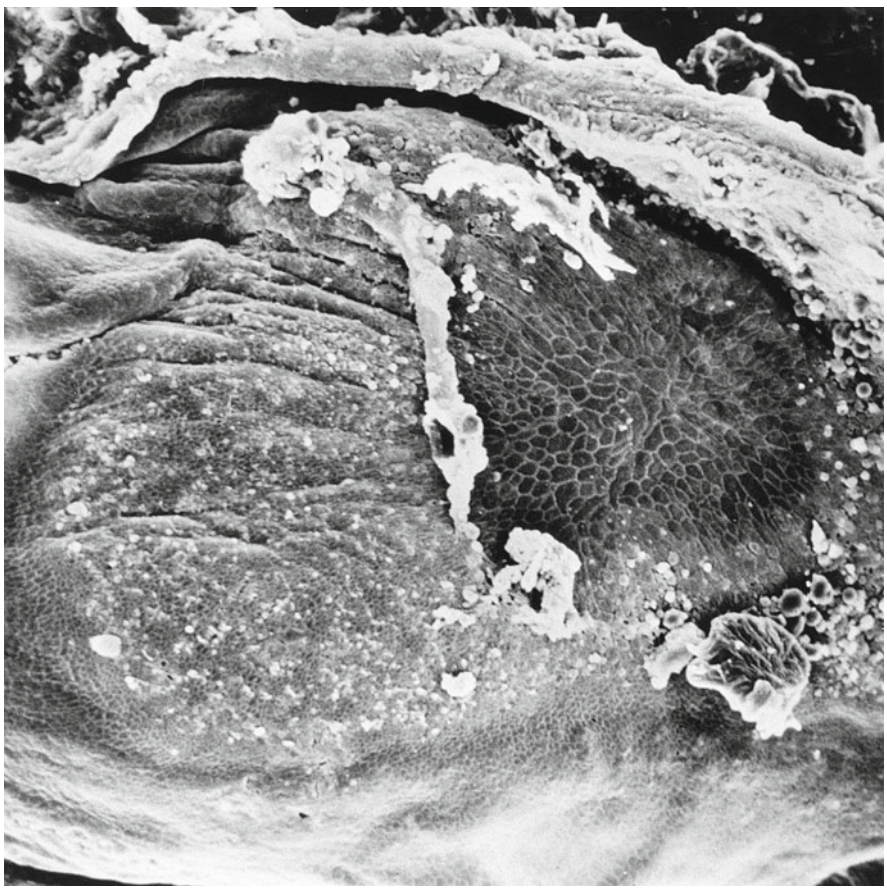

Fig. 7.18 Loss and repair of the utricular sensory epithelium [12]. Degeneration of the sensory epithelium had progressed toward the periphery of the macula. The area has been replaced by polygonal cells. Three weeks after irradiation (1 W×0.5 s). Guinea pig (original ×300)

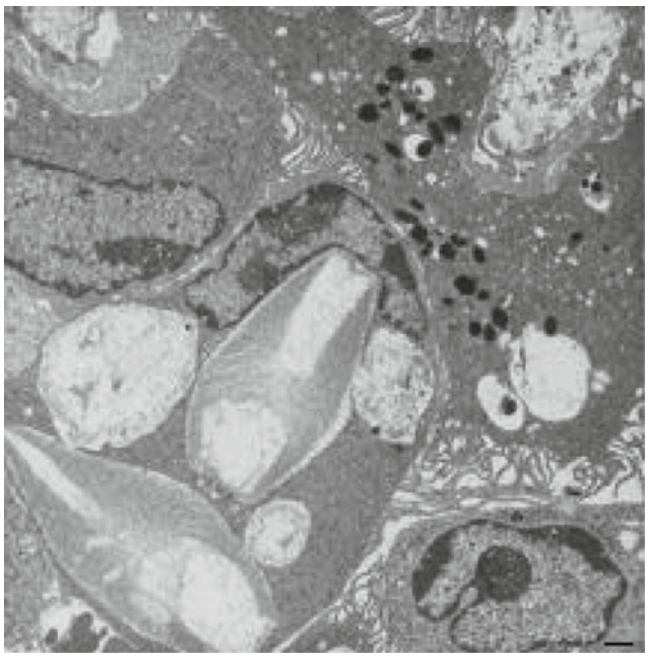

Fig. 7.19 Changes in the utricular otoliths after laser irradiation [15]. Macrophages surround, trap, and disintegrate the otoliths. Scale: 1 μm

In another specimen, a single layer of cells with microvilli covered the irradiated saccular macula 10 weeks after irradiation (Fig. 7.21). Whether the microvilli were related to the remaining stereocilia is unknown.

The vestibular ganglion cells became atrophic and decreased in number (Fig. 7.22).

7.2.3 The Semicircular Canal

7.2.3.1 Laser Irradiation of the Semicircular Canal

In one study, argon laser was applied to the semicircular canals of guinea pigs. The configuration of the three semicircular canals is easily identified and the bony wall is thin. The laser can be applied directly to the canal. Char formation may not occur at the target until after repeated irradiation. However, the temperature rises inside the canal despite little change in its appearance. If black ink is painted on the target, carbonization will occur easily.

The purpose of laser irradiation of the semicircular canal is to constrict the semicircular duct by heat. Constriction results in immobilization of endolymph in the irradiated semicircular canal.

In this experiment, one of the three semicircular canals was irradiated one to several times with an argon laser (1.0–1.5 W×0.5 s). The target sites were the semicircular canal away from the ampulla and the ampulla itself.

Histopathological examination of the temporal bones immediately after irradiation revealed carbonization of the irradiated bony canal, extreme constriction of the semicircular duct and complete disappearance of the trabecular mesh.

The semicircular duct constricts when heated, yet argon laser passes through the membranous labyrinth without causing any damage. When lasing the canal wall, it is hard to know how the duct is heated. Char formation at the bony wall suggests that enough heat was transmitted to the duct to cause constriction.

The hand-held probe laser system used in this study was an ME-648 HGM Laser System (Salt Lake City, UT, USA). Irradiation of the semicircular canal of guinea pigs caused a defect approximately 350 μm in diameter where the bony canal had carbonized and vaporized. The semicircular duct markedly constricted without carbonization or vaporization (Fig. 7.23) [16]. The basement membrane thickened. The epithelial cells were swollen and partly detached from the basement membrane (Fig. 7.24). The trabecular mesh disappeared. The mesothelial cells lining the inside of the bony canal were either absent or necrotic (Fig. 7.23).

Constriction of the duct also occurred longitudinally; the duct became shorter. Thus, the irradiated portion of the duct moved away from the original outer side toward the inner side (Figs. 7.23 and 7.25) [16]. Auditory brainstem response measurements showed no change with the power, duration, and iterations of argon laser application used in these experiments [17].

The semicircular canal became fibrotic and gradually ossified, and had become completely occluded within several weeks after irradiation (Figs. 7.26, 7.27, and 7.28) [17, 18].

7.2.3.2 Laser Irradiation of the Ampulla of the Semicircular Canal

Argon laser irradiation (1 W×0.5 s) of the bony ampulla caused destruction and disappearance of the sensory epithelium and nerve fibers. The sensory epithelium of the irradiated site was severely damaged, sometimes detaching from the crista ampullaris, and sometimes gradually disappearing with the nerve fibers. The transitional area and dark cell area were also destroyed and replaced by a single cell layer (Figs. 7.29 and 7.30). Beneath the irradiated dark cell area, small particles of melanin were found scattered toward the base of the crista ampullaris [17].

7.3 Clinical Applications

7.3.1 Irradiation of the Semicircular Canal

Several surgical methods are used to treat intractable benign paroxysmal positional vertigo (BPPV), including singular neurectomy, canal plugging, and laser irradiation. Canal plugging requires a fenestra in the affected canal wall and occlusion of the lumen with a piece of fascia or connective

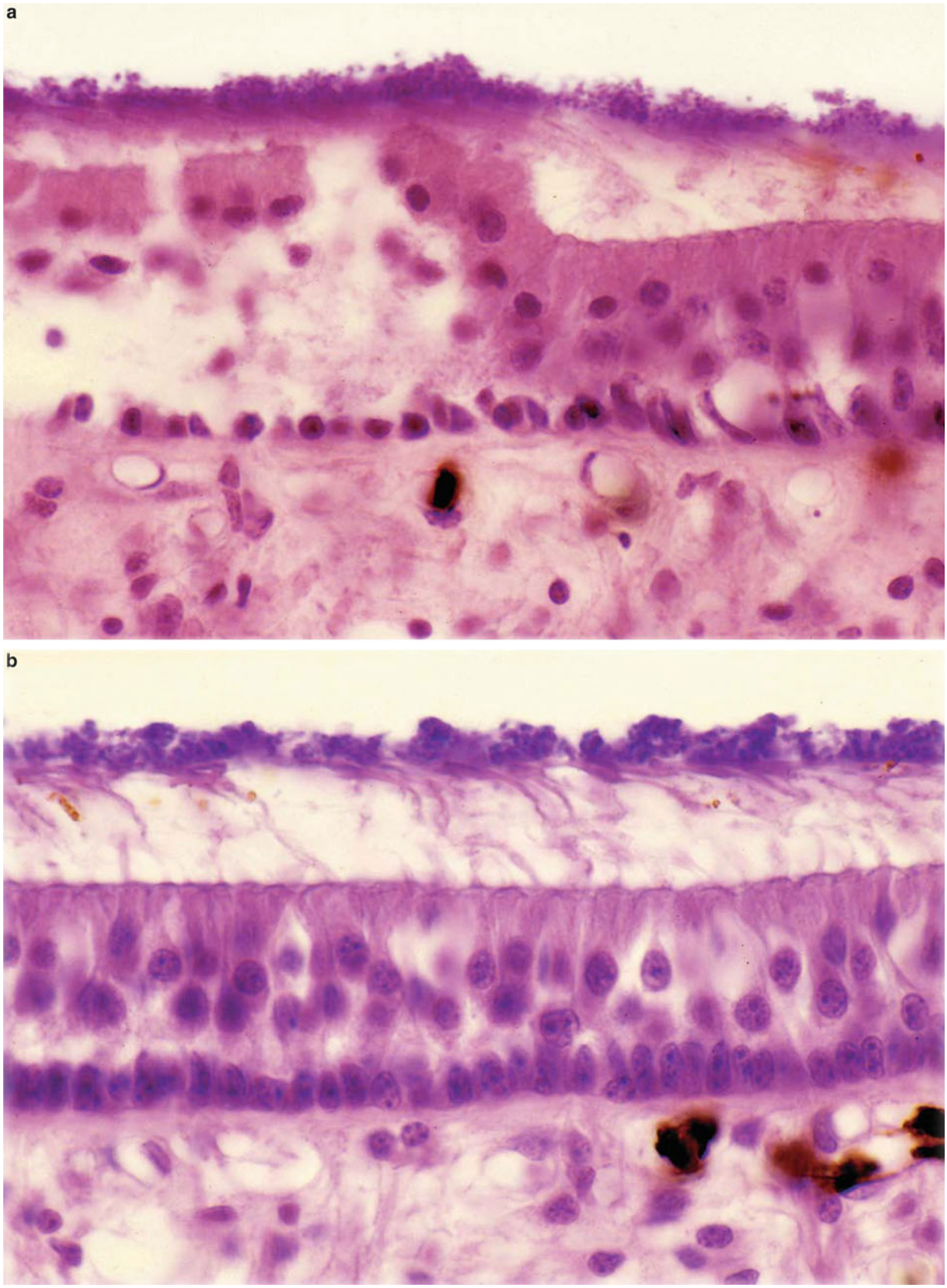

Fig. 7.20 The saccular macula immediately after irradiation (1 W × 1 s × 3 times) [14]. (**a**) Sensory cells are destroyed and elevated in an area 300 μm in diameter. Supporting cells are destroyed. The nuclei are pyknotic and remain on the basement membrane. These changes resulted from microexplosion within the sensory epithelium. The otolithic membrane is elevated. (**b**) Control: Cynomolgus monkey (original ×40)

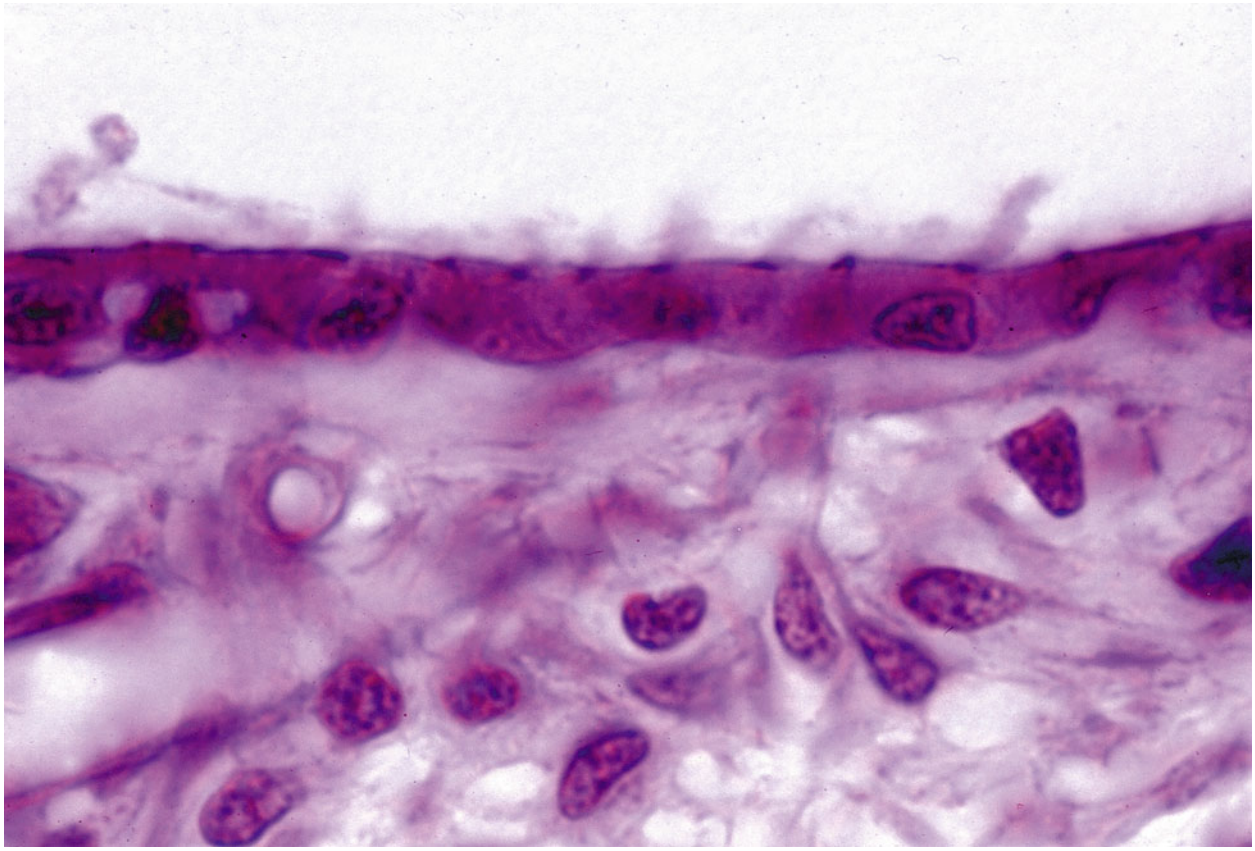

Fig. 7.21 The saccular macula 10 weeks after irradiation (1 W × 1 s). Sensory epithelia and nerve fibers have disappeared. A single layer of cells with microvilli covers the sensory epithelium. Cynomolgus monkey (original ×40)

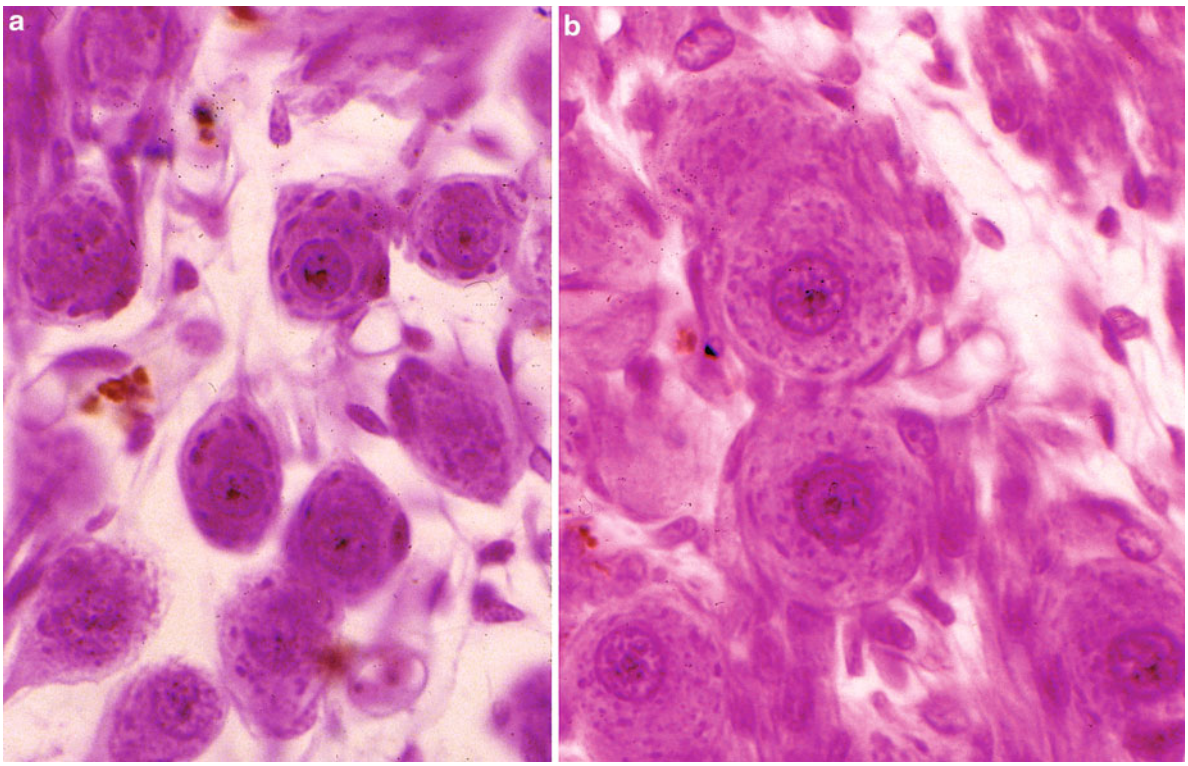

Fig. 7.22 The vestibular ganglion cells. Ten weeks after irradiation of the saccular macula. The ganglion cells are atrophic and their numbers are decreased. (**a**) Control: The ganglion cells of the opposite, non-irradiated side. Cynomolgus monkey (original ×40)

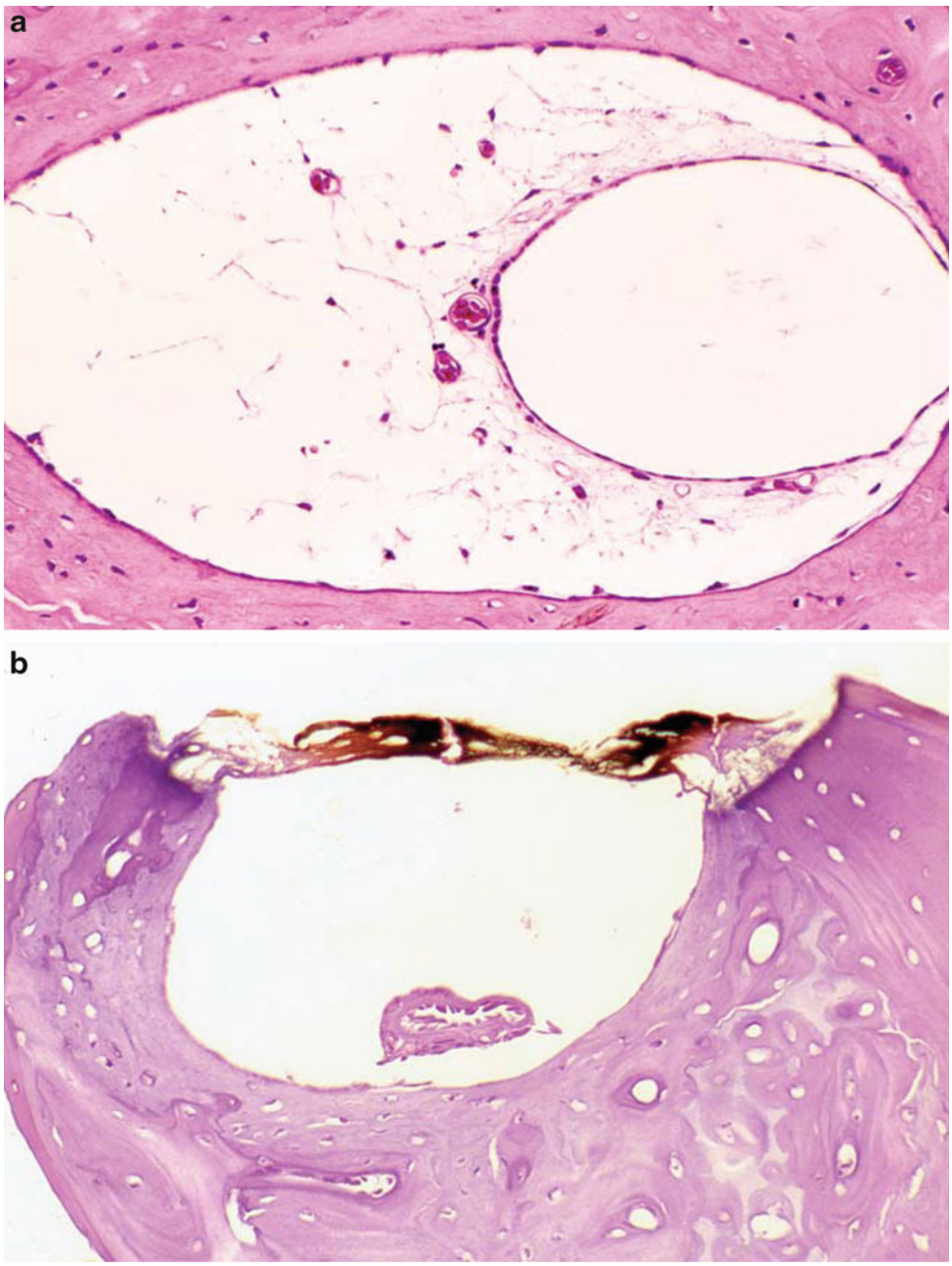

Fig. 7.23 Irradiation of the semicircular canals [16]. (**a**) Normal: The trabecular mesh is seen in the perilymphatic space. (**b**) Immediately after irradiation of the anterior canal (1 W × 0.5 s × 8 times). The bony wall is carbonized and vaporized. The semicircular duct is markedly constricted. The trabecular mesh has disappeared. Guinea pig (original ×16)

tissue to compress the semicircular duct. MRI images show evidence of occlusion.

As described in the above experiments, the semicircular canal can be completely occluded with canal wall irradiation. The same method may be applied in patients with BPPV. However, complete occlusion by ossification as we saw in guinea pigs is difficult to achieve in people. The diameter of the semicircular canal is larger in humans than in guinea pigs. The laser needs much more energy to occlude the canal. We estimated the percentage of irradiated semicircular canal that showed narrowing by ossification 16 years after laser surgery in a patient with BPPV.

The history of this patient has been previously reported [19]. Therefore, only a summary will be given here. This is the case history of a woman who was 68 years old when she visited us for the first time.

Fig. 7.24 High-power view of Fig. 7.23 [16]. (**a**) High power view of Fig. 7.23b, showing marked constriction of the semicircular duct. The basement membrane is thickened. Swollen epithelial cells have partly detached from the basement membrane. (**b**) High power view of Fig. 7.23a. Normal control: The semicircular duct is lined with an epithelial cell layer inside (original ×40)

This woman was using an ear pick to clean her left ear when her grandson bumped her, causing the ear pick to penetrate her middle and inner ear. She lost hearing in the left ear. Six months later she developed severe vertigo. With a diagnosis of BPPV, the woman was treated with argon laser irradiation of the posterior and lateral canals of the left ear to occlude the canals (Fig. 7.31). The postoperative course was uneventful. The patient noticed on the second postoperative day that her vertigo had subsided. After the procedure, she was free from vertigo for 16 years. The woman had a normal caloric response after surgery.

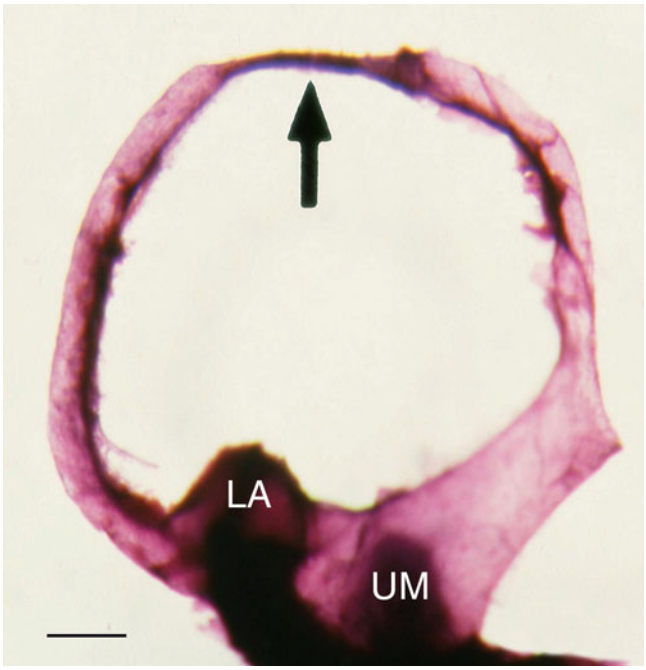

Fig. 7.25 Constriction of the lateral semicircular duct (*arrow*) [16]. Seven days after argon laser irradiation. The laser beam was applied consecutively to the lateral canal (1 W×0.5 s×5 times). *LA* lateral ampulla, *UM* utricular macula HE staining, scale: 0.5 mm. Guinea pig

With laser surgery, we attempted to occlude the semicircular canal including the duct. Occlusion of the canal takes a long time, probably weeks or months, depending on the power applied and the age of the patient.

Based on this patient's post-operative course, it is more likely that occlusion of the semicircular duct brought her relief from intractable vertigo. Unlike the canal, the duct constricts instantaneously with irradiation.

The area of the bilateral posterior canals were measured using a film of the patient CT. It was found that the size of the irradiated posterior canal was 72 % that of the non-irradiated canal. Statistical evaluation indicated that this difference was significant, assuming that the canals had been equal in size prior to irradiation [20].

This reduction in canal size is far from complete occlusion. However, perfect canal occlusion is not necessary for a good clinical outcome. Occlusion of the semicircular duct is necessary. The semicircular duct of this patient was occluded, immobilizing the endolymph. The patient was free of vertigo for 16 years after irradiation.

Based on experimental and clinical experience, one of the easiest and least traumatic surgical procedures for BPPV is laser irradiation of the semicircular canal. No opening of the canal is necessary. Heat produced by burning the canal wall constricts the duct, which degenerates, possibly becoming scar tissue. In animal experiments, we can expect complete closure of the lased canal by new bone, but this is hard to accomplish and unnecessary in clinical use.

7.3.1.1 Surgical Procedure

Irradiation of the semicircular canal is indicated for patients with intractable positional vertigo after identification of the responsible semicircular canal. Disabling vertigo other than BPPV may also be considered an indication for laser treatment.

Irradiation of the Posterior Canal

After mastoidectomy, identify the lateral and posterior canals. Using a diamond burr, clear the mastoid cells between the sigmoid sinus wall and the solid angle. It is essential to expose the blue line before irradiating the canal. The intersection between the blue line of the posterior canal and Donaldson's line is the center of the site of irradiation.

The semicircular duct adheres to the periosteum (endosteum) of the semicircular canal (Fig. 7.32). This point is the best site for irradiation because heat produced at the otic capsule will be immediately transmitted to the semicircular duct. When irradiated, the site is carbonized and a small amount of hot inner ear fluid splashes up. Irradiation of a 3 mm length along the blue line is sufficient. Several consecutive applications are needed to cover 3 mm (Fig. 7.31a). A pause of 20 s between applications prevents the temperature in the inner ear from rising excessively. Do not remove the carbonized portion. A piece of fascia is placed over the irradiated area.

Irradiation of the Lateral Canal

The irradiation site for the lateral canal is as far from the lateral ampulla as possible (Fig. 7.31). The site should be far from the course of the facial nerve and from the crista ampullaris. The semicircular duct is located at the outer circumference of the canal (Fig. 7.33). This means that the blue line to be irradiated is at the outermost part of the canal. After irradiation, a piece of fascia is used to cover the irradiated area without cleaning the bony surface.

7.3.2 Irradiation of the Otolithic Organ

7.3.2.1 Susceptibility of the Human Utricular Wall

The utricular wall consists of two cell layers. The epithelial cell layer faces the endolymph, and the mesothelial cell layer faces the perilymph. Argon laser beams pass through the utricular wall without causing damage except in the sensory

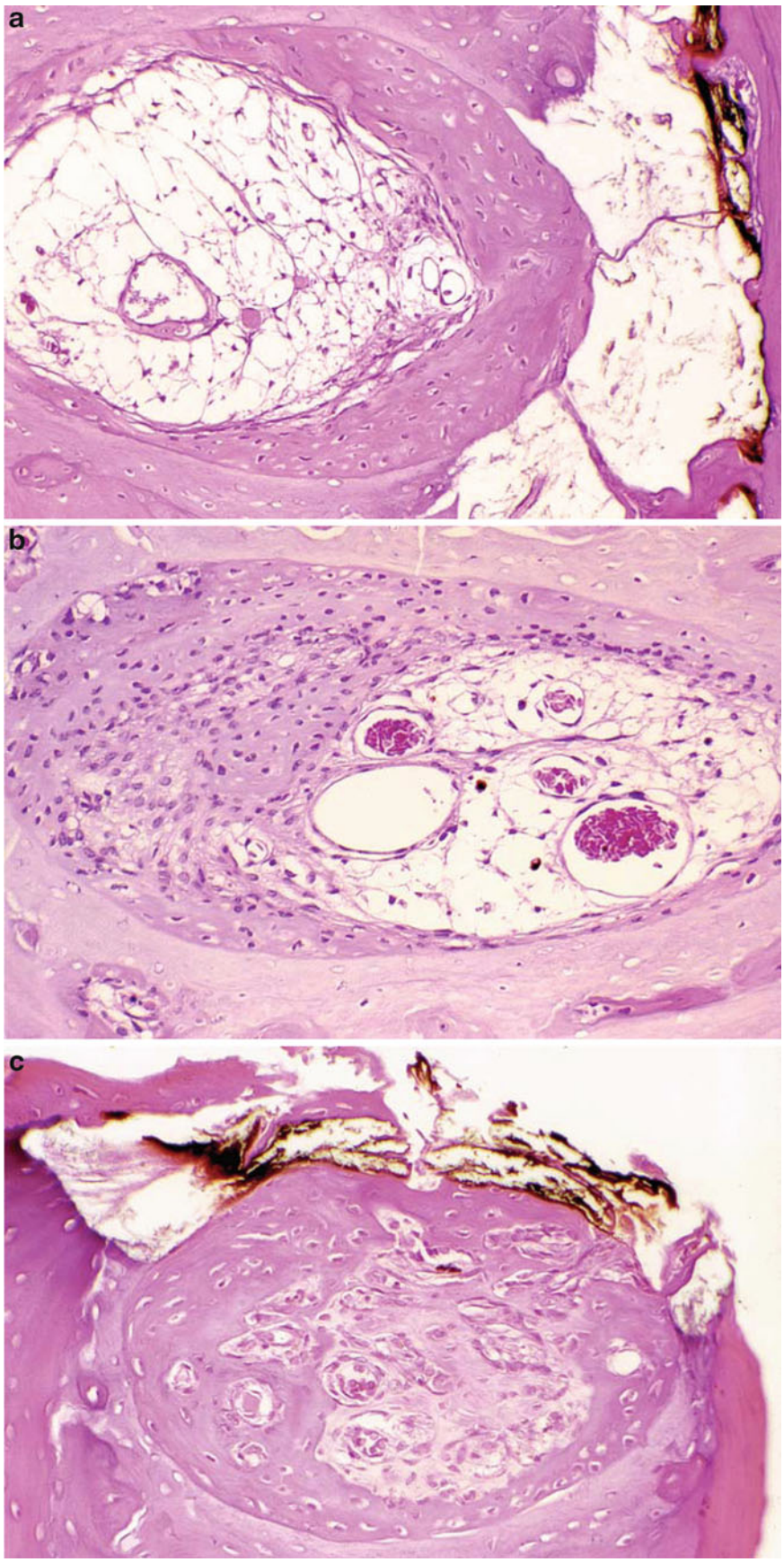

Fig. 7.26 Irradiation of semicircular canals. (**a**) Seven weeks after irradiation (1 W × 0.5 s × 5 times). New bone formation and marked fibrosis are seen in the canal. The area beneath the charred region is vaporized. The semicircular duct is constricted. (**b**) Five weeks after irradiation (1 W × 0.5 s × 4 times). Half of the canal is ossified, the other half is fibrotic. (**c**) Five weeks after irradiation (1 W × 0.5 s × 2 times). The canal is completely occluded by new bone (original ×16)

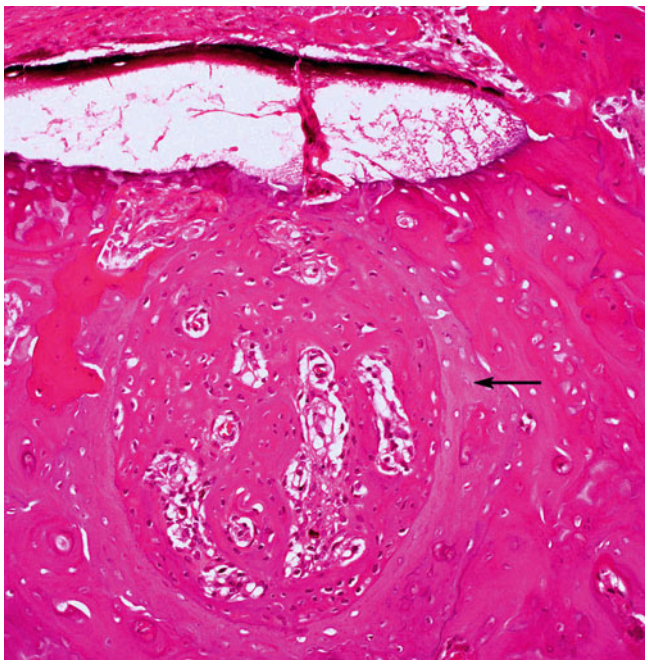

Fig. 7.27 Completely ossified posterior canal (*arrow*). Quite often vascular strands connect the outside and inside of the irradiated site through the charred and vaporized area. Adjacent to the medial part of the carbonized and vaporized area the repair process is underway. Thirty-five days after irradiation (1 W×0.5 s×6 times). Guinea pig (original ×10)

epithelium and dark cell area. The former is the most vulnerable to the argon laser but can be destroyed without perforating the utricular wall. The latter is easily destroyed, resulting in wall perforation (Fig. 7.34).

7.3.2.2 Susceptibility of the Human Saccular Wall

Unlike the utricular wall, the saccular wall has no dark cell areas. However, the human saccular wall, particularly in elderly patients, contains pigment granules (Fig. 7.35).

To determine the properties of these granules, Nakamura et al. [21] performed histochemical studies on the human saccular wall.

The saccular walls from 20 temporal bones were examined. The bones came from individuals ranging in age from 52 to 91 years (average, 82.7 years). Nine staining methods were employed, and results from the following four methods are described here:

1. Nile blue staining (Lillie), blue
2. Nile blue staining after acetone extraction, brown
3. PAS staining, red
4. Ziehl-Neelsen staining, red

The results revealed that the granules were lipofuscin, not melanin. The granules were relatively large and were distributed mainly in the epithelial cell layer of the saccular wall. In the mesothelial cells, lipofuscin granules were present, but were very small in size and few in number. No granules were found in the connective tissue of the reinforced area (Fig. 7.36).

The saccular walls of the elderly patients (71–91 years old) had more lipofuscin granules than those of a younger patient (52 years old). The granules did not contain melanin.

Transmission electron microscopy showed granules varying in size from 0.2 to 2.5 μm aggregated in the epithelial cells. The granule interior was amorphous. Electron density was low in the central area compared to the marginal area. No melanocytes or melanosomes were observed.

Because of the presence of these lipofuscin granules, care should be taken not to irradiate the saccular macula of elderly people. The granules are distributed throughout the saccular wall, including in the reinforced area. Argon laser irradiation will cause rupture of the saccular wall in these individuals. The saccular wall shows sieve-like perforations (Fig. 7.37), whereas the dark cell area has a large perforation [11, 21]. The difference in the size of the perforations is mainly due to differences in the density of melanin or lipofuscin. Perforation of the saccular wall will cause hearing impairment with or without formation of cochlear hydrops [22].

Temperature Change in the Vestibule after Irradiation

Nomura et al. [11] measured the temperature elevation in the vestibule using a thermocouple probe (copper-constantan) placed close to the site of irradiation of the utricular macula. When an argon laser (1.5 W×0.5 s) was used to irradiate the utricular macula within a human temporal bone that was kept in a basin of saline, the temperature within the saline-filled vestibule rose 6 °C, from 36 °C to 42 °C. The temperature gradually returned to 36 °C over 20 s. Continuous laser application increased the temperature in the vestibule. In this experiment, ten continuous applications caused an elevation of 20 °C. Approximately 50 s were required for the temperature to return to baseline (Fig. 7.38).

7.3.3 Surgical Procedure

7.3.3.1 Irradiation of the Utricular Macula

After stapedectomy, the laser hand probe is introduced into the vestibule and advanced to the utricular macula, which may be visualized as a white plaque in the superior portion (Fig. 7.39). It is important not to touch the area of the utricular macula. Because nerve fibers originate from the base to fan out beneath the sensory epithelia, an irradiation site near the base is preferable. When suction is needed in the vestibule and around the oval window, care should be taken not to dry out the vestibule.

After lasing, the oval window is sealed and a stapes prosthesis is anchored.

The optimum laser power for this procedure has not been established and may vary depending on the distance from the tip of the laser probe to the target, the target site, and number of applications. Laser powers of 1.0 W [23] and 3.5 W [6] have been reported.

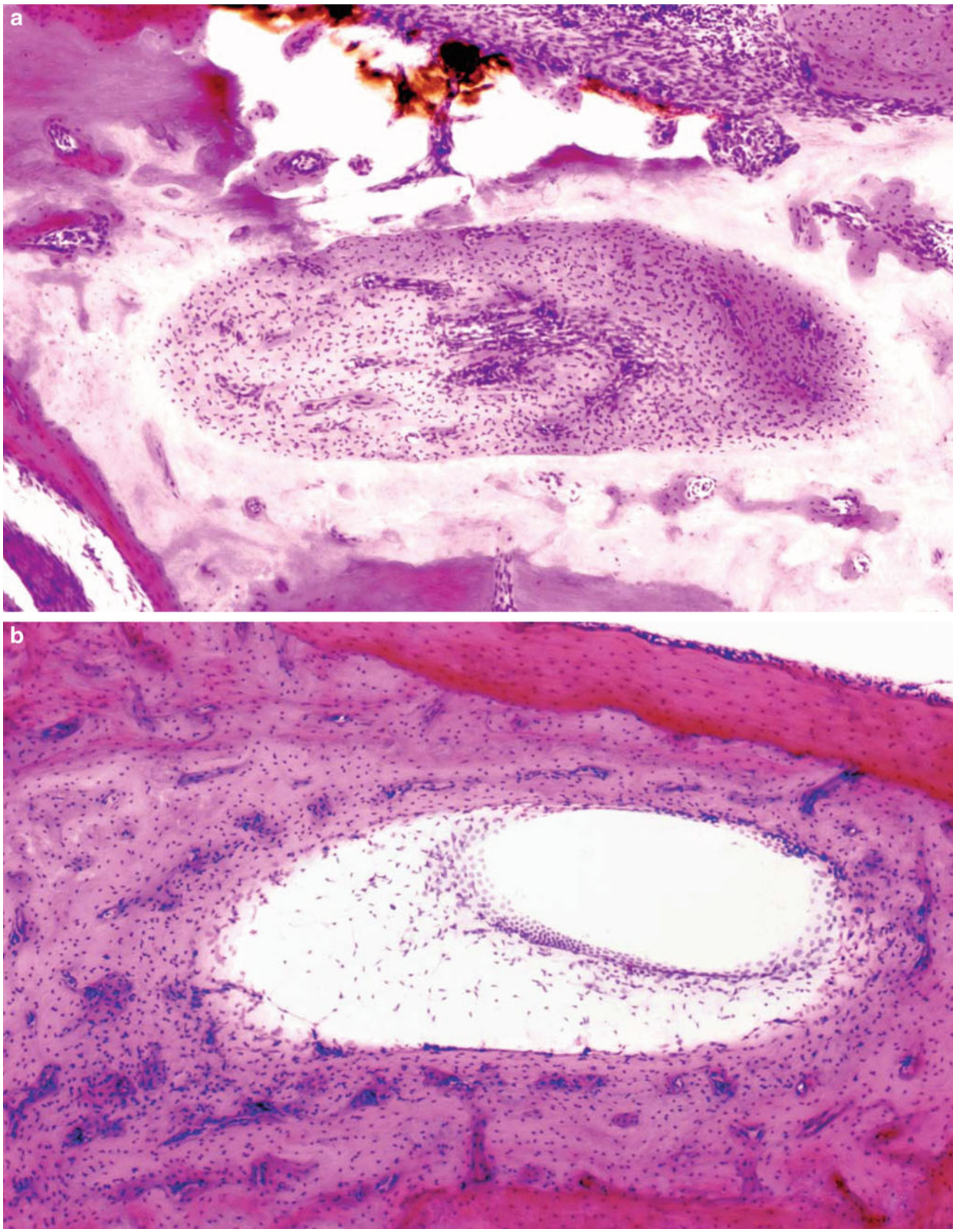

Fig. 7.28 Irradiation of the lateral canal [18]. (**a**) Forty-three days after irradiation (1 W × 0.5 s × 15 times). The canal is completely ossified. The vaporized area is seen nearby. No caloric response was observed with irrigation of 5 mL of ice water to the ear canal of the irradiated side. (**b**) Control: This ear showed a good caloric response (original ×6.5)

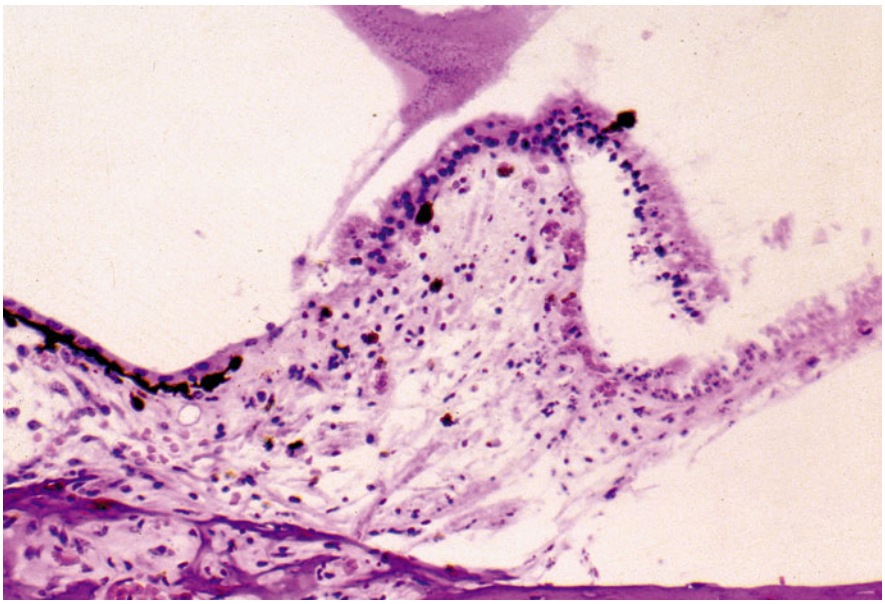

Fig. 7.29 Irradiation of the lateral ampulla. Ten days after irradiation (1 W×0.5 s×3 times). Destroyed epithelium has partly detached from the crista (original ×16)

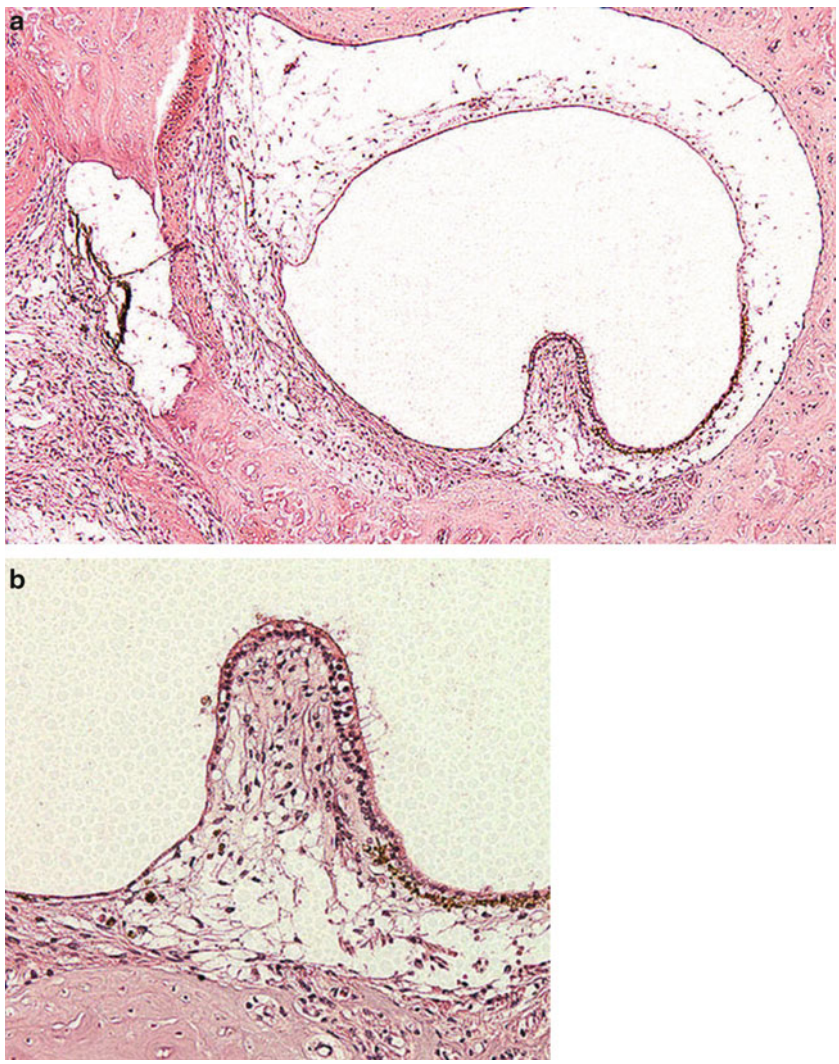

Fig. 7.30 Irradiation of the posterior ampulla. (**a**) Thirty days after irradiation (1 W×0.5 s×5 times). The irradiated side of the sensory epithelium shows more severe damage than the opposite side. Nerve fibers are completely missing. The transitional area and dark cell area have disappeared completely (original ×2.5). (**b**) High power view of the irradiated crista ampullaris shown in (**a**), (original ×6.5)

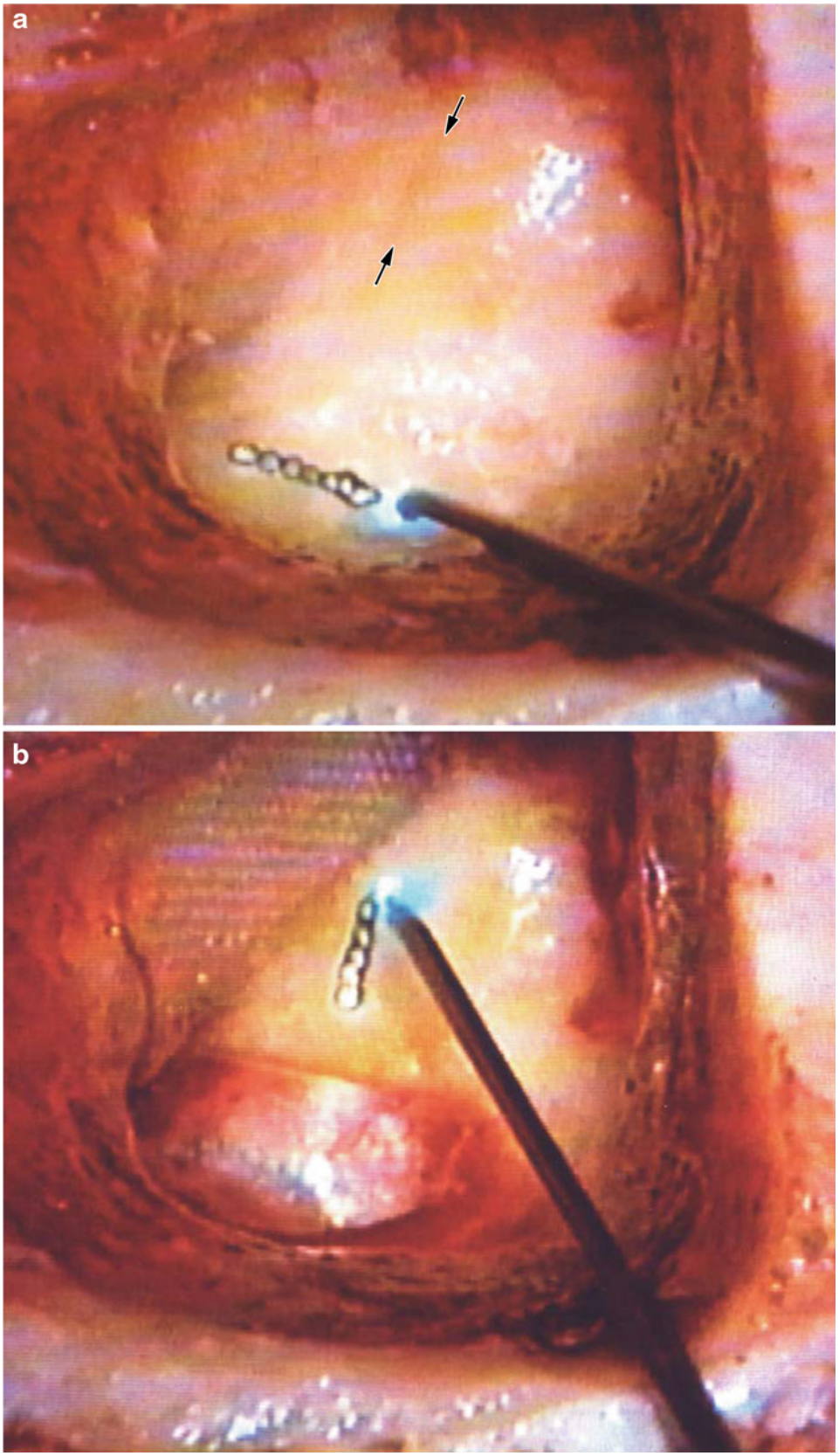

Fig. 7.31 Laser irradiation of posterior and lateral canals of a patient with traumatic benign paroxysmal positional vertigo [19]. (**a**) The left mastoid cavity is widely open. Seven laser applications (1.5 W × 0.5 s each) were administered to the left posterior canal. The guide light was blue. The *blue line* of the lateral canal is indicated between *arrows*. (**b**) The probe approaches the lateral canal *blue line* for irradiation. The irradiated posterior canal was covered by fascia

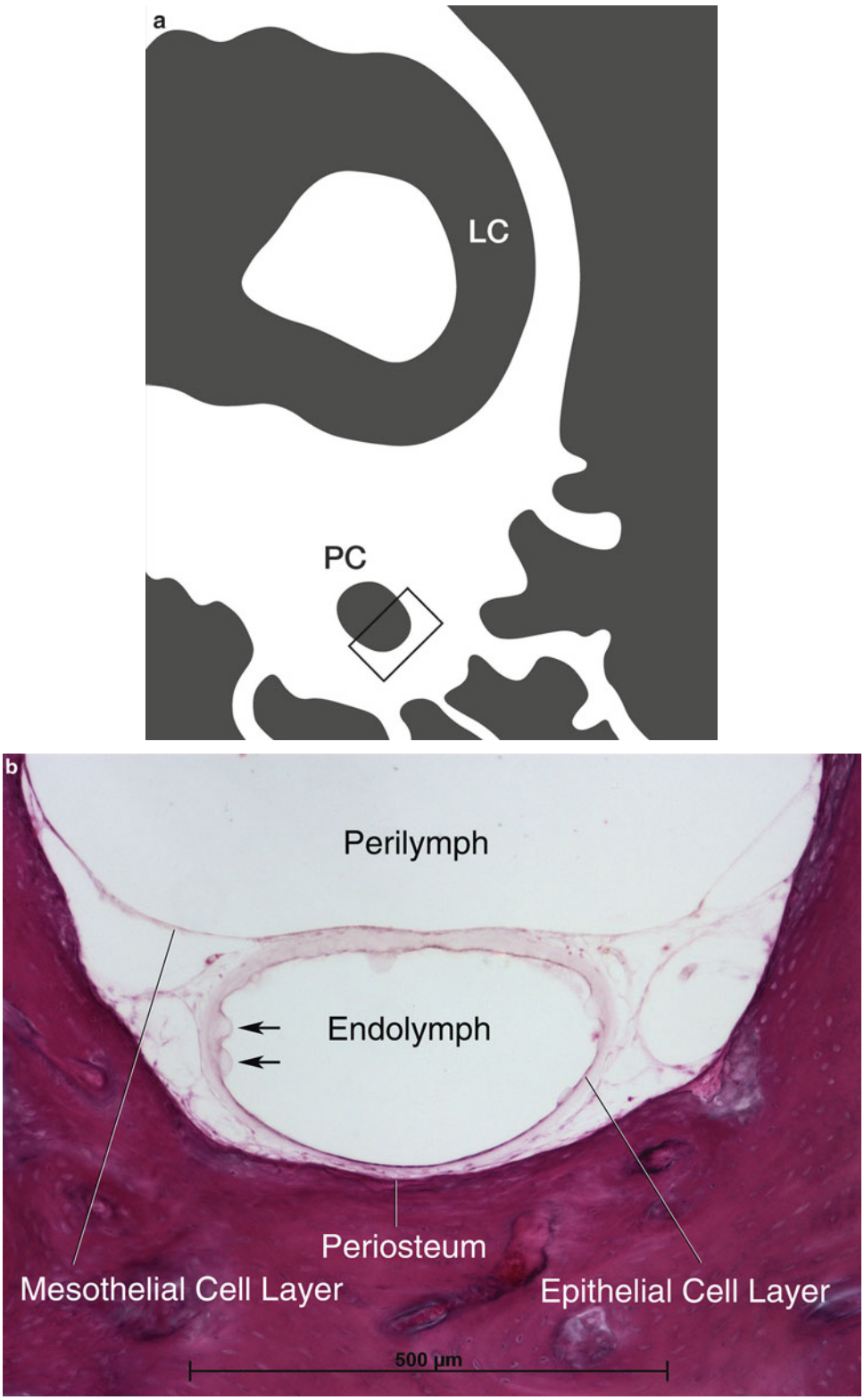

Fig. 7.32 Cross section of the human posterior canal and duct. (**a**) A schema showing a CT image including the lateral and posterior canals. *LC* lateral canal, *PC* posterior canal. (**b**) High power view of the *inset* in (**a**). The semicircular duct adheres to the periosteum (endosteum). *Arrows*: vesiculation

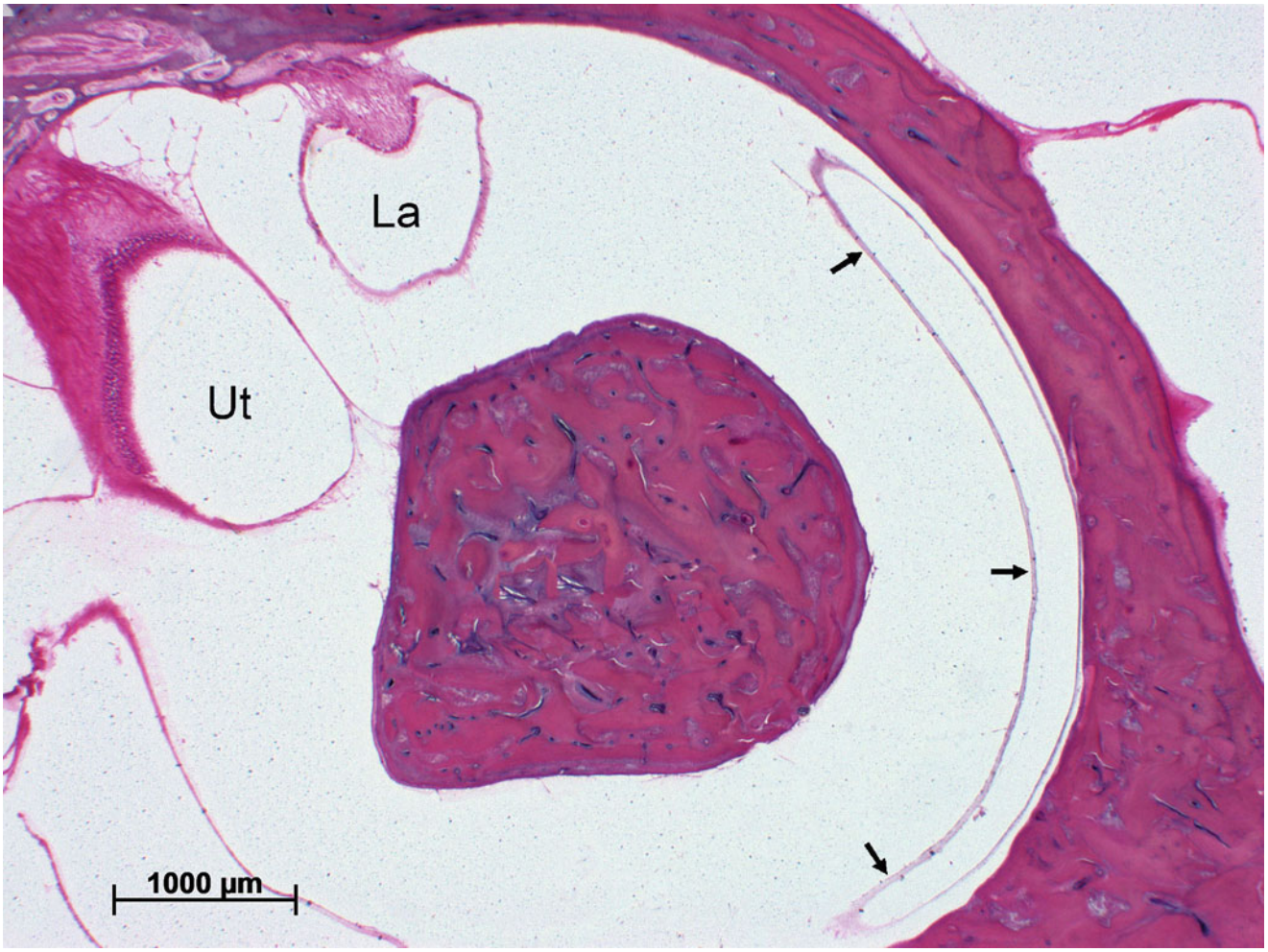

Fig. 7.33 The lateral semicircular canal and duct in a human temporal bone specimen. *Arrows* indicate the semicircular duct. It adheres to the periosteum (endosteum) of the outer circumference of the canal. *Ut* utricle, *La* lateral ampulla (original ×1)

7.3.3.2 Case Presentation [23]

A 51-year-old woman presented to our hospital in March 1981, complaining of vertigo and a sensation of deviation while walking. Four months earlier, she had tripped and struck the left part of her forehead without loss of consciousness. Nine hours after her fall, the woman had developed clock-wise vertigo of 30 min' duration with vomiting.

On examination, the patient's eardrums were normal. The pure tone average of the right ear was 25.0 dB of sensorineural hearing loss, and that of the left ear was 8.3 dB. Caloric testing showed normal values in both ears. Spontaneous, positional, and positioning nystagmus were not observed. No sign or symptoms of fistula were present. In June 1982, the patient felt unsteady. Hearing loss of 68.3 dB in the right ear with positive Metz test and a score of 100 % on the SISI test were noted. Eustachian tube catheterization of the right ear made the patient dizzy. Exploratory tympanotomy was performed with a suspected diagnosis of perilymphatic fistula of the right ear. A fistula was found in the lower margin of the annular ligament and was treated by covering the defect with a small piece of fascia. The patient's hearing improved by about 20 dB, and her sensations of ear fullness and dizziness improved.

In October 1985, the patient noticed vertigo when positioned with her right ear inferiorly. In May 1991, the patient's vertigo became disabling. Labyrinthine pathology associated with the perilymphatic fistula seemed to have progressed, leading to a "floating" labyrinth (Fig. 2.33). Partial laser labyrinthectomy consisting of singular neurectomy, utricular macula ablation, and irradiation of the utriculoampullary nerve going to the anterior and lateral ampullae was attempted.

Utricular macula ablation was performed using argon laser (1.0 W×0.5 s×15 times) after stapedectomy (Figs. 7.40 and 7.41). The saccular macula was not irradiated. After irradiation, the oval window was sealed using tragal perichondrium. A Teflon piston (0.6×4 mm) was

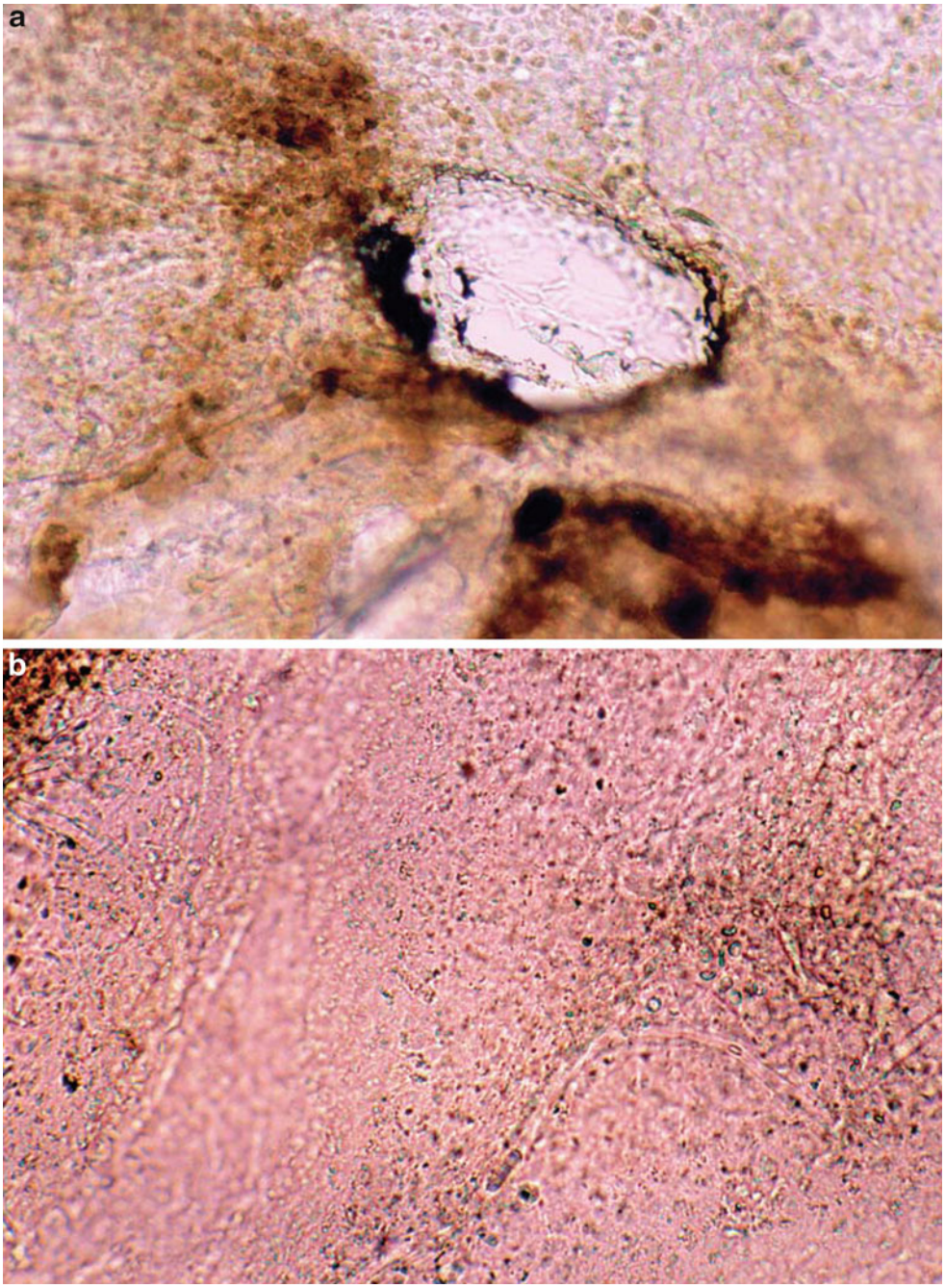

Fig. 7.34 Argon laser irradiation of the utricular wall. (**a**) The dark cell area shows perforation by irradiation (1.5 W × 0.5 s). (**b**) The laser beam penetrated the utricular wall without causing any damage. Immediately after irradiation. Human (original ×16)

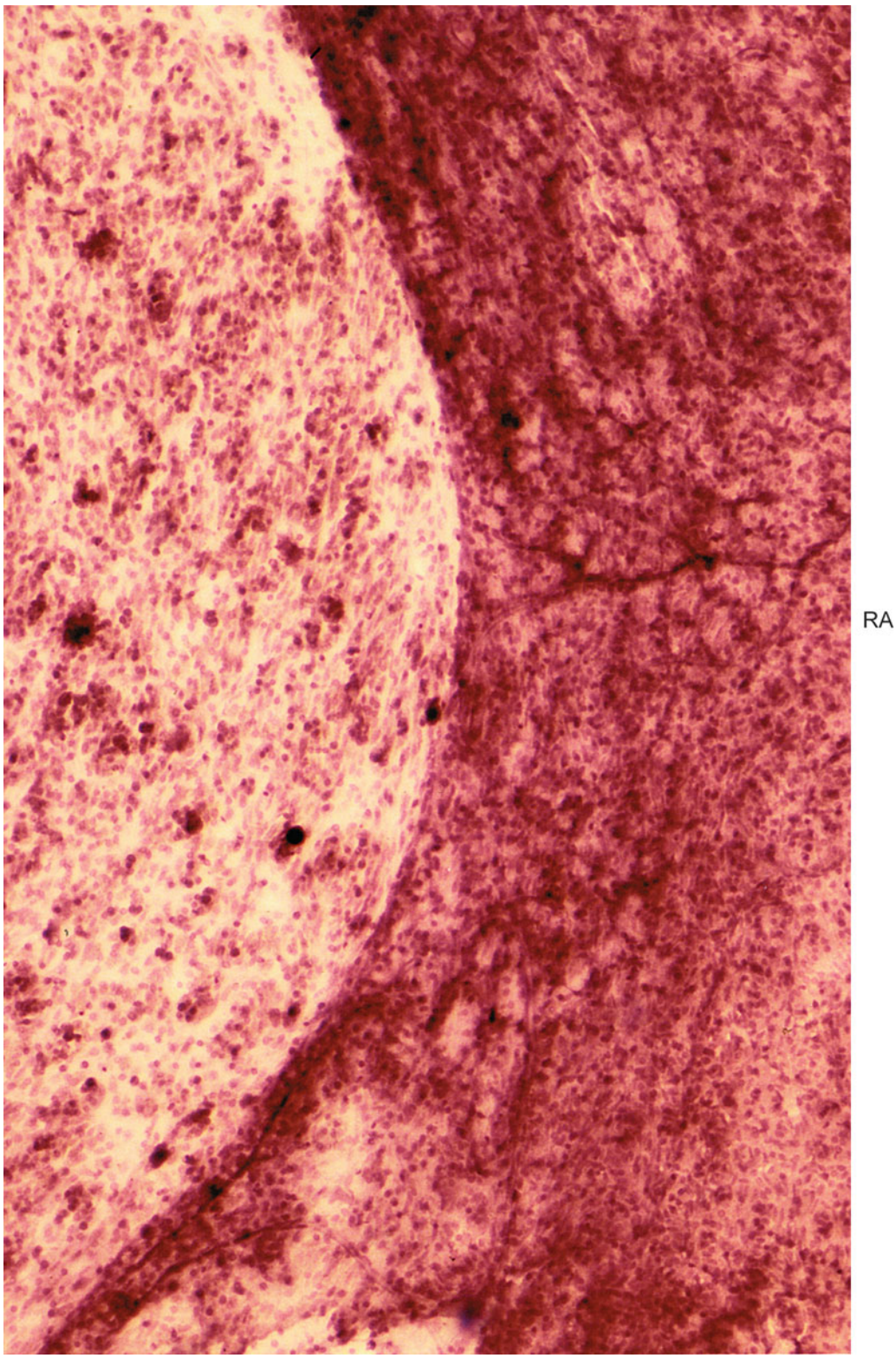

Fig. 7.35 The human saccular wall. There are many lipofuscin granules throughout the saccular wall. *RA* reinforced area. Surface preparation (original ×100)

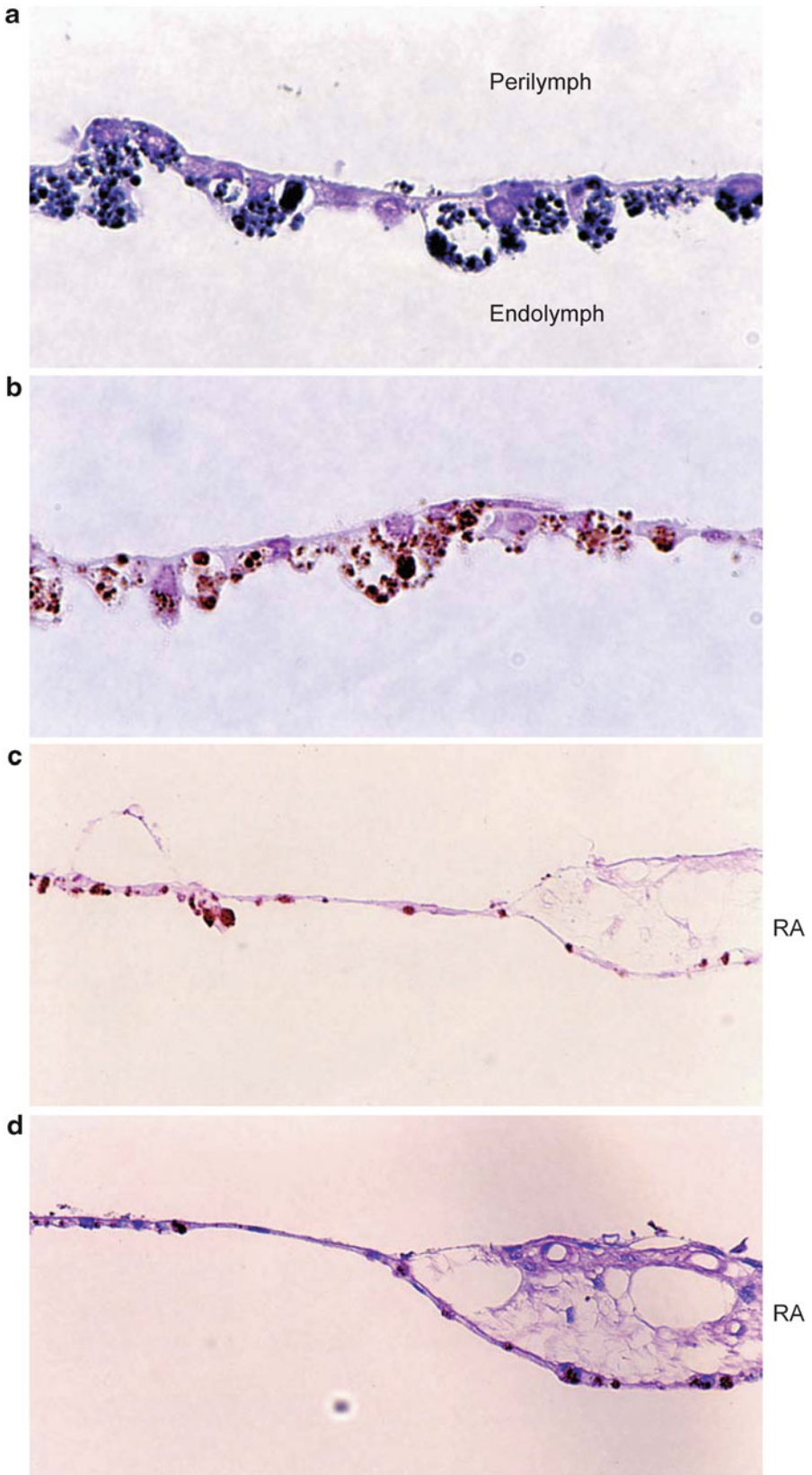

Fig. 7.36 Histochemical staining of the saccular wall [21]. (**a**) Nile blue staining (Lillie's method). Granules are stained blue. (**b**) Nile blue staining after extraction with acetone. Granules are stained yellowish-brown. (**c**) PAS staining. Granules are stained red-purple. (**d**) Ziehl–Neelsen staining, positive stains pale red. *RA* reinforced area. The epithelial cell layer (facing the endolymph) contains lipofuscin granules. Human; (**a**), (**b**): ×250; (**c**), (**d**): ×100

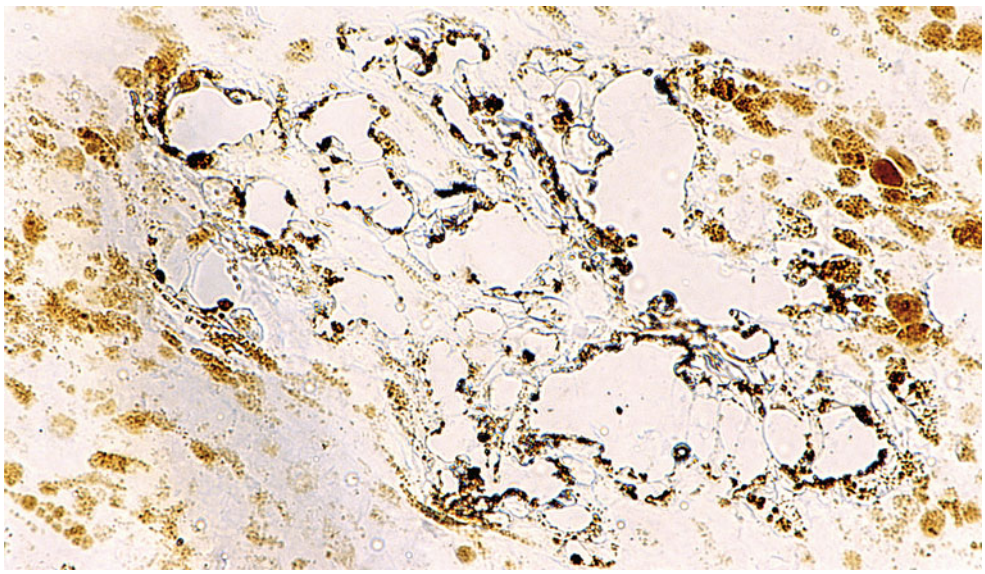

Fig. 7.37 Laser irradiation of the saccular wall with lipofuscin granules [21]. Perforations were induced by laser irradiation of the lipofuscin granules. 1.5 W×0.5 s, human, ×200

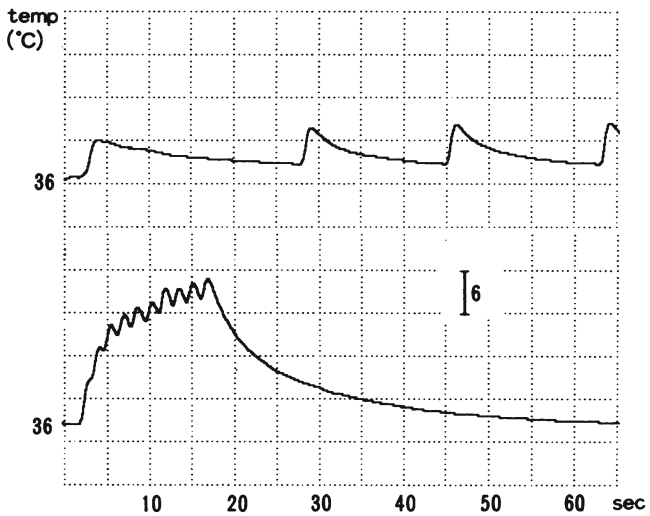

Fig. 7.38 Measurements of temperature change in the human vestibule [11]. A thermocouple was placed 1 mm from the site of laser application. The hand probe was 1 mm from the posterior aspect of the utricular macula. *Upper*: A single application (1.5 W×0.5 s) with a pause raised the temperature 6 °C each time *Lower*: Ten continuous applications cause a marked temperature increase of 20 °C

Fig. 7.39 A composite showing lasing of the utricular macula. The tip of the probe is in the vestibule and irradiates the utricular macula. *UM* utricular macula, *SA* saccule

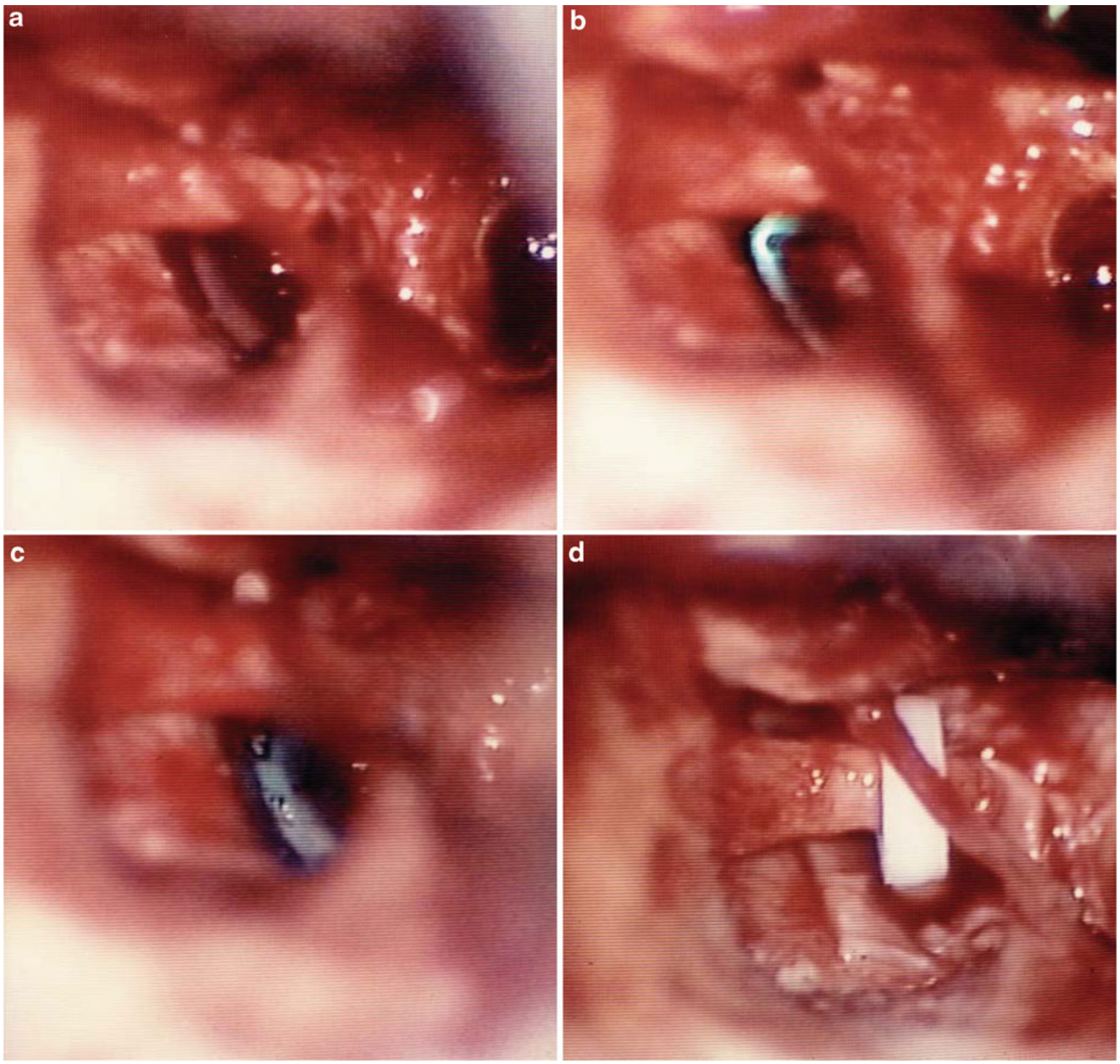

Fig. 7.40 Ablation of the utricular macula. Photographs were captured from video [23]. (**a**) The stapes is removed from the oval window. The white plaque is the utricular macula. (**b**) A laser hand probe approaches the utricular macula. *Blue color* is the guide light of the laser system. (**c**) Several irradiated spots are seen in the utricular macula area. (**d**) The oval window is sealed with perichondrium. A Teflon piston is anchored to the long process of the incus

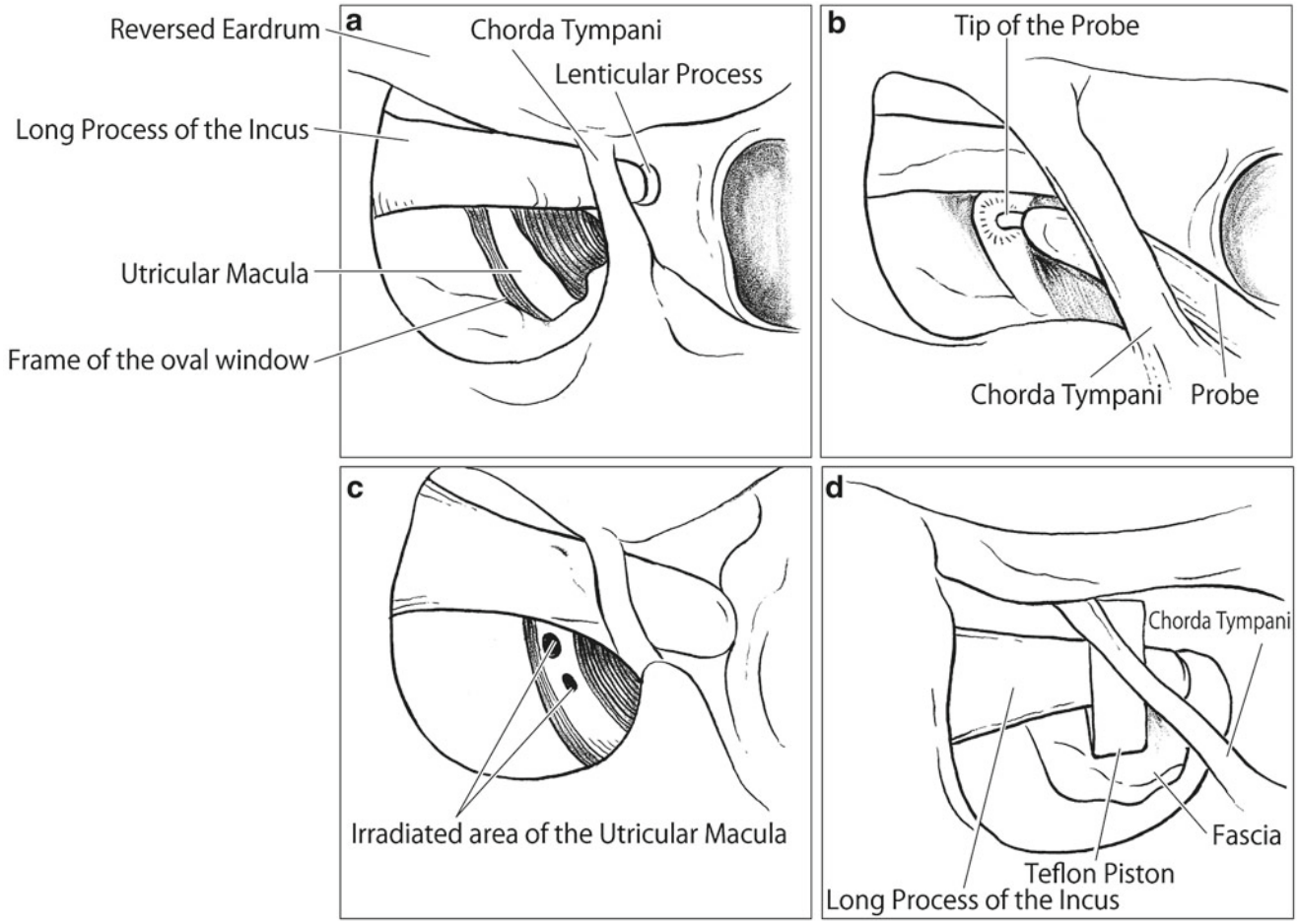

Fig. 7.41 Explanation of Fig. 7.40

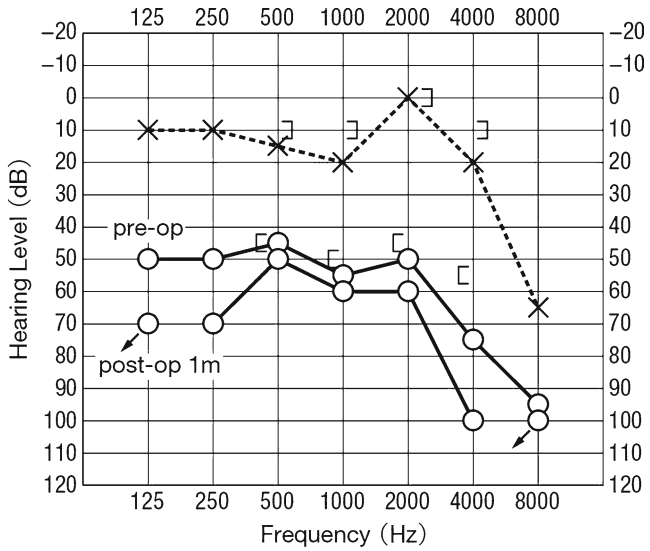

Fig. 7.42 Audiograms taken before and 1 month after laser surgery [23]

used to connect the long process of the incus with the perichondrium. One month after surgery, the patient's hearing had almost recovered to the pre-operative level (Fig. 7.42). She had no further positional vertigo or vertiginous attacks, and she was able to move quickly and rotate her head without symptoms.

References

1. Stahle J, Högberg L (1965) Laser and the labyrinth. Some preliminary experiments on pigeons. Acta Otolaryngol 60:367–374
2. Stahle J, Högberg L, Engström B (1972) The laser as a tool in inner ear surgery. Acta Otolaryngol 73:27–37
3. Wilpizeski C, Sataloff J, Doyle C, Leonard J, Behrendt T (1972) Selective vestibular ablation in monkeys by laser irradiation. Laryngoscope 82:1045–1058
4. Wilpizeski CR (1981) Feasibility of lasers for performing otologic surgery. Laryngoscope 91:834–837
5. Anthony PF (1991) Partitioning of the labyrinth: application in benign paroxysmal positional vertigo. Am J Otol 12:388–393
6. Anthony PF (1996) Utricular macular ablation for benign paroxysmal positional vertigo. Ear Nose Throat J 75:416–421
7. Namba G, Nomura Y (1997) Morphological effects of laser irradiation on the cochlea. Showa Univ J Med Sci 9:25–32
8. Nomura Y, Hara M, Okuno T (1988) Application of argon laser to the inner ear. Acta Otolaryngol (Stockh) 105:439–444
9. Ocho S, Iwasaki S, Umemura K, Hoshino T (2000) A new model for investigating hair cell degeneration in the guinea pig following damage of the stria vascularis using a photochemical reaction. Eur Arch Otorhinolaryngol 257:182–187
10. Hoshino T (1999) Morphology and function of localized strial lesion in the cochlea. Tokyo-Igakusha, Tokyo
11. Nomura Y, Okuno T, Young Y-H, Hara M (1991) Laser labyrinthectomy in humans. Acta Otolaryngol (Stockh) 111:319–326
12. Okuno T, Nomura Y, Young Y-H (1991) Ablation of otolithic organs with argon laser. Acta Otolaryngol 481(Suppl):607–609
13. Okuno T, Nomura Y, Young Y-H, Hara M (1990) Argon laser irradiation of the otolithic organ. Otolaryngol Head Neck Surg 103:926–930
14. Okuno T, Nomura Y, Hara M (1988) Partial labyrinthectomy with argon laser. Acta Otolaryngol 456(Suppl):111–116
15. Okuno T, Nomura Y, Hara M, Young Y-H (1991) Histological changes of the utricular otolith after laser irradiation. Otol Jpn 1:60
16. Nomura Y, Ooki S, Kukita N, Young Y-H (1995) Laser labyrinthectomy. Acta Otolaryngol (Stockh) 115:158–161
17. Oki S, Nomura Y, Sugio Y, Young Y-H (1996) Occlusion of the semicircular canal using argon laser. J Clin Laser Med Surg 14:393–398
18. Sugio Y, Nomura Y, Oki S (1997) Argon laser irradiation to the semicircular canal. Laryngoscope 107:1107–1111
19. Nomura Y (2002) Argon laser irradiation of the semicircular canal in two patients with benign paroxysmal positional vertigo. J Laryngol Otol 116:723–725
20. Nomura Y, Kobayashi H (2012) Laser irradiation of the semicircular canal: occlusion of the canal or duct. Acta Otolaryngol 132:106–111
21. Nakamura M, Nomura Y, Suzaki H (2000) Study of the characteristics of pigments and laser permeability of the human saccular wall. Showa Univ J Med Sci 60:285–294
22. Nomura Y, Hara M, Funai H, Okuno T (1987) Endolymphatic hydrops in perilymphatic fistula. Acta Otolaryngol (Stockh) 103:469–476
23. Nomura Y, Okuno T, Hara M, Young Y-H (1992) "Floating" labyrinth. Pathophysiology and treatment of perilymph fistula. Acta Otolaryngol (Stockh) 112:186–191

Presbycusis

8

Abstract

Presbycusis occurs mainly as a result of aging of the cochlea and the central auditory system. This chapter presents observations made using unconventional techniques to evaluate the nerve fibers in the organ of Corti, the basilar membrane, the stereocilia of the outer hair cells, and the stria vascularis in elderly people. Stained surface preparations of nerve fibers in the organ of Corti and the osseous spiral lamina were observed. Afferent and efferent nerve fibers were reduced in number in the lower basal turn in the elderly. Swellings of the efferent nerve fibers crossing the tunnel of Corti were occasionally observed. These swellings resembled the torpedoes seen in Purkinje cell degeneration. The medial fiber is considered an efferent fiber, and sometimes extends laterally beyond the outer hair cell area.

The stereocilia of the outer hair cells showed various types of degeneration with aging. Loss of individual hairs, fusion of several hairs, and giant cilia were common findings. After complete disappearance of the stereocilia, the surface of the cuticular plate showed remnants of equally-sized stumps, suggesting the breaking point of each hair.

In strial atrophy, the cells composing the stria vascularis disappeared with the strial capillaries. The basilar membrane of elderly people showed lipid deposits in the basal turn. These deposits were composed of neutral fat and cholesterol and were located along the filaments of the pars pectinata. As for prevention of presbycusis, an animal experiment revealed that caloric restriction prevented the age-related loss of spiral ganglion cells.

Keywords

Aging • Basilar membrane • Caloric restriction • Cochlea • Nerve fiber • Organ of Corti • Stereocilia • Strial atrophy

8.1 Nerve Fibers in the Osseous Spiral Lamina

The axons of the spiral ganglion cells leave Rosenthal's canal, and join at the central bony axis, the modiolus, to form the cochlear nerve. The dendrites of the spiral ganglion cells pass between the upper and lower shelves of the osseous spiral lamina as they head toward the organ of Corti. Near the end of the spiral lamina are small foramina called habenula perforata, through which unmyelinated nerve fibers pass to the inner and outer hair cells.

In young people, the cochlea contains abundant nerve fibers leaving Rosenthal's canal, their bundles gradually fanning out radially in the osseous spiral lamina (Fig. 8.1). Spiral fibers intermingle with the radial fibers in the osseous spiral lamina.

In elderly people, the cochlea shows loss of radial and spiral fibers, particularly in the lower basal turn, with less loss toward the apex (Fig. 8.2).

Histochemical staining for acetylcholinesterase specifically stains the efferent nerve fibers, leaving the afferent fibers unstained. From spiral bundles, fibers radiate outward, eventually terminating primarily on the outer hair cells. In the organ of Corti, the outer spiral bundle shows acetylcholinesterase activity, though postmortem autolysis may obscure details (Fig. 8.3a, b) [1, 2]. In the lower basal turn of a 59-year-old man, most of the afferent and efferent nerve

Y. Nomura, *Morphological Aspects of Inner Ear Disease*, DOI 10.1007/978-4-431-54204-9_8,

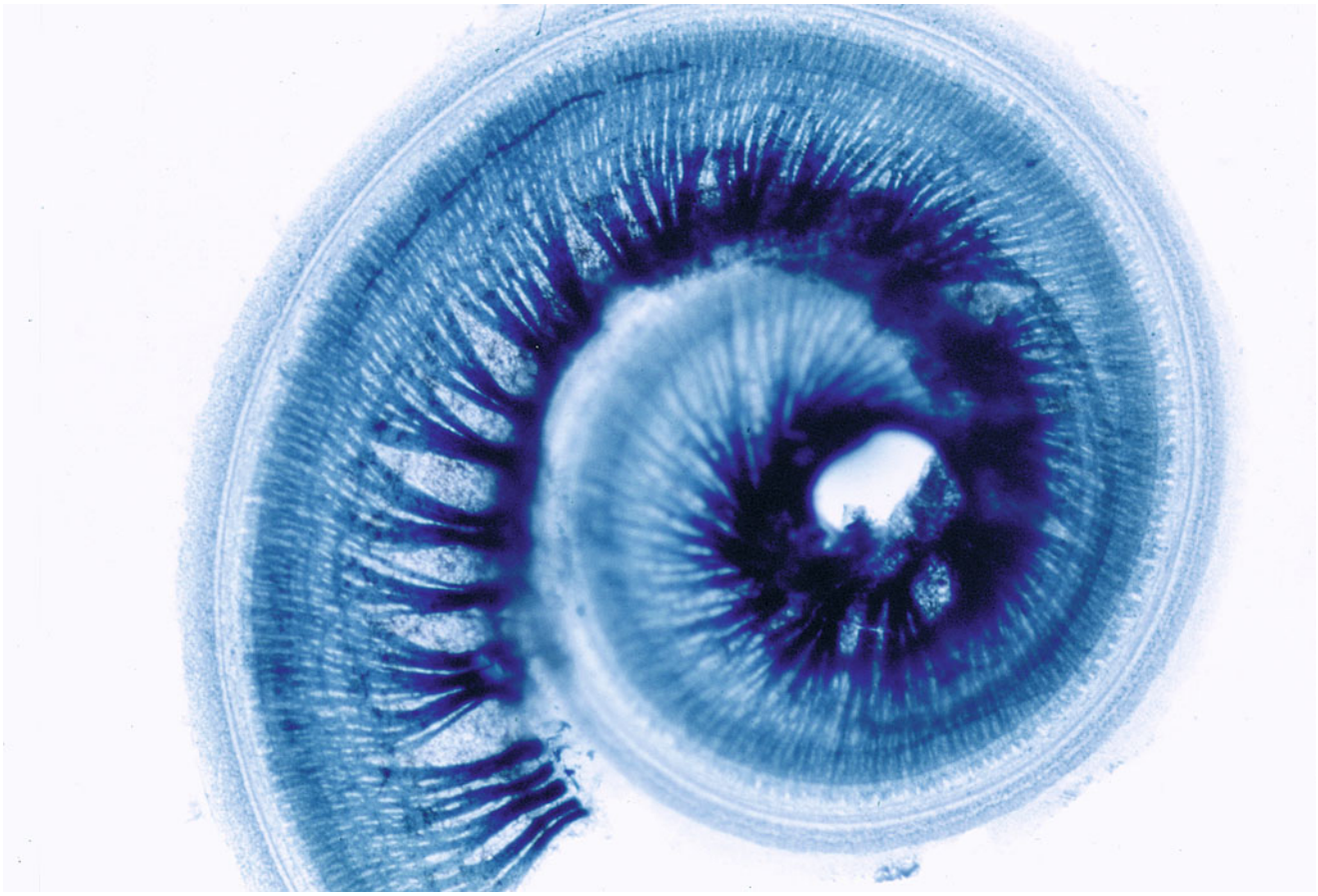

Fig. 8.1 Myelinated nerve fibers of the human cochlea. The organ of Corti is at the periphery of the specimen. Sudan Black B staining

fibers had disappeared, with only a few fibers remaining (Fig. 8.3c). The course of the afferent fibers was relatively simple. By contrast, the efferent fibers followed a complicated course (Fig. 8.4). No efferent fibers were seen in the osseous spiral lamina of the cochlea (Fig. 8.5). Clinical data were not available for this individual.

Gacek [3] reported a case in which the cochlea showed only efferent fibers.

8.2 Nerve Fibers in the Organ of Corti

It is difficult to follow nerve fibers in the organ of Corti in serial temporal bone specimens. However, they are easier to follow in properly stained surface specimens of the cochlea. When observed as a surface preparation, the tunnel of Corti is seen as a wide, clear belt because of its sparse cellularity. Individual nerve fibers can be clearly observed here (Figs. 8.6 and 8.7). The medial fiber and basilar fiber cross the tunnel of Corti. The medial fiber crosses the medial part of the tunnel, and is the efferent fiber [4]. The basilar fiber crosses the tunnel at its base and is the afferent fiber (Fig. 1.19).

According to Spoendlin [5], 90 % of the afferent fibers in the cat terminate on the inner hair cells, while 10 % terminate on the outer hair cells.

A similar finding was observed in a human organ of Corti, where only the basilar fiber was observed in the tunnel of Corti in a 6-month-old fetus after Holmes staining. The basilar fibers ran at the base of the tunnel, maintaining regular spacing. Evaluation revealed that 10–15 % of the nerve fibers crossed the tunnel to reach the outer hair cells after passing through the habenula perforata (Fig. 8.8) [6].

Some efferent fibers have the appearance of a gigantic old tree. Perhaps the composing fibers loosen in the process of degeneration (Fig. 8.9).

A striking finding in the medial fibers is the presence of spindle-shaped swellings, similar in appearance to torpedoes (Figs. 8.10–8.12). These fibers are generally thick, and after forming a torpedo shape they bifurcate before joining the outer spiral bundles.

The spindle-shaped swelling observed in the efferent fibers appears similar to Purkinje cell axonal torpedoes. According to Louis et al. [7], a prominent finding in the cerebellum of patients with essential tremor is an abundance of torpedoes, swellings that result from the mis-accumulation

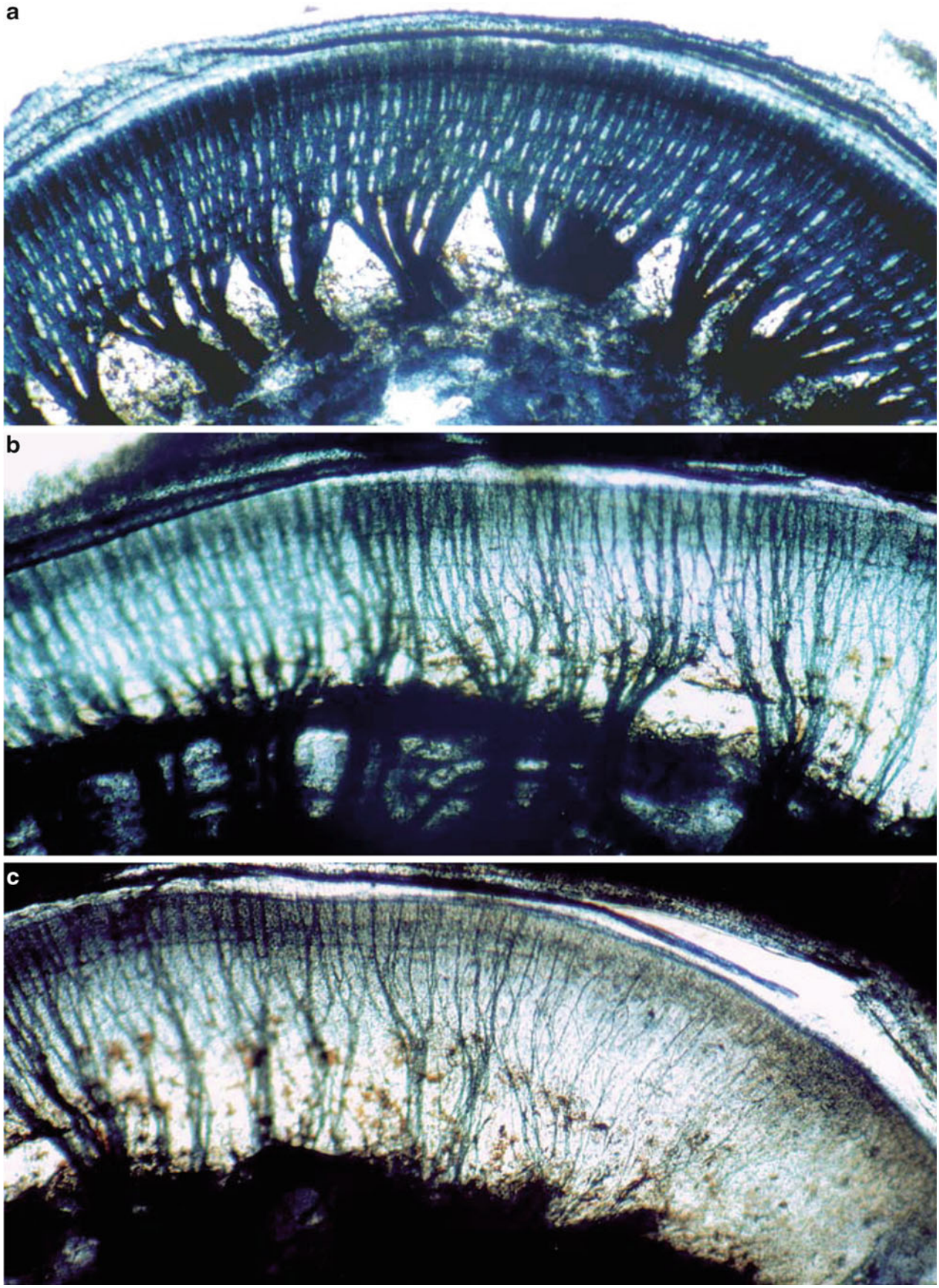

Fig. 8.2 Myelinated nerve fibers in the osseous spiral lamina. Bundles of nerve fibers emerge from Rosenthal's canal, and fan out in the osseous spiral lamina. (**a**) The radial and spiral fibers are densely intermingled in the lamina of the middle turn. (**b**) Both radial and spiral fibers are reduced in the basal turn. (**c**) Almost no fibers remain near the basal end. Seventy-five-year-old woman, Sudan Black B staining, ×10

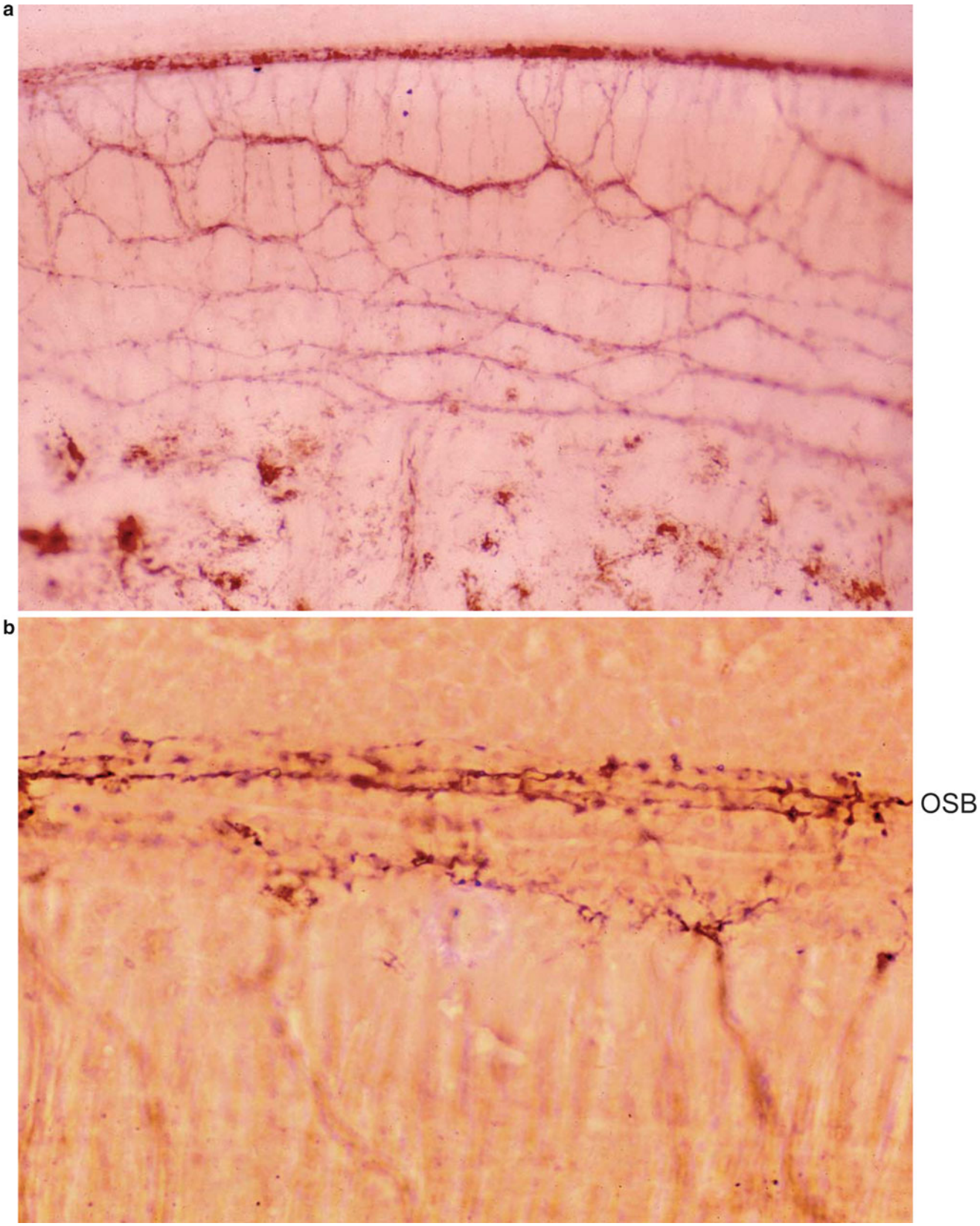

Fig. 8.3 Distribution of efferent fibers in the organ of Corti and osseous spiral lamina. (**a**) Strong staining at the top of the photograph indicates acetylcholinesterase activity in the organ of Corti (×45). (**b**) High power view of the organ of Corti. Sparse enzyme activity due to marked loss of the organ of Corti and postmortem changes. *OSB* outer spiral bundles (×160). (**c**) A single efferent fiber (*white arrow*) and a few afferent fibers (*black arrow*) remain in the lower basal turn (×160). Fifty-nine-year-old man, staining for acetylcholinesterase

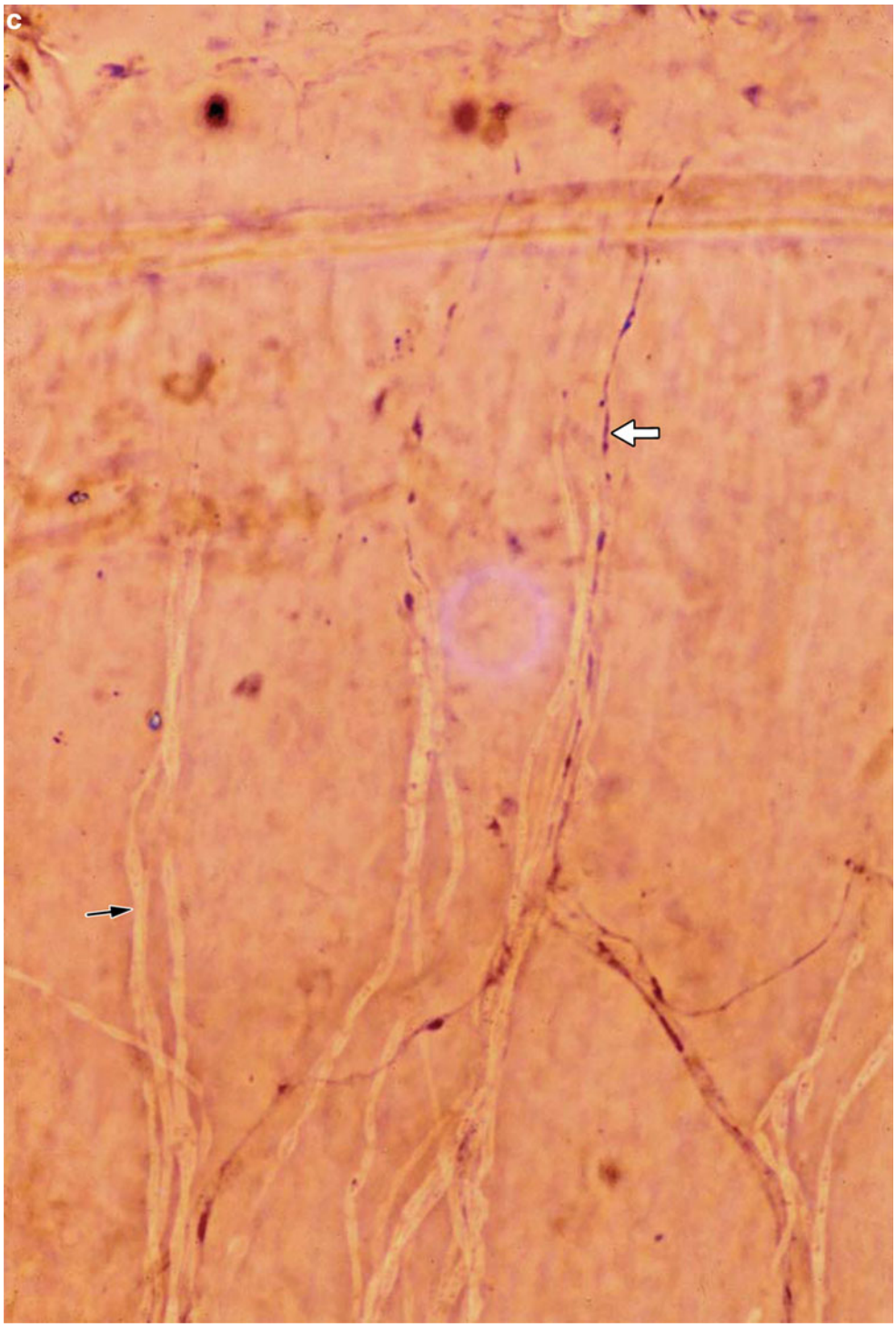

Fig. 8.3 (continued)

of cell constituents. Immunoreactivity for phosphorylated neurofilament protein revealed clear labeling of torpedoes. On electron microscopy, torpedoes were packed with randomly arranged 10–12 nm neurofilaments. Mitochondria and smooth endoplasmic reticulum were abundant at the periphery of the torpedoes. The authors concluded that the torpedoes in essential tremor represent the mis-accumulation of disorganized neurofilaments and other organelles.

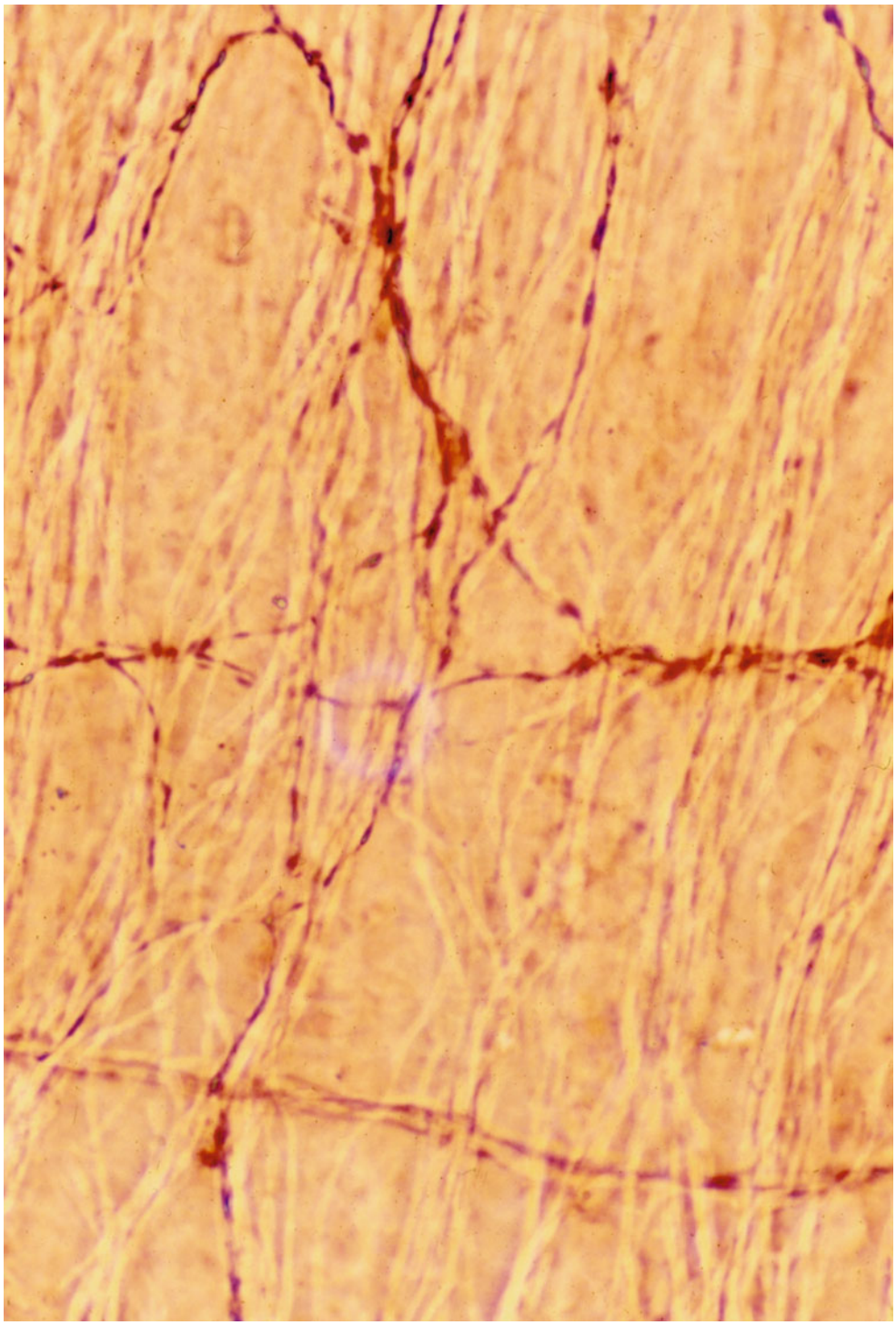

Fig. 8.4 Efferent and afferent fibers in the osseous spiral lamina. Because of the difficulty of pursuing the course of an individual fiber, an area with reduced fibers is selected for observation. Generally, the afferent fibers run radially, whereas the efferent fibers run spirally with a complicated course before taking a radial course to the organ of Corti. *unstained fiber* afferent fiber, *stained fiber* efferent fiber ×160

Efferent nerve fibers run spirally in the osseous spiral lamina toward the apex. In the cochlea of elderly people, both afferent and efferent fibers show the greatest loss in the lower basal turn. The torpedoes were rarely observed in aged cochleae, whereas they sometimes appear in younger individuals, where they are evenly distributed throughout the cochlea. The torpedoes might suggest a degenerative process of the nuclei of the efferent fibers.

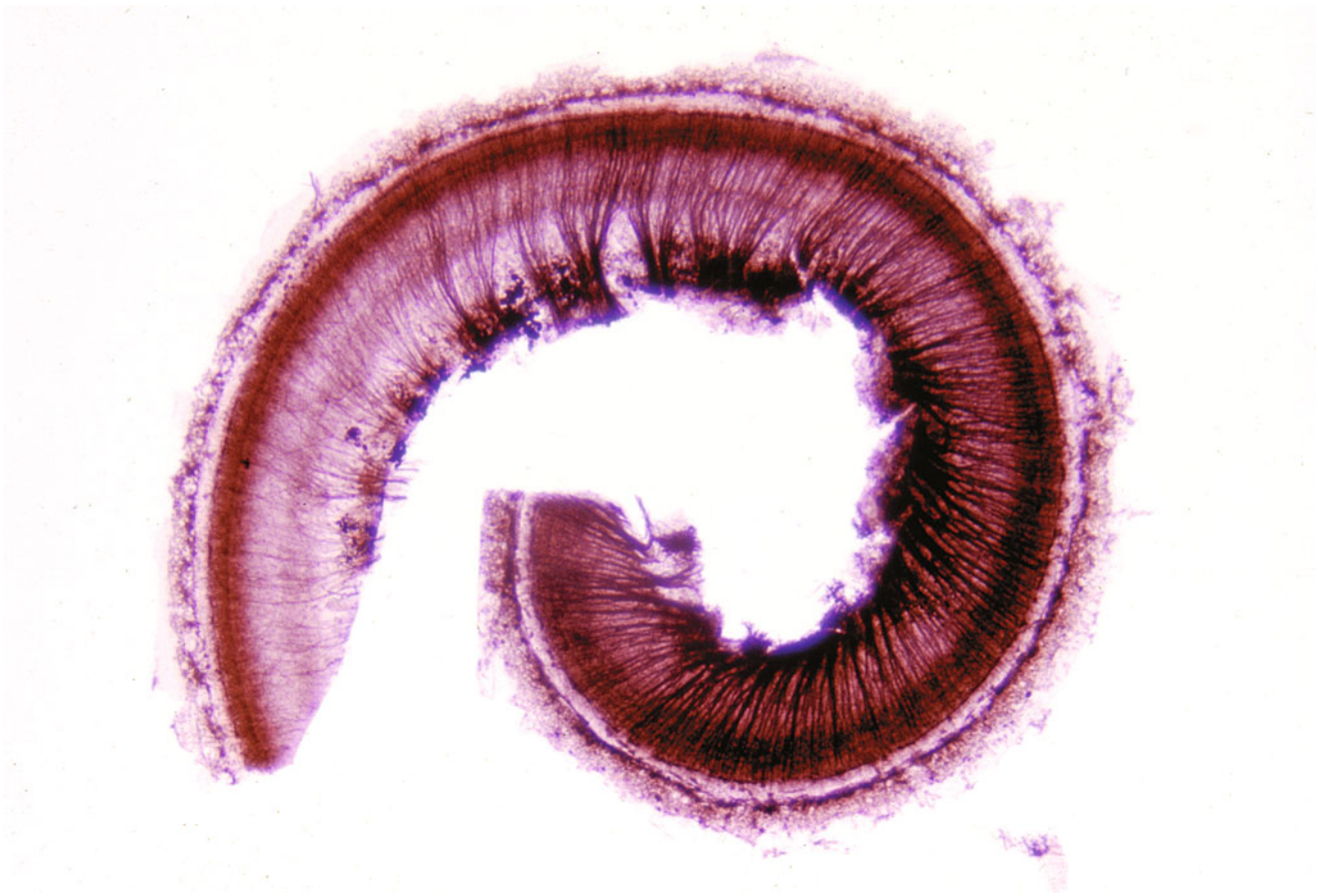

Fig. 8.5 The cochlea shows reduced numbers of afferent fibers, particularly in the basal turn, and complete loss of the efferent fibers. Seventy-eight-year-old man with severe hearing loss, OTAN staining

8.3 Nerve Fibers Running Lateral to the Hair Cell Area

Occasionally, the medial fibers run laterally, away from the outer spiral bundles. The fibers bifurcate and run tortuously in the Hensen's cell or Claudius' cell area, but never extend to the spiral ligament. The termination of these fibers has not yet been determined (Figs. 8.13, 8.14, and 8.15).

8.4 Degeneration of Sensory Hairs on the Outer Hair Cells

Surface preparations of the organ of Corti of elderly people show loss of hair cells. The arrangement of hair cells and supporting cells becomes irregular with advancing age (Fig. 8.16). Details of the stereocilia cannot be clarified at the light microscopic level.

One study evaluated the surface of the outer hair cells of elderly patients, aged 80–91 years, using a scanning electron microscope [8]. Fifteen temporal bones were studied within a 1–1.5 h postmortem interval. The organ of Corti from the upper basal turn to the middle turn was examined in this study.

The surface of the membrana reticularis showed normal stereocilia as well as hairs with varying degrees and types of degeneration (Fig. 8.17). Pathological changes of the stereocilia were mainly loss of hairs and giant cilia formation [8]. Cytoplasmic protrusion was another pathological change on the surface of the outer hair cells.

Hair loss occurred in all regions of the stereocilia, i.e., in the peripheral area, the central area, or a mixture of the two. There was no particular pattern of loss distribution in different parts of the organ of Corti (Fig. 8.18).

Total hair loss was also seen, and this is a terminal stage before the stereocilia disappear. After disappearance of the stereocilia, remnants persisted on the surface of the cuticular plate. These were of uniform hemispherical shape and size, with a diameter of approximately 0.1 μm, suggesting a natural breaking point in each stereocilium. The remnants sometimes coexisted with a few remaining abnormal stereocilia.

A W-configuration could still be recognized in this case. As the degenerative process continues, the cuticular plate begins to

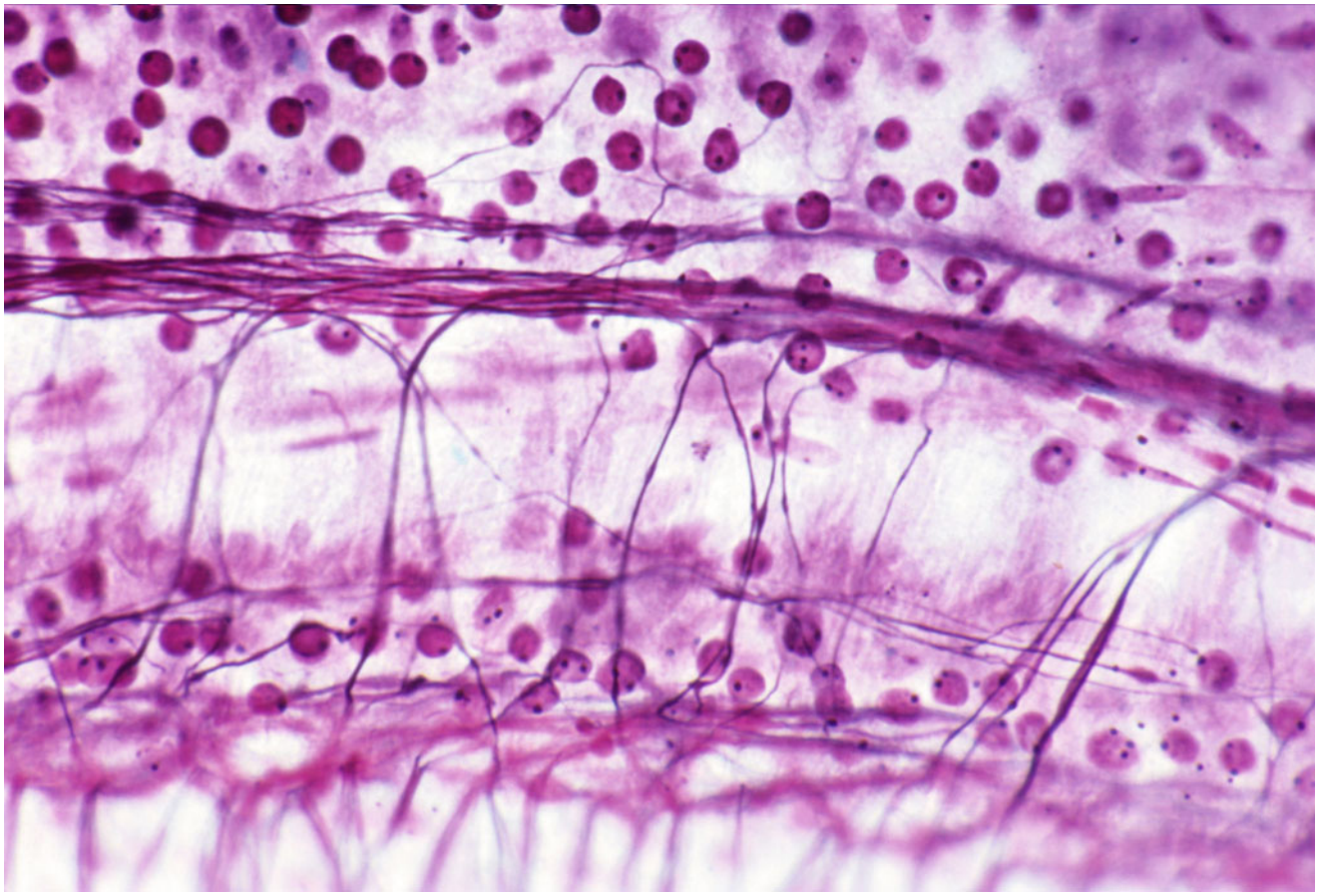

Fig. 8.6 Nerve fibers in the organ of Corti of the apical turn. There are fewer fibers near the apical end. Holmes staining (original ×40)

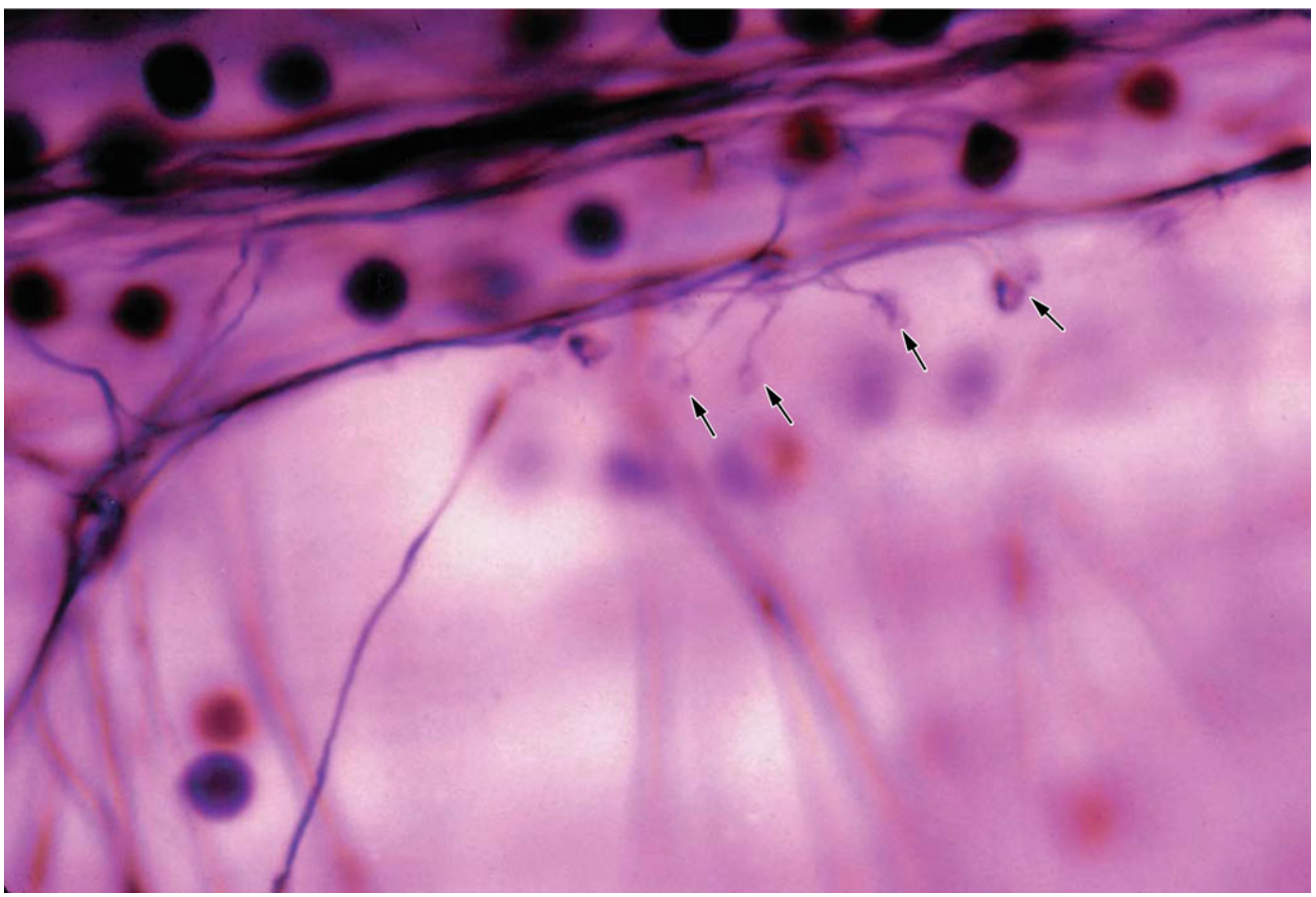

Fig. 8.7 Nerve endings (*arrows*) at the first row of the outer hair cells. Holmes staining (original ×100)

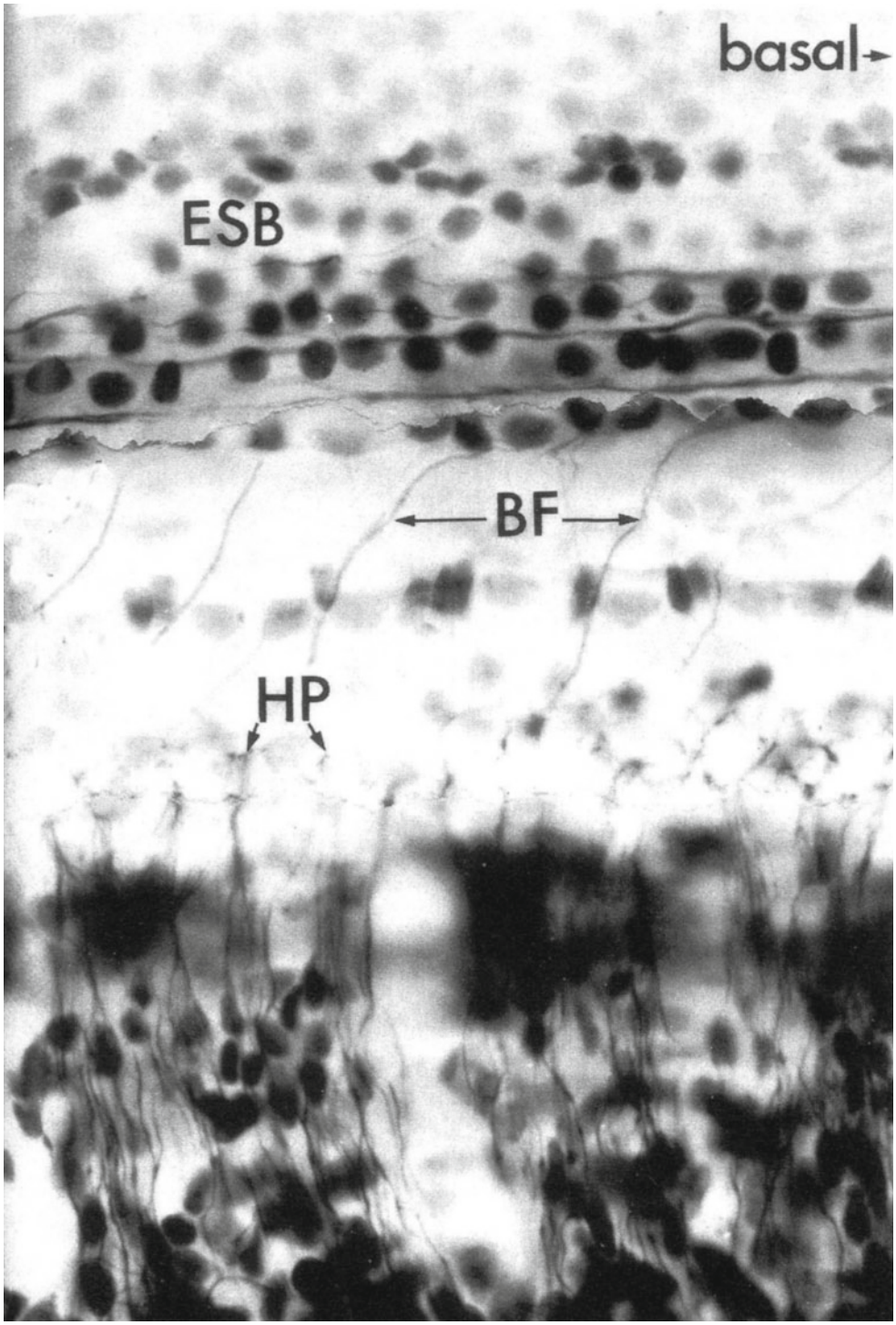

Fig. 8.8 Basilar fibers crossing the tunnel, maintaining a regular interval. No medial fibers are seen [6]. *ESB* external (outer) spiral bundle, *BF* basilar fiber, *HP* habenula perforata. The basal direction is to the right in the figure. Six-month-old fetus, Holmes staining

disappear and the number of remnants decreases. The W-configuration becomes eccentric as surrounding cells invade the cuticular plate. Eventually, the hair cell surface is replaced by supporting cells. In this case there was a shallow depression indicating almost complete disappearance of the outer hair cells and replacement by the phalanx of Deiters' cells and outer pillar cells (Fig. 8.19) [9]. The membrana reticularis consists of the cuticle, the phalanx of Deiters' cells, and the outer pillar cells.

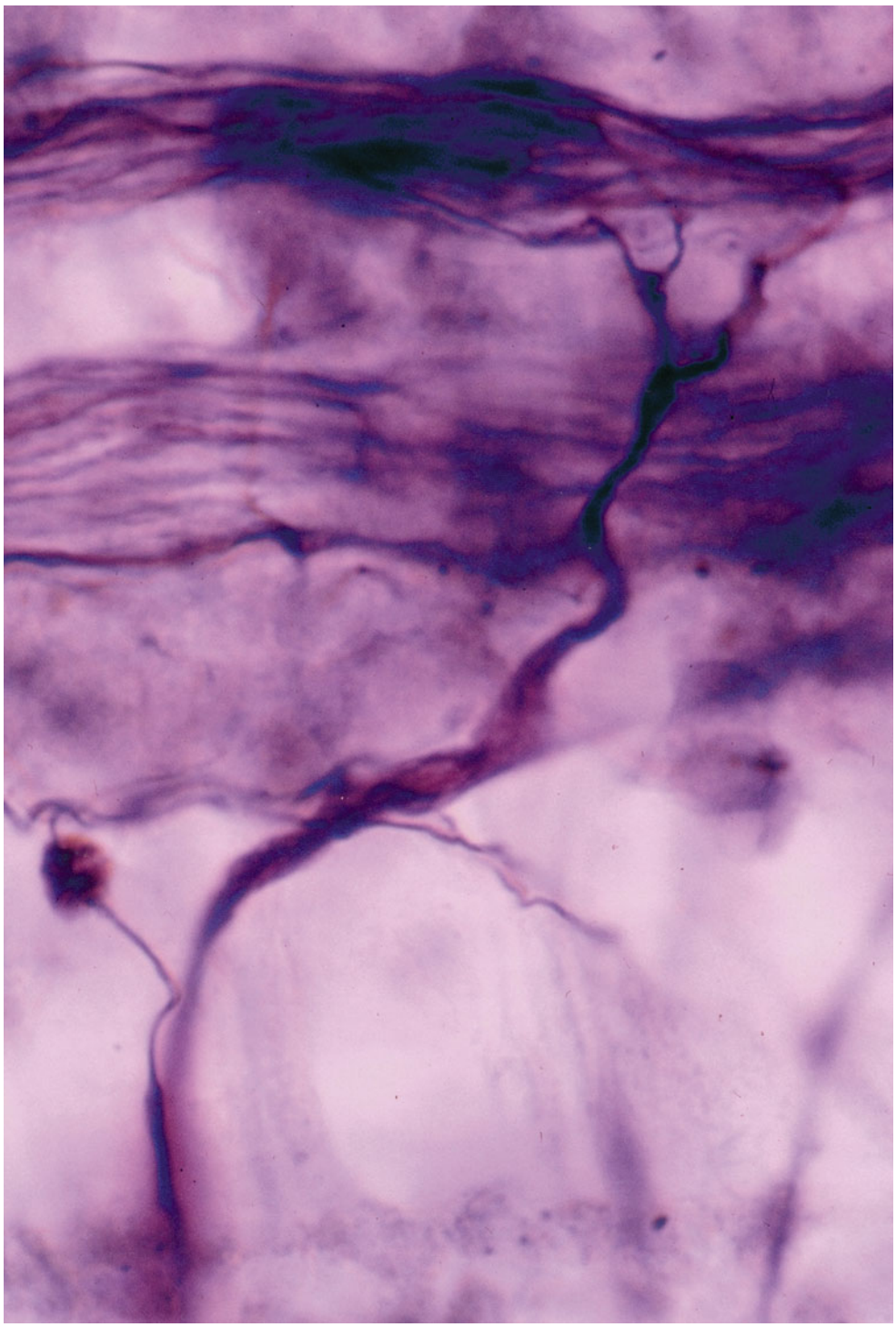

Fig. 8.9 Gigantic efferent fibers join the outer spiral bundles. Possibly in the process of degeneration. Eighty-four-year-old woman, Holmes staining (original ×100)

A giant cilium is produced through fusion of hairs. Reorganization takes place within the fused hair. The length of the giant cilium is indicative of its growth. This can be interpreted as a premortem change rather than a postmortem change or artifact.

8.5 Strial Atrophy

Aging is one cause of degeneration of the stria vascularis. Schuknecht and Gacek [10] proposed defining strial pres-

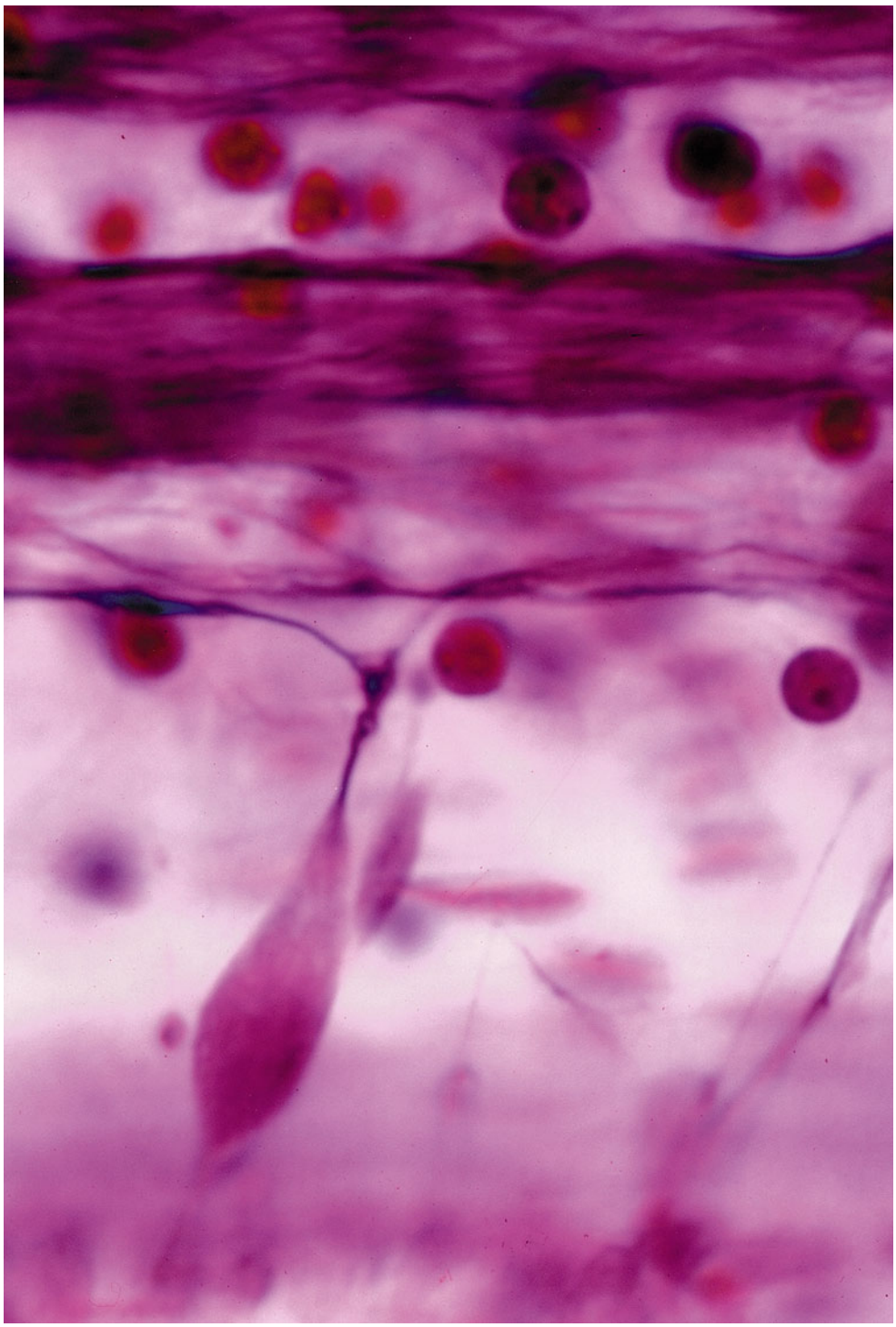

Fig. 8.10 Axonal swelling of an efferent fiber creating a torpedo. Maximal diameter is about 8 μm. Many torpedoes were present in this specimen. The patient had no neurological disease. Forty-six-year-old woman, Holmes staining (original ×100)

bycusis as the loss of at least 30 % of the strial tissue. Typically strial atrophy is patchy and is more pronounced in the middle and apical turns. On audiometry, flat elevations or slightly descending pure tone thresholds are seen in patients with strial atrophy, with preservation of good speech discrimination scores.

When fresh stria vascularis was stained for alkaline phosphatase and observed as a surface preparation, it was found that the remaining strial tissue always surrounded the strial capillary in the atrophic area. No strial capillary was found without surrounding strial tissue (Figs. 8.20, 8.21, and 8.22). Complete loss of a localized area of the stria vascularis sug-

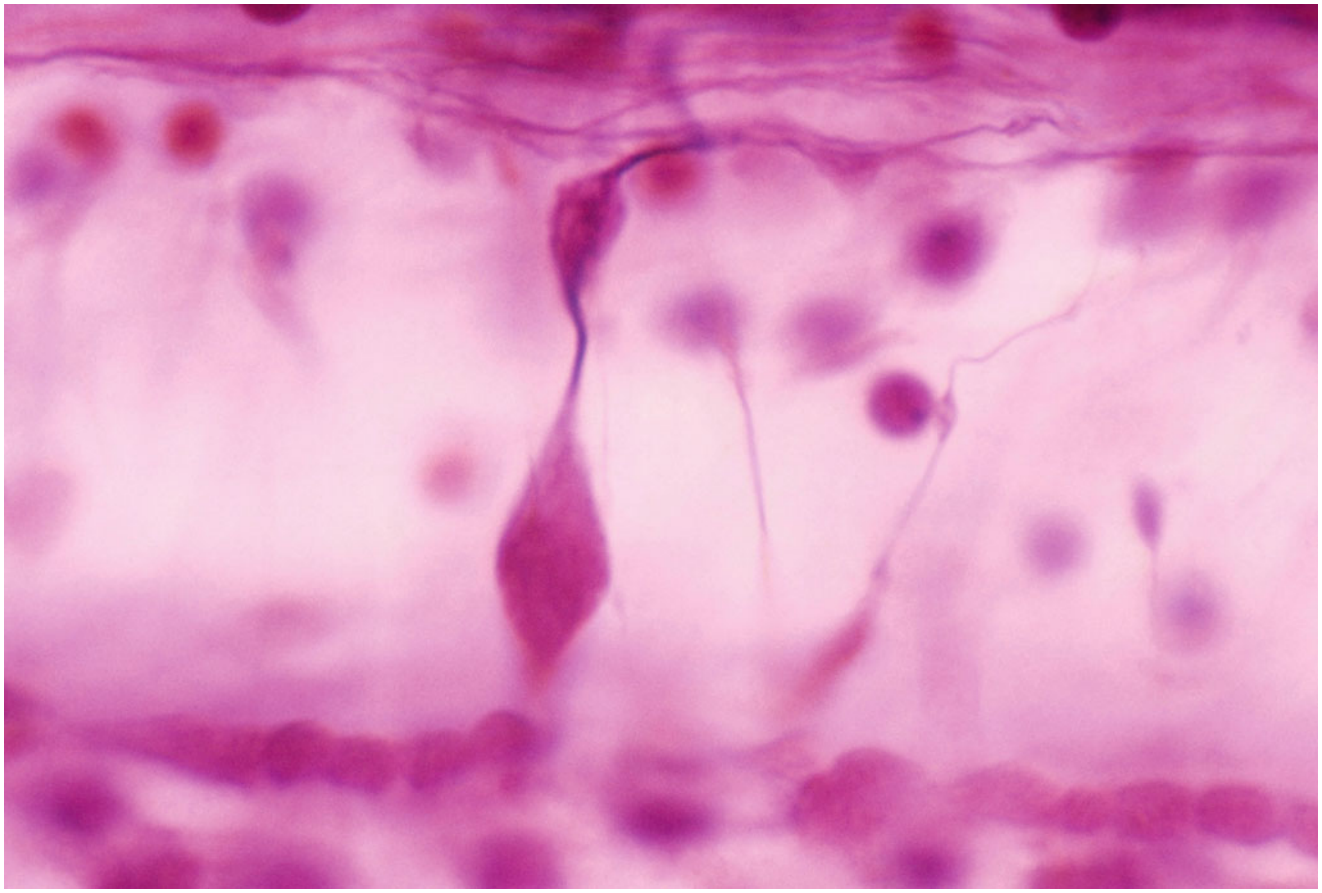

Fig. 8.11 Two torpedoes connected in the same nerve fiber. Forty-six-year-old woman (original ×100)

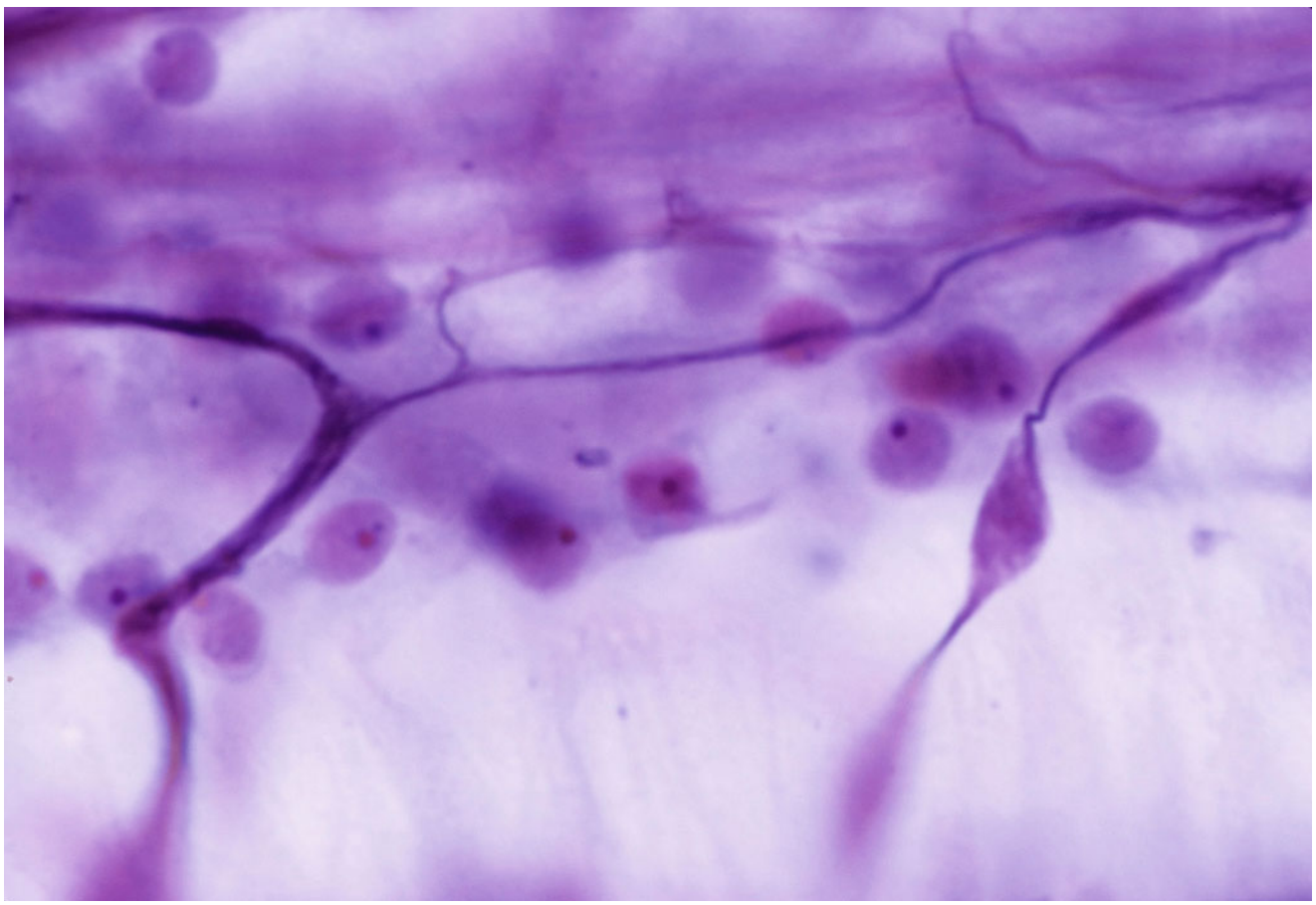

Fig. 8.12 Branching of the medial fiber in the outer hair cell area (×100)

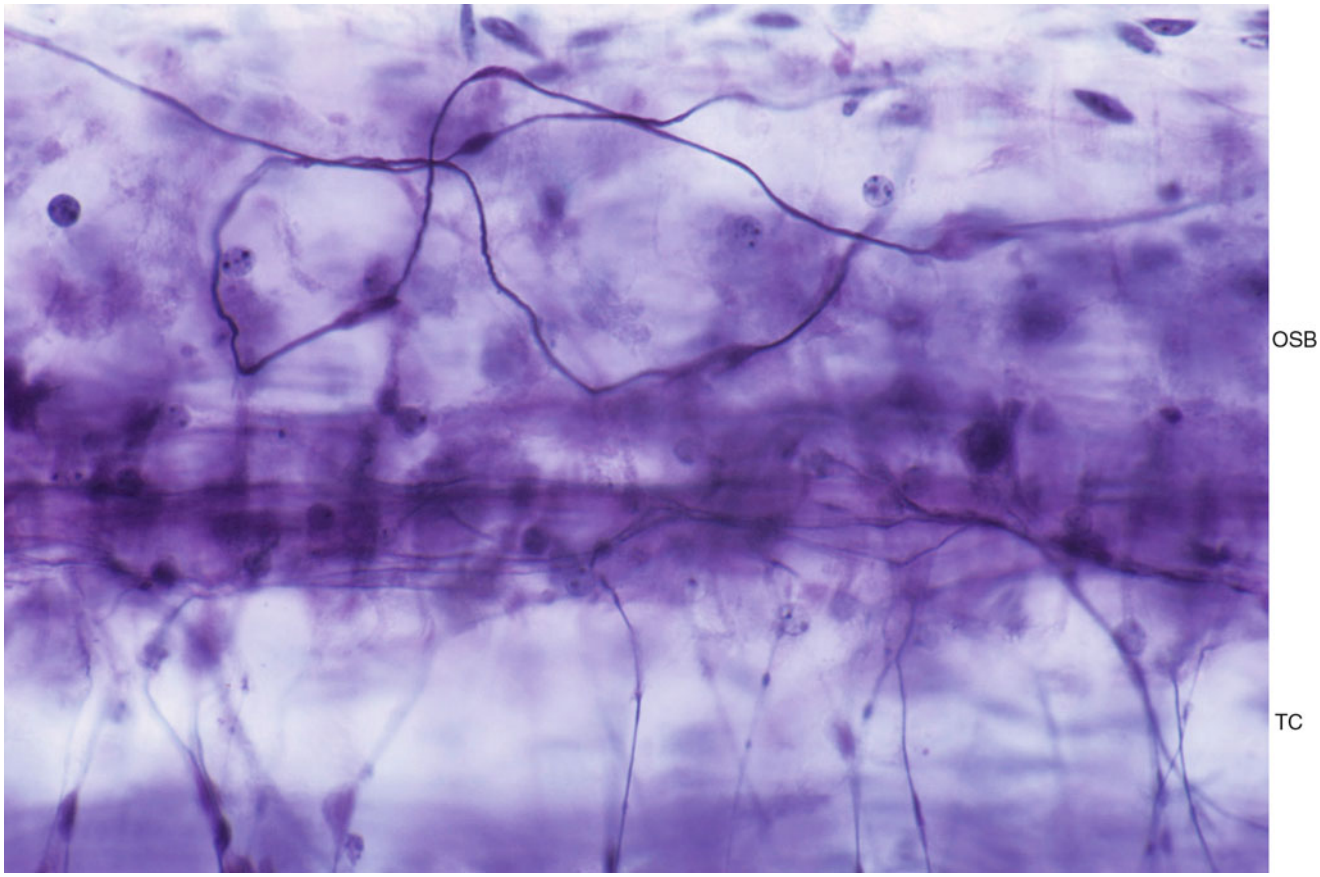

Fig. 8.13 Aberrant fibers. The medial fiber runs lateral to the outer spiral bundles. *OSB* outer spiral bundles, *TC* tunnel of Corti (original ×40)

gests atrophy of the spiral prominence as a result of loss of the vas spirale (Fig. 8.23).

8.6 Lipidosis of the Basilar Membrane

Precipitates are found in the basilar membrane of elderly people.

Twenty-four human temporal bones from 20 patients ranging in age from 71 to 95 years were studied. After fixation in 10 % formalin and decalcification with a 5 % solution of trichloroacetic acid, the temporal bones were trimmed and the membranous labyrinth was exposed.

The following staining procedures were employed: 1. Osmium tetroxide-α-naphthylamine (OTAN) method, 2. Sudan III staining, 3. Nile blue sulfate method, 4. PAS reaction, 5. Smith-Dietrich reaction, 6. Observations under ultraviolet light and polarized light [11].

In some cases ultrasonic shaking was performed to disintegrate and detach the organ of Corti from the basilar membrane, before or after staining. Stained tissue was washed in distilled water and mounted as a flat specimen in polyvinyl pyrrolidone medium.

There were lipid deposits along the filamentous structure of the pars pectinata in the lower basal turn. Nine ears from 12 patients showed lipid deposits in the basilar membrane. Six cochleae from three younger patients, aged 1, 24, and 37 years, did not show any deposits at all. In specimens in which the organ of Corti was detached by ultrasonic shaking, the lipid deposits were more clearly observed. Deposits were most prominent in the basal turn from the vicinity of the basal end to the 5–10 mm area, and were more heavily distributed near the basal end than apically. The apical and middle turns failed to show deposits in the basilar membrane.

The following test results were obtained. The deposits were soluble in ether-alcohol. They were sudanophilic, stained pink by Nile blue sulfate, and showed partial birefringence under crossed nicols. Deposits were composed mainly of neutral fat with small amounts of cholesterol. No reaction was seen with the PAS or Smith-Dietrich methods, indicating the absence of glucolipid and phospholipid, respectively. Because the deposit did not fluoresce, the presence of lipofuscin was not likely. Formalin solution is not the best fixative for lipids, so it is possible that certain constituents were lost during fixation (Figs. 8.24, 8.25, and 8.26).

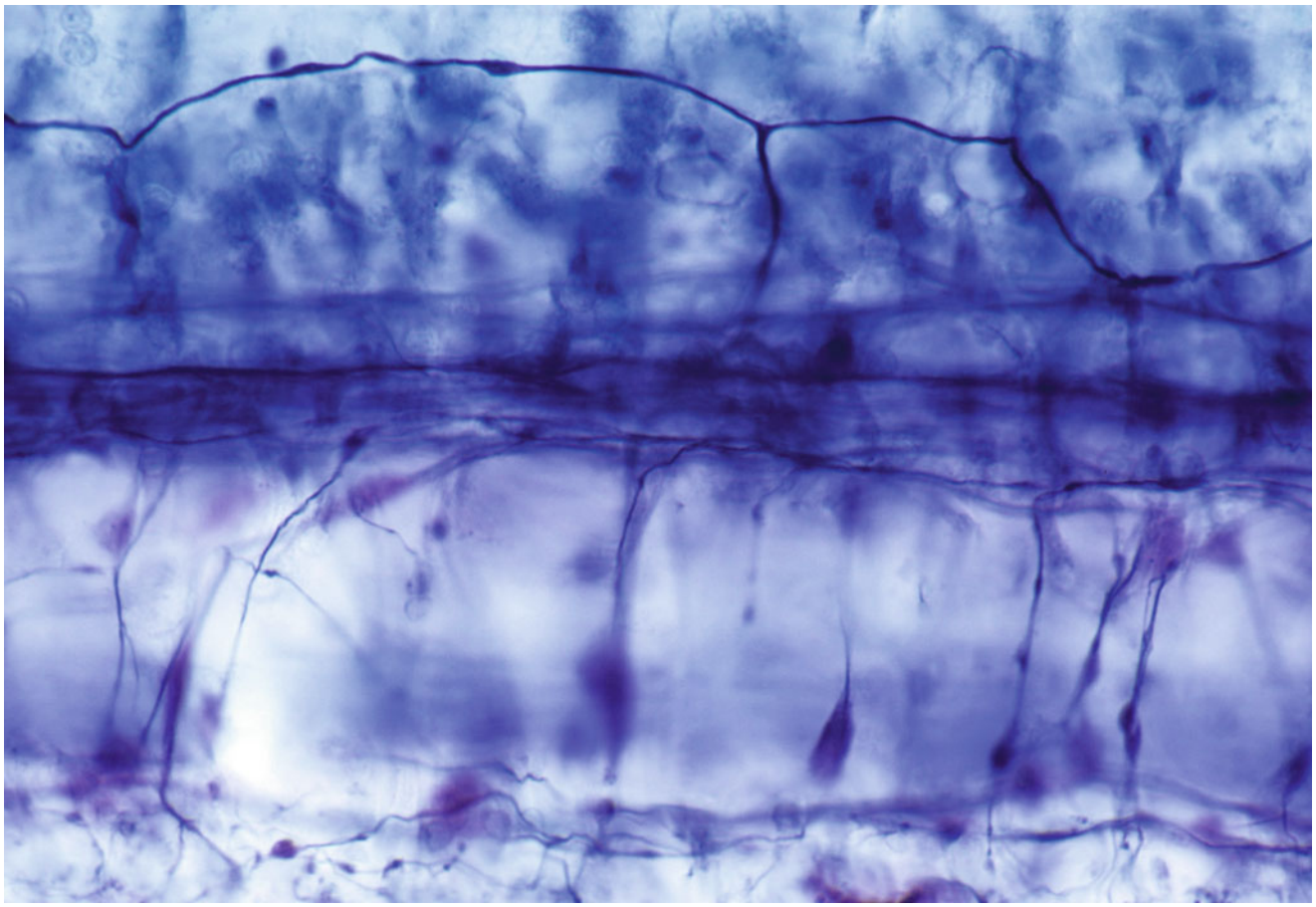

Fig. 8.14 Aberrant fibers. The medial fiber traverses the tunnel. It bifurcates beyond the outer spiral bundles. Many torpedoes are seen in the tunnel of Corti (original ×40)

The basilar membrane is composed of ground substance, filaments, and a few connective tissue cells. The inner part, the pars tecta, is formed of radially arranged filaments, which are not grouped in bundles but lie side by side in scant ground substance. Beneath the filaments is cottony ground substance without filaments. The outer part of the basilar membrane, the pars pectinata, is thicker and striated. It is formed of compactly arranged, grouped filaments, all of which run radially. The space between filaments is filled with scant ground substance. The fibers are separated from each other by abundant cottony ground substance and are arranged in two strata [12, 13].

Mayer [14] reported that people over 60 years of age showed thickening of the basilar membrane. According to Mayer, calciferous deposits and occasional ossification was also observed in the thickened membrane. He believed that basilar membrane rigidity was the anatomical basis for presbycusis.

The basilar membrane is a tissue usually devoid of discernible lipids [15]. The formation of fat in tissue other than adipose tissue is called aberrant lipogenesis, which is thought to be related to fatty degeneration and atheromatosis [16].

It is not clear how lipids are deposited in the basilar membrane. The serum cholesterol levels of these patients had no correlation with the presence of lipid deposits. Because the deposits occurred in the lower basal turn, degeneration of the organ of Corti might be responsible for their formation. However, lipid deposits were also found in regions of the basilar membrane where the organ of Corti was intact. Because the basilar membrane from younger individuals did not show these deposits, aging may be closely related to the formation of the lipids. The motion of traveling waves in the basilar membrane may be influenced by the presence of the lipids, and the deposits may alter the membrane structure.

8.7 Prevention of Presbycusis

There is a paper suggesting that caloric restriction can prevent loss of spiral ganglion cells and hair cells in the organ of Corti. According to Lee et al. [17], most rodents demonstrate delayed onset of age-related pathological changes and have

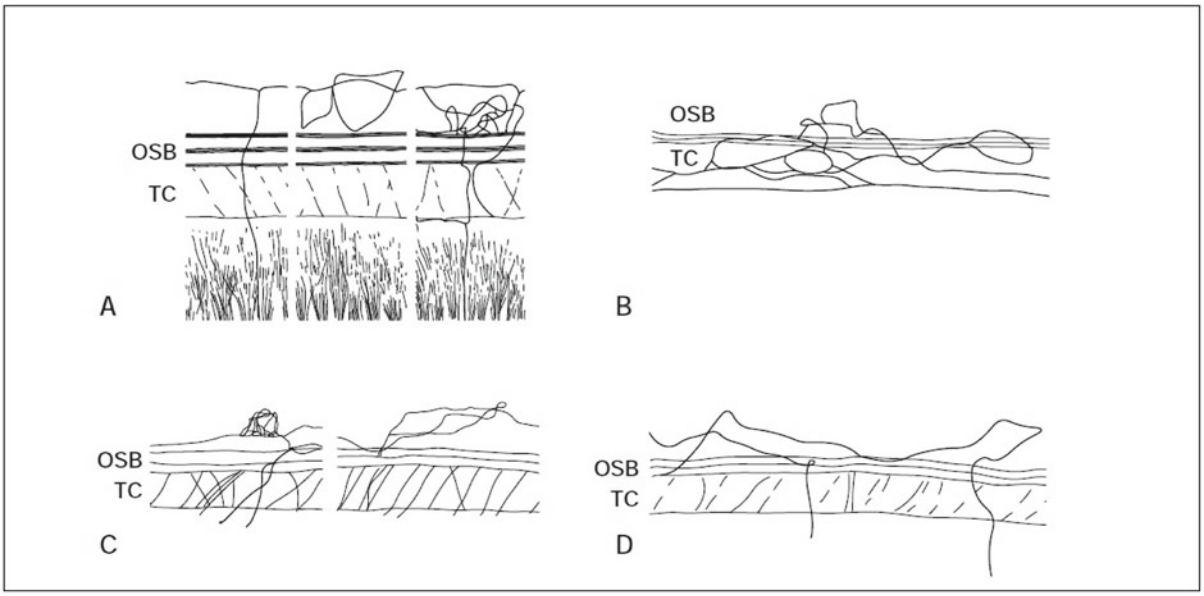

Fig. 8.15 Drawings of aberrant fibers. *OSB* outer spiral bundles, *TC* tunnel of Corti

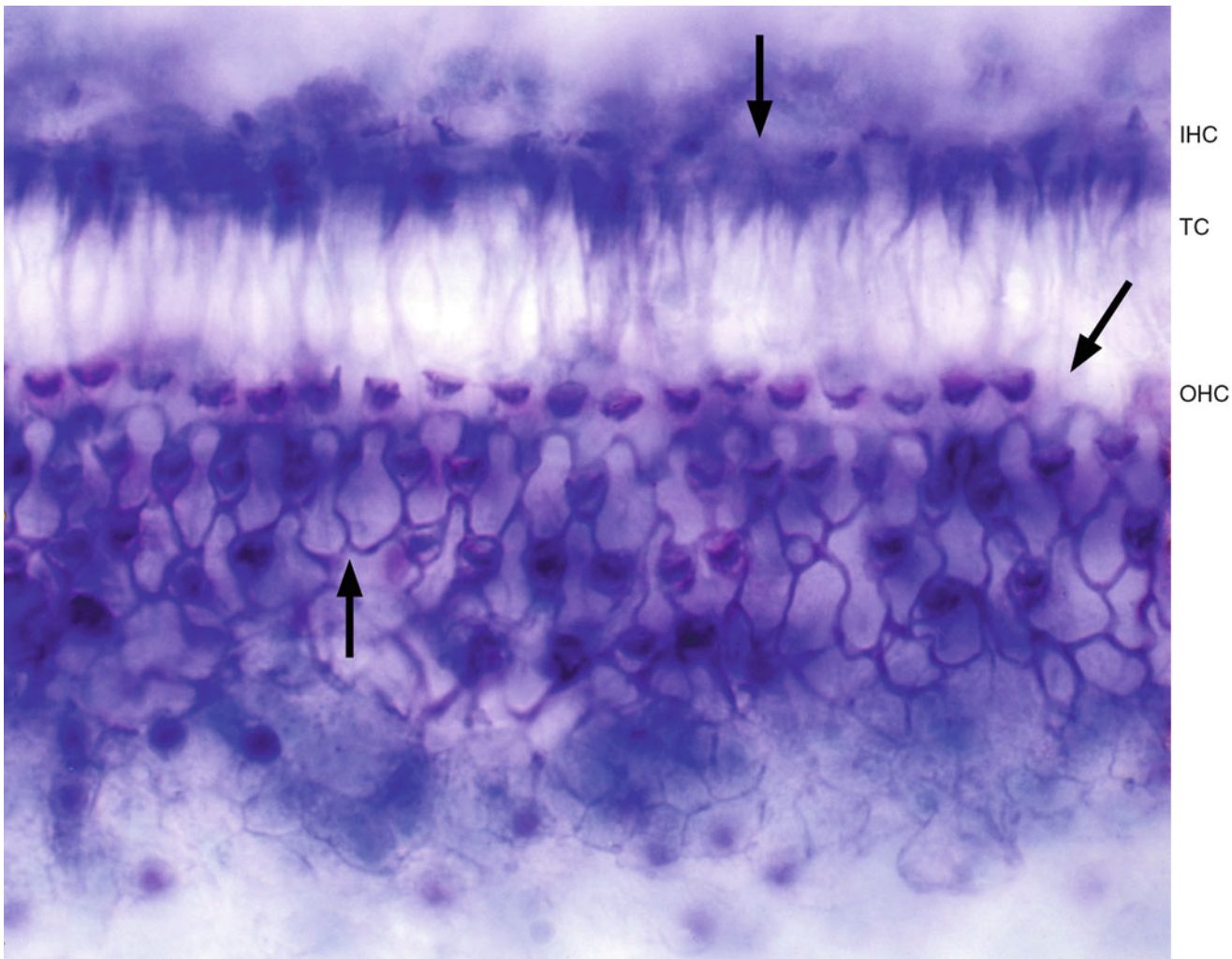

Fig. 8.16 Surface specimen of the lower basal turn. Partial loss of inner and outer hair cells. *Arrows* point to areas of loss of inner hair cells and of outer hair cells in the first and third rows. *IHC* inner hair cell area, *TC* tunnel of Corti, *OHC* outer hair cell area. Seventy-one-year-old man, trichrome staining (×40)

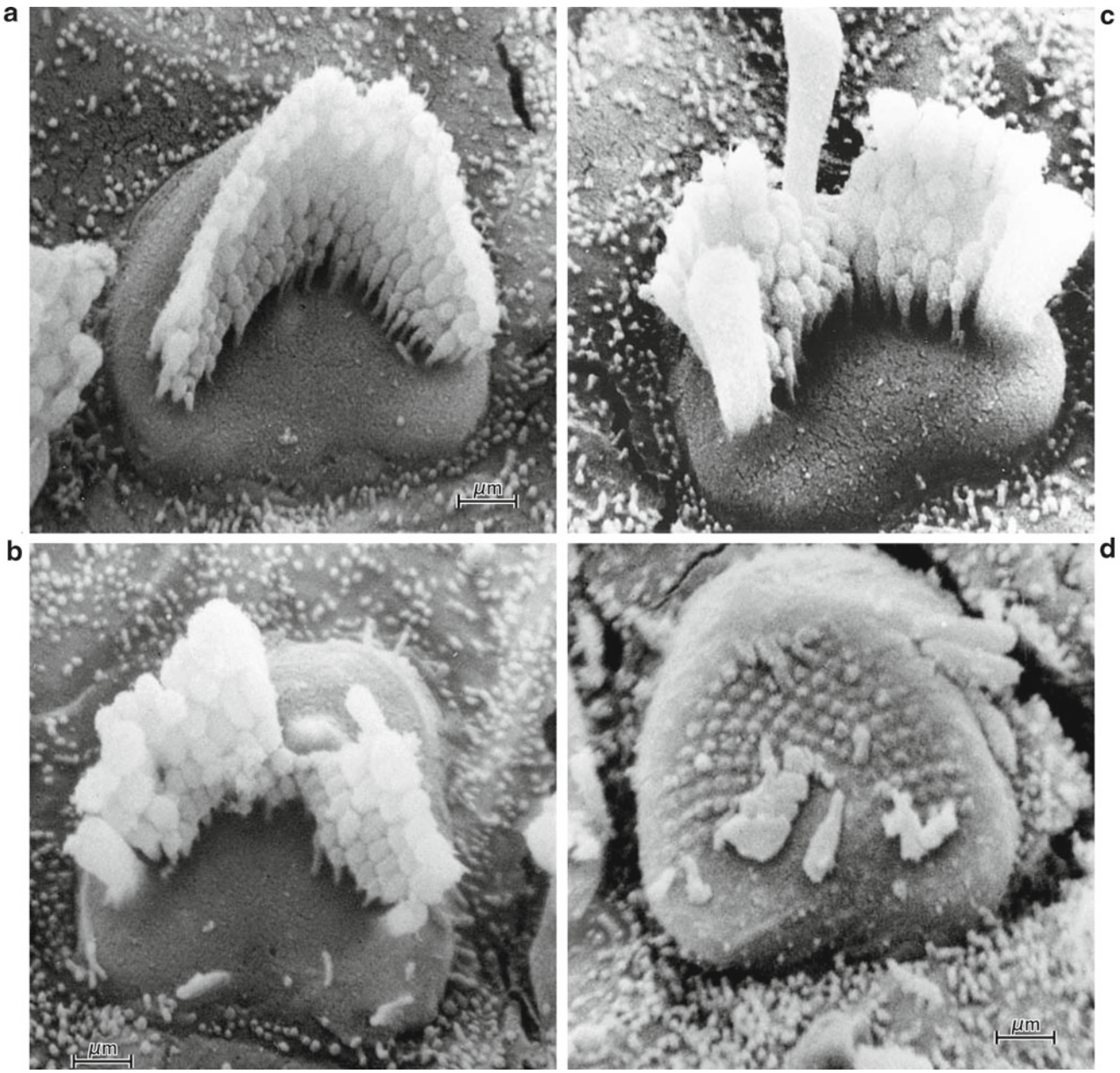

Fig. 8.17 Changes in the stereocilia of the outer hair cells [8]. (**a**) Normal stereocilia of the outer hair cell. (**b**) Marked defect of the central stereocilia. Two giant stubs are seen at the center and a side of the stereocilia. (**c**) Marked loss of the central stereocilia around the giant cilium. (**d**) After loss of the stereocilia, remnants of equal size and shape are seen. Eighty-six-year-old woman, scale: 1 μm × 7500

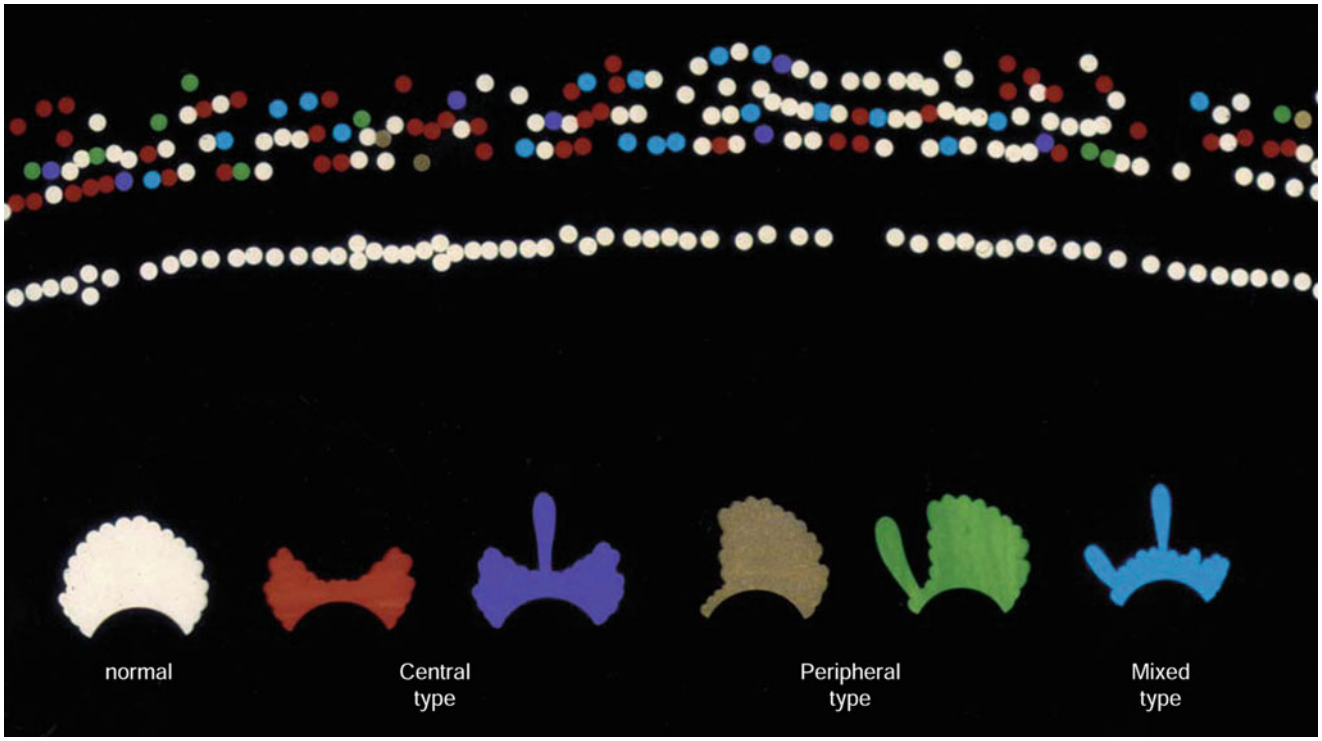

Fig. 8.18 Distribution and pathologic changes in stereocilia of human outer hair cells. There is no pattern of distribution or type of pathology

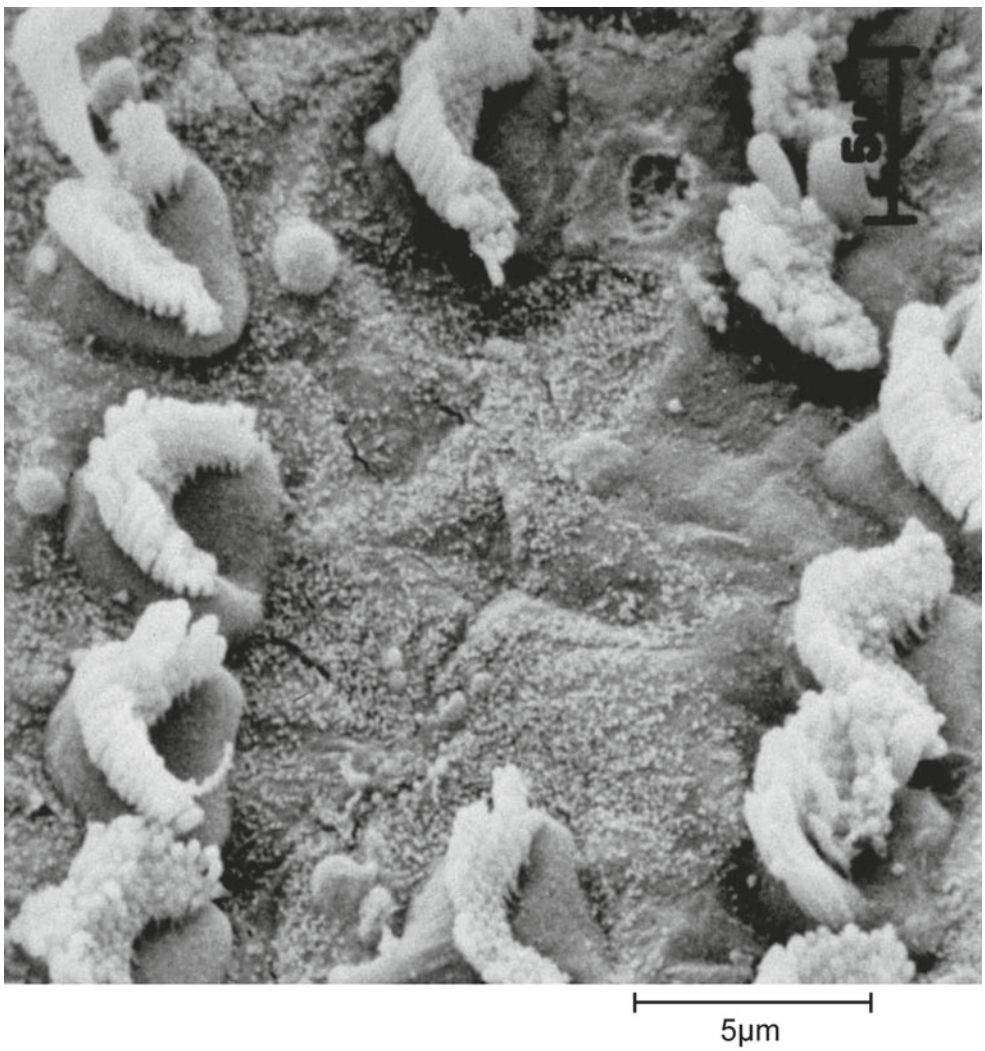

Fig. 8.19 Repair of the membrana reticularis [9]. Two outer hair cells have disappeared in the second row. Eighty-six-year-old woman, scale: 5 µm, (×3,300)

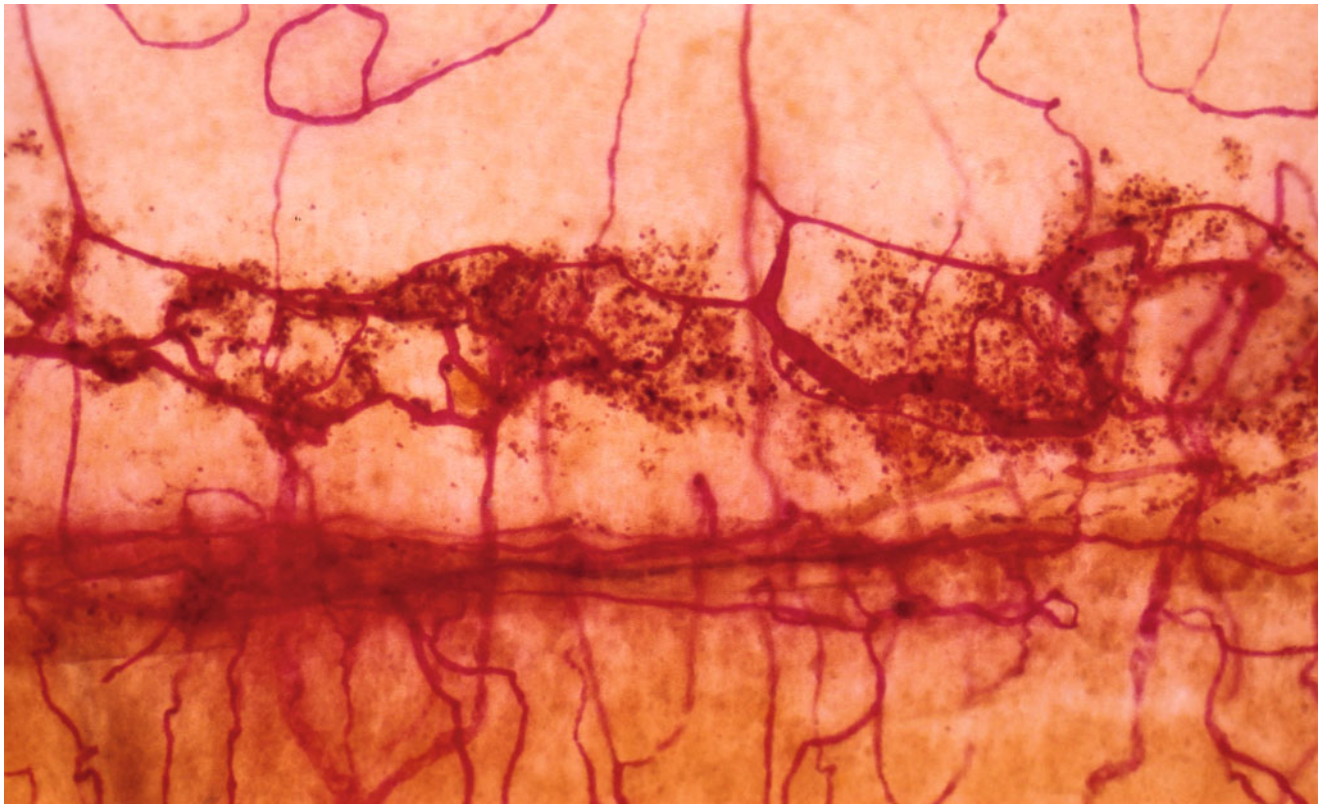

Fig. 8.20 Strial atrophy. There is marked loss of the stria vascularis with its capillaries. Eighty-six-year-old woman, alkaline phosphatase staining (original ×6.5)

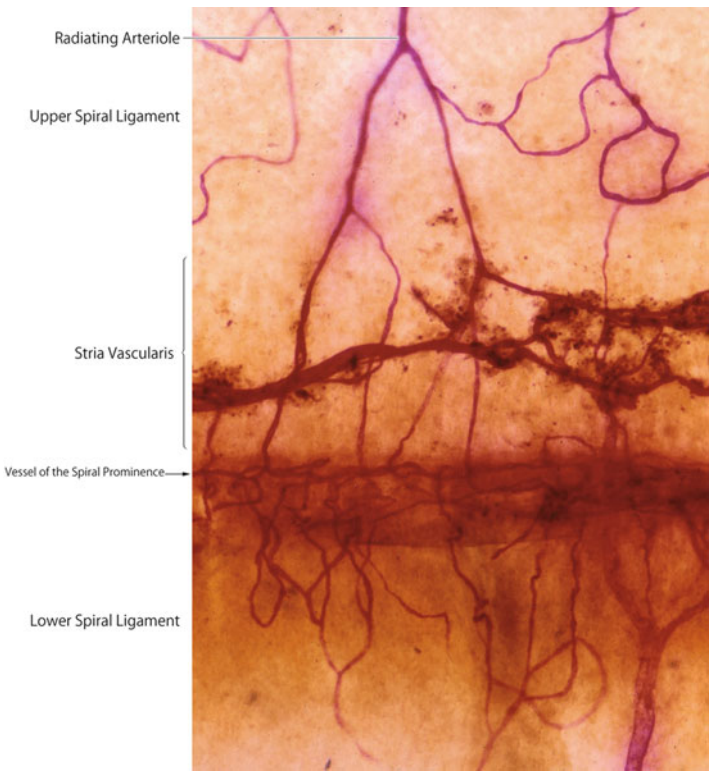

Fig. 8.21 Strial atrophy. Marked loss of strial tissue and capillaries is observed. The blood vessel of the spiral prominence remains

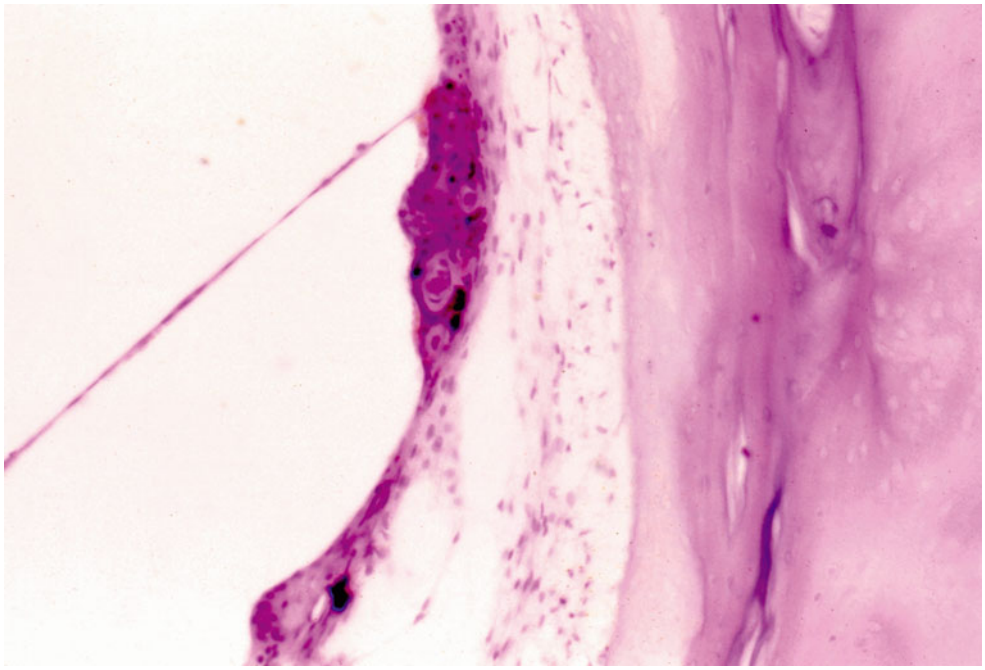

Fig. 8.22 Partial strial atrophy. Part of the stria vascularis remains, but appears pathologic. The spiral ligament is atrophic. Eighty-six-year-old woman

Fig. 8.23 Strial atrophy. Complete loss of a localized area of the stria vascularis. The vas prominence (vessel of the spiral prominence) seems to have disappeared. Atrophy of the spiral prominence is suggested

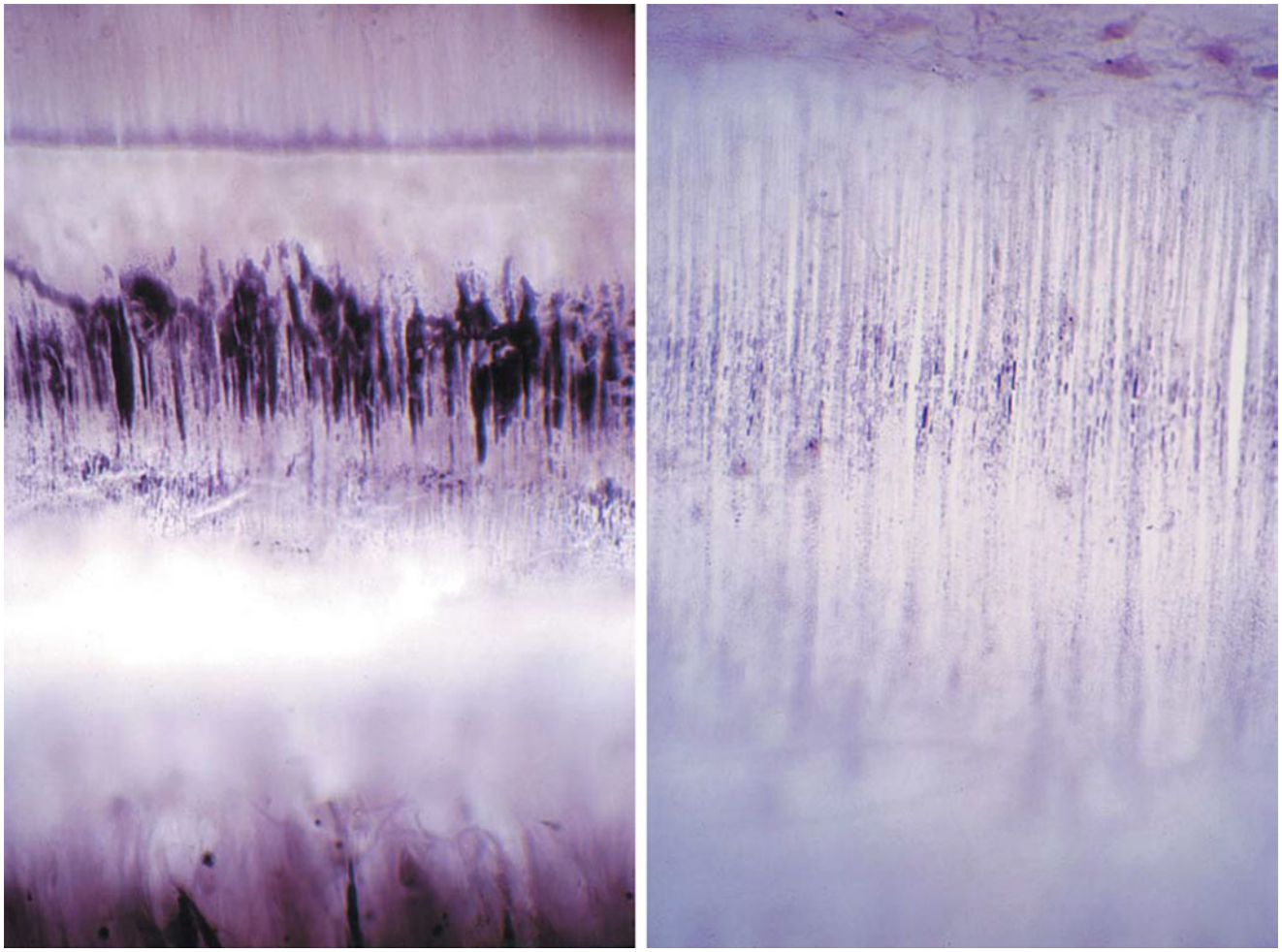

Fig. 8.24 Lipidosis of the basilar membrane [11]. *Left*: 3 mm area of the lower basal turn. *Right*: 9 mm area. Marked lipid deposits are present in the 3 mm area. Eighty-six-year-old woman, osmium tetroxide-α-naphthylamine (OTAN) method (×400)

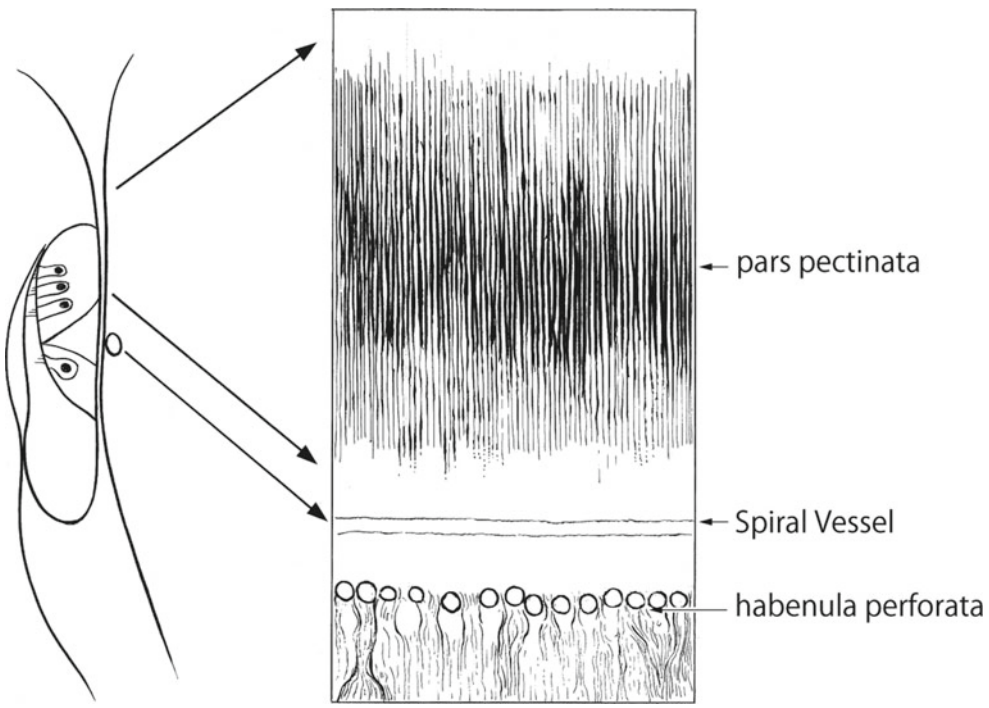

Fig. 8.25 A schema showing lipid deposits in the basilar membrane

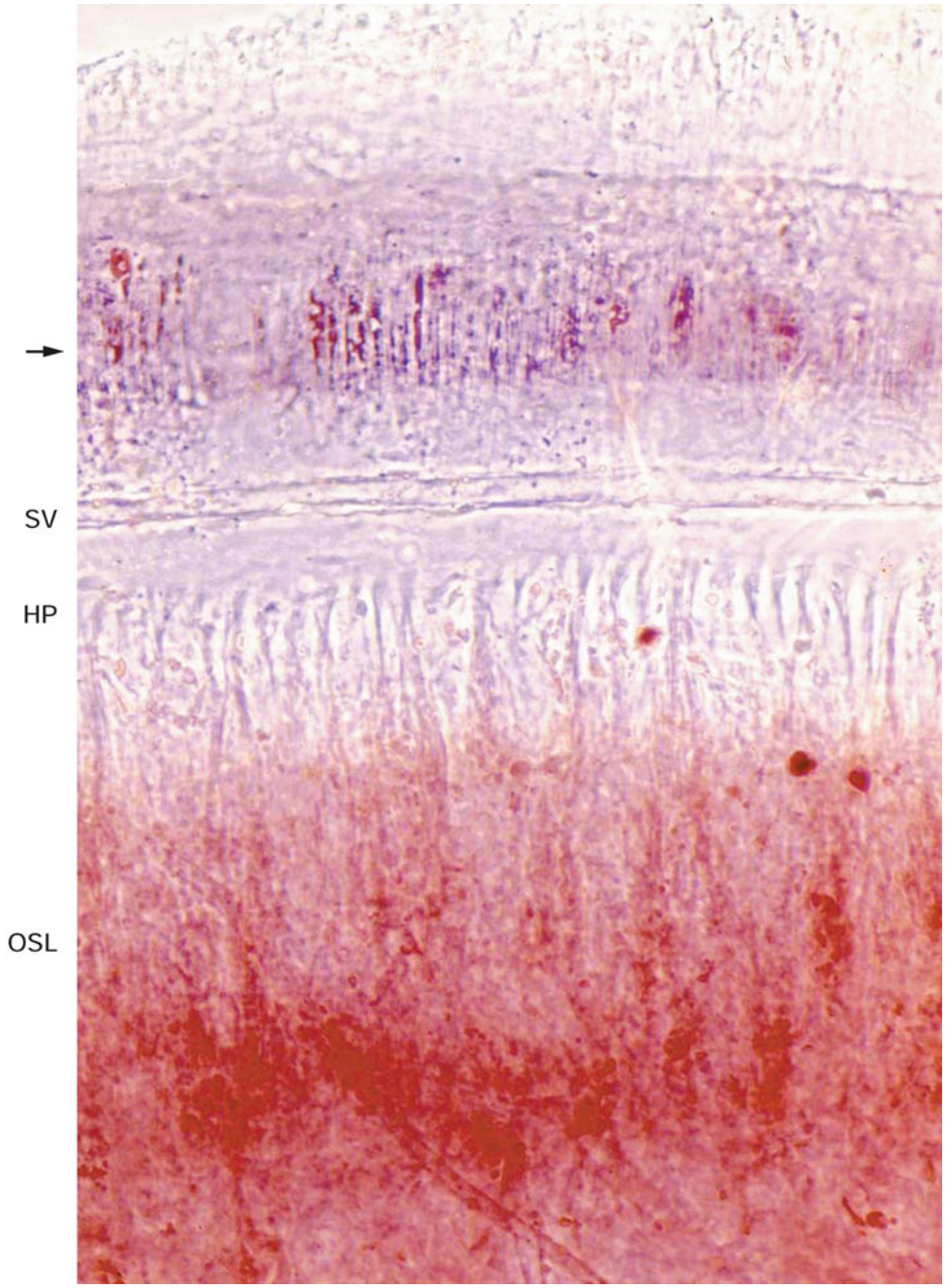

Fig. 8.26 Lipidosis of the basilar membrane. *Arrow* indicates lipid precipitate stained by Sudan III. *SV* spiral vessel, *HP* habenula perforata, *OSL* osseous spiral lamina. Eighty-six-year-old woman (×160)

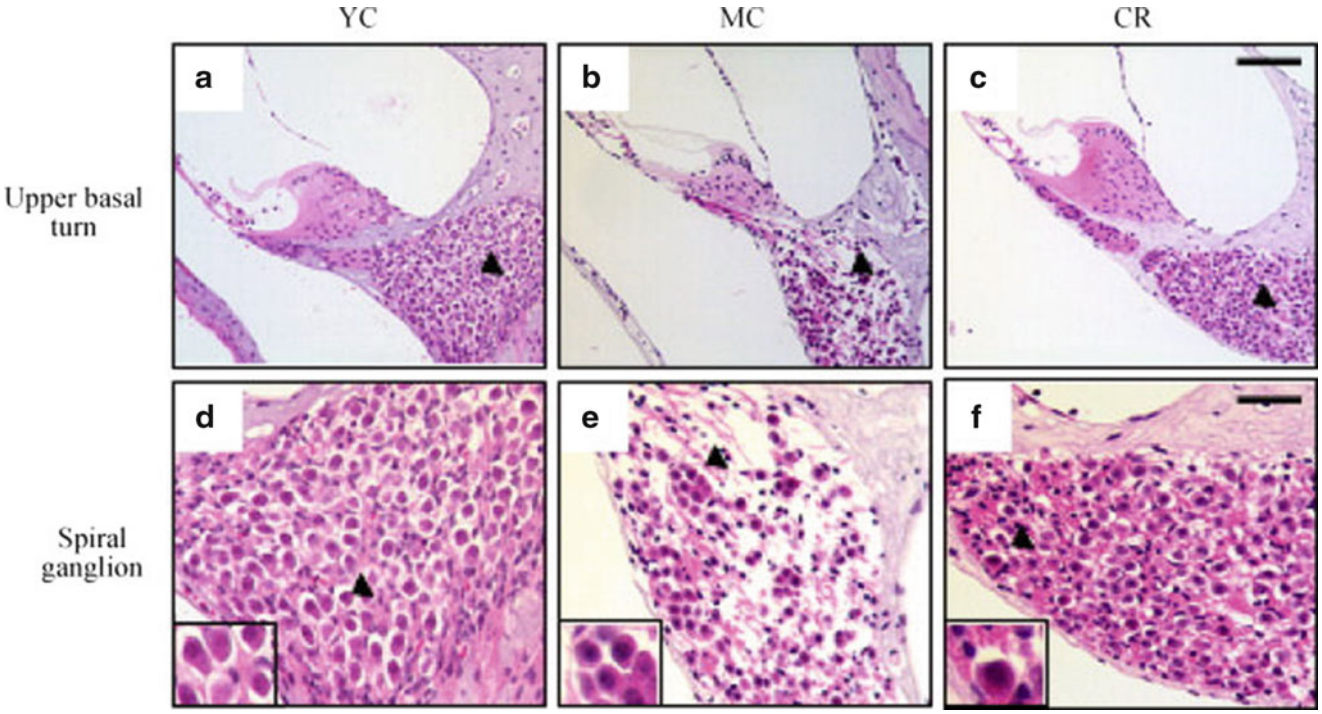

Fig. 8.27 Caloric restriction prevents presbycusis [18]. *YC* 4-month-old young control group, *MC* 15-month-old control group, *CR* 15-month-old caloric restricted group. *Arrowheads* in panels (**a**)–(**c**) indicate the spiral ganglion regions. *Arrowhead* in panel (**d**) indicates normal neurons. *Arrowheads* in panels (**e**) and (**f**) indicate neurons with marked chromatin condensation, a morphological characteristic of apoptosis. MC mice displayed severe degeneration of spiral ganglion cells, decreased cell body size, and chromatin condensation. CR mice displayed no significant degeneration of spiral ganglion cells, showing that caloric restriction prevented cochlear degeneration. CR mice showed no significant cell shrinkage, but did display some chromatin condensation ((**c**) and (**f**)). Scale: 50 μm (*upper panel*), 100 μm (*lower panel*) (Courtesy of Dr. Yamasoba)

extended maximum lifespans when subjected to a long-term 20–50 % reduction in caloric intake without essential nutrient deficiency.

Someya et al. [18] observed the effects of caloric restriction on cochlear degeneration in mice. They restricted the caloric intake of experimental mice to 74 % that of control animals in early adulthood, and maintained this dietary regimen until the mice were 15 months of age. The mean weight of the 15-month-old caloric restriction mice was significantly lower than that of the 15-month-old control mice, but was not different from the mean weight of young control mice. ABR threshold measurements revealed that the young control mice exhibited normal hearing, whereas the 15-month-old control mice exhibited significant age-related hearing loss. In contrast, the 15-month-old caloric restricted mice displayed normal hearing.

The cochleae of the 15-month-old control mice showed the morphological characteristics of apoptosis, such as cell shrinkage and chromatin condensation in the spiral ganglion cells (Fig. 8.27b, e), indicating that apoptosis was associated with the development of presbycusis. The cochleae of the caloric restriction mice did not show cell shrinkage, but showed some chromatin condensation (Fig. 8.27c, f). The cochleae of young control mice showed no cell shrinkage or chromatin condensation (Fig. 8.27a, d).

Caloric restriction mice also showed a significant reduction in the number of TUNEL-positive cells and cleaved caspase-3-positive cells relative to the 15-month-old control mice. Microarray analysis revealed that caloric restriction down-regulated the expression of 24 apoptotic genes. Suppression of apoptosis by caloric restriction can prevent presbycusis.

References

1. Nomura Y, Kirikae I (1967) Innervation of the human cochlea. Ann Otol Rhinol Laryngol 76:57–68
2. Nomura Y, Kirikae I (1968) Presbyacusis. A histological-histochemical study of the human cochlea. Acta Otolaryngol 66:17–24
3. Gacek RR (1961) The efferent cochlear bundle in man. Arch Otolaryngol 74:690–694

4. Spoendlin H, Gacek R (1963) Electron microscopic study of the efferent and afferent innervation of the organ of corti in the cat. Ann Otol Rhinol Laryngol 72:660–686
5. Spoendlin H (1985) Anatomy of cochlear innervation. Am J Otolaryngol 6:453–467
6. Nomura Y (1976) Nerve fibers in the human organ of corti. Acta Otolaryngol 82:317–324
7. Louis ED, Yi H, Erickson-Davis C, Vonsattel JP, Faust PL (2009) Structural study of Purkinje cell axonal torpedoes in essential tremor. Neurosci Lett 450:287–291
8. Nomura Y, Kawabata I (1978) The pathology of sensory hairs in the human organ of corti, Scanning Electron Microscopy 1978/II. IITRI, Chicago, pp 417–422
9. Nomura Y, Kawabata I (1979) Loss of stereocilia in the human organ of corti. Acta Otorhinolaryngol 222:181–185
10. Schuknecht HF, Gacek MR (1993) Cochlear pathology in presbycusis. Ann Otol Rhinol Laryngol 102:1–16
11. Nomura Y (1970) Lipidosis of the basilar membrane. Acta Otolaryngol 69:352–357
12. Iurato S (1962) Functional implictions of the nature and submicroscopic structure of the tectorial membrane and basilar membrane. J Acoust Soc Amer 34:1386–1395
13. Iurato S (1967) Submicroscopic structure of the inner ear. Pergamon, Oxford
14. Mayer O (1920) Das anatomisches Substrat der Altersschwerhörighkeit. Arch Ohr Nas Kehlkopfheilk 105:1–13
15. Schätzle W, von Westernhagen B (1967) Lipidnachweis in der Cochlea. Pract Otorhinolaryngol (Basel) 29:75–84
16. Cogan DG, Kuwabara TK (1960) Aberrant lipogenesis. Nutr Rev 18:225–227
17. Lee CK, Klopp RG, Weindruch R, Prolla TA (1999) Gene expression profile of aging and its retardation by caloric restriction. Science 285:1390–1393
18. Someya S, Yamasoba T, Weindruch R, Prolla TA, Tanokura M (2007) Caloric restriction suppresses apoptotic cell death in the mammalian cochlea and leads to prevention of presbycusis. Neurobiol Aging 28:1613–1622

Anomalies

9

Abstract

This chapter discusses cochlear hyperplasia, hypophosphatasia, Alagille syndrome, Scheibe dysplasia, and Mondini dysplasia. Anomalies of the inner ear usually derive from arrested embryonic organ development. Cochlear hyperplasia results from excessive development of the organ of Corti and cochlear duct. Because the bony cochlea is normal in shape, the overdeveloped cochlear duct with the organ of Corti reverses at its apical end and heads backwards into the scala tympani, producing a mirror image of the organ of Corti. The case of hypophosphatasia described here showed immature ossification of the bony labyrinth with abnormal tissue formation in the lateral wall of the membranous cochlea. The parents of this patient were consanguineous and their sera showed low alkaline phosphatase activity. Alagille syndrome is a systemic malformation, in which the posterior semicircular canal shows a partial deficit. In cases of Scheibe dysplasia the bony labyrinth develops normally, but the cochleosaccular portion of the membranous labyrinth is dysplastic. Mondini dysplasia is relatively common, but no two cases are identical in detail.

Keywords

Alagille syndrome • Cochlear hyperplasia • Hypophosphatasia • Mondini dysplasia • Scheibe dysplasia

9.1 Cochlear Hyperplasia

9.1.1 Introduction

Various anomalies may be seen in the cochlea of humans and other animals. Jackler et al. [1] classified congenital malformations of the cochlea as follows:

1. Complete labyrinthine aplasia (Michel deformity)
2. Cochlear aplasia: no cochlea, normal or malformed vestibule and semicircular canals
3. Cochlear hypoplasia: small cochlear bud, normal or malformed vestibule and semicircular canals
4. Incomplete partition: small cochlea with incomplete or no interscalar septum, normal or malformed semicircular canals
5. Common cavity: cochlea and vestibule form a common cavity without internal architecture; normal or malformed semicircular canals

These malformations result from arrested maturation during one of the stages of inner ear embryogenesis. Other malformations may result from aberrant development.

9.1.2 Cochlear Hyperplasia

In a series of experiments using guinea pig cytomegalovirus (GPCMV), Nomura et al. [2] found a strange cochlear anomaly: hyperplasia of the organ of Corti with the scala media. They inoculated GPCMV into the cochlea of a female guinea pig through the round window membrane. Shortly after inoculation the animal became pregnant and 2 months later bore a litter of four. One of the offspring showed an anomalous right cochlea. The bony cochlea had normal coils. The organ of Corti, however, did not end at the apex, but together with the scala media continued backwards into the scala tympani. Graphic reconstruction revealed that the cochlea

Y. Nomura, *Morphological Aspects of Inner Ear Disease*, DOI 10.1007/978-4-431-54204-9_9,

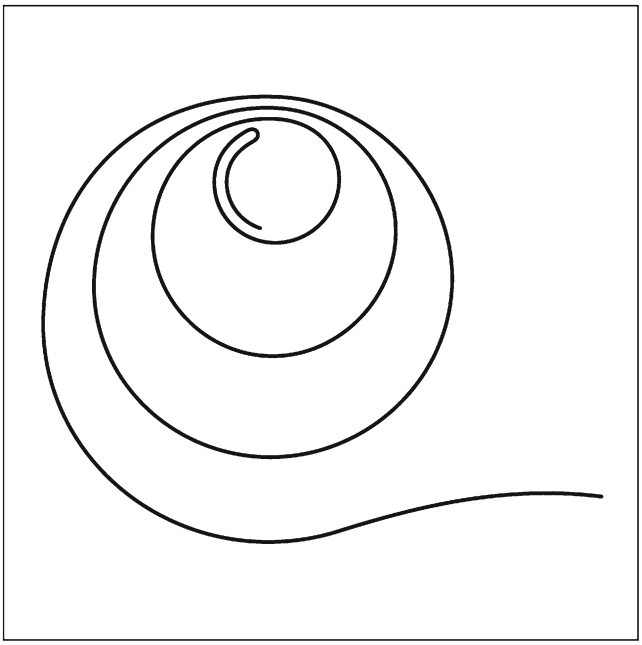

Fig. 9.1 Graphic reconstruction of the cochlear coils showing hyperplasia of the organ of Corti. Of a total length of 24 mm, the excessive organ of Corti occupies 1 mm [2]

had a total length of 24 mm, including an overgrowth of 1 mm (Fig. 9.1). Therefore, the organ of Corti showed a symmetrical mirror image, sharing a common scala tympani at the apical turn (Fig. 9.2). The inverted organ of Corti and scala media intruded into the space normally occupied by the scala tympani. The outer hair cells seemed excessive in number and the Deiters' cells beneath these hair cells were either hypoplastic or absent (Figs. 9.3 and 9.4). The limbus spiralis, inner sulcus, osseous spiral lamina, and nerve fibers were hypoplastic in the inverted portion. The inner ear structures other than the cochlea were normal.

Merchant and Nadol [3] reported a similar case from the human temporal bone collection at the University of Zurich. The bone came from an 18-year-old man with congenital syphilis, who died of unknown causes. In his left ear, the organ of Corti of the shortened apical turn was inverted so that its cuticular plate faced the cuticular plate of the second turn. The limbus spiralis was present. The normal and inverted portions shared a common tectorial membrane. Hair cells were present. The stria vascularis was hypoplastic in the region of the anomaly. In this case, the inverted organ of Corti shared the scala media of the second turn, whereas in the guinea pig, the scala media itself was inverted, together with all other constituents.

Some viruses are known to cause anomalous development of the inner ear. These include *Herpesviridae*, *Togaviridae*, and *Bunyaviridae*. A virus may attack the anlage, killing or degenerating part of it. Because the anlage is the first step of organ formation, cessation of cell division or decreased rate of cell division occur and cause further changes in the anlage. Malformations are usually due to cessation of development or partial loss of the organ.

In contrast to the usual developmental anomalies, the cochlea described above is characterized by excessive development of the cochlear duct, which returned at the apex with the scala vestibuli down into the space normally occupied by the scala tympani. Perhaps in this case the signals to create the normal organ of Corti were not turned off, resulting in its hyperplasia. Whether or not GPCMV induced mutation in the gamete is uncertain.

9.2 Hypophosphatasia

9.2.1 Introduction

Hypophosphatasia, named by Rathbun in 1948 [4], is a rare genetically determined metabolic disease characterized by defective bone and tooth mineralization. The disease results from mutations in the liver/bone/kidney alkaline phosphatase gene encoding tissue-nonspecific alkaline phosphatase. The diagnosis is based on laboratory assays and DNA sequencing of the *ALPL* gene [5].

Hypophosphatasia is characterized by (1) abnormal mineralization of bone (2) lowered serum and tissue alkaline phosphatase activity, and (3) increased urinary excretion of phosphoethanolamine. Age of onset varies considerably from before birth to adulthood. The earlier the onset of pathology, the more severe the lesions. There is no curative treatment for hypophosphatasia.

Fraser [6] divided hypophosphatasia cases into three groups, based on the estimated time of development of demonstrable bone lesions:

Group 1: Infants with lesions present at birth or within the first 6 months of life

Group 2: Children with lesions gradually becoming apparent after the age of 6 months

Group 3: Individuals with lesions appearing in adulthood

9.2.2 Case Report

9.2.2.1 Clinical Findings

Nomura and Mori [7] reported a case of hypophosphatasia belonging to Group 1 of Fraser's classification.

A full term girl was born to consanguineous parents. The delivery was normal. The baby weighed 2,140 g at birth and died 1 h later. Her 29-year-old mother had no obvious disturbances in the course of pregnancy. Examinations had indicated an uneventful pregnancy. The fetal outline, however, could not be identified and radiography had failed to show the skull and skeleton.

Fig. 9.2 Mirror image of the organ of Corti [2]. *Arrow* indicates the common narrow scala tympani. The inverted scala media together with the scala vestibuli lies in the space normally occupied by the scala tympani. Nerve fibers are fewer in number toward the inverted organ of Corti (original ×2.5)

Autopsy revealed the following findings:

1. The baby had stunted extremities: arms and legs measured 5 cm and 6 cm, respectively. No malformations were found in the face, head, or neck.
2. Bones were soft. Histology found inhibited calcification of the cartilaginous bone. The epiphyses were irregular and thick. These findings were similar to those of rickets.

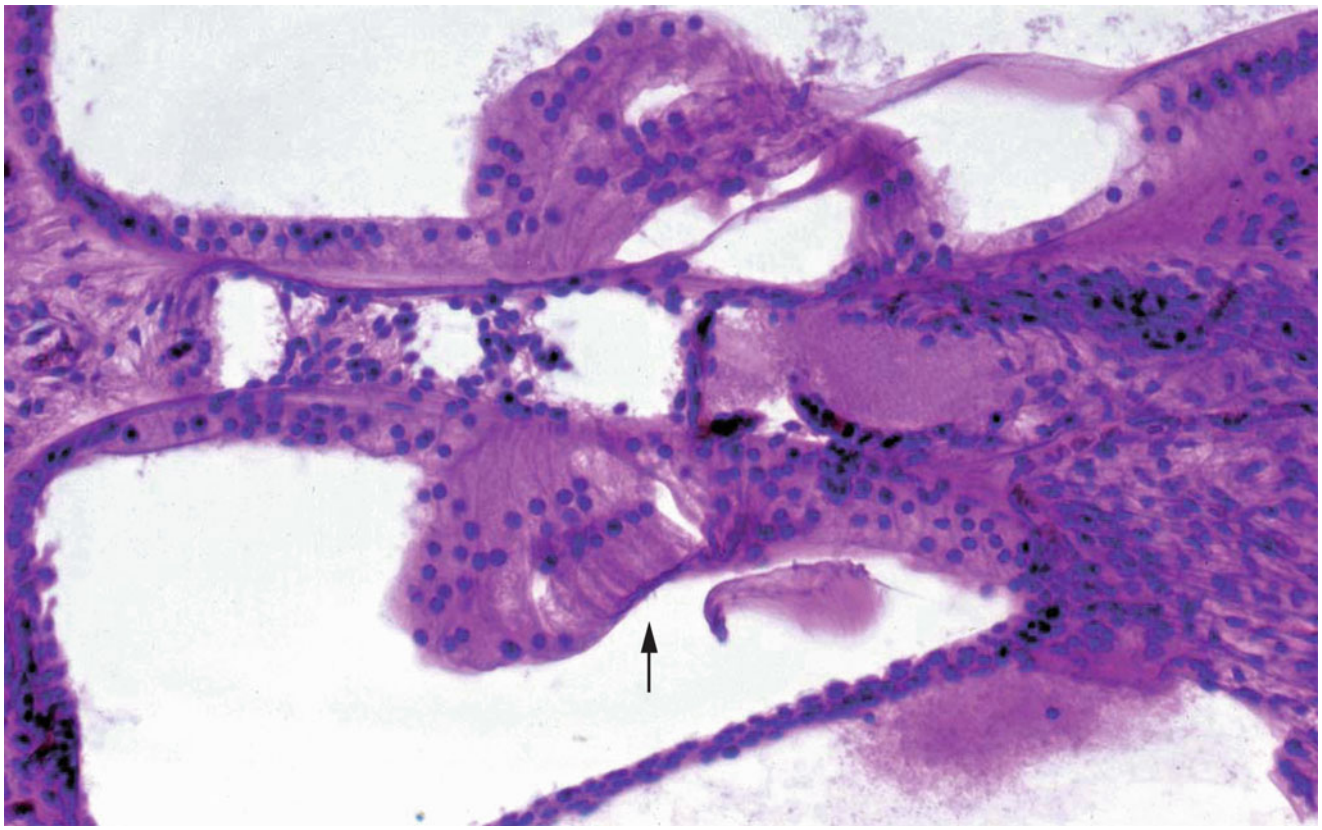

Fig. 9.3 Higher power view of Fig. 9.2. Excessive outer hair cells are present (*arrow*). The inner sulcus is absent. The osseous spiral lamina and nerve fibers are hypoplastic. The inverted limbus is not well developed. The detached tectorial membrane shows small projections toward the limbus. The stria vascularis is atrophic (original ×16)

3. The skull was peculiarly soft.
4. There was enamel hypoplasia of the deciduous teeth.
5. The scapulae were partly ossified.
6. The lungs showed marked dystelectasis.

Serum alkaline phosphatase could not be measured because of the infant's early death. The enzyme levels were low in her parents (father 1.5 units/100 mL, mother 2.0 units/100 mL, normal 3–13 King-Armstrong units/100 mL).

9.2.2.2 Histopathology of the Temporal Bones

Temporal bones were removed and submitted for histopathological study. The bones were easily severed from the skull with scissors. Decalcification was not necessary for temporal bone sectioning. The specimens were embedded in celloidin and sliced into serial sections 20 μm thick.

The Middle Ear

The malleus, incus, and stapes were present as usual in the middle ear cavity, which was occupied by mesenchymal tissue. The ossicles were osteoid. Bone marrow was also present.

The Inner Ear

The otic capsule was composed of red (eosin) osteoid tissue and bone marrow. The membranous labyrinth of the pars superior and pars inferior was well developed. The organ of Corti appeared fairly normal. The populations of hair cells and ganglion cells were normal.

The spiral ligament showed a peculiar change. A portion of the spiral ligament underlying the stria vascularis was densely stained blue by hematoxylin (Fig. 9.5). This seemed to be calcified tissue, with an occasional blood vessel running through it (Fig. 9.6). The tissue was continuous and most striking from the upper basal turn to the upper middle turn.

In the left cochlea the densely staining tissue was continuous for 9.4 mm from the 10 mm area of the basal turn. In the right ear the tissue extended for 9.6 mm from the 8 mm area. The total lengths of the left and right cochleae were 28.5 and 28.3 mm, respectively. The tissue lay beneath the stria vascularis, however, an amorphous tissue zone was present between the stria and the blue haematoxylin tissue. Various staining methods were employed, revealing the tissue to be

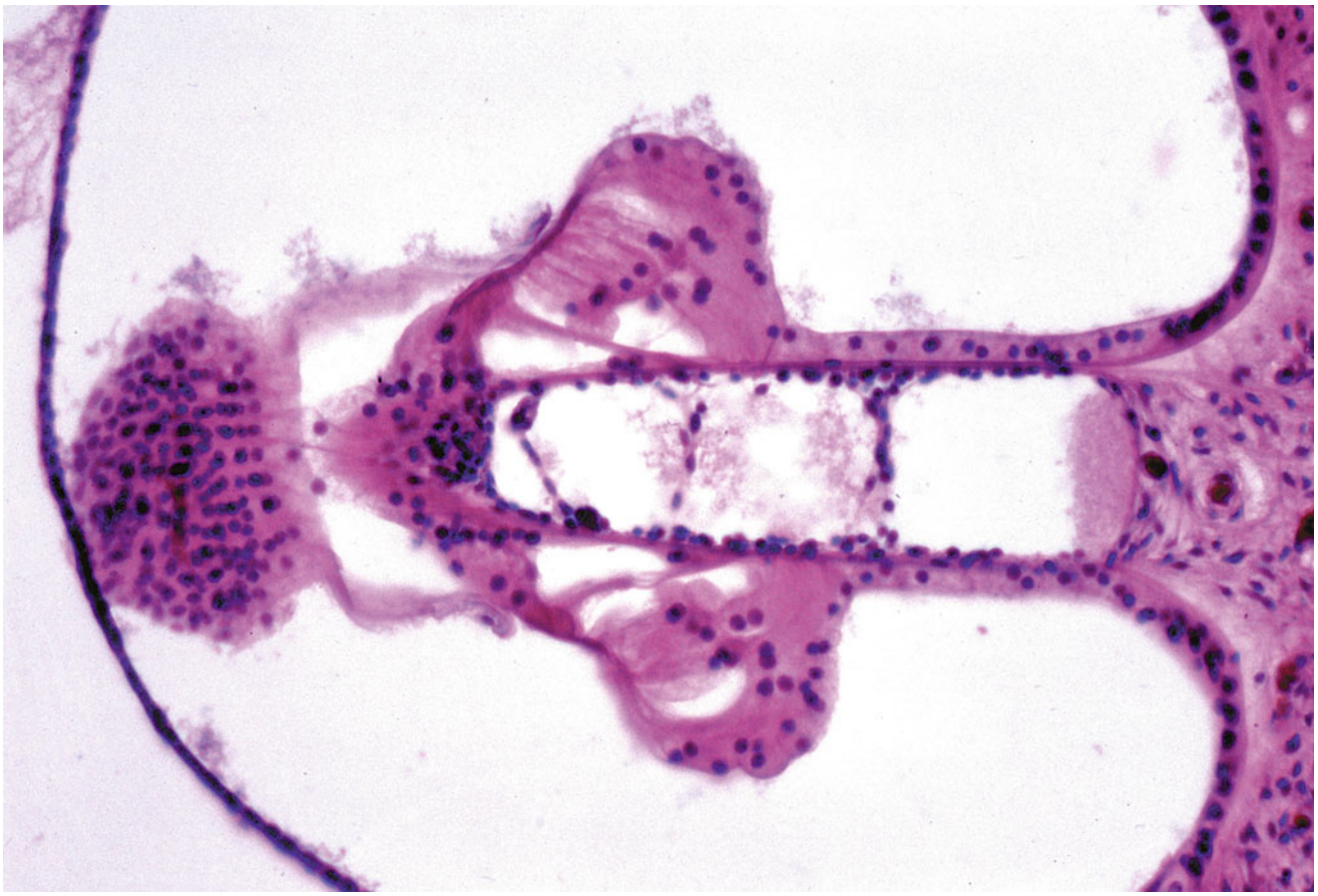

Fig. 9.4 Mirror image of the organ of Corti. Deiters' cells beneath the outer hair cells are partly missing. Cellular bridges in the common scala tympani connect the upper and lower tympanic lamella. No nerve fibers are observed in the organ of Corti (original ×16) [2]

PAS positive, blue by Azan, Hale's colloid iron negative, and with no metachromasia by toluidine blue. This material was interpreted to be either calcification or hyaline degeneration. Varying amounts of amorphous substance existed between this tissue and the stria vascularis (Fig. 9.7).

Hypophosphatasia is caused by mutations in the *ALPL* gene. This gene codes for an enzyme called alkaline phosphatase, which plays an essential role in bone and tooth mineralization. Mutations in the *ALPL* gene lead to the production of an abnormal version of alkaline phosphatase, which cannot function in the normal process of mineralization.

It is generally thought that elevation of serum alkaline phosphatase activity in the absence of liver disease reflects osteoblastic activity. Enzyme levels are highest during the most rapid growth phase and become abnormally elevated when osteoblast activity increases in such bone diseases as rickets, hyperparathyroidism, and Paget's disease. Phosphoethanolamine is considered the true substrate for alkaline phosphatase.

Although serum alkaline phosphatase and phosphoethanolamine levels were not determined in this case, the following factors made it possible to diagnose hypophosphatasia: (1) abnormal mineralization of bone as evidenced by radiography (2) histologically-demonstrated bony changes similar to rickets, though congenital rickets was ruled out, and (3) consanguineous parents showing low levels of serum alkaline phosphatase activity.

The histologic lesions of hypophosphatasia are characterized by two abnormalities [6]: (1) disturbance in the normal calcification process of cartilage and bone, (2) excessive production and disordered arrangement of preosseous cartilage and of osteoid. It has been stressed that the lesions of hypophosphatasia are morphologically indistinguishable from those of simple rickets unless special stains are performed to demonstrate phosphatase.

As far as the otic capsule is concerned, typical changes in rickets are confined to the periosteal layer with newly formed bone lamellae. In marrow spaces the newly formed bone lamellae are poorly calcified and show a red-eosinophilic osteoid border. Osteoid is the unmineralized, organized portion of the bone matrix. The endochondral layer remains normal unless active bone resorption occurs. The inner ear remains normal.

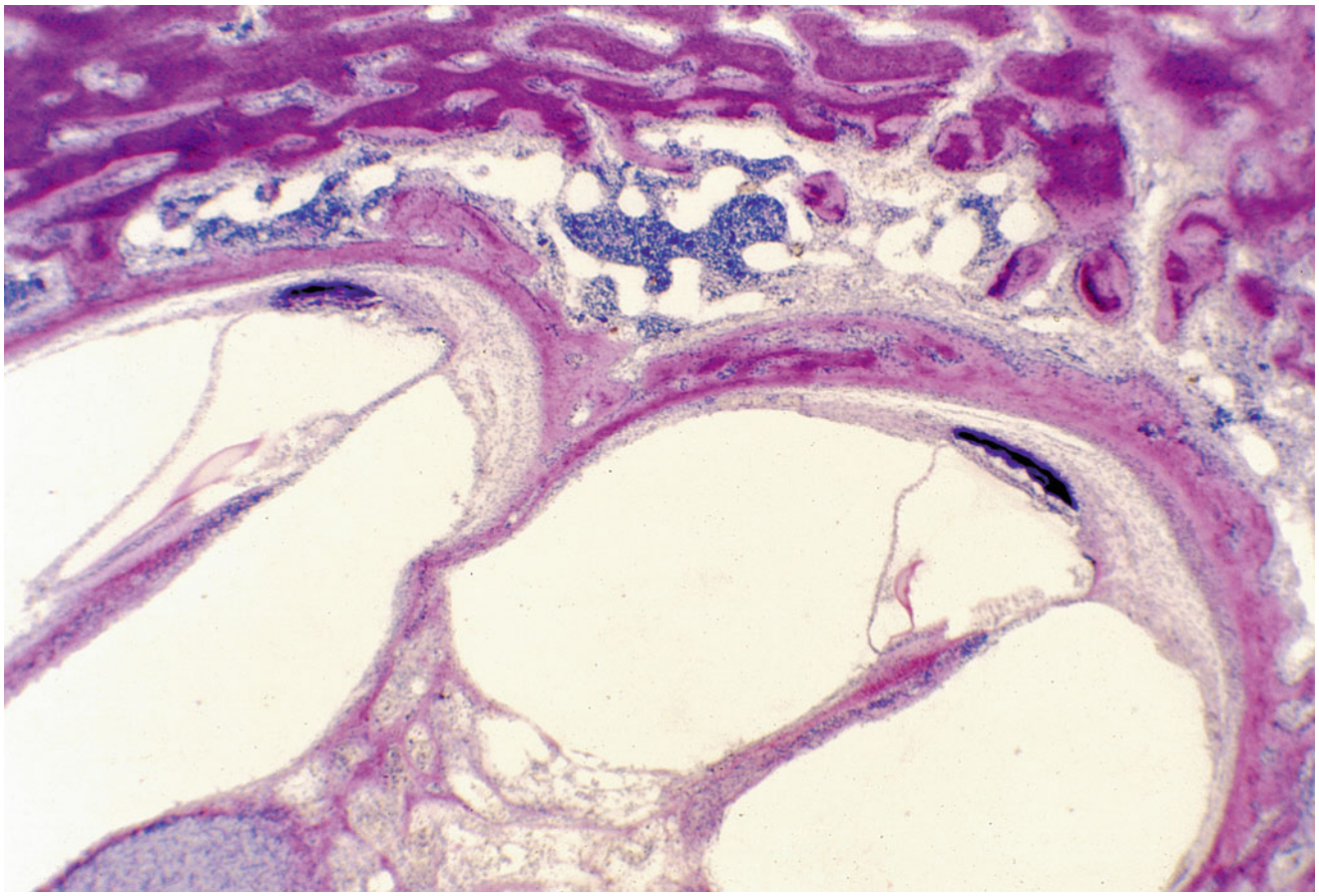

Fig. 9.5 Temporal bone from a patient with hypophosphatasia [7]. Between the stria vascularis and the spiral ligament, there is tissue densely stained by haematoxylin. The otic capsule is red-eosinophilic osteoid. The organ of Corti and dendrites in the osseous spiral lamina are normal. HE staining (original ×2.5)

The PAS positive tissue in the spiral ligament in this case is strange and might be pathognomonic of hypophosphatasia. PAS positive material in the stria vascularis has occasionally been reported [8–11] and has been interpreted as hyaline cartilage or calcification. The present case did not show such changes in the stria. The PAS positive tissue in the spiral ligament was not hyaline, but was possibly calcified tissue.

Dr. Schuknecht examined the specimen and observed that the region of the spiral ligament underlying the stria vascularis showed changes consistent with strial atrophy. Rauch [12] described strong alkaline phosphatase activity in the spiral ligament of guinea pig embryos. His histochemical study demonstrated that the enzyme was abundant in this particular perilymph-endolymph junction area. The finding of abnormal tissue in the spiral ligament was difficult to explain in relation to alkaline phosphatase. This tissue may be comparable to pseudocalcinosis of the brain.

9.3 Alagille Syndrome

9.3.1 Phylogenesis of the Semicircular Canal

Phylogenetically, a single semicircular canal appeared in the hagfish (*Myxinoidea*), an eel-like animal, during the Cambrian Period some 530 million years ago (Fig. 9.8) [13]. The single canal has two ampullae and a macula communis. It is in the hagfish that the first true vestibular apparatus developed.

The lamprey (*Petromyzontida*) shows higher development of the inner ear, with two vertical canals and three ampullae. The vestibulum has become more complex than in the hagfish (Fig. 9.9a, b). The hagfish and lamprey belong to the order Cyclostomata. The former are found only in salt water, and the latter in both salt and fresh water. Both have cartilaginous capsules.

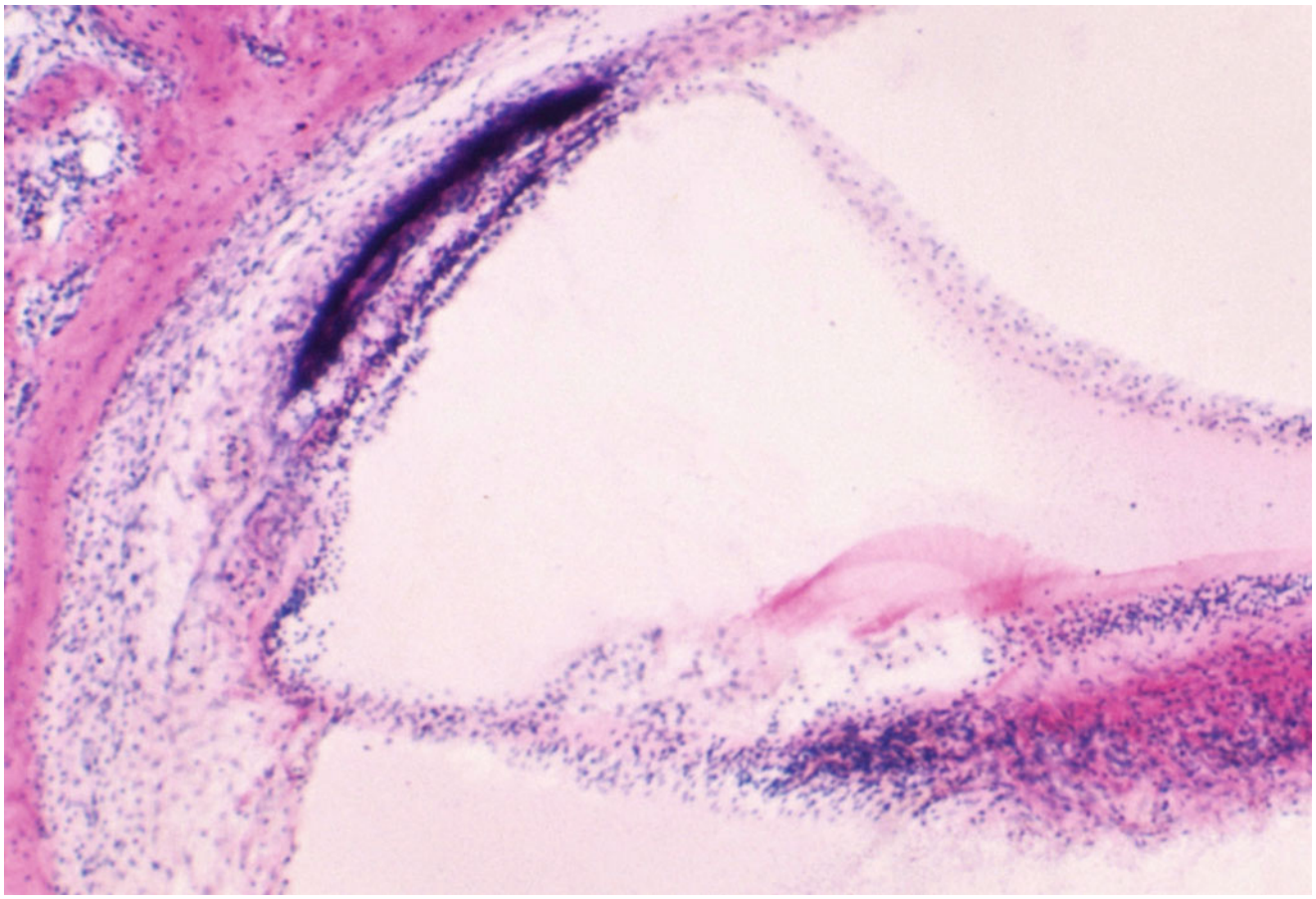

Fig. 9.6 High power view of the stria vascularis and spiral ligament. The stria vascularis is thin. The densely stained tissue is behind, but not directly bordering, the stria. There is hypocelluar area between them. A capillary runs through the densely stained tissue. The spiral ligament contains a hypocellular zone. HE staining (original ×6.5)

Three semicircular canals appeared in fish that must have developed in the Devonian Period of the Paleozoic Era, about 350 million years ago. The Japanese eel (*Anguilla japonica*) has three canals. The general arrangement of the membranous labyrinth in all bony fishes is very similar. An extremely large utricule is found in the lungfish (*Protopterus annectens*) (Fig. 9.10). In the sturgeon (*Acipenser sturio*) the recessus utriculi is much smaller, as is the saccule. The European perch (*Perca fluviatilis*) possesses an elongated sinus superior utriculi, a small main utricular body, and a large saccule (Fig. 9.11). The sinus superior utriculi is a part of the utricle, and a predecessor of the crus commune. The lateral canal appeared later and is shorter than the two vertical canals [14].

The membranous labyrinth of the frog (amphibian) and dove (avian) are shown in Figs. 9.12 and 9.13. The hearing organ begins its evolution. The pars basilaris makes its appearance in the amphibian ear. In birds the pars basilaris has elongated as the membrana basilaris, which becomes so extensive in mammals that it needs to form a spiral to find space. The very ancient balance organ reached perfection in primitive animals, whereas the hearing organ has continuously evolved along with mammals, keeping pace with the needs of the various life forms [14].

The entire labyrinth is exposed equally to aging, metabolic disturbances, and viral attack, while the phylogenetically older pars superior (utricle and canals) is rarely affected [15].

The human semicircular canals (SCC) begin development during the sixth week of embryonic growth [16]. The budding of the SCC forms a semicircular evagination from the vestibular anlage. The central protrusion adheres, leaving a peripheral semicircular tube. When this central adhesion fails to occur, SCC dysgenesis results. SCC aplasia arises from a failure in the development of the vestibular anlage before the sixth week.

Siebenmann stated that gross malformation of the semicircular canals can occur with or without other anomalies.

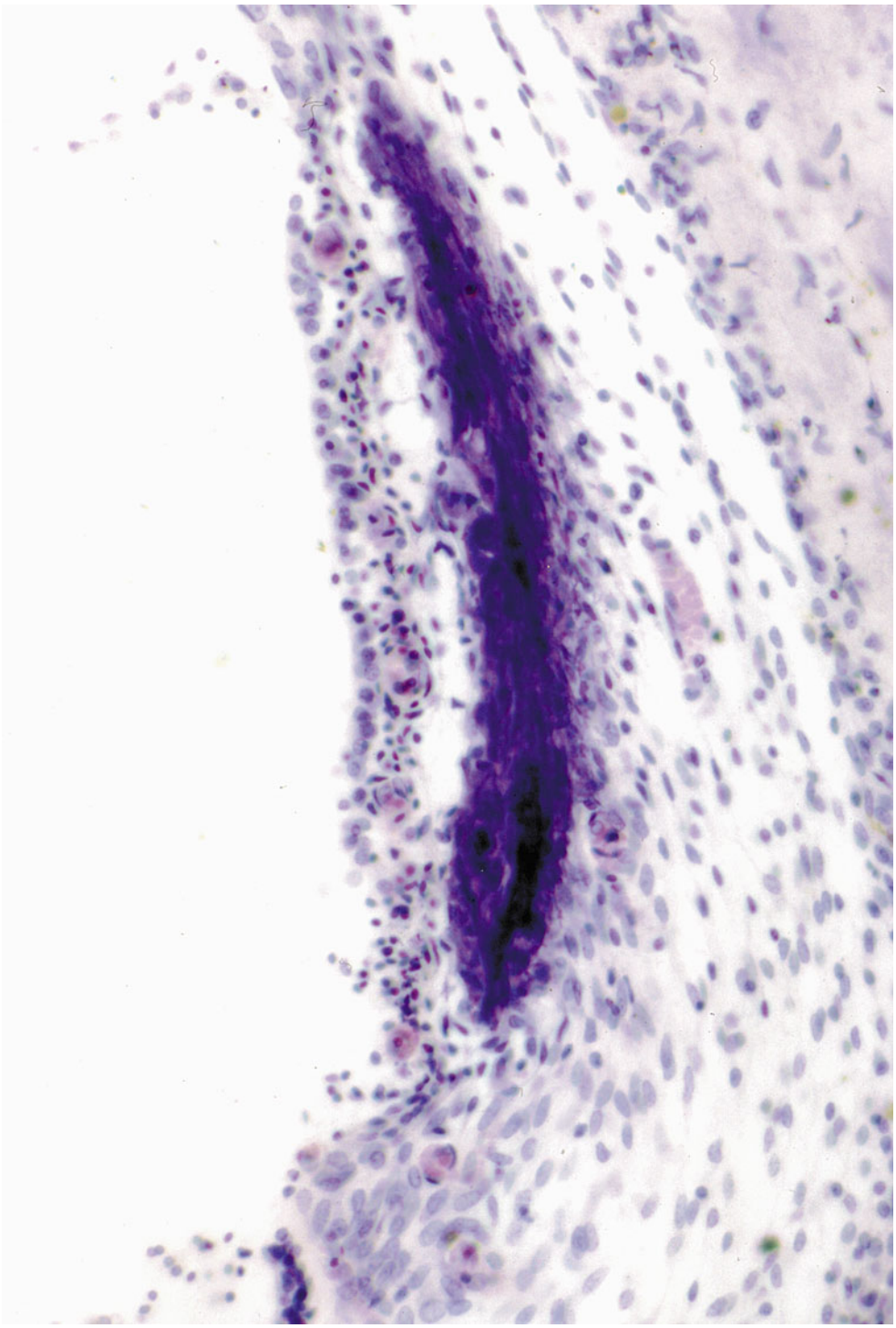

Fig. 9.7 High power view of the densely stained tissue [7]. There is a lucent area between the stria vascularis and the blue-stained tissue. The stria vascularis and spiral prominence seem underdeveloped, although several capillaries are observed in cross-section. The spiral ligament is hypocellular. HE staining (original ×16)

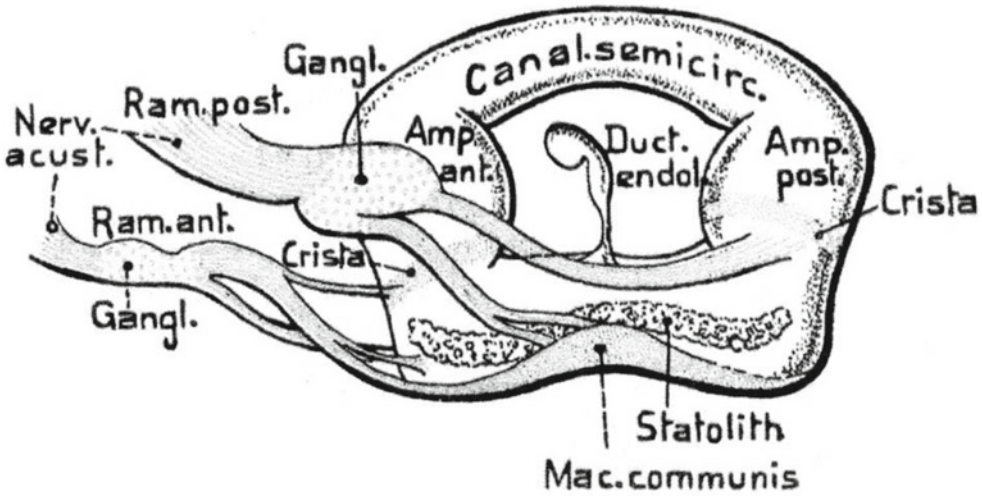

Fig. 9.8 Hagfish—left membranous labyrinth. From Bütschli after Retzius [13]

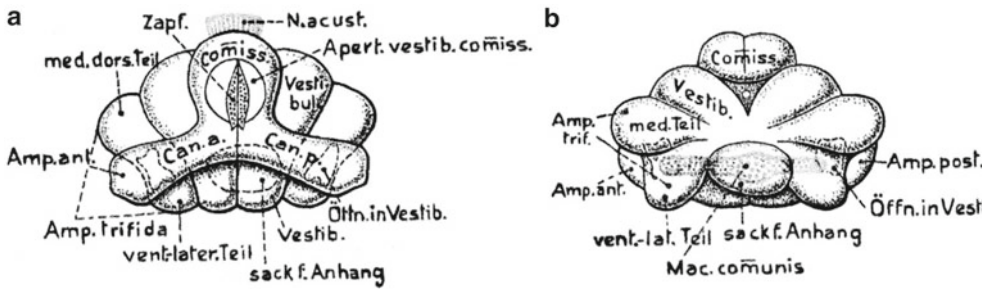

Fig. 9.9 Lamprey—left membranous labyrinth. (**a**) Dorsal view, (**b**) ventral view. From Bütschli after Retzius [13]

Among the three semicircular canals, the most frequently involved is the lateral canal [3, 17]. Anomalies of the semicircular canals are found in patients with CHARGE syndrome, trisomy 13 and 18, Waardenburg syndrome type II, and Alagille syndrome.

9.3.2 Anomalies of the Semicircular Canal

9.3.2.1 CHARGE Syndrome

CHARGE syndrome, first described independently by Hall [18] and Hittner et al. [19] in 1979, is an acronym for a complex constellation of anomalies: coloboma, heart defects, choanal atresia, mental retardation, genitourinary hypoplasia and ear defects. Additional anomalies have been reported, including facial palsy or asymmetry, esophageal and laryngeal abnormalities, renal malformations, and facial clefts.

Morimoto et al. [20] studied CT images of 13 patients with CHARGE syndrome, and found that the lateral, superior, and posterior SCCs were absent in 25 of 26 patients. Murofushi et al. [21] described five patients with CHARGE syndrome. All six semicircular canals were aplastic in each of the patients. The authors confirmed absent vestibular function with the presence of bony cochlea. These findings are probably pathognomonic of CHARGE syndrome with preservation of some cochlear function.

9.3.2.2 Alagille Syndrome

Alagille syndrome is an autosomal dominant disorder that affects the liver (paucity of intrahepatic bile ducts), heart, kidney, and other body systems [22]. Mutations in the *JAG1* and *NOTCH2* genes cause the syndrome. The estimated incidence of Alagille syndrome is 1:70,000, according to the Genetic Home Reference of the U.S. Library of Medicine.

Patients with Alagille syndrome show partial absence of the posterior semicircular canal. Koch et al. [23] reviewed the imaging findings and embryology of the semicircular canals, and suggested that this abnormality was specific to patients with Alagille or Waardenburg syndromes.

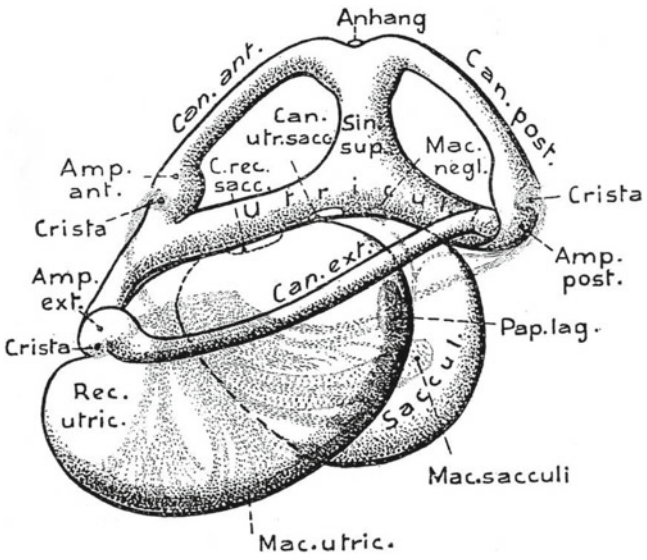

Fig. 9.10 *Protopterus annectens*——lungfish Left labyrinth, lateral view From Bütschli after Retzius [13]

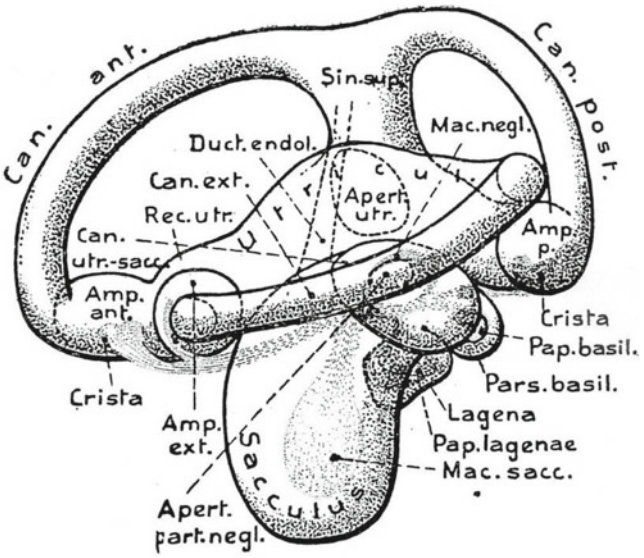

Fig. 9.12 *Rana esculenta*——common water frog. Left labyrinth. From Bütschli after Retzius [13]

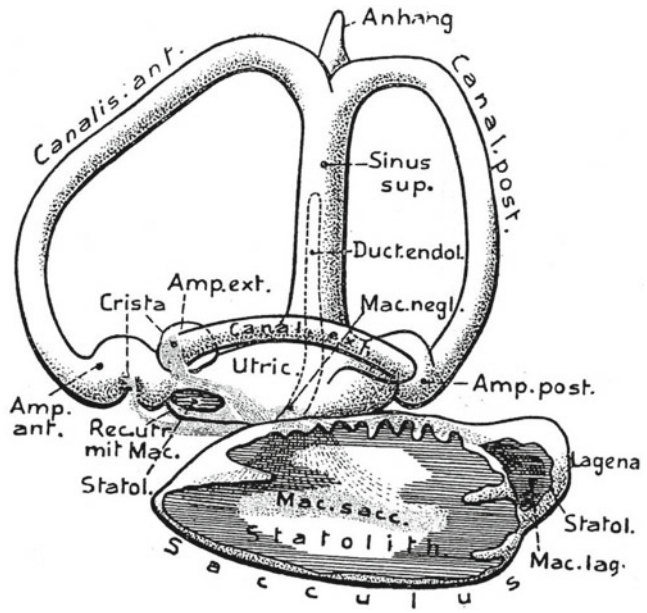

Fig. 9.11 *Perca fluviatilis*——European perch. Left labyrinth, lateral view *Mac. negl.*, macula neglecta. From Bütschli after Retzius [13]

Okuno et al. [24] studied six temporal bones from four individuals with Alagille syndrome, aged 4 months and 3, 6, and 7 years. They found that both the bony and membranous structures of the posterior semicircular canal were partially or totally absent in all cases (Fig. 9.14). In three ears, the structures of the superior semicircular canal were also partially absent. The lateral semicircular canal was normal in all cases. The cochlea was shortened in only one case (patient 1).

One of the cases (patient 2) showed a strange anomaly: the ampullated and nonampullated ends of the posterior canal were absent, but an isolated pouch containing the membranous labyrinth remained (Fig. 9.15).

In addition to the SCCs, the cochlear aqueducts, ossicles, and subarcuate fossae showed anomalies. Inflammation of various degrees was found in the middle ear in more than half of the temporal bones.

9.4 Scheibe Dysplasia

9.4.1 Introduction

Scheibe dysplasia was first described in a paper by Arno Scheibe of Munich in 1892 [25]. He reported the histopathological findings from the case of a 47-year-old deaf man. Marked dysplasia was observed in the membranous cochlea and saccule. The cochlear nerve and inferior division of the vestibular nerve were also hypoplastic. The utricle and semicircular canals were normal. The superior division of the vestibular nerve was preserved.

Because histopathologic findings in Scheibe dysplasia show changes limited to the pars inferior, cochleosaccular dysplasia is another commonly used term for the disorder. One of the characteristic findings is the presence of lacunae in the modiolus, empty areas in Rosenthal's canal and the osseous spiral lamina (Fig. 9.16). Some atrophic spiral ganglion cells remain attached to the medial-inferior parts of the canal. The organ of Corti is rudimentary or absent. The stria vascularis is aplastic with cyst-like structures. Reissner's membrane is collapsed and may be indiscernible.

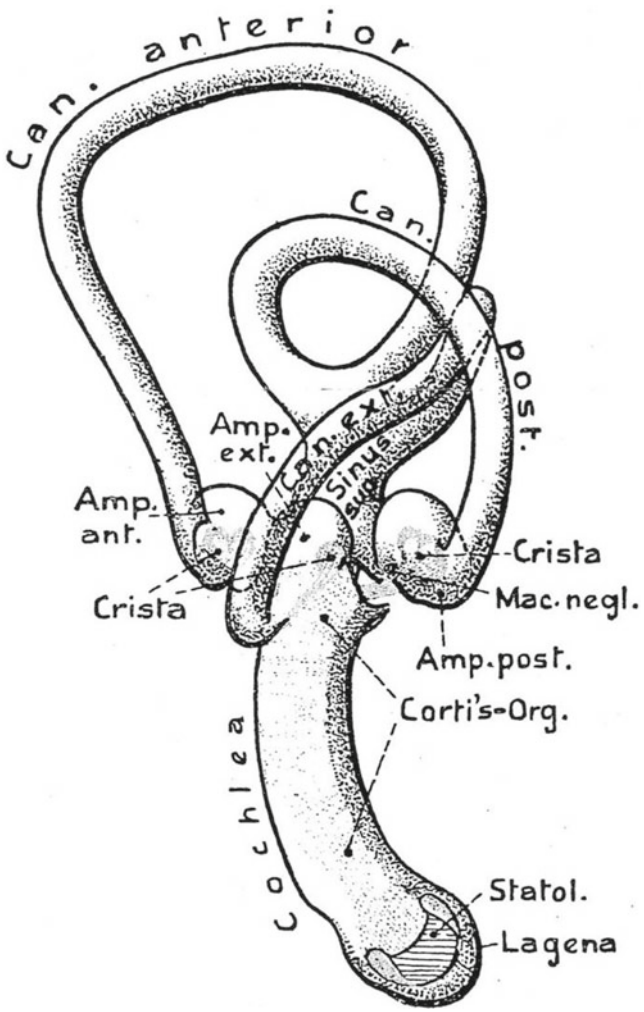

Fig. 9.13 *Columba domestica*——domestic pigeon Left labyrinth. From Bütschli after Retzius [13]

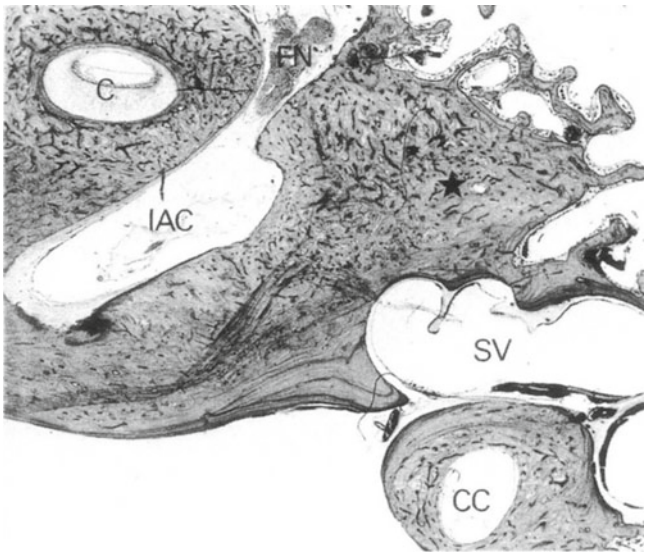

Fig. 9.14 Horizontal section through the right ear of patient 1 (aged 6 years). The ampullated end of the superior semicircular canal is missing (*star*). *C* cochlea, *CC* crus commune, *FN* labyrinthine portion of the facial nerve, *IAC* internal auditory canal, *SV* large vein in the subarcuate fossa. HE stain (original ×13.5) [24]

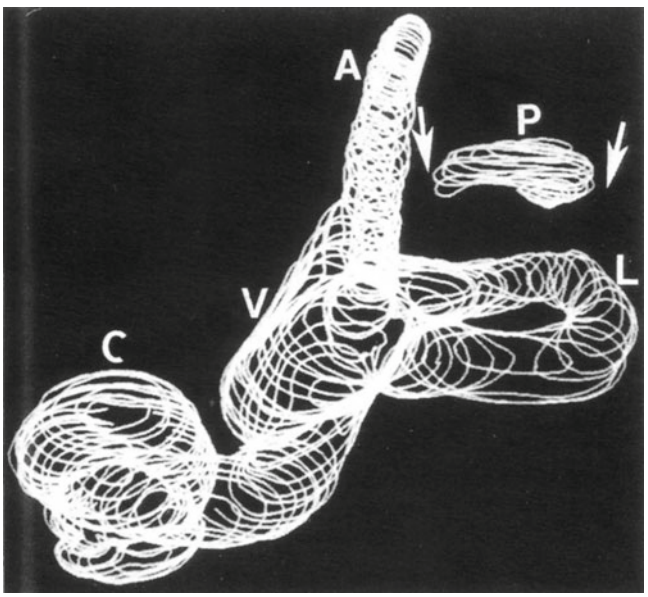

Fig. 9.15 Computer-aided three-dimensional reconstruction of the bony labyrinth of the left ear of patient 2 (aged 4 months), viewed from the anterolateral superior direction. Both the ampullated and nonampullated ends (*arrows*) of the posterior semicircular canal (*P*) were absent. The canal thus appears as a small, isolated, doubly blind pouch. No distinct anomalies were present in other parts of the bony labyrinth. *A* superior semicircular canal, *C* cochlea, *L* lateral semicircular canal, *V* vestibule [24]

9.4.2 Dysplasia and Degeneration

Schuknecht et al. [15] attributed cochleosaccular degeneration to various causes, including genetically inherited anomalies, viral labyrinthitis, and aging. Nadol and Burgess [26] described "Scheibe dysplasia" or "cochleosaccular dysplasia" as disordered development causing congenital deafness. In contrast, the term "Scheibe degeneration" or "cochleosaccular degeneration" refers to postnatal degeneration of a normally developed inner ear, causing progressive sensorineural hearing loss.

9.4.3 Case Report [27]

The following histopathological findings were from an 85-year-old deaf woman who died of rectal cancer.

The inner ears showed essentially similar findings bilaterally. There was no abnormality in the bony labyrinth. The membranous cochlea and saccule showed extensive pathology (Fig. 9.17). The lengths and number of cochlear turns were normal. The organ of Corti was either missing or rudimentary.

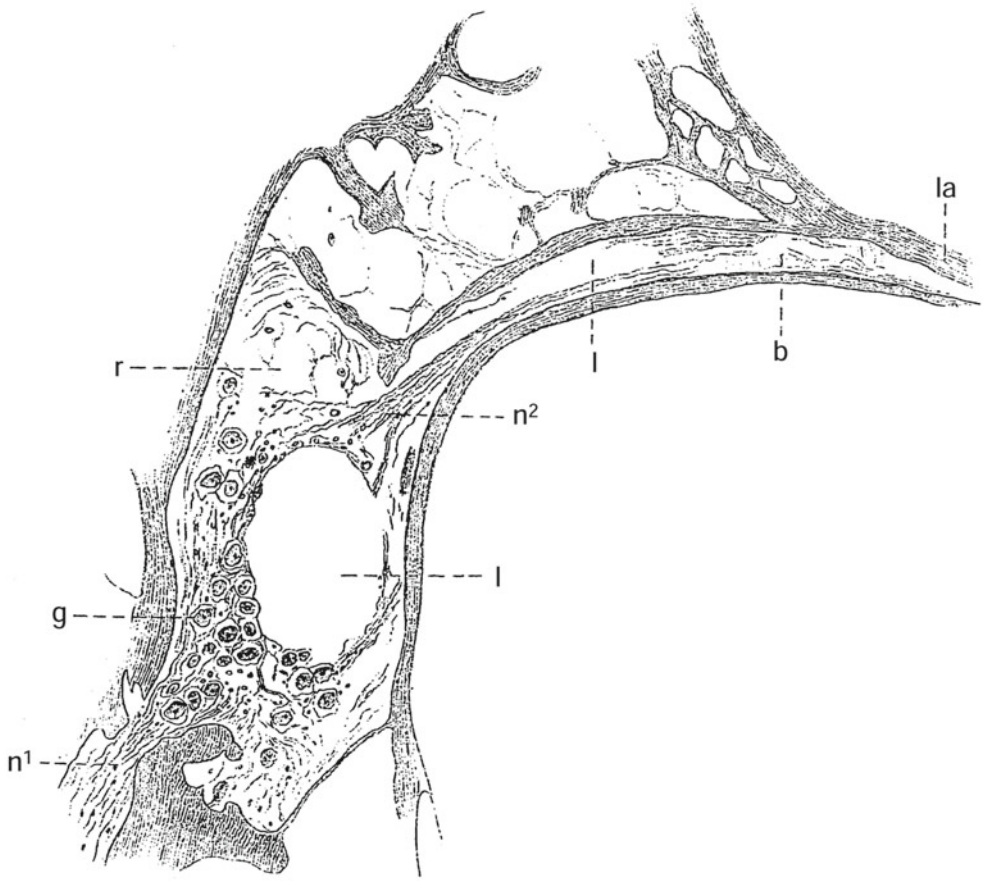

Fig. 9.16 Scheibe's original figure. *l* lacuna, *r* Rosenthal's canal, *la* osseous spiral lamina, *g* spiral ganglion cells, n^1 entering nerve fibers, n^2 departing nerve fibers, *b* connective tissue [25]

Structures of the utricle and semicircular canals were normal, although age-related changes were recognized.

9.4.3.1 The Left Labyrinth

In the left cochlea, there was a basophilic, round, lamellated mass at the location of the organ of Corti in the area 20 mm from the basal end (Fig. 9.18). The cochlear duct was collapsed. An extremely thin Reissner's membrane covered a small number of otoconia lying on the limbus, tectorial membrane, and rudimentary organ of Corti, except in the lower basal turn (Figs. 9.19 and 9.22).

The stria vascularis was aplastic and contained cyst-like structures with eosinophilic colloidal inclusions. There were one to four cysts within the aplastic stria vascularis. The contents of the cysts were PAS positive and stained red with Azan staining method (Figs. 9.20 and 9.21). The cysts seemed to be covered by thin Reissner's membrane. Every section contained cysts, forming ridges on and/or within the aplastic stria vascularis. There was pronounced epithelial atrophy in the external sulcus. The spiral ligament was sponge-like in appearance (Fig. 9.22). The limbus showed a loss of cellular elements. The tectorial membrane was disintegrated, with a portion resting on the internal sulcus, which had no epithelial lining.

The modiolus appeared empty because of the absence of nerve fibers. Rosenthal's canal was occupied by lacunae, which were lined by a few atrophic neurons and a thin membrane with scattered nuclei of connective tissue (Fig. 9.23). The blood vessels in the modiolus were sparse.

The saccular wall was collapsed onto the otolithic membrane except in the reinforced area. However, there was no sensory epithelium beneath the otolithic membrane. Several round masses, similar to those observed in the stria vascularis, were noted on and under the disintegrated otolithic

Fig. 9.17 The organ of Corti, cochlear nerve, and Reissner's membrane are not seen in this photograph. Cysts are present in the aplastic stria vascularis of the upper turn. Right ear [27]

membrane (Fig. 9.24). The utricle and cristae of the semicircular canals were normally shaped, but the neuroepithelia were atrophic, with marked loss of nerve fibers in the utricular and ampullary nerves. The subepithelial tissue of the utricular macula was atrophic (Fig. 9.25).

The endolymphatic duct and sac contained masses similar to those observed in the stria vascularis (Fig. 9.26). The utriculo-endolymphatic valve was normal.

9.4.3.2 The Right Labyrinth

The otolithic membrane was absent in the saccule, but atrophic sensory epithelium was preserved. The utricle and cristae of the semicircular canals were essentially normal in structure, although the neuroepithelia and their nerve fibers showed age-related changes. Dark cell areas were present.

Other parts of the inner ear showed changes similar to those of the left side.

9.4.4 Comment

It is hard to estimate the original structures of the inner ear from the temporal bones in this particular case, because pathologic changes were modified by aging. The changes were restricted to the membranous inner ear of the pars inferior. Scheibe dysplasia is the most common deformity in deaf children with radiographically normal inner ears.

Various changes have been reported in the stria vascularis in Scheibe dysplasia. In Scheibe's case, a ridge-like elevation was present with a broad base on the stria, higher than the spiral prominence. This consisted of cells, pigment, and vessels, with a few fissures between them. In general, the stria vascularis may be absent and replaced by flat epithelium or hyaline masses. These masses have been described as "colloid" or "mucoid" [28]. According to Buch and Jorgensen [8], colloid formation in the stria results from secretory or meta-

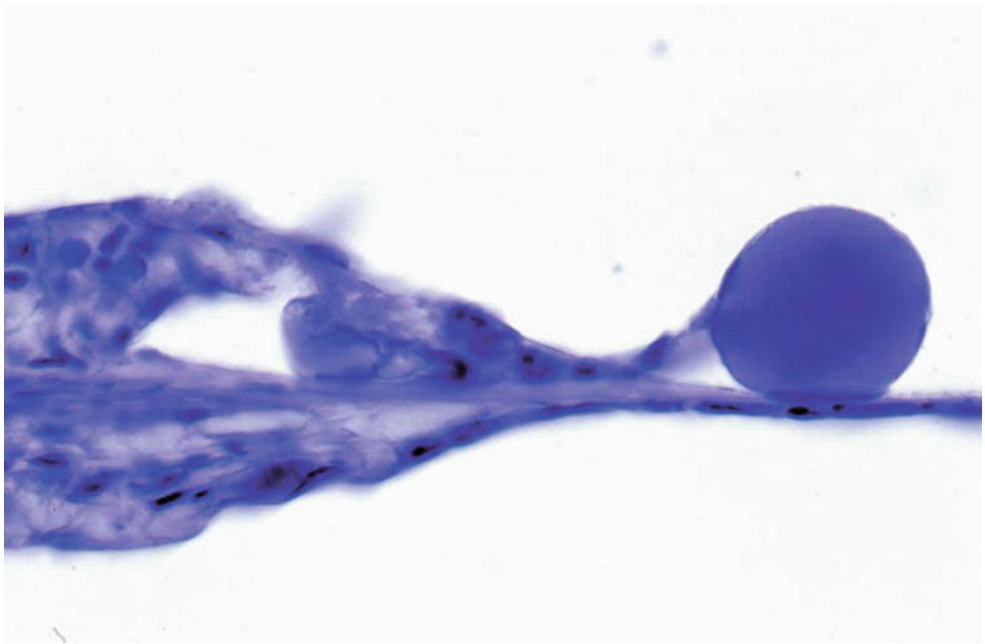

Fig. 9.18 The organ of Corti is missing and a round mass sits in its place (×160) [27]

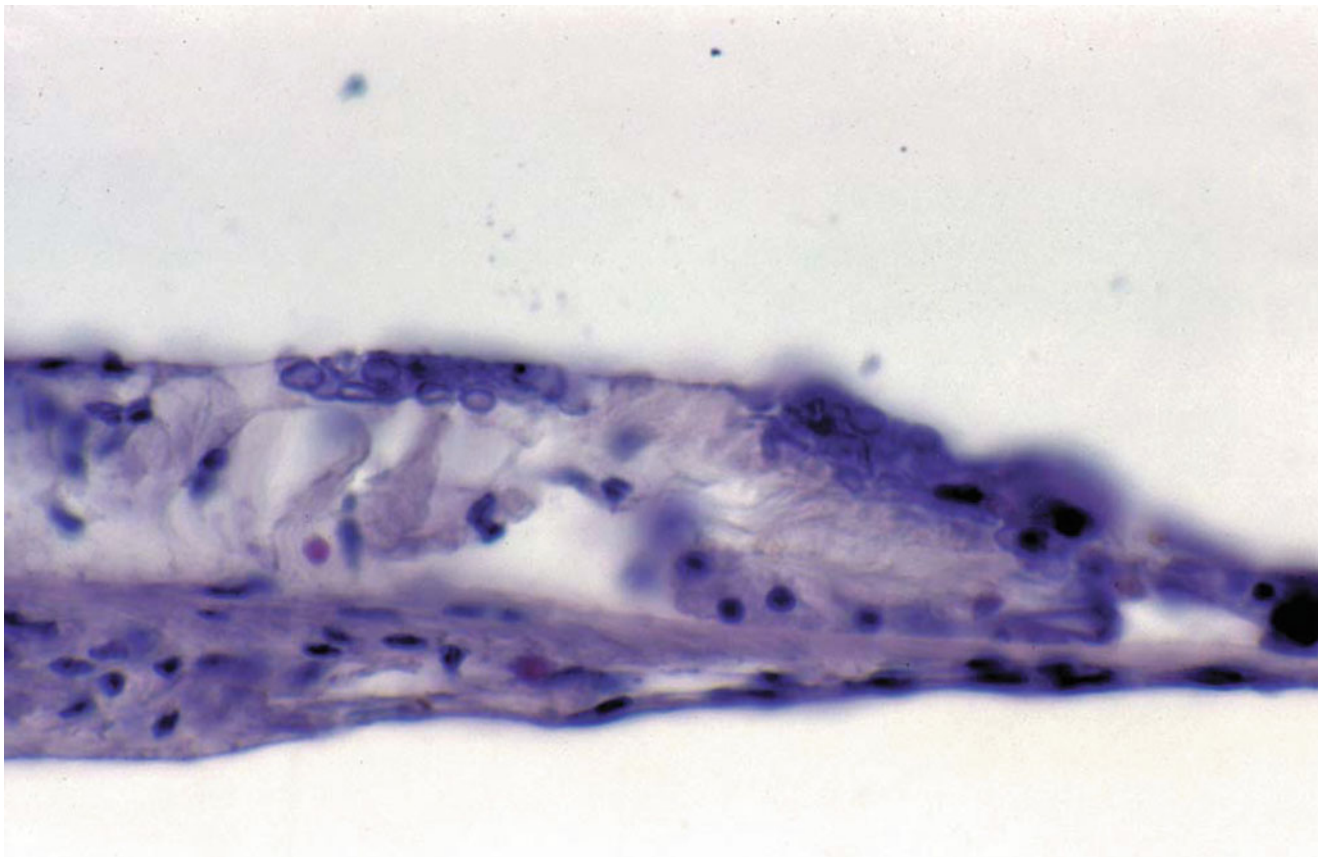

Fig. 9.19 Otoconia are observed between the collapsed Reissner's membrane and the rudimentary organ of Corti of the left ear. The organ of Corti seems to have ceased development at about the 20th week of gestation (×160) [27]

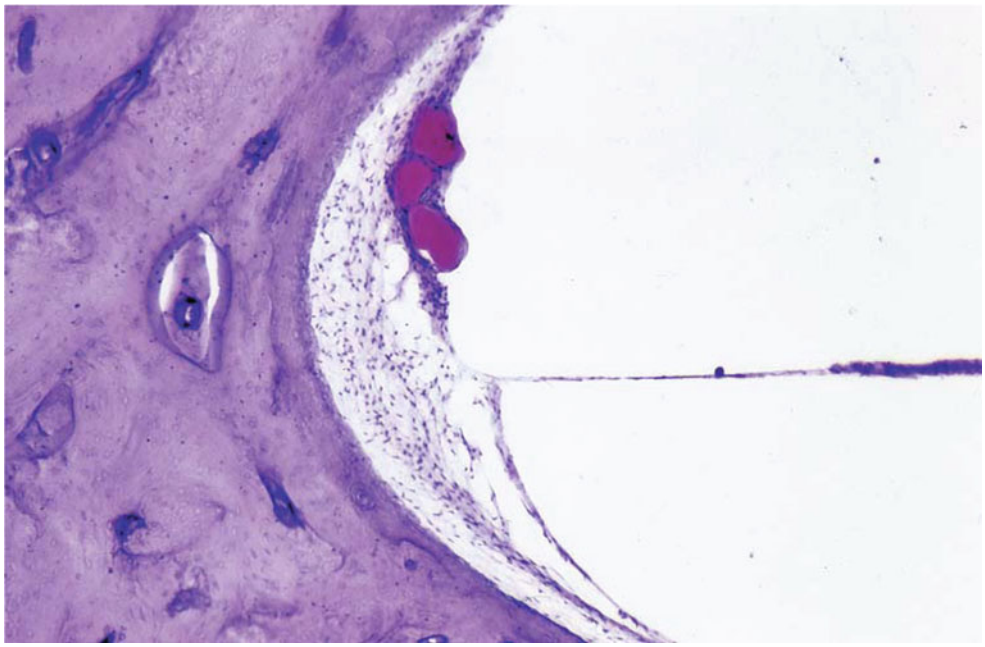

Fig. 9.20 Aplasia of the stria vascularis with cysts. The spiral ligament is hypoplastic. Reissner's membrane is indiscernible. The organ of Corti is missing. Left ear [27]

bolic products of the avascular and immature group of cells, which would secrete endolymph under normal conditions.

Scheibe described a lacuna in Rosenthal's canal [25]. He mentioned that lacunae resulted more from disturbed development than degeneration of ganglion cells. A marked loss of the spiral ganglion cells can be seen without formation of lacunae in the temporal bones of patients with various diseases. This suggests that lacuna formation is not due to ganglion cell degeneration, but is a developmental anomaly.

The presence of otoconia in the cochlea seems quite strange. Sugiura and Hilding [29] reported the presence of otoconia in Reissner's membrane between the perilymphatic and endolymphatic layers in Hedlund white mink. They thought that the otoconia had escaped from the saccule into the perilymph and had drifted into the cochlea, because the perilymphatic layer was often found to have separated.

Scheibe dysplasia has been seen in the temporal bones of patients with Jervell-Lange-Neilsen, Down, Refsum, Usher, Waardenburg, and congenital rubella syndromes.

Scheibe dysplasia is known to occur in animals such as the Dalmatian dog, deaf white cat, the Hedlund white mink, and various mouse mutants [30].

9.5 Mondini Dysplasia

9.5.1 Introduction

Carlo Mondini (1729–1803) was an Italian anatomist. Mondini dysplasia is the name given to a condition described in his paper "Anatomica surdi nati sectio" (Anatomical section of a boy born deaf) (Fig. 9.27) [31] published in 1791, 60 years before Corti's publication. His name Carlo Mondini was translated as Carolus Mundinus in Latin. "Opuscula Caroli Mundini" on the top page of his paper means "Minor works of Carlo Mondini."

Mondini reported the case of an 8-year-old deaf boy, who was struck on the foot by a speeding wagon. The wound in his leg became infected and he died of gangrene. Mondini dissected the boy's temporal bones to clarify the cause of his deafness.

Mondini found no abnormalities in the external and middle ears. In the inner ear, the semicircular canals appeared normal but the cochlea had only one and a half turns. The cochlear nerve was present. Mondini thought that the reduced number of cochlear turns could not fully explain the boy's deafness and that other causative factors must have existed in the periphery of the cochlea or inner ear fluid.

Mondini found an enlarged vestibular aqueduct in the same temporal bone. The dura mater was widely swollen in the area corresponding to the vestibular aqueduct. He opened the area circularly with a scalpel and found a small hole anteriorly connecting to the labyrinth. He was convinced that this was nothing but the vestibular aqueduct (Fig. 9.28).

A short cochlea results from arrest of cochlear development during embryogenesis of the inner ear. As a result, the cochlea may be composed of a short, curved tube. Even in more developed cochleae, the middle and apical turns may occupy a common space or cloaca. There are various possible changes in the inner ear in patients with Mondini dysplasia.

Alexander [32] was first to describe the microscopic findings of Mondini dysplasia.

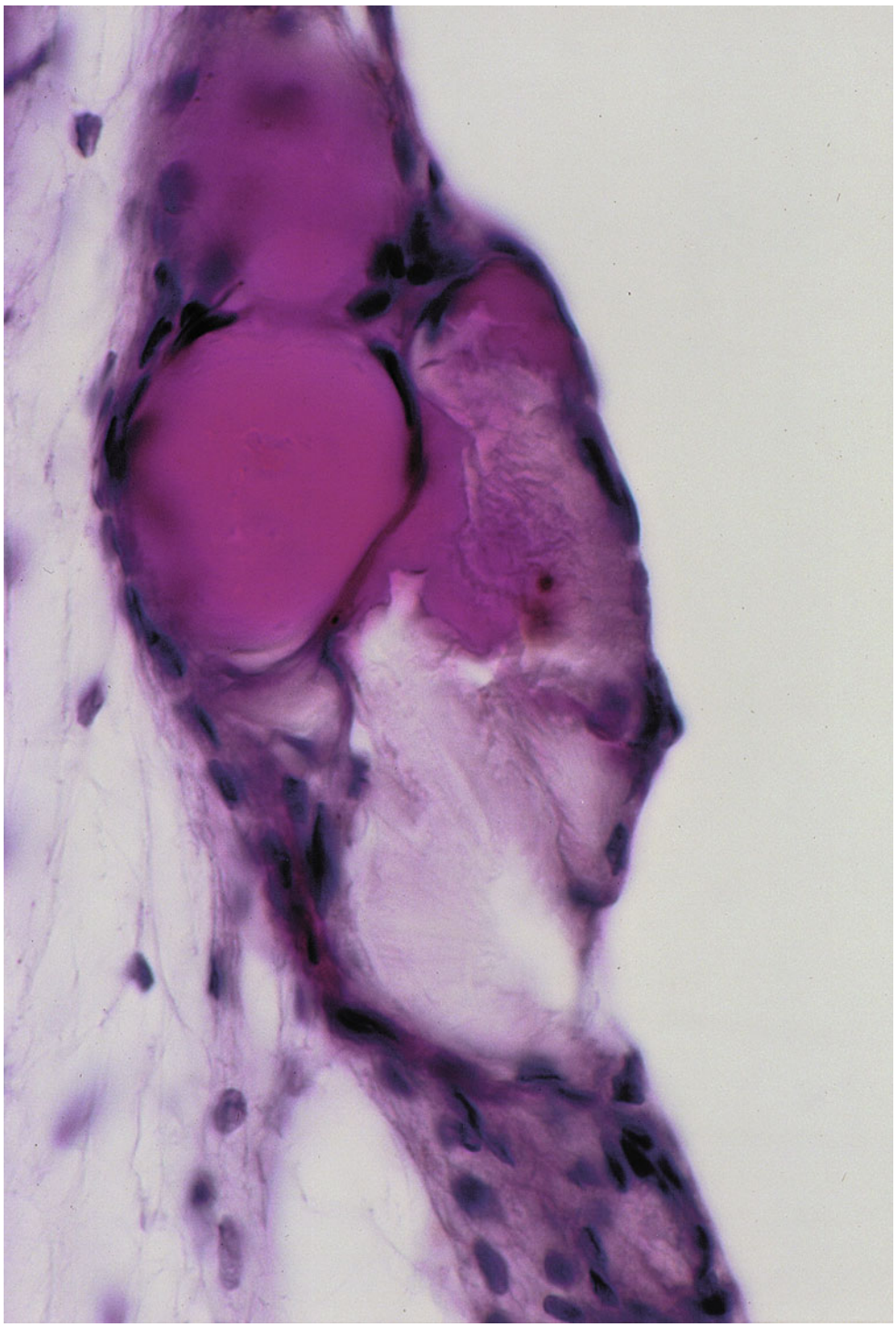

Fig. 9.21 High power view of the stria vascularis. The contents of the cysts is partly homogeneous, partly heterogeneous. The homogeneous component is eosinophilic, while the heterogeneous, white lamellar component is grey. Left ear [27]

9.5.2 Characteristics of Mondini Dysplasia

1. Mondini dysplasia usually occurs bilaterally. However, there are occasional reports of bilateral differences. Fraser [33] reported the case of a patient with Mondini dysplasia in one ear, and Michel dysplasia, complete labyrinthine aplasia, in the other.
2. The number of coils is reduced. The case Mondini reported had one and a half cochlear turns. However, the cochlear turns reported in other cases vary from flat to

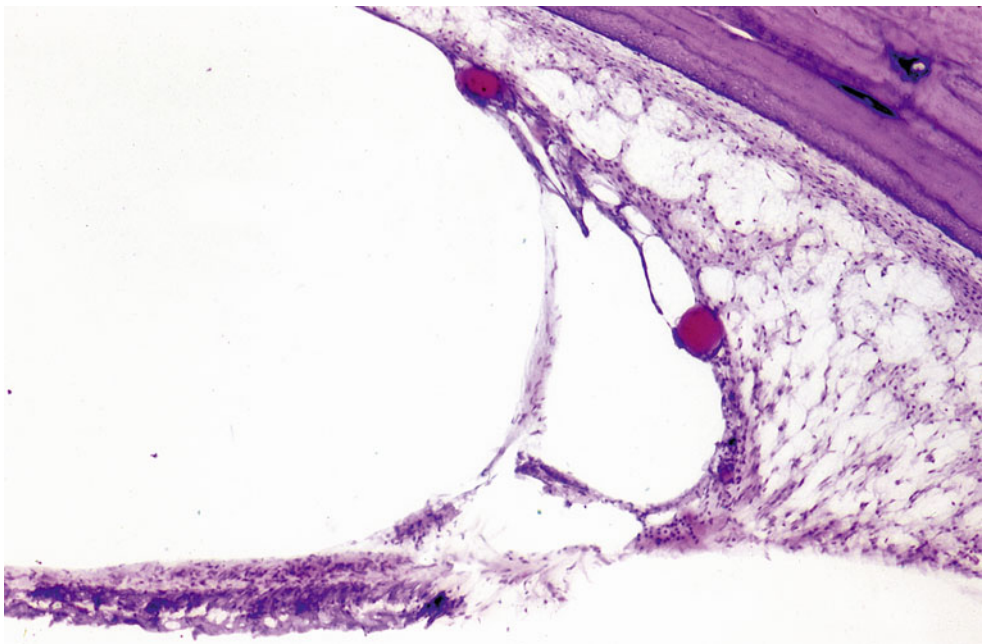

Fig. 9.22 The stria vascularis is disintegrated and includes two cysts. The spiral ligament has a sponge-like appearance. Reissner's membrane is observed in the lower basal turn. Left ear

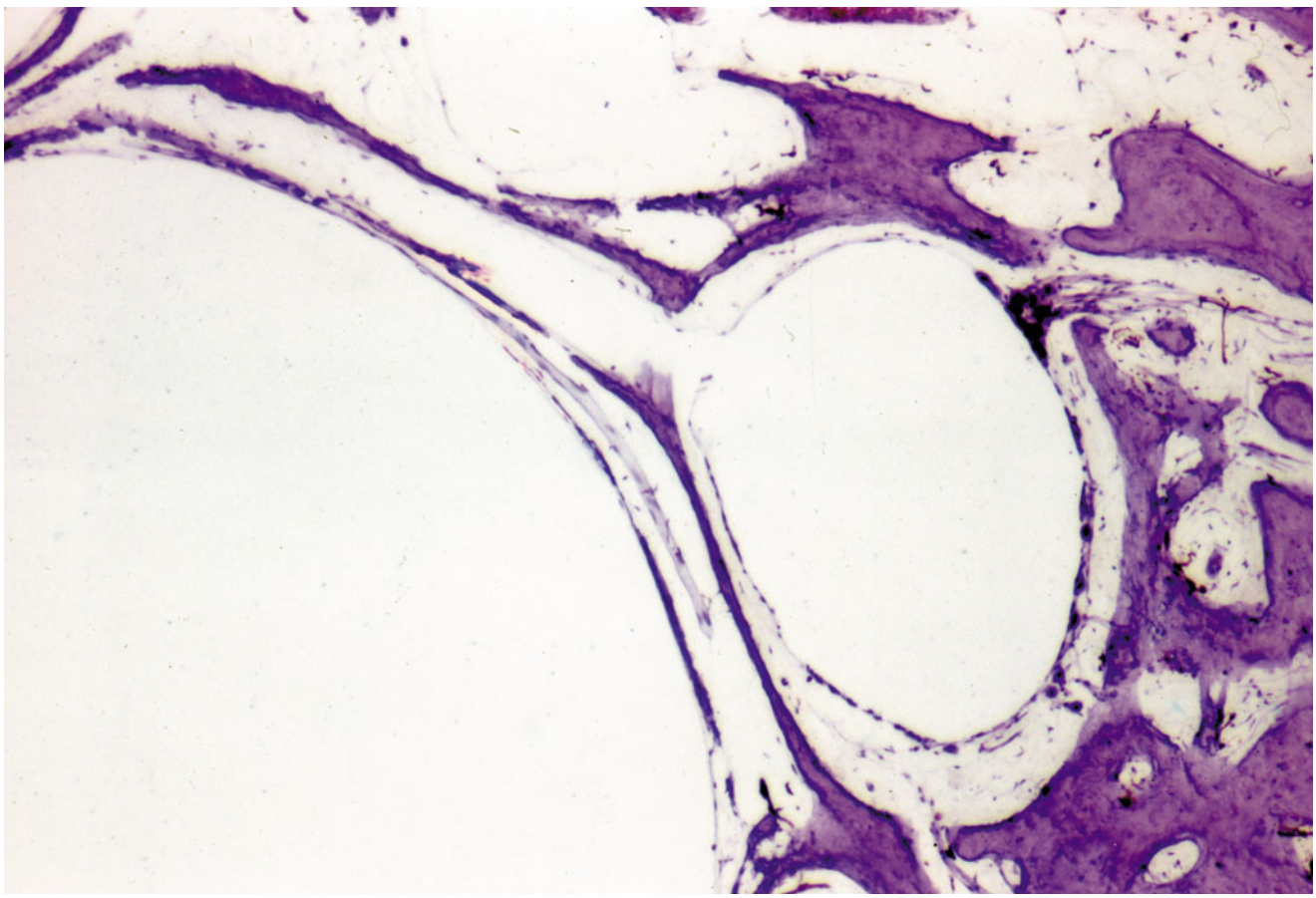

Fig. 9.23 Empty space (lacuna) from Rosenthal's canal to the osseous spiral lamina. The lacuna was named by Scheibe. Remnants of atrophic spiral ganglion cells are seen along the medial part of lacuna (×6.5)

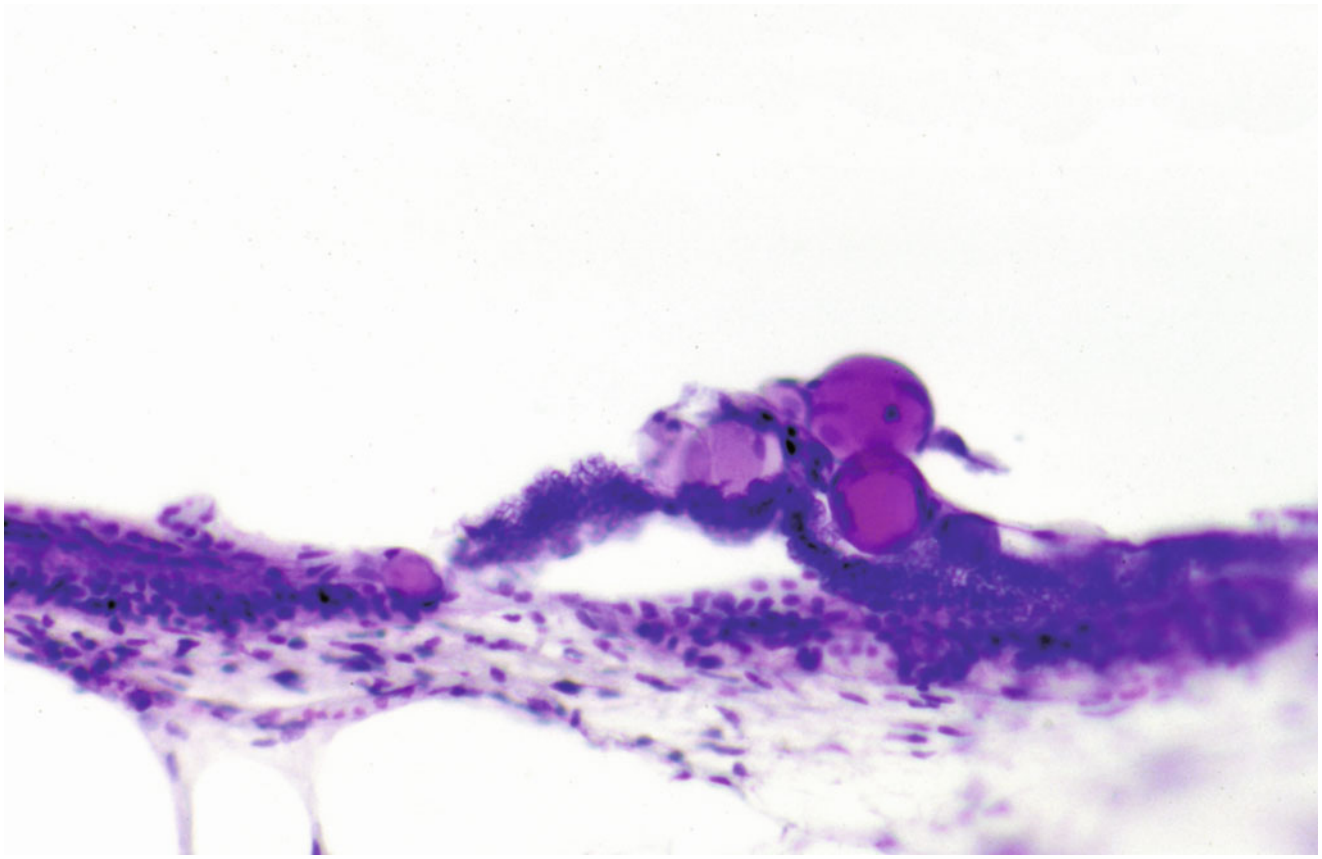

Fig. 9.24 No neuroepithelium is seen in the macula sacculi but cystic masses are present

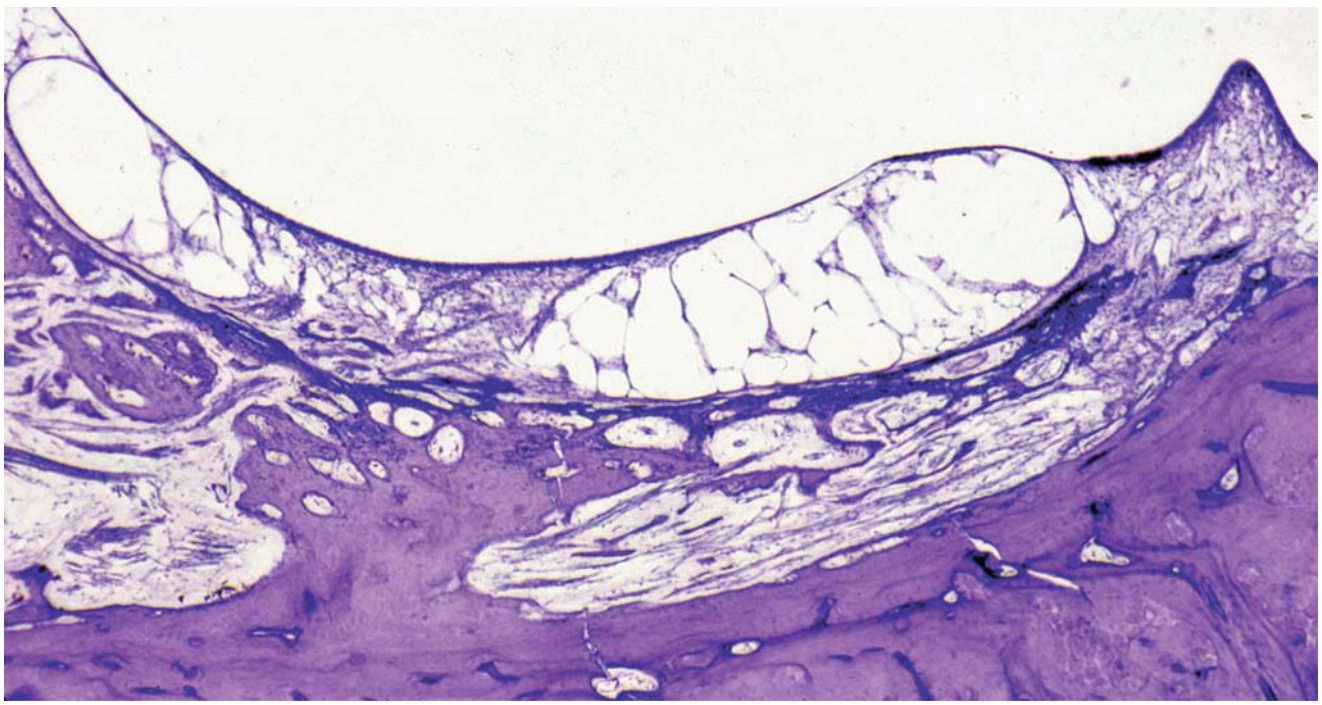

Fig. 9.25 The macula utriculi and lateral crista have normal structure, although there is a marked decrease in the neuroepithelia and nerve fibers. The area outside the utricle is fibrotic. Left ear

Fig. 9.26 The endolymphatic duct. The lumen contains a colloidal mass similar to those in the stria vascularis. Left ear [27]

normal. In the latter case, normal scalae were only found in the basal turn. The upper turns showed loss of the interscalar septum, resulting in formation of a scala communis. The modiolus and osseous spiral lamina were partly missing.

3. The deformed scala media of the second turn is hydropic and distends to the osseous spiral lamina of the upper turn.
4. The stria vascularis and spiral ligament are atrophic.
5. There is a decreased number of fibers in the cochlear nerve and spiral ganglion.
6. The saccule, utricle, ductus endolymphaticus, and endolymphatic sac are enormously dilated.
7. Many patients with Mondini dysplasia have profound hearing loss, while some have fairly good hearing.

9.5.3 Case Reports

Case 1: A 2-month-old girl died of bronchopneumonia. She had hydrocephalus (head circumference 41.5 cm; average for a 2-month-old girl, 38 cm). Histologic findings in both ears were similar [34]. The external and middle ears were normal. The internal carotid artery protruded into the middle ear bilaterally. The cochleae were short and semicircular in shape (Figs. 9.29 and 9.30). The left cochlea was 9.5 mm long; the right was 8.5 mm. In both ears, the stria vascularis was atrophic with PAS positive deposits between the spiral ligament and the basal cells of the stria. The external sulcus was wide and the stria vascularis was narrow. The saccule showed collapse. The semicircular canals were normal. The left cochlear aqueduct was large.

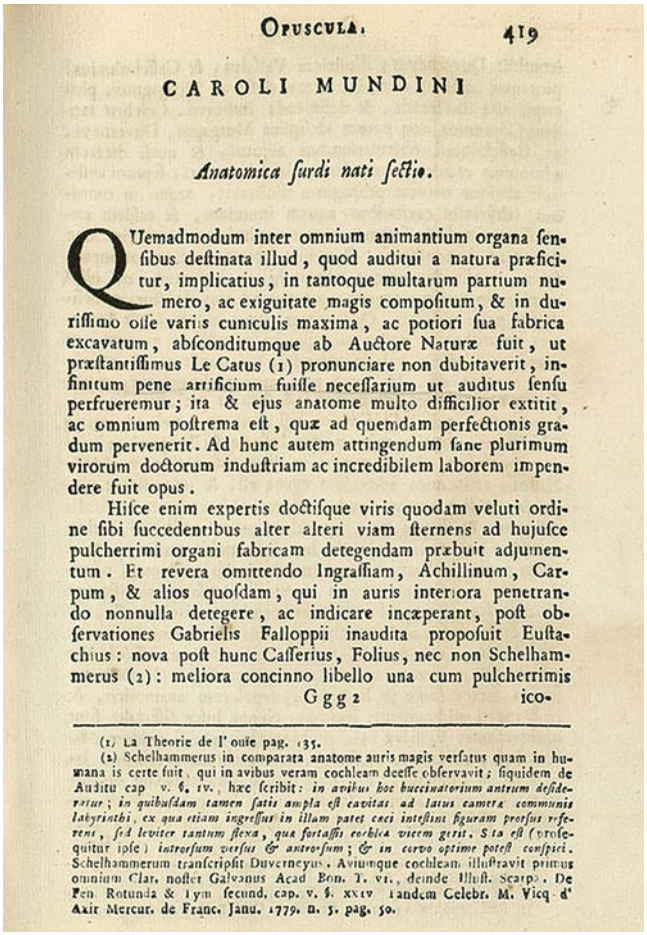

OPUSCULA. 419

CAROLI MUNDINI

Anatomica ſurdi nati ſectio.

QUemadmodum inter omnium animantium organa ſenſibus deſtinata illud, quod auditui a natura præficitur, implicatius, in tantoque multarum partium numero, ac exiguitate magis compoſitum, & in duriſſimo oſſe variis cuniculis maxima, ac potiori ſua fabrica excavatum, abſconditumque ab Auctore Naturæ fuit, ut præſtantiſſimus Le Catus (1) pronunciare non dubitaverit, infinitum pene artificium fuiſſe neceſſarium ut auditus ſenſu perfrueremur; ita & ejus anatome multo difficilior extitit, ac omnium poſtrema eſt, quæ ad quemdam perfectionis gradum pervenerit. Ad hunc autem attingendum ſane plurimum virorum doctorum induſtriam ac incredibilem laborem impendere fuit opus.

Hiſce enim expertis doctiſque viris quodam veluti ordine ſibi ſuccedentibus alter alteri viam ſternens ad hujuſce pulcherrimi organi fabricam detegendam præbuit adjumentum. Et revera omittendo Ingraſſiam, Achillinum, Carpum, & alios quoſdam, qui in auris interiora penetrando nonnulla detegere, ac indicare incæperant, poſt obſervationes Gabrielis Falloppii inaudita propoſuit Euſtachius: nova poſt hunc Caſſerius, Folius, nec non Schelhammerus (2): meliora concinno libello una cum pulcherrimis

Ggg 2 ico-

(1) La Theorie de l'ouïe pag. 135.

(2) Schelhammerus in comparata anatome auris magis verſatus quam in humana is certe fuit, qui in avibus veram cochleam deeſſe obſervavit; ſiquidem de Auditu cap. v. §. IV., hæc ſcribit: *in avibus hoc buccinatorium antrum deſideretur; in quibuſdam tamen ſatis ampla eſt cavitas ad latus cameræ communis labyrinthi, ex qua etiam ingreſſus in illam patet cæci inteſtini figuram prorſus referens, ſed leviter tantum flexa, qua fortaſſis cochlea vicem gerit. Sita eſt* (proſequitur ipſe) *introrſum verſus & antrorſum; & in cervo optime poteſt conſpici.* Schelhammerum tranſcripſit Duvernеyus. Aviumque cochleam illuſtravit primus omnium Clar. noſter Galvanus Acad. Bon. T. VI., deinde Illuſt. Scarpa. De Fen. Rotunda & Lym. ſecund. cap. V. §. XXIV. Tandem Celebr. M. Vicq d'Azir Mercur. de Franc. Janu. 1779. n. 3. pag. 30.

Fig. 9.27 Mondini's original paper published in 1791 [31]

In the normal cochlea, the width of the basilar membrane at the 7, 8, and 9 mm areas is less than 200 μm. In this case, the widths at these regions in the right ear were 360, 300, and 330 μm, respectively. These values correspond to those usually observed in the 20–25 mm region. This means that areas in the short cochlea in Mondini cases may not correspond functionally with the same areas in the normal cochlea.

Case 2: A 17-month-old boy died of bronchopneumonia. He had a cleft lip and palate, and microcephaly (brain, 495 g; head circumference, 37 cm). Family history revealed that the mother had had gestational toxicosis. There was no familial hearing loss. The pediatrician had estimated the boy's hearing to be fairly good, although hearing tests were not performed.

The left temporal bone was removed 6 h postmortem and studied [36]. There were no changes in the external and middle ears except protrusion of the bony carotid canal into the tympanic cavity. The graphic reconstruction demonstrated a short cochlea, measuring 26.7 mm (Fig. 9.30). The hook portion was missing. There was a defect of the interscalar septum between the middle and apical turns, resulting in formation of a scala communis in the region 8.2–12.6 mm from the basal end. The cochlear duct in this region was remarkably distended but was relatively flat in the lower basal turn. The distended Reissner's membrane reached to the spiral lamina and basilar membrane of the upper turn (Figs. 9.31 and 9.32).

The organ of Corti appeared well preserved. The usual modiolus was not seen but was separated and arboreous. In the basal turn, the spiral ganglion cells were arranged in a plane facing the fundus of the internal auditory canal. In the middle and apical turns, ganglion cells were scattered and ascended along strands of nerve fiber. There was no Rosenthal's canal. The spiral ganglion cells were generally decreased in number.

The stria vascularis was markedly hypoplastic. It had a papillar extension onto Reissner's membrane in the lower middle and apical turns.

The vestibular membranous labyrinth showed hydrops in the large vestibule, so that the perilymphatic space in the vestibular system was almost missing (Fig. 9.33).

The utricular macula was displaced inferiorly to the annular ligament. The utricular nerve entered the utricular macula as the two bundles subdivided.

The saccular wall was enlarged and was almost in contact with the footplate of the stapes.

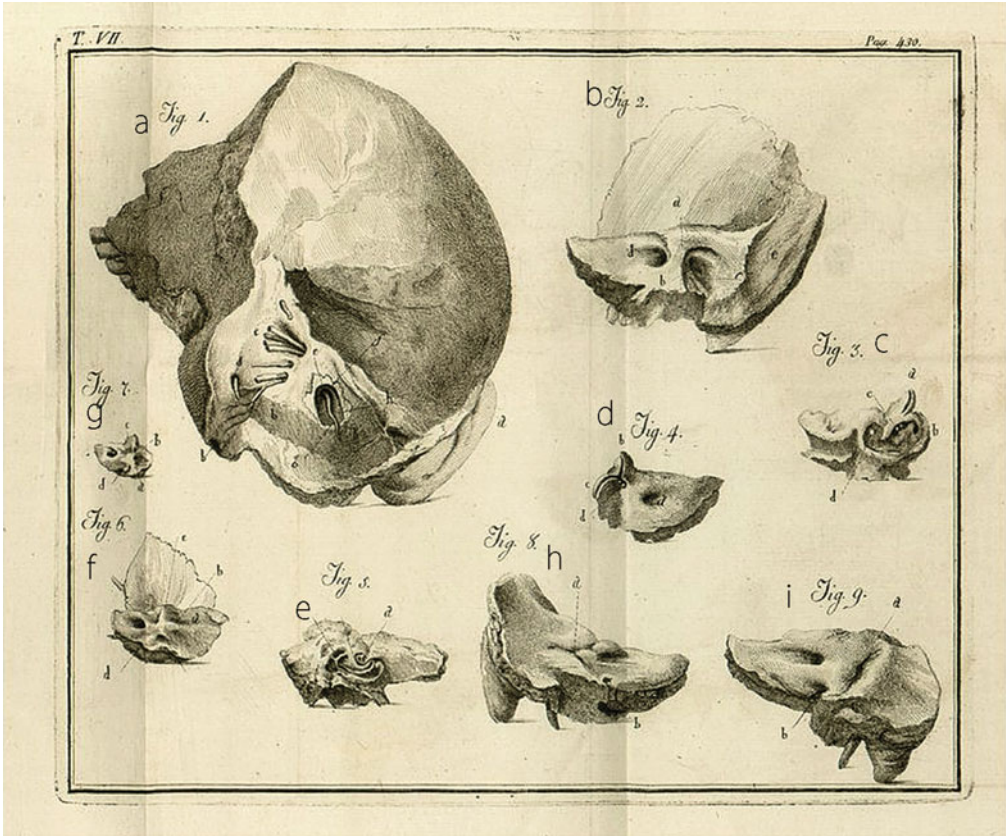

Fig. 9.28 Figures in Mondini's original paper. (**a**) The right posterior cranial fossa. The dura mater over the vestibular aqueduct is removed. *a:* auricle, *b:* sigmoid sinus, *c:* VIIth cranial nerve, *d:* VIIIth cranial nerve, *e:* open vestibular aqueduct, *f:* extremely enlarged vestibular aqueduct, *g:* a small vein, *h:* part of the posterior semicircular canal. (**b**) The right temporal bone. *a:* at the location of the vestibular aqueduct, defect of the bony wall covering the large cavity. Usually the bony wall forms the external aperture near the sigmoid sinus. *b:* abnormally enlarged entry of the vestibular aqueduct, *c:* part of the posterior semicircular canal, *d:* opening for the VIIth cranial nerve, *e:* sigmoid sinus. (**c**) The left labyrinth showing the superior and lateral canals, vestibule, and the basal turn of the cochlea. (**d**) The same as shown in (**c**). The superior and lateral semicircular canals and common crus are observed. (**e**) The right cochlea had one and a half turns. (**f**) The right temporal bone of a 9-month-old fetus. (**g**) The petrous bone of a 7-month-old fetus. (**h**) The left temporal bone of an adult (**i**) The right temporal bone with a large external aperture of the vestibular aqueduct

The endolymphatic duct and sac were greatly enlarged.

The facial canal showed dehiscence. The facial nerve was small in diameter.

Hydrops of the cochlear duct was restricted to the area of the scala communis. During cochlear development, the endolymphatic space develops first, surrounded by mesodermal tissue. The perilymphatic space is produced by absorption of mesodermal tissue. Its over-differentiation produces the scala communis. When Reissner's membrane is involved in this process marked hydrops formation results [36].

The scala communis is not pathognomonic of Mondini dysplasia. It was also found in a patient with 18 trisomy syndrome [37]. Because the blood vessels feeding the stria vascularis and spiral ligament run through the interscalar septum, defects there result in poor development of these tissues.

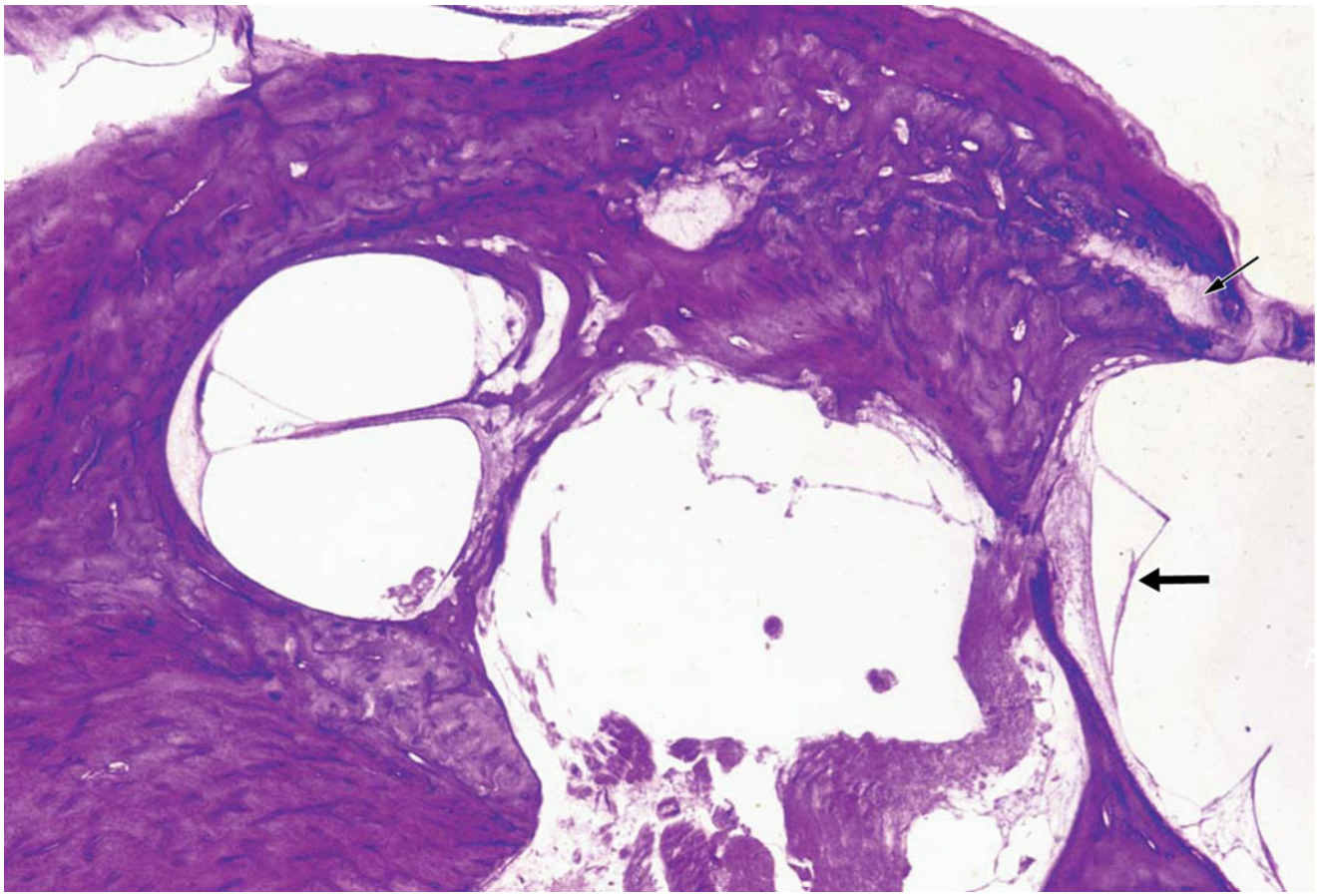

Fig. 9.29 Mondini dysplasia in case 1 (2-month-old girl). The cochlea is short and the saccule collapsed (*large arrow*). The small arrow indicates fissula ante fenestram [34]

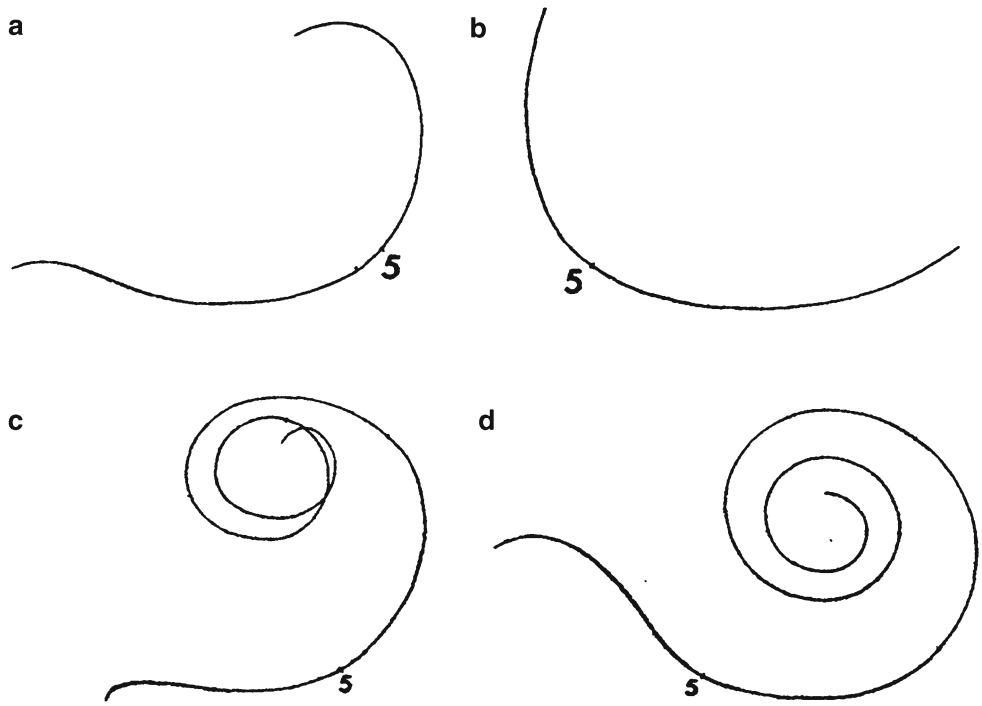

Fig. 9.30 Mondini dysplasia. The cochleae were graphically reconstructed. (**a**) The left cochlea of case 1. (**b**) The right cochlea of case 1. (**c**) The left cochlea of case 2. (**d**) Normal adult cochlea *5*: This indicates the area of the cochlea 5 mm from the basal end. Magnification of (**a**) and (**b**) is different from that of (**c**) and (**d**)

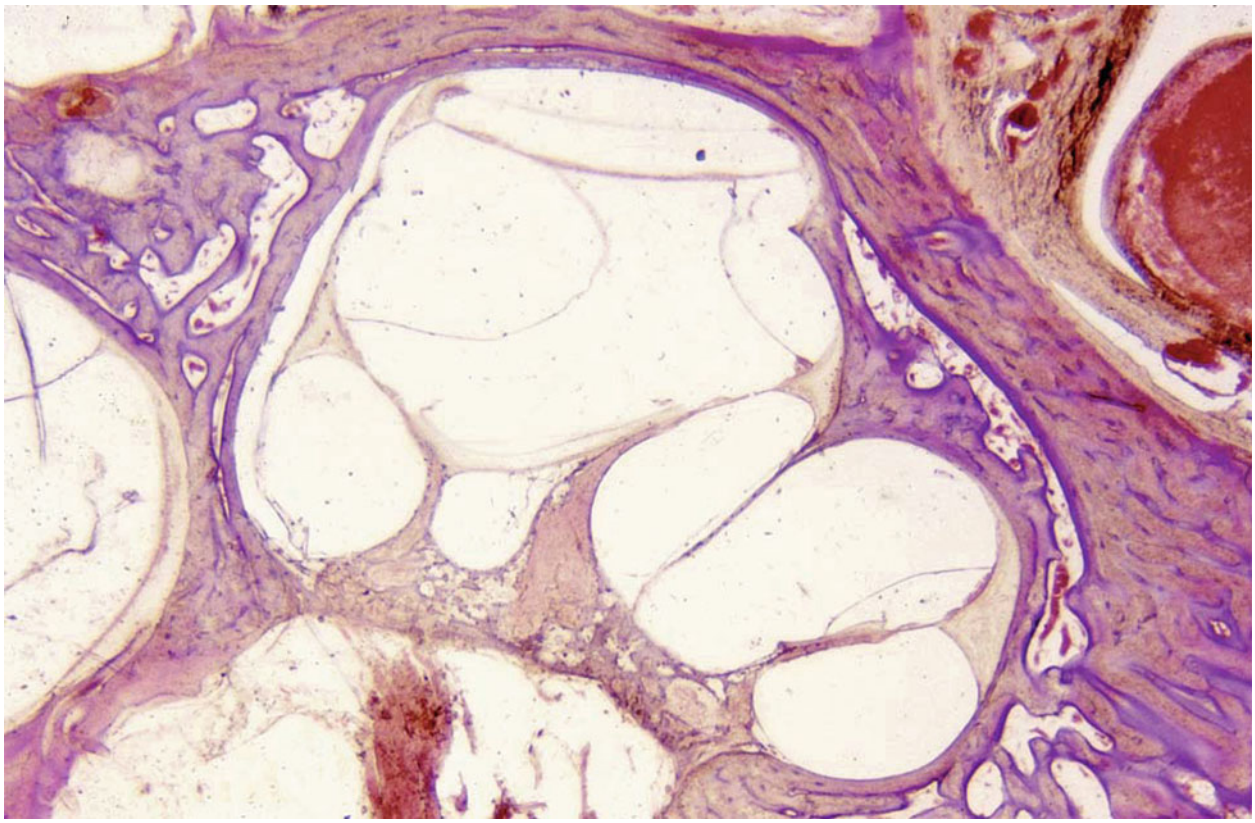

Fig. 9.31 Mondini dysplasia in case 2 (17-month-old boy). The modiolus and interscalar septum are missing; instead a scala communis has formed. The ballooned Reissner's membrane of the middle turn is attached to the basilar membrane of the apical turn. The stria vascularis and spiral ligament are either hypoplastic or aplastic. Cochlear nerves branch soon after passing the fundus of the internal acoustic meatus [35]

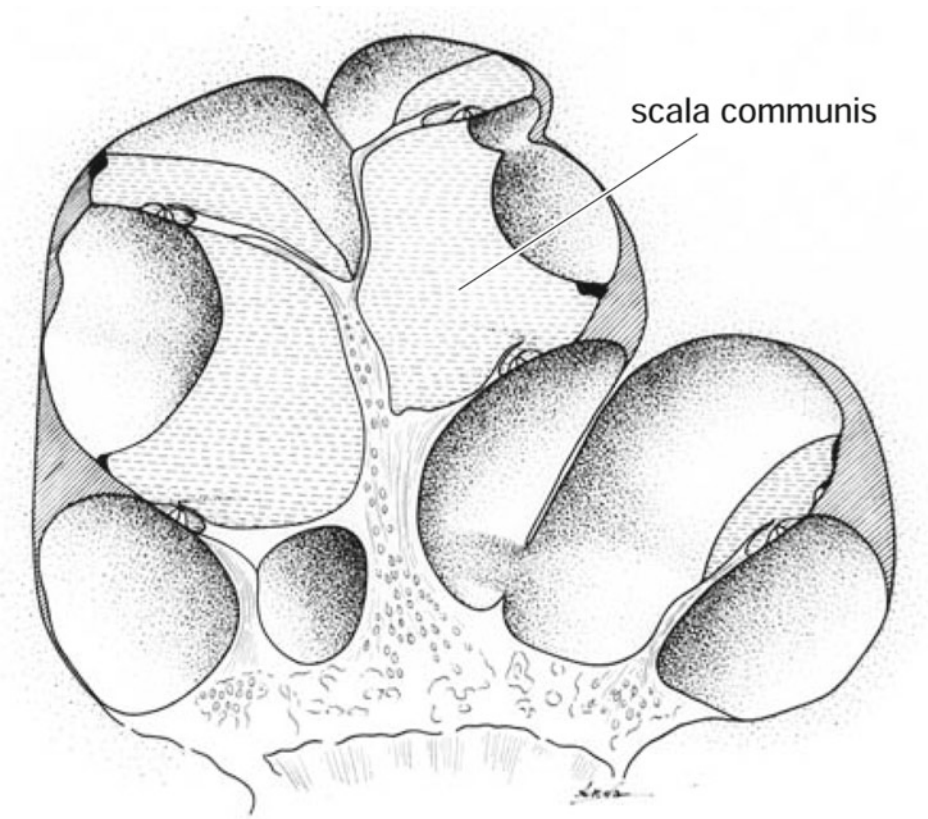

Fig. 9.32 Schematic drawing of the cochlea in Mondini dysplasia in case 2 [34]

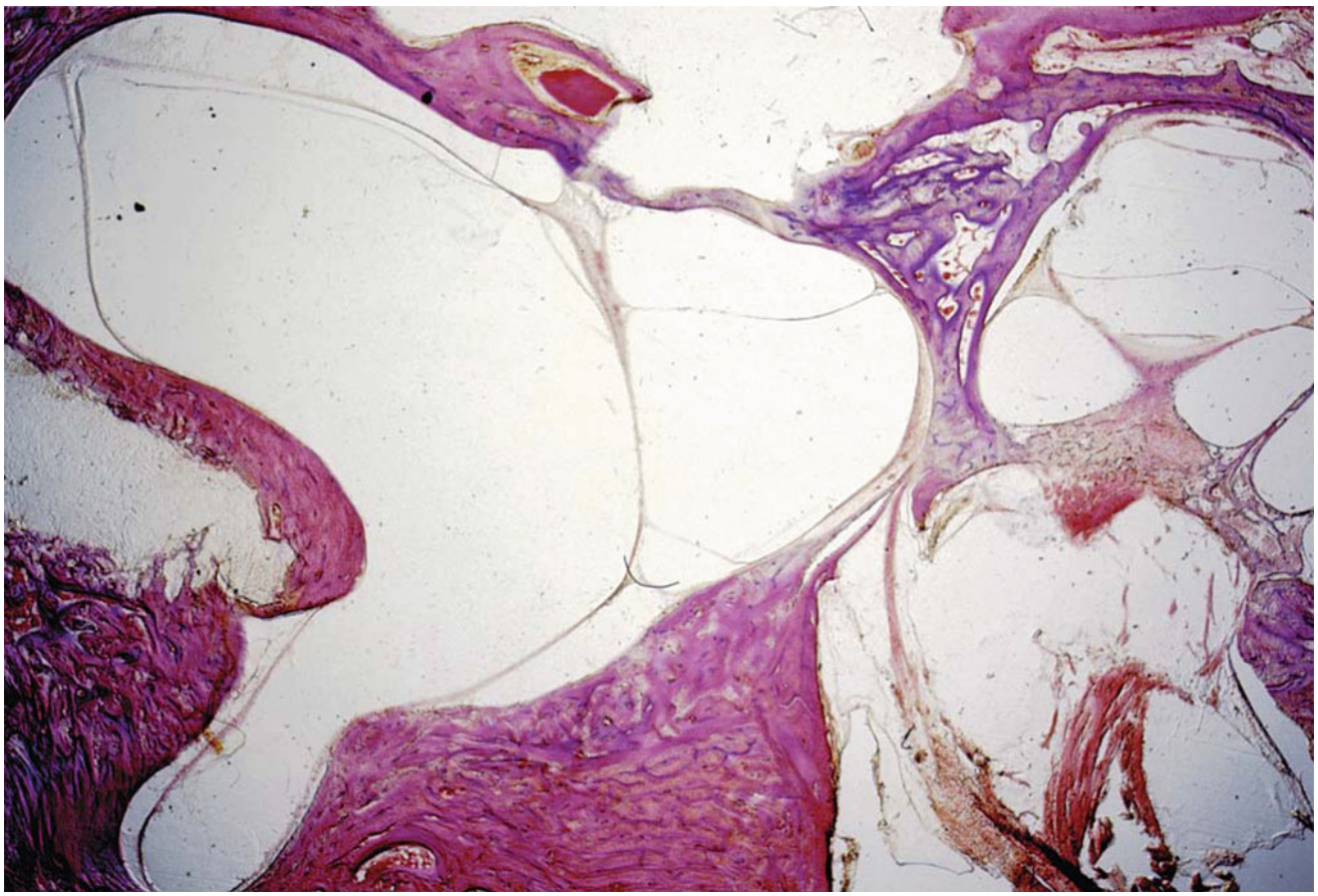

Fig. 9.33 Mondini dysplasia in case 2. The hydropic utricle, semicircular canal, and saccule occupy the enlarged vestibule. There is almost no perilymphatic space in the vestibule [35]

References

1. Jackler RK, Luxford WM, House WF (1987) Congenital malformations of the inner ear: a classification based on embryogenesis. Laryngoscope 97(Suppl 40):2–14
2. Nomura Y, Harada T, Hara M (1988) Viral infection and the inner ear. ORL J Otorhinolaryngol 50:201–211
3. Merchant SN, Nadol JB Jr (2010) Schuknecht's Pathology of the Ear, 3rd edn. People's Medical Publishing House, Shelton
4. Rathbun JC (1948) Hypophosphatasia; a new developmental anomaly. Am J Dis Child 75:822–831
5. Mornet E (2007) Hypophosphatasia. Orphanet J Rare Dis 4:2–40
6. Fraser D (1957) Hypophosphatasia. Am J Med 22:730–746
7. Nomura Y, Mori W (1968) Hypophosphatasia. Histopathology of human temporal bones. J Laryngol Otol 82:1129–1136
8. Buch NH, Jorgensen MB (1963) Pathological studies of deafmutes. Arch Otolaryngol 77:246–253
9. Balslev Jorgensen M (1964) Changes of aging in the inner ear, and the inner ear in diabetes mellitus. Histological studies. Acta Otolaryngol 188(Suppl):125–128
10. Altmann F (1964) The inner ear in genetically determined deafness. Report and analysis of 2 new cases. Acta oto-laryngol (Stockh) 187(Suppl):1–39
11. Friedmann I, Fraser GR, Froggatt P (1966) Pathology of the ear in the cardioauditory syndrome of Jervell and Lange–Nielsen (recessive deafness with electrocardiographic abnormalities). J Laryngol Otol 80:451–470
12. Rauch S (1964) Biochemie des Hörorgans. Thieme, Stuttgart
13. Bütschli O (1921) Vorlesungen über vergleichende Antomie. Band 1. Verlag von Julius Springer, Berlin
14. Guggenheim L (1948) Phylogenesis of the ear. Murray & Gee, Inc., Culver City
15. Schuknecht HF, Igarashi M, Gacek RR (1965) The pathological types of cochleo-saccular degeneration. Acta Otolryngol 59: 154–167
16. Anson BJ, Donaldson JA (1981) Surgical anatomy of the temporal bone, 3rd edn. WB Saunders Company, Philadelphia, pp 162–170
17. Sando I, Takahara T, Ogawa A (1984) Congenital anomalies of the inner ear. Ann Otol Rhinol Laryngol 93(Suppl 112):110–117
18. Hall BD (1979) Choanal atresia and associated multiple anomalies. J Pediatr 95:395–398
19. Hittner HM, Hirsh NJ, Kreh GM, Rudolph AJ (1979) Colobomatous microphthalmia, heart disease, hearing loss, and mental retardation-a syndrome. J Pediatr Ophthalmol Strabismus 16:122–128
20. Morimoto AK, Wiggins RH III, Hudgins PA, Hedlund GL, Hamilton B, Mukherji SK, Telian SA, Harnsberger HR (2006)

Absent semicircular canals in CHARGE syndrome: radiologic spectrum of findings. Am J Neuroradiol 27:1663–1671
21. Murofushi T, Ouvrier RA, Parker GD, Graham RI, Da Silva M, Halmagyi GM (1997) Vestibular abnormalities in CHARGE association. Ann Otol Rhinol Laryngol 106:129–134
22. Alagille D, Odievre M, Gautier M, Dommergues JP (1975) Hepatic ductular hypoplasia associated with characteristic facies, vertebral malformations, retarded physical, mental, and sexual development, and cardiac murmur. J Pediatr 86:63–71
23. Koch B, Goold A, Egelhoff J, Benton C (2006) Partial absence of the posterior semicircular canal in Alagille syndrome: CT findings. Pediatr Radiol 36:977–979
24. Okuno T, Takahashi H, Shibahara Y, Hashida Y, Sando I (1990) Temporal bone histopathologic findings in Alagille's syndrome. Arch Otolaryngol Head Neck Surg 116:217–220
25. Scheibe A (1892) A case of deaf-mutism, with auditory atrophy and anomalies of development in the membranous labyrinth of both ears. Arch Otol 21:12–22
26. Nadol JB Jr, Burgess B (1982) Cochleosaccular degeneration of the inner ear and progressive cataracts inherited as an autosomal dominant trait. Laryngoscope 92:1028–1037
27. Nomura Y, Kawabata I (1980) Scheibe dysgenesis of the inner ear. J Laryngol Otol 94:1345–1352
28. Fraser JS (1922) The pathological and clinical aspects of deaf-mutism. J Laryngol Otol: 13–38, 57–75, and 126–139
29. Sugiura A, Hilding DA (1970) Cochleo-saccular degeneration in hedlund white mink. Acta Otolaryngol 69(1):126–137
30. Steel KP, Bock GR (1983) Hereditary inner ear abnormalities in animals. Relationships with human abnormalities. Arch Otolaryngol 109(1):22–29
31. Mondini C (1791) Anatomica surdi nati sectio. De Bononiensi Scientarium et Artium, 7. Instituto Atque Academia Commentarii, Bologna, pp 419–431
32. Alexander G (1904) Zur pathologie und pathologischen Anatomie der kongenitalen Taubheit. Arch kiln exp Ohren Nasen Kehlkopfheilkd 61:183–219
33. Fraser JS (1927) A case of congenital deafness, showing malformations of bony and membranous labyrinths on both sides. J Laryngol 42:315–321
34. Nomura Y, Hiraide H (1972) Congenital anomalies of the inner ear. Audiol Japan 5:165–172
35. Sugiura S, Nomura Y (1970) Histological findings in a case of Mondini anomaly of the inner ear. Ann Otol Rhinol Laryngol 79:1139–1142
36. Guild SR (1929) A case of bilateral scala communis cochleae uncomplicated by other defects. An embryological interpretation of this and associated anomalies. Anat Rec 42:19
37. Kos AO, Schuknecht HF, Singer JD (1966) Temporal bone studies in 13–15 and 18 trisomy syndromes. Arch Otolaryngol 83:439–445

Index

A
Aging, 190, 194
Alagille syndrome, 210–214
Alkaline phosphatase, 55, 206
Alphaherpesvirinae, 117
ALPL gene, 206
Aortic arch syndrome, 74
Aplastic anemia, 63–64
Argon laser, 148
Arteriovenous arcade, 59
Asymptomatic mumps, 92, 137
Attic, 17
Autoimmune disease, 75
Avascular canal, 55
Azan staining, 55

B
Basilar afferent fiber, 16
Basilar fiber, 16, 182
Basilar membrane, 193–194
Benign paroxysmal positional vertigo (BPPV), 147
Betaherpesvirinae, 117, 122
Bill's bar, 16
Bindegewebesbalken, 2
Breaking point, 181, 187
Buerger's disease, 64–67
Bunyaviridae, 206

C
Caloric irregularity, 38
Caloric restriction, 202
Canaliculi perforantes Schuknechtii, 24, 25
Canal plugging, 160
Carbonic anhydrase, 29, 33
Carbonization, 160
Cerebrospinal fluid pressure (CSF-P), 37
Cervical VEMP (cVEMP), 109
CHARGE syndrome, 213
Chorda tympani, 17
CMV. *See* Cytomegalovirus (CMV)
Coagulation necrosis, 88
Cochlea, 10–17, 182, 186, 187
Cochlear aqueduct, 27
Cochlear hyperplasia, 205
Cochlear neuronitis, 92
Cochleosaccular degeneration, 214
Cochleosaccular dysplasia, 214
Cochlin-tomoprotein, 34
Coiled arteriole, 51
Common cavity, 205
Complement-fixation testing (CFT), 118
Congenital rubella syndrome, 219
Cortilymph, 30
Cortilymphatic hydrops, 27, 29, 30, 38, 42
Cowdry type A inclusion bodies, 119
Crista transversa, 16
Crus commune, 211
Cryoglobulinemia, 67–69
CSF pressure, 34
Cyclostomata, 210
Cytomegalic inclusion disease, 122, 126
Cytomegalovirus (CMV), 117, 122–137
  screening program, 126
Cytoplasmic protrusion, 187

D
Dalmatian dog, 219
Dark cell area, 152, 160
Deaf white cat, 219
3D-FLAIR gadolinium MRI, 113
Diabetes mellitus, 78
Diagnosis of mumps deafness, 143
Diagnosis of sudden deafness, 98–99
Dissociation of ampullary wall, 38, 48
D-JNK-1, 112
Donaldson's line, 165
Dove, 211
Down syndrome, 219

E
Efferent fibers, 182
Efferent innervation, 13
Emperipolesis, 118, 119
Endolymph, 23, 30
Endolymphatic hydrops, 39, 102, 121
Endolymphatic sac surgery, 113
Endolymph of Breschet, 23
Enlarged vestibular aqueduct, 219
Epithelial cell layer, 130
Epitympanic recess, 17
Epstein-Barr virus (EBV), 117
Essential cryoglobulinemia, 68
Esterase, 3
European perch *(Perca fluviatilis)*, 211

Y. Nomura, *Morphological Aspects of Inner Ear Disease*, DOI 10.1007/978-4-431-54204-9,

Experiment, 111, 112
Experimental cytomegalic labyrinthitis, 128–137
Experimental endolymphatic hydrops, 107
Experimental HSV labyrinthitis, 118–121
Experimental mumps labyrinthitis, 140–142
Experimental perilymphatic fistula, 36, 39
Experimental viral labyrinthitis, 90, 141
Explosive route, 34
External ear, 17

F
Floating labyrinth, 172
Floating (irritable) labyrinth, 38, 45
Foramen rotundum, 2
Frog, 211
Full type inclusion bodies, 119

G
Gadolinium, 104
Gadolinium 3D-FLAIR image, 104
Gadolinium-diethylene-triamine pentaacetic acid (Gd-DTPA), 104
Gadolinium MRI, 103–106, 113
Gammaherpesvirinae, 117
Gd-DTPA-BMA, 104
Gentamicin, 110–114
Giant cilia/cilium, 187, 190
GJB2 mutation, 126
Grenzmembran, 3
Guinea pig cytomegalovirus (GPCMV), 128, 205

H
Habenula perforata, 13, 181
Hagfish *(Myxinoidea)*, 210, 213
Hale's colloid iron, 209
Hedlund white mink, 219
Hensen-Deiters' junction, 25
Hensen-Deiters' split, 25
Hensen's cell cyst, 27
Herpes classification, 117
Herpes simplex virus (HSV), 117–122
  antigen, 118
  human, 86
Herpes simplex virus-1 (HSV-1), 117
Herpes simplex virus-2 (HSV-2), 117
Herpesviridae, 206
HSV. *See* Herpes simplex virus (HSV)
Human vestibule, 176
Huschke's teeth, 11, 14
Hypophosphatasia, 206

I
Idiopathic perilymphatic fistula, 38
Idiopathic sudden deafness, 85
Immunofluorescence, 112, 118, 141
Implosive route, 34
Inclusion-bearing cells, 126
Inferior cochlear vein, 51
Inner ear, 147–179
  anatomy, 1–7
  blood vessel, 52, 55, 63, 67, 73, 74, 80, 81
Interdental cell, 71, 86–87
Internal auditory canal, 16
Interscalar septum, 52, 223

J
Jacobson's nerve, 16
JAG1, 213
Japanese eel *(Anguilla japonica)*, 211
Jervell-Lange-Neilsen syndrome, 219
c-Jun N-terminal kinase (JNK), 112

K
Kaposi's sarcoma-associated herpesvirus (KSHV), 117
K^+ cycling, 107

L
Labyrinth, 1, 38
Labyrinthine artery, 51
Lacuna/lacunae, 214, 219
Lagena cochleae, 1
Lamprey *(Petromyzontida)*, 210, 213
Laser labyrinthectomy, 172
Leukemia, 63
Limbus spiralis, 29
Lipidosis, 193–194
Lipofuscin, 167
Lipofuscin granule, 167
Liquid of Cotugno, 23
Low-tone sensorineural hearing loss, 38
Lungfish *(Protopterus annectens)*, 211
Lymphocryptovirus, 117

M
Macula communis, 210
Mammalian cochlea, 1
Medial efferent fiber, 16
Medial fiber, 16, 182
Melanin, 167
Melanocyte, 52
Membrana limitans, 2–7, 113
Membrana reticularis, 27, 30, 187, 189, 197
Meniere's disease, 101–114
Mesothelial cell, 160
Mesothelial cell layer, 130
Metachromasia, 209
Michel deformity, 205
Michel dysplasia, 220
Middle ear, 16
Middle ear pressure (ME-P), 34, 38
Mild hydrops, 152
Mixed cryoglobulinemia, 71
Mondini dysplasia, 219
Mononuclear phagocyte system, 137
MRI, 103–107
Mumps, 137
Mumps IgM test, 97
Mumps meningoencephalitis, 144
Myeloid leukemia, 63

N
Nasopharyngeal pressure (NP-P), 38
Nerve fiber, 192
Neurofilament, 185
Neutralization testing (NT), 118
Nile blue staining, 167
Nile blue sulfate, 193
NOTCH2 genes, 213

O
Ocular VEMP (oVEMP), 109
Optical coherence tomography (OCT), 107–109
Organ of Corti, 3, 4, 11, 13, 14, 16, 18, 182–188, 193, 194
Osmium tetroxide-α-naphthylamine (OTAN), 193
Osseous labyrinth, 2
Osteoid tissue, 208
Otic capsule, 153
Otoconia, 10
Outer spiral vessel, 59

P
Pars basilaris, 1
Pars inferior, 7–16
Pars pectinata, 193, 194
Pars superior, 2–7, 211
Pars tecta, 193, 194
Partitioning, 147
PAS, 193, 209
PAS staining, 167
Penetration depth, 148
Perilymph, 23
  leakage, 30
Perilymphatic fistula, 30, 172
Periosteum, 165
Petromyzontidae, 1
Phenazine methosulfate, 25
Phosphoethanolamine, 209
Photochemical reaction, 151
Phylogenesis, 1, 210–213
Planum semilunatum, 62
Promunturium/*promontorium*, 10
Pseudocalcinosis, 210
Pulseless disease, 74

R
Reactivation of latent infection, 90
Refsum syndrome, 219
Reinforced area, 167
Reinforced area of the saccular membrane, 7
Relapsing polychondritis, 90
Reptiles, 121
Rhadinovirus, 117
Rickets, 207
Rolled-up, 86, 128
  tectorial membrane, 86, 117
Root cell, 59, 107
Roseolovirus, 117
Round window, 2
  membrane, 148, 149
  niche membrane, 31

S
Saccular hydrops, 103
Saccular macula, 157
Saccular wall, 167
Saccule, 1, 7–10
Scala communis, 223, 224
Scheibe degeneration, 214, 215
Scheibe dysplasia, 214–219
Secondary tympanic membrane, 2
Semicircular canal, 2, 163, 210–213
Semicircular duct, 62, 165
Seronegative animal, 137
Seropositive animal, 137
Short cochlea, 219
Silent mumps, 137, 144
Simplex virus, 117
Singular neurectomy, 160
Sinus superior utriculi, 2, 211
Smith-Dietrich reaction, 193
Spatium perilymphaticum, 2
Spatium perilymphaticum inferius, 2
Spatium perilymphaticum superius, 2
Spiral ganglion, 13
Spiral prominence, 59
Spiral vessel under the tunnel of Corti, 59
Stapes gusher, 29, 32
Statocyst, 1
Stereocilia, 187, 196, 197
Strial atrophy, 190–193
Strial presbycusis, 190–191
Sturgeon *(Acipenser sturio)*, 211
Subcuticular region, 112
Succinic dehydrogenase, 25
Sudan III, 193
Sudden deafness, 67, 80, 85–99, 118, 143

T
Takayasu's arteritis, 74–78
Tectorial membrane, 86–87
Temporal bone histopathology, 102–103
The otic capsule adjacent to, 153
Thermocouple probe, 167
Thromboangiitis obliterans, 64
Togaviridae, 206
TORCH complex, 122
Torpedoes, 182
Trabecular mesh, 3, 43
Transverse crest, 16
Trisomy 13, 213
Trisomy 18, 213, 225
Tunnel spiral bundle, 16
Tympanic nerve, 16

U
Usher syndrome, 219
Utricle, 2
Utricular endolymphatic hydrops, 103
Utricular hydrops, 111
Utricular macula, 152, 167
Utricular macula ablation, 172
Utricular wall, 165
Utriculoampullary nerve, 172
Utriculo-endolymphatic valve, 98, 110

V
Vaporization, 160
Varicella zoster virus (VZV), 117
Vasculoepithelial zone, 29
Vas prominence, 193
Vas spirale, 59
Vein of the cochlear aqueduct, 51
VEMPs dissociation, 109

Vertical crest, 16
Vertigo, 164–165, 172, 173
Vessel wall ratio, 78
Vestibular anlage, 211
Vestibular atelectasis, 38
Vestibular collapse, 44
Vestibular evoked myogenic potential (VEMP), 109
Vestibular ganglion cell, 160
Vestibular membrane, 23
Vestibulum, 2
Viral labyrinthitis, 85, 86, 88, 90, 91, 99
Virion, 142
Visualization of hydrops, 104
Voit's nerve, 10

W
Waardenburg syndrome, 213, 219

Z
Ziehl-Neelsen staining, 167